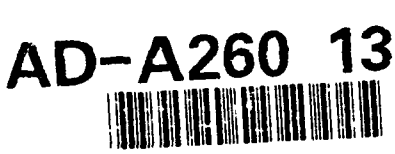

BEHAVIOR OF UNSATURATED CLAYEY SOILS AT HIGH STRAIN RATES

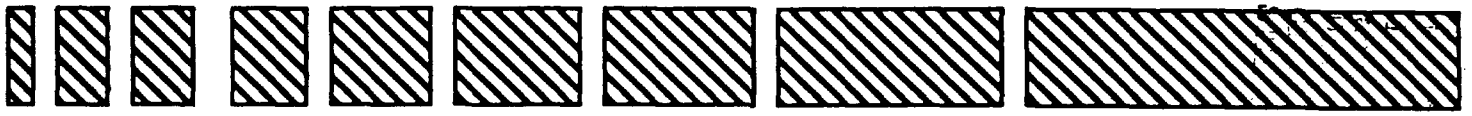

FINAL REPORT
for
CONTRACT NO. F49620-89-C-0077
1989-1992

for
The Air Force Office of Scientific Research
Building 410
Bolling AFB, DC 200332-6448

October 1992

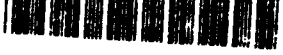

CENTER FOR GEOTECHNICAL & HIGHWAY MATERIALS RESEARCH
THE UNIVERSITY OF TEXAS AT EL PASO
EL PASO, TEXAS 79968
(915)747-5464

REPORT DOCUMENTATION PAGE

Form Approved
OMB No. 0704-0188

1. AGENCY USE ONLY (Leave blank)	2. REPORT DATE	3. REPORT TYPE AND DATES COVERED
	October, 1992	Final Report June 89-Aug 92

4. TITLE AND SUBTITLE

Behavior of Unsaturated Clayey Soils at High Strain Rates

5. FUNDING NUMBERS

F 49620-89-C-0077
PE 61102F
PR 2302-CS

6. AUTHOR(S)

Miguel Picornell and Soheil Nazarian

7. PERFORMING ORGANIZATION NAME(S) AND ADDRESS(ES)

Center for Geotechnical and Highway Materials Research
University of Texas at El Paso
El Paso, Texas 79968-0516

8. PERFORMING ORGANIZATION REPORT NUMBER

9. SPONSORING/MONITORING AGENCY NAME(S) AND ADDRESS(ES)

Air Force Office for Scientific Research / N.A
Building 410
Bolling AFB, DC 20032-6448

10. SPONSORING/MONITORING AGENCY REPORT NUMBER

F49620-89-C-0077

11. SUPPLEMENTARY NOTES

12a. DISTRIBUTION/AVAILABILITY STATEMENT

*

DISTRIBUTION STATEMENT A
Approved for public release
Distribution Unlimited

12b. DISTRIBUTION CODE

13. ABSTRACT (Maximum 200 words)

Specimens of clayey soils with a controlled pore solution chemistry were prepared, consolidated, and equilibrated at three different soil suction levels. Some specimens were subjected to creep/recovery tests in conventional triaxial cells. These results were used to select viscoelastic models that could explain the specimen behavior. Duplicate specimens equilibrated at the same soil suction levels were tested in a dynamic triaxial test system. For this purpose, the specimen was subjected to a series of stress controlled pulses of 50msec duration and consisting of a ramp-up to a peak deviatoric stress and a ramp-down to zero. The peak stress was increased for successive pulses. The response of the specimen, and the strain-time history, was then recorded. The non-linear viscoelastic models fitted to creep-recovery tests were used in combination with the modified superposition principle to predict the expected response of the specimen. The viscoelastic models that were fitted to the steady creep phase did not provide the best match. It was rather necessary to use the models fitted to the initial part of the transient creep phase.

14. SUBJECT TERMS	15. NUMBER OF PAGES
Creep, High Strain Rates, Unsaturated Clayey Soils	417
	16. PRICE CODE

17. SECURITY CLASSIFICATION OF REPORT	18. SECURITY CLASSIFICATION OF THIS PAGE	19. SECURITY CLASSIFICATION OF ABSTRACT	20. LIMITATION OF ABSTRACT
Unclassified	Unclassified	Unclassified	UL

FINAL REPORT
for
CONTRACT NO. F49620-89-C-0077
1989-1992

BEHAVIOR OF UNSATURATED CLAYEY SOILS AT HIGH STRAIN RATES

for

The Air Force Office of Scientific Research
Building 410
Bolling AFB, DC 200332-6448

By
M. Picornell and S. Nazarian
Center for Geotechnical and Highway Materials Research
The University of Texas at El Paso
El Paso, Texas 79968-0516
915/747-5464

ABSTRACT

A sample of soil from the flood plain of the Rio Grande was collected and subjected to engineering and physicochemical characterization tests. The soil was cleaned of soluble components and organic matter. Then a soil suspension stock was prepared with a precisely known and controlled chemistry of the pore solution. This soil suspension was used as a stock to provide soil to prepare specimens for testing.

The first step in specimen preparation consisted of the centrifugation of the soil suspension to reduce water content and reduce the volume changes that the suspension would have to experience during consolidation. For this purpose, the soil cake recovered from the centrifuge bottle was placed on a glass plate and was thoroughly mixed. Then the mixed soil cake was placed in a rubber membrane and consolidated in a triaxial cell under 50 psi confining pressure, at constant temperature, and for a fixed length of time.

The test specimens were trimmed from the consolidated material to cylindrical specimens 1.4 in. in diameter. These in turn were placed in a triaxial cell over a high air entry porous stone to equilibrate the specimen to predetermined soil suction levels. Upon reaching the equilibration point some specimens were destined to perform creep/recovery tests, while the rest were used for dynamic tests at high strain rates.

The creep tests were performed on specimens equilibrated at three soil suction levels and several deviatoric stress levels. The results of these tests were used to find viscoelastic models that could explain the observed behavior. The test matrix was selected to provide information on how the model parameters depended on deviatoric stress and soil suction levels.

The specimens destined for the dynamic tests were prepared following the same procedure and under conditions that duplicated the creep tests. The specimen was placed in a dynamic triaxial test system and was subjected to successive load pulses of increasing peak load intensity. During the test, the load-time and the strain-time histories were recorded for each load pulse.

The load-time history recorded was used in conjunction with non-linear viscoelastic models developed from the creep tests to predict the strain-time history of the specimens tested in the dynamic triaxial test. The best model was found to be a power law of time with the coefficient and the exponent being functions of the deviatoric stress and soil suction levels.

The predictions using this power law in conjunction with a modified superposition principle compare favorably with the recorded data at low deviatoric stress levels. However, at the peak loads, the predictions consistently are larger than the measured strain levels by factors from two to three. Although some of these discrepancies might be due to limitations of the viscoelastic model, the results of the present study suggest that a large part of the discrepancies might be due to inaccurate records of the load-time history applied on the specimen. The

major concern being the friction between the push rod and the bushing of the triaxial cell.

In summary, the results of the present study suggests that the long term creep records do not provide the best models to predict the high strain rate behavior of unsaturated clayey soils. Nevertheless, it appears that the records of the transient creep phase can be advantageously used to model the soil behavior at high strain rates; although further research is necessary to further investigate this point.

TABLE OF CONTENTS

LIST OF TABLES

LIST OF FIGURES

CHAPTER ONE

INTRODUCTION

1.1 PROBLEM STATEMENT

In order to properly analyze the survivability of military or security sensitive structures, the soil-structure interaction under extreme loading conditions, such as those caused by a conventional or nuclear attack, should be understood and accurately modeled. Under these conditions, the strain levels as well as strain rates experienced by the soil are extremely high. Furthermore, many of these structures rest on or is surrounded by soils that are in the unsaturated state. For a realistic prediction of the soil response, it is necessary to develop appropriate constitutive equations that account for the high strain rates imposed on the soil and should include the effects of the soil suction.

Strength and constitutive behavior of soils are known to be strain-rate dependent. This dependency is more pronounced for clayey soils than for granular soils. In the existing technical literature, the bulk of research has been directed towards the study of the strength and constitutive behavior of saturated clayey soils. However, most of those investigations have been performed at small strain-rates. Further more, a very limited amount of work has been performed to elucidate the effect of soil suction on the constitutive behavior of unsaturated clayey soils.

1.2 OBJECTIVES AND APPROACH

The main focus of the present report has been to evaluate the possibility of using low-strain rate test results and models to predict the behavior of unsaturated clayey soils at high-strain-rates. The study consisted of performing creep/recovery test on soil specimens equilibrated to these preselected soil suction levels. These results are then used to develop constituting models to explain the soil behavior at low strain rates. In a second phase, specimens of "identical" characteristics were subjected to high strain rates with a concurrent variation of the deviatoric stress in a MTS dynamic soil testing facility. Finally, the constitutive models developed from the creep-recovery tests were used to predict the behavior of the tests performed at high strain rates. The validity of the existing models were investigated by comparing the predictions to the actual measurements.

1.3 ORGANIZATION

This section provides a brief overview of the organization of this report that includes eight chapters. Chapter Two contains a review of the mechanics of unsaturated soils and the basis for the analysis of the creep and recovery tests. A detailed description of the test set-up, specimen preparation, creep and recovery test and data reduction are presented in Chapter Three. In Chapter Four, the static properties and index properties of the materials are described. The constitutive models at constant loading conditions are proposed in Chapter Five. Chapter Six describes the MTS dynamic testing facility, and the dynamic testing procedure. The

predictions of the behavior at high strain rates using the proposed models as well as the evaluation are contained in Chapter Seven. Chapter Eight is the closure, which contains a summary of the report, conclusions and recommendations for future studies. The results of individual tests are presented in the appendices.

CHAPTER TWO

BACKGROUND

2.1 INTRODUCTION

The purpose of the present study is to predict the dynamic behavior of unsaturated clayey soils. Accordingly, the basic considerations on the mechanics of unsaturated soils, and the time-dependent stress-strain behavior of soils and existing rheological models are described and discussed in this chapter.

2.2 BASIC UNSATURATED SOIL CONCEPTS

Unsaturated soils are composed of three phases, i.e. solid, liquid, and gaseous. When the pore pressure in the liquid phase is positive, any gaseous phase present in the soil can only exist as trapped gas at a higher pressure than the ambient air pressure on the soil. This gas will tend to diffuse out of the soil system and the soil will tend to reach a fully saturated condition with all the pore spaces completely filled with water. On the other hand, when the water table is drawn below the ground surface, decreasing pore water pressure and evapo-transpiration result in larger air bubbles in the pore space. Under these conditions, the pore pressure becomes negative, that is, below atmospheric pressure. A measure of the affinity of soil for water is the magnitude of the negative pressure or soil suction of the pore water.

In soil science, soil suction is defined as a thermodynamic variable. The International Society of Soil Science defines soil suction as follows: Soil suction, (h), is the negative pressure, relative to the external gas pressure acting on the soil water (normally atmospheric pressure), to which a pool of pure and free water at the same elevation and temperature must be subjected in order to be in equilibrium with the soil water.

Soil suction can be measured based on the relative humidity of air in thermodynamic equilibrium with soil water according to the following relationship:

$$h_t = -\frac{RT}{v_w}\ln\frac{p}{p_0} \qquad (2.1)$$

where

h_t = total suction

R = universal gas constant

T = absolute temperature

v_w = volume of a mole of liquid water

p/p_0 = relative humidity

p = partial pressure of water vapor

p_0 = partial pressure of saturated water vapor

Total suction is the algebraic sum of matric and osmotic suctions given by:

$$h_t = h_m + h_s \tag{2.2}$$

where

h_m = matric suction

h_s = osmotic or solute suction

Osmotic suction results from the presence of soluble salts in the pore water. Matric suction is related to the negative pore water pressure or capillary stress in soil, which is given by:

$$h_m = u_a - u_w \tag{2.3}$$

where

u_a = pore air pressure

u_w = pore water pressure

Pore air pressure is usually taken as zero for atmospheric pressure.

Changes of osmotic suction with water content are small relative to matric suction as indicated by the results shown in Figure 2.1. These results suggests that matric suction gradients can be approximately substituted for total suction gradients. Furthermore, osmotic suction gradients do not affect water flow unless a semipermeable barrier prevents the movements of the electrolyte.

In 1965, Hilf proposed a Mohr-Coulomb strength relation for unsaturated

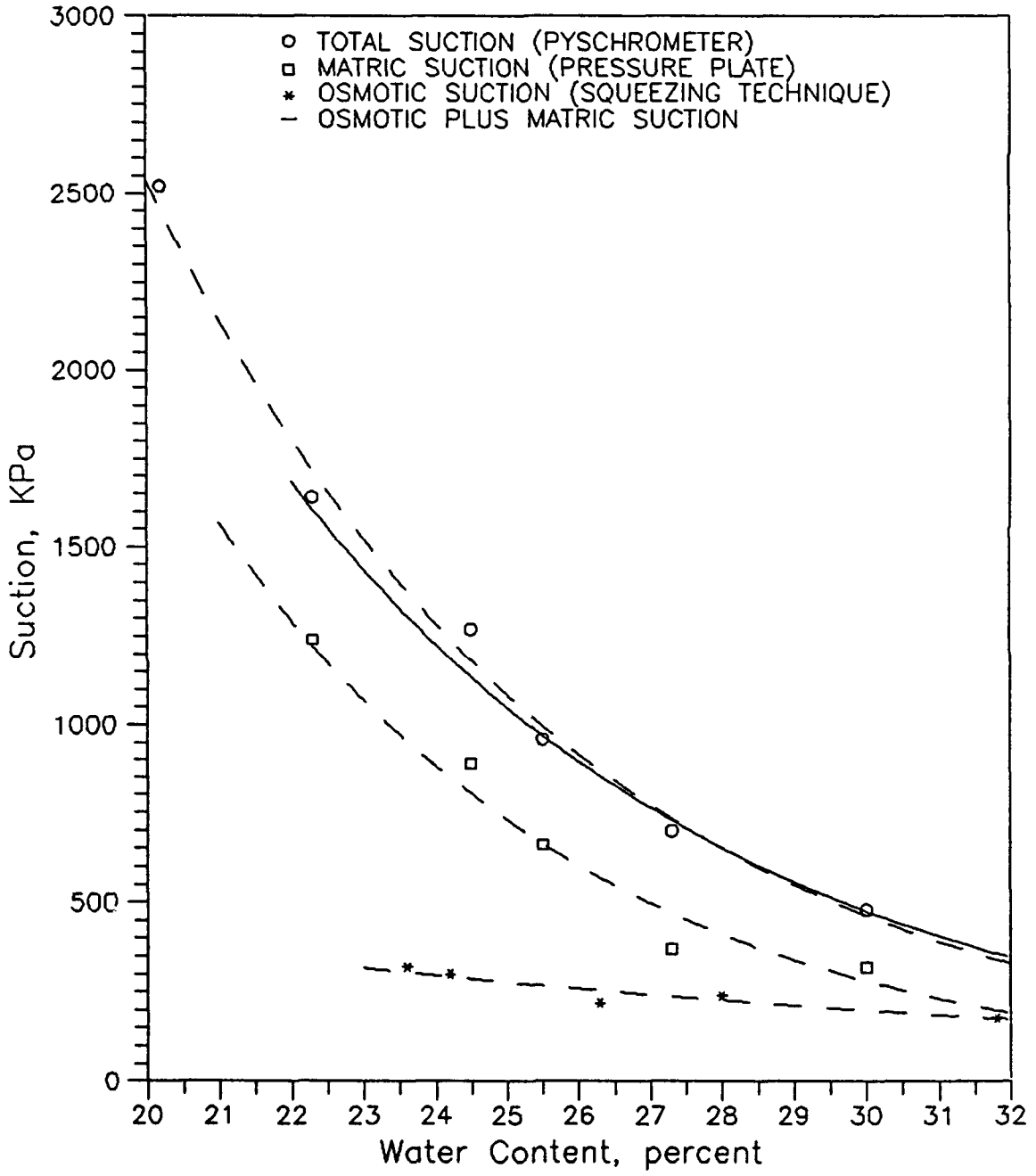

Figure 2.1 **Variations of Total, Matric, and Osmotic Suction with Water Content for Regina Clay (Fredlund, 1979)**

soils:

$$\tau = c' + \sigma' \tan\phi' \tag{2.4}$$

$$\sigma' = (\sigma - u_a) - u_c \tag{2.5}$$

$$u_c = -(u_a - u_w) \tag{2.6}$$

where

τ = shear strength

c' = apparent cohesion in terms of effective stress

ϕ' = angle of internal friction in terms of effective stress

σ' = effective stress

σ = total normal stress

u_c = capillary stress.

Guided by the success of the effective stress equation for saturated soils, Bishop (1960) suggested the following effective stress relationship for partially saturated soils:

$$\sigma' = (\sigma - u_a) + \chi(u_a - u_w) \tag{2.7}$$

where

σ' = effective stress

σ = total stress

u_a = pore air pressure

u_w = pore water pressure

χ = parameter dependent on the degree of saturation with a value of 1.0 for 100% saturation and a value of 0 for dry soil

The shear strength of unsaturated soil was expressed as:

$$\tau = c' + [(\sigma - u_a) + \chi(u_a - u_w)]\tan\phi' \qquad (2.8)$$

In relatively recent time, Fredlund has suggested that the unsaturated soil was composed of the following four-phase system: solids, water, air and contractile skin (or air-water interface) as shown in Figure 2.2. It was assumed that the air phase generally becomes continuous at degrees of saturation less than approximately 85% to 90%. This fact can be supported by a stress analysis consistent with multiphase continuum mechanics. Conceptually, Fredlund suggested that the shear strength of unsaturated soil could be expressed in the form of an extended or three dimensional, Mohr-Coulomb strength relationship:

$$\tau = c' + (\sigma - u_a)\tan\phi' + (u_a - u_w)\tan\phi^b \qquad (2.9)$$

where

τ = shear strength

c' = cohesion intercept when the two stress state variables are zero

$\sigma - u_a$ = stress state variable, applied stress

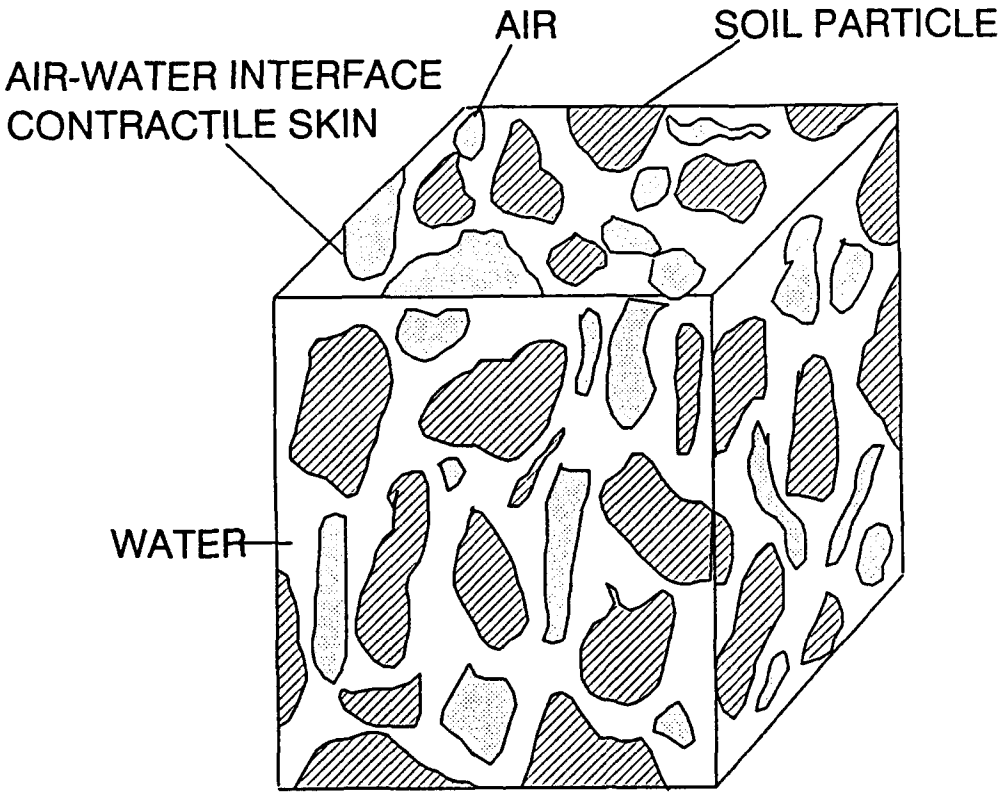

Figure 2.2 An Element of Unsaturated Soil (Fredlund, 1979)

u_a-u_w = stress state variable, matrix suction

ϕ' = angle of friction with respect to applied stress

ϕ^b = angle of friction with respect to matric suction

This relationship is illustrated in Figure 2.3. In this relationship, two independent stress tensors were proposed, that is σ-u_a, and u_a-u_w. As the degree of saturation approaches 100%, the pore air pressure reaches to the pore water pressure. Therefore, the matrix suction term goes to 0.0 and the pore air term in the first stress tensor becomes the pore-water pressure.

2.3 GENERAL STRESS-STRAIN-TIME BEHAVIOR OF SOIL

Creep is the time-dependent deformation of a material under constant stress. It is very important in a variety of geotechnical problems where long term behavior is of concern. The creep behavior of soils is dependent on stress history, drainage conditions, type of stress system and other factors.

In many cases, the application of a constant stress to a soil specimen leads to following strain phases also shown in Figure 2.4:

(1) Initial instantaneous stage. Immediately upon loading an initial elastic strain occurs. If the applied stress exceeds the yield stress, an initial plastic strain also takes place.

(2) Transient or primary stage where the rate of creep strain decrease with time as a result of strain hardening or time hardening.

(3) Steady or secondary creep stage. The creep strain rate is essentially

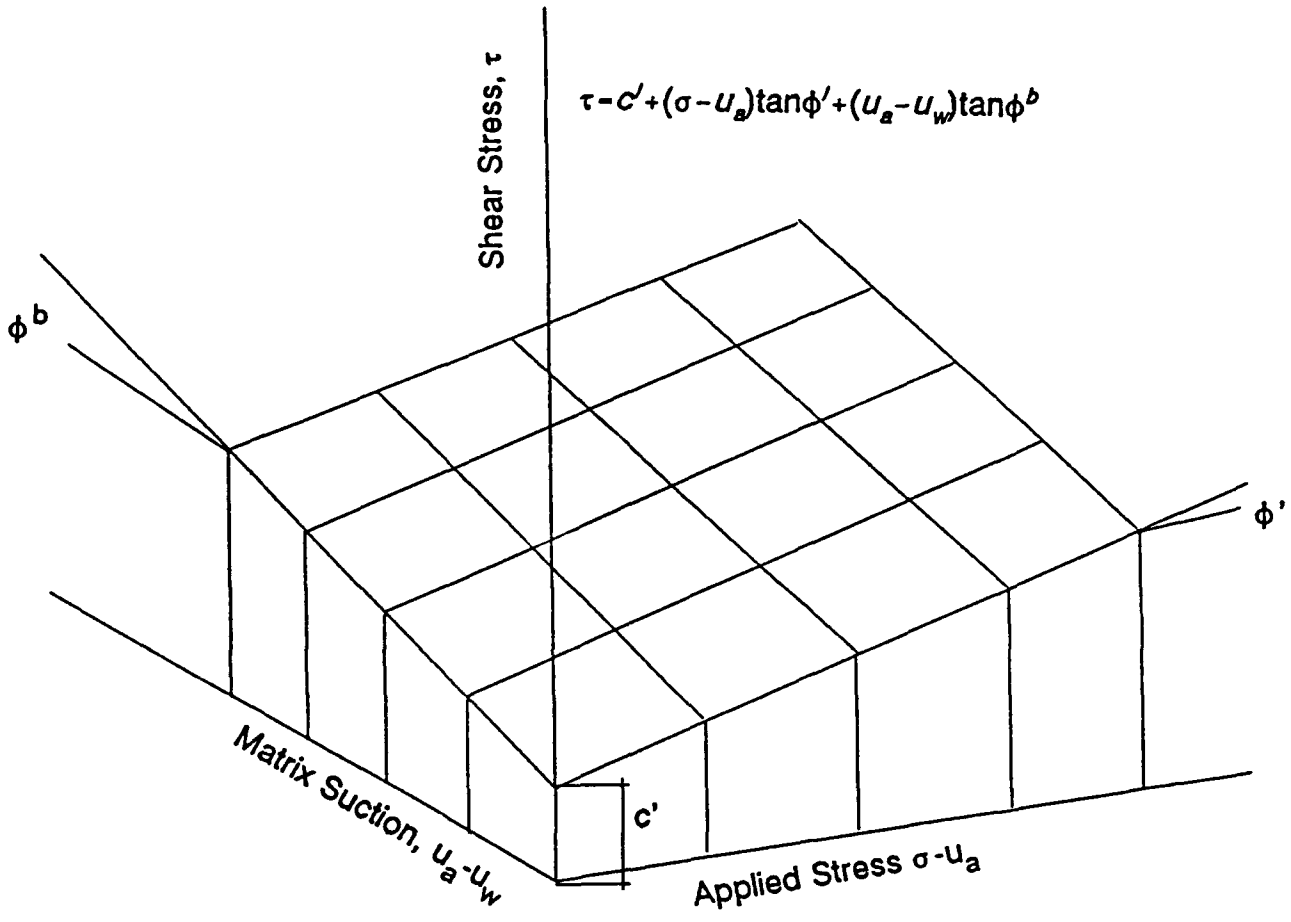

Figure 2.3 Extended Mohr-Coulomb Strength Relationship for Unsaturated Soil (Fredlund, 1979)

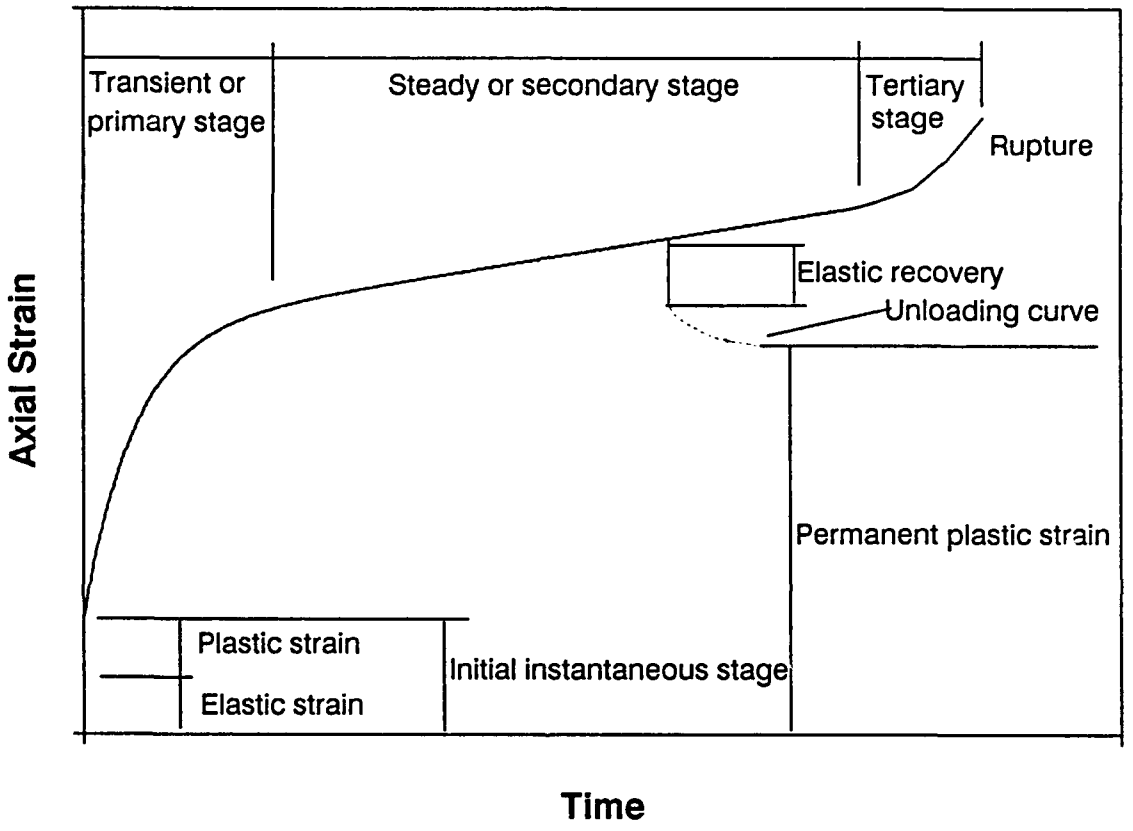

Figure 2.4 General Creep Development Stages

constant in this region. In many instances it is actually decreasing slowly, but the data are frequently approximated nicely by a straight line.

(4) Tertiary is the final stage. The creep strain rate increases leading to failure of the specimen.

If loading is removed at some point, all of the elastic strain is recovered instantaneously plus some of the creep strain over an interval of time.

2.4 SOIL DEFORMATION AS A RATE PROCESS

Rate process theory was originally proposed by Glasstone, Laidler and Eyring (1941) for the time-dependent rearrangement of matter and polymers. Later, Mitchell and Singh (1968), Christensem and Wu (1964), applied this theory to study the creep behavior of soil specimens. These studies provided insights into the fundamental nature of soil strength and functional forms for the influence of certain variables on soil behavior.

The rate process theory is based on the fact that atoms, molecules and/or particles participate in a time-dependent flow of deformation process as "flow units". These units are constrained from movement relative to each other by virtue of energy barriers separating adjacent equilibrium positions, as depicted schematically in Figure 2.5.

The displacement of flow units to new positions requires the introduction of sufficient energy to surmount the barrier, which is referred to the activation energy,

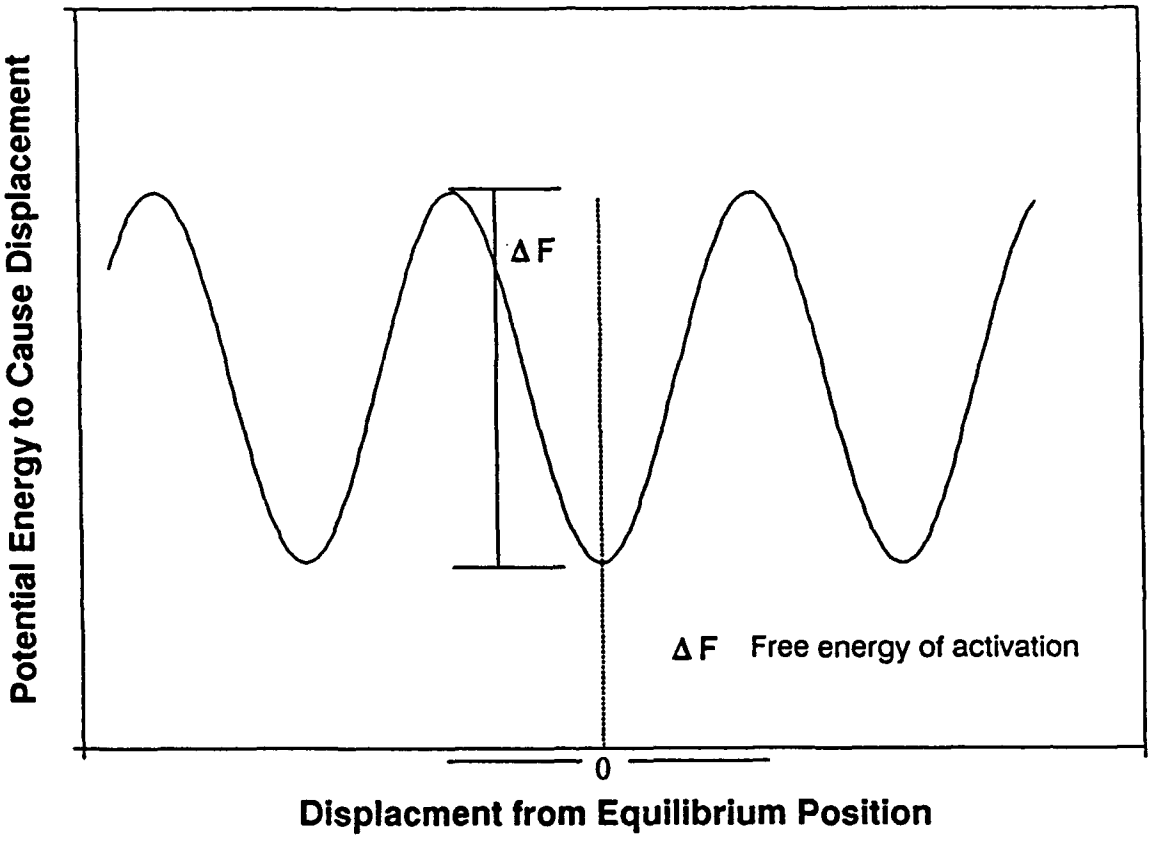

Figure 2.5 Energy Barriers and Activation Energy (Mitchell, 1964)

ΔF. The value of the activation energy depends on the material and type of process and is supplied by thermal energy and various applied potentials. By using this basic concept, Mitchell, Campanella, and Singh (1968) developed the expression of a rate process for most soil deformation problems:

$$\dot{\epsilon} = X\frac{kT}{h}\exp(-\frac{\Delta F}{RT})\exp(\frac{f\lambda N}{2RT}) \qquad (2.10)$$

where

ϵ = rate of creep strain

X = parameter may be both time and structure dependent

k = Boltzman's constant (1.38×10^{-16} erg-° K^{-1})

T = absolute temperature (° K)

h = Planck's constant (6.625×10^{-27} erg Sec^{-1})

ΔF = activative energy (erg)

R = universal gas constant (1.98 cal K^{-1} $mole^{-1}$)

N = Avogadro's number (6.02×10^{23})

λ = distance between successive equilibrium positions (Å)

f = force acting on the flow unit (g/cm^2)

Equation (2.10) is valid except for very small stress intensities.

The preceding equation for the rate of strain in soil implies that the creep rate, among other factors, is related to axial load and temperature. Based on rate process theory, Singh and Mitchell proposed phenomenological equations for the

description of creep deformation over the range of stresses of engineering interest for various types of clayey soils. This strain-stress-time function is given by:

$$\dot{\epsilon} = A e^{\alpha D} \left(\frac{t_1}{t}\right)^m \qquad (2.11)$$

where

$\dot{\epsilon}$ = creep strain rate

t = time

D = stress intensity which is the ratio of deviatoric stress to ultimate axial strength

A = strain rate at time t_1 and D=0.0

α = value of the slope of the mid-range linear portion of a plot of logarithmic strain rate versus deviatoric stress all points corresponding to the same time after load application

m = slope of a logarithmic strain rate versus logarithmic time straight line

t_1 = reference time

Taking t_1 as unity, equation (2.11) becomes:

$$\dot{\epsilon} = A e^{\alpha D} \left(\frac{1}{t}\right)^m \qquad (2.12)$$

Integration of equation (2.12) yields:

$$\epsilon = \epsilon_1 + \frac{A}{1-m} e^{\alpha D}(t^{1-m}-1), \qquad m \neq 1 \tag{2.13}$$

$$\epsilon = \epsilon_1 + A e^{\alpha D} \ln(t), \qquad m=1, t=1 \tag{2.14}$$

where ϵ_1 is creep strain at unit time.

2.5 LINEAR VISCOELASTIC MODELS

2.5.1 Linear Viscoelastic Behavior

Viscoelasticity is concerned with materials which exhibit strain rate effects in response to applied stress. These effects are manifested by the phenomena of creep under constant stress and stress relaxation under constant strain. Viscoelasticity combines elasticity (spring) and viscosity (dashpot or viscous flow).

The material is said to be linearly viscoelastic if stress is proportional to strain at a given time and the linear superposition principle holds. These linear requirements can be stated mathematically in two equations:

$$\epsilon[c\sigma(t)] = c\epsilon[\sigma(t)] \tag{2.15}$$

$$\epsilon[\sigma_1(t) + \sigma_2(t-t_1)] = \epsilon[\sigma_1(t)] + \epsilon[\sigma_2(t-t_1)] \tag{2.16}$$

where

$\sigma(t)$ = stress input

ϵ = strain output

c = constant

The second requirement is usually called the Boltzman superposition principle. Equation (2.15) and (2.16) are illustrated in Figure 2.6 and 2.7.

The linear theory of viscoelasticity yields a mathematically tractable representation for stress-strain-time relations which permits reasonably simple solutions for many stress analysis problems.

2.5.2 Linear Models

All linear viscoelastic models are made up of linear spring and linear viscous dashpots.

In the linear spring element shown in Figure 2.8

$$\sigma = E\epsilon \tag{2.17}$$

where E can be interpreted as a linear spring constant or Young's modulus. The spring element exhibits instantaneous elasticity and recovery.

A linear viscous dashpot element is shown in Figure 2.9.

$$\sigma = \eta \frac{d\epsilon}{dt} = \eta\dot{\epsilon} \tag{2.18}$$

where the constant η is the viscosity of the dashpot.

Equation (2.18) implies that the dashpot will be deformed continuously at

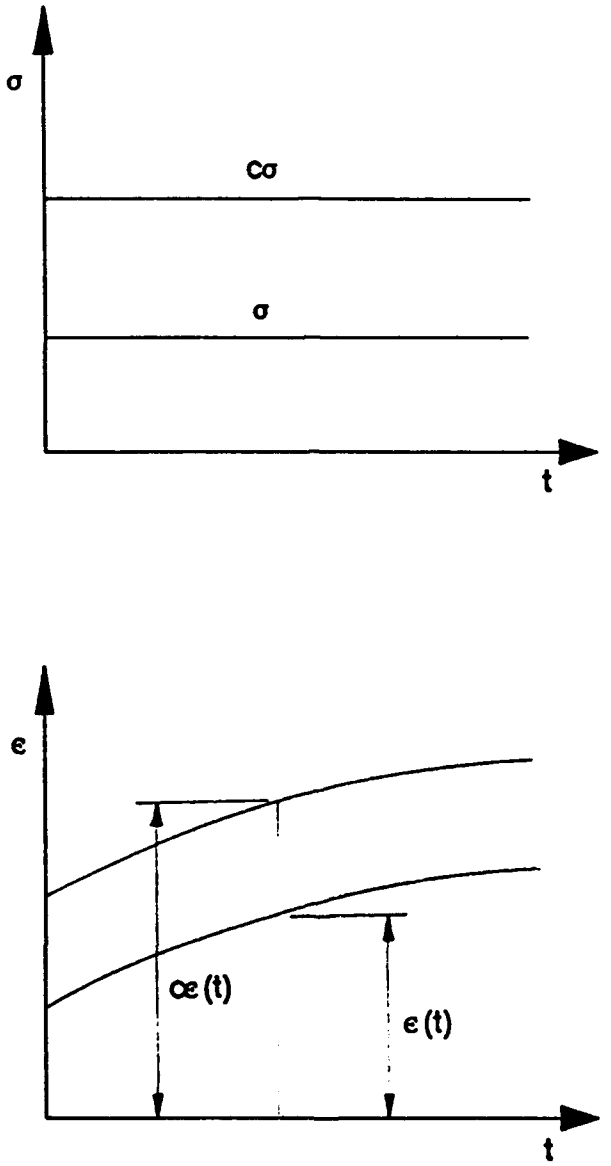

Figure 2.6 Illustration of the Behavior of Linear Viscoelastic Materials, Eq. (2.15)

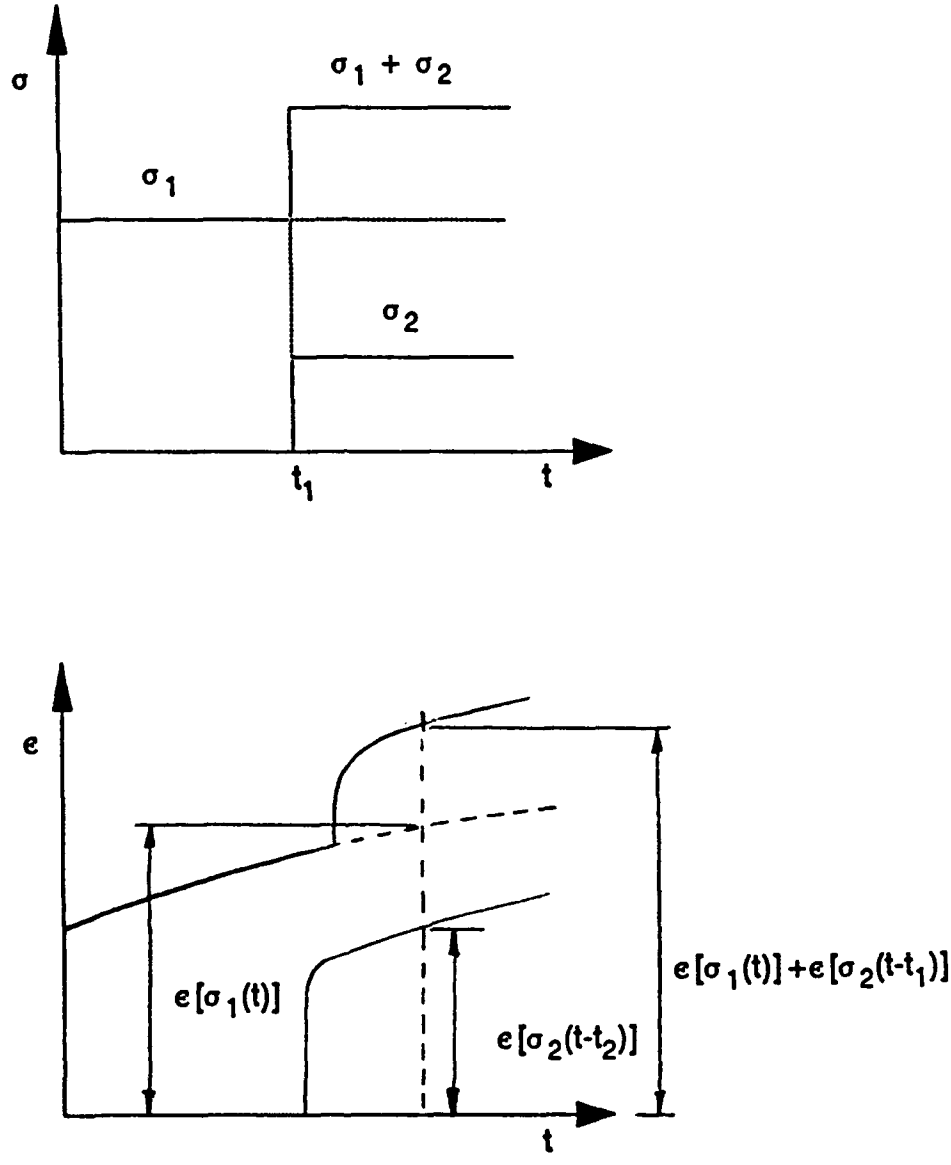

Figure 2.7 Illustration of the Behavior of Linear Viscoelastic Materials, Eq. (2.16)

a constant rate when it is subjected to a step of constant stress.

Maxwell Model

The Maxwell model is a two-element model consisting of a linear spring element and a linear viscous dashpot element connected in series as shown in Fig. 2.10.

The stress-strain rate relation for the Maxwell Model can be obtained as follows:

$$\dot{\epsilon} = \frac{\dot{\sigma}}{E} + \frac{\sigma}{\eta} \tag{2.19}$$

The strain-time relations under various stress conditions and stress-time relations under given strain input can be obtained by solving the differential equation (2.19).

For the simple model shown in Fig 2.10, the strain-time relation is given by:

$$\epsilon(t) = \frac{\sigma_0}{E} + \frac{\sigma_0}{\eta} t \tag{2.20}$$

where σ_0 is the constant applied stress.

Kelvin Model

The Kelvin model is illustrated in Fig.2.11 and consists of a spring element

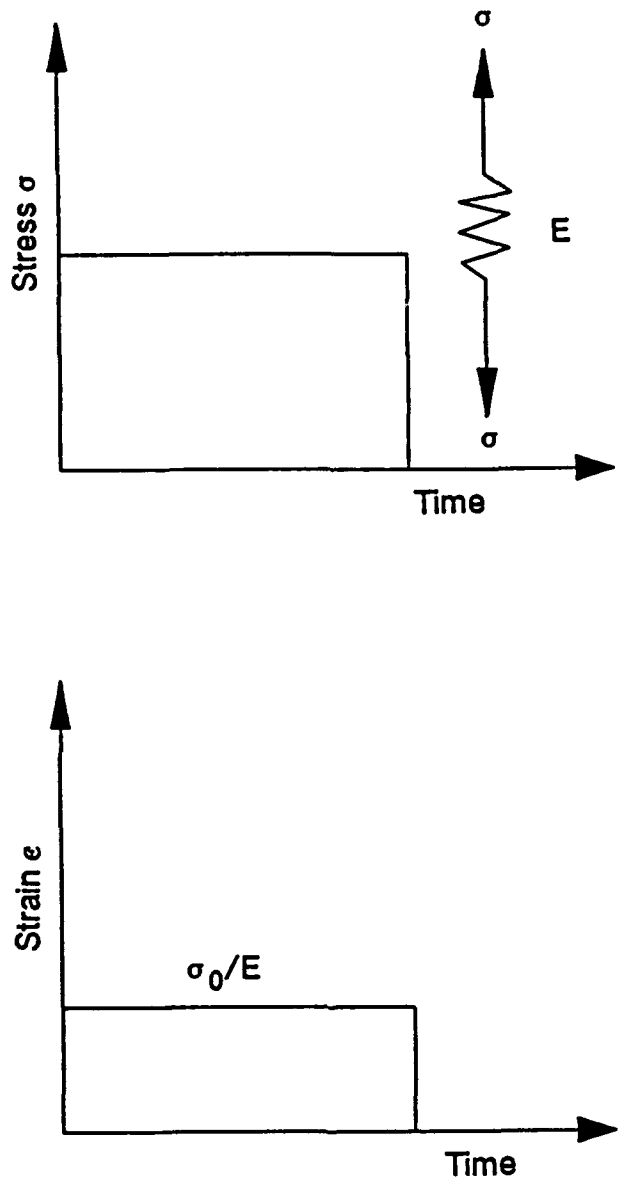

Figure 2.8 Behavior of Linear Spring

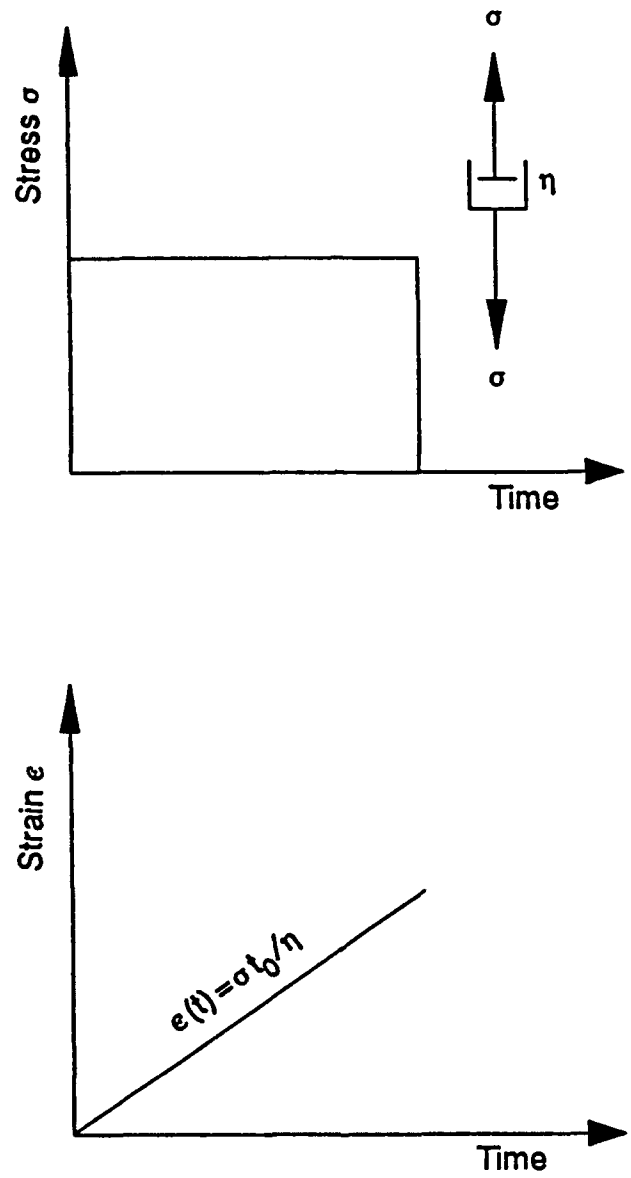

Figure 2.9 Behavior of Linear Dashpot

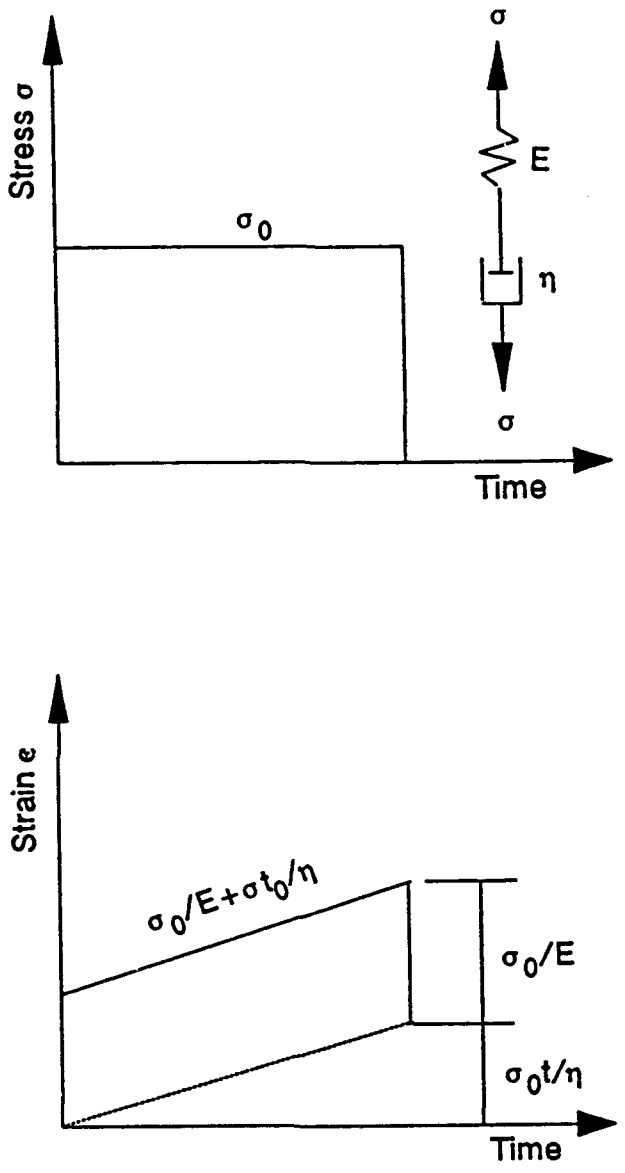

Figure 2.10 Behavior of Maxwell Model

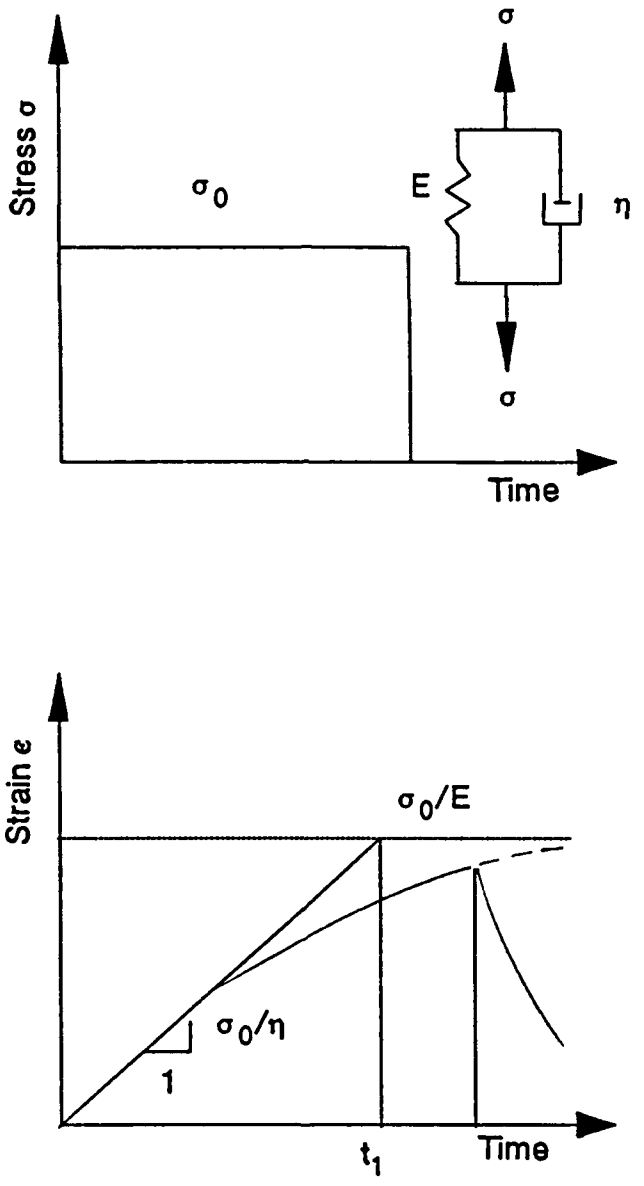

Figure 2.11 Behavior of Kelvin Model

and a dashpot element connected in parallel.

The differential relationship between strain and stress is given by the following expression:

$$\dot{\epsilon}+\frac{E}{\eta}\epsilon=\frac{\sigma}{\eta} \qquad (2.21)$$

The solution of equation (2.21) has the following form for creep under constant stress applied at t=0:

$$\epsilon=\frac{\sigma_0}{E}(1-e^{-\frac{E}{\eta}t}) \qquad (2.22)$$

As shown in Figure 2.11, the strain increases with a decreasing rate and approaches asymptotically the value of σ_0/E for t approaching infinity. The response of this model to an abruptly applied stress is that the stress is at first carried entirely by the viscous element, η. Under the stress the viscous element then elongates, thus transferring a greater and greater portion of the load to the elastic element E. Finally, the entire stress is carried by the elastic element. This behavior is called delayed elasticity.

If the stress is removed at time t_1, the superposition principle yields the strain ϵ for $t>t_1$ during recovery:

$$\epsilon = \frac{\sigma_0}{E} e^{-\frac{E}{\eta}t}(e^{\frac{E}{\eta}t_1}-1), \qquad t>t_1 \tag{2.23}$$

When t tends to infinity, the recovery tends to zero.

Burger's Model

The Burger's model is shown in Fig.2.12. It consists of a Maxwell and a Kelvin model connected in series.

The constitutive equation between stress σ and strain ϵ for the Burger's model can be given as follows:

$$\sigma+(\frac{\eta_1}{E_1}+\frac{\eta_1}{E_2}+\frac{\eta_2}{E_2})\dot{\sigma}+\frac{\eta_1\eta_2}{E_1E_2}\ddot{\sigma}=\eta_1\dot{\epsilon}+\frac{\eta_1\eta_2}{E_2}\ddot{\epsilon} \tag{2.24}$$

in which E_1, η_1, E_2 and η_2 are material constants.

The creep behavior of the Burger's model under constant stress σ_0 can be obtained by solving the above second order differential equation with two initial conditions $\epsilon=\sigma_0/E_1, t=0$ and $\epsilon=\sigma_0/\eta_1+\sigma_0/\eta_2$, $t=0$, which yields:

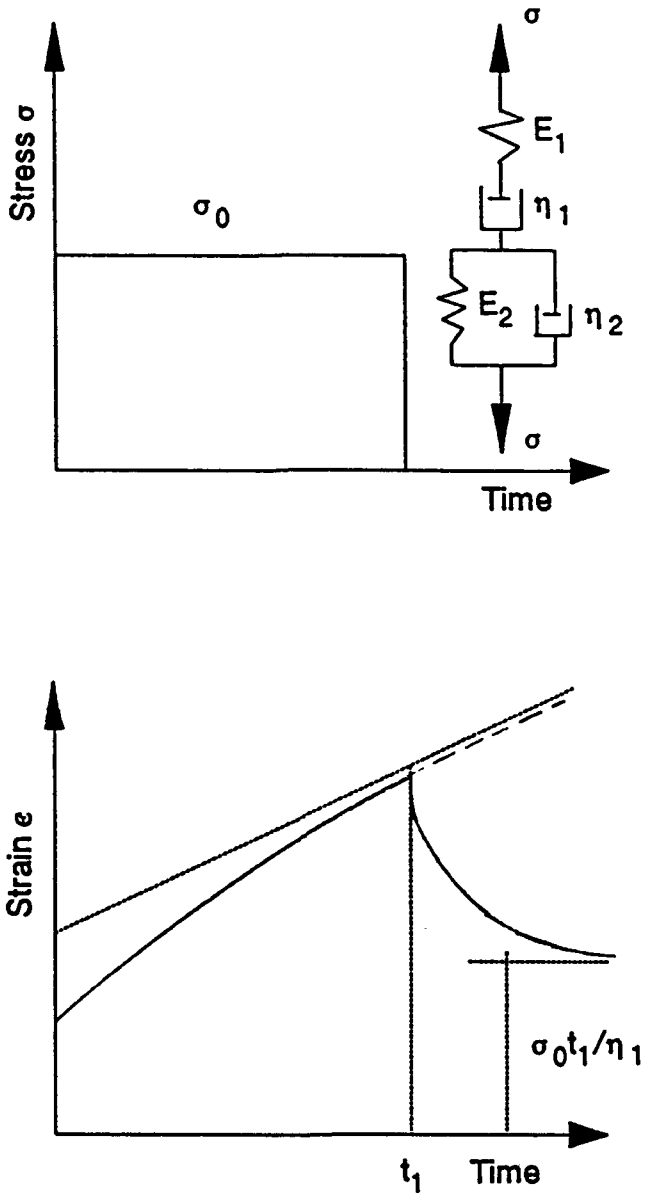

Figure 2.12 Behavior of Burgers Model

$$\epsilon(t) = \frac{\sigma_0}{E_1} + \frac{\sigma_0}{\eta_1} t + \frac{\sigma_0}{E_2}(1 - e^{-\frac{E_2}{\eta_2} t}) \tag{2.25}$$

where σ_0 is applied constant stress.

It is obvious that the creep behavior of the Burger's model is the sum of the creep behavior of the Maxwell and Kelvin models. The relationship between the stress and strain is linear in the Burger's model.

If the constant stress σ_0 is removed at time t_1, the recovery strain can be obtained in terms of the superposition principle, which is as follows:

$$\epsilon(t) = -\frac{\sigma_0}{\eta_1} t_1 + \frac{\sigma_0}{E_2}(e^{\frac{E_2}{\eta_2} T_1} - 1) e^{\frac{E_2}{\eta_2} t}, t > t_1 \tag{2.26}$$

The recovery as shown in Figure 2,12 has an instantaneous elastic recovery followed by creep recovery at a decreasing rate. The recovery approaches asymptotically to $\sigma_0 t_1 / \eta_1$ as t approaches infinity.

2.6 NONLINEAR VISCOELASTIC MODELS

2.6.1 General Ideas

By way of contrast to linear viscoelastic materials, the strain of nonlinear viscoelastic materials exhibit a highly nonlinear dependence on stress. So far the nonlinear viscoelastic theory is still under development. This section presents some

basic theory as summarized by Shames and Cozzarelli (1992).

In Figure 2.13, the development of creep strain under constant uniaxial stress is shown to consist of three periods of deformation characterized respectively by an "instantaneous" response, a decreasing strain rate, and a constant strain rate. Tertiary creep has not been included because it is not pertinent to the purpose of the study.

The creep strain due to constant uniaxial stress under constant temperature can be expressed as a superposition of three components:

$$\epsilon(t) = \epsilon_I + \epsilon_s(t) + \epsilon_t(t), \quad t > 0 \qquad (2.27)$$

where

$\epsilon(t)$ = total creep strain

ϵ_I = instantaneous strain component

$\epsilon_t(t)$ = transient creep strain component

$\epsilon_s(t)$ = steady creep strain component

The instantaneous strain ϵ_I is independent of time. It is all elastic or part elastic and some plastic response. The transient component $\epsilon_t(t)$ is a function of time starting from zero at t=0 and the derivative approaches zero as time approaches infinity. the steady creep component $\epsilon_s(t)$ is linear with time, giving a constant steady creep strain rate. Based on these considerations, equation 2.27 can be also expressed in following way:

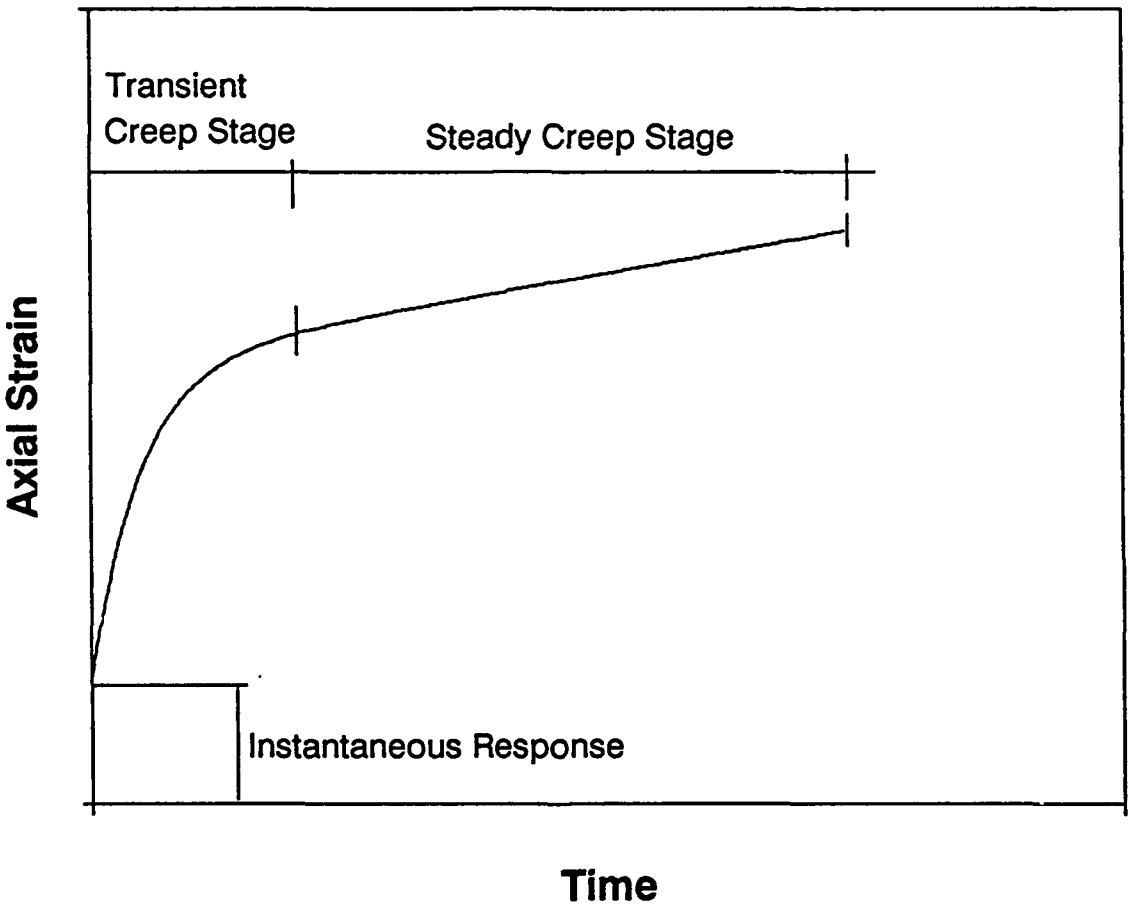

Figure 2.13 Idealized Creep Curve

$$\epsilon(t) = f_i(\sigma) + f_s(\sigma)t + f_t(\sigma)g(t) \qquad (2.28a)$$

where $f_i(\sigma)$, $f_s(\sigma)$ and $f_t(\sigma)$ are stress functions, and g(t) is a transient time function. These stress functions and time function can have a wide variety of monotonically increasing forms for various nonlinear viscoelastic materials. However, the transient time function , has to satisfy the following additional requirements:

$$g(0) = 0 \qquad \lim_{t \to \infty} \frac{dg}{dt} = 0 \qquad (2.28b)$$

For the recovery stage, the "modified superposition method" proposed by Findlay et al (1968), may be employed to describe the nonlinear behavior. According the superposition principle, the strain during recovery at zero stress is given by:

$$\epsilon_r(t) = f(\sigma, t-t_0) - f(\sigma_0, t-t_1), t > t_1 \qquad (2.29)$$

where

$\epsilon_r(t)$ = strain after removal of load

σ_0 = constant applied stress during creep stage

t_0 = time of application of σ_0

t_1 = time of removal of σ_0

Equation (2.29) is illustrated in Figure 2.14.

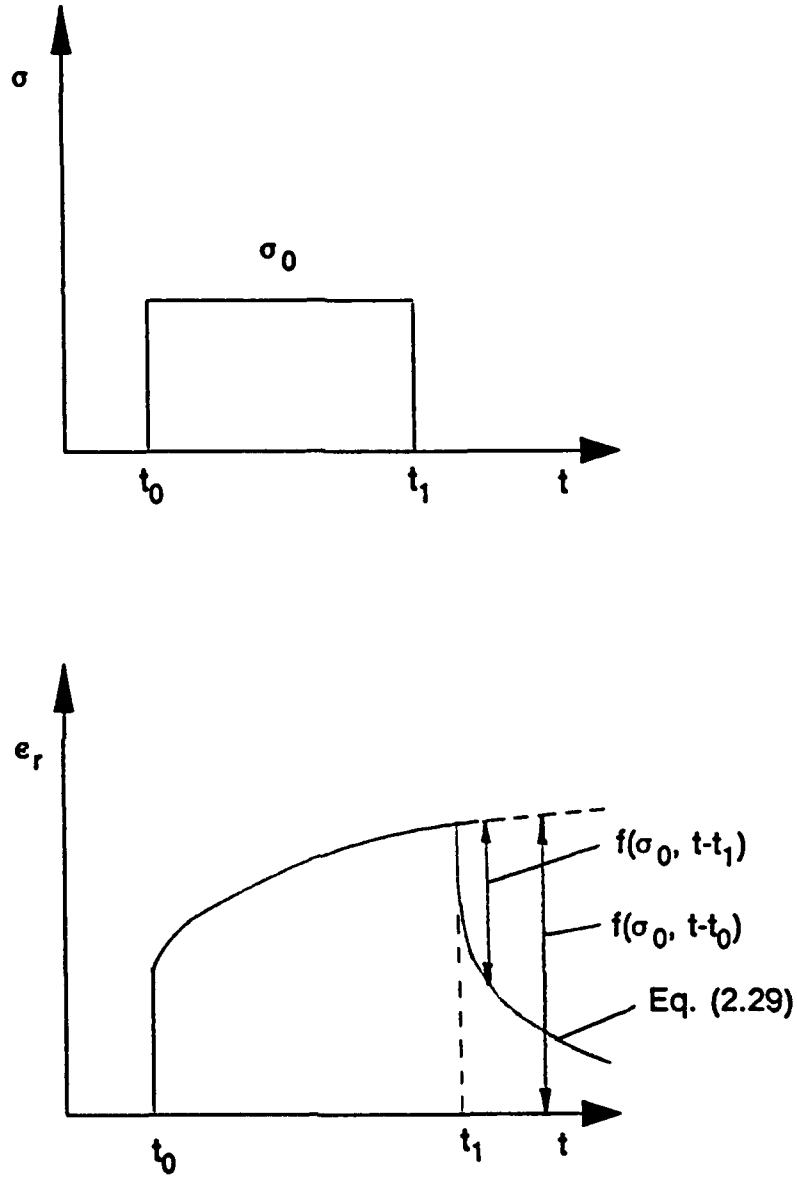

Figure 2.14 Illustration of Modified Superposition Principle for Recovery

2.6.2 Nonlinear Viscoelastic Models Under Constant Uniaxial Stress

If the applied stress is relatively small, the instantaneous stress function $f_1(\sigma_0)$ is linear with applied stress σ_0, which can be simply assumed as:

$$f_1(\sigma_0) = \frac{\sigma_0}{E} \tag{2.30}$$

where E is the Young's modulus of the material. For the relatively larger stress, the expression of stress function can be obtained from test data, as a combination of elastic and plastic strains.

Two forms of stress function for the steady creep are widely used in soil creep behavior, each involving two material constants. These are the following:

$$f_s(\sigma_0) = A\sigma_0^n \tag{2.31}$$

$$f_s(\sigma_0) = Be^{\alpha\sigma_0} \tag{2.32}$$

where A, n, B, and α are material constants. Based on these functions, the stress power law for the steady creep component is as follows:

$$\epsilon_s(t) = A\sigma_0^n t \tag{2.33}$$

and the stress exponential law for the steady creep component is the following:

$$\epsilon_s(\sigma_0) = Be^{\alpha\sigma_0}t \tag{2.34}$$

The transient creep stress function also can be expressed as a stress power function. That is,

$$f_t(\sigma_0) = C\sigma_0^m \tag{2.35}$$

where C, and m are material constants obtained from creep test data.

The functions commonly used to satisfy the conditions 2.28b are the time exponential function and a time power function. These are given respectively as follow:

$$g(t) = 1-e^{-pt} \tag{2.36}$$

$$g(t) = t^q, \quad 0<q<1 \tag{2.37}$$

where p and q are material constants. Therefore, the transient strain component can adopt either of the following two expressions:

$$\epsilon_t(t) = C\sigma_0^m(1-e^{-pt}) \tag{2.38}$$

$$\epsilon_t(t) = C\sigma_0^m t^q, \quad 0<q<1 \tag{2.39}$$

Based on the above considerations, the total creep strain for constant stress can adopt any of the following two forms:

$$\epsilon(t) = f_I(\sigma_0) + A\sigma_0^n t + C\sigma_0^m [1 - e^{-pt}] \qquad (2.40)$$

$$\epsilon(t) = f_I(\sigma_0) + A\sigma_0^n t + C\sigma_0^m t^q \qquad (2.41)$$

2.6.3 Nonlinear Viscoelastic Models Under Variable Uniaxial Stress

In order to analyze the behavior of nonlinear viscoelastic materials under variable stress, the strain-hardening hypothesis and time-hardening hypothesis are employed.

The strain-hardening hypothesis consists of considering that the creep strain rate is a function of the stress and accumulated creep strain. That is:

$$\dot{\epsilon}(t) = f[\epsilon(t), \sigma(t)] \qquad (2.42)$$

in which $\epsilon(t)$ may refer either to the total creep strain or to each component of creep strain, but normally excluding the elastic strain. This hypothesis implies that the creep model obtained from a particular stress (a constant stress σ_0 could be such a stress) is still valid for any stress variation $\sigma(t)$. The strain-hardening hypothesis works well for those materials which experience relatively minor changes in microscopic structure during creep deformation.

The time-hardening hypothesis assumes that creep strain rate is a function

of stress and time in the following fashion:

$$\dot{\epsilon}(t) = f[\sigma(t), t] \qquad (2.43)$$

This hypothesis is used to predict the creep behavior for materials which experience significant microscopic change. It implies that if the creep model for an "aging" material (for some particular stress function such as the constant stress σ_0) is manipulated into the form of equation (2.43), then the creep model is also valid for any stress function $\sigma(t)$.

In the rest of this section, the general expressions obtained for the creep components from strain-hardening or time hardening hypothesis are discussed separately.

2.6.3.1 Transient Creep Component from Strain-Hardening Hypothesis (Exponential Law)

Differentiation of equation (2.38) with respect to time yields:

$$\dot{\epsilon}_t(t) = pC\sigma_0^m e^{-pt} \qquad (2.44)$$

at the same time, solving equation (2.38) leads to the following expression:

$$\exp(-pt) = 1-\frac{\epsilon_t(t)}{C\sigma_0^m} \qquad (2.45)$$

Substituting equation (2.45) into equation (2.44), it is finally found:

$$\dot{\epsilon}_t(t) = -p\epsilon_t(t)+pC\sigma_0^m \qquad (2.46)$$

This equation is of the form assumed in the strain-hardening hypothesis. Thus the constant stress can be replaced by a variable stress σ (t) . Rearrangement gives the following differential equation:

$$\dot{\epsilon}_t(t)+p\epsilon_t(t) = pC[\sigma(t)]^m \qquad (2.47)$$

The solution of this differential equation provides the strain hardening transient creep strain component.

2.6.3.2 Transient Creep Component from Strain-Hardening hypothesis (Power Law)

As described earlier, the time power transient creep component under constant uniaxial stress is given by equation (2.39). This equation can be rearranged as follows:

$$[\epsilon_f(t)]^{\frac{1}{q}} = [C\sigma_0^m]^{\frac{1}{q}} t \tag{2.48}$$

Differentiating equation (2.48) respect to time it is found:

$$\frac{\partial[\epsilon_f(t)]^{\frac{1}{q}}}{\partial t} = [C\sigma_0^m]^{\frac{1}{q}} \tag{2.49}$$

which also can be written as:

$$\dot{\epsilon}_f(t) = q[C\sigma_0^m]^{\frac{1}{q}}[\epsilon_f(t)]^{1-\frac{1}{q}}, \quad 0<q<1 \tag{2.50}$$

Eq.(2.50) indicates that the strain rate decreases as the strain increases, satisfying the strain-hardening hypothesis. Therefore, σ_0 can be replaced by σ (t). Eq.(2.49) becomes:

$$\frac{\partial[\epsilon_f(t)]^{\frac{1}{q}}}{\partial t} = [C\sigma(t)^m]^{\frac{1}{q}} \tag{2.51}$$

Integration of Eq.(2.51) gives:

$$\epsilon_t(t) = \left[\int_o^t [C\sigma(t')^m]^{\frac{1}{q}} dt'\right]^q \qquad (2.52)$$

which is the integral form of time power transient creep strain component.

2.6.3.3 Transient Creep Component from Time-Hardening Hypothesis (Exponential Law)

The time exponential transient creep strain rate component is given by Eq.(2.38) for the constant uniaxial stress σ_0. Taking derivatives with respect to time it is found the following:

$$\dot{\epsilon}_t(t) = pC\sigma_o^m e^{-pt} \qquad (2.53)$$

This equation contains the explicit dependence on time required by the time-hardening hypothesis. Accordingly, the constant stress σ_0 can be replaced by the variable stress σ(t) to obtain the strain rate equation:

$$\dot{\epsilon}_t(t) = pC[\sigma(t)]^m e^{-pt} \qquad (2.54)$$

By direct integration, the corresponding transient creep strain component is:

$$\epsilon_t(t) = pC\int_o^t [\sigma(t')]^m e^{-pt'} dt' \tag{2.55}$$

2.6.2.4 Transient Creep Component from Time-hardening Hypothesis (Power Law)

At constant stress σ_0 the time power transient creep component is given by Eq.(2.39). Differentiating with respect to time, the following expression is obtained for the strain rate:

$$\dot{\epsilon}_t(t) = Cq\sigma_0^m t^{q-1} \tag{2.56}$$

This is in the form required by the time-hardening hypothesis. So, the general expression is:

$$\dot{\epsilon}_t(t) = qC[\sigma(t)]^m t^{q-1} \tag{2.57}$$

Direct integration yields:

$$\epsilon_t(t) = \int_0^t qC[\sigma(t')]^m t'^{q-1} dt' \tag{2.58}$$

2.7 EXISTING LITERATURE REVIEW

Different rheological models have been proposed to describe the stress-

strain-time behavior of soils. All these models are composed of combination of linear springs, linear and nonlinear dashpots and sliders.

In 1956, Murayama and Shibata developed a mechanical model to explain the viscosity, elasticity, and internal resistance of clay as shown in Figure 2.15. It consists of a spring element in series with a modified Voigt element (E_2, σ_0, η_2). The relationship between total strain ϵ and time t can be given by the following expression:

$$\epsilon = \frac{\sigma}{E_1} + \frac{(\sigma-\sigma_0)}{E_2}\log\left(\frac{A_2}{2}B_2E_2t\right), 0<\epsilon_2<\frac{\sigma-\sigma_0}{2B_2E_2}(2B_2-1) \qquad (2.59)$$

$$\epsilon = \frac{\sigma}{E_2} + \frac{(\sigma-\sigma_0)}{E_2}, \qquad \epsilon_2>\frac{(\sigma-\sigma_0)}{2B_2E_2}(2B_2-1) \qquad (2.60)$$

where A_2 and B_2 are material constants determined by rate process. E_1, E_2, η_2 and σ_0 are illustrated in Figure 2.15. Equations (2.59) and (2.60) show that the flow of clay ϵ is proportional to the logarithm of time at first but should approach the asymptotic value equation (2.60) for the time approaching infinity as shown in Figure 2.16.

In 1964, a rheological model similar to the Kelvin-Maxwell model was proposed by Christensen and Wu, which is illustrated in Figure 2.17. The spring k_2 represents the effect of the nonflow stress. The combination of spring k_1 and dashpot β represent the response of the particle structure of the flow stress.

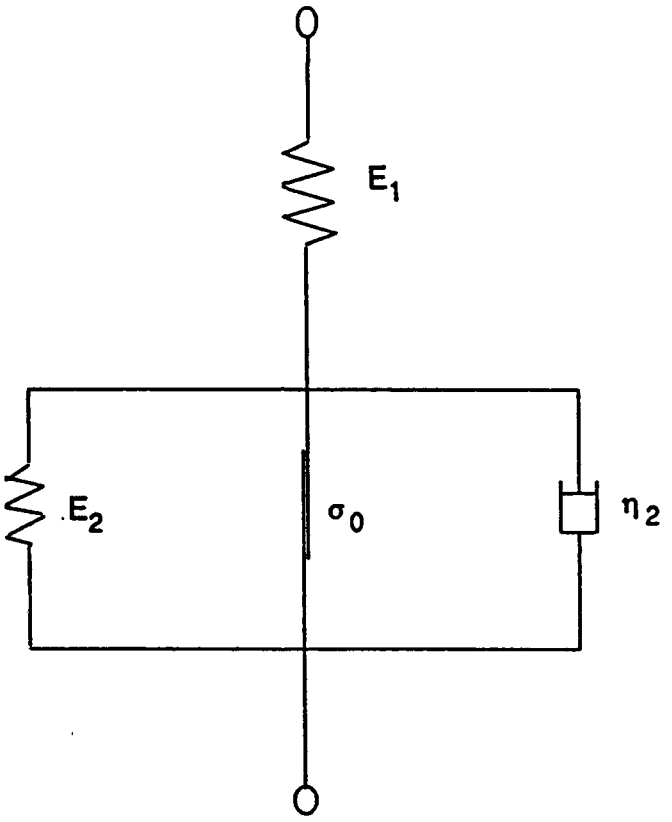

Figure 2.15 Rheological Model for Clays (Murayama and Shibata, 1956)

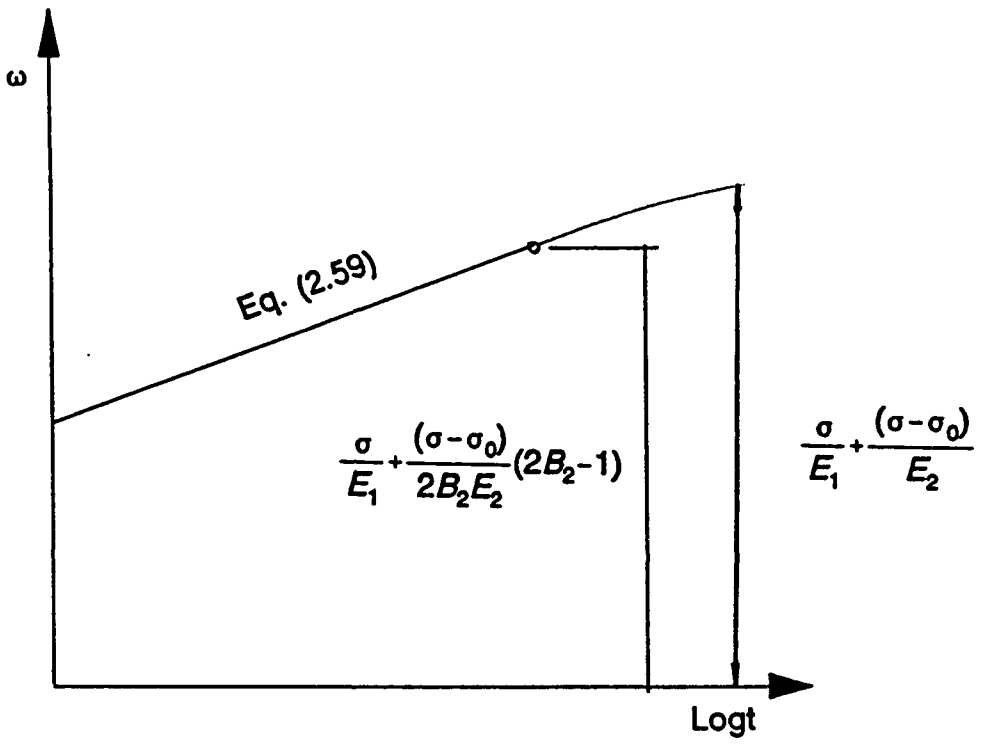

Figure 2.16 Relationship between Flow Strain and Time (Murayama and Shibata, 1956)

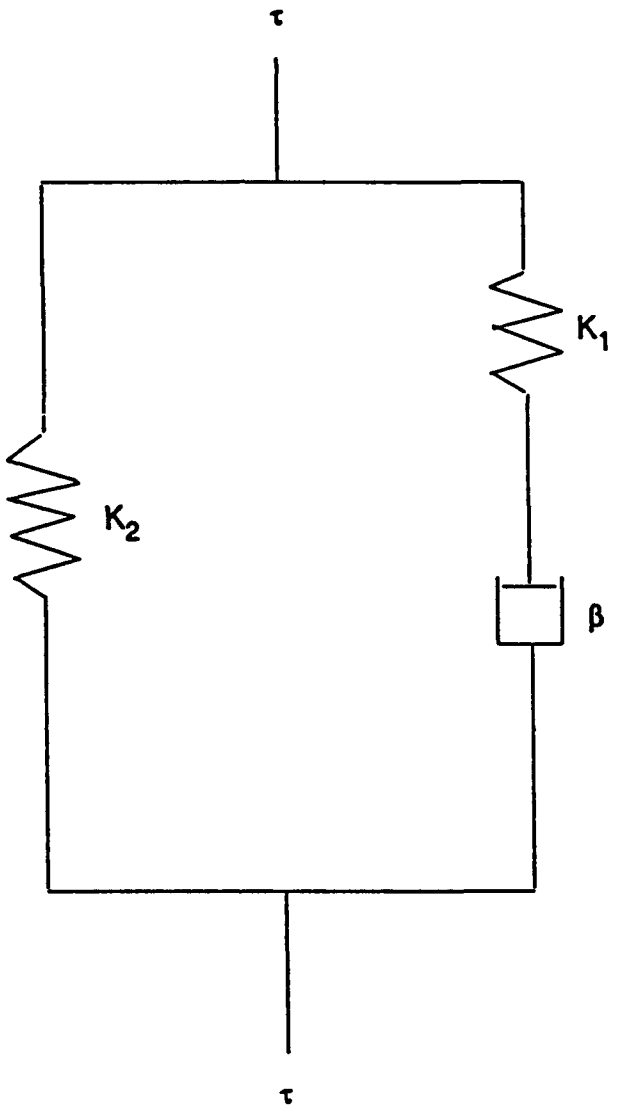

Figure 2.17 Rheological Model (Christensen and Wu, 1964)

In terms of the rate process theory, the total strain can be obtained from the following expression:

$$\gamma = \frac{1}{k_1}\tau + \frac{1}{\alpha k_2} \ln \tanh\left[\frac{1}{2}\alpha\beta\frac{k_1 k_2}{k_1 + k_2}t + \tanh^{-1} e^{\left(\frac{\alpha k_1 \tau}{k_1 + k_2}\right)}\right] \qquad (2.61)$$

where

γ = shear strain

τ = shear stress

α, β = dashpot parameters in rheological model

k_1, k_2 = spring constants in rheological model

In 1966, a five-element rheological model shown in Figure 2.18 was introduced by Abdel-Hady and Herrin to describe the behavior of compacted soil-asphalt mixtures. Base on the typical creep curve, the total creep strain at any time was the superposition of four deformation components. That is as follows:

$$\epsilon = \epsilon_0 + \epsilon_f + \epsilon_d + \epsilon_p \qquad (2.62)$$

where

ϵ = total strain at any time

ϵ_0 = instantaneous elastic strain

ϵ_i = instantaneous elastic strain

ϵ_d = transient creep strain

ϵ_p = secondary (constant) creep strain

In the above equation, the instantaneous strain $\epsilon_0+\epsilon_1$, on application of the load is represented in the model by the elastic elongation of spring E and the irrecoverable elongation of the spring E_1. The transient creep strain ϵ_p and the secondary creep strain ϵ_d are represented in the model by the action dashpot, K, α, in series with the parallel unit composed of the spring E_p and the dashpot K_p, α_p.

Based on elastic theory, the instantaneous strains caused by the applied stress σ are:

$$\epsilon_0 = \frac{\sigma}{E} \qquad (2.63)$$

$$\epsilon_1 = \frac{\sigma}{E_1} \qquad (2.64)$$

where

σ = stress applied on the five-element model

E = spring modulus

E_1 = constant specifying the response of a spring element that has irrecoverable deformation

According to the experimental strain-time curves on different stress level, the total instantaneous strains, instantaneous recovery strain, and instantaneous irrecoverable strain can be evaluated. Therefore, the mean value of E and E_1 can

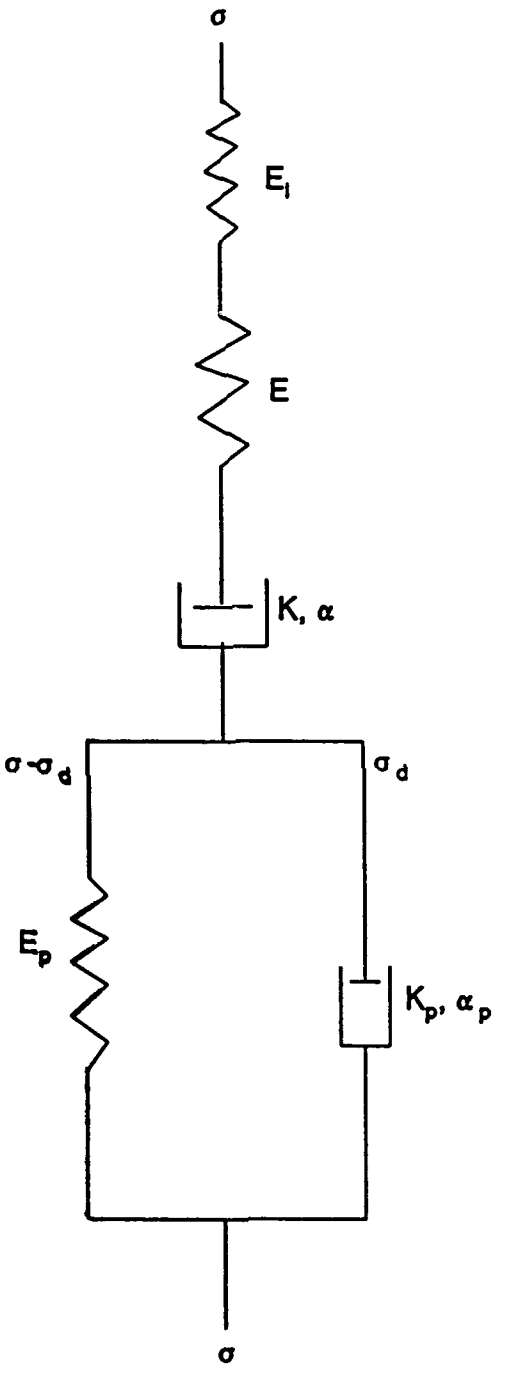

Figure 2.18 Rheological Model (Abdel-Hady and Herrin, 1966)

be obtained using equations (2.63) and (2.64).

With the elapse of time, the transient and secondary creep strains can be obtained respectively in terms of the rate process theory:

$$\ln(\dot{\epsilon}_d) = \ln(\frac{k}{2}) + \alpha\sigma \qquad (2.65)$$

$$\dot{\epsilon}_p = K_p \sinh(\alpha_p \sigma_d) \qquad (2.66)$$

where

ϵ_d = rate of transient creep strain

ϵ_p = rate of secondary creep strain

K = constant specifying the rate of flow of the dashpot, in sec^{-1}

α = constant specifying the response as the resistance of the dashpot to force, in psi^{-1}

σ = stress applied to the five-element model, in psi

K_p, α_p = properties of the parallel spring and dashpot

σ_d = stress acting on the parallel viscous element

The value of K and α can be obtained from the curve of constant creep rate versus stress level in terms of Equation (2.55). The values of K_p and α_p can be determined from the experimental data of a single strain-time curve using rate process theory.

In the Murayama and Shibata, Abdel-Hady and Herrin, Christensen and Wu

models, the dashpots are nonlinear with stress-flow rate behavior governed by the functional forms dictated by rate process theory.

In 1974, a new rheological model for soil behavior was proposed by Komamura and Huang(1974). This model describes the deformation behavior of soil under various conditions of stress and water content. The basic visco-plastic-elastic model consists of Voight and Bingham elements in series as shown in Figure 2.19. This model was proposed to account for the behavior of soil with water contents below the visco-plastic limit for applied stresses larger than the critical stress. The stress- strain-time relationship can be expressed as follows:

$$\epsilon = \frac{1}{\eta_1}(\sigma-\sigma_0)\,t+\frac{\sigma}{E}(1-e^{-\frac{E}{\eta_2}t}), \qquad \sigma>\sigma_0 \qquad (2.67)$$

where

ϵ = axial strain

t = time

σ = stress level, $\sigma > \sigma_0$

σ_0 = critical stress

η_1 = Bingham viscosity

η_2 = Voigt viscosity

E = modulus of elasticity, spring constant for rheological model

If the applied stress level is below the critical stress σ_0, the maximum

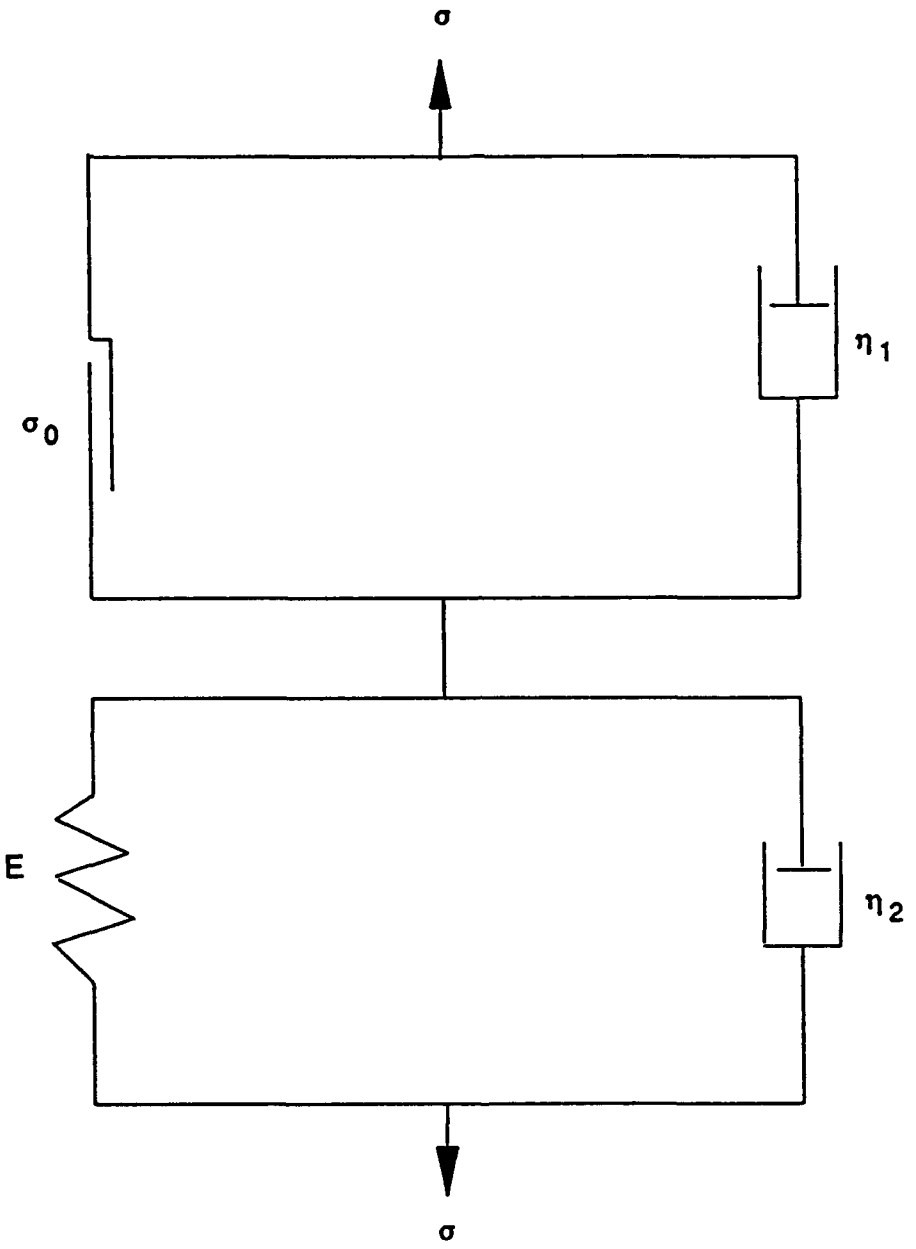

Figure 2.19 Rheological Model (Komamura and Huang, 1974)

resistance of the slider element exceeds the applied stress. Consequently, only the Voigt model shown in Figure 2.20 is used to describe the stress-strain-time relationship, that is as follows:

$$\epsilon = \frac{\sigma}{E}(1-e^{-\frac{e}{\eta_2}t}), \qquad \sigma<\sigma_0 \tag{2.68}$$

At a higher water content than the visco-plastic limit, the modulus of elasticity of the spring in the Voight unit is zero. Under these conditions the visco-plastic model reduces to that shown in Figure 2.21. The stress-strain-time relationship may be expressed as follows:

$$\epsilon = \frac{\sigma-\sigma_0}{\eta_1}t+\frac{\sigma}{\eta_2}t \tag{2.69}$$

At water contents higher than the liquid limit, the rheological model for the soil become the viscous model shown in Figure 2.22. The stress-strain-time relationship is then as follows:

$$\epsilon = (\frac{1}{\eta_1}+\frac{1}{\eta_2})\sigma t \tag{2.70}$$

The rheological coefficients of soil in these models vary with the water content.

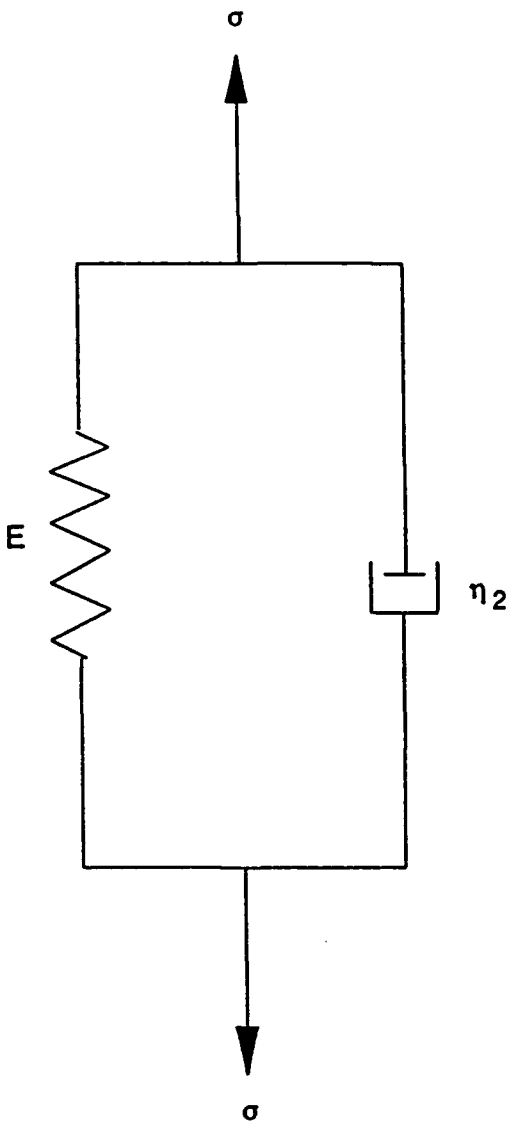

Figure 2.20 Visco-Elastic Model for Small Levels (Komamura and Huang, 1974)

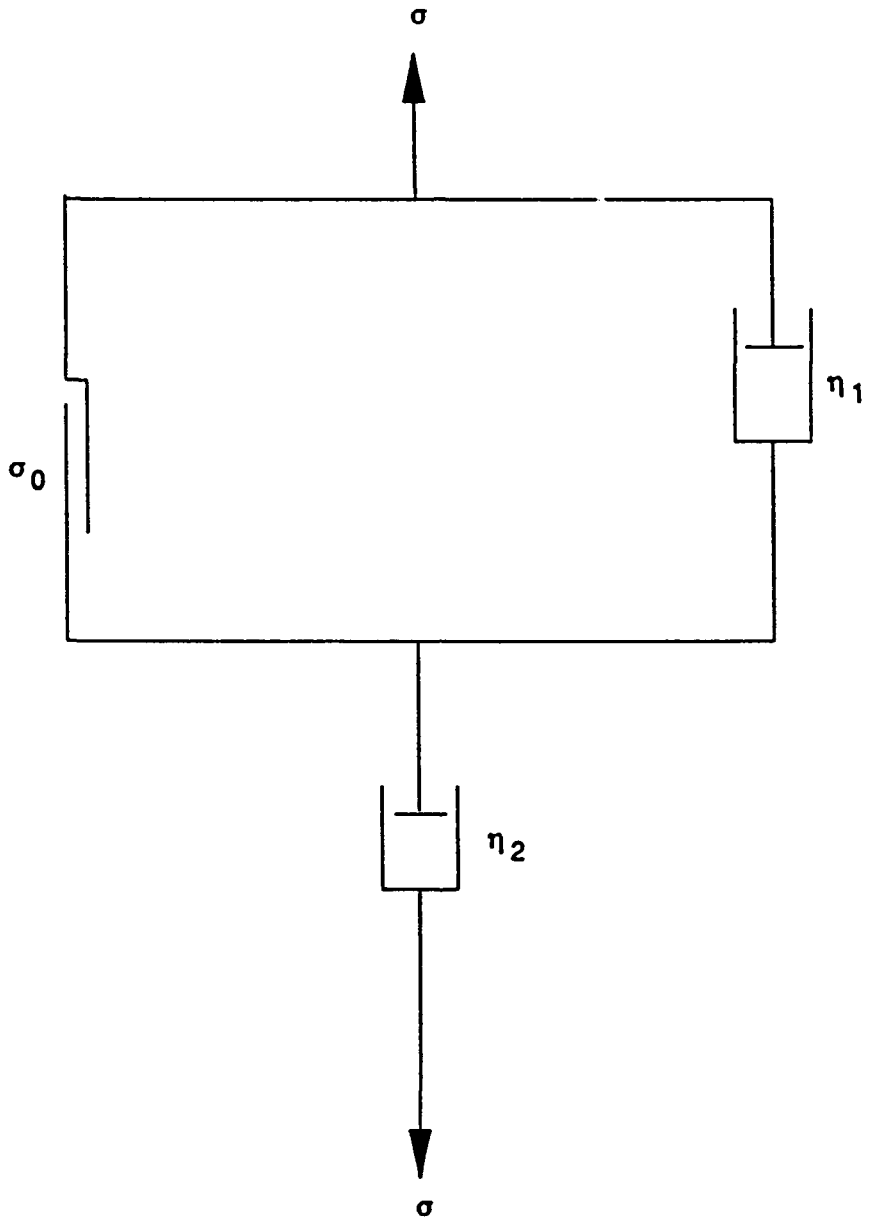

Figure 2.21 Visco-Plastic Model for Water Content Above the Visco-Plastic Limit (Komamura and Huang, 1974)

Figure 2.22 Viscous Model for Water Contents Higher Than the Liquid Limit (Komamura and Huang, 1974)

CHAPTER THREE

SPECIMEN PREPARATION AND CREEP RECOVERY TESTING

3.1 INTRODUCTION

The sample preparation procedure, the test set-up used in the creep tests, the calibrations, and the results of the tests performed are described and discussed in this chapter.Creep and recovery tests were performed in conventional triaxial cells to evaluate the strain-stress-time behavior of unsaturated clayey soil specimens, with an initial cylindrical shape 3 inches long and 1.4 inches in diameter. The moisture conditions were controlled by equilibrating the soil at three soil suction levels of 15 psi, 40 psi and 70 psi. All these creep and recovery tests were conducted in a constant temperature room at 20 ° C.

3.2 PREPARATION OF SPECIMENS

3.2.1 Soil Stock Preparation

For the purpose of this study, a 50 lb sample of clayey soil was collected from the flood plain of the Rio Grande, in El Paso, Texas. This soil sample was subjected to a treatment in four phases to remove all soluble matter and afford a strict control of the chemical make-up of the pore fluid.

Phase 1

Initially, the soil was crushed and sieved through a number 40 sieve. Following this, the soil was repeatedly washed with distilled water in flasks. The soil was mixed with distilled water in a beaker for 24 hours. Sodium Chloride solution was added to the soil during the washes to speed up the flocculation of the soil suspension. The clear supernatant was siphoned off after the soil had flocculated. This procedure was repeated five times to ensure that gypsum if present would have been completely removed. At the end of this cleaning procedure, the soil was left with excess sodium chloride in the interstitial fluid.

Phase 2

Following the distilled water wash, the soil was sieved through a number 200 sieve. This step was taken to ensure that only particles less than 75 microns were used in the tests. The soil that was sieved was then placed in a fume hood and titrated with hydrochloric acid. The purpose of the addition of acid was to react and dissolve the carbonates.

The pH of the soil suspension was always maintained at 5, as at this pH, the carbonate reaction can be completed without the clay being affected. Addition of acid was stopped when the reaction with carbonates was not observed visually. A pH meter was used subsequently to monitor the pH levels. This phase was prolonged until the 5 pH of the soil suspension did not increase in a period of 24 hours.

Phase 3

Following the complete removal of all carbonates, hydrogen peroxide 30% by volume was added to the soil. The hydrogen peroxide was added to oxidize all the organic matter present in the soil. The soil suspension with peroxide was placed aside for a period of approximately 24 hours and then heated gently in a water bath. The remaining peroxide was allowed to react completely in the bath to accelerate the reaction.

This procedure was repeated until visible signs of reaction were not observed. Distilled water was then added to the soil to flush out the remaining hydrogen peroxide and hydrochloric acid. At the end of the cleaning cycle, the soil attained a reddish-brown tint indicating the presence of iron oxides. Particles of iron oxide slightly magnetic were removed by repeatedly inserting and removing a magnetic stirring bar into the soil slurry.

Phase 4

The next step involved the removal of soluble salts from the pore water. The suspension of soil and distilled water was placed in a container. Inside the container, cellulose membranes or dialysis bags were attached and filled with distilled water. The membranes were connected in series to a distilled water source. The purpose of this setup was to allow the distilled water to pass through the membranes continuously. Soluble salts from the surrounding soil then had to pass into the membrane due to the differential salt concentration between the

distilled water and the soil. A conductivity meter was used to monitor the salt concentration of the effluent from the membranes. Unfortunately the cleaning process was extremely lengthy and a different approach had to be adopted.

The new approach consisted of flushing the sample repeated times with a 0.01 molal solution of calcium chloride. The process consisted of dispersing the soil into a container using 0.01 molal calcium chloride solution. After completing the dispersion, the soil suspension is allowed to flocculate and sediment on the bottom of the container. The clean supernatant was decanted and the process repeated until the electrical conductivity of the supernatant approached the electrical conductivity of the fresh salt solution which is 1900 micromhos/cm. The records of electrical conductivities of the supernatant during this cleaning are presented in Table 3.1.

3.2.2 Centrifuging of Soil Suspension

After the above four-phase cleaning, the remaining soil suspension was placed in centrifuge bottles and centrifuged at 2,000 rpm for 15 minutes. The clear supernatant was discarded and the soil cake left in the bottles was recovered and placed on a glass plate. At this point, the soil slurry was thoroughly mixed to homogenize the segregated soil cake created by the centrifugation. A photographic view of the mixed soil slurry is shown in Figure 3.1. The goal of this step was to reduce the soil moisture in the suspension, and, thus, reduce consolidation time and control specimen volume changes during the consolidation

Table 3.1

Records of the Electrical Conductivity of the Supernatant
During Cleaning of Soil Stock

Date	Electrical Conductivity (micromhos/cm)		
	Container 1	Container 2	Container 3
Sep.17, 90	6600	4800	20000
Sep.18, 90	6400	3000	14000
Sep.19, 90	6800	3000	13600
Sep.20, 90	4200	2600	8400
Sep.21, 90	4200	2600	8400
Sep.22, 90	3200	2350	4600
Sep.24, 90	2700	2200	4200
Sep.25, 90	2400	1900	5100
Sep.26, 90	2400	2200	4100
Sep.27, 90	2400	1900	3400
Sep.29, 90	2400	1900	3300
Sep.30, 90	2400	2300	3300
Oct.1, 90	2200	2200	2000
Oct.2, 90	2600	2300	3200
Oct.3, 90	2400	2100	200
Oct.4, 90	2300	2100	2500
Oct.5, 90	2100	2300	2300
Oct.6, 90	2000	2050	2000
Electrical conductivity of 0.01 molal solution of $CaCl_2$ = 1900 micromhos/cm			

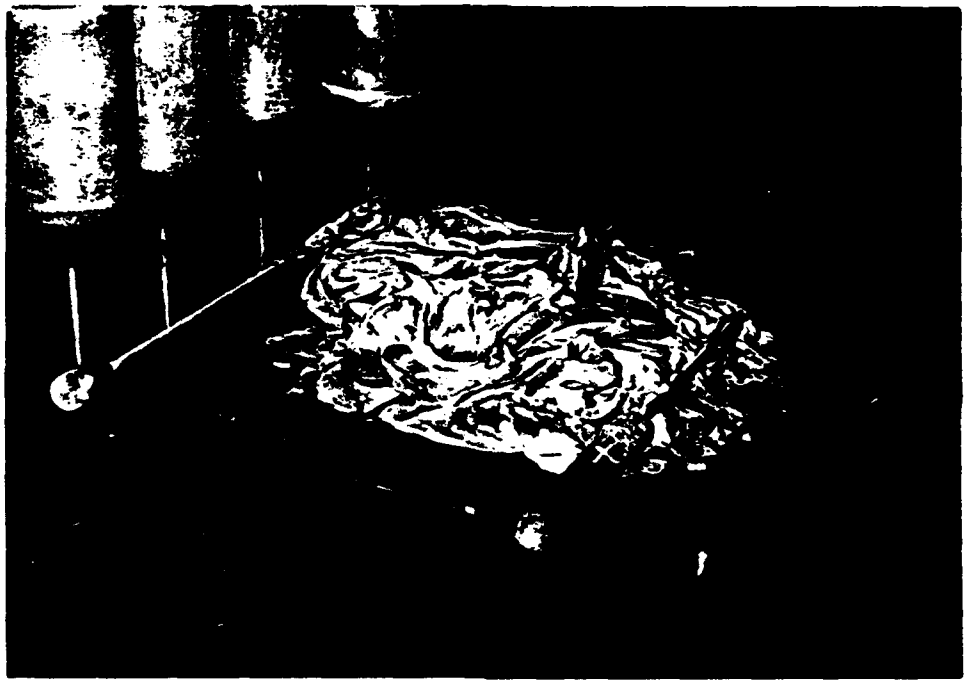

Figure 3.1 A Photographic View of Mixed Soil Slurry

phase.

3.2.3 Specimen Consolidation

The homogenized slurry was then placed inside a rubber membrane attached to a 2.8 inch in diameter pedestal and top cap. The specimen was initially built to a 2.8 inch in diameter, and was then consolidated under 50 psi cell pressure in a conventional triaxial cell, which is shown photographily in Figure 3.2. During the consolidation, the outflow from the specimen was directed towards a burette and a record was kept of the volume of water expelled from the specimen with time.

A total of 46 specimens have been consolidated. The records of volume of water expelled from each specimen with time are included in Appendix A. A summary of the conditions during the consolidation phase of all these 46 specimens is presented in Table 3.2. The time invested in the consolidation phase ranged for 72 to 300 hours. The initial specimen was consolidated for nearly 200 hours. The consolidation curve suggested that from 2,000 to 3,000 minutes are necessary to reach the 100% "primary consolidation". Because of this, the time of consolidation was reduced to 72 hours for Specimens 7 to 8. The curve presented for Specimen 8 indicates that this was the appropriate time; however, the consolidation curves for Specimens 7, 9, and 10 do not show signs of having reaching the 100% primary consolidation point. Consequently, starting from Specimen 11, consolidation time of most specimens were controlled ranging from

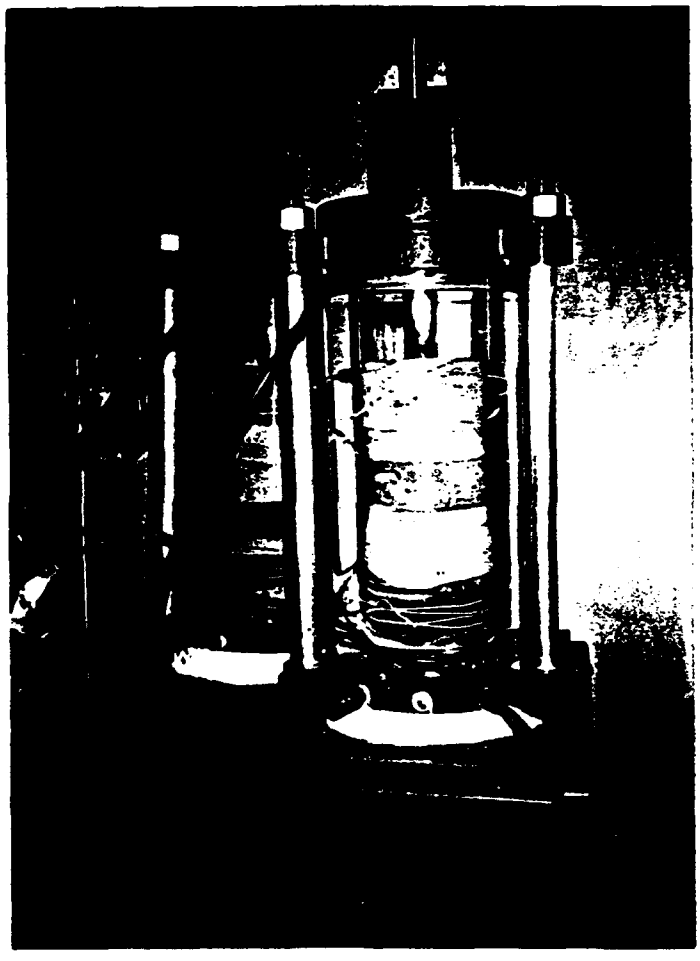

Figure 3.2 A Photographic View of the Specimen Consolidation Set Up

Table 3.2
Conditions and Results of Specimen Consolidation

Specimen No.	Consolidation Time, hrs.	Water Outflow, ml	Specimen No.	Consolidation Time, hrs.	Water Outflow, ml
1	179	187	24	162	168
2	310	178	25	164	174
3	110	178	26	162	171
4	110	171	27	162	163
5	193	199	28	162	164
6	198	155	29	162	178
7	72	149	30	162	177
8	72	141	31	164	183
9	72	187	32	164	188
10	72	162	33	170	189
11	164	160	34	170	197
12	164	173	35	164	188
13	172	146	36	164	168
14	172	169	37	166	184
15	212	165	38	166	184
16	162	163	39	174	185
17	164	172	40	174	161
18	164	180	41	164	170
19	164	166	42	164	160
20	168	170	43	161	179
21	168	173	44	161	180
22	166	178	45	167	194
23	162	170	46	167	200

160 to 170 hours, that is around 6 to 7 days. For all the consolidation curves obtained afterwards, it appears that 100 hours is the time when the 100% "primary consolidation" point is reached.

The total water outflow measured during the consolidation phase of each specimen is listed in Table 3.2. These results indicated that the specimens were not exactly the same. The reasons for this variability are not evident but would be related to losing water during mixing of slurry and/or water squeezing through the drainage tube when the triaxial cell was being filled with water. However, the consolidation process was not controlled by the total amount of outflow water, but rather by the length of time and by the reaching the 100% primary consolidation point.

3.3 TEST SET-UP

3.3.1 General Description

A triaxial cell was used in this study. A schematic of the triaxial cell used to performed the creep test is presented Figure 3.3. In order to equilibrate the specimens to predetermined soil suctions, a high air entry disk was used to control independently the pore water pressure and pore air pressure in the specimen. The high air entry porous disk is made of ceramic which allows the slow passage of water but does not permit the flow of free air as long as the difference between the air and water pressures does not exceed the air entry value of the disk. Such a disk placed underneath the soil specimen serves to separate the pore air pressure

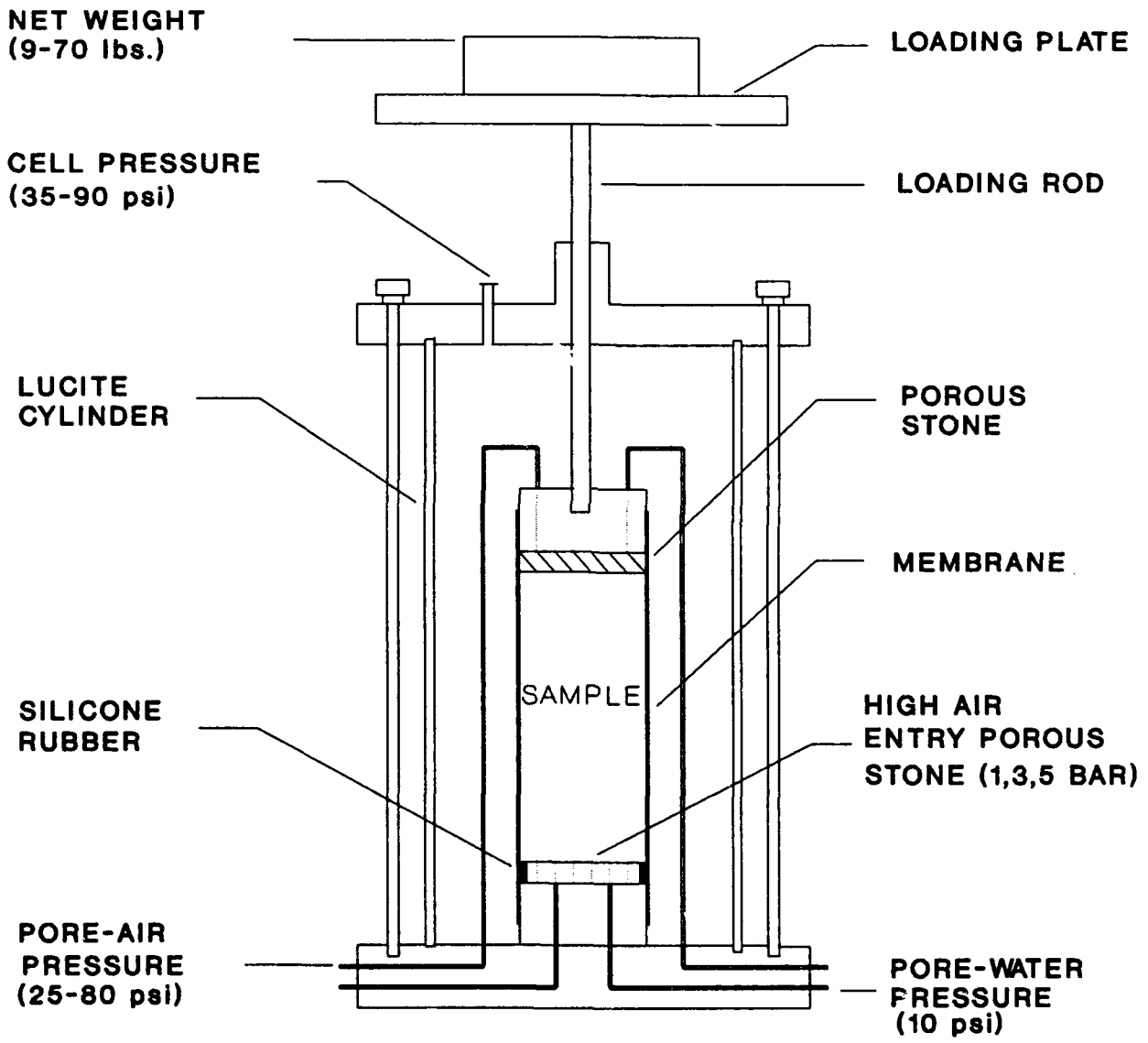

Figure 3.3 Test Set-Up for Creep and Recovery Testing

and pore water pressure. So long as the difference between the pore-air pressure and pore-water pressure does not exceed the air entry value of the disk, there is a continuous column of water from the specimen to the water below the high air entry porous disk. This allows that the pore water pressure can be independently controlled. Before doing any tests, the high air entry porous disk was saturated with deaired distilled water to obtain the continuous water flow. Three types of ceramic disks were used in this study, the characteristics of these dicks are shown in Table 3.3.

Table 3.3
Characteristics of High Air Entry Porous Disks Used in This Study

Air Entry Value	Diameter, in	Thickness, in
1 bar (14.7 psi)	1.125	0.28
3 bar (44.7 psi)	1.175	0.35
5 bar (73.5 psi)	1.115	0.31

3.3.2 Calibration of Test Set Up

The cell pressure and the friction between the rod and bushing affect the load transmitted by the rod to the specimen under testing. A calibration of the four cells used in the creep tests was conducted to allow the separation of these effects. This process consisted of two independent calibration methods to evaluate quantitatively the load needed on the platform to balance cell pressure and friction. In both methods, a synthetic dummy specimen was used inside the cell, the rod was clamped, and the calibration started.

The first approach consisted of placing a container with sand on the loading platform shown in Figure 3.3. The amount of sand used was large enough to keep the rod resting on the top cap. A dial gage was attached to the rod and sand from the container was slowly removed while the gage was monitored. When the gage started to indicate a quick exit (upward movement) of the rod from the cell it was taken as the equilibration point. The load of sand on the platform was recorded as the load necessary to equilibrate the cell pressure. These steps were then repeated for other cell pressure covering the expected range of cell pressures.

In the second approach, the load necessary to push the rod into the cell was measured. This was accomplished locking the rod just above the specimen. Under these conditions, the load of sand on the loading platform was slowly increased. The rod was momentaneously unloaded to observe the tendency of movement of the rod. When a quick penetration of the rod was indicated by the dial gage, the load of sand on the platform was recorded as the weight needed to equilibrate the cell pressures.

The calibration data for each of the four cells are presented in Appendix B. These results show that the two sets of measurements are fairly close. A single regression line was fitted to all the data points measured. The four linear regression equations used to calculate the loads necessary to balance cell pressure and friction, are summarized in Table 3.4. These lines were used to calculate the fraction of the gross load on the loading platform that was actually applied on the specimen to cause creep. The loads reported in this report are "net"

loads; that is, the load after discounting the effect of the cell pressure on the rod.

Table 3.4
Regression Equation To Calculate The Load Necessary
to Balance Cell Pressure and Friction

Cell No.	Regression Equation
1	Y=0.10052X-1.663494
2	Y=0.10182X-1.985027
3	Y=0.09133X-1.546964
4	Y=0.09093X-1.393695
X=Cell Pressure, psi	Y=Balanced Load, Kg

3.4 SPECIMEN EQUILIBRATION TO PREDETERMINED SOIL SUCTIONS

After the consolidation process was completed, the specimen was extracted from the membrane and trimmed down to 1.4 inch diameter and 3.0 inch length. A specimen before and after the trimming is shown photographily in Figure 3.4 and Figure 3.5, respectively. The shavings produced in this trimming process were used to determine the water content of the specimen after the consolidation phase. These values of water content are presented and discussed in Chapter 4 in more detail.

Upon trimming, the specimen was placed in triaxial cell enclosed with a rubber membrane. The set-up used is illustrated in Figure 3.3. The air pressure was applied on the top of the specimen and the water pressure was controlled through the bottom high air entry porous disk. The soil suction level imposed on

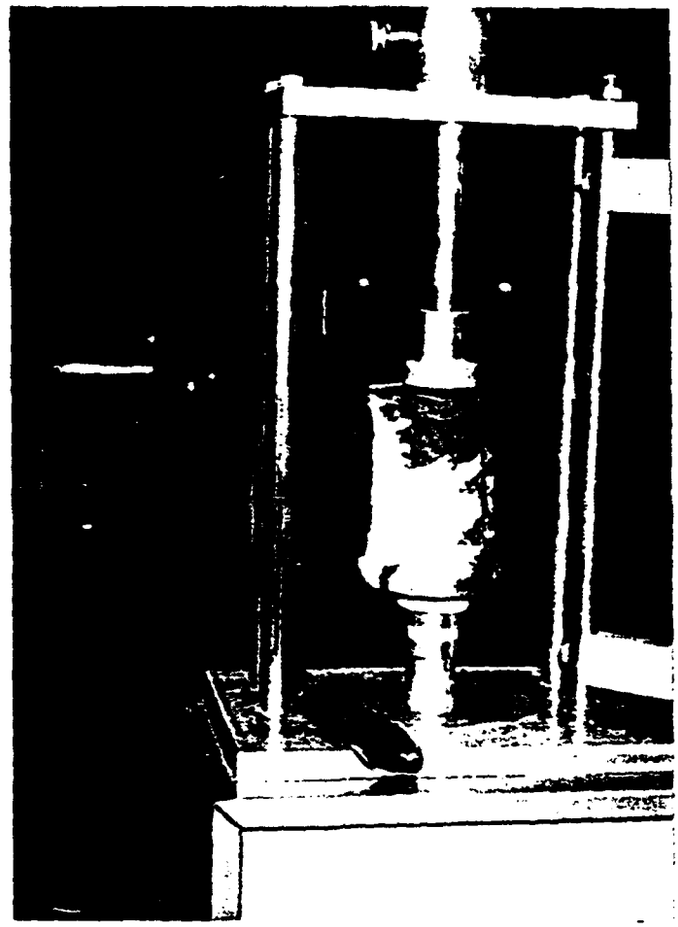

Figure 3.4 Specimen before the Trimming

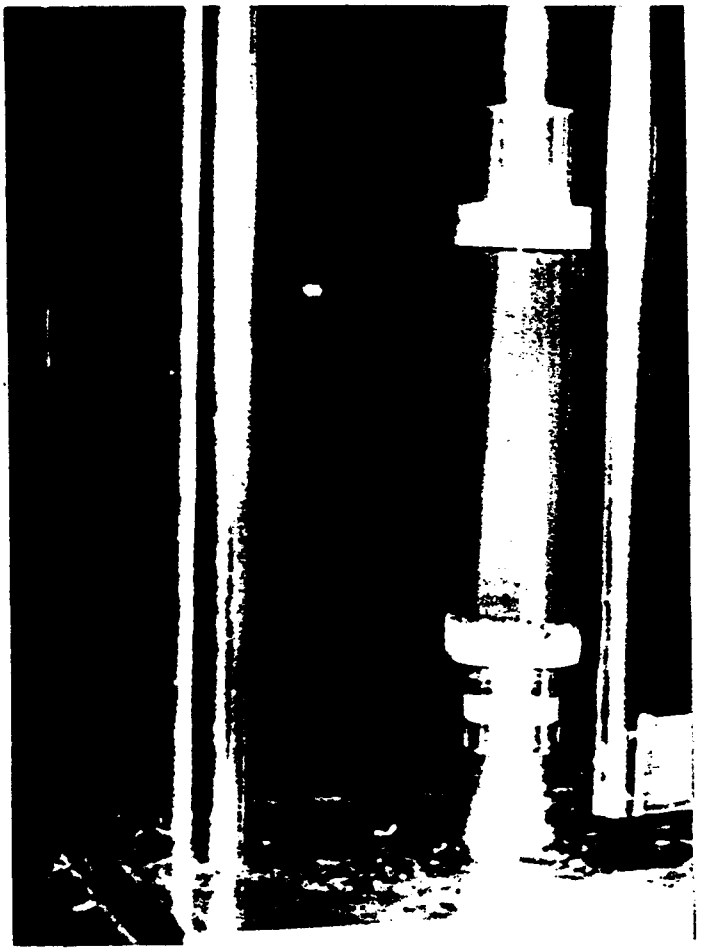

Figure 3.5 Specimen after the Trimming

the specimen was the difference between the air and pore water pressures. The cell pressure was applied through the top valve of the cell.

Under these conditions, the specimen was allowed to equilibrate while the pore fluid being expelled or imbibed was monitored. A summary of the conditions imposed on all the specimens performed is presented in Table 3.5. The individual records of volume of pore fluid expelled or imbibed with time for each specimen are included in Appendix C.

From Specimen 1 to 6, the pore-water pressure was 5 psi, and the pore-air pressure was controlled at 19 psi, so the soil suction was 14 psi. The cell pressure was kept at 20 psi. As indicated in Table 3.5, starting from Specimen 7, the pore-water pressure for all specimens was kept at 10 psi. The three soil suction levels used were 15, 40 and 70 psi. From Specimen 7 on, the cell pressure was always 10 psi larger than the respective pore-air pressure. The volume of pore water being expelled during the equilibration phase for 15 psi soil suction ranges form 0.05 to 0.8 ml. Specimens 30 and 32 experienced an overall gain of pore fluid during this equilibration phase, as illustrated in Figure 3.6. From Specimen 1 to 6, the specimen was left saturating for 24 hours before the soil suction equilibration phase. Therefore, the volume of pore water expelled from these specimen, except for Specimen 3 was more than for the rest. The pore water outflow for the specimens equilibrated at 40 psi soil suction range form 1.3 to 9.2 ml. The only exception is Sample 8 that imbibed 0.2 ml water. These results are shown graphically in Figure 3.7. The pore water being expelled from the specimens

Table 3.5
Conditions during the Specimen Equilibration Phase
to a Constant Soil Suction

Specimen No.	Pore-water Pressure psi	Pore-air Pressure psi	Soil Suction psi	Cell Pressure psi	Equilibration Time hour	Pore-water Movement ml
1	5	19	14	20	375	3.24
2	5	19	14	20	169	0.92
3	5	19	14	20	540	-3.25
4	5	19	14	20	834	2.89
5	5	19	14	20	573	7.60
6	5	19	14	20	580	2.20
7	10	50	40	60	258	2.95
8	10	50	40	60	258	-0.20
9	10	50	40	60	422	3.75
10	10	50	40	60	422	6.15
11	10	80	70	90	480	4.70
12	10	80	70	90	480	10.70
13	10	50	40	60	429	8.86
14	10	50	40	60	429	9.20
15	10	80	70	90	285	35.90
16	10	50	40	60	496	4.05
17	10	50	40	60	496	4.17
18	10	80	70	90	397	10.15
19	10	80	70	90	396	5.92
20	10	25	15	35	333	0.80
21	10	25	15	35	333	0.20
22	10	80	70	90	439	8.52
23	10	25	15	35	285	0.53
24	10	25	15	35	285	0.44

Table 3.5 (continued)
Conditions During the Specimen Equilibration Phase
to a Constant Soil Suction

Specimen No.	Pore-water Pressure psi	Pore-air Pressure psi	Soil Suction psi	Cell Pressure psi	Equilibration Time hour	Pore-water Movement ml
25	10	50	40	60	378	1.70
26	10	50	40	60	362	1.62
27	10	50	40	60	257	7.90
28	10	80	70	90	264	10.05
29	10	25	15	35	110	0.18
30	10	25	15	35	110	-0.80
31	10	80	70	90	283	6.97
32	10	25	15	35	327	-0.47
33	10	25	15	35	212	0.05
34	10	80	70	90	308	6.80
35	10	80	70	90	479	4.95
36	10	50	40	60	379	1.30
37	10	50	40	60	355	6.27
38	10	50	40	60	355	2.20
39	10	50	40	60	260	1.63
40	10	80	70	90	431	11.8
41	10	50	40	60	378	1.50
42	10	25	15	35	260	0.21
43	10	50	40	60	310	5.38
44	10	50	40	60	430	0.67
45	10	50	40	60	430	3.93
46	10	50	40	60	337	4.00

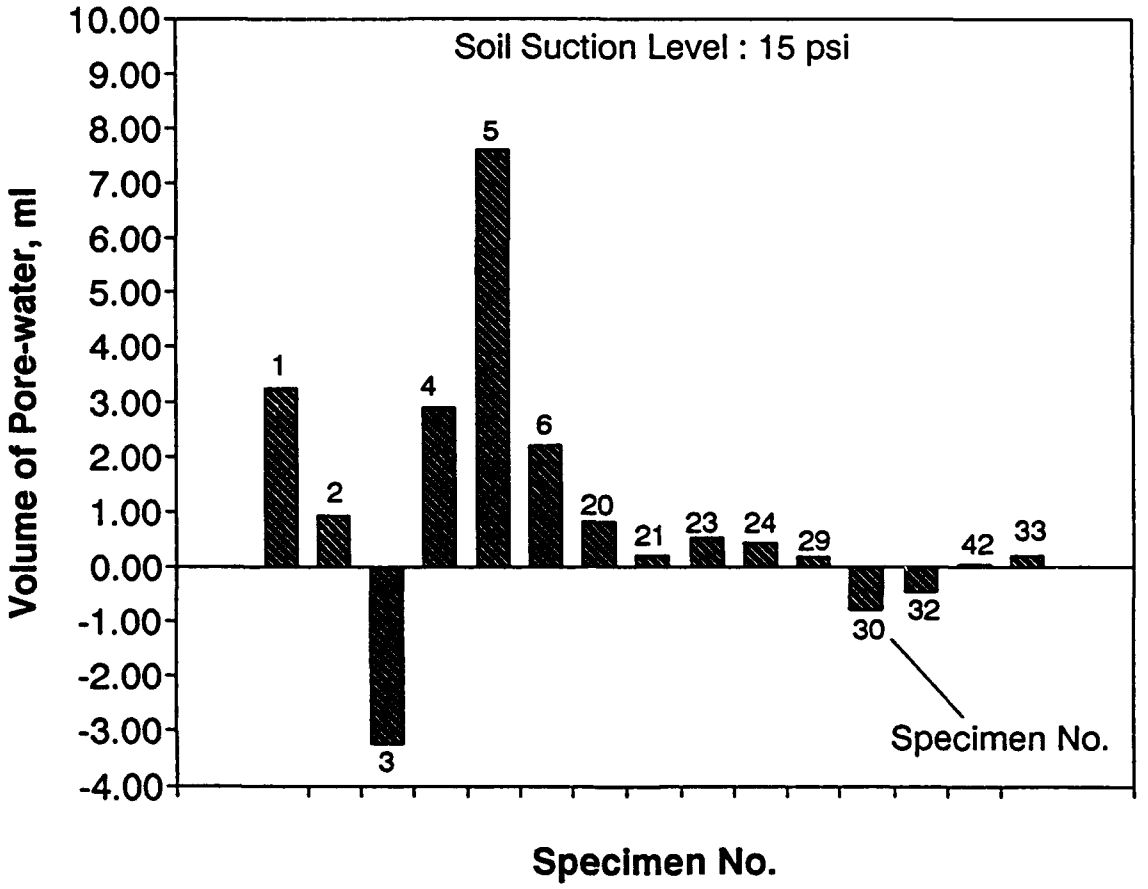

Figure 3.6 Volume of Pore-water Movement During Equilibration at 15 psi Soil Suction

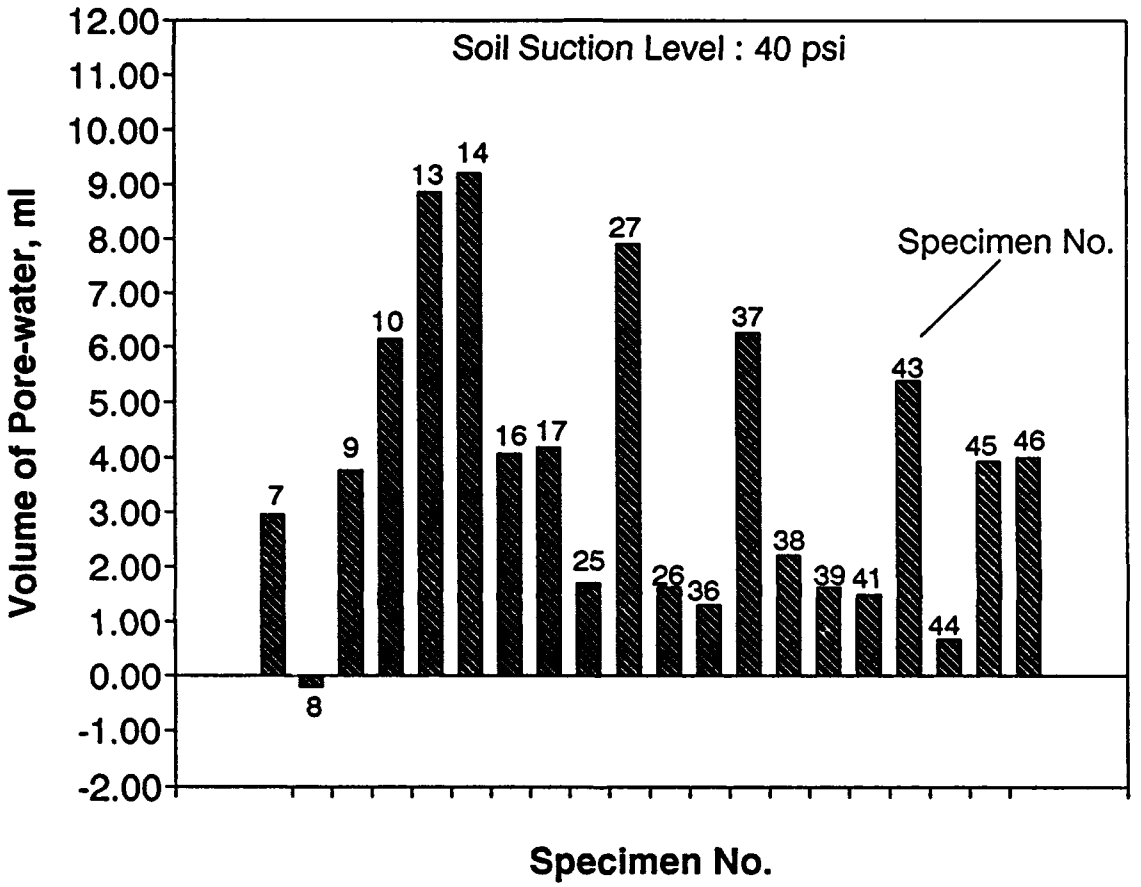

Figure 3.7 Volume of Pore-water Movement During Equilibration at 40 psi Soil Suction

equilibrated at 70 psi soil suction are shown in Figure 3.8. The volumes of water expelled varied from 4.7 to 10.7 ml expect for Specimen 15.

The results presented in Table 3.5 indicate that specimens equilibrated at 15 psi soil suction may imbibe pore fluid during equilibration phase. The reasons for this fact are not evident. Nevertheless, at higher suction levels most equilibration phases resulted in more pore fluid being expelled from the specimen.

The criteria used to stop the equilibration phase was to make sure that the movement of the pore water in or out of the specimen had leveled off. This was achieved in many of the specimens where the movement of pore water seems to stop. However, there were some exceptions such as Specimens 2, 3, 6, 8, 11, 20, 21, 30, and 33, in which the pore fluid flow reached a peak and then the water flow appears to reverse with water moving out or into the specimen. Most of these case occurred in the equilibration phase at 15 psi soil suction level. Further discussion of this occurrence will be deferred until the presentation of the water contents before and after the creep tests in Chapter Four.

3.5 CREEP AND RECOVERY TESTS

Upon completion of the soil suction equilibration phase, the desired gross load was applied on the loading platform shown in Figure 3.3 and the displacements experienced were recorded using a dial gage with a readability of 0.0001 inches. The goal of the study was to monitor the specimens until the "steady state" creep had been reached.

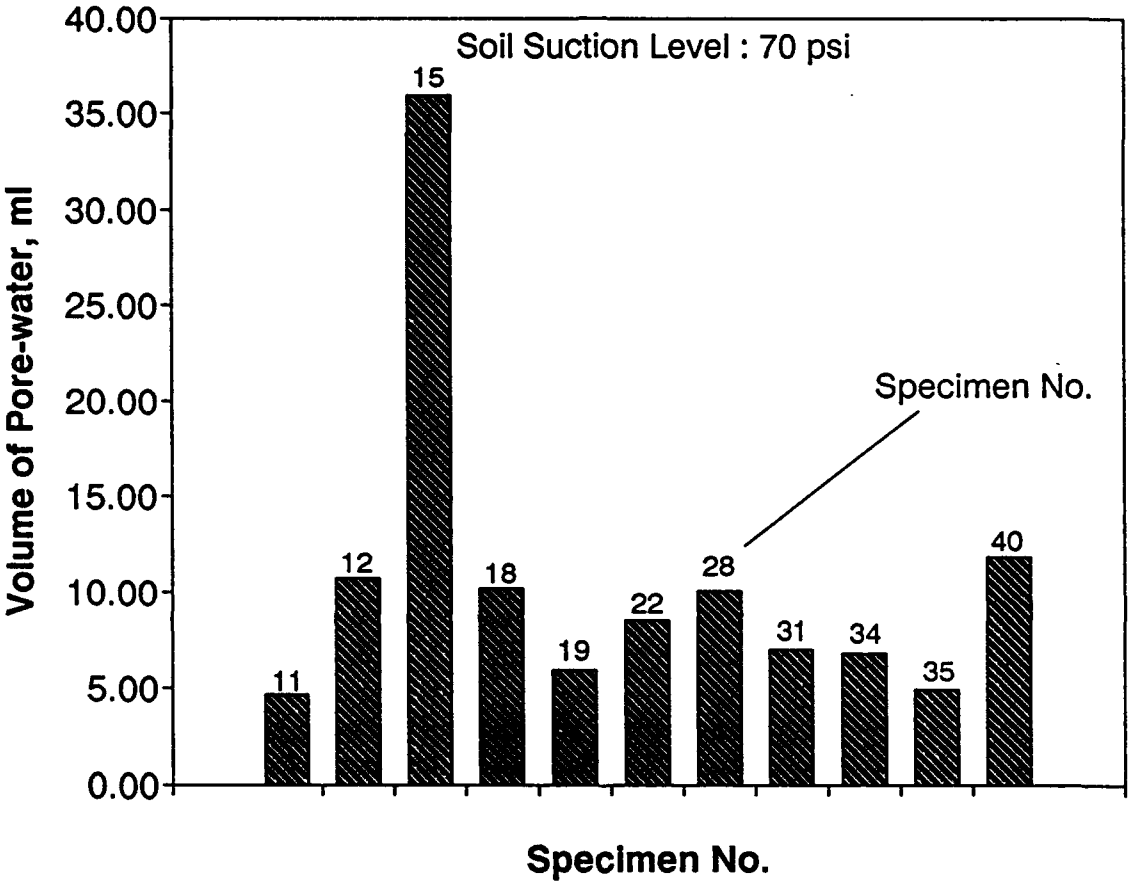

Figure 3.8 Volume of Pore-water Movement During Equilibration at 70 Soil Suction

The conditions of the creep and recovery tests conducted are summarized in Table 3.6. The records of each creep and recovery test are presented in Appendix D. Each record is presented in two figures. In the first figure the time scale is natural and in the second figure the time scale is logarithmic. The purpose of the dual graph is to provide an aid in the identification of the steady creep phase. For the first specimens (from No.1 to No.6), small variations of cell pressure coupled with the small deviatoric stresses applied on the specimens resulted in poorly defined creep curves. A typical example is specimen No.1. In the early stages of this study, large changes of temperature took place due to mal function of the temperature room. This resulted in large changes of strain of several specimens. Examples are specimens No.2 and 5 which exhibit large sudden changes of strain coinciding with the temperature changes.

Most of the specimens exhibited the general development of creep as discussed in Chapter 2. The time to reach the steady state creep was about 5000 minutes or 3.5 days for most specimens and suction levels. A large part of the creep strain occurred in the primary stage. No tertiary phase was ever observed, even for the largest devitoric stresses applied on Specimen 24. This specimen experienced very large strain, of about 13%, in the primary creep stage. Nevertheless, the load was not sustained for a long enough period of time to reach the steady state creep, due to the large transversal strains experienced by the specimen.

Table 3.6
Conditions of The Creep / Recovery Tests

Specimen No.	Soil Suction psi	Pore-air Pressure psi	Cell Pressure psi	Deviatoric Stress psi	Time for Creep min	Time for Recovery min
1	14	19	20	0.93	39550	no
2	14	19	20	1.03	15575	no
3	14	19	20	5.33	46310	no
4	14	19	20	5.23	46310	no
5	14	19	20	5.23	20464	no
6	14	19	20	5.33	19210	no
7	15	25	35	3.32	15980	1090
8	15	25	35	3.08	15980	no
9	40	50	60	5.20	13330	no
10	40	50	60	5.83	13330	no
11	70	80	90	5.73	15925	4550
12	70	80	90	11.46	15920	4550
13	40	50	60	11.46	22785	7240
14	40	50	60	17.19	22763	6937
15	70	80	90	22.92	20026	4238
16	40	50	60	22.92	21700	9025
17	40	50	60	28.65	21699	8579
18	70	80	90	40.12	27254	no
19	70	80	90	28.65	27263	2745
20	15	25	35	11.46	28920	8580
21	15	25	35	17.19	28864	8605
23	15	25	35	22.92	21550	2880
24	15	25	35	28.65	40	1250
29	15	25	35	14.30	20208	8800

Table 3.6 (continued)
Conditions of The Creep / Recovery Tests

Specimen No.	Soil Suction psi	Pore-air Pressure psi	Cell Pressure psi	Deviatoric Stress psi	Time for Creep min	Time for Recovery min
30	15	25	35	5.73	20218	8800
35	70	80	90	17.19	24330	1350
36	40	50	60	5.73	20150	10045
37	40	50	60	11.43	20155	7170
38	40	50	60	17.19	31394	7325
40	70	80	90	40.12	25860	10140
45	40	50	60	22.92	25940	9860
46	40	50	60	34.38	34480	5738

3.6 REPEATABILITY OF CREEP/RECOVERY TESTS

Due to some of the problems, described later, encountered with the creep/recovery tests on specimens equilibrated at 40 psi soil suction, it was decided to perform duplicates of five creep/recovery tests for deviatoric stresses ranging from 5.76 psi to 28.65 psi. These duplicates afford the opportunity to evaluate the repeatability of the creep/recovery tests. The results of the two repetitions for a deviatoric stress of 5.76 psi are compared graphically in Figure 3.9. The same comparison for the two repetitions for a deviatoric stress of 11.46 psi is presented in Figure 3.10. The two creep/recovery curves for a deviatoric stress of 17.19 psi are presented in Figure 3.11. Finally, the two creep curves obtained at deviatoric stress of 22.92 psi and 28.65 psi are compared to the duplicates in Figure 3.12 and 3.13, respectively.

For the deviatoric stress of 17.19 psi, the creep curves are remarkably similar. Nevertheless, the recovery tests are sensibly different. For the rest of the deviatoric stress, the long term creep strains are nearly twice as large as the corresponding first trial. Differences of the same order of magnitude in term of a percentage are also observed in the recovery phase. The differences illustrated in Figures 3.9 through 3.13 suggests the need to build a data base with several repetitions for each soil suction and deviatoric stress in order to properly characterize average values and variability of the creep/recovery tests. This objective was not possible to be achieved in the present study due to the large number of tests required and the long duration of each test.

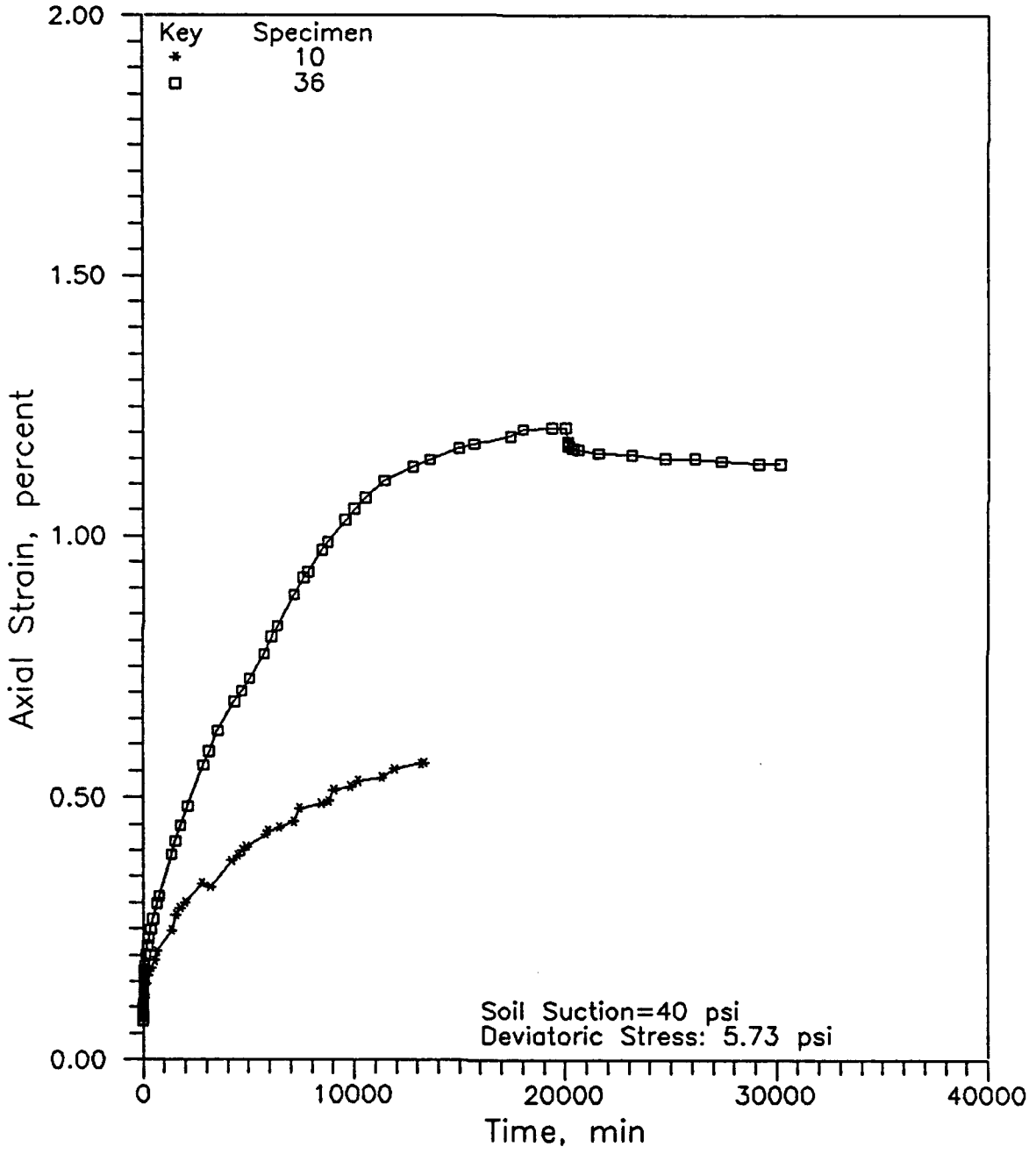

Figure 3.9 Comparison of Creep/Recovery Tests at 40 psi Soil Suction and 5.76 psi Deviatoric Stress

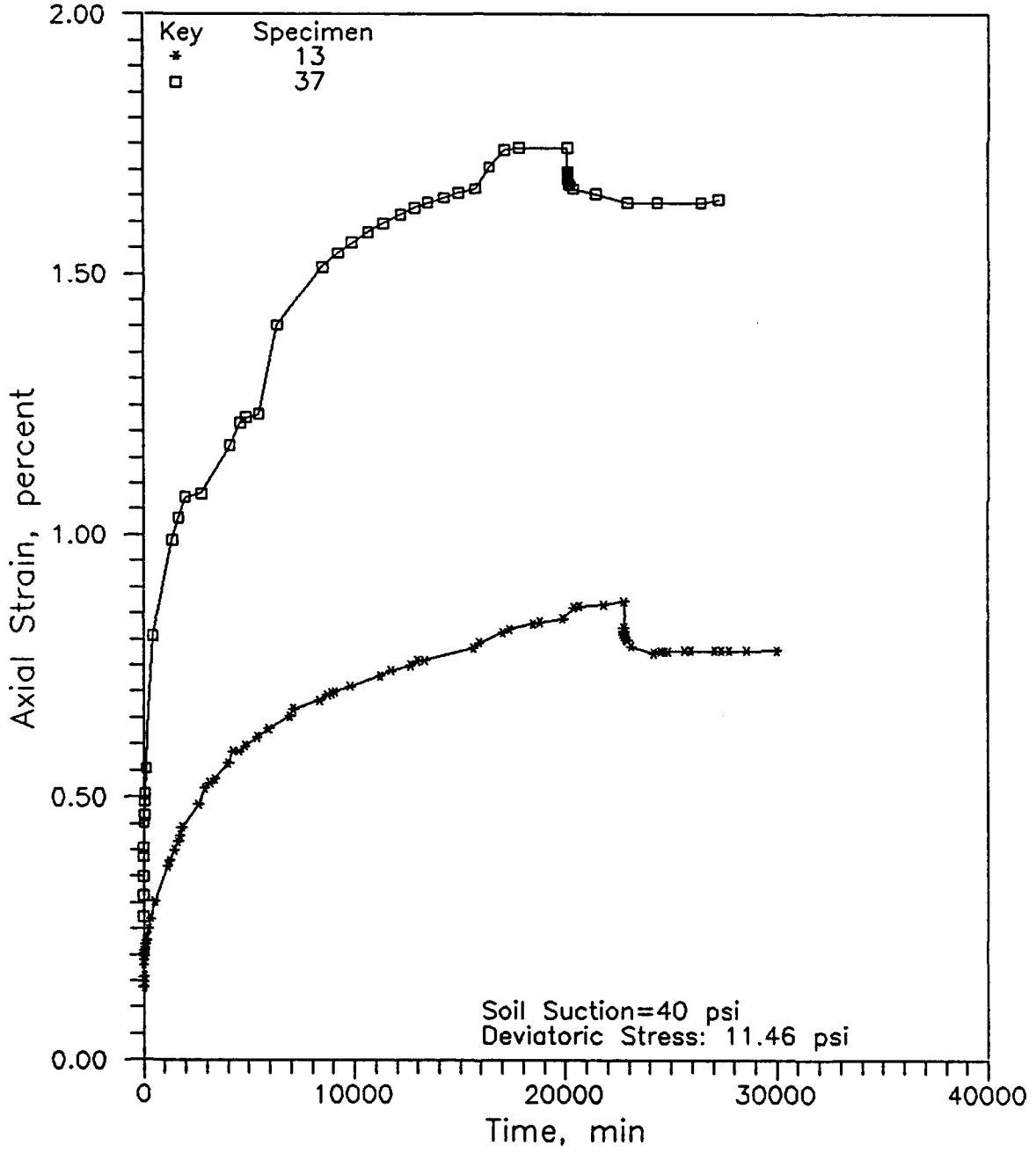

Figure 3.10 Comparison of Creep/Recovery Tests at 40 psi Soil Suction and 11.46 psi Deviatoric Stress

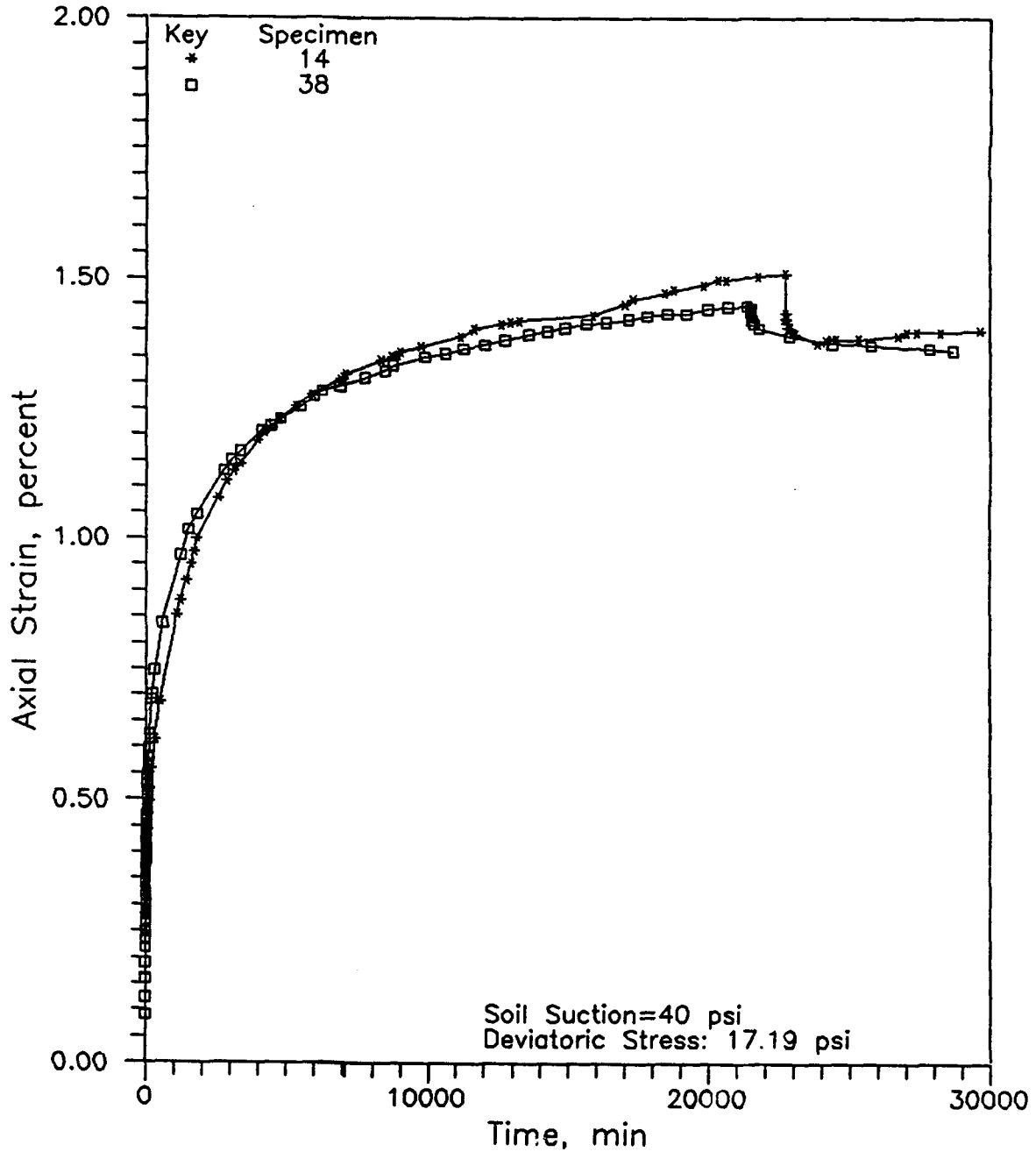

Figure 3.11 Comparison of Creep/Recovery Tests at 40 psi Soil Suction and 17.19 psi Deviatoric Stress

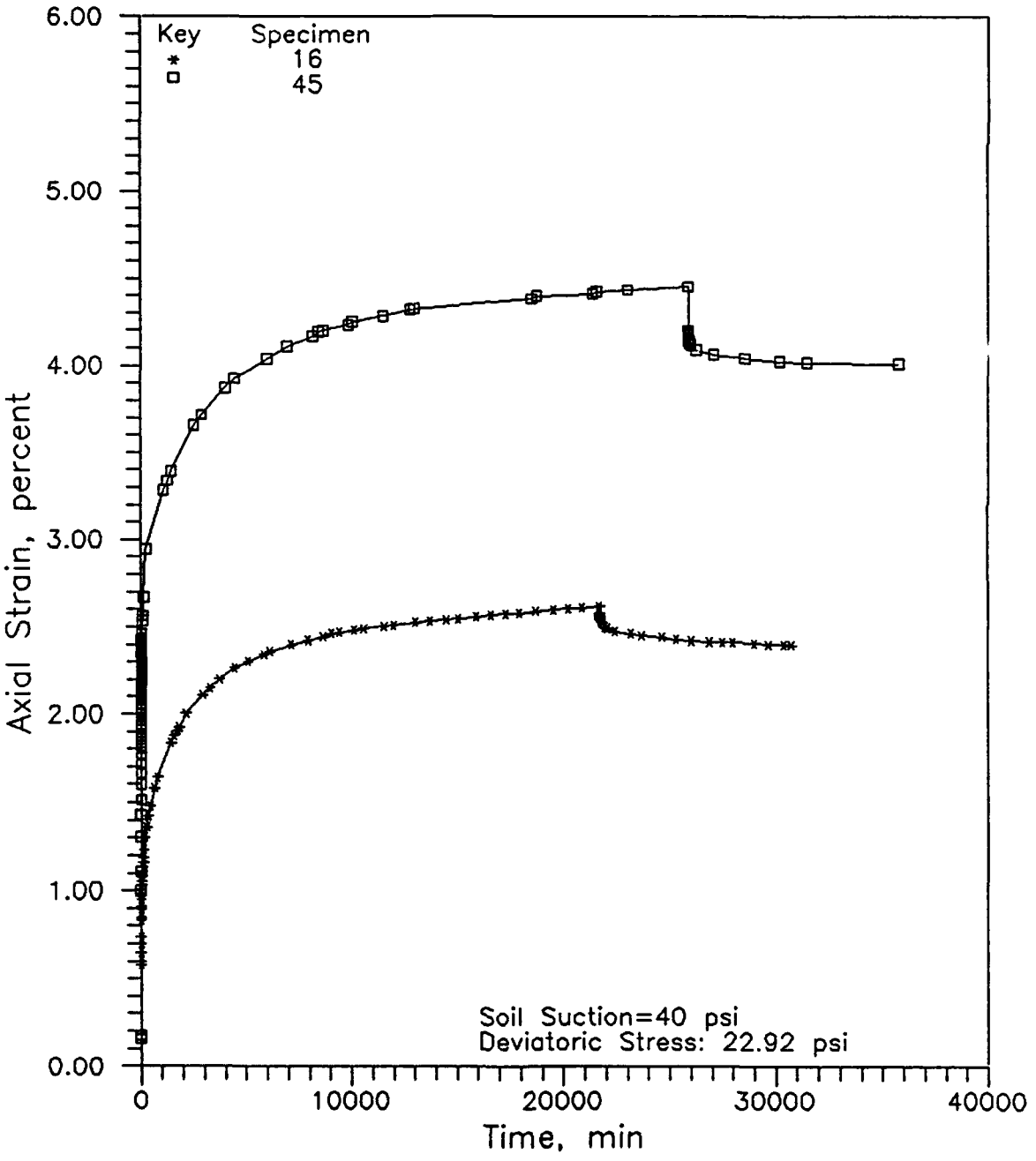

Figure 3.12 Comparison of Creep/Recovery Tests at 40 psi Soil Suction and 22.92 psi Deviatoric Stress

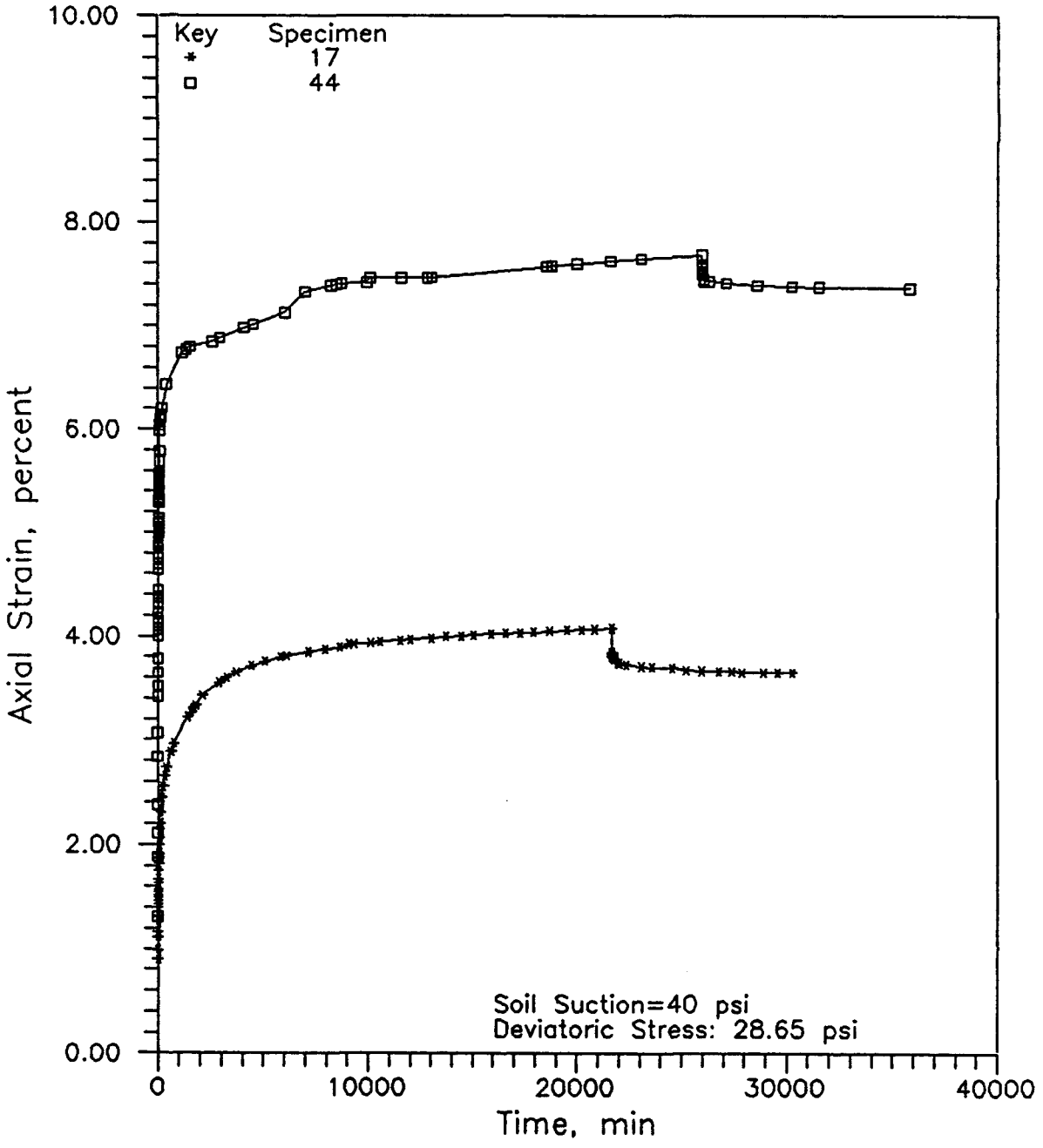

Figure 3.13 Comparison of Creep/Recovery Tests at 40 psi Soil Suction and 28.65 psi Deviatoric Stress

CHAPTER FOUR

INDEX PROPERTIES OF THE SOIL STOCK AND SPECIMENS

4.1 INTRODUCTION

Identification tests were performed early in this study to characterize the soil stock to be used in the test program. Furthermore, some tests such as grain size distribution and water content were performed on the tested specimens to permit an evaluation of the repeatability of the soil stock being used in the preparation of specimens. The results of these tests are summarized in this chapter.

4.2 SPECIFIC GRAVITY OF THE SOLIDS

The specific gravity of the solids for most specimens was determined as a basic index properties of the soils. The measured specific gravities are presented in Table 4.1. These results show that the measured specific gravities are almost the same, close to an average value of 2.75.

4.3 GRAIN SIZE DISTRIBUTION

Specimen of the soil stock already were used to perform grain size distribution analyses. Since the soil stock had been sieved through sieve No. 200, the grain size analyses were performed with the hydrometer test. The hydrometer analysis is used to determine the particle size, and the distribution of those

Table 4.1
Specific Gravity of the Solids

Specimen	Specific Gravity	Specimen	Specific Gravity
1	2.78	16	2.77
2	2.75	17	2.77
3	2.75	18	2.82
4	2.75	19	2.75
5	2.64	20	2.76
6	2.75	21	2.80
7	2.65	22	2.79
8	2.61	23	2.80
9	2.63	24	2.75
10	2.67	25	2.74
11	2.95	26	2.73
12	2.61	27	2.77
13	2.88	28	2.73
14	2.75	29	2.79
15	2.67	30	2.76
Average value is 2.75			

particles, that pass the No. 200 sieve. The hydrometer analysis is based on the terminal velocity of solid particles falling through a liquid, since individual particles settle at different velocities depending on their size, shape and weight. Hydrometer test were performed according to ASTM test designation D422-63 method. The sample was prepared by mixing 50 grams of soil with a sodium carbonate solution as a dispersant. The soil and sodium carbonate solution was mixed in an electric malt-mixer to form a slurry. The slurry was poured into the test cylinders and placed in a constant temperature room at 20^0 C for 24 hours. A calibrated 152H hydrometer was used to perform the four tests. Hydrometer calibration with sodium carbonate solution was performed for the following corrections:

1) meniscus correction; determined to be +1.0 and

2) zero correction; determined to be 0.0

Readings were taken and upon completion, the slurry from the hydrometer was placed in an oven. The oven dry weight of the soil was recorded.

Four specimens of the soil-stock were analyzed and the results are presented in Figure 4.1. The results for all four specimens are very close, indicating that 33% of the stock soil are clay size particles (less than 2 microns) and the remaining 67% are silt size particles.

As the creep tests and the dynamic tests were being performed, some sixteen soil specimens left over after testing were used to perform hydrometer analyses. The grain size distributions calculated from these tests are included in Appendix E. The extreme results of these tests are shown in Figure 4.2 together

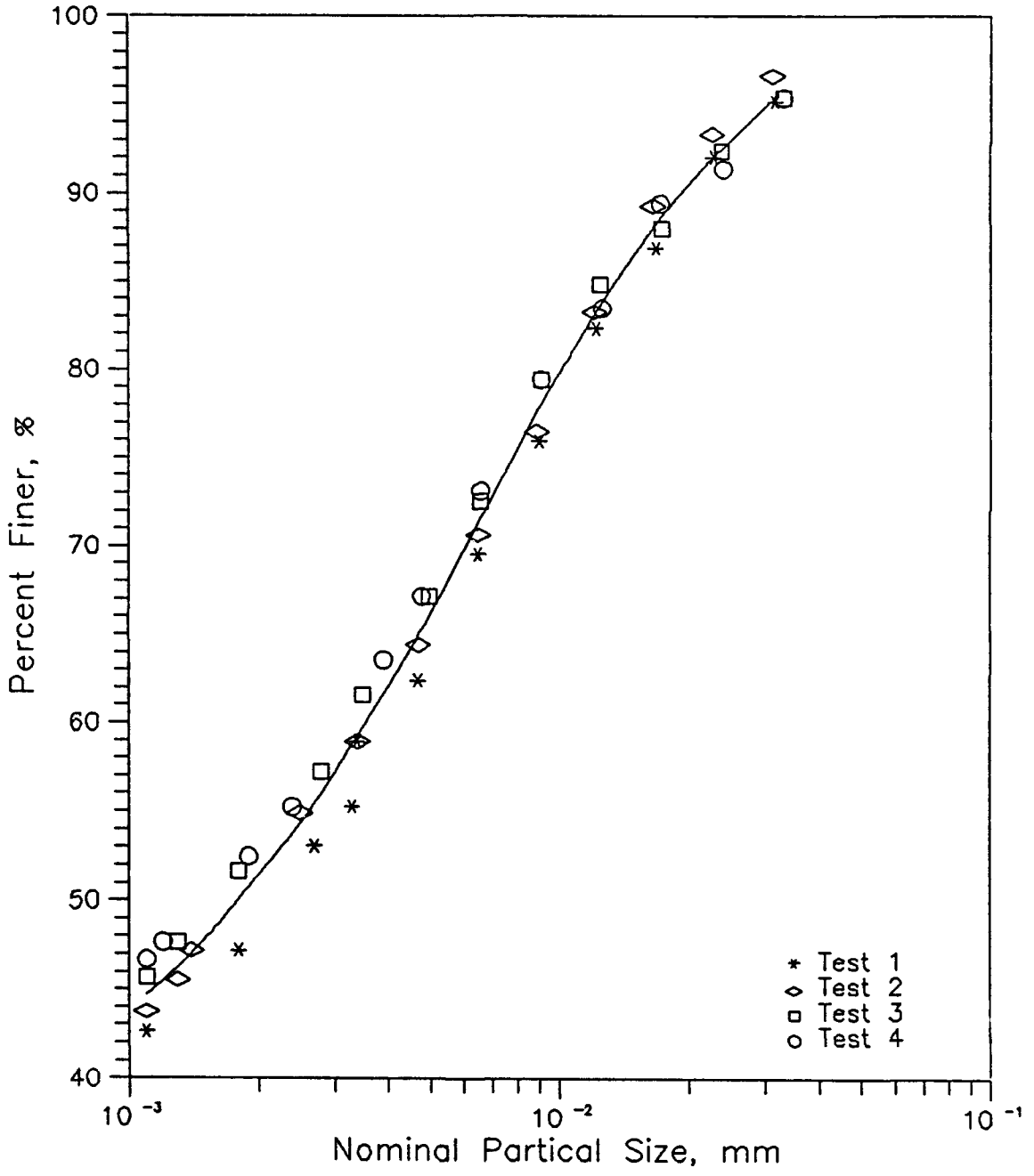

Figure 4.1 Hydrometer Test Results on the Soil Stock

with the hydrometer tests performed initially on the soil stock. These results indicate that differences between specimens exists that could possibly be responsible of the difference in behavior observed in the consolidation and saturation phases described earlier.

It is apparent in Figure 4.2 that the percentage of clay sizes appear to be several percentage points lower for the specimens. This difference could be attributed to the fact that the pore solution in the specimens was 0.01 N $CaCl_2$ while the soil stock was essentially electrolyte free. In this sense, it is believed that the results on the soil stock are more reliable and, thus, give a more representative percentage of clay sizes in the soil stock.

4.4 SOIL PLASTICITY CHARACTERISTICS

Two specimen of the cleaned soil stock were used to perform a two series of Atterberg Limits determinations. For this purpose, the two specimen were flushed repeatedly with 0.001N solutions of Lithium and Aluminum-Chloride, respectively. The flushing was repeated until the electrical conductivity of the supernatant was the same as the electrical conductivity of the fresh salt solution used in the flushing.

After the flushing process was completed the specimens were thoroughly mixed and six determinations of the Liquid and Plastic Limits were performed for each specimen. These determinations were performed in accordance with ASTM test designation D4318-84 method. The results of these determinations with the

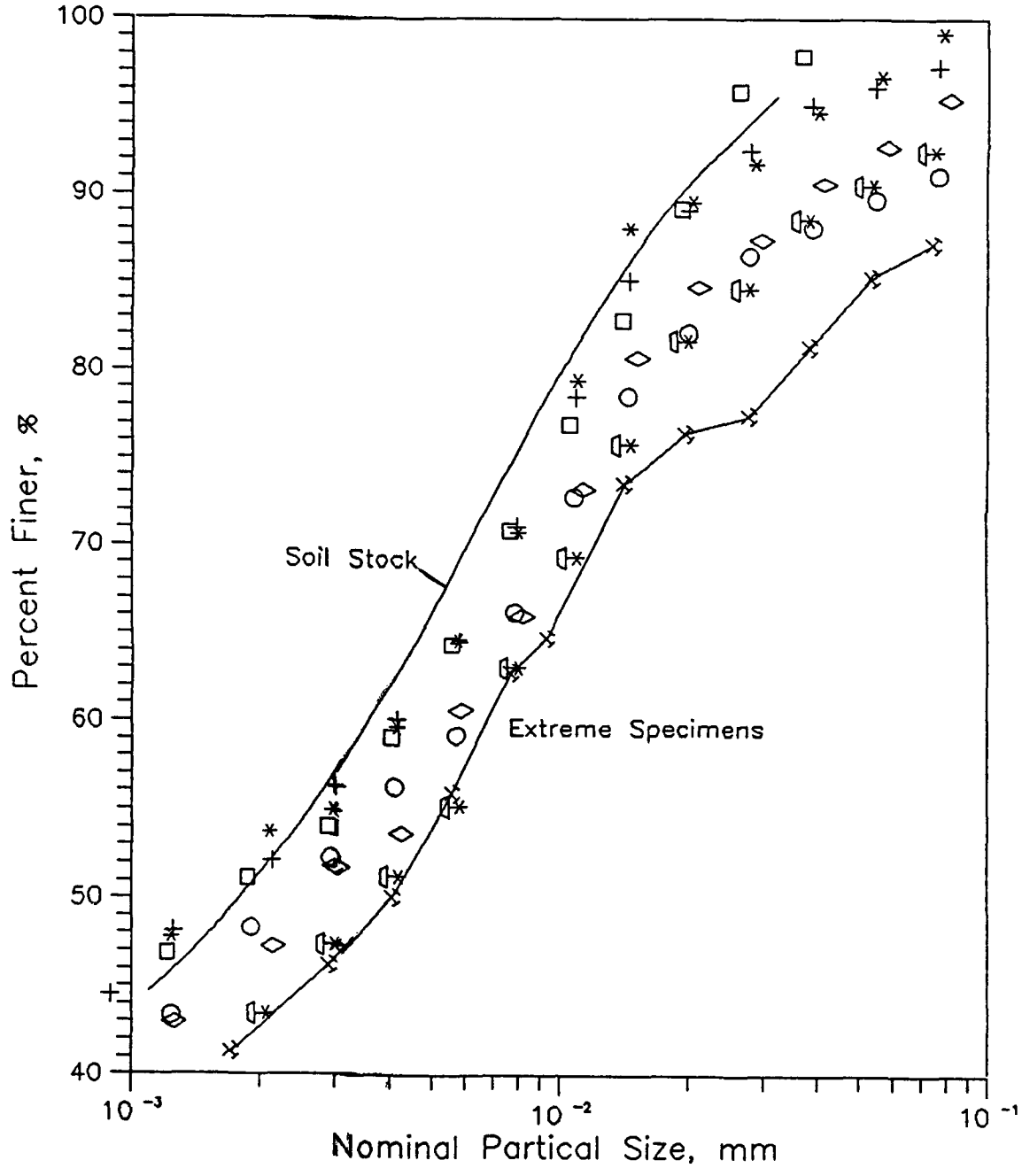

Figure 4.2 Illustration of the Scatter Measured in the Grain Size Distribution of the Specimen

specimens saturated with Lithium Chloride are summarized in Table 4.2 and the results of the determinations on the specimens saturated with Aluminum Chloride are summarized in Table 4.3.

Table 4.2
Atterberg Limits of The Soil Stock Saturated With Lithium Chloride

Test No.	Liquid Limit (%)	Plastic Limit (%)	Plasticity Index (%)
1	63.7	24.6	39.1
2	61.1	21.4	39.7
3	60.8	27.8	33.0
4	61.3	23.8	37.5
5	60.7	23.5	37.2
6	61.8	23.1	38.7

Table 4.3
Atterberg Limits of The Soil Stock Saturated With Aluminum Chloride

Test No.	Liquid Limit (%)	Plastic Limit (%)	Plasticity Index (%)
1	58.7	25.6	33.1
2	60.7	25.1	35.6
3	58.3	25.9	32.4
4	61.9	25.0	36.9
5	58.6	25.4	33.2
6	59.4	25.5	33.9

All these results have been plotted on a Casagrande's Plasticity chart and are presented in Figure 4.3. This figure illustrates that PI's of the soil stock with the exchange complex saturated with Lithium are slightly higher than the PI's of the soil stock with the exchange complex saturated with Aluminum. The average PI ranges from 37.5% with Lithium on the exchange complex to 34.2% with aluminum on the exchange complex. These two cations were selected to cover the possible range of PI to be expected for different saturating cations on the soil stock exchange complex.

4.5 CATION EXCHANGE CAPACITY

The cation exchange capacity of the soil stock was measured saturating the exchange complex with potassium and, then , displacing the potassium with calcium.

The first part of the determination was saturating the exchange complex of the soil stock with potassium. This consisted of five washes of a 0.2 gram specimen with a 1N potassium chloride solution. Each wash consisted of dispersing the specimen in 40 ml of solution, first; then, a centrifugation and decantantion of the clear supernatant. A second series of washes with a 0.01N potassium chloride solution was performed. After five more washes the specimen with the interstitial fluid was weighted and a sample of 0.01N solution was collected to determine the potassium concentration.

The specimen was then washed ten times with 20 ml of a 1N calcium

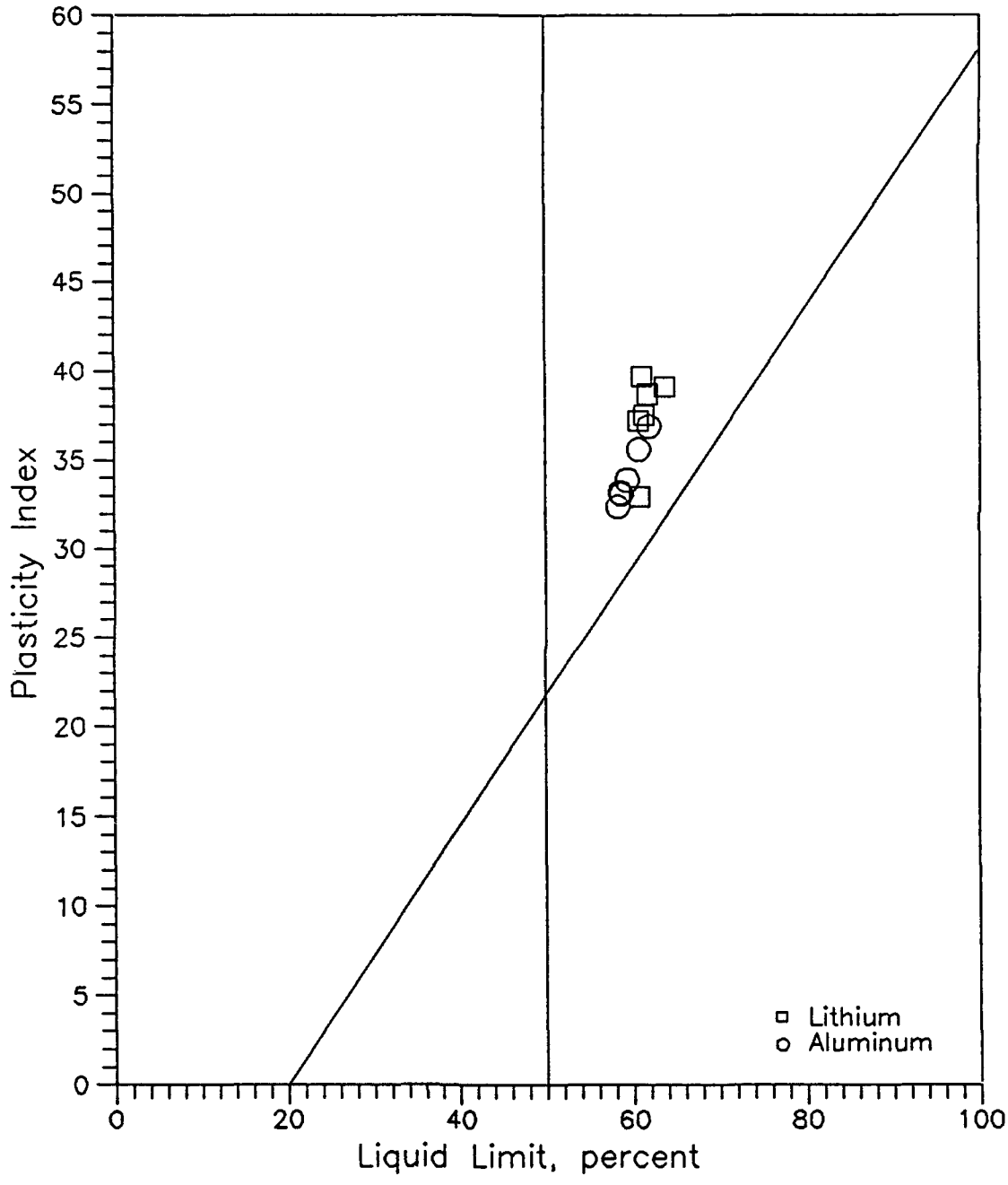

Figure 4.3 Plasticity Characteristics of the Soil Stock with the Exchange Complex Saturated with Lithium and Aluminum

chloride solution. After each wash, the clear supernatant was collected into a 250ml flask. After the last wash, the flask was filled to the 250 ml mask with the stock calcium chloride solution. Samples of the collected wash, the 1N, and the 0.01N potassium chloride solutions were subjected to determinations of the potassium concentration. The potassium concentration of the collected supernatant times the volume of the flask (250 ml) provides the total potassium present. The actual potassium on the exchange complex is the total potassium minus the potassium present in the 250 ml of 1N calcium chloride solution and the potassium present in the interstitial water of the filter cake formed after the last wash with the 0.01N potassium chloride solution.

Three specimens of soil stock were subject to this determination and the calculated cation exchange capacities are included in Table 4.4.

Table 4.4
Cation Exchange Capacity Measurements

Test No.	Capacity (Meg/100 grams)
1	47.54
2	52.22
3	46.29
Average: 48.68	

4.6 CLAY MINERAL IDENTIFICATION

Approximately 0.5 grams of soil that did not contain carbonates or organic matter and passing the number 200 sieve was placed into two test tubes. Four

different sets of samples were prepared. The soil was washed with sodium carbonate solution as a dispersant. The soil suspension was then centrifuged at 2000 rpm for 3 minutes, and the supernatant was collected. This procedure was repeated until the supernatant was clear. The supernatant collected included the clay size fraction. The soil remaining in the centrifuge tubes consisted of silt size particles. After this first separation was completed, the clay was dispersed with sodium carbonate solution and centrifuged at 2500 rpm for 15 minutes. The supernatant collected contained the fine clay (particles smaller than 0.2 microns) and the remaining clay in the tubes contained the coarse clay (particles between 2.0 and 0.2 microns). The two clay fractions and silt were then washed with distilled water and dialyzed with cellulose membranes in a distilled water bath.

The fine and coarse clay samples of each specimen were split into two parts. One part of the fine clay was saturated with a potassium chloride solution and the other portion was saturated with a magnesium chloride solution. The saturation process consisted of adding the solution, dispersing with a vortex mixer, centrifuging for 15 minutes at 3000 rpm, and decanting the clear supernatant. This procedure was repeated for the coarse clay fraction. Slides were prepared with the fine clay saturated with potassium chloride, fine clay saturated with magnesium chloride, coarse clay saturated with potassium chloride, coarse clay saturated with magnesium chloride and the clean silt specimens. The slides were air-dried and labeled. A 10% solution of glycerol was prepared and a drop of this solution was placed on the slides containing magnesium saturated clays.

Finally the slides were x-rayed at room temperature and peaks recorded. In addition, the slides containing the potassium chloride clays were heated to 300^0 C and x-rayed. Following this procedure, the slides were heated again to 600^0 C and x-rayed.

The x-ray diffraction patterns recorded for both clay fractions of all the specimen x-rayed have been assembled into Appendix F. For each group of patterns, the diagnostic peaks used to identify the minerals are indicated together with the coversponding d-spacings in Amstrongs. The patterns for all the specimens indicate consistent results. In this sense, minerals positively identified include the following:

1) KAOLINITE

   This clay is identified by x-ray peaks at 7.25Å and 3.60Å with all treatments and the disappearance of these peaks when the slide are heated beyond 550^0 C.

2) CHLORITE

   This mineral is identified by x-ray peaks at approximately 14Å with all treatments. Specifically if this peak does not disappear when the slide is heated to 550^0 C. This is precisely the case in almost all the x-ray patterns presented in Appendix F.

3) QUARTZ

   This mineral is unaquivocally identified by the x-ray peaks at 3.33Å and 4.27Å and the stability of these peaks against all the treatments

used on the slides.

4) MICAS

The presence of micas is indicated by peaks at 10Å under the Mg plus glycerol solvation treatment.

5) SMECITES

The presence of this mineral is not clearly indicated by the x-ray patterns recorded. Nevertheless, it appears that some smecites might be present for several reasons. The first reason is that some slides show broad peaks at about 19Å in the Mg slide. The second reason is the reinforced intensity experienced by the 10Å as the k slide is gradually heated to higher temperatures.

The third reason is related to the cation exchange capacities measured. Kaolinites typically have capacities of 5 meg/100gr and chlorites have capacities of 10 to 40 meg/100gr while quatz and mica have no exchange capacity. Since the average exchange capacity measured is near 48 meg/100gr, the minerals listed above cannot explain this capacity. Smecites have capacities of 105 meg/100gr, thus, even small amounts of this mineral could boost the overall exchange capacity to the measured values.

In summary, the x-ray analysis and the cation exchange capacity indicate that the minerals making up the soil-stock are: kaolinites, chlorites, micas, quartz, and to some extent smectite.

4.7 WATER CONTENTS OF THE SPECIMENS

Water content determinations were performed on the specimens before starting the equilibration phase and after completing the creep or the dynamic tests. The complete set of water contents together with soil suction levels imposed on the specimens are presented in Table 4.5.

For most specimen, the water contents before the equilibration phase are between 28% and 32%, with an average value of 29.94%. The histogram of water contents before the equilibration phase is shown in Figure 4.4. These results indicate that for more than 50% of the cases, the water content falls in the very narrow range from 29.5% to 30.5%. Thus the variability of the specimens after consolidation appears to be quite small.

The water contents of the specimens after testing have been plotted as a function of the soil suction imposed during the equilibration phase and are shown in Figure 4.5. The average water content for each suction levels seems to suggest a linear relationship between water content and soil suction. These results seem to indicate a lower variability of the water content after testing.

Table 4.5
Specimen Conditions Before & After Tests

Specimen	Water Content Before Tests,%	Water Content After Tests,%	Soil Suction psi
1	28.98	30.10	14
2	27.89	30.07	14
3	25.08	27.30	14
4	27.15	30.21	14
5	24.70	27.32	14
6	27.66	28.09	15
7	27.96	29.36	15
8	30.39	30.24	15
9	29.33	27.64	40
10	30.22	28.64	40
11	30.54	25.78	70
12	31.20	28.20	70
13	31.12	28.32	40
14	30.48	28.07	40
15	31.18	24.42	70
16	29.91	28.13	40
17	30.17	28.35	40
18	29.58	23.34	70
19	32.36	23.34	70
20	32.26	31.30	15
21	29.86	30.15	15
22	28.41	25.10	70
23	30.26	30.26	15

Table 4.5 (continued)
Specimen Conditions Before & After Tests

Specimen	Water Content Before Tests,%	Water Content After Tests,%	Soil Suction psi
24	29.78	30.32	15
25	31.18	30.00	15
26	28.52	28.51	40
27	29.62	29.32	70
28	31.02	25.02	70
29	30.70	30.65	15
30	29.53	31.13	15
31	29.21	25.80	70
32	30.99	31.32	15
33	30.24	31.11	15
34	30.16	24.95	70
35	30.21	25.39	70
36	29.74	28.03	40
37	29.71	28.00	40
38	30.32	27.80	40
39	28.65	28.01	40
40	30.61	24.10	70
41	30.72	28.07	40
42	30.82	30.53	15
43	31.25	28.18	40
44	29.28	28.10	40
45	30.23	27.98	40
46	32.10	28.05	40

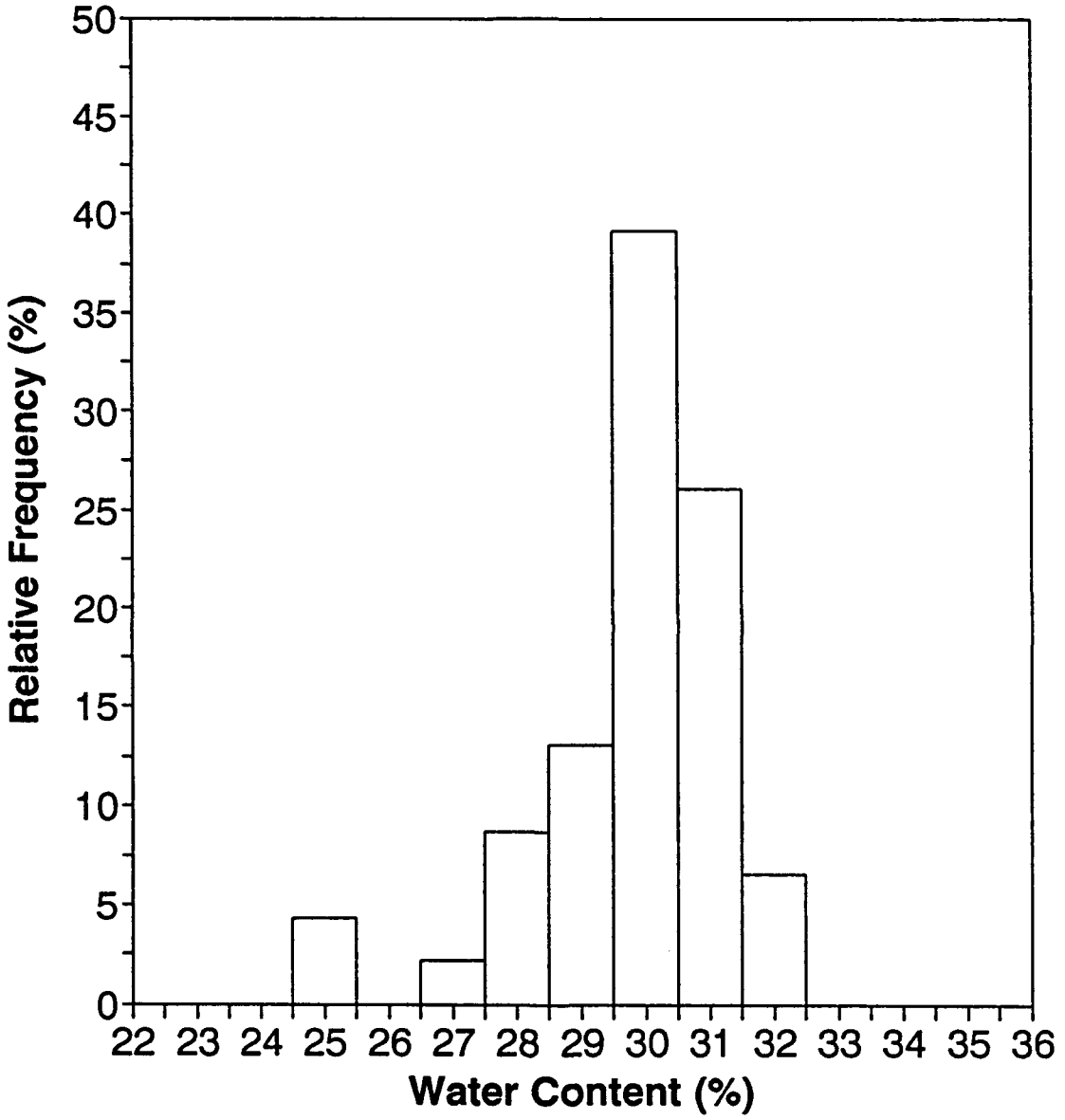

Figure 4.4 Distribution of Water Contents of the Specimens Before the Equilibration Phase

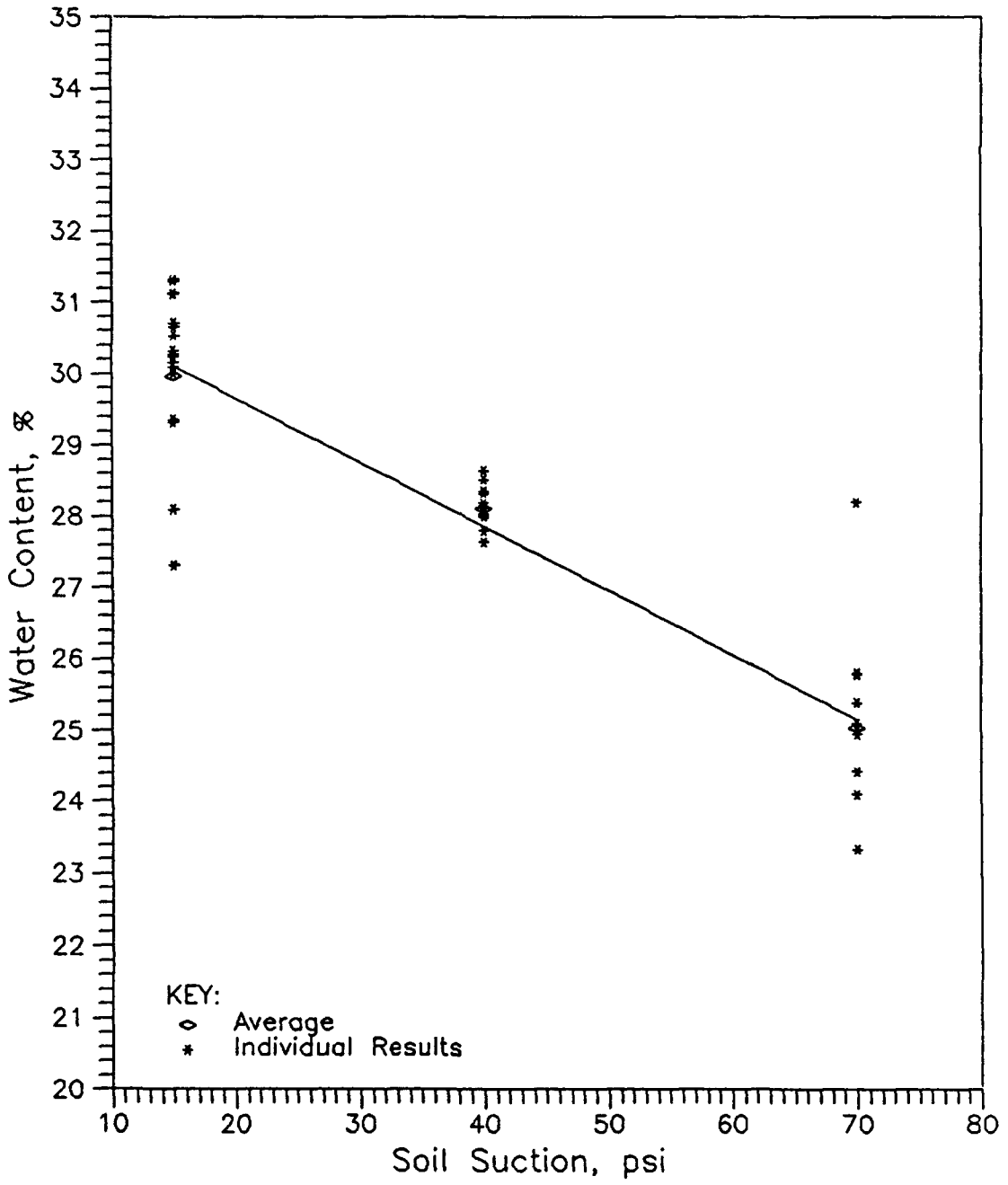

Figure 4.5 Water Content of the Specimens after Testing

CHAPTER FIVE

SELECTION OF CREEP AND RECOVERY MODELS

5.1 INTRODUCTION

The results of creep/recovery tests performed and presented earlier in Chapter Three have been used to select potential viscoelastic models that could explain the observed behavior.

The test program was designed to illustrate the effects that the deviatoric stress and the soil suction level had on the creep/recovery of the specimen. To illustrate these effects representative creep/recovery records for different deviatoric stress and soil suction levels have been plotted in Figures 5.1, 5.2, and 5.3. These results are used to define the dependence of the model parameters on soil suction and deviatoric stress levels.

The simple analytical functions fitted to the observed variation of model parameters are then also used to predict the creep/recovery phases for the conditions of the test specimens to afford a qualitative description of goodness of fit of the models assembled.

Three basic models have been tried consisting of one linear viscoelastic model based on Burgers model and two non-linear viscoelastic models based on power and exponential laws.

5.2 FOUR-PARAMETER EXPONENTIAL MODEL

5.2.1 Proposed Model

The strain-time data illustrated in Figures 5.1, 5.2, and 5.3 indicate that a large portions of strain occurred very fast and was followed by a time-dependent deformation. The strain rate varied continuously through the period of sustained load and approached a steady strain rate. Under the applied deviatoric stress, the creep deformations continued more or less indefinitely. This strain-time relationship may be expressed by a four-parameter exponential function of the following form:

$$\epsilon = A+Bt+C(1-e^{-Dt}) \qquad (5.1)$$

where

ϵ = axial creep strain,

t = elapsed time,

A, B, C = parameters which in the Burgers Model are linear functions of the applied deviatoric stress, and

D = a material parameter

Equation (5.1) can be rearranged to the following form:

$$\epsilon = Bt+(A+C)\left(1-\frac{C}{A+C}e^{-Dt}\right) \qquad (5.2)$$

Defining $P_1=A+C$ and $P_2=C/(A+C)$ and substituting Equation (5.2) can be

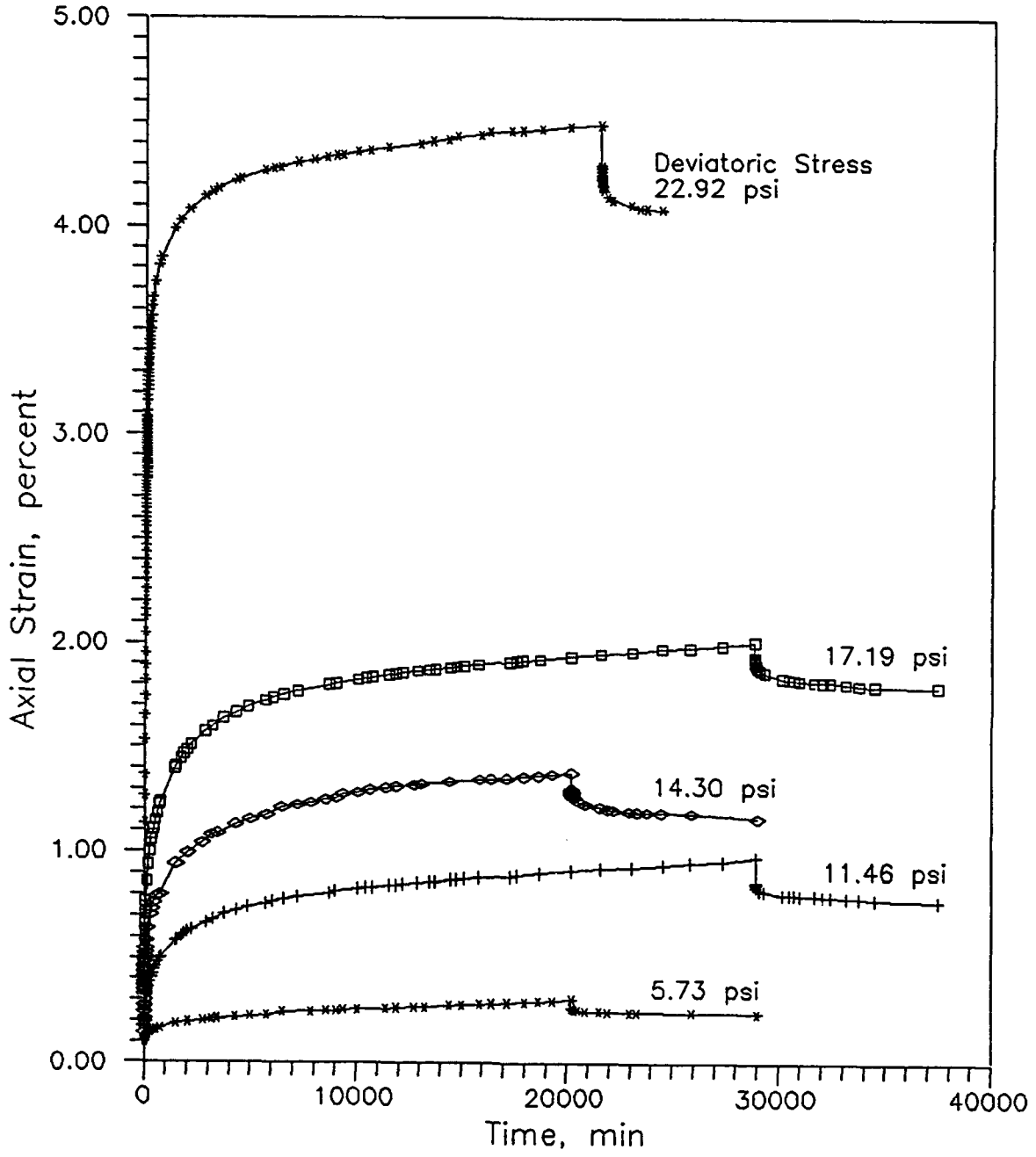

Figure 5.1 Creep/Recovery Tests on Specimens Equilibrated at 15 psi Soil Suction

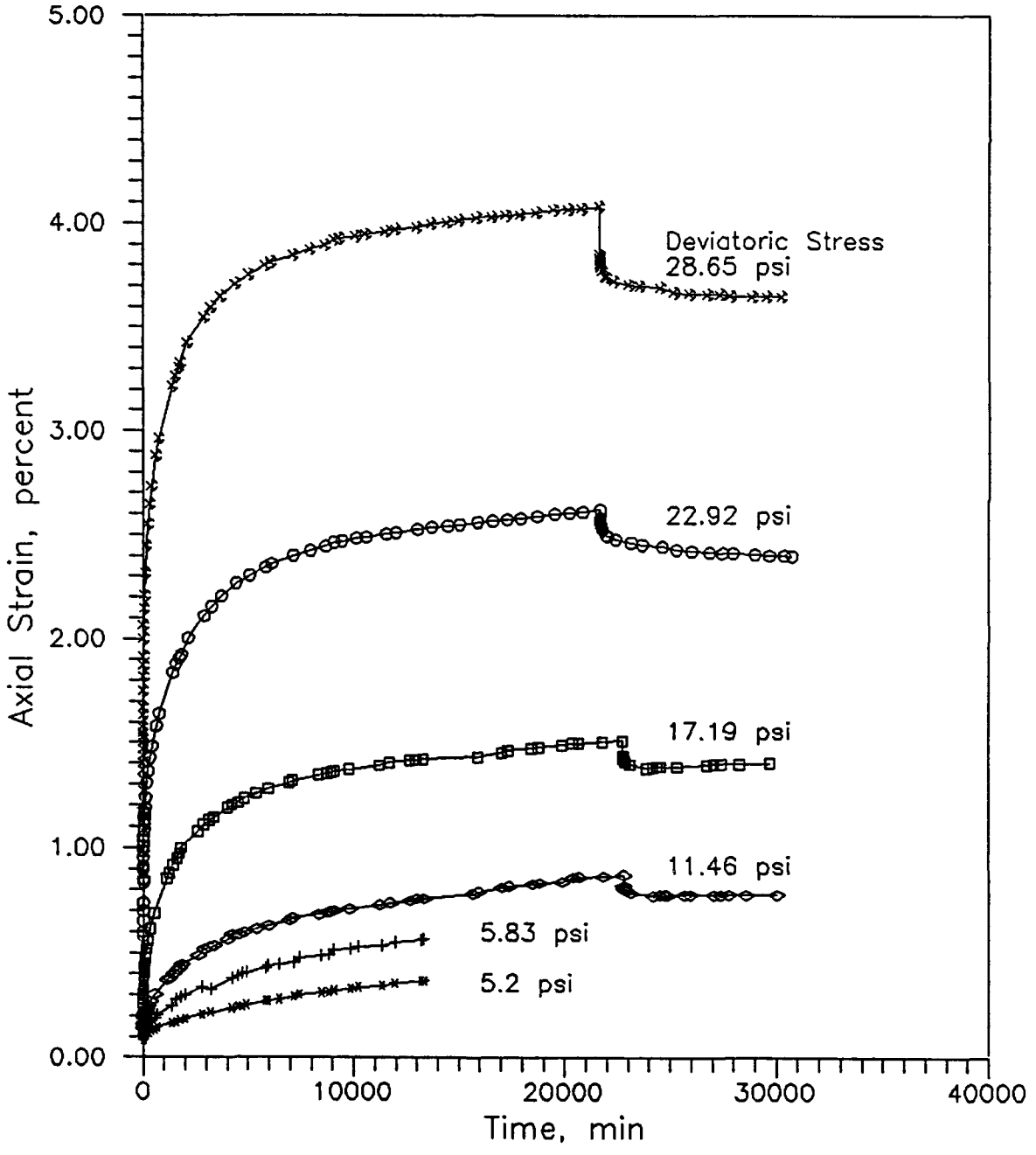

Figure 5.2 Creep/Recovery Tests on Specimens Equilibrated at 40 psi Soil Suction

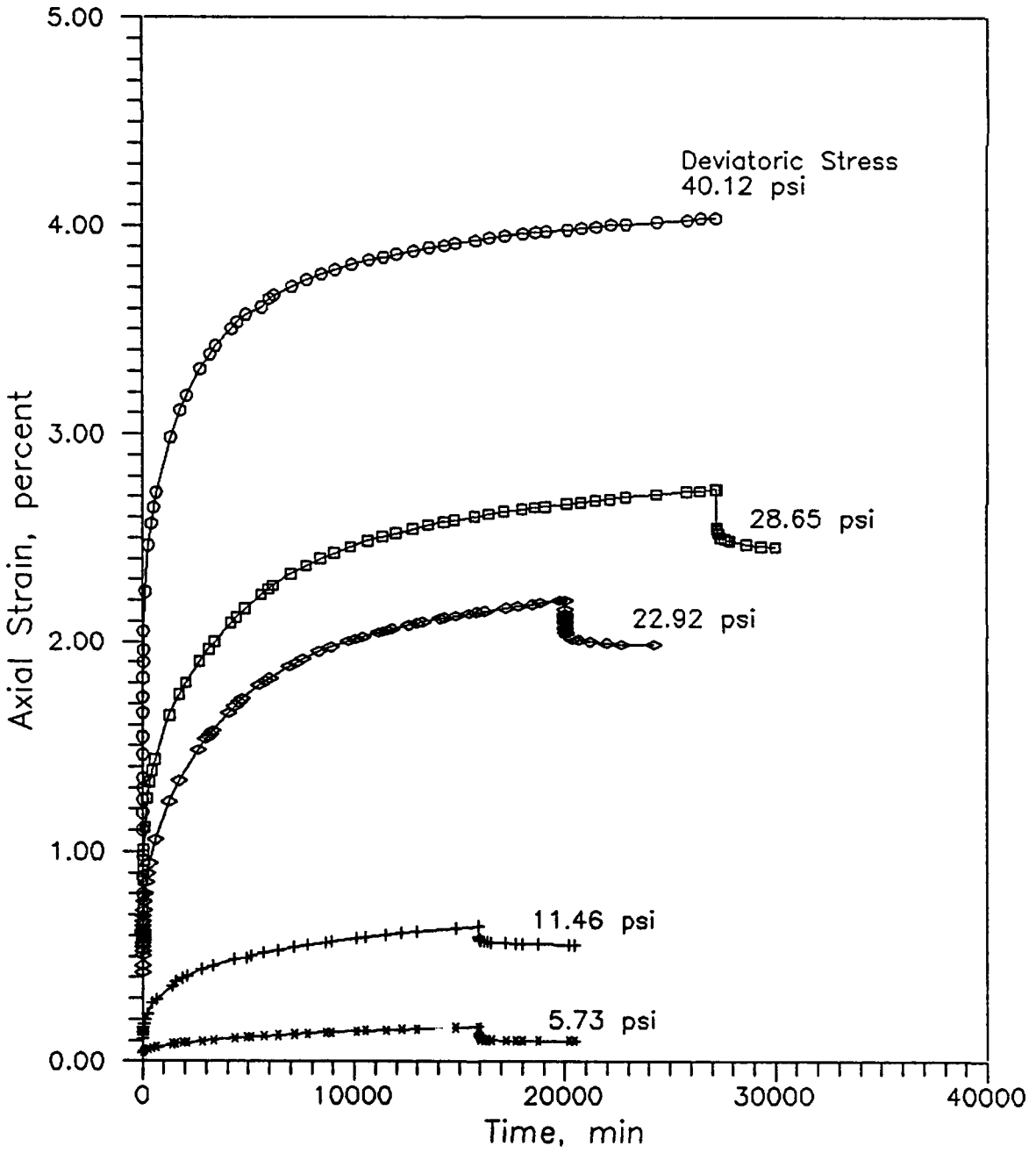

Figure 5.3 Creep/Recovery Tests on Specimens Equilibrated at 70 psi Soil Suction

rewritten as follows:

$$\epsilon = Bt + P_1(1 - P_2 e^{-Dt}) \qquad (5.3)$$

for large times, Equation 5.3 approaches an asymptote $\epsilon_a = Bt + P_1$. The values of the parameters B and P_1 can be obtained from the slope and intercept of the asymptote. Therefore, these parameters can be obtained from the steady creep phase by measuring the slope and intercept of the straight line fitted to these data.

The values of the parameters D and P_2 can be determined from the transient creep stage data using the following linear regression method. First, Equation (5.3) is reorganized as follows:

$$\frac{P_1 + Bt - \epsilon}{P_1} = P_2 e^{-Dt} \qquad (5.4)$$

Taking natural logarithm of both sides, yields:

$$\ln \frac{P_1 + Bt - \epsilon}{P_1} = -Dt + \ln P_2 \qquad (5.5)$$

For each transient creep data points the two variables $\ln[(P_1 + Bt_i - \epsilon_i)/P_1]$ and t_i are calculated. The parameter D and P_2 can then be evaluated by the linear regression method.

This approach has been used for all the creep tests and the calculated

model parameters: A, B, C, and D are listed in Table 5.1 in correspondence with the test conditions.

The effects of soil suction and deviatoric stress on the model parameters is evident in the results shown in Table 5.1. The relationships of parameter A with deviatoric stress for each suction level is presented in graphical form in Figure 5.4. The results shown in this figure do not support the linear variation of A with deviatoric stress that the Burgers model would require, thus, indicating that the linear viscoelastic model is not appropriate. This fact requires the use of the four parameter exponential model that is a non-linear viscoelastic model. The relationship between the parameter A and the deviatoric stress (σ_d) can be better modeled with the following exponential relationship:

$$A = a_1 e^{a_2 \sigma_d} \qquad (5.6)$$

where a_1 and a_2 are functions of the soil suction level. The identified values of a_1 and a_2 using regression analysis for the three soil suction levels are listed in Table 5.2.

Table 5.2
Values of Parameters a_1 and a_2 for Different Soil Suction Levels

Soil Suction, psi	Constant a_1	Constant a_2
15	0.035451	0.1827
40	0.044853	0.1311
70	0.041863	0.1001

Table 5.1
Regression Values of Parameters A, B, C, and D
and the Corresponding Test Conditions

Specimen No.	Deviatoric Stress, psi	A in/in,%	B 1/min	C in/in,%	D 1/min
Soil Suction 15 psi					
30	5.73	0.1152	5.39×10^{-6}	0.0826	8.08×10^{-4}
20	11.46	0.2807	7.66×10^{-6}	0.4750	4.76×10^{-4}
29	14.30	0.4341	1.13×10^{-5}	0.7295	5.20×10^{-4}
21	17.19	0.6856	1.20×10^{-5}	1.0052	6.72×10^{-4}
23	22.92	2.8063	1.68×10^{-5}	1.3641	1.27×10^{-4}
24	28.65	-	-	-	-
Soil Suction 40 psi					
9	5.2	0.0911	1.11×10^{-5}	0.1295	4.13×10^{-4}
10	5.83	0.1117	1.18×10^{-5}	0.2968	3.59×10^{-4}
13	11.46	0.1984	1.26×10^{-5}	0.3974	3.89×10^{-4}
14	17.19	0.3882	1.28×10^{-5}	0.8472	5.62×10^{-4}
16	22.92	1.0273	1.38×10^{-5}	1.3063	5.26×10^{-4}
17	28.65	1.8376	1.55×10^{-5}	1.9286	6.69×10^{-4}
Soil Suction 70 psi					
11	5.73	0.0486	3.94×10^{-6}	0.0555	4.00×10^{-4}
12	11.46	0.1690	1.14×10^{-5}	0.3002	5.27×10^{-4}
15	22.92	0.5674	1.35×10^{-5}	1.3645	3.54×10^{-4}
19	28.65	0.9655	1.49×10^{-5}	1.3883	3.43×10^{-4}
18	40.12	1.6870	1.88×10^{-5}	1.9091	5.86×10^{-4}

$$e(t) = A + Bt + C(1 - e^{-Dt})$$

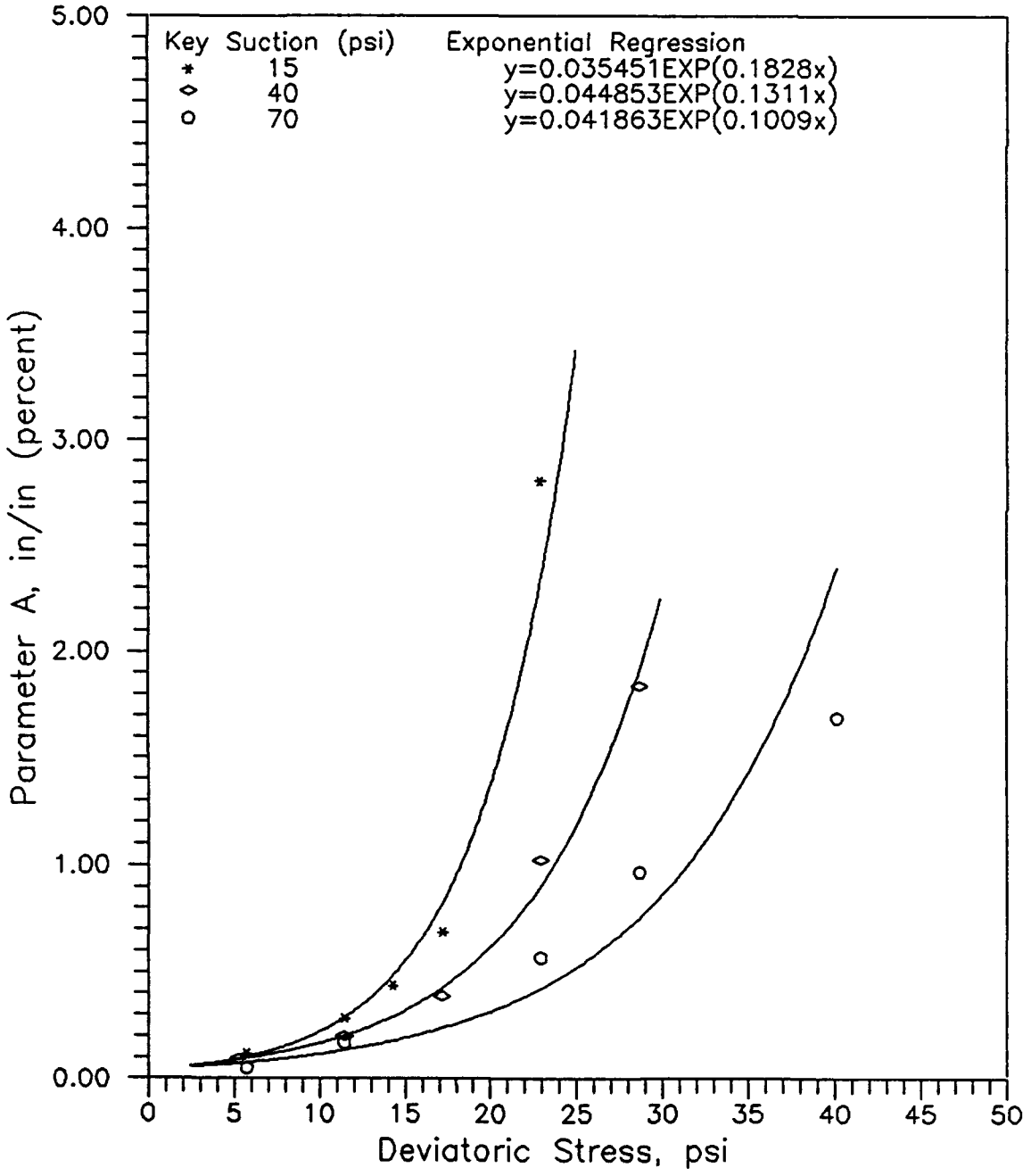

Figure 5.4 **Relationship between Parameter A and Deviatoric Stress for Three Soil Suction Levels**

It is felt that not enough suction levels have been tested to permit a reasonable definition of the variability of the parameter A with suction. This function is not critical in the present study because the dynamic tests are performed at constant suction levels.

The dependence of parameter B on the deviatoric stress level (σ_d) is shown in graphical form in Figure 5.5. The results for a suction level of 40 psi are unexplainably different from the trends indicated at the other two levels. It has been considered that parameter B_1 depends on the applied deviatoric stress in a power law fashion as indicated by the following relationship:

$$B = b_1 \sigma_d^{b_2} \qquad (5.7)$$

where b_1 and b_2 are functions of soil suction. The values selected from regression analysis are presented in Table 5.3.

Table 5.3
Values of Parameters for Different Soil Suction Levels

Soil Suction, psi	b_1	b_2
15	1.21×10^{-6}	0.8183
40	8.21×10^{-6}	0.1734
70	1.35×10^{-6}	0.7328

These results again suggest the need to perform tests at other soil suction levels to allow some more insight on the shape or type of variability of these parameters on the soil suction level.

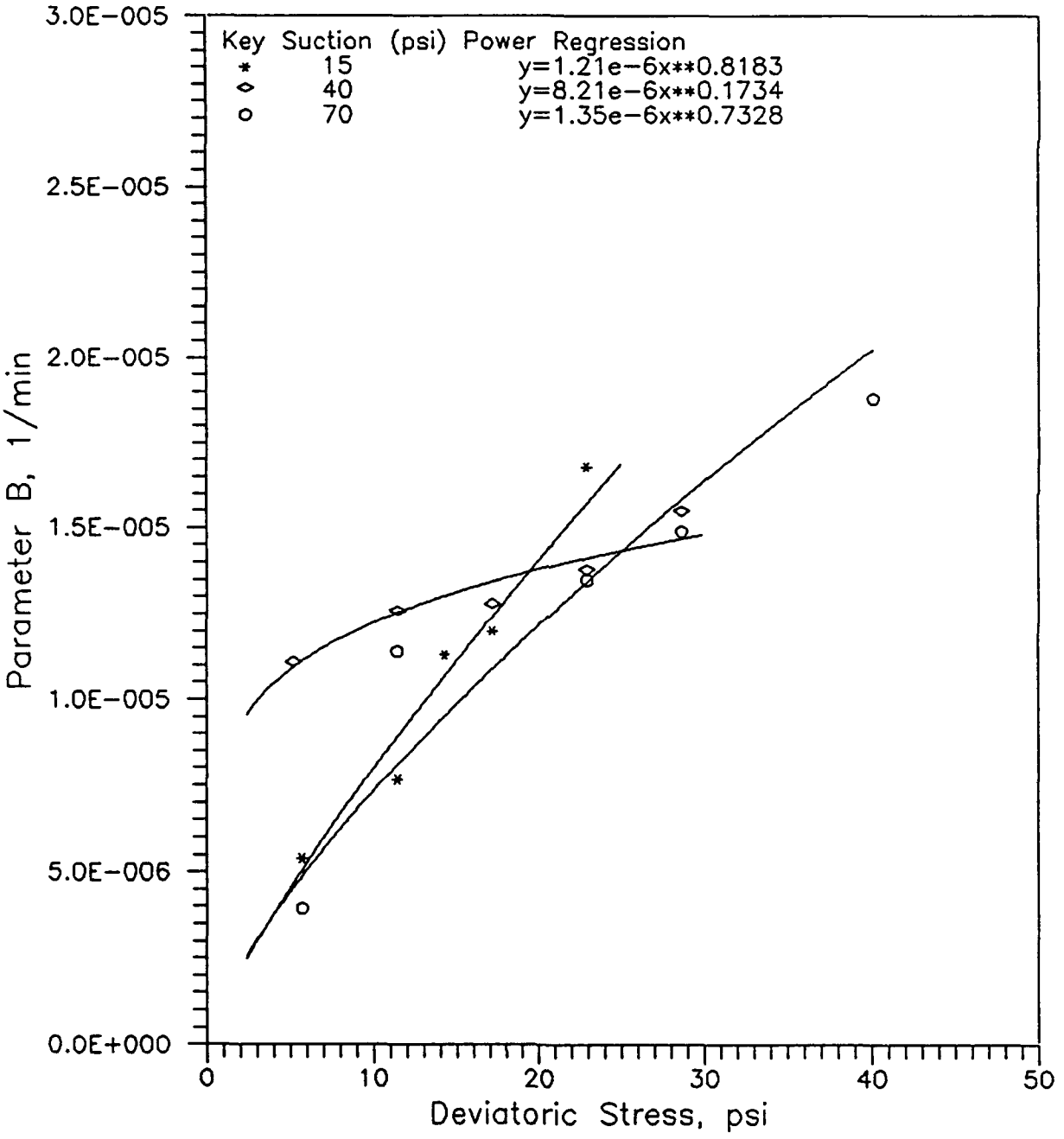

Figure 5.5 **Relationship between Parameter B and Deviatoric Stress for Three Soil Suction Levels**

The variation of parameter C with the deviatoric stress level is presented in Figure 5.6. The observed variability can be best expressed analytically with a power law of the deviatoric stress as follows:

$$C = c_1 \sigma_d^{c_2} \qquad (5.8)$$

where c_1 and c_2 are functions of soil suction. The values of c_1 and c_2 are summarized in Table 5.4.

Table 5.4
Values of Parameters c_1 and c_2 for Different soil Suction Levels

Soil Suction, psi	c_1	c_2
15	2.51×10^{-3}	2.0826
40	9.02×10^{-3}	1.5899
70	2.64×10^{-3}	1.8710

As for the values of B, these results indicate some discrepancy between the specimens equilibrated at 40 psi and the specimens at 15 psi and 70 psi. Further testing would be required to check the validity of the 40 psi results or to define with more certainty the form of the dependence of these parameters on soil suction.

The parameter D is a material constant, independent of the applied stress and soil suction levels. As indicated in Table 5.1, the value of D ranges from 1.2×10^{-4} 1/min. to 8.1×10^{-4} 1/min. However, for the majority of the creep tests, D is within 3.5×10^{-4} 1/min.to 6.5×10^{-4} 1/min. The average value for all the tests performed is 4.80×10^{-4} 1/min.

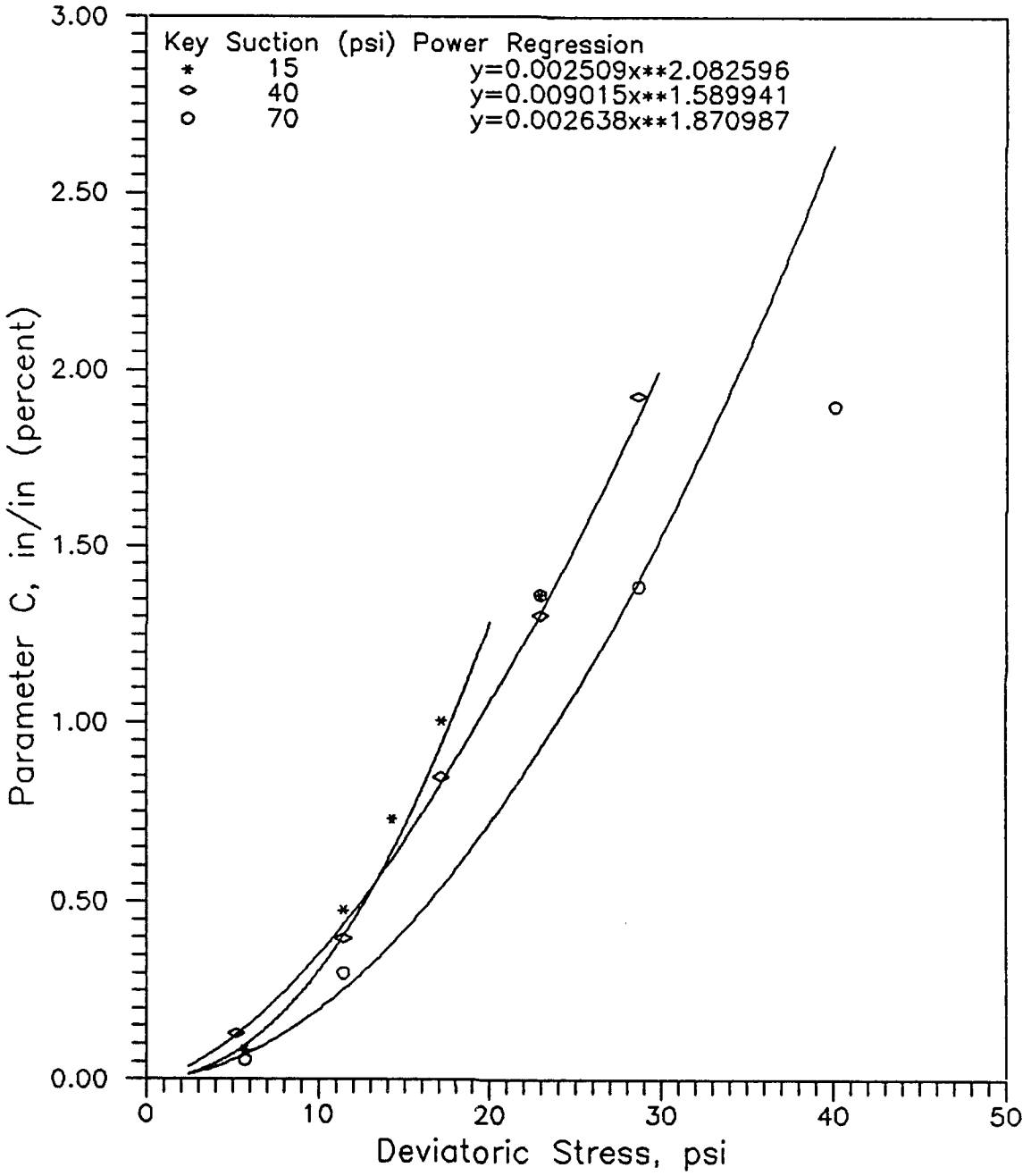

Figure 5.6 **Relationship between Parameter C and the Deviatoric Stress for Three Soil Suction Levels**

This parameter has been considered constant and set a the average value.

In summary, the four-parameter exponential model results in the following stress time relationship during creep:

$$\varepsilon = a_1 e^{a_2 \sigma_d} + b_1 \sigma_d^{b_2} t + c_1 \sigma_d^{c_2} (1 - e^{-Dt}) \qquad (5.9)$$

with the values indicated in Table 5.5 for all the model parameters.

Table 5.5
Parameters Selected for the Four-Parameter Exponential Model

Soil Suction psi	a_1	a_2	b_1	b_2	c_1	c_2
15	0.0355	0.1828	1.21×10^{-6}	0.8183	2.51×10^{-3}	2.0826
40	0.0445	0.1311	8.21×10^{-6}	0.1734	9.02×10^{-3}	1.5899
70	0.0299	0.1255	1.35×10^{-6}	0.7328	2.64×10^{-3}	1.8726
$D = 4.80 \times 10^{-4}$						

5.2.2 Capabilities of the Proposed Model

To illustrate the abilities of the model indicated by equation (5.9) with the parameters listed in Table 5.5, the predictions of the model are compared with the actual creep test results. The complete set of results is presented in Appendix G. From this comparison it is evident that the capabilities of the method are much better in the steady state creep phase than in the initial part of the transient creep phase.

Since the purpose of the test is to develop viscoelastic models that could

be applied to very fast rates of loading, it seems imperative that the initial transient creep phase is the critical portion of the creep curve that should be closely approximated by the viscoelastic model. Based on this consideration, this four-parameter model was not considered appropriate to predict the dynamic soil behavior. The need thus arose to select alternative models based on simple exponential or power laws.

5.3 INITIAL POWER LAW

5.3.1 Proposed Model

As indicated previously, the four-parameter exponential model yields a nice fit to the testing data at relatively large times. But it lost some accuracy at very early time, especially within the initial 60 minutes. This phenomena may be due to the drainage conditions during the creep test at large times. To improve the approximation of the model to the initial part (first sixty minutes) of the creep phase, the following power law model was fitted to the laboratory data:

$$\epsilon(t) = \alpha t^{\beta} \qquad (5.10)$$

where

ϵ = initial creep strain, percent

t = elapsed time, min.

α, β = functions of the deviatoric stress and soil suction

The power law fits the experimental data in a better fashion than the previously tried model. To illustrate this effect, the initial creep curves at 70psi suction level are plotted in Figure 5.7. This figure shows the linear trend is clearly seen in the data. But contrary to other materials the exponent of the power is found to be a function of the deviatoric stress level.

Taking natural logarithms of Equation (5.10) yields the following:

$$\ln[\epsilon(t)] = \beta \ln t + \alpha \qquad (5.11)$$

The values of $\ln[\epsilon(t)]$ and $\ln(t)$ can be calculated from the results of the creep tests during the first 60 minutes. Thus, the values of parameters, α and β can be obtained from linear regression analysis. The values of parameters α and β for all the tests performed are presented in Table 5.6. These results indicate that the values of α increase with the applied deviatoric stress. The form of this dependence is shown in Figures 5.8 and 5.9. In Figure 5.8 the parameter α has been fitted with a power law of the deviatoric stress of the following form:

$$\alpha = \alpha_1 \sigma_d^{\alpha_2} \qquad (5.12)$$

In Figure 5.9 the values of parameter α have been fitted with an exponential law of the following form:

$$\alpha = \alpha_1 e^{\alpha_2 \sigma_d} \qquad (5.13)$$

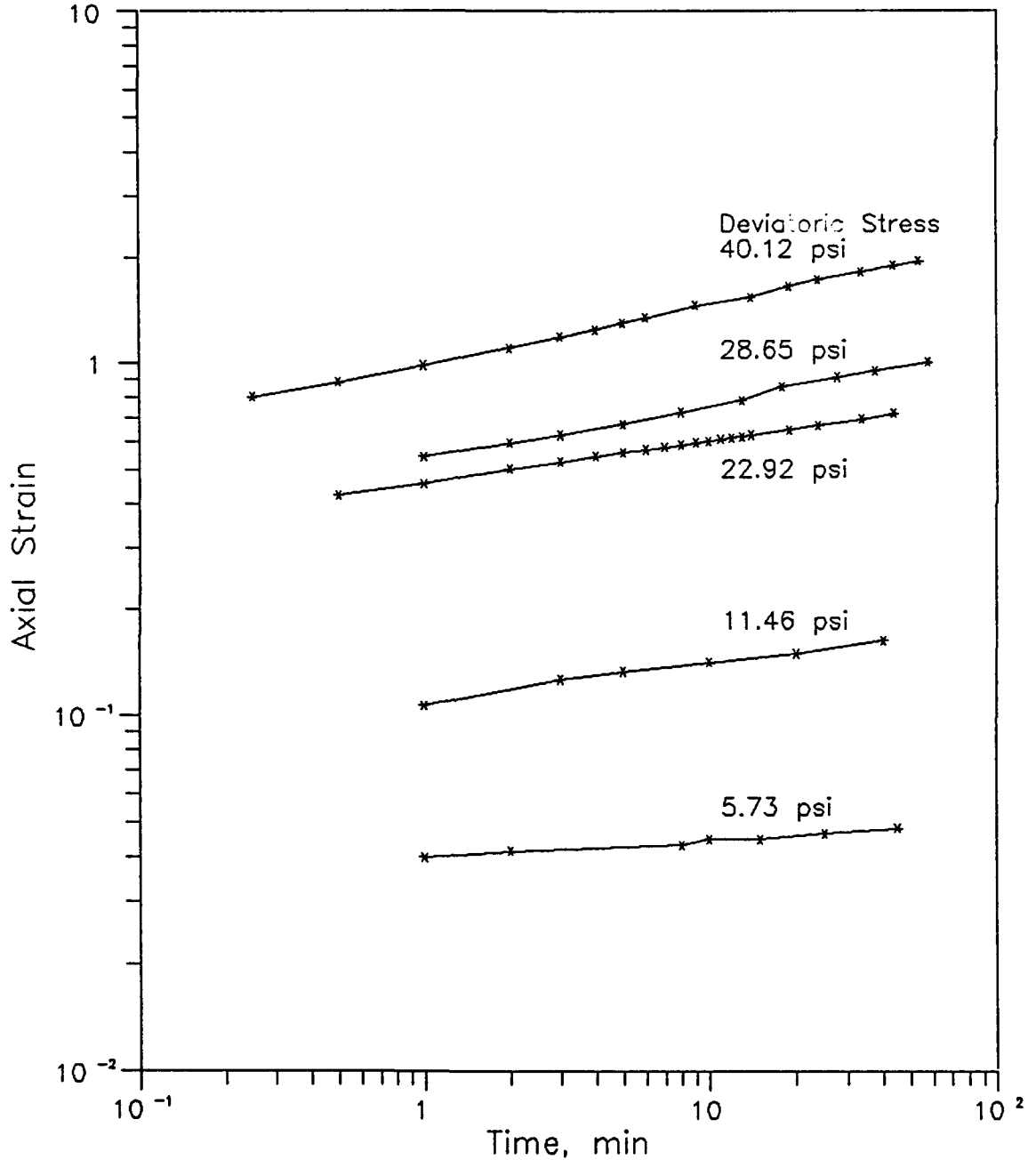

Figure 5.7 Initial Creep Phase for the Specimens Equilibrated at 70 psi

Table 5.6
Values of Parameters α and β with the Corresponding Test Conditions

Specimen No.	Deviatoric Stress, psi	α	β
Soil Suction 15 psi			
30	5.73	0.0989	0.0486
20	11.46	0.1714	0.1103
29	14.30	0.2038	0.2462
21	17.19	0.4119	0.1457
23	22.92	1.1854	0.1803
24	28.65	6.3960	0.1803
Soil Suction 40 psi			
9	5.2	0.0876	0.0361
36	5.73	0.0876	0.1664
10	5.83	0.1043	0.0355
13	11.46	0.1404	0.0965
14	17.19	0.2738	0.1117
16	22.92	0.6584	0.1314
17	28.65	0.9098	0.1806
Soil Suction 70 psi			
11	5.73	0.0400	0.0475
12	11.46	0.1095	0.1098
15	22.92	0.4607	0.1179
19	28.65	0.5324	0.1581
18	40.12	0.9920	0.1709

$e(t) = \alpha t^{\beta}$

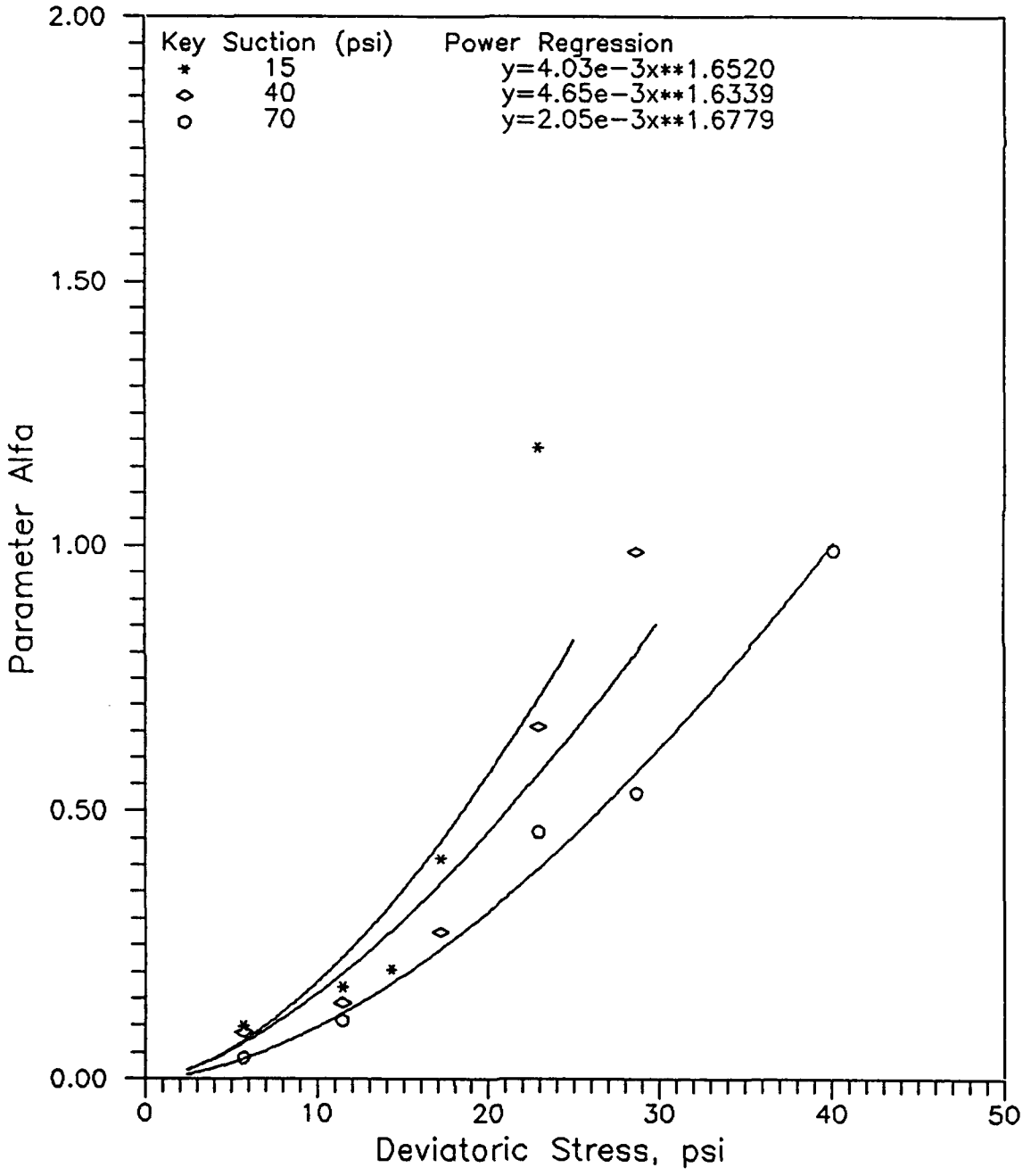

Figure 5.8 **Power Relationship between Parameter α and the Deviatoric Stress for Three Soil Suction Levels**

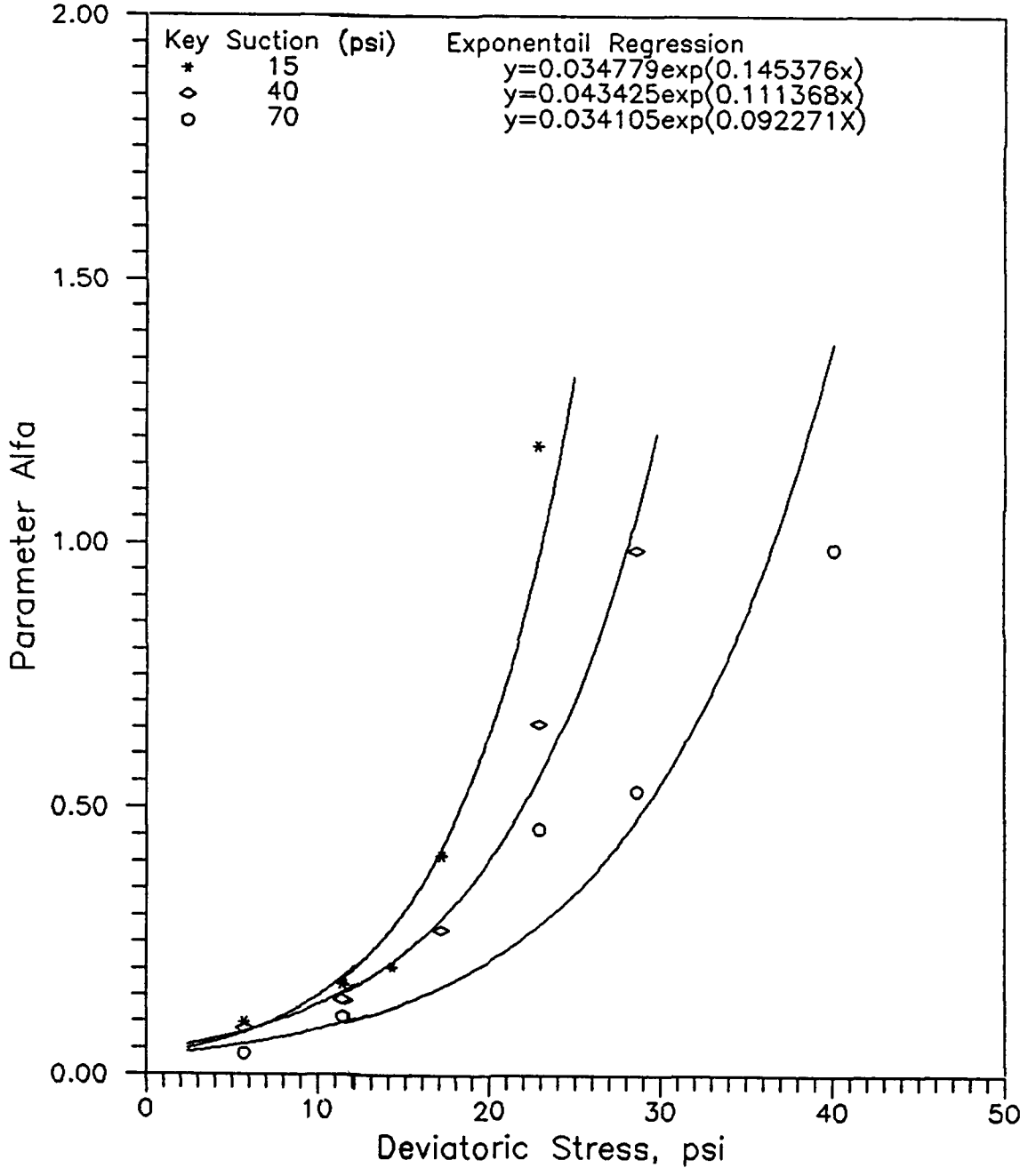

Figure 5.9 Exponential Relationship between Parameter α and the Deviatoric Stress for Three Soil Suction Levels

The values of α_1 and α_2 obtained from regression analysis for the three suction levels are summarized in Table 5.7.

Table 5.7
Values of Parameters α_1 and α_2 for Different Soil Suction Levels

Soil Suction psi	α_1		α_2	
	Power	Exponential	Power	Exponential
15	4.034×10^{-3}	0.03478	1.6520	0.1454
40	4.659×10^{-3}	0.04325	1.6339	0.1114
70	2.051×10^{-3}	0.03411	1.6779	0.0923

From a comparison of Figure 5.8 and 5.9, it is evident that the power law fits best the change of α with deviatoric stress for some suction level. However, for other suction levels the exponential provides a better fit.

The results of the parameter β shown in Table 5.6 do indicate that the parameter β is independent of soil suction and only depends on deviatoric stress. The average values of parameter β at each deviatoric stress level are presented in Table 5.8.

Table 5.8
Variation of Average Values of Parameter β

Deviatoric Stress psi	Average β Value	Deviatoric Stress psi	Average β Value
7.73	0.0411	22.92	0.1686
11.46	0.1055	28.65	0.1612
17.19	0.1287	40.12	0.2350

This variation of the average value of parameter β with deviatoric stress is illustrated in Figure 5.10.

Since the values calculated for the parameter β range in a fairly narrow range, it was decided to approximated the relationship with the following linear regression:

$$\beta = 0.003623\sigma_d + 0.055131 \qquad (5.14)$$

In summary, two proposed models, one a power law and the other an exponential function, were fitted to the creep data of the initial 60 minutes. These models are represented by the following analytical expressions:

$$\epsilon_I(t) = \alpha_1 \sigma_d^{\alpha_2} t^{(0.003623\sigma_d + 0.055131)} \qquad (5.15)$$

The values of the parameters α_1 and α_2 for each model are summarized in Table 5.7.

5.3.2 Evaluation of Model Capacities

Although the power law fits exceedingly well the initial creep curve, the adequacy of the power law and exponential function of the deviatoric stress has been evaluated by predicting the creep for the actual test conditions used in the laboratory program. The comparison of the creep curve measured in the lab and the predictions with the two models described above are shown in Appendix H.

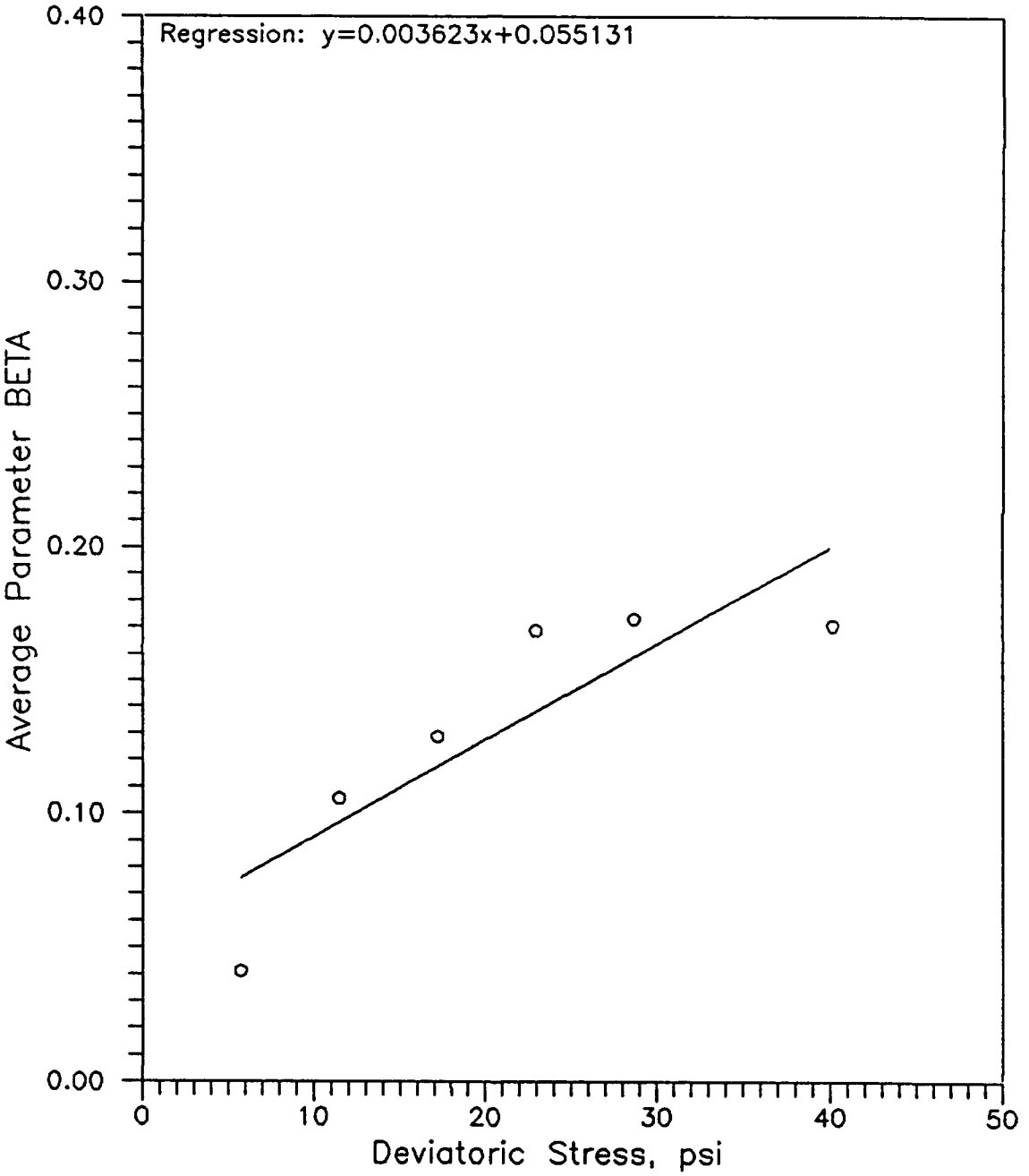

Figure 5.10 Variation of Parameter β with the Deviatoric Stress Level

From the comparison it is evident that the shapes of the predicted curves are very close to the shapes of measured creep curves. Nevertheless, in some cases there is a clear shift of one or both predictions relative to the test data. These shifts are due to inadequacies of the stress function filled to the data. In order to improve the stress function in explaining the variation of creep with deviatoric stress it would be necessary to increase the data base, specifically repetitions at already tested stress levels to check whether the results already obtained contain a large testing errors.

These problems can be traced back to the results shown in Figure 5.8 and 5.9. Since in these figures it was not possible to fit all the data points with a single model. In fact, the power law of stress was best in some case and the exponential functions of the stress was best in another case. Despite of this problem it is felt that the power of time is definitely the model to fit the measured creep data. This non-linear viscoelastic model has been used later in this report to model the loading phase of the dynamic tests.

5.4 RECOVERY POWER LAW

5.4.1 Proposed Model

For the purpose of the analysis, the test data recorded during the recovery phase was transformed by changing the strain and time origin. In this sense, the time zero was set at the beginning of the unloading and the strain at this time was set to zero. Thus the strains experienced during the recovery become negative.

A power law of time fits exceedingly well the experimental data. To illustrate this effect, the recovery curve at 70psi soil suction are shown in Figure 5.11. This figure clearly indicates the linear trend of the transformed data.

The strains experienced during the recovery phase of the tests have been fitted with the following power law of time:

$$\epsilon_R(t) = -\alpha_R t^{\beta_R} \tag{5.16}$$

where

$\epsilon_R(t)$ = recovery strain, percent, that occurs from the time of unloading,

t = elapsed time, min, from the time of unloading,

α_R = parameter,

β_R = parameter,

By taking logarithms of both sides of Equation (5.16), the following relationship is obtained:

$$\ln|\epsilon_R(t)| = \ln\alpha_R + \beta_R \ln t \tag{5.17}$$

According to Equation (5.17), the parameters α_R and β_R can be evaluated using linear regression methods. The results obtained from all recovery tests performed are summarized in Table 5.9.

The results shown in Table 5.9 indicate that deviatoric stress has an influence on the value of parameter α_R. This effect is illustrated graphically in

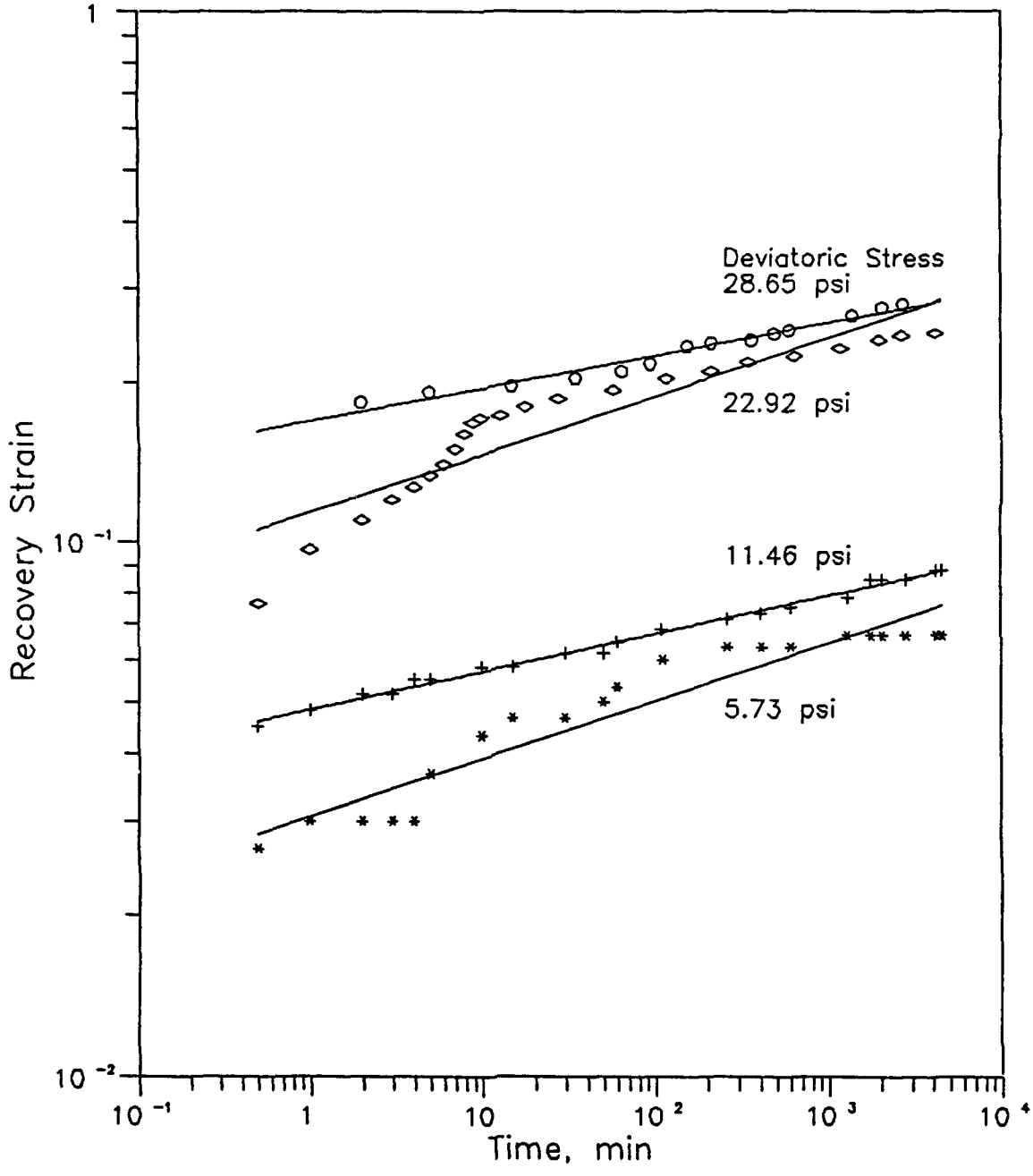

Figure 5.11 Recovery Phase for Specimens Equilibrated at 70 psi

Table 5.9
Regression Values of Recovery Phase

Soil Suction 15 psi			
Specimen No.	Deviatoric Stress, psi	Parameter α_R	Parameter β_R
30	5.73	0.0398	0.0526
20	11.46	0.0644	0.0904
29	14.30	0.0766	0.1063
21	17.19	0.0734	0.1204
23	22.92	0.2108	0.0835
24	28.65	1.5629	0.0254
Soil Suction 40 psi			
13	11.46	0.0519	0.0755
14	17.19	0.0782	0.0531
16	22.92	0.1568	0.0831
17	28.65	0.2258	0.0708
Soil Suction 70 psi			
11	5.73	0.0306	0.1081
12	11.46	0.0484	0.0713
15	22.92	0.1135	0.1094
19	28.65	0.1691	0.0614

Figures 5.12 and 5.13. The existing results have been fitted with an exponential function of deviatoric stress in Figure 5.12 and with a power law of the deviatoric stress in Figure 5.13. Although there is some scatter in the results, it appears that the exponential function of deviatoric stress would provide a more consistent fit to all the data. Nevertheless, for consistency with the model for the creep phase, the two functions of stress have been retained in this study.

The actual analytical functions used to represent the influence of the deviatoric stress level are the following:

$$\alpha_R = \alpha_{R1}\sigma_d^{\alpha_{R2}}$$

$$\alpha_R = \alpha_{R1}e^{\alpha_{R2}\sigma_d} \qquad (5.18)$$

where α_{R1} and α_{R2} are functions of soil suction level. The values of α_{R1} and α_{R2} obtained from regression analysis for the three suction levels are summarized in Table 5.10.

Table 5.10
Values of α_{R1} and α_{R2} for Different Soil Suction Levels

Soil Suction, psi	α_{R1}		α_{R2}	
	Power	Exponential	Power	Exponential
15	5.73×10^{-3}	0.0218	1.0220	0.0218
40	8.47×10^{-4}	0.0183	1.6524	0.0891
70	4.37×10^{-3}	0.0218	1.0558	0.0745

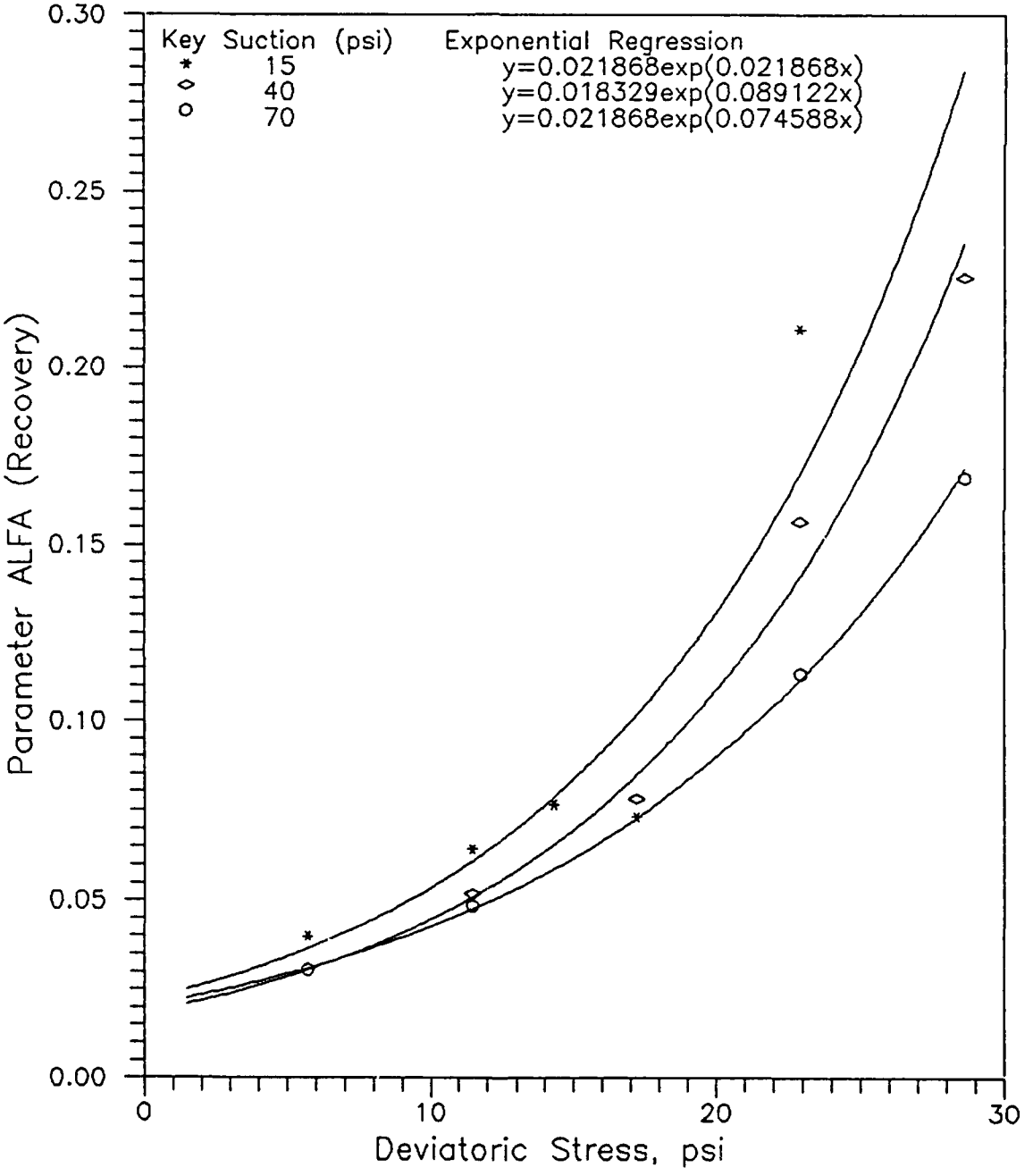

Figure 5.12 Exponential Regression between Parameter α_R and Deviatoric Stress

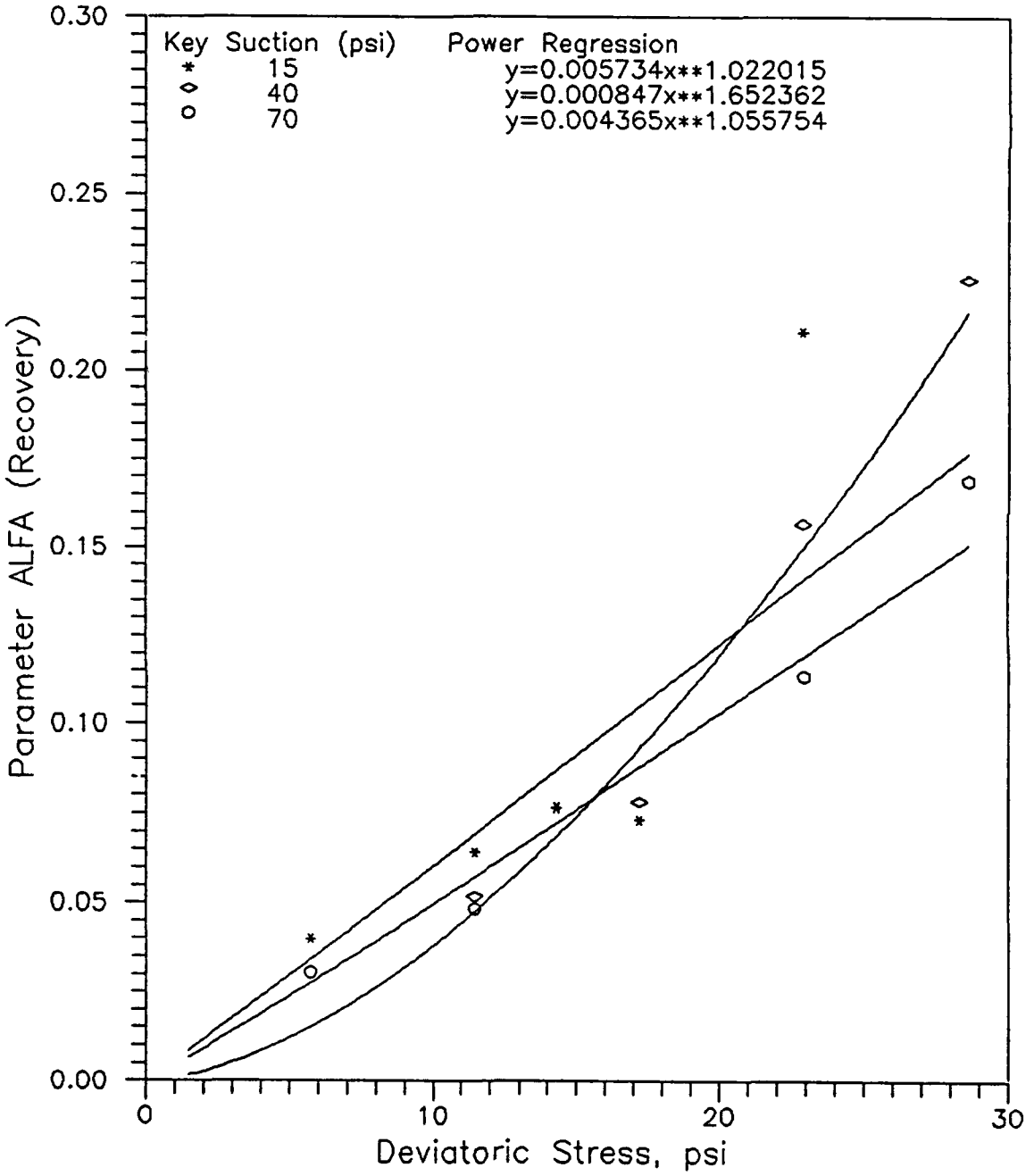

Figure 5.13 Power Law Regression between Parameter α_R and Deviatoric Stress

The results of parameter β_R shown in Table 5.9 appear to indicate that the parameter is independent of deviatoric stress and soil suction. The variability observed appears to be random and covers a very narrow range from 0.05 to 0.120. Because of these considerations the parameter β_R has been assumed to be constant and equal to the average of all results at 0.076.

The proposed model for the unloading phase is a power law of time with an exponent that is constant and equal to 0.076. The coefficient of this power law is found to be a function of the deviatoric stress and soil suction and two proposed models exists to account for this effect. The general analytical expression for these models are the following:

$$\epsilon_R(t) = \alpha_{R1}\sigma_d^{\alpha_{R2}}t^{0.076}$$

$$\epsilon_R(t) = \alpha_{R1}e^{\alpha_{R2}\sigma_d}t^{0.076} \qquad (5.19)$$

with the values of parameters α_{R1} and α_{R2} listed in Table 5.10.

5.4.2 Evaluation of Model Capabilities

A comparison of the model parameters for the creep and the recovery phase (shown in Table 5.7 and 5.10, respectively) indicate that the model are sensibly different and in order to model the unloading of the soil it might be necessary to retain the recovery model also.

The capabilities of the model fitted to the recovery phase has been

evaluated through using the model selected in predicting the response to be expected for the specific conditions of the recovery cases actually monitored. The comparison of the lab data and the model predictions are shown in Appendix I for all the tests with recovery phase.

In general all the predictions with the power law of time with a coefficient that is a power law of deviatoric stress provides the best fit to the experimental data. For a couple of specimens No. 23 and 24, the deviations are very large. These specimens were subjected to excessively large deviatoric stresses and part of the deformation has to be attributed to plastic deformation of the specimen.

In a similar fashion as for the other models, it appears that the parameters obtained for the specimens equilibrated at 40 psi soil suction are out of the pattern indicated by the other two soil suction levels, 15 psi and 70 psi. These considerations suggest the need to extend the range and the number of test conditions in order to provide a better indication of the variation of model parameters with soil suction and deviatoric stress.

CHAPTER SIX

HIGH STRAIN RATE EQUIPMENT AND TEST PROGRAM

6.1 INTRODUCTION

Specimens equilibrated to the same three soil suction levels were subjected to dynamic tests. These tests were performed in a closed-loop servovalve MTS test system. Each test consisted of several pulses being applied on the specimen under stress controlled conditions. Each stress pulse lasted 50 milliseconds and consisted of a ramp-up loading to a peak stress and a ramp-down unloading. The peak stress was increased from a pulse to the next. The present chapter describes the specimen preparations, the testing equipment, the testing methodology, the data reduction and presents the test program and results.

6.2 SPECIMEN PREPARATION

The specimens subjected to the dynamic test were consolidated from a slurry in an identical process as the one followed for the creep recovery tests. Upon consolidation of the slurry, the specimen was trimmed and placed in the test cell for equilibration to the desired suction level. After equilibration was judged completed, all the cell valves were closed and the cell with the specimen was moved from the constant temperature room to the MTS test facility. At this point, the cell was connected again to water and air pressure lines to the same pressures

as it had during the equilibration process.

Since the MTS test facility did not have a temperature chamber, the test was performed at room temperature. Nevertheless, since the cell and water were in the temperature control room, it is believed they afforded some thermal insulation thus protecting the specimen from temperature changes during the dynamic test. After the cell was removed from the temperature controlled room, the assembly and testing proceeded rapidly to guard the specimen from temperature changes.

6.3 TEST EQUIPMENT

A closed-loop servovalve system manufactured by MTS, Inc, was used to perform the high strain rate tests. The system consists of several interacting units that can be grouped into four main components: 1) Load Unit, 2) Controller, 3) MicroProfiler, and 4) Hydraulic Power Supply.

The Load Unit consists of two stiff columns that join two stiff structural members; i.e. a movable crosshead and a fixed platen. The crosshead is vertically adjustable to accommodate specimens of varying lengths. The vertical load is applied to the specimen using a hydraulic actuator. The actuator is mounted on the crosshead.

The Triaxial cell is fixed to the lower platen. The triaxial cell push-rod is rigidly mounted to the actuator via a load cell. The position of the push-rod is monitored by a linear variable differential transformer (LVDT). A shut-off valve manifold at the base of the triaxial cell provides control for the soil suction levels.

pressure is applied through a shut-off valve on the top plate of the cell.

An additional service manifold is attached to the load frame to accommodate reservoirs for the confining fluid and the pore fluid. Compressed air (obtained form an external air compressor) applied on the water in the pore fluid reservoir causes the water to flow into the specimen. In this study, the pore fluid reservoir was used as source of pore water pressure. Pore air pressure was applied from a tubing connected to the valve for the confining pressure reservoir. A valve and a pressure gage are provided to control the pore water and pore air pressures respectively.

The controller consists of a MicroConsole that controls and monitors the operation of the load unit. It also provides chassis connections for functional plug-in modules. Jacks on the rear panel are provided for transducers, servovalves, hydraulic service manifold, etc.

Three plug-in modules are provided: an AC controller, a DC controller, and an Auxiliary span-control. The Auxiliary Span-Control was not used in this study. Either the AC controller or the DC controller can be used to operate the actuator mounted at the top of the load frame. The AC controller and DC controller control the movement of and the load applied by the actuator rod, respectively. Depending on the selected active controller, the test can be run in strain- or stress- controlled mode.

The MicroProfiler on the front panel of the Controller, is a microprocessor-based, single output precision waveform generation device, which command the

AC or DC controllers for tests in stress, strain, temperature and other test control parameters. Unique waveforms can be programmed with the front panel controls or from a personal computer through an RS232 serial interface. The MicroProfiler creates a waveform by linking together a series of programmed segments which include ramp, haversine and hold time segments. Segments can also be linked together to form a block. A block allows a sequence of segments to be programmed and blocks to be repeated a specific number of times or continuously. The wave form used in the present study was preprogrammed in the Micro Profiler as a ramp up lasting 25 milliseconds followed by a ramp-down also lasting 25 milliseconds.

The Hydraulic Power Supply provides the high pressure fluid required for the operation of the system. The high pressure fluid is applied to one side of the actuator piston, causing it to move. A servovalve controls the movement of the actuator, by opening or closing in response to the Controller. The valve can be opened in either of two directions allowing the high pressure fluid to flow into the cylinder on either side of the piston. This causes movement of the piston in either of two directions.

6.4 TESTING METHODOLOGY

First the cell was fixed on the platen of the load unit and air and water pressures then were reconnected to the cell and specimen. A short time of equilibration was allowed and then the controller was switched on in a strain-

controlled mode. The push rod is connected rigidly with the load cell and, then, the output of the DC transducer is adjusted to zero so that the desired deviatoric stress could be applied on the specimen. At this moment, control is transferred to the stress mode.

At the time, the output of the AC module was adjusted to zero and the test set up was ready for the load cycles. The stress pulse was applied using the Micro-Profiler. The first pulse consisted of a ramp-up to 5.73 psi in 25 msec. and a ramp-down back to 0.0 psi in 25 msec. Then the peak deviatoric stress was gradually increased up to 85.97 psi in the steps indicated in Table 6.1. After each load pulse, the AC controller was adjusted to zero in order to start at zero displacement at the beginning of each stress pulse.

Three channels of data were collected during each stress pulse: Load cell, LVDT, displacement of the push rod, and the Microprofiler output signal. The data was collected with an analyzer. The analyzer was triggered 48 msec. before the stress pulse was applied and collected approximately 136 msec. of data. A total of 4096 data points per channel were collected. These data were then saved for future reduction.

After subjecting the specimen to all the stress pulses listed in Table 6.1, the specimen was removed from the cell and it was subjected to determinations of water content and sporadically to hydrometer analysis and dry density.

Table 6.1
Load Pulses Applied to the Specimen

Time Span: 50 msec		
Load Pulse No.	Peak Deviatoric Stress psi	Rate psi/min
1	5.73	13752
2	11.46	27504
3	17.19	41256
4	22.92	55008
5	28.65	68760
6	34.38	82512
7	40.12	96288
8	45.85	110040
9	51.58	130992
10	57.31	137544
11	63.04	151296
12	68.77	165048
13	74.50	178800
14	80.24	192576
15	85.97	306328

6.5 DATA REDUCTION

After completing the high strain rate test, the data collected was reduced. Since there were large amounts of data for each test, a computer program was developed to automatically obtain the strain-time and stress-time relationships. The program is written in FORTRAN 77 and was named "hstrain". A FORTRAN listing of this program is presented in Appendix J.

The main tasks performed by the computer program HSTRAIN include the following sequence:

1) The voltage data collected is smoothed. This is performed by replacing the value of the voltage at a certain time with the average voltage between the replaced voltage and the voltage at the previous time.

2) The next step is to convert the voltage to stresses and strains. The voltage from the load cell is first transformed to load, and this load divided into the undeformed cross section area of the specimen provides the stress. The voltage from the LVDT is first transformed to displacement, and this displacement divided into the initial length of the specimen provides the strain.

3) The third step is to identify time zero when the waveform was initialized. This is accomplished scanning the stress and strain time series of data.

4) The program forms two files one with the stress-time history detected

by the load cell and the second with the strain-time history detected by the LVDT of the push rod.

The output file contains the information on the loading sequence such as desired peak stress, peak deviatoric stress actually measured by the load cell, peak strain for each loading step, and stress-time and strain-time histories for each pulse of stress applied on the specimen.

6.6 TEST PROGRAM AND RESULTS

At least three repetitions have been performed for each of the three soil suction levels. The measured peak deviatoric stresses and peak strain levels for each specimen are summarized in Table 6.2 for the specimens equilibrated at 15 psi; in Table 6.3 for the specimens equilibrated at 40 psi; and in Table 6.4 for the specimens equilibrated at 70 psi soil suction.

The results presented in Table 6.2 are shown in graphic form in Figure 6.1. Those in Table 6.3 are plotted in Figure 6.2 and the results of Table 6.4 are plotted in Figure 6.3. In general, these figures illustrated that the repetitions provided fairly close results with the exception of specimens 32 and 33 equilibrated at 15 psi soil suction. These specimens exhibited strain several times higher than the result on the other three repetitions. The reason for this large difference is not apparent at this time.

It is worth noting that for the same specimen as in Figure 6.4, the peak values shown in Table 6.2 at larger deviatoric stresses indicate that the differences

Table 6.2

Results of Dynamic Tests for Specimens Equilibrated at 15 psi

Load Pulse No.	Desired Peak Stress psi	Measured Peak Stress psi				Measured Peak Strain %			
		Specimen				Specimen			
		25	33	32	42	25	33	32	42
1	5.73	4.28	5.34	4.75	3.69	0.026	0.00066	0.005	0.027
2	11.46	7.62	10.89	8.84	6.66	0.061	0.00144	0.036	0.072
3	17.19	10.79	13.11	12.14	11.29	0.111	0.015	0.077	0.135
4	22.92	15.59	16.20	16.20	13.67	0.193	0.040	0.140	0.183
5	28.65	17.33	18.92	16.23	16.65	0.266	0.071	0.163	0.254
6	34.38	21.66	22.97	18.01	18.83	0.353	0.124	0.219	0.323
7	40.12	25.02	25.18	19.99	23.78	0.459	0.213	0.304	0.474
8	45.85	26.30	26.97	21.88	23.96	0.573	0.288	0.409	0.589
9	51.58	29.08	28.48	24.00	25.58	0.702	0.362	0.546	0.717
10	57.31	29.48	29.73	25.54	26.84	0.851	0.434	0.684	0.827
11	63.04	none	31.02	26.59	27.42	none	0.568	0.826	0.957
12	68.77	none	32.01	27.31	27.68	none	0.686	0.991	1.067
13	74.50	none	33.87	28.27	27.35	none	0.843	1.148	1.201
14	80.24	none	33.48	28.84	27.33	none	0.967	1.265	1.323
15	85.97	none	33.96	29.60	27.74	none	1.140	1.438	1.465

Table 6.3

Results of Dynamic Tests for Specimens Equilibrated at 40 psi

Load Pulse No.	Desired Peak Stress psi	Measured Peak Stress psi				Measured Peak Strain %			
		Specimen				Specimen			
		26	27	39	41	26	27	39	41
1	5.73	4.48	4.28	4.30	4.81	0.015	0.022	0.025	0.022
2	11.46	8.81	8.01	7.25	9.04	0.036	0.053	0.065	0.052
3	17.19	13.00	11.32	11.33	12.35	0.067	0.086	0.130	0.087
4	22.92	16.09	20.17	15.06	19.42	0.103	0.158	0.206	0.152
5	28.65	23.20	20.18	none	21.17	0.173	0.220	none	0.195
6	34.38	25.05	22.82	21.56	24.82	0.218	0.285	0.376	0.258
7	40.12	27.44	26.88	24.80	28.95	0.280	0.362	0.466	0.338
8	45.85	30.85	30.63	27.79	33.41	0.348	0.451	0.576	0.409
9	54.58	33.87	34.92	29.63	34.92	0.431	0.553	0.704	0.504
10	57.31	35.46	40.17	31.32	41.43	0.524	0.564	0.809	0.609
11	63.04	none	41.44	33.94	40.51	none	0.687	0.924	0.740
12	68.77	39.31	43.20	34.23	42.38	0.653	0.804	1.022	0.861
13	74.50	41.44	43.97	35.61	42.35	0.910	0.945	1.136	1.015
14	80.24	41.10	43.68	34.80	42.07	1.019	1.068	1.223	1.132
15	85.97	41.77	45.17	35.84	43.14	1.173	1.206	1.359	1.279

Table 6.3 (continued)

Results of Dynamic Tests for Specimens Equilibrated at 40 psi

Load Pulse No.	Desired Peak Stress psi	Measured Peak Stress psi	Measured Peak Strain %
		Specimen	Specimen
		43	43
1	5.73	3.10	0.028
2	11.46	6.60	0.071
3	17.19	10.75	0.129
4	22.92	14.24	0.184
5	28.65	18.37	0.232
6	34.38	22.87	0.288
7	40.12	27.21	0.353
8	45.85	30.12	0.417
9	54.58	34.15	0.511
10	57.31	37.38	0.612
11	63.04	39.95	0.713
12	68.77	42.00	0.807
13	74.50	42.24	0.935
14	80.24	42.21	1.030
15	85.97	42.31	1.159

Table 6.4

Results of Dynamic for Specimens Equilibrated at 70 psi

Load Pulse No.	Desired Peak Stress psi	Measured Peak Stress psi				Measured Peak Strain %			
		Specimen				Specimen			
		22	28	31	34	22	28	31	34
1	5.73	5.03	3.69	4.53	2.05	0.015	0.014	0.013	0.053
2	11.46	9.68	6.16	9.17	6.51	0.033	0.075	0.034	0.096
3	17.19	14.14	10.59	12.92	11.01	0.058	0.080	0.061	0.126
4	22.92	16.50	15.78	16.65	15.90	0.083	0.147	0.092	0.141
5	28.65	19.34	19.68	21.92	16.69	0.109	0.207	0.142	0.125
6	34.38	26.24	23.27	21.49	22.03	0.168	0.267	0.135	0.174
7	40.12	28.19	26.87	25.80	24.09	0.233	0.344	0.191	0.208
8	45.85	31.37	30.51	28.11	27.71	0.301	0.404	0.242	0.253
9	51.58	33.70	34.27	30.61	31.18	0.383	0.492	0.299	0.315
10	57.31	35.23	39.19	33.93	34.55	0.465	0.561	0.384	0.405
11	63.04	36.05	41.39	37.05	38.25	0.544	0.659	0.462	0.484
12	68.77	39.92	44.34	38.97	41.55	0.673	0.742	0.553	0.566
13	74.50	39.80	44.98	41.15	44.16	0.819	0.866	0.651	0.668
14	80.24	41.11	46.76	42.47	46.25	0.931	0.952	0.745	0.759
15	85.97	42.65	47.11	44.02	48.27	1.072	1.105	0.858	0.885

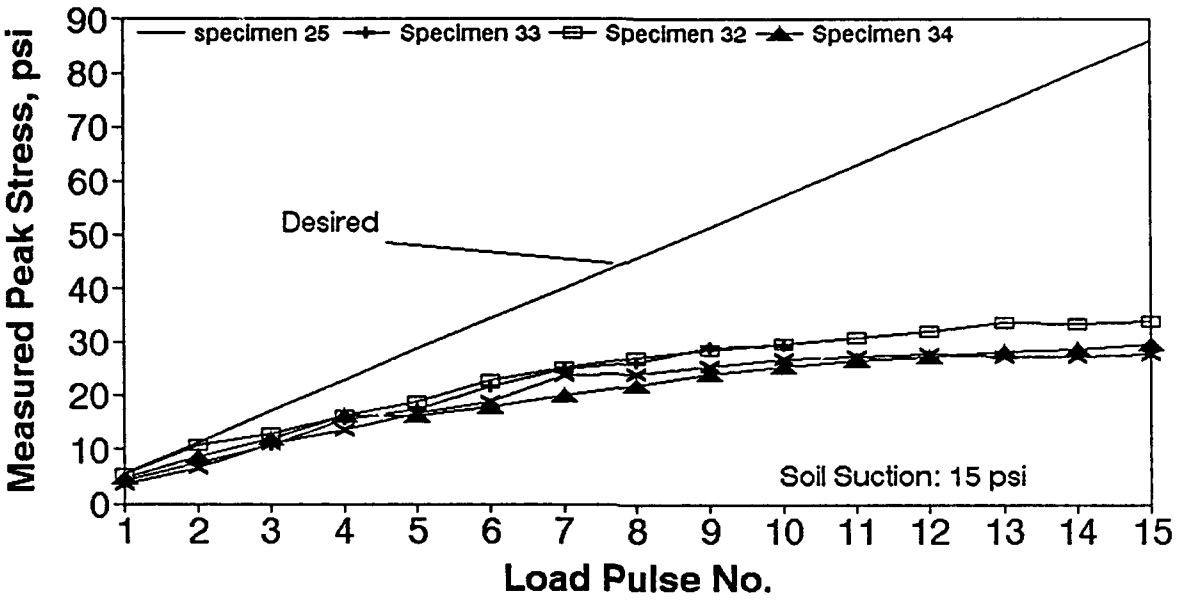

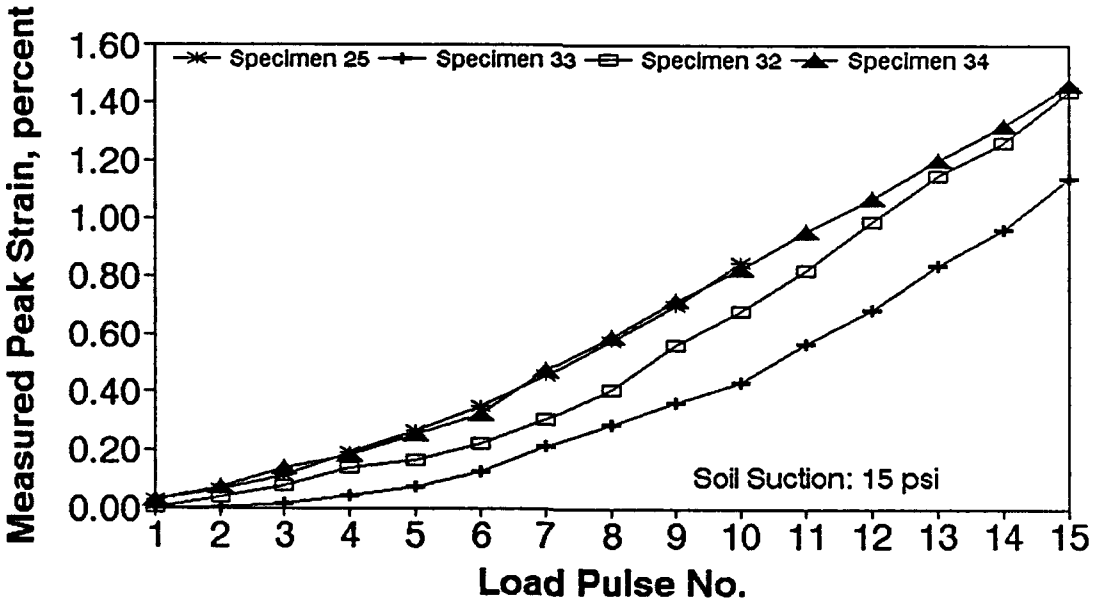

Figure 6.1 Dynamic Test Results for Specimens at 15 psi Soil Suction

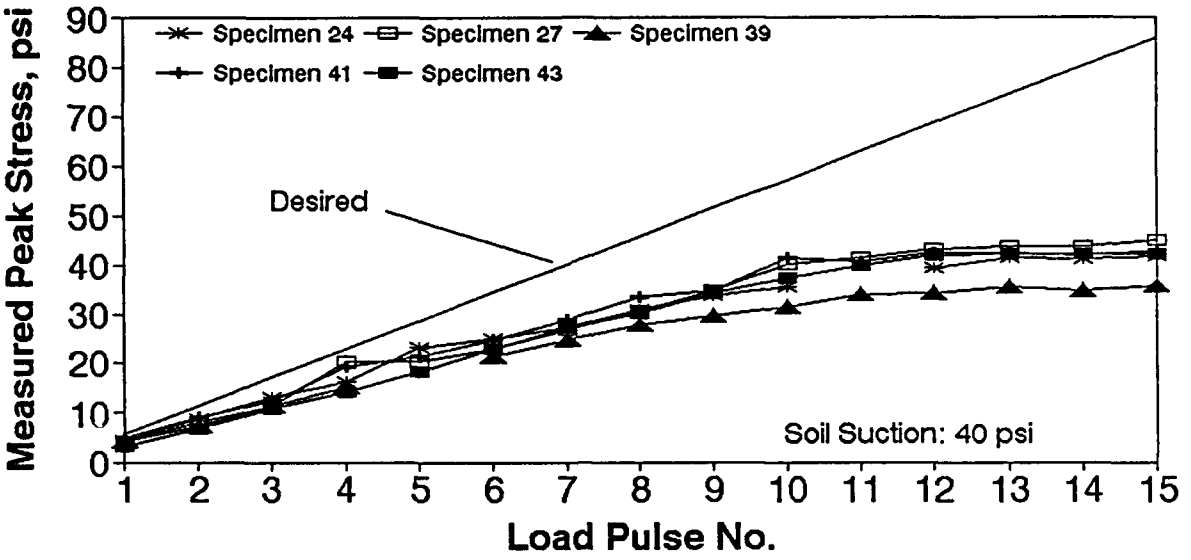

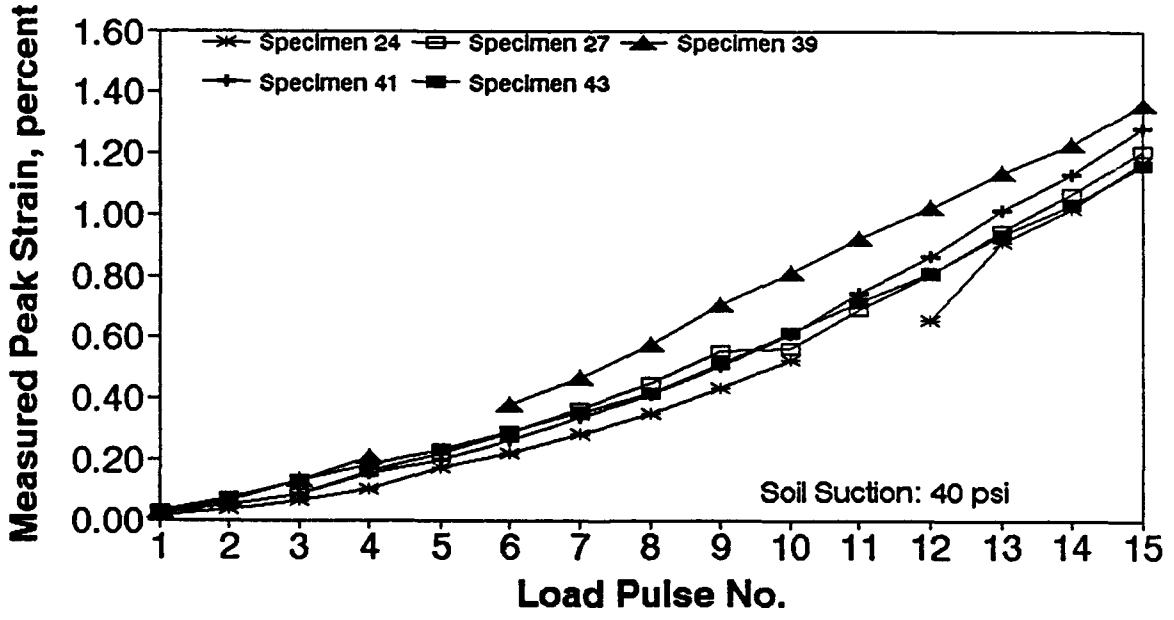

Figure 6.2 Dynamic Test Results for Specimens at 40 psi Soil Suction

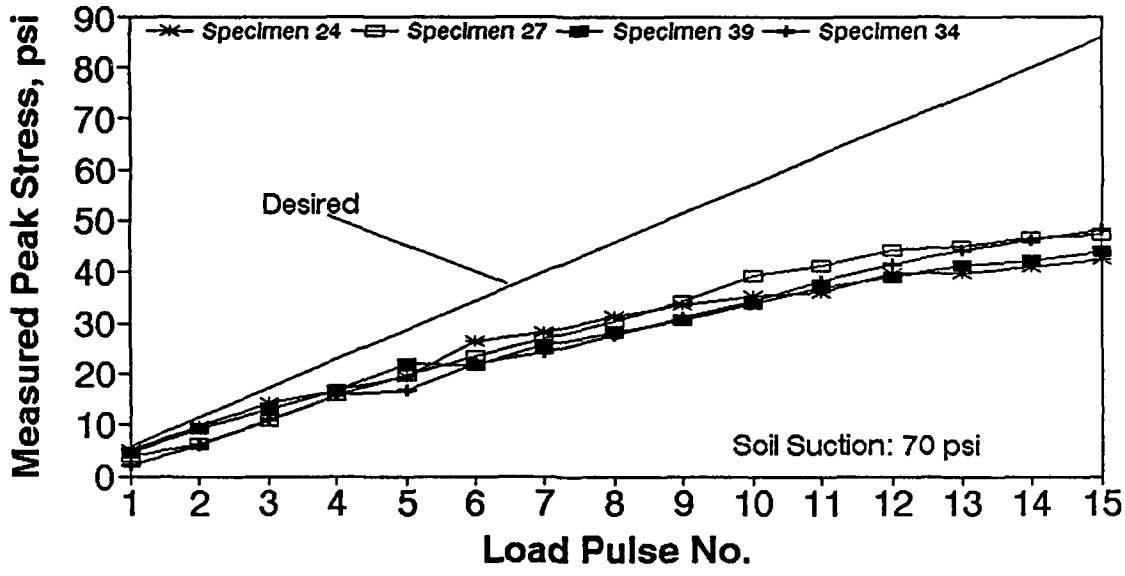

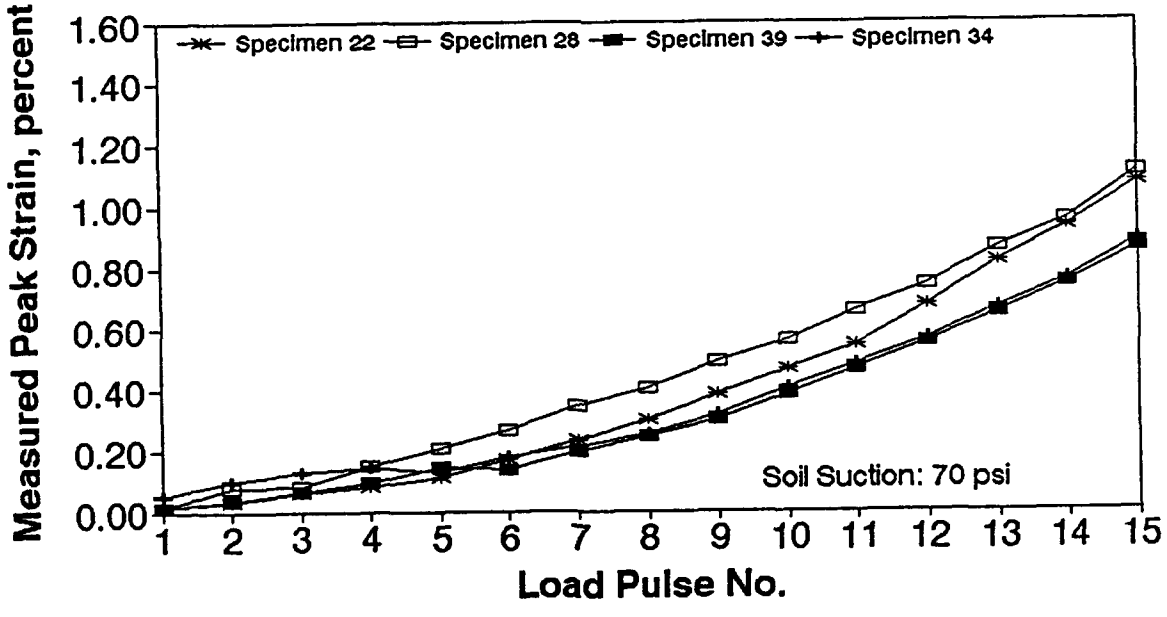

Figure 6.3 Dynamic Test Results for Specimens at 70 psi Soil Suction

become progressively smaller.

A comparison of the full stress and strain time histories for the specimens at 15 psi soil suction for the load Pulse No. 2 are shown in Figure 6.4. This case is one of the worst cases registered in the present study. It is worth noticing that for the specimens in Figure 6.4, the peak values shown in Table 6.2 indicate progressively smaller differences. This figure illustrates the shortcomings of the test system used that could not respond fast enough to reproduce the wave pulse desired. Furthermore, as the stiffness of the specimen increases the system does not have to deform as much (as illustrated by specimen No. 32) and, thus, it can very readily accomplish the desired peak deviatoric stress.

For larger deviatoric stresses, the system cannot adjust fast enough and "ringing" near the peak load becomes progressively a very dominant feature providing a wave form that does not resemble the stress pulse desired. Nevertheless, since the specimen had already been subjected to several stress pulses, it is questionable whether the properties of the undisturbed specimen could explain the behavior of the specimen at that stage.

The individual test results for each combinations of soil suction and deviatoric stress levels are shown in appendices. These appendices only include the test results for the deviatoric stress levels where the peak instabilities are reasonably small. The results on specimens equilibrated at 15 psi soil suction are presented in Appendix K, those at 40 psi are shown in Appendix L, and the 70 psi specimens are included in Appendix M.

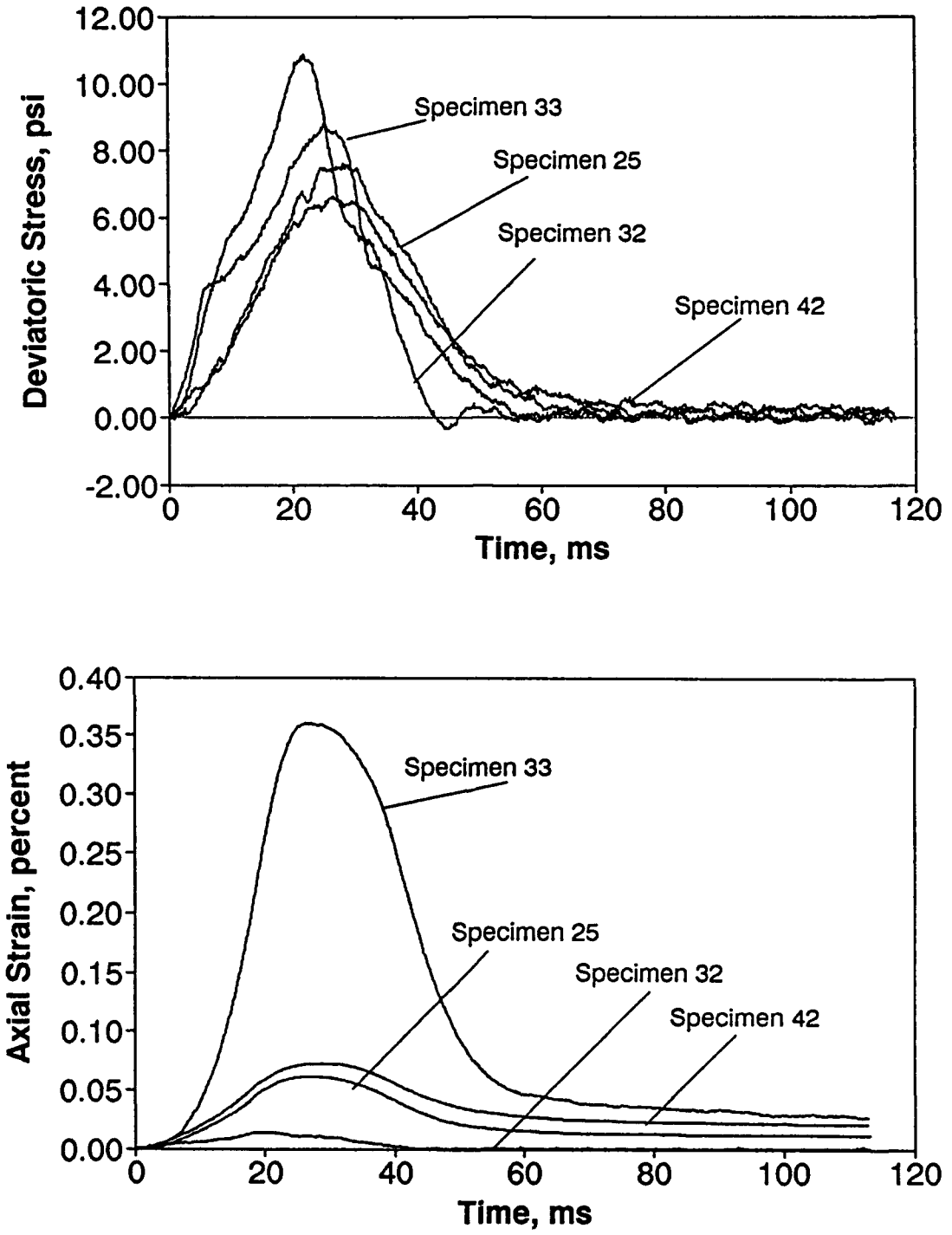

Figure 6.4 Comparison of Stress and Strain Time Histories for Specimens at 15 psi

CHAPTER SEVEN

COMPARISON OF PREDICTED AND MEASURED DYNAMIC BEHAVIOR

7.1 INTRODUCTION

The power laws fitted to the creep/recovery data have been used to predict the response of the specimens to the pulses of load applied during the dynamic tests. This decision was based on the believe that the initial part of the transient creep phase would be the model with the most possibilities to explain the dynamic test behavior. In this sense, the initial and the recovery power models have been used in conjunction with the indirect methods proposed by Shames and Cozarelli (1991) which are based on strain hardening hypotheses and with the modified superposition principle (Findley et al, 1976) for non-linear viscoelastic materials.

The best approached found consisted of using the modified superposition principle with the power law model of the initial transient creep strain. The rest of the present chapter presents only the comparisons obtained using the modified superposition and the initial power law.

7.2 PREDICTION METHODOLOGY

The actually recorded load pulse was used as the input to predict the specimen response. For this purpose, the recorded load pulse was approximated by a step like functions of constant stress during every millisecond of the 50 msec.

duration of the load pulse. For times beyond 50 msec., the noise recorded from the load cell was neglected and the deviatoric stress was fixed at zero. An example of a load pulse recorded with the step-like approximation superimposed is shown in Figure 7.1.

The predictions were calculated using the modified superposition principle as described by Findley et al (1976). In this approach every step is added in full at the beginning of the step (that is from zero to the full value of the deviatoric stress) and subtracted in full at the end of the step. The response at any time is the result of the superposition of all the additions and substractions from previous steps. In algebraic form, a step-like function of the following type:

1) σ_1 from t_1 / t_2

2) σ_2 from t_2 / t_3

.....

n) σ_n from t_n / t_{n+1}

used in combination with the following power law:

$$\epsilon(t) = \alpha_1 (\sigma_d)^{\alpha_2} t^{\beta} \qquad (7.1)$$

Then the modified superposition principle would become the following relationship:

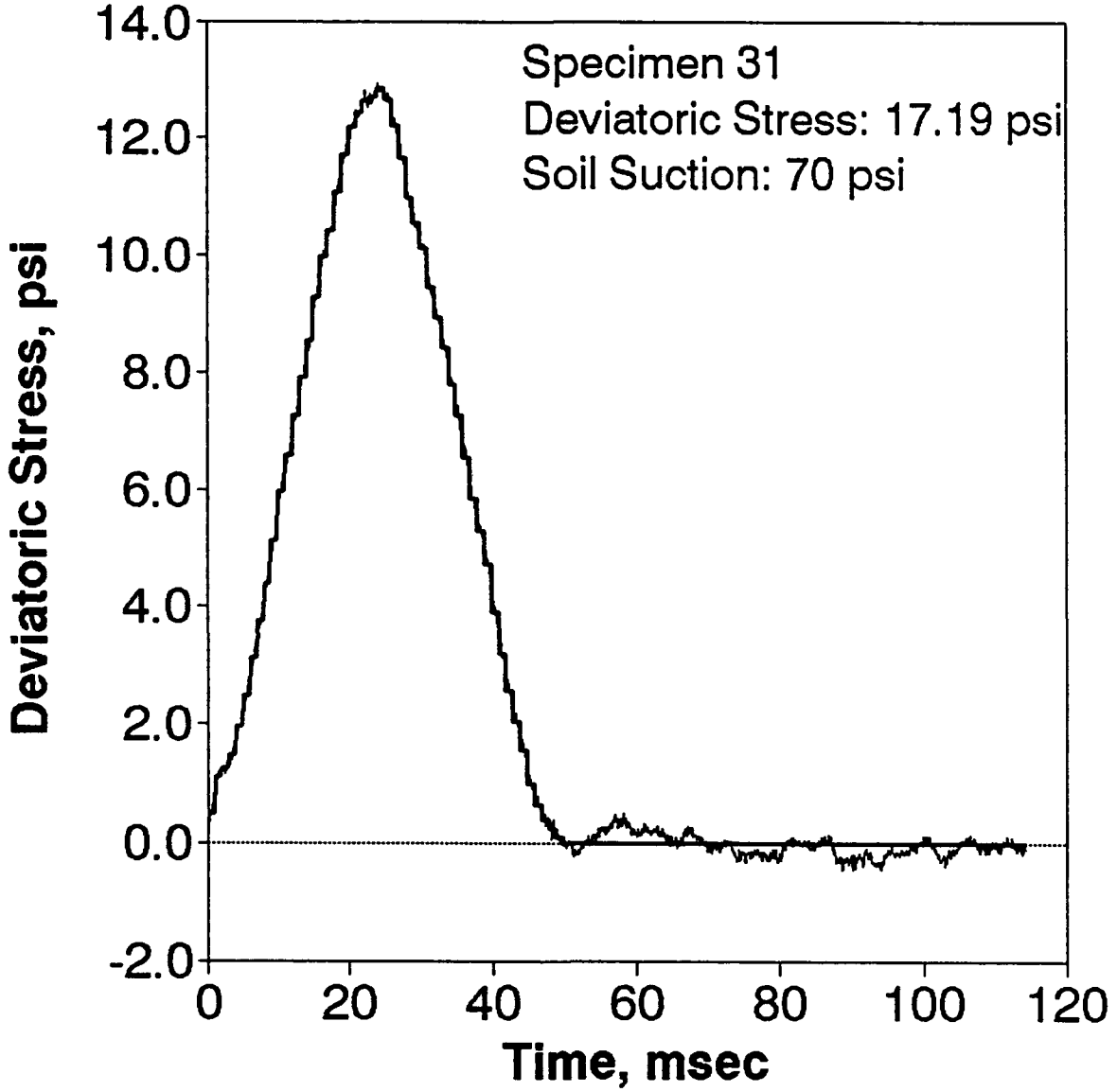

Figure 7.1 Example of the Approximation of the Load Pulse Used in the Predictions

$$\epsilon_p(t) = \alpha_1 (\sigma_1)^{\alpha_2} (t-t_1)^{\beta} + \sum [-\alpha_1 (\sigma_1)^{\alpha_2} (t-t_{i+1})^{\beta} +$$

$$\alpha_1 (\sigma_{i+1})^{\alpha_2} (t-t_{i+1})^{\beta}] \quad \text{for } t_{n+1} \leq t \leq t_{n+2} \tag{7.2}$$

Equation (7.2) has been programmed and the predictions described in the present chapter were calculated with this approach. Specifically, the modelling consisted of the following steps:

1)Reading the deviatoric stress-time history and forming the step-like function by averaging the stress readings within one millisecond, for the first 50 milliseconds, and

2)Using this stress function in conjunction with Equation (7.2) to predict the strain-time history for the specimen.

7.3 RESULTS AND DISCUSSION

The model described in the previous section was used to predict the response of all the specimens tested in dynamic tests. Examples of the comparison of measured versus predicted strain histories for a specimen equilibrated at 15 psi soil suction are presented in Figure 7.2 and 7.3.

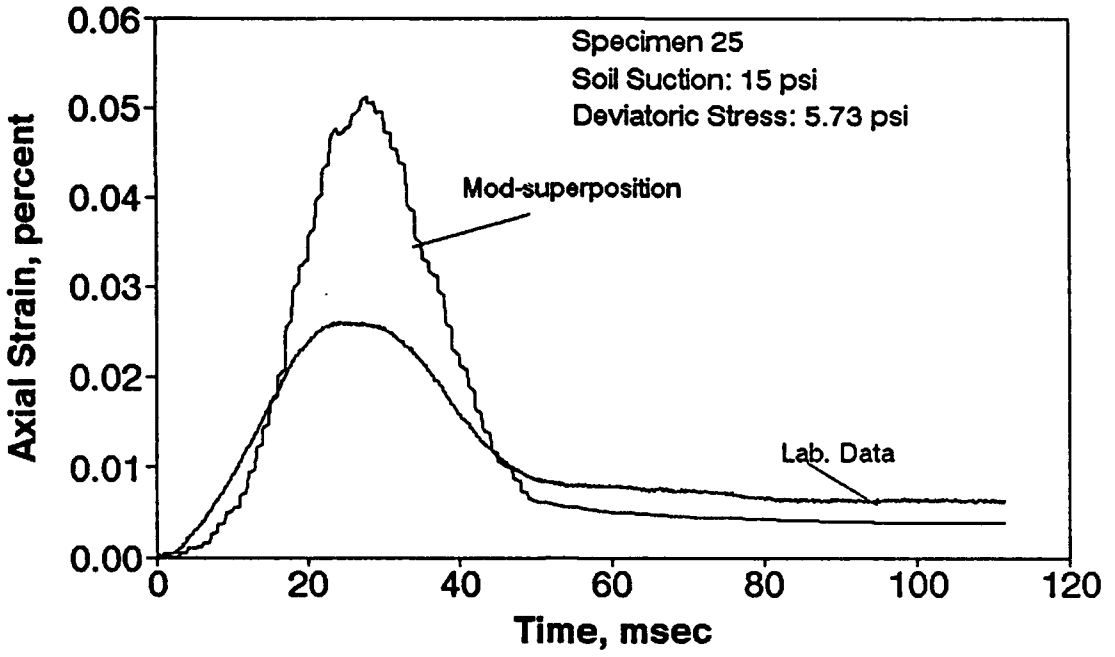

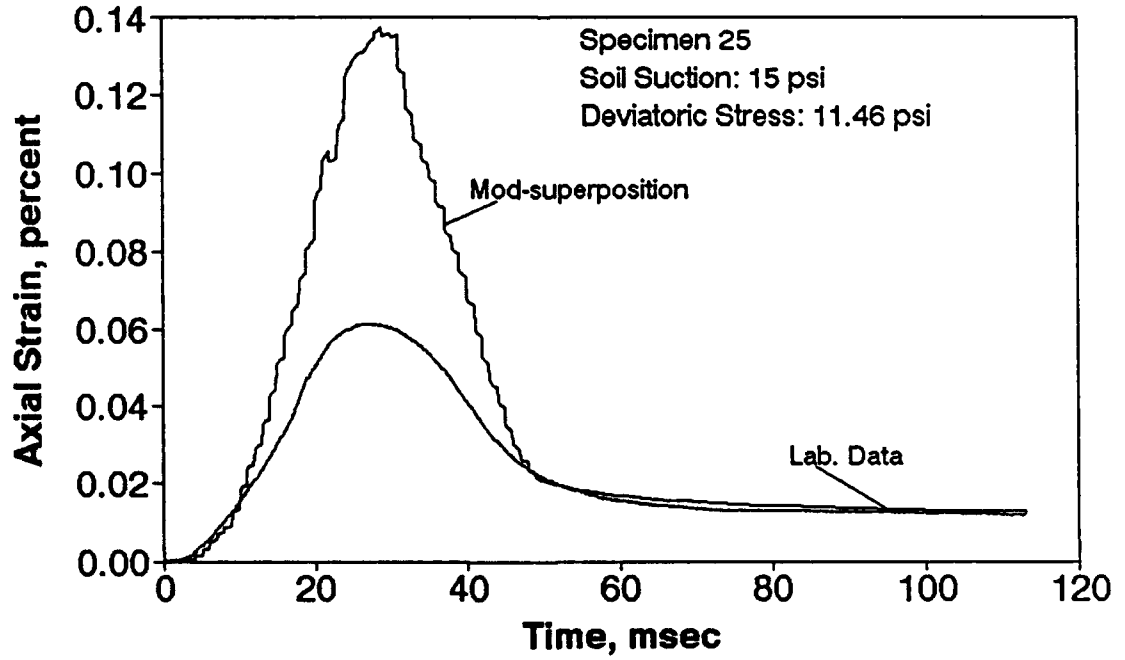

Figure 7.2 Predicted vs Measured Strain Histories, Soil Suction 15 psi and Peak Deviatoric Stresses 5.73 and 11.46 psi

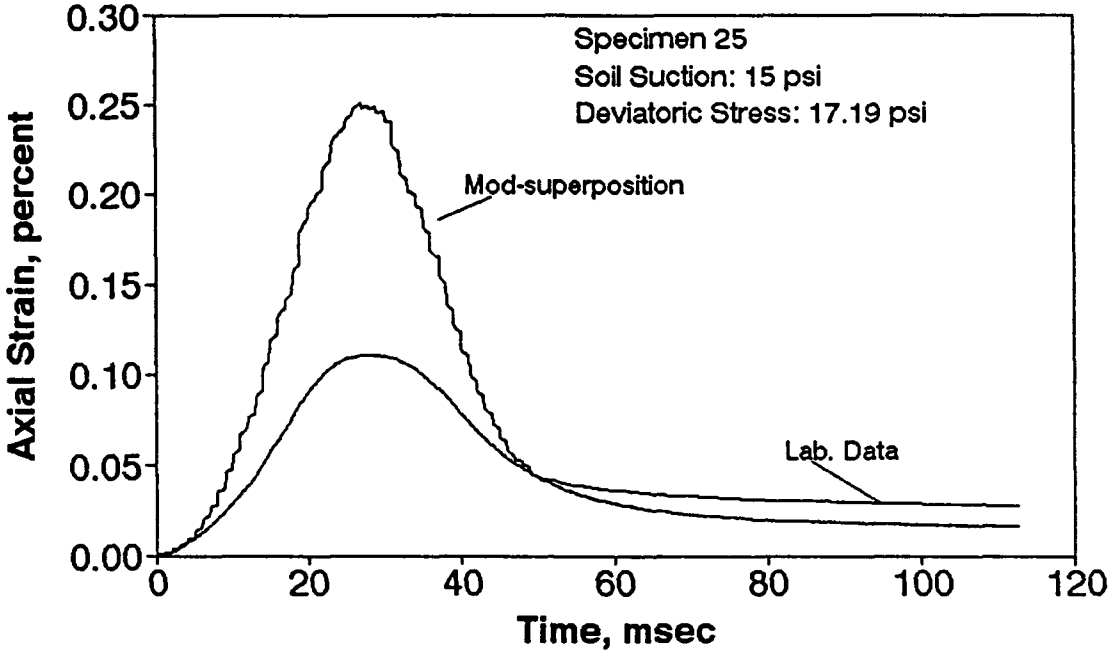

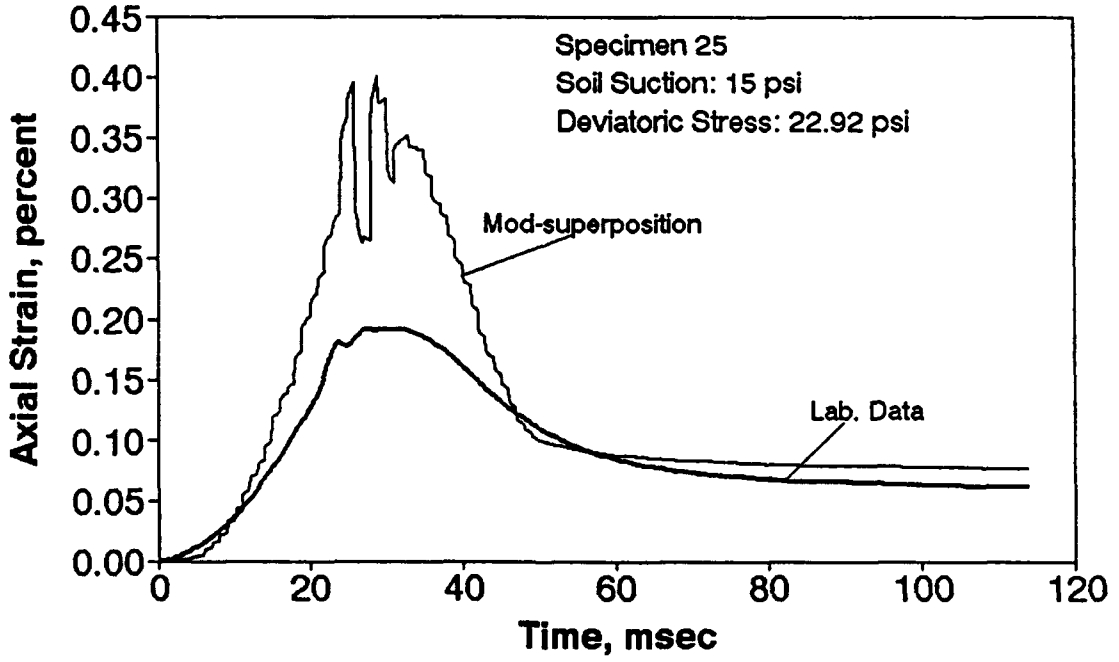

Figure 7.3 Predicted vs Measured Strain Histories, Soil Suction 15 psi and Peak Deviatoric Stresses 17.19 and 22.92 psi

The results shown in these figures indicate that the predicted strain levels near the peak of the load pulse are larger than the measured strains by a factor of roughly two. Nevertheless, it is relevant to notice that at very low deviatoric stress levels, that is, at the beginning and at the end of the stress pulse, the agreement between prediction and measurement is much better. Specifically, the plastic strains predicted are remarkably close to the recorded values.

Comparisons of the measured versus predicted strain histories for a specimen equilibrated at 70 psi soil suction are presented in Figure 7.4 and 7.5. These figures show results exhibiting very similar patterns as those discussed for Figures 7.2 and 7.3. In this sense, the predicted and measured data are in fairly good agreement at low deviatoric stress levels, that is, at the beginning and at the end of the stress pulse. Near the peak of the stress pulse , the predictions suggests strain levels about three times as large as the strains measured.

There are two possible sources of error that could help explain the differences between the predicted and measured strain histories. The first possibility is related to the constitutive relations developed in Chapter Five. The comparisons between the model predictions and the individual test results described in that chapter illustrate the variability of the creep/recovery tests. Thus some of the differences should then be attributed to shortcomings of the initial power law model used in the predictions.

The second possibility is related to errors in the stress-time histories recorded in the dynamic tests. It is worth mentioning that the dynamic tests were

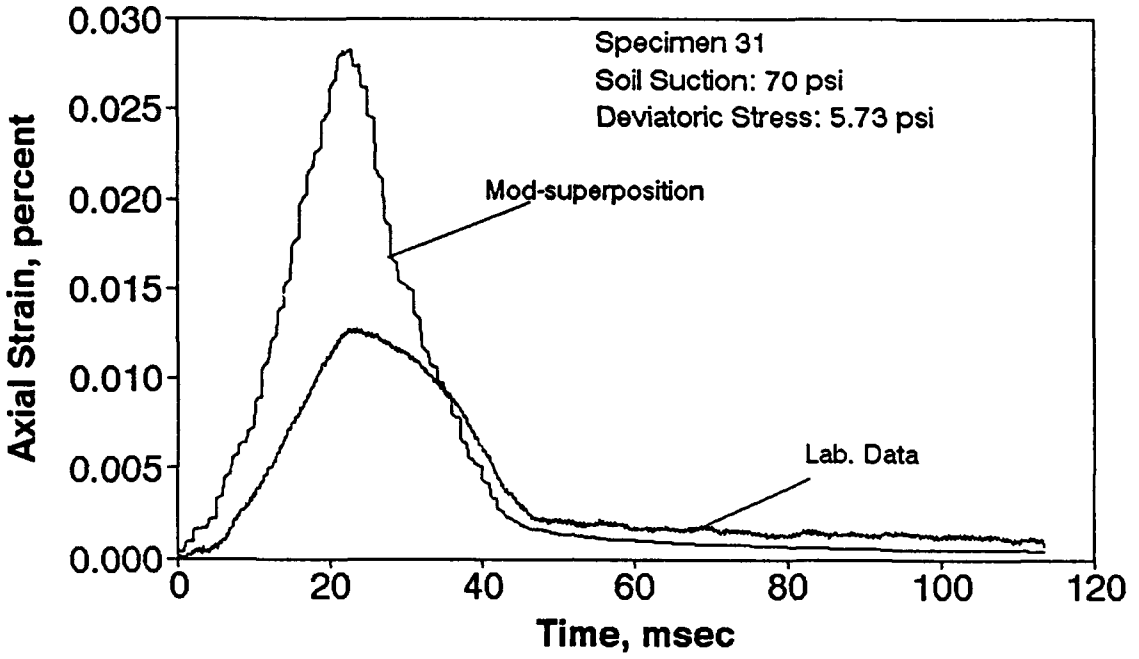

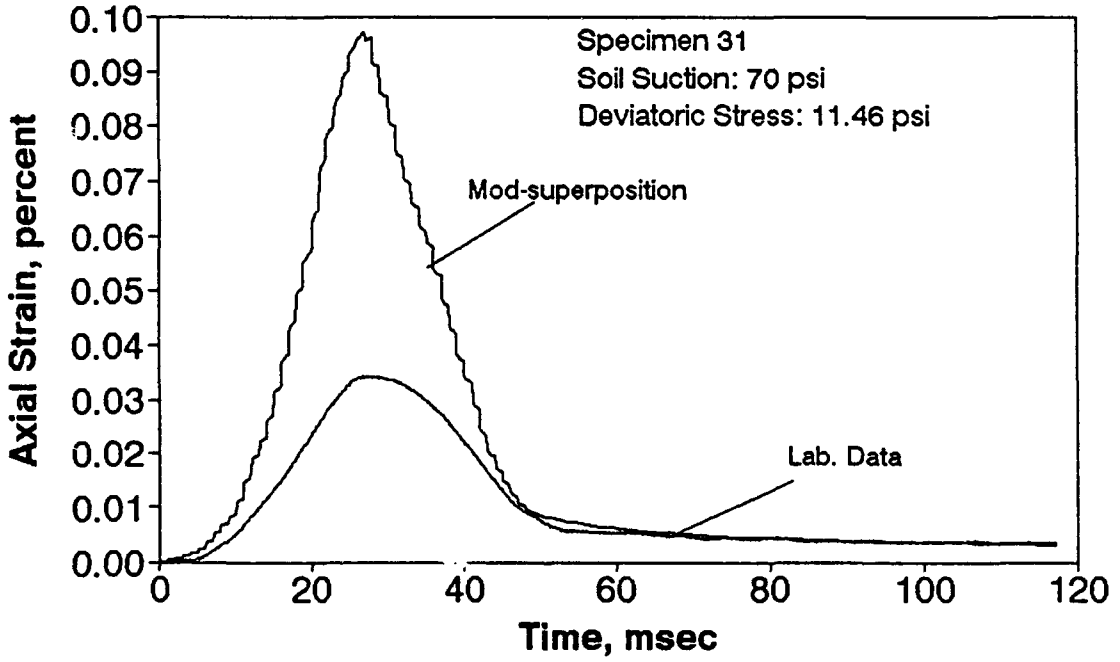

Figure 7.4 Predicted vs Measured Strain Histories, Soil Suction 70 psi and Peak Deviatoric Stresses 5.73 and 11.46 psi

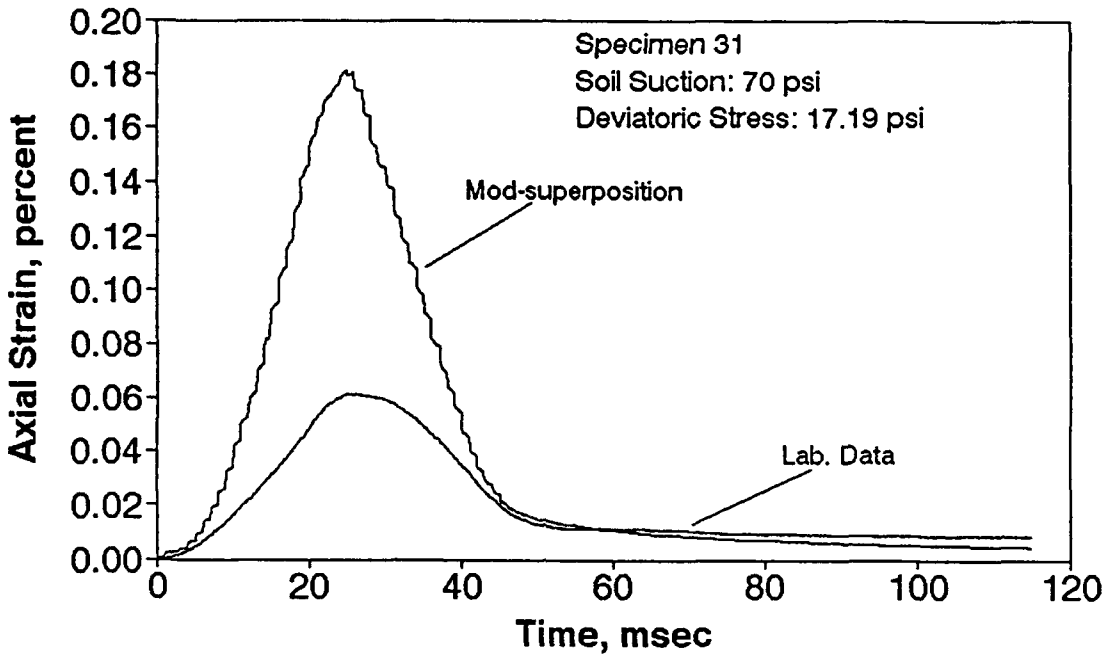

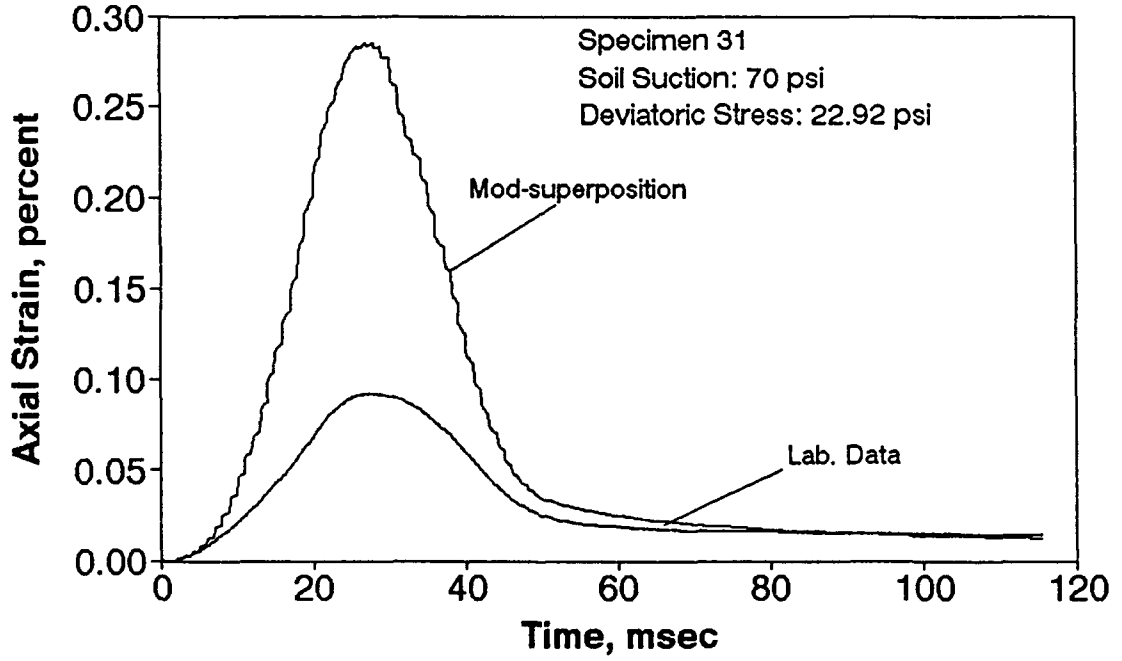

Figure 7.5 Predicted vs Measured Strain Histories, Soil Suction 70 psi and Peak Deviatoric Stresses 17.19 and 22.92 psi

performed with the triaxial cell partially filled with an air gap, nearly one inch of air under pressure, to ensure that the penetration of the push rod into the cell did not cause undue confining pressure changes on the specimen. However, the load cell was installed in the push rod but outside of the triaxial cell; thus, the loads experienced by the load cell can be expected to be somewhat different that the loads actually applied on the specimen.

One cause of the difference in loads is the friction at the bushing as the push rod penetrates into the triaxial cell. The responsible element is a rubber O-ring that braces the push rod and prevents the cell fluid from leaking. This mechanism implies that the friction force would be different for different confining pressures. In this sense, it is worth recalling from Table 3.5, that the confining pressure of Specimen 25 was 60 psi while for Specimen 31 it was 90 psi. This difference in pressure could explain some of the differences described earlier from the comparison of predicted versus measured strain histories; that is , the over prediction of strain near the peak load was a factor of two for Specimen 25 and a factor of three for Specimen 31. Furthermore, the good agreement between prediction and measurement at low strain levels (Specifically the close agreement in plastic deformation of the specimen after each stress pulse) is an indication that the differences observed can probably be attributed mainly to friction at the bushing. This friction is at a minimum when there is no displacement of the rod relative to the cell.

An additional cause of the differences that could exists between the loads registered by the load cell and the loads experienced by the specimen is the result of the inertia of the push rod placed between the load cell and the specimen. The push rod is made out of steel and possesses considerable mass of several kilograms. This large mass subjected to stress changes in fractions of a millisecond would add and/or subtract the inertia force to the load experienced by the load cell. The fact is that when the inertia is added to the load cell record is simultaneously subtracted of the stress experienced by the specimen. The results shown in Figure 7.3 for the deviatoric stress level of 22.92 psi are a clear demonstration of this effect. While the prediction experienced large oscillations of strain associated with large oscillations of stress recorded by the load cell, the strains experienced by the specimen are negligible . Furthermore, the results shown in Figures 7.2 through 7.5 show a pattern of increasing the over prediction of strain for the increasing displacements implied by the increasing strain levels in successive stress pulses.

In summary, there is concern that the constitutive model derived from the creep/recovery tests needs improvements and might be responsible for some of the over predictions of strain. Nevertheless, it seems that a considerable part of the over prediction can be attributed to the conditions of the test set up used in the dynamic tests; specifically the friction push-rod/ bushing of the triaxial cell and the inertial forces introduced by the accelerations/ deceleration of the push rod during the dynamic tests.

CHAPTER EIGHT

CONCLUSIONS AND RECOMMENDATIONS

8.1 SUMMARY

A bulk sample of clayey soil was treated to remove all soluble materials and equilibrated at a known and constant chemical composition of the pore solution. Cylindrical specimens were prepared from this soil suspension stock by consolidating the suspension in a triaxial cell under constant temperature, isotropic pressure, and for a specified length of time. The specimens were then trimmed and equilibrated to specified soil suction levels. A total of 46 specimens were prepared and tested in the present study.

Some specimens were subjected to creep/recovery tests and the results of these tests were used to fit viscoelastic models to the observed soil behavior. Other specimens were subjected to dynamic tests in an MTS dynamic testing facility. In the dynamic tests, the specimen was subjected to a controlled load pulse made with a ramp-up to the peak deviatoric stress and a ramp-down to zero deviatoric stress. The imposed load-time history was recorded together with the strain-time history experienced by the specimens.

The viscoelastic models fitted to the creep/recovery data were then used to predict the response of the specimen to the load pulses applied in the dynamic

tests. The comparison of predicted versus measured strain-time histories was used to select the best constitutive model to explain the dynamic soil behavior.

8.2 CONCLUSIONS

The specimens tested were prepared from a stock of soil suspension consisting of approximately 33% clay size particles and 67 % of silt size particles. The liquid limit of the soil was approximately 60% and the plasticity index 35%. The cation exchange capacity of the soil averaged 48.7 meq/100 gr. and the major mineral components included kaolinite, chlorite, quartz, mica, and smectite.

One of the major concerns of the present study was the possibility of preparing repeatable specimens, thus, permitting to test specimens of identical conditions in creep/recovery tests and in the dynamic triaxial equipment. Some differences between specimens became evident at the time of equilibration the specimen at a fixed soil suction. In this stage, specimens apparently subjected to identical treatment and conditions resulted in different behavior pertaining to the release or absorption of water during this phase and, then, ended up with water contents of the specimen that in some cases were noticeably different.

The only difference observed in these specimens is some variability of the particle make up indicated by the results of hydrometer analysis. These results suggest a maximum difference of about 5% in the grain size distribution curve. This fact appears to indicate that the specimen preparation steps to be concerned with include the sampling of the soil suspension stock and the mixing operation of the

centrifuge cakes. Nevertheless, the majority of specimens fell in what normally would be considered a very narrow range of moisture contents.

For a series of specimens equilibrated at 40 psi soil suction, it was possible to perform repetitions for identical test conditions. This was meant to illustrate test variability. These results showed creep strain changes by a factor of two for specimens with water contents ranging in a half a percentage point to a full percentage point. Two specimens (numbers 14 and 38) exhibited very similar behavior and their water contents differed only in a tenth of a percentage point. These results suggests that it is necessary to reproduce the water contents of the specimens in a much narrower range than it was achieved in the present study. These differences in water content would be justified in view of the differences in particle make up of the specimens. In this fashion, larger percentages of clay particles would result in a larger affinity for water of the soil and could explain the higher moisture content left by the combined centrifugation and consolidation processes.

The results of the creep/recovery tests have been attempted to be explained using linear viscoelastic models. Specifically, the four parameter Burgers Model was fitted to the transient and steady state creep phase. The fitting process was implemented by non-linear regression of the laboratory data. The dependence of the model parameters on deviatoric stress level was found not to be linear and, thus, the model developed turned out to be non-linear viscoelastic. This model fits exceedingly well the long term creep in the steady state creep phase, but it does

not match well the initial part of the transient creep phase.

A very good fit of the initial part of the transient creep phase was possible with power laws of time with the coefficient and exponent being functions of soil suction and applied deviatoric stress levels. No attempt has been made to generalize the dependence of these parameters on soil suction due to the small number of soil suction levels tested. The exponent has been assumed to depend on deviatoric stress level through a linear relationship. The coefficient has been assumed to depend on deviatoric stress level through a power law of deviatoric stress and also through an exponential function of deviatoric stress level.

The two alternatives considered for the coefficient of the power law have some advantages and some disadvantages. There is not one alternative that is a clear cut choice. A comparison is documented that shows the predictions of the model together with the results of the actual creep tests. In some cases the differences are considerable. At this stage, it is not clear whether these differences can be attributed to an inadequate stress function or that the results of the individual creep test are not representative.

These considerations illustrate the need to develop a much larger data base of creep/recovery tests with several repetitions for each set of test conditions. This would allow the selection of a stress function with a much higher confidence level. Furthermore, the extension of the range and number of soil suction levels would permit the definition of the dependence of the model parameters on soil suction level.

Several repetitions were performed for each dynamic test . The repeatability of these tests seems to be better than for the results of the creep/ recovery tests. The measured strain-time histories of these specimens was compared to the predictions based on the several non-linear viscoelastic models fitted to the creep tests. The best alternative constitutive model was a power law of time with a coefficient being a power law of the deviatoric stress level. This model can predict quite approximately the behavior of the specimens at low deviatoric stress levels, and specially can explain the plastic strain remaining for the specimens after the application of a load pulse.

The main shortcoming of the model is that it over predicts, by a factor ranging from two to three, the peak strains in the vicinity of the peak of the stress pulse. Although some of this disagreement might be attributable to the selected stress function, there are reasons to believe that the testing methodology could account for a sizeable portion of the difference. Specifically, the friction and inertia forces introduced by the push rod might be responsible of the major part of the differences in strain levels predicted and measured.

Although it cannot be categorically stated, there are reasons to believe that the results of creep tests can be used advantageously to predict the behavior of specimens subjected to high strain rates. Nevertheless, this would require to use constitutive models appropriate for the test conditions in such a manner that it can duplicate the no drainage conditions present in the high strain rate tests.

8.3 RECOMMENDATIONS

The specimen preparation steps need to be revised to impose a stricter control on the grain size distribution of the specimens. It appears that the process of sampling of the soil stock should be modified. At the same time, it is felt that the steps of consolidation of the soil stock and the equilibration to a soil suction level should be somewhat extended in order to better ensure that the same point has been reached for each specimen. The drawback is that these processes already take up a considerable amount of time. These times have been cut to the minimum lengths in the present study to allow the preparation of enough specimens for the creep/recovery tests and the dynamic tests.

The repeatability of specimens documented in the present study suggests the need to perform several repetitions for each combination of test conditions. This would be intended to provide statistical evidence to select average values with a higher level of confidence. It is also evident that the number of soil suction levels to be tested should be increased to provide evidence about the form of the dependence of the model parameters on the soil suction level. These tasks would have consumed much longer time than it was available in the present study.

Relative to the dynamic tests at high strain rates there are two major areas that need improvement. One is relative to the stability of the test system, the second is related to the method of measurement of the loads imposed on the specimen. The testing system was not stable at high deviatoric stresses due to the large displacements than the actuator had to produce in short time intervals. This

resulted in excessive "ringing" of the load-time history and was also limiting the peak deviatoric stress that could be imposed on the specimen. The time span of 50 msec. of each load pulse was selected as a compromise to achieve some load pulses approximately resembling the desired ramp-up and ramp-down.

The testing system can be definitely improved with a larger servovalve that would permit a larger flow rate towards the actuator and, thus, allow for a faster response of the system. Additionally, the use of an smaller capacity load cell would reduce considerably the noise levels.

The second area that needs improvement is related to the calibration and/or elimination of friction at the bushing where the push rod penetrates into the triaxial cell. The safest approach would consists of placing the load cell inside the triaxial cell. In this manner, the friction on the rod would not take place between the load cell and the specimen and, thus, would not influence the load cell record. Furthermore, this approach would also results in the reduction of the mass of the push rod between the load cell and the specimen, thus, reducing the inertia forces that might affect the load cell record.

REFERENCES

1. Abdel-Hady, M. and Herrin, M., "Characteristics of Soil-Asphalt as a Rate Process," Journal of the Highway Division, Proceedings of the American Society of Civil Engineers, Vol. 92, No. HW1, March 1966, pp. 49-69.
2. Aitchison, G. D., "Some Preliminary Studies of Unsaturated Soils," Second Australia-New Zealand Conference Soil Mechanics and Foundation Engineering, pp. 173-204, 1956.
3. Aitchison, G. D., and Richards, B. G., "A Broad Scale Study of Moisture Conditions in Pavement Subgrades throughout Australia, Part 4." Moisture Equilibria and Moisture Changes in Soils Beneath Covered Areas, A Symposium in Print, Butterworths, Australia, 1965.
4. Christensen, R.W. and Wu, T.H., "Analysis of Clay Deformation as a Rate Process," Journal of the Soil Mechanics and Foundations Division, Proceedings of the American Society of Civil Engineers, Vol. 90, No. SM6, November 1964, pp. 125-157.
5. Conway, J.B., "Numerical Methods for Creep and Rupture Analysis," Gordon and Breach, Inc., New York.
6. Findley, W.N., Lai, J.S. and Onaran, K., "Creep and Relaxation of Nonlinear Viscoelastic Materials," North-Holland Publishing Company, 1976.
7. Fredlund, D.G., "A Diffused Air Volume Indicator for Unsaturated Soils," Canadian Geotechnical Journal, Vol. 12, No. 4, 1975, pp. 533-539.

8. Fredlund, D.G., "Appropriate Concepts and Technology for UnsaturatedSoils, "Second Canadian Geotechnical Colloquium, Canadian Geotechnical Journal, Vol. 16, No. 1, 1979, pp. 121-139.

9. Fredlund, D.G. and Morgenstern, N.R., "Stress State Variables for Unsaturated Soils," Journal of the Geotechnical Engineering, Vol. 103, No. GT5, May 1977, pp. 447-467.

10. Fredlund, D.G., Morgenstern, N.R. and Widger, R.A., "The Shear Strength of Unsaturated Soils," Canadian Geotechnical Journal, Vol. 15, No. 3, August 1978, pp. 313-321.

11. Gan, K.J. and Fredlund, D. G., "Multistage Direct Shear Testing of Unsaturated Soils," Geotechnical Testing Journal, GTJODL, Vol. 11, No. 2, June 1988, pp. 132-138.

12. Geyze, E. and Tan, T.K., "The Mechanical Behavior of Clays," Proceedings, 2nd International Congress of Rheology, Oxford, 1953, pp. 247-259.

13. Ho, D.Y.F. and Fredlund, D. G., "A Multistage Triaxial Test for Unsaturated Soils," Geotechnical Testing Journal, GTJODJ, Vol. 5, No. 1/2, March/June 1982, pp. 18-25.

14. Kavazanjian, E.Jr. and Mitchell, J.K., "Time-Dependent Deformation Behavior of Clays," Journal of the Geotechnical Engineering Division, Proceedings of the American Society of Civil Engineers, Vol. 106, No. GT6, June 1980, pp. 611-630.

15. Komamura, F. and Huang, R.J., "New Rheological Model for Soil Behavior," Journal of the Geotechnical Engineering Division, Proceedings of the American Society of Civil Engineers, Vol. 100, No. GT7, July 1974, pp. 807-824.

16. Mitchell, J.K., "Shearing Resistance of Soils as a Rate Process," Journal of the Soil Mechanics and Foundations Division, Proceedings of the American Society of Civil Engineers, Vol. 90, No. SM1, January 1964, pp. 29-61.

17. Mitchell, J.K., Campanella, R.G. and Singh, A., "Soil Creep as a Rate Process," Journal of the Soil Mechanics and Foundation Division, Proceedings of the American Society of Civil Engineers, Vol. 94, No. SM1, January 1968, pp. 231-253.

18. Murayama, S. and Shibata, T., "On the Rheological Characteristic of Clay, Part I," Bulletin No. 26, Disaster Prevention Research Institute, Kyoto University, Japan, 1958.

19. Murayama, S. and Shibata, T., "Rheological Properties of Clays," Proceedings, 5th International Congress on Soil Mechanics and Foundations, Paris, 1961, PP. 269-273.

20. Murayama, S. and Shibata, T., "Flow and Stress Relaxation of Clays (Theoretical Studies on the Rheological Properties of Clay-Part I)," Proceedings, Rheology and Soil Mechanics Symposium of the International Union of Theoretical and Applied Mechanics, Grenoble, France, April, 1964.

21. Peterson, R.W., "Interpretation of Triaxial Compression Test Results on Partially Saturated Soils," Advanced Triaxial Testing of Soil and Rock, ASTM STP 977, Robert T. Donahe, Ronald C. Chaney, and Marshall L. Silver, Eds., American Society for Testing and Materials, Philadelphia, 1988, pp. 512-538.

22. Shames, I.H. and Cozzarelli, F.A., "Elastic and Inelastic Stress Analysis," Prentice Hall, New Jersey, 1991.

23. Singh, A. and Mitchell, J.K., "General Stress-Strain-Time Function for Soils," Journal of Soil Mechanics and Foundations Division, Proceedings of the American Society of Civil Engineers, Vol. 94, No. SM1, January 1968, pp. 21-47.

APPENDIX A

RECORDS OF SPECIMEN CONSOLIDATION

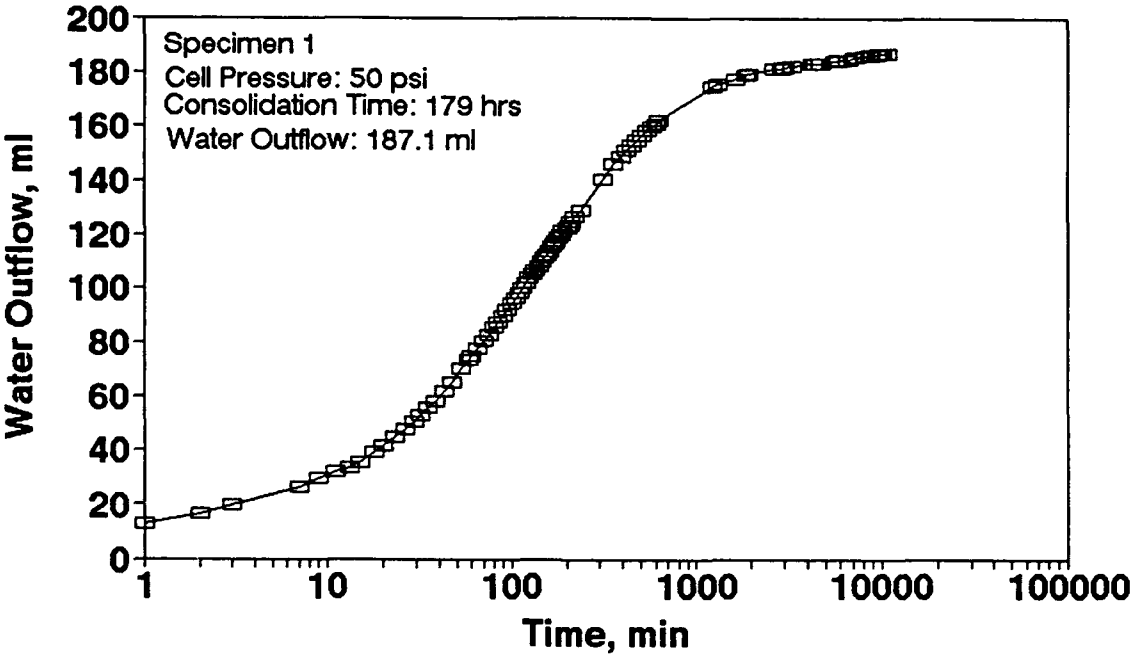
Specimen 1
Cell Pressure: 50 psi
Consolidation Time: 179 hrs
Water Outflow: 187.1 ml
Water Outflow, ml
200
180
160
140
120
100
80
60
40
20
0
1
10
100
1000
10000
100000
Time, min

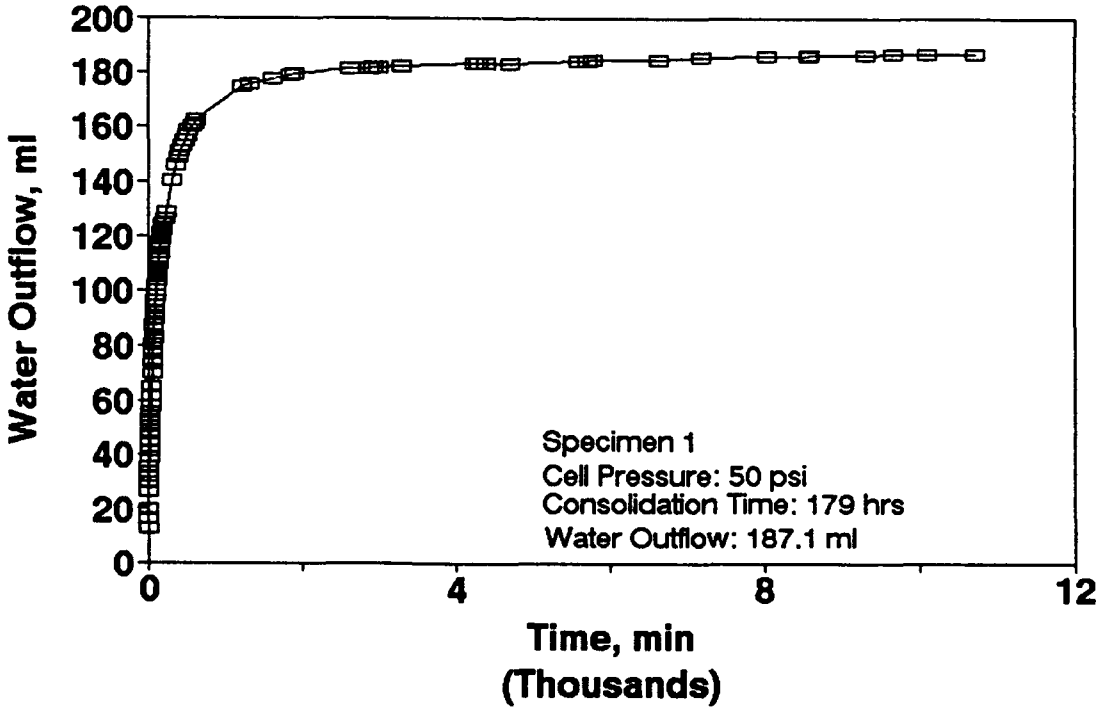
Water Outflow, ml
200
180
160
140
120
100
80
60
40
20
0
Specimen 1
Cell Pressure: 50 psi
Consolidation Time: 179 hrs
Water Outflow: 187.1 ml
0
4
8
12
Time, min
(Thousands)

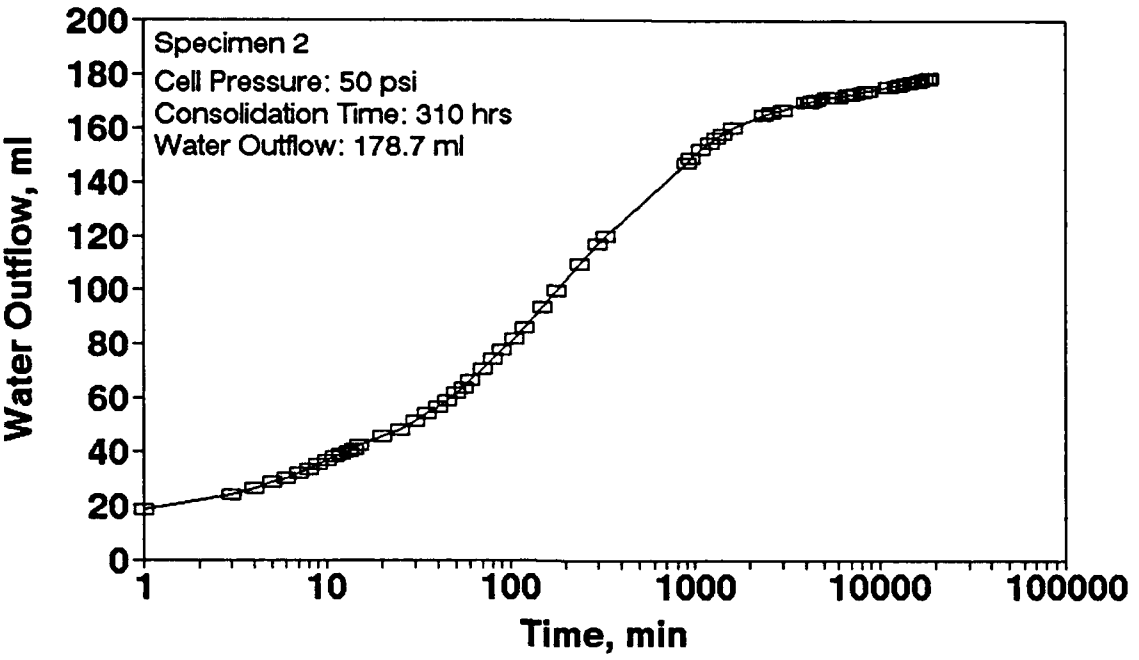
Specimen 2
Cell Pressure: 50 psi
Consolidation Time: 310 hrs
Water Outflow: 178.7 ml
Water Outflow, ml
Time, min
0
20
40
60
80
100
120
140
160
180
200
1
10
100
1000
10000
100000

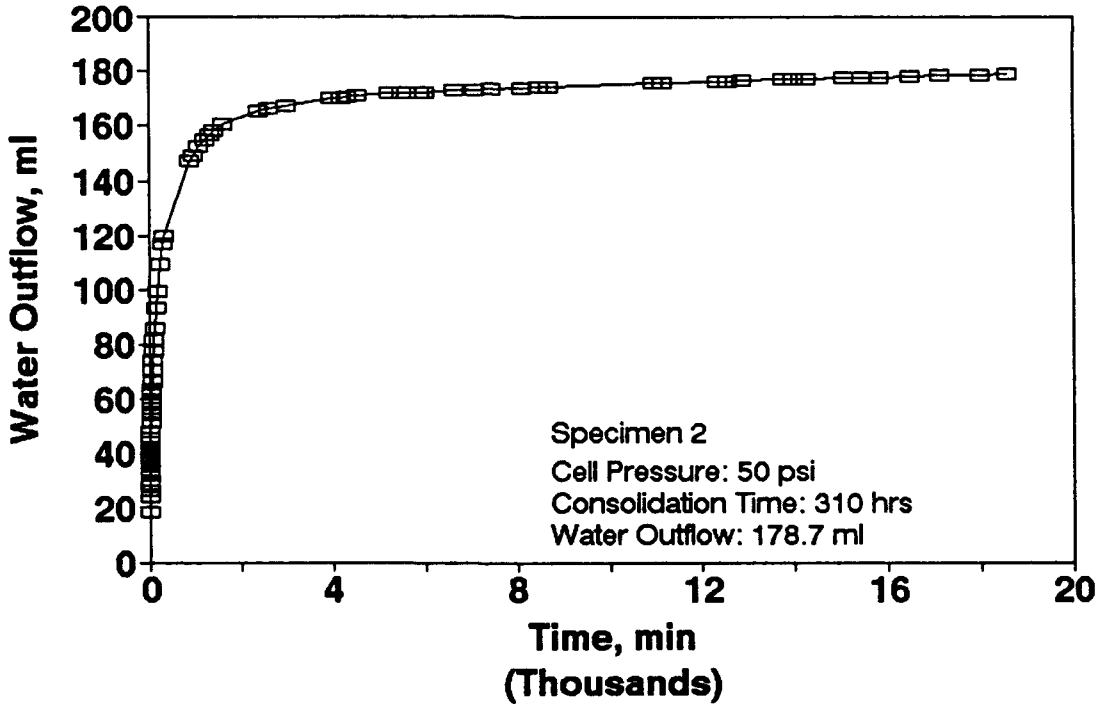
Specimen 2
Cell Pressure: 50 psi
Consolidation Time: 310 hrs
Water Outflow: 178.7 ml
Water Outflow, ml
Time, min
(Thousands)
0
20
40
60
80
100
120
140
160
180
200
0
4
8
12
16
20

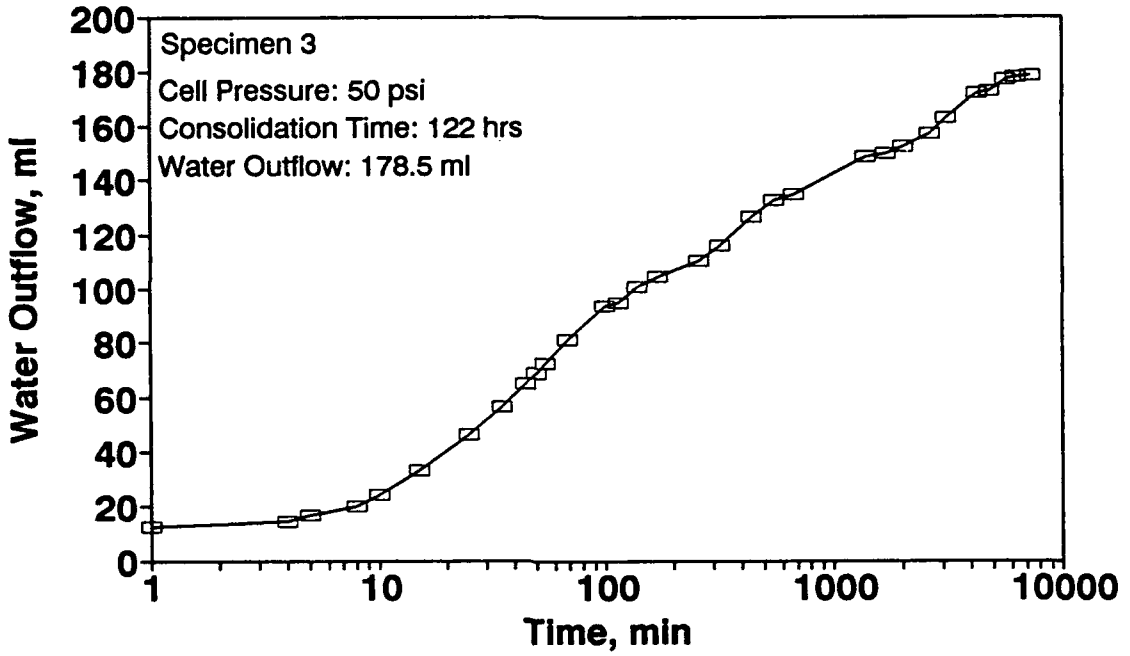
Specimen 3
Cell Pressure: 50 psi
Consolidation Time: 122 hrs
Water Outflow: 178.5 ml
Water Outflow, ml
Time, min
200
180
160
140
120
100
80
60
40
20
0
1
10
100
1000
10000

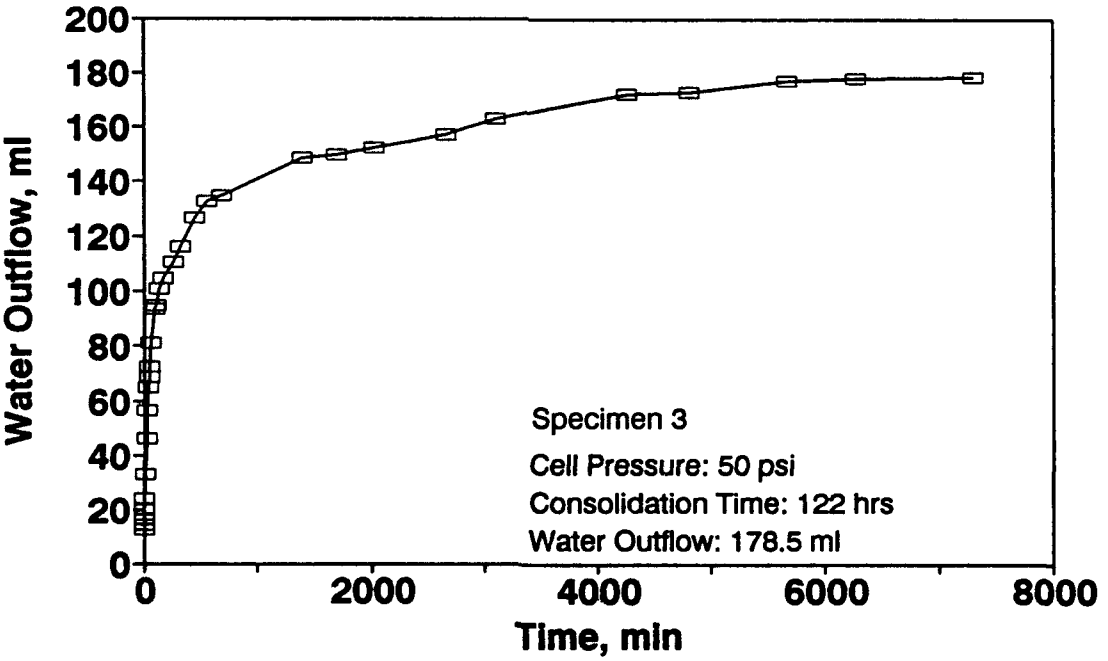
Specimen 3
Cell Pressure: 50 psi
Consolidation Time: 122 hrs
Water Outflow: 178.5 ml
Water Outflow, ml
Time, min
200
180
160
140
120
100
80
60
40
20
0
0
2000
4000
6000
8000

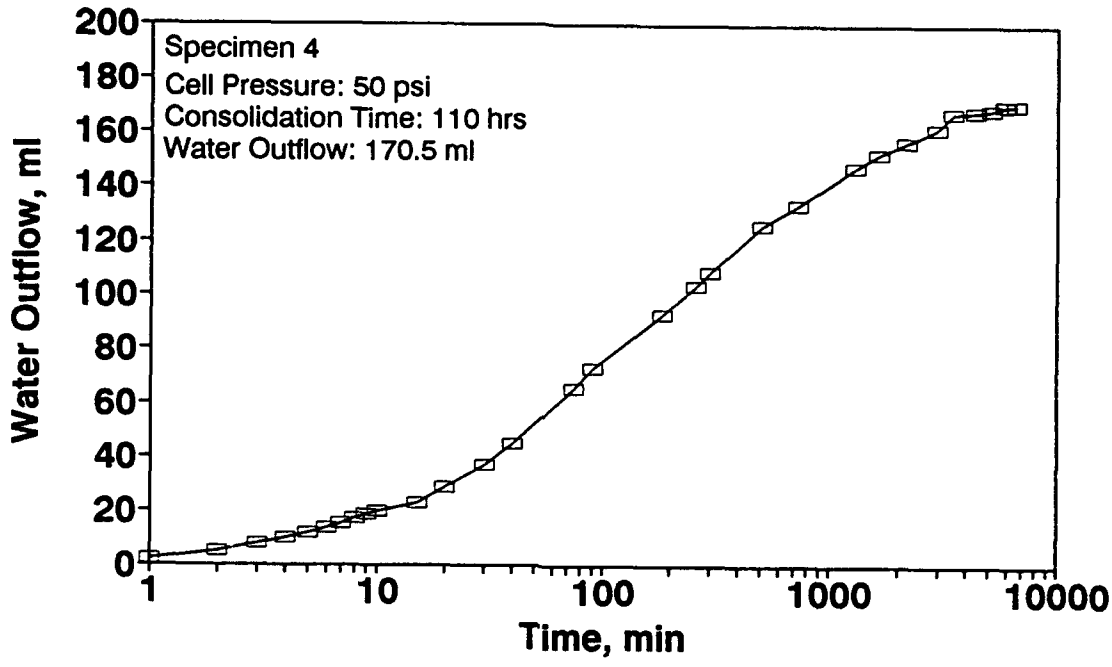
Specimen 4
Cell Pressure: 50 psi
Consolidation Time: 110 hrs
Water Outflow: 170.5 ml
Water Outflow, ml
Time, min
200
180
160
140
120
100
80
60
40
20
0
1
10
100
1000
10000

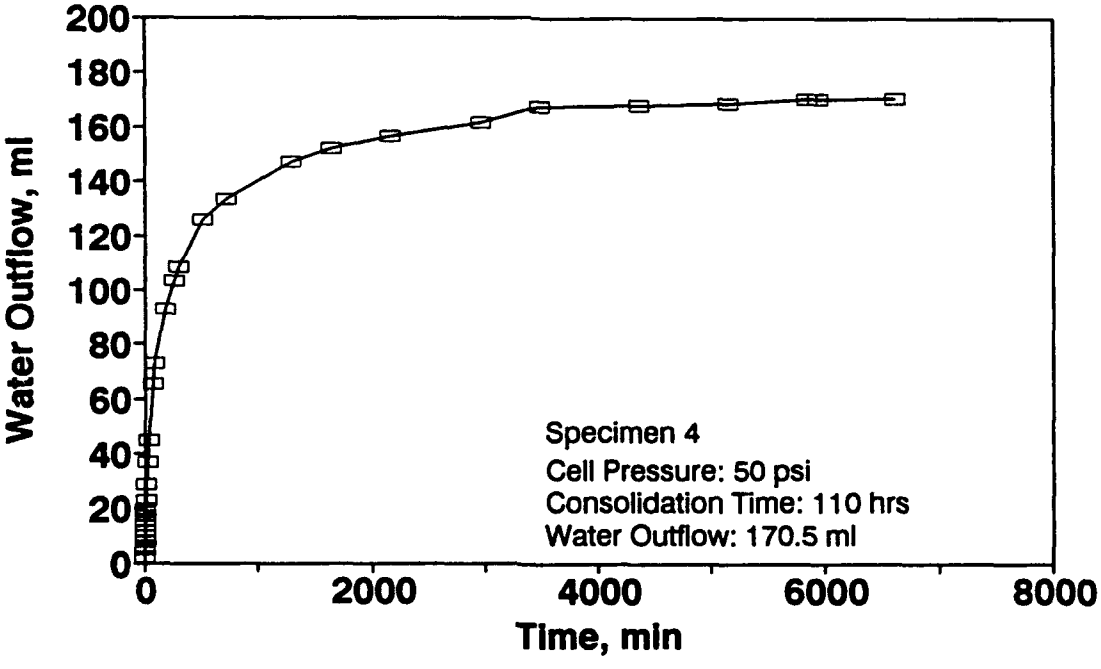
Specimen 4
Cell Pressure: 50 psi
Consolidation Time: 110 hrs
Water Outflow: 170.5 ml
Water Outflow, ml
Time, min
200
180
160
140
120
100
80
60
40
20
0
0
2000
4000
6000
8000

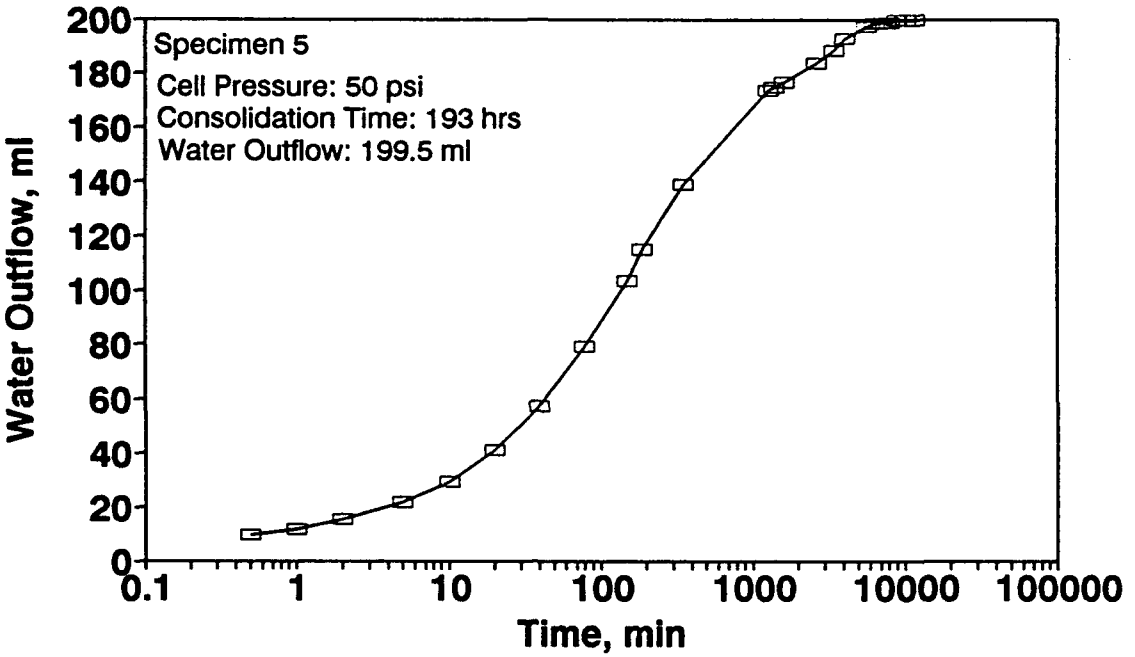
Specimen 5
Cell Pressure: 50 psi
Consolidation Time: 193 hrs
Water Outflow: 199.5 ml
Water Outflow, ml
200
180
160
140
120
100
80
60
40
20
0
0.1
1
10
100
1000
10000
100000
Time, min

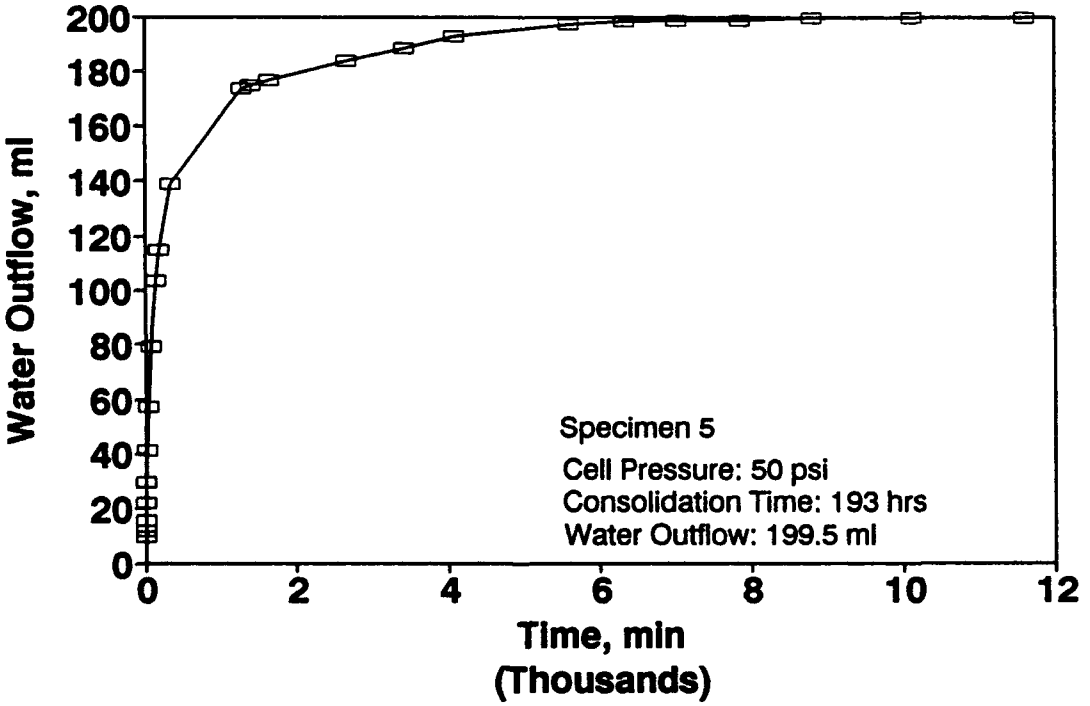
Water Outflow, ml
200
180
160
140
120
100
80
60
40
20
0
Specimen 5
Cell Pressure: 50 psi
Consolidation Time: 193 hrs
Water Outflow: 199.5 ml
0
2
4
6
8
10
12
Time, min
(Thousands)

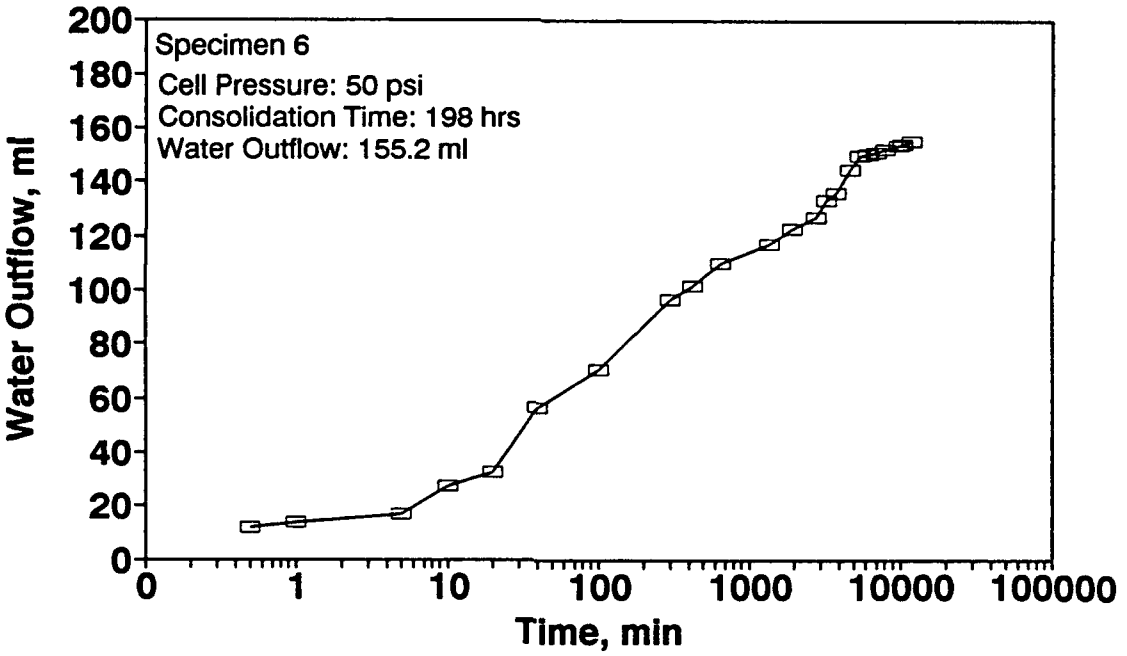
Specimen 6
Cell Pressure: 50 psi
Consolidation Time: 198 hrs
Water Outflow: 155.2 ml
Water Outflow, ml
200
180
160
140
120
100
80
60
40
20
0
0
1
10
100
1000
10000
100000
Time, min

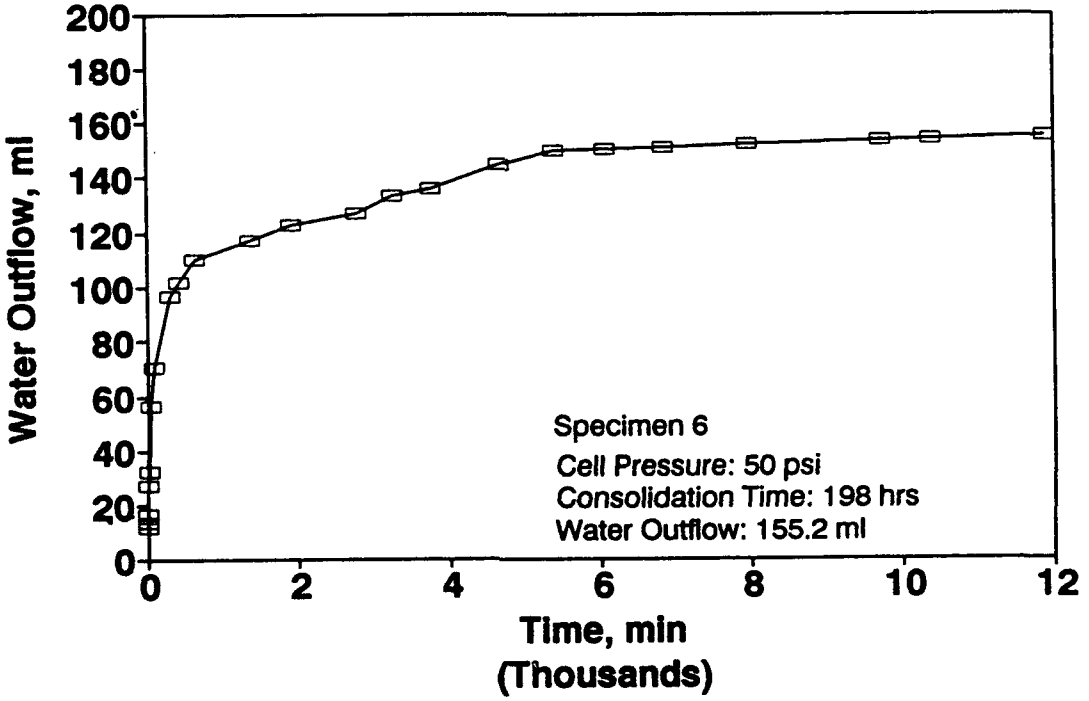
Water Outflow, ml
200
180
160
140
120
100
80
60
40
20
0
Specimen 6
Cell Pressure: 50 psi
Consolidation Time: 198 hrs
Water Outflow: 155.2 ml
0
2
4
6
8
10
12
Time, min
(Thousands)

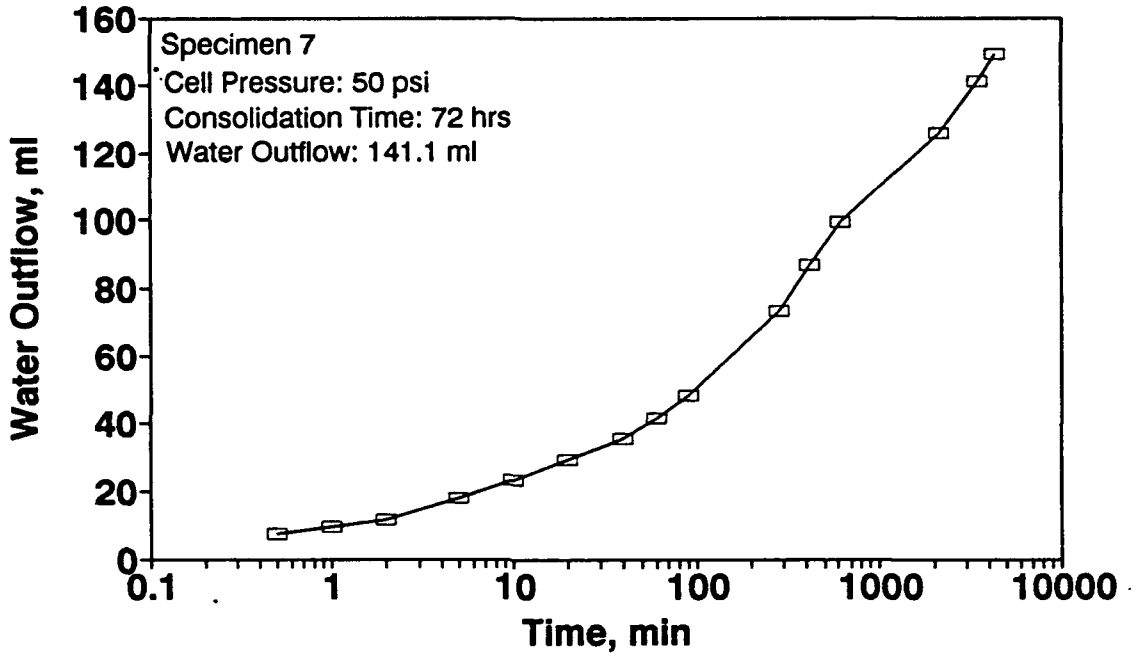
Specimen 7
Cell Pressure: 50 psi
Consolidation Time: 72 hrs
Water Outflow: 141.1 ml
Water Outflow, ml
160
140
120
100
80
60
40
20
0
0.1
1
10
100
1000
10000
Time, min

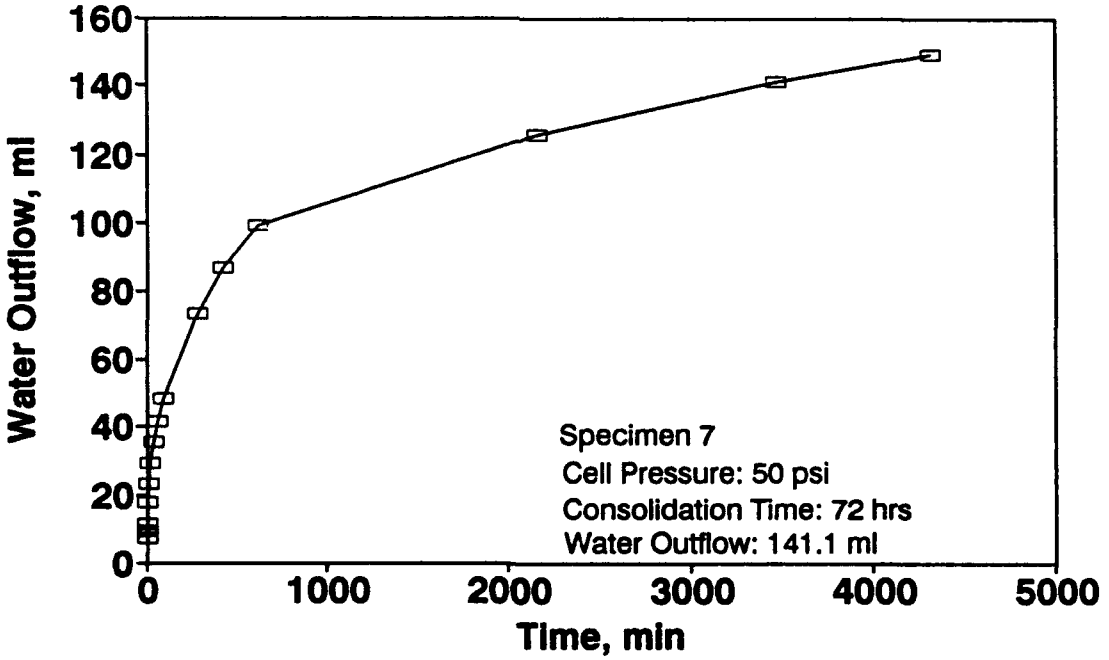
Water Outflow, ml
160
140
120
100
80
60
40
20
0
0
1000
2000
3000
4000
5000
Time, min
Specimen 7
Cell Pressure: 50 psi
Consolidation Time: 72 hrs
Water Outflow: 141.1 ml

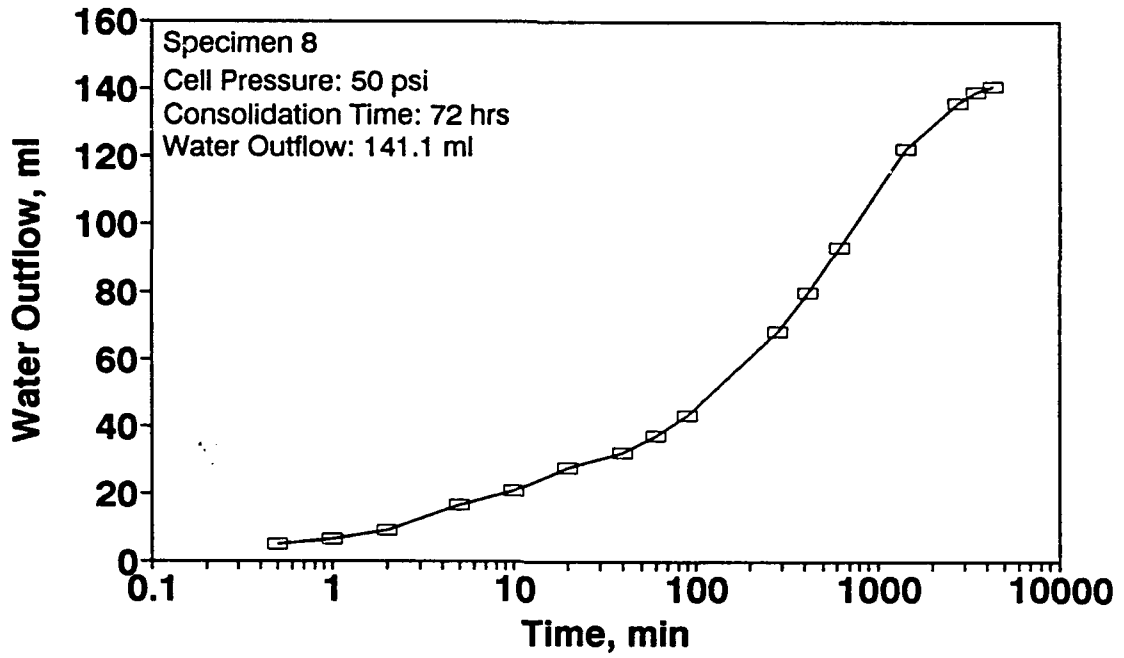
Specimen 8
Cell Pressure: 50 psi
Consolidation Time: 72 hrs
Water Outflow: 141.1 ml
Water Outflow, ml
Time, min
0
20
40
60
80
100
120
140
160
0.1
1
10
100
1000
10000

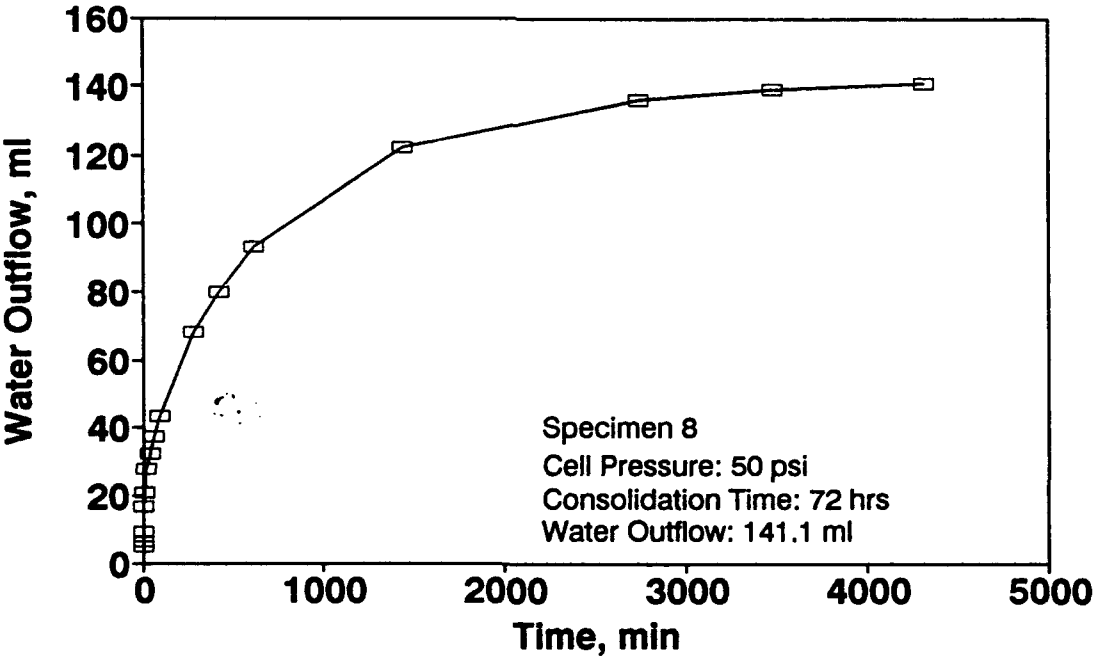
Specimen 8
Cell Pressure: 50 psi
Consolidation Time: 72 hrs
Water Outflow: 141.1 ml
Water Outflow, ml
Time, min
0
20
40
60
80
100
120
140
160
0
1000
2000
3000
4000
5000

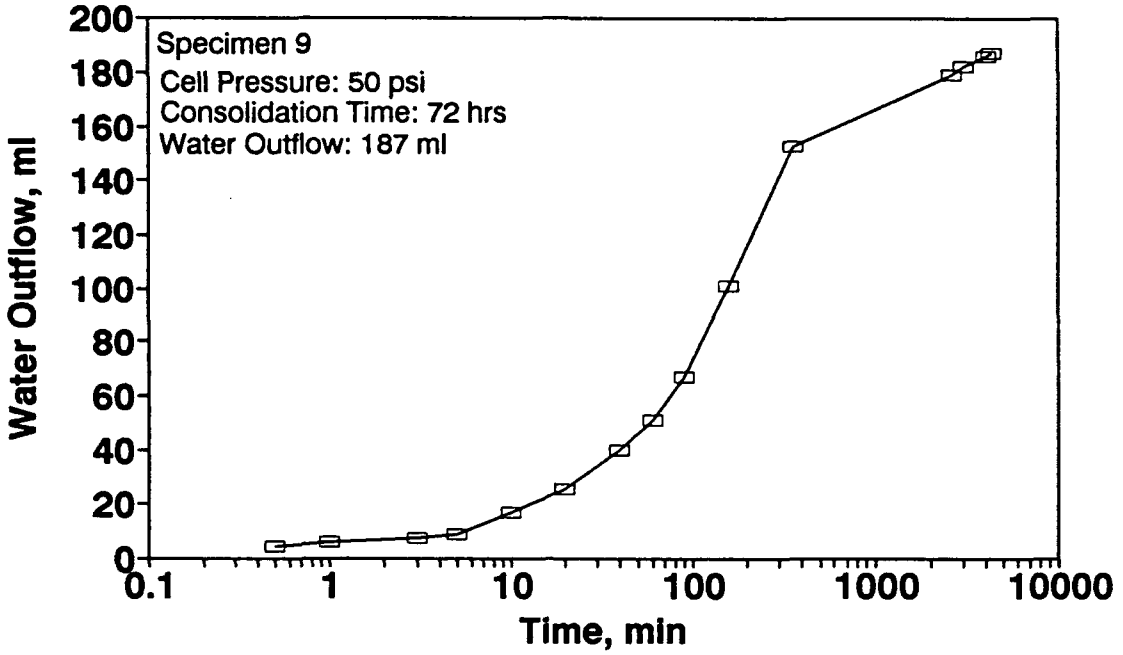
Specimen 9
Cell Pressure: 50 psi
Consolidation Time: 72 hrs
Water Outflow: 187 ml
Water Outflow, ml
Time, min
200
180
160
140
120
100
80
60
40
20
0
0.1
1
10
100
1000
10000

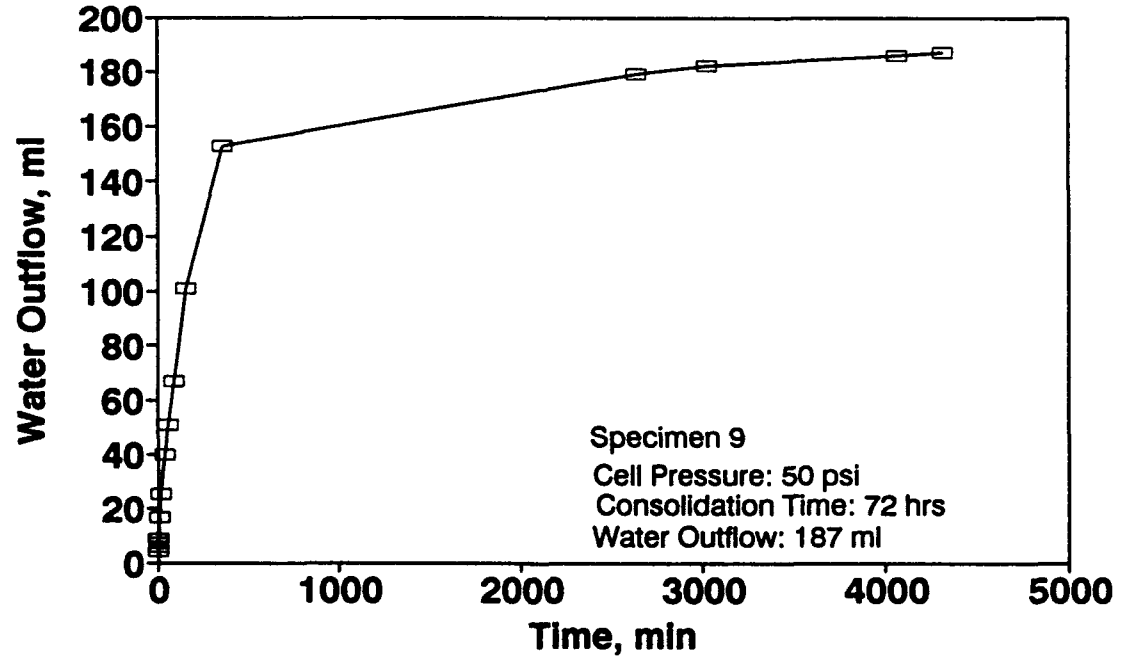
Specimen 9
Cell Pressure: 50 psi
Consolidation Time: 72 hrs
Water Outflow: 187 ml
Water Outflow, ml
Time, min
200
180
160
140
120
100
80
60
40
20
0
0
1000
2000
3000
4000
5000

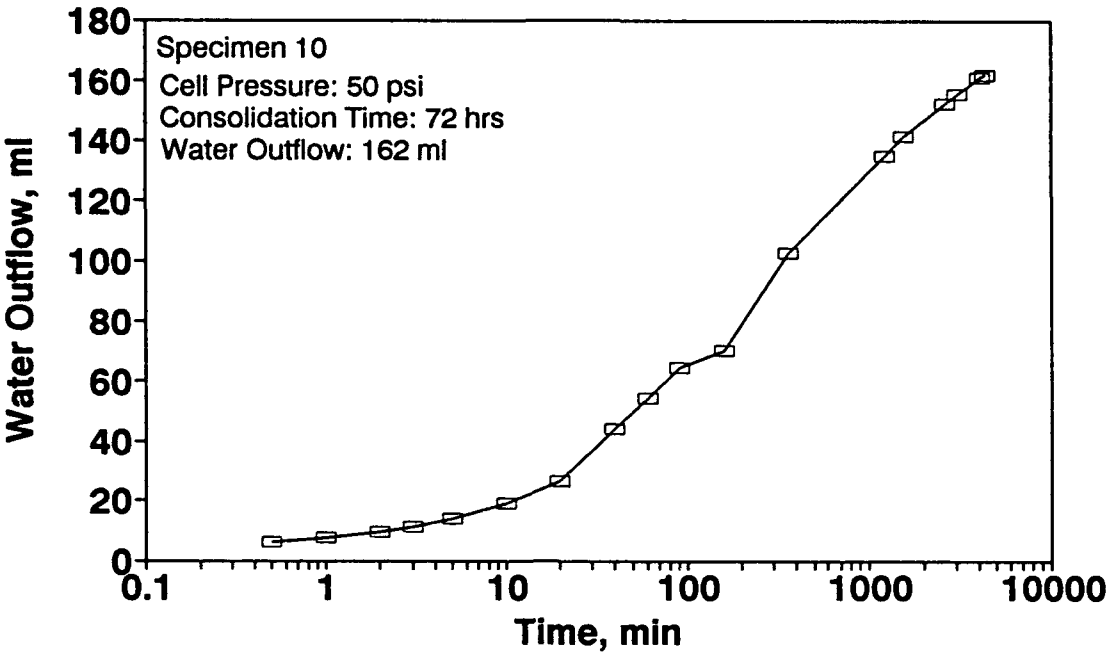
Specimen 10
Cell Pressure: 50 psi
Consolidation Time: 72 hrs
Water Outflow: 162 ml
Water Outflow, ml
Time, min
0
20
40
60
80
100
120
140
160
180
0.1
1
10
100
1000
10000

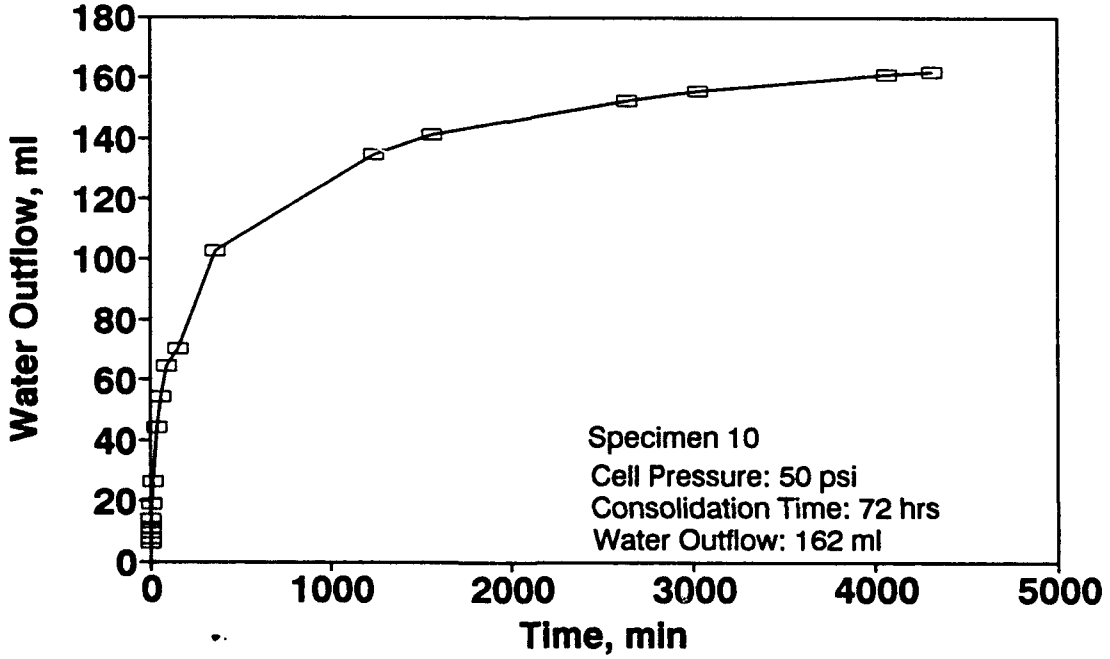
Specimen 10
Cell Pressure: 50 psi
Consolidation Time: 72 hrs
Water Outflow: 162 ml
Water Outflow, ml
Time, min
0
20
40
60
80
100
120
140
160
180
0
1000
2000
3000
4000
5000

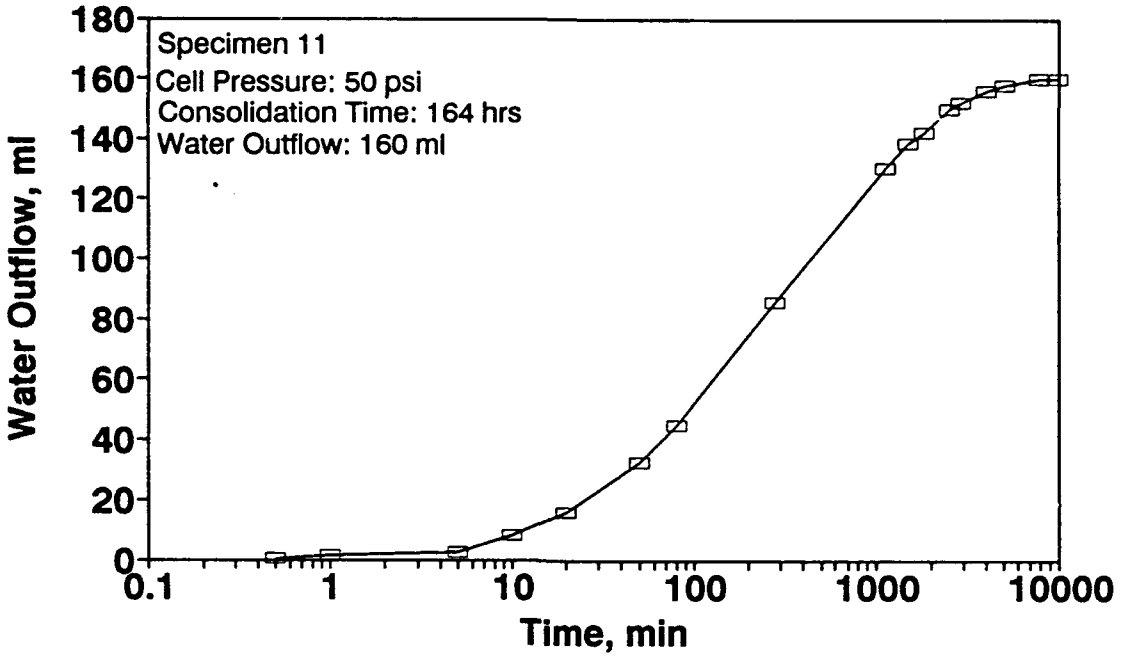
Specimen 11
Cell Pressure: 50 psi
Consolidation Time: 164 hrs
Water Outflow: 160 ml
Water Outflow, ml
Time, min
180
160
140
120
100
80
60
40
20
0
0.1
1
10
100
1000
10000

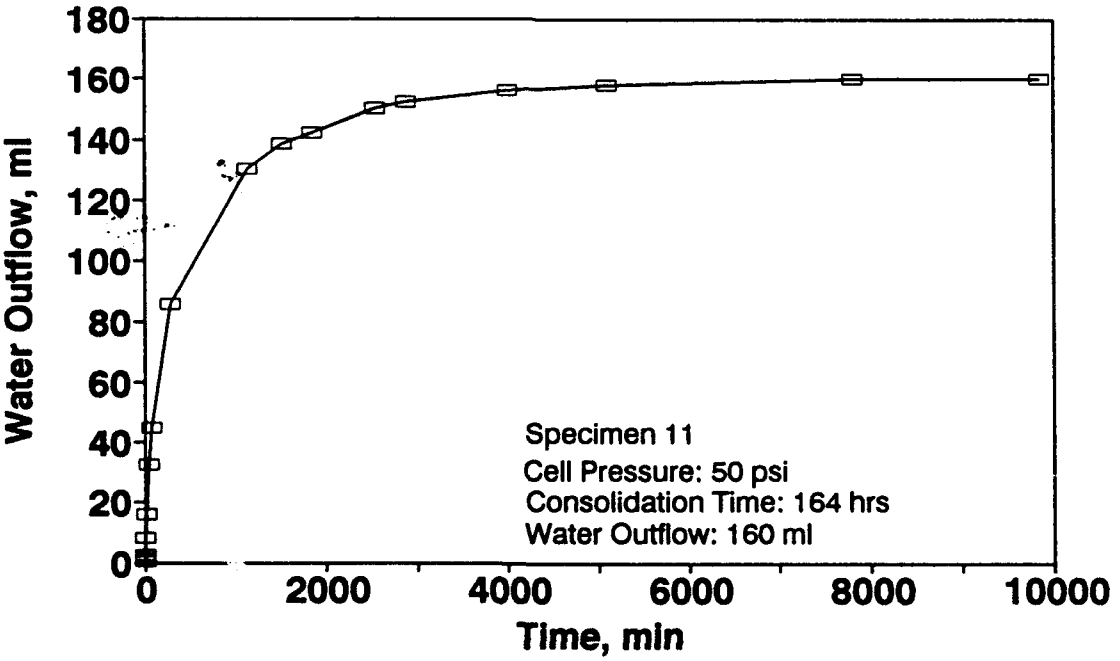
Specimen 11
Cell Pressure: 50 psi
Consolidation Time: 164 hrs
Water Outflow: 160 ml
Water Outflow, ml
Time, min
180
160
140
120
100
80
60
40
20
0
0
2000
4000
6000
8000
10000

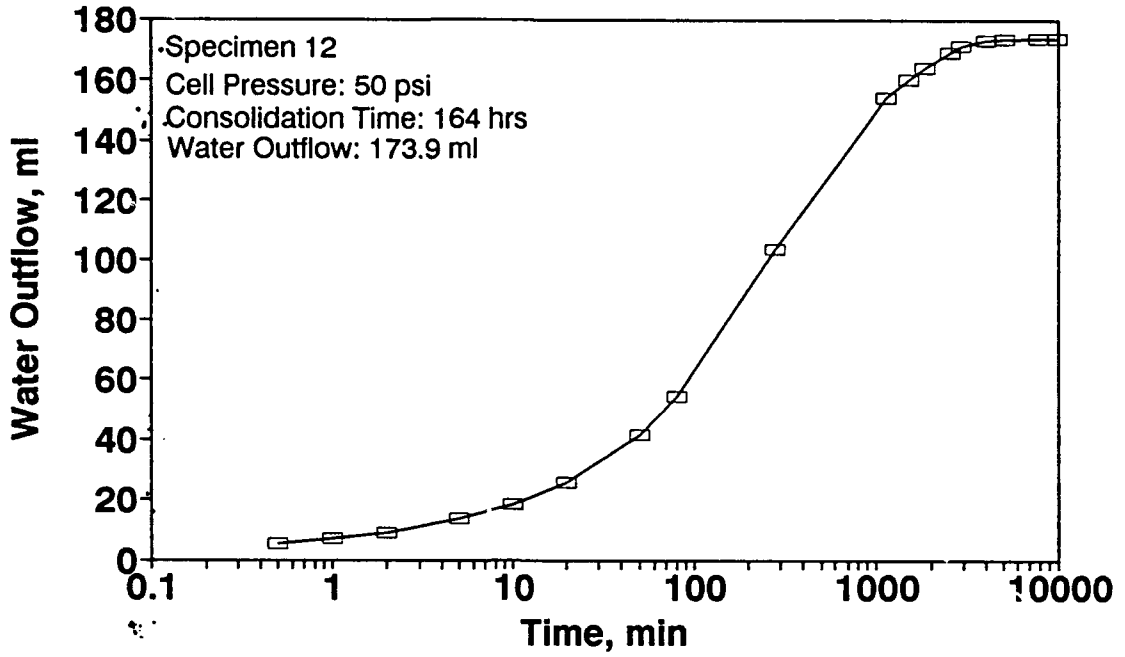
Specimen 12
Cell Pressure: 50 psi
Consolidation Time: 164 hrs
Water Outflow: 173.9 ml
Water Outflow, ml
Time, min
0
20
40
60
80
100
120
140
160
180
0.1
1
10
100
1000
10000

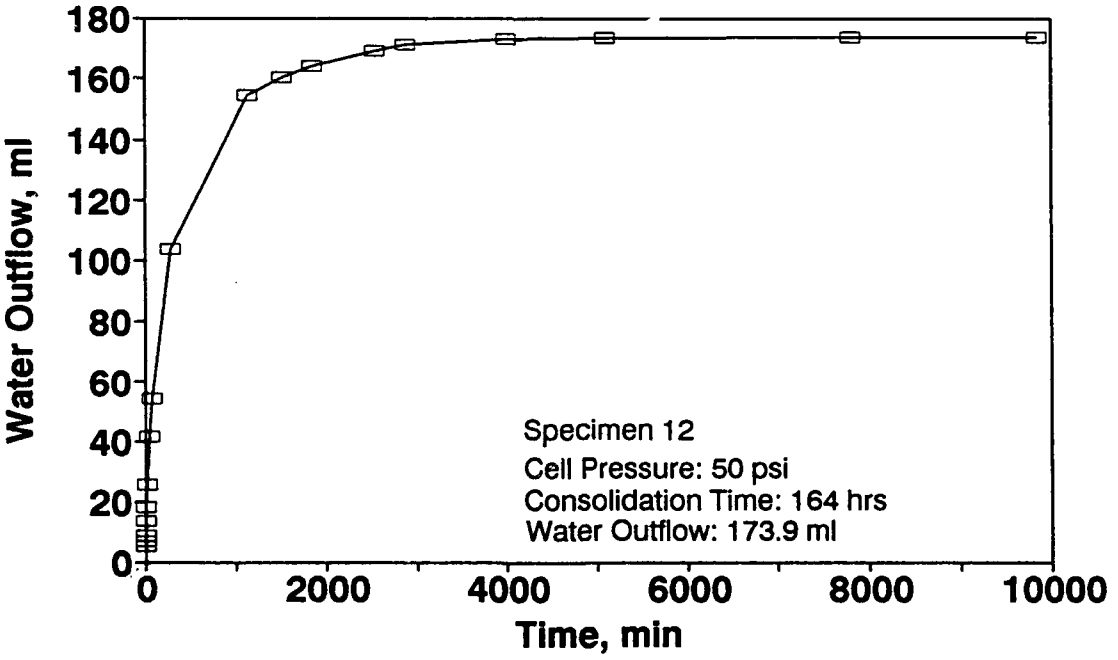
Specimen 12
Cell Pressure: 50 psi
Consolidation Time: 164 hrs
Water Outflow: 173.9 ml
Water Outflow, ml
Time, min
0
20
40
60
80
100
120
140
160
180
0
2000
4000
6000
8000
10000

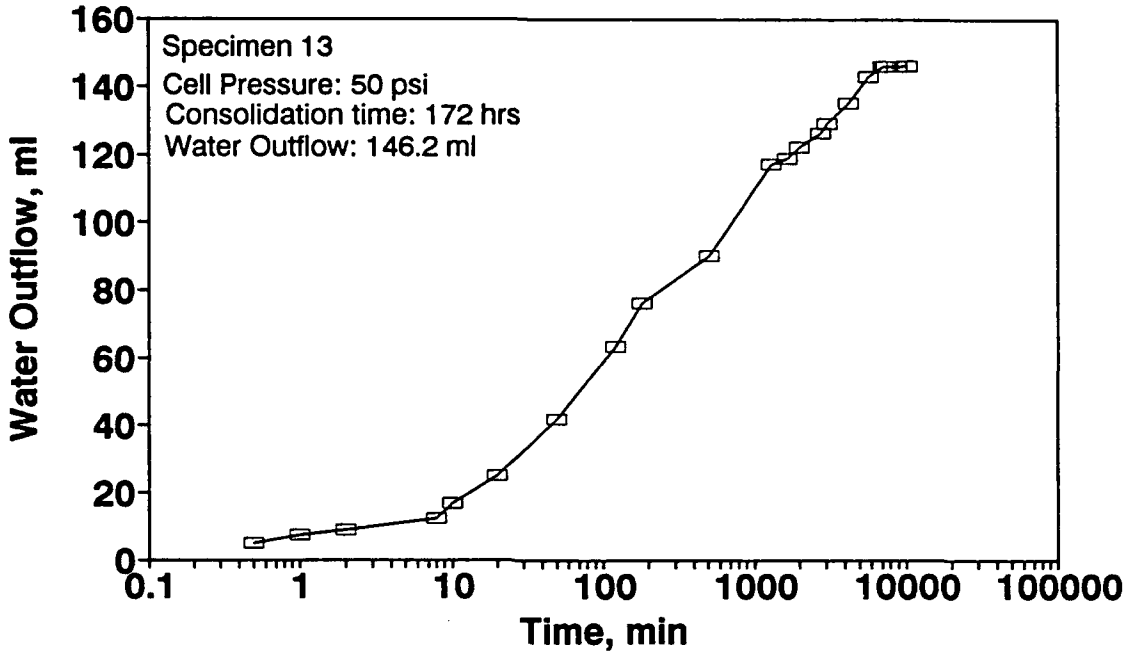
Specimen 13
Cell Pressure: 50 psi
Consolidation time: 172 hrs
Water Outflow: 146.2 ml
Water Outflow, ml
160
140
120
100
80
60
40
20
0
0.1
1
10
100
1000
10000
100000
Time, min

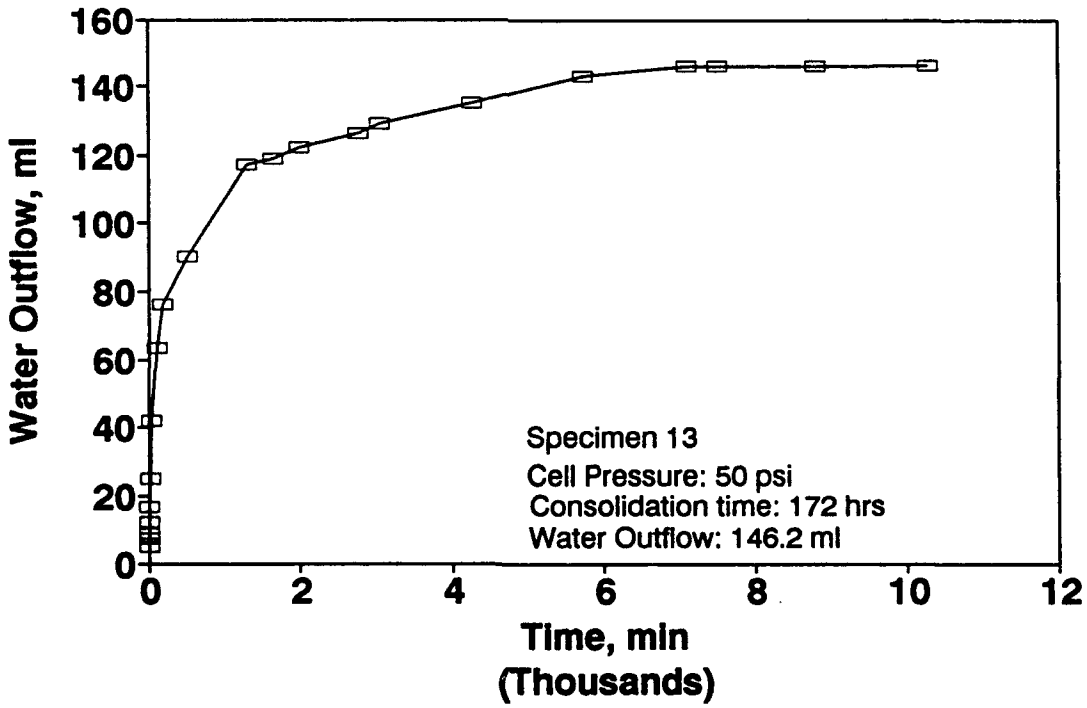
Water Outflow, ml
160
140
120
100
80
60
40
20
0
Specimen 13
Cell Pressure: 50 psi
Consolidation time: 172 hrs
Water Outflow: 146.2 ml
0
2
4
6
8
10
12
Time, min
(Thousands)

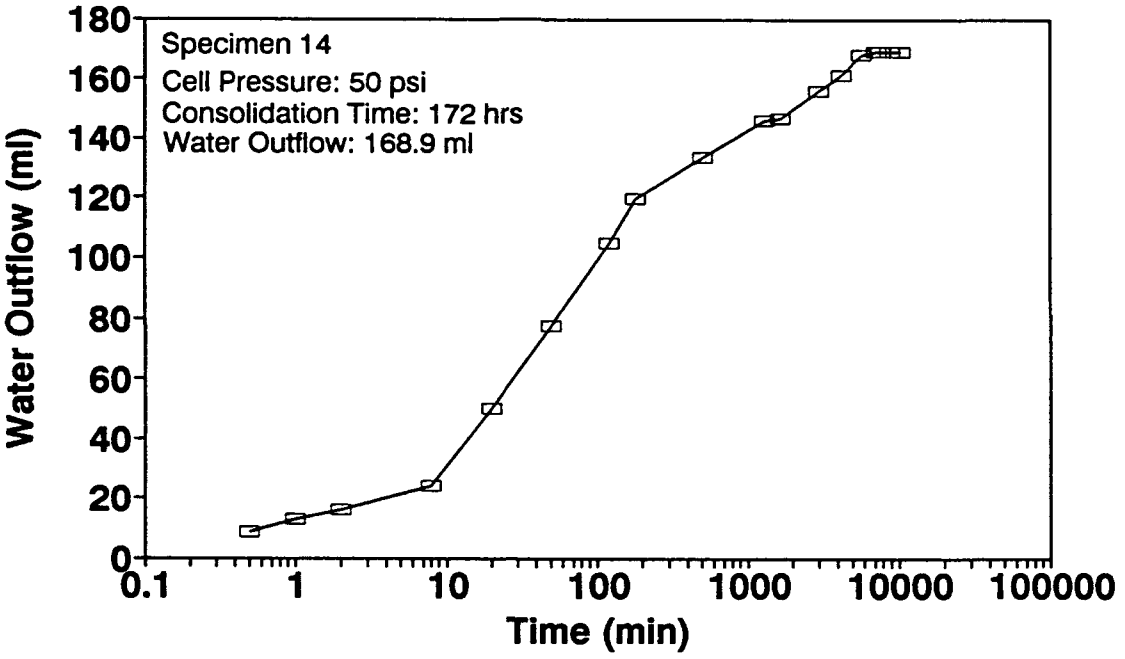
Specimen 14
Cell Pressure: 50 psi
Consolidation Time: 172 hrs
Water Outflow: 168.9 ml
Water Outflow (ml)
180
160
140
120
100
80
60
40
20
0
0.1
1
10
100
1000
10000
100000
Time (min)

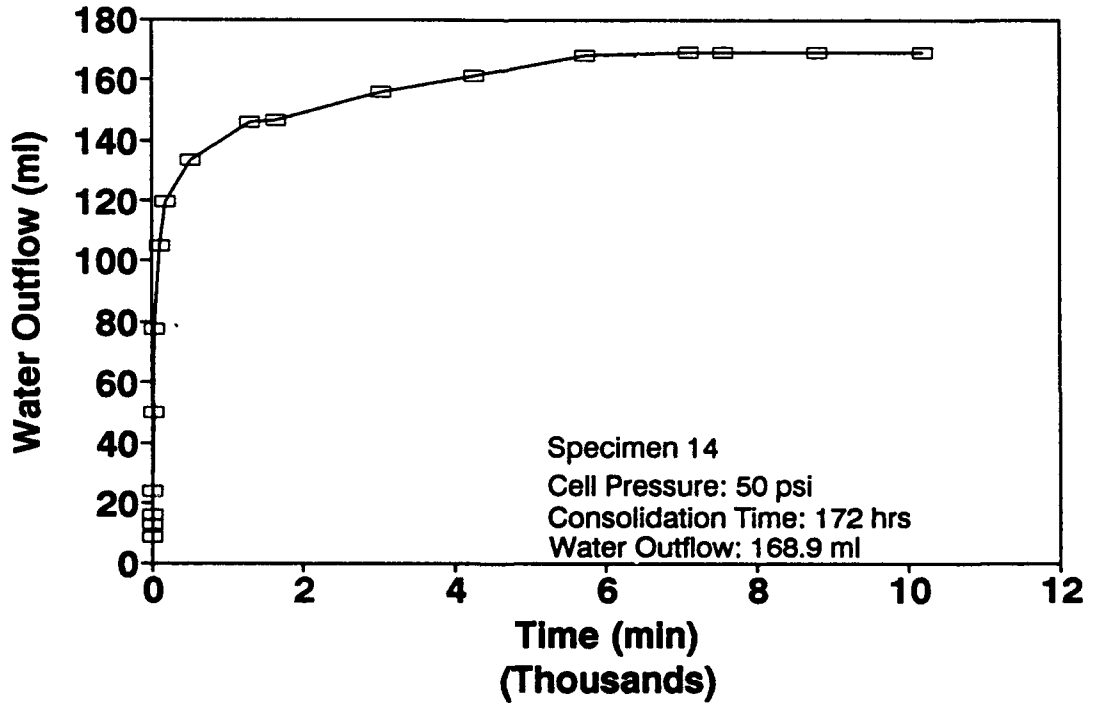
Water Outflow (ml)
180
160
140
120
100
80
60
40
20
0
Specimen 14
Cell Pressure: 50 psi
Consolidation Time: 172 hrs
Water Outflow: 168.9 ml
0
2
4
6
8
10
12
Time (min)
(Thousands)

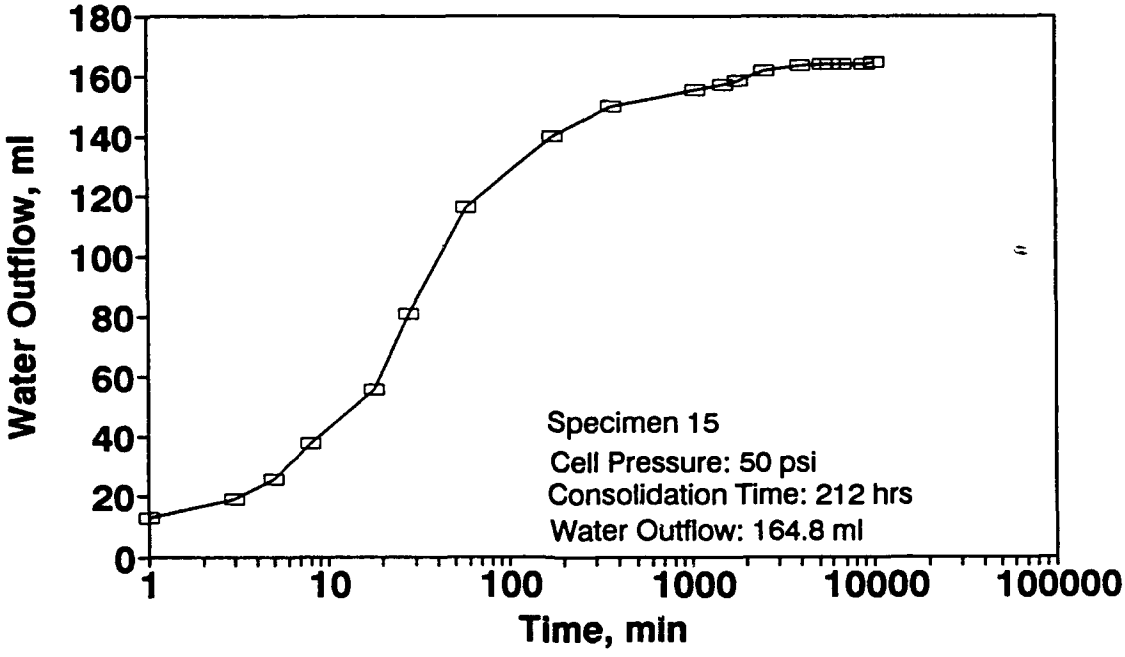
Water Outflow, ml
180
160
140
120
100
80
60
40
20
0
1
10
100
1000
10000
100000
Time, min
Specimen 15
Cell Pressure: 50 psi
Consolidation Time: 212 hrs
Water Outflow: 164.8 ml

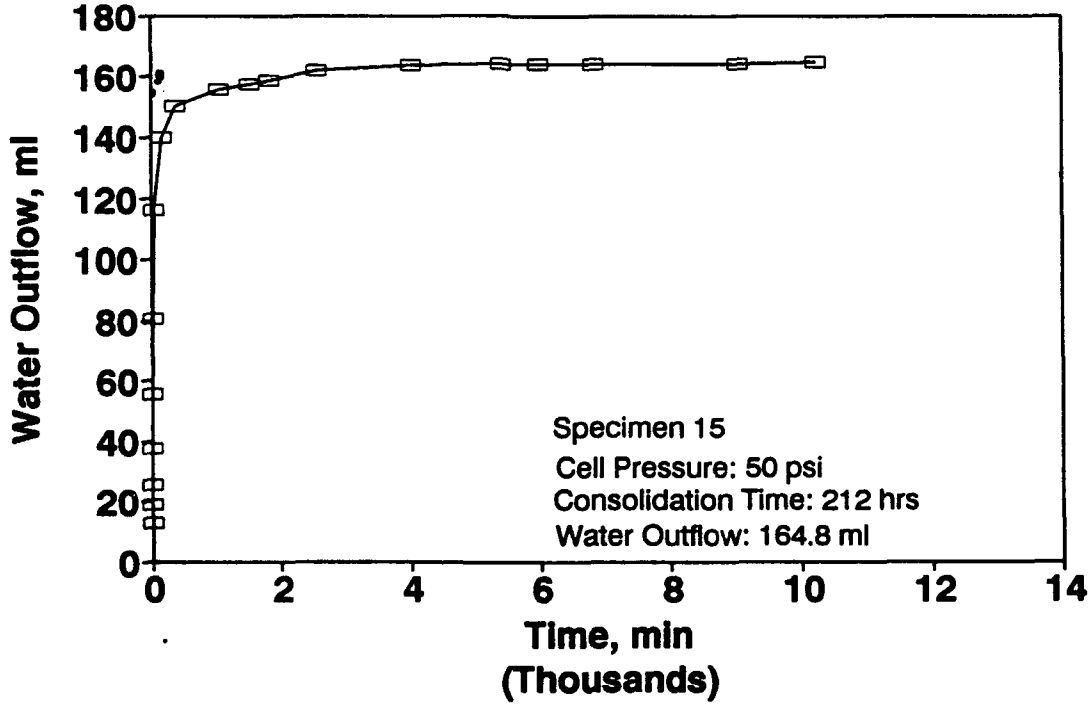
Water Outflow, ml
180
160
140
120
100
80
60
40
20
0
0
2
4
6
8
10
12
14
Time, min
(Thousands)
Specimen 15
Cell Pressure: 50 psi
Consolidation Time: 212 hrs
Water Outflow: 164.8 ml

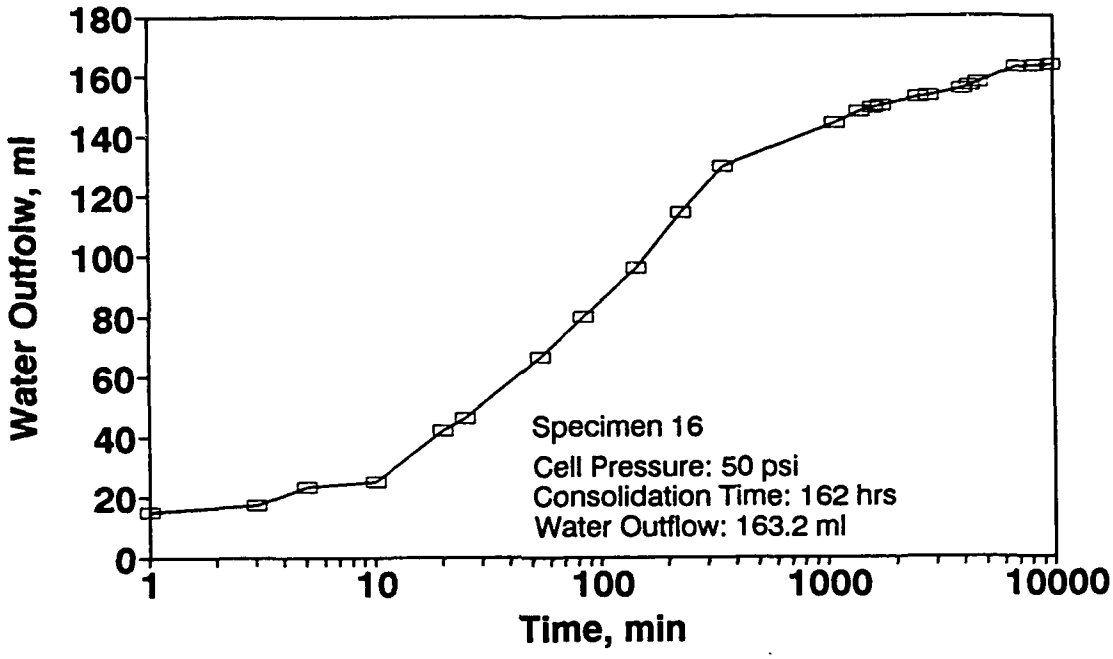
Water Outfolw, ml
180
160
140
120
100
80
60
40
20
0
1
10
100
1000
10000
Time, min
Specimen 16
Cell Pressure: 50 psi
Consolidation Time: 162 hrs
Water Outflow: 163.2 ml

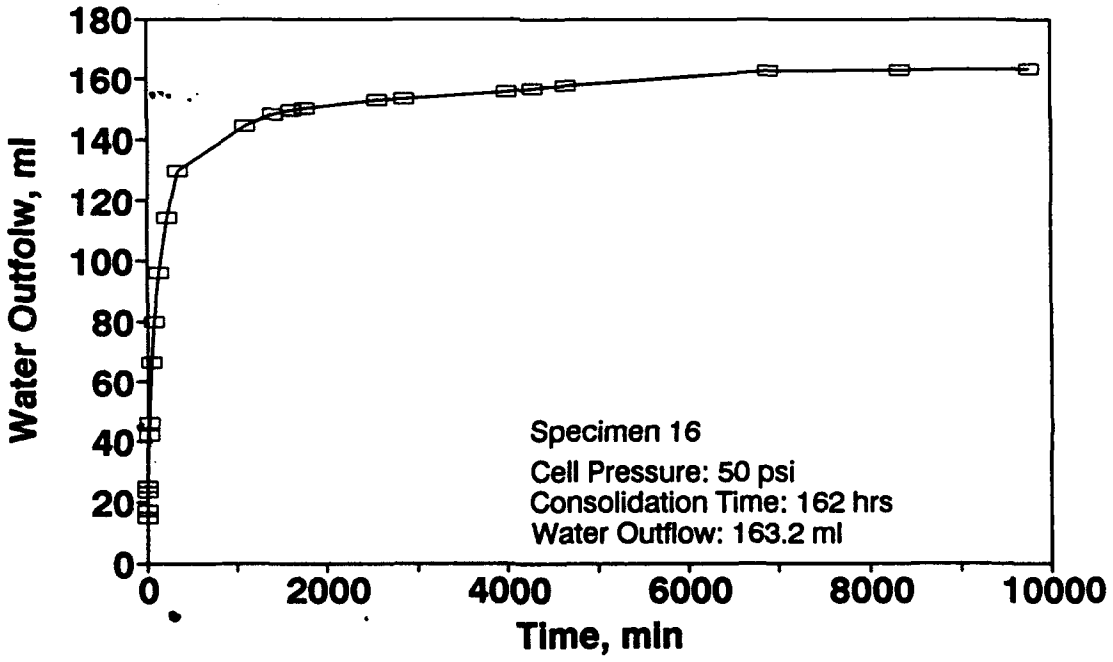
Water Outfolw, ml
180
160
140
120
100
80
60
40
20
0
0
2000
4000
6000
8000
10000
Time, min
Specimen 16
Cell Pressure: 50 psi
Consolidation Time: 162 hrs
Water Outflow: 163.2 ml

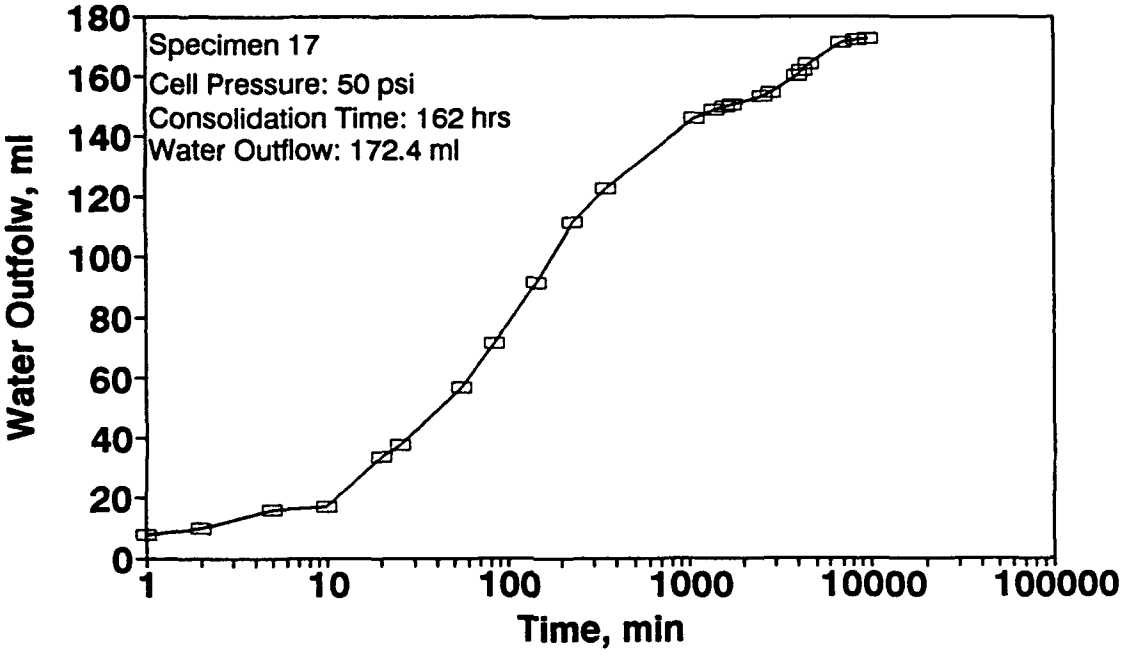
Specimen 17
Cell Pressure: 50 psi
Consolidation Time: 162 hrs
Water Outflow: 172.4 ml
Water Outfolw, ml
Time, min
0
20
40
60
80
100
120
140
160
180
1
10
100
1000
10000
100000

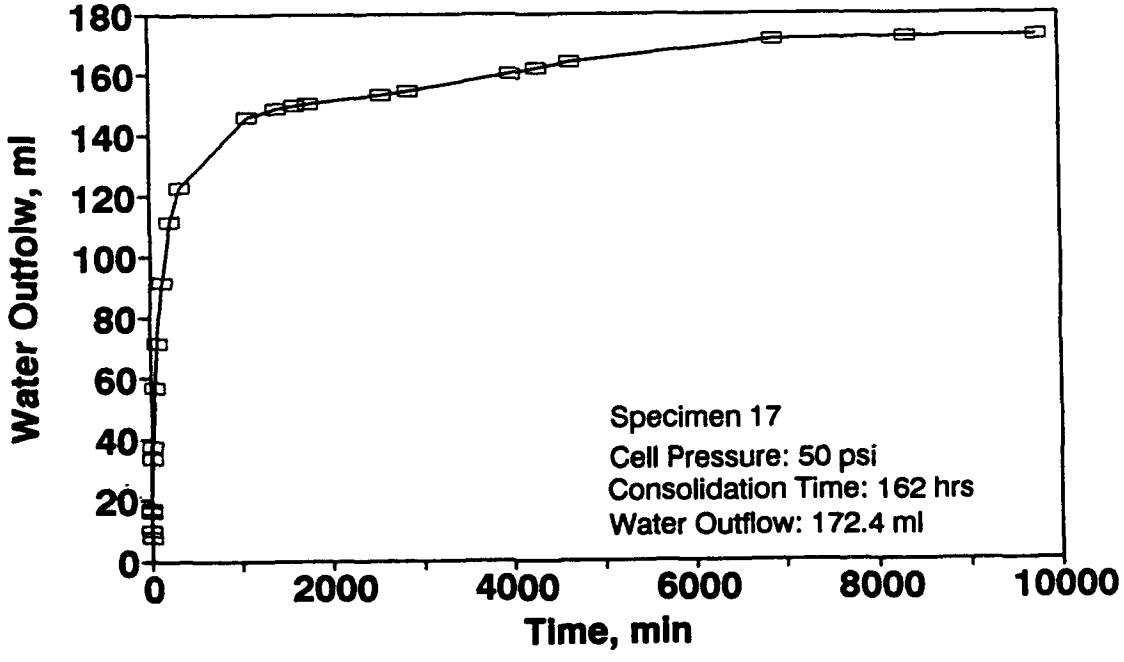
Specimen 17
Cell Pressure: 50 psi
Consolidation Time: 162 hrs
Water Outflow: 172.4 ml
Water Outfolw, ml
Time, min
0
20
40
60
80
100
120
140
160
180
0
2000
4000
6000
8000
10000

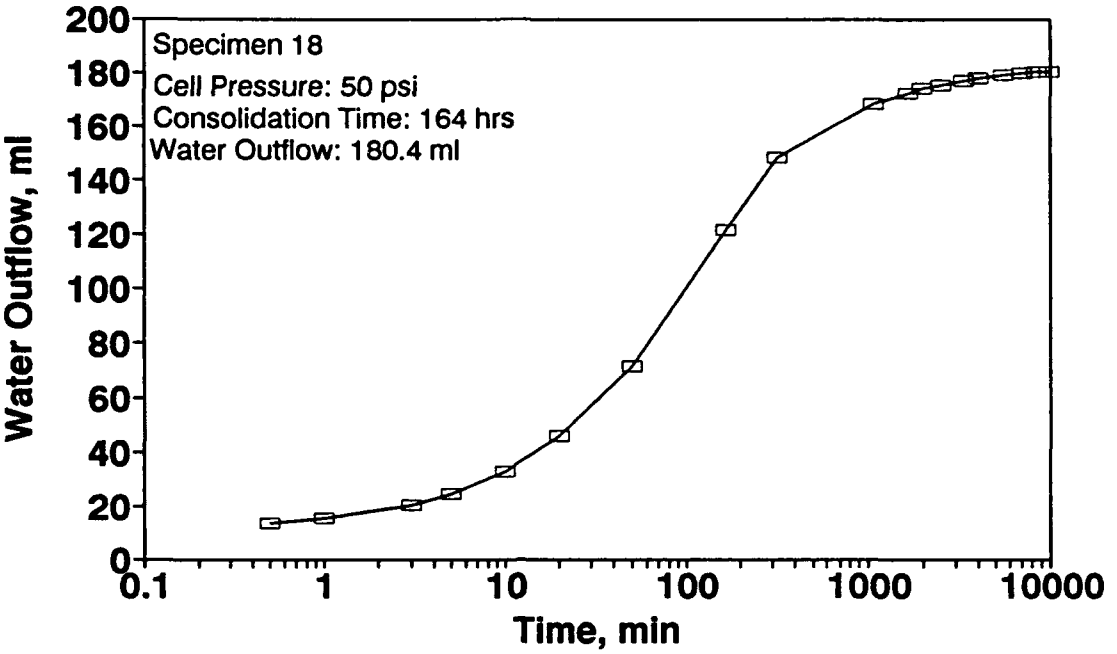
Specimen 18
Cell Pressure: 50 psi
Consolidation Time: 164 hrs
Water Outflow: 180.4 ml
Water Outflow, ml
Time, min
200
180
160
140
120
100
80
60
40
20
0
0.1
1
10
100
1000
10000

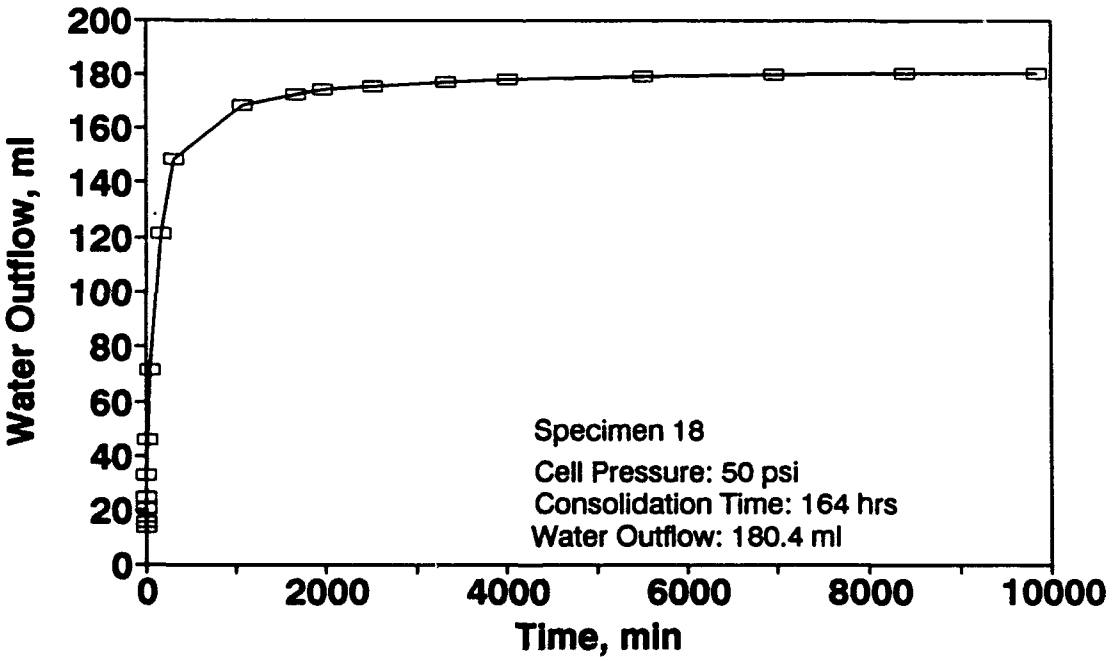
Specimen 18
Cell Pressure: 50 psi
Consolidation Time: 164 hrs
Water Outflow: 180.4 ml
Water Outflow, ml
Time, min
200
180
160
140
120
100
80
60
40
20
0
0
2000
4000
6000
8000
10000

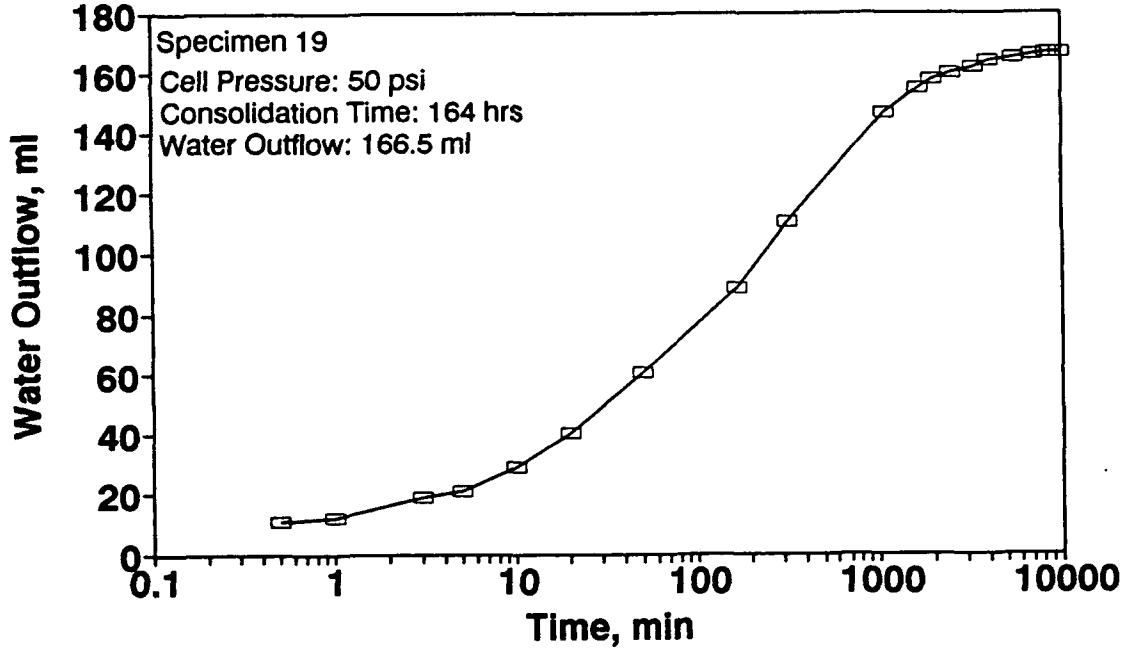
Specimen 19
Cell Pressure: 50 psi
Consolidation Time: 164 hrs
Water Outflow: 166.5 ml
Water Outflow, ml
Time, min
0
20
40
60
80
100
120
140
160
180
0.1
1
10
100
1000
10000

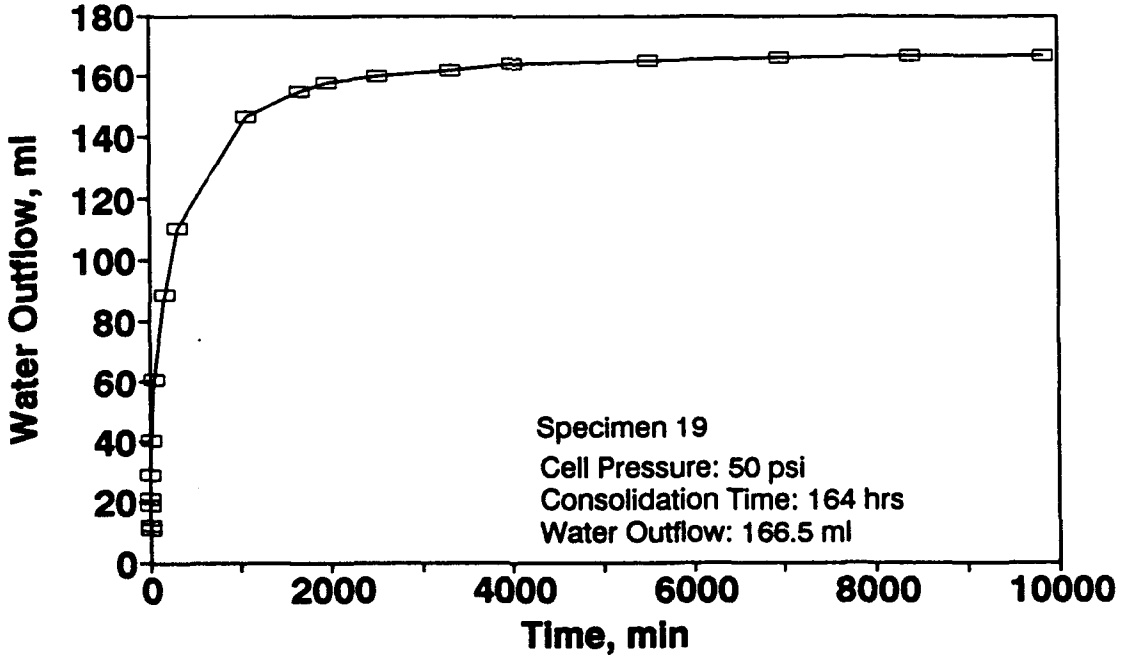
Specimen 19
Cell Pressure: 50 psi
Consolidation Time: 164 hrs
Water Outflow: 166.5 ml
Water Outflow, ml
Time, min
0
20
40
60
80
100
120
140
160
180
0
2000
4000
6000
8000
10000

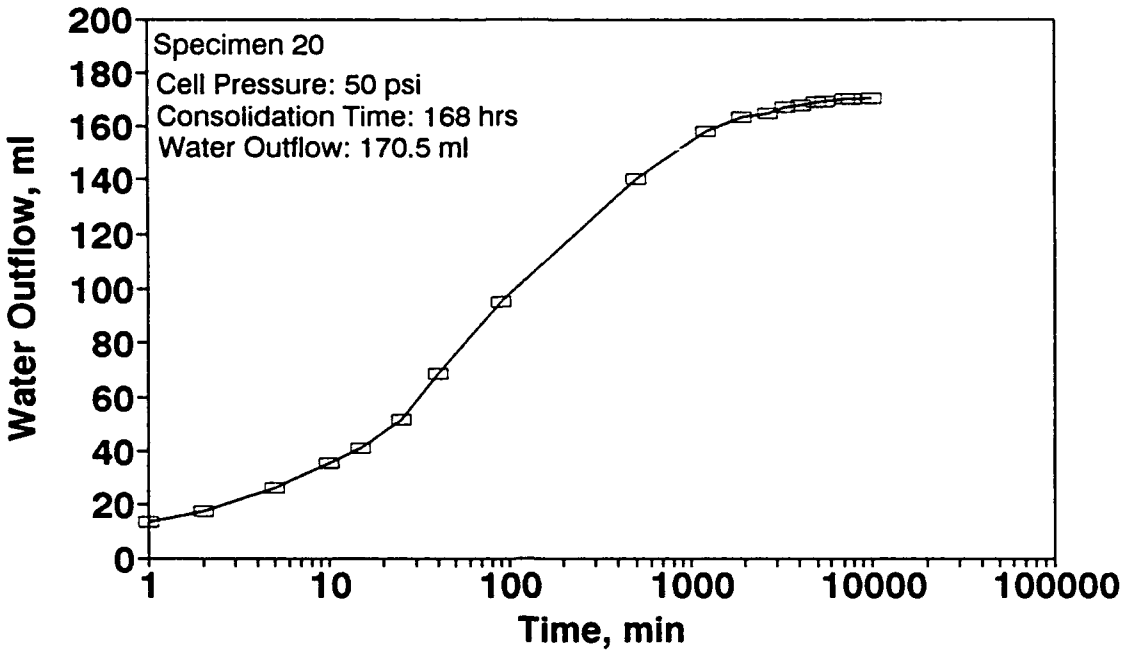
Specimen 20
Cell Pressure: 50 psi
Consolidation Time: 168 hrs
Water Outflow: 170.5 ml
Water Outflow, ml
Time, min
200
180
160
140
120
100
80
60
40
20
0
1
10
100
1000
10000
100000

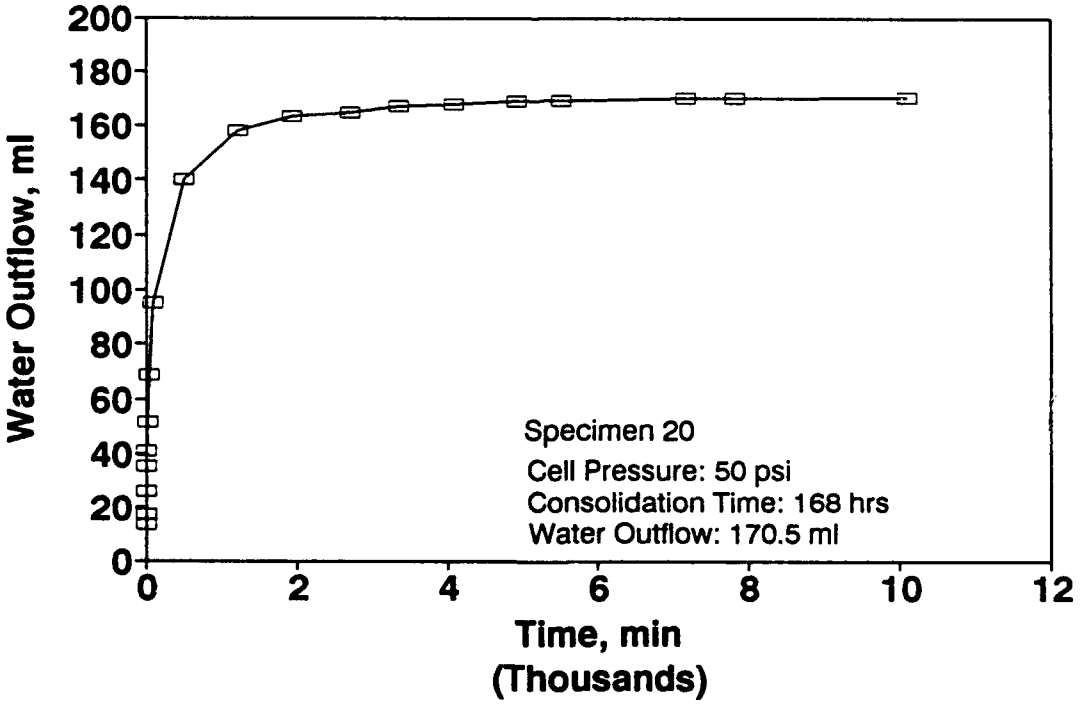
Specimen 20
Cell Pressure: 50 psi
Consolidation Time: 168 hrs
Water Outflow: 170.5 ml
Water Outflow, ml
Time, min
(Thousands)
200
180
160
140
120
100
80
60
40
20
0
0
2
4
6
8
10
12

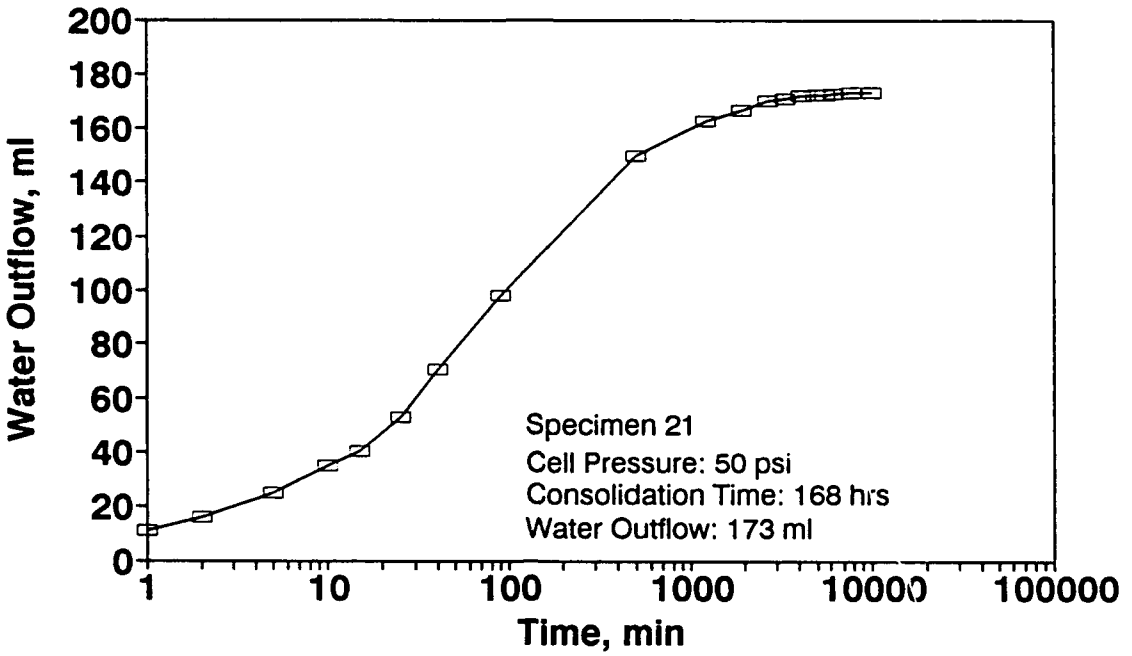
Water Outflow, ml
200
180
160
140
120
100
80
60
40
20
0
1
10
100
1000
10000
100000
Time, min
Specimen 21
Cell Pressure: 50 psi
Consolidation Time: 168 hrs
Water Outflow: 173 ml

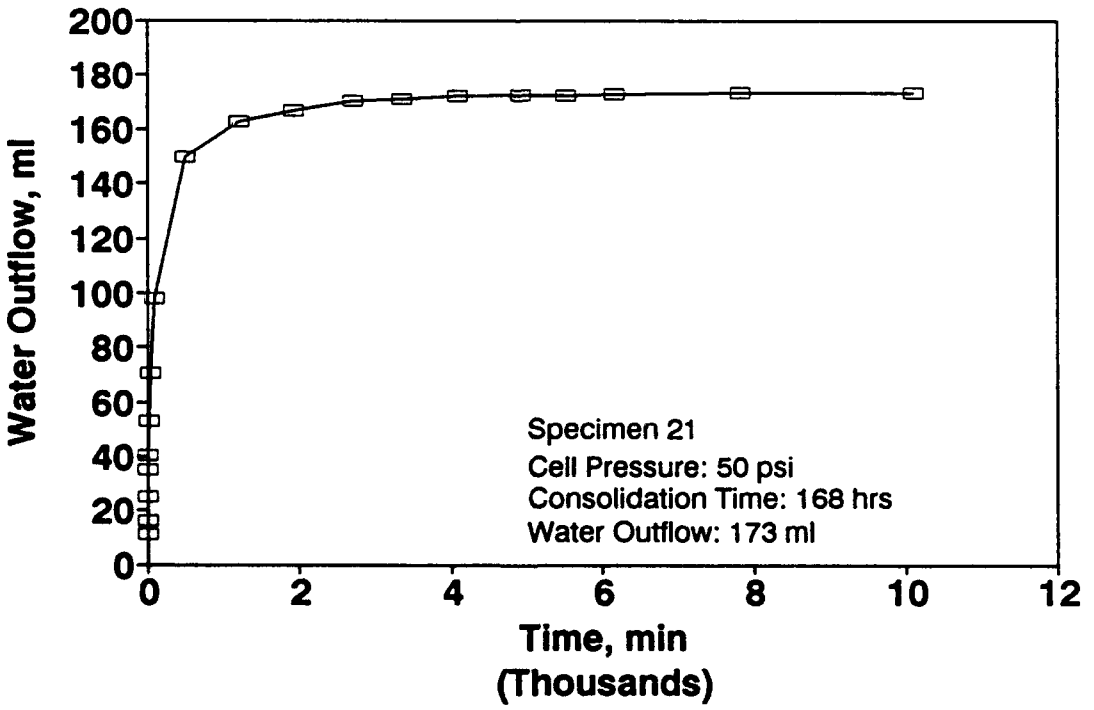
Water Outflow, ml
200
180
160
140
120
100
80
60
40
20
0
0
2
4
6
8
10
12
Time, min
(Thousands)
Specimen 21
Cell Pressure: 50 psi
Consolidation Time: 168 hrs
Water Outflow: 173 ml

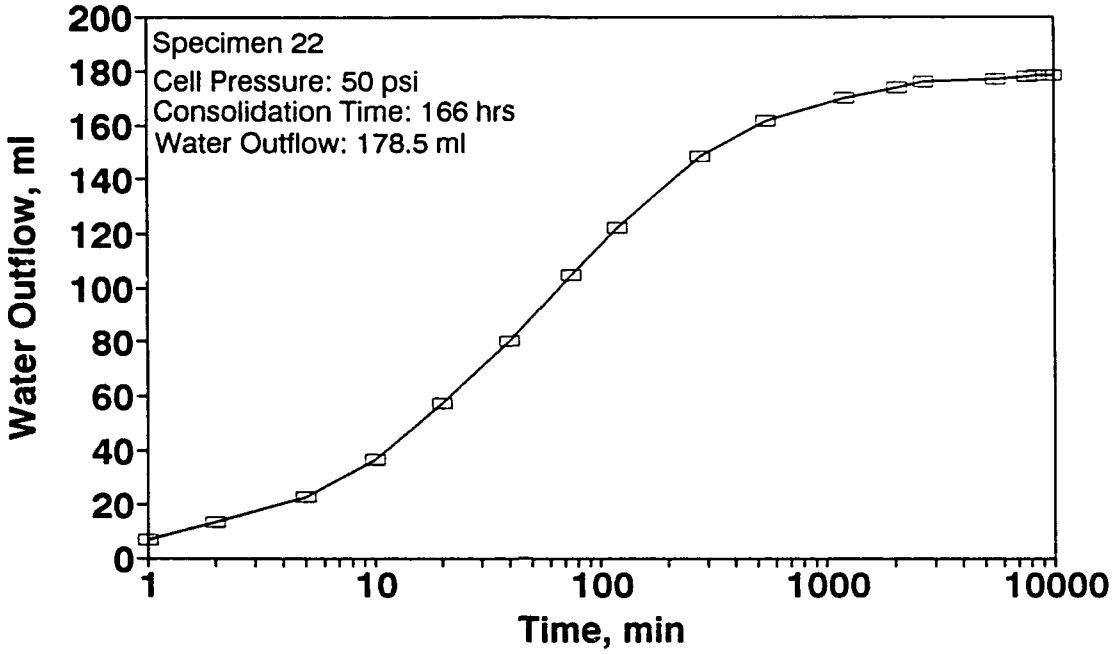
Specimen 22
Cell Pressure: 50 psi
Consolidation Time: 166 hrs
Water Outflow: 178.5 ml
Water Outflow, ml
Time, min
200
180
160
140
120
100
80
60
40
20
0
1
10
100
1000
10000

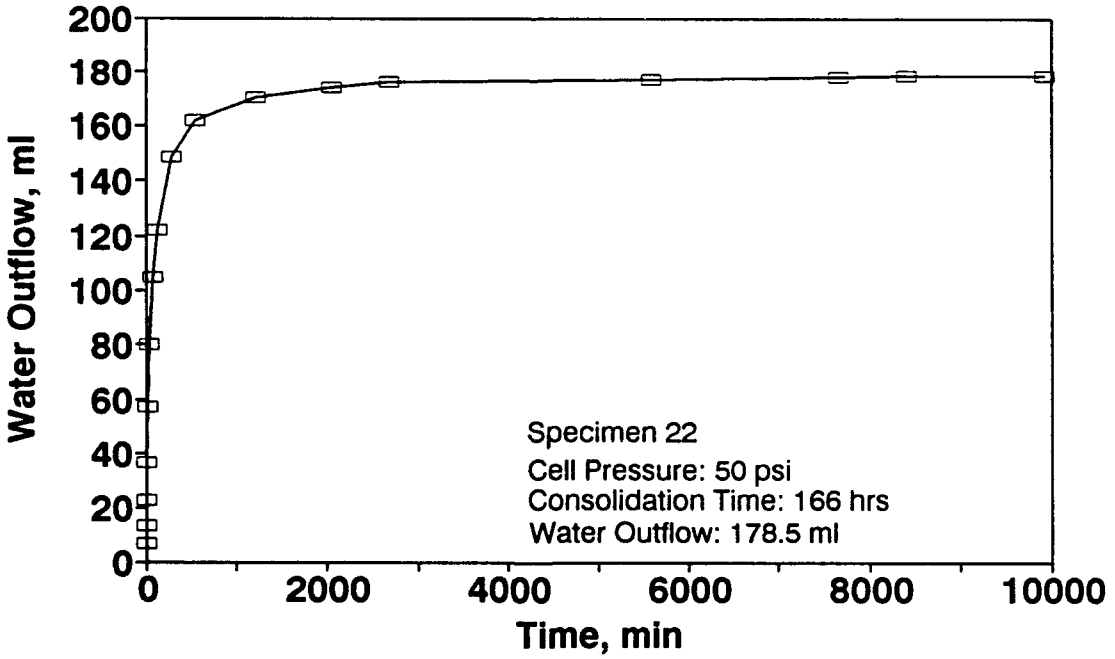
Specimen 22
Cell Pressure: 50 psi
Consolidation Time: 166 hrs
Water Outflow: 178.5 ml
Water Outflow, ml
Time, min
200
180
160
140
120
100
80
60
40
20
0
0
2000
4000
6000
8000
10000

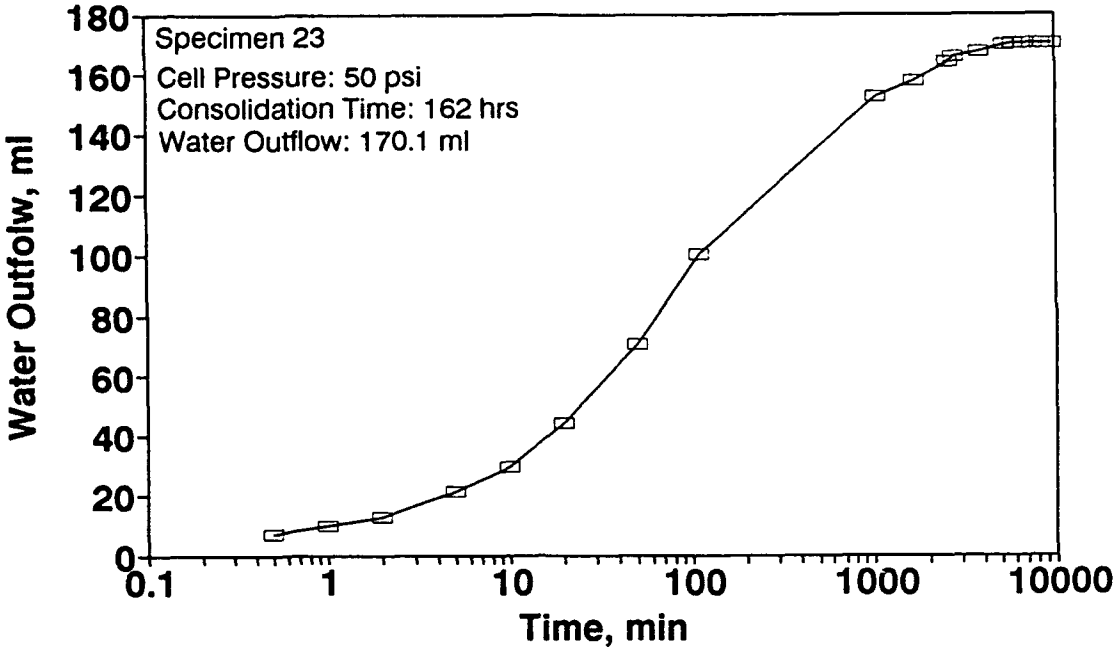
Specimen 23
Cell Pressure: 50 psi
Consolidation Time: 162 hrs
Water Outflow: 170.1 ml
Water Outfolw, ml
180
160
140
120
100
80
60
40
20
0
0.1
1
10
100
1000
10000
Time, min

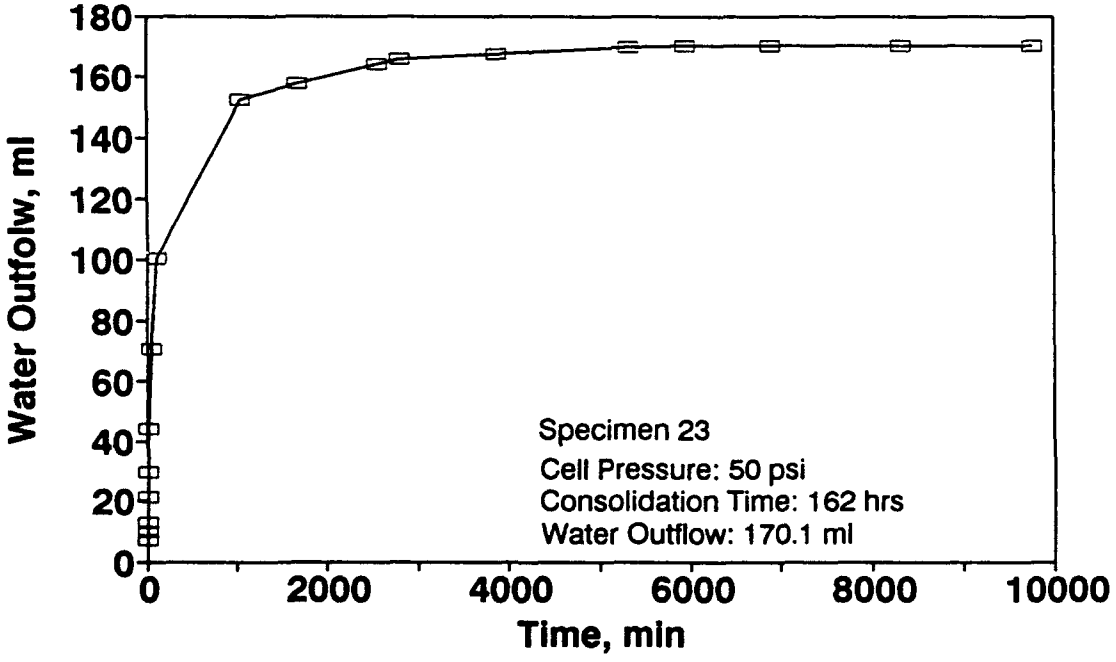
Specimen 23
Cell Pressure: 50 psi
Consolidation Time: 162 hrs
Water Outflow: 170.1 ml
Water Outfolw, ml
180
160
140
120
100
80
60
40
20
0
0
2000
4000
6000
8000
10000
Time, min

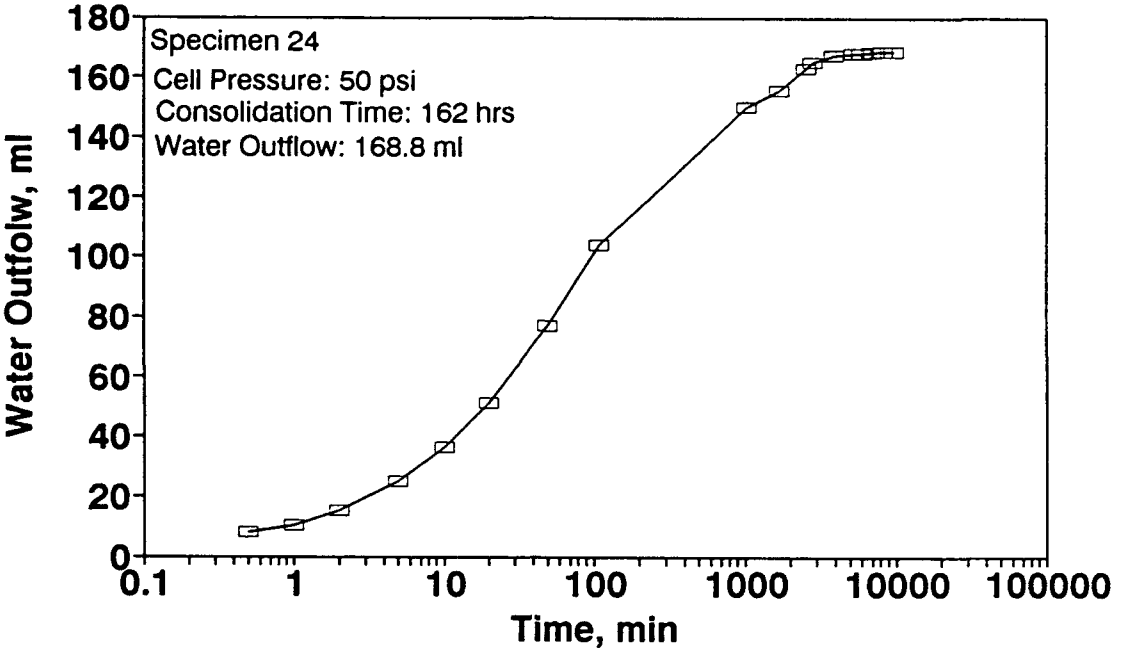
Specimen 24
Cell Pressure: 50 psi
Consolidation Time: 162 hrs
Water Outflow: 168.8 ml
Water Outfolw, ml
Time, min
0
20
40
60
80
100
120
140
160
180
0.1
1
10
100
1000
10000
100000

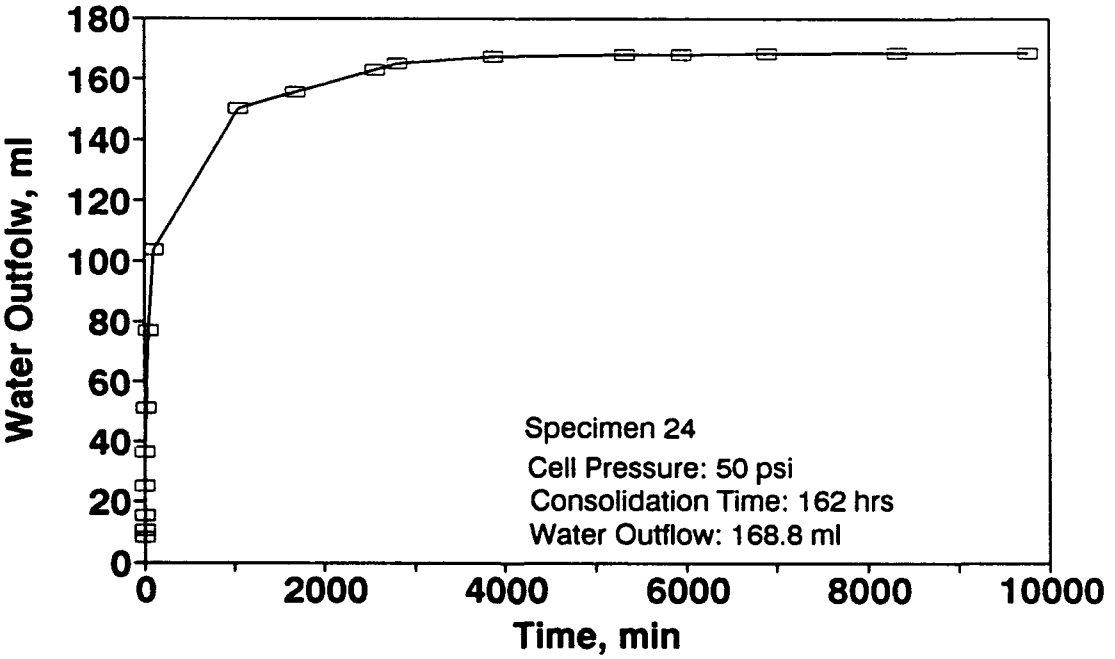
Specimen 24
Cell Pressure: 50 psi
Consolidation Time: 162 hrs
Water Outflow: 168.8 ml
Water Outfolw, ml
Time, min
0
20
40
60
80
100
120
140
160
180
0
2000
4000
6000
8000
10000

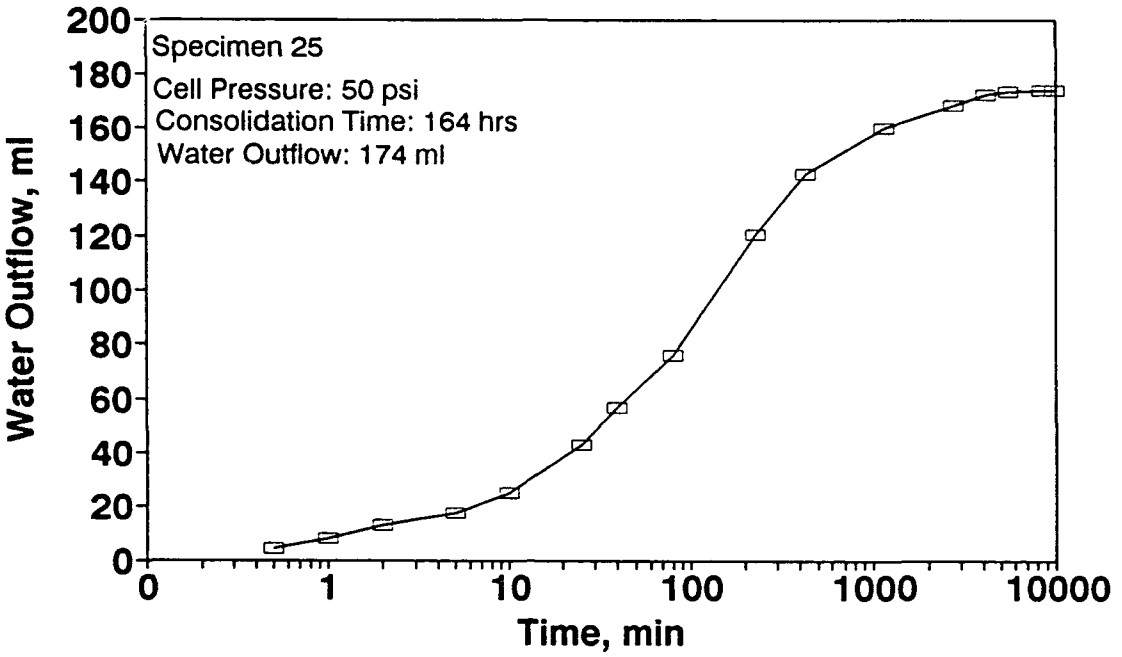
Specimen 25
Cell Pressure: 50 psi
Consolidation Time: 164 hrs
Water Outflow: 174 ml
Water Outflow, ml
Time, min
0
20
40
60
80
100
120
140
160
180
200
0
1
10
100
1000
10000

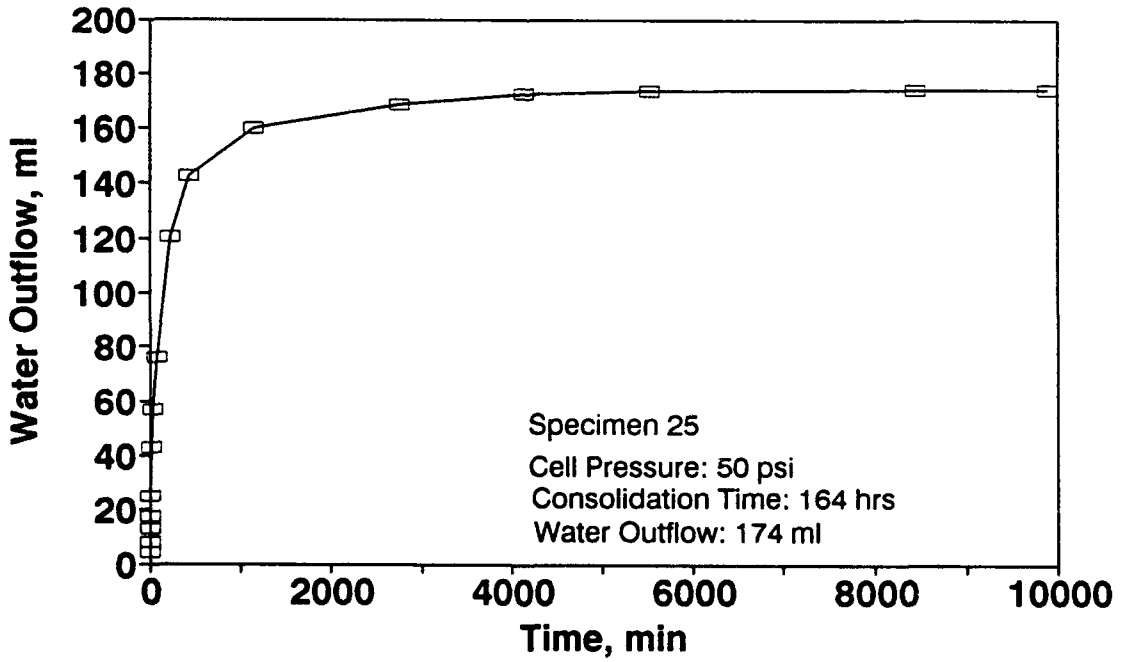
Specimen 25
Cell Pressure: 50 psi
Consolidation Time: 164 hrs
Water Outflow: 174 ml
Water Outflow, ml
Time, min
0
20
40
60
80
100
120
140
160
180
200
0
2000
4000
6000
8000
10000

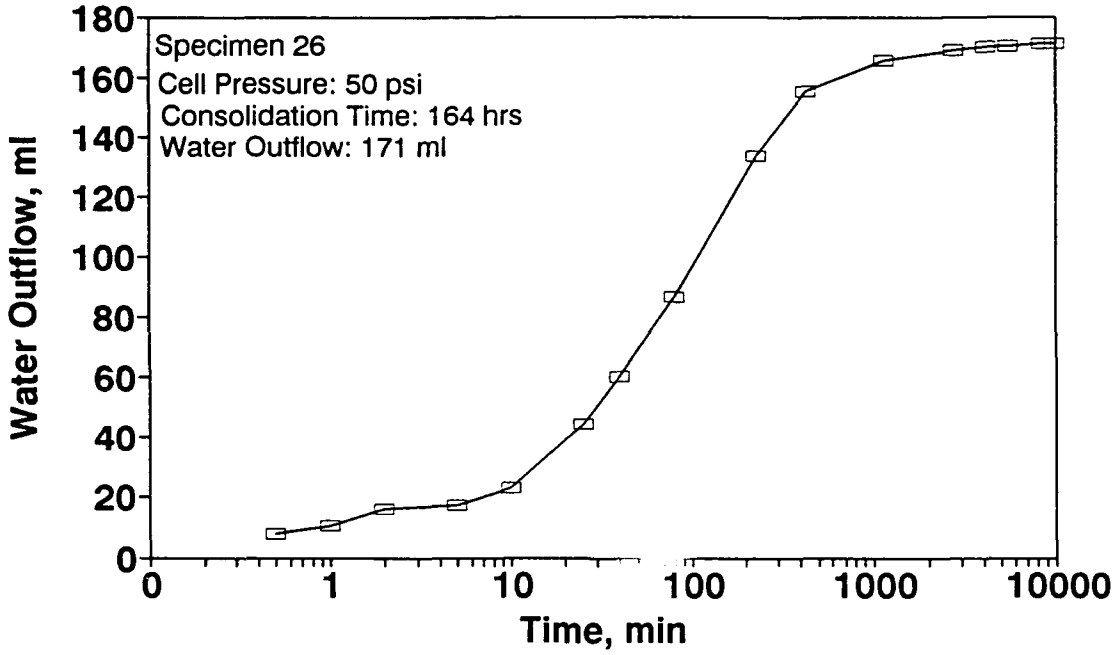
Specimen 26
Cell Pressure: 50 psi
Consolidation Time: 164 hrs
Water Outflow: 171 ml
Water Outflow, ml
Time, min
0
20
40
60
80
100
120
140
160
180
0
1
10
100
1000
10000

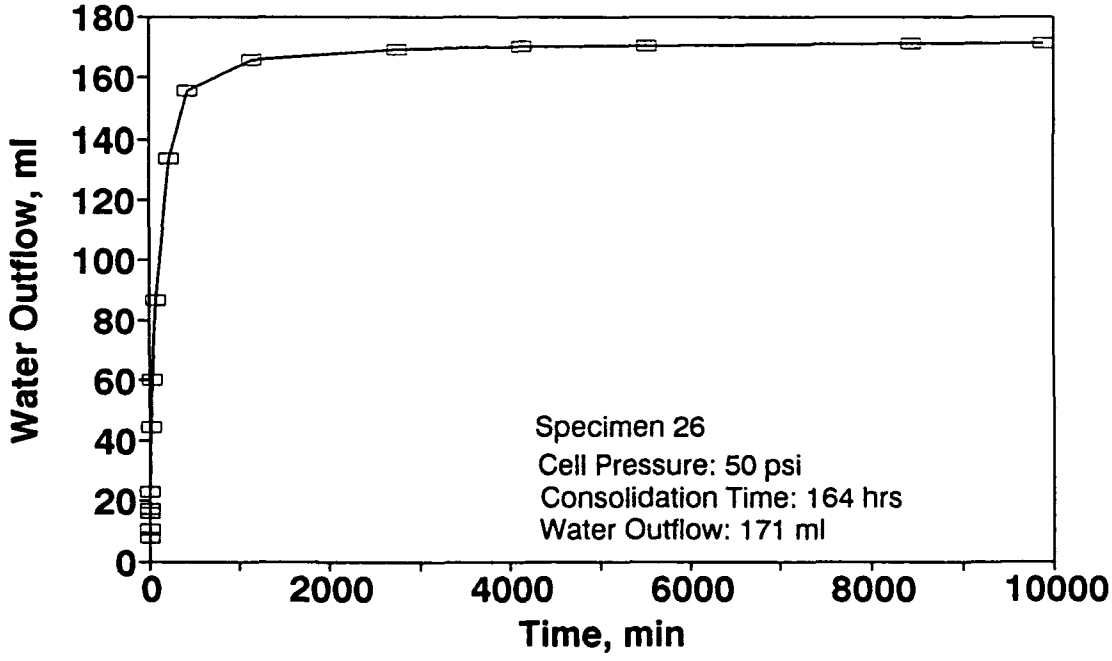
Specimen 26
Cell Pressure: 50 psi
Consolidation Time: 164 hrs
Water Outflow: 171 ml
Water Outflow, ml
Time, min
0
20
40
60
80
100
120
140
160
180
0
2000
4000
6000
8000
10000

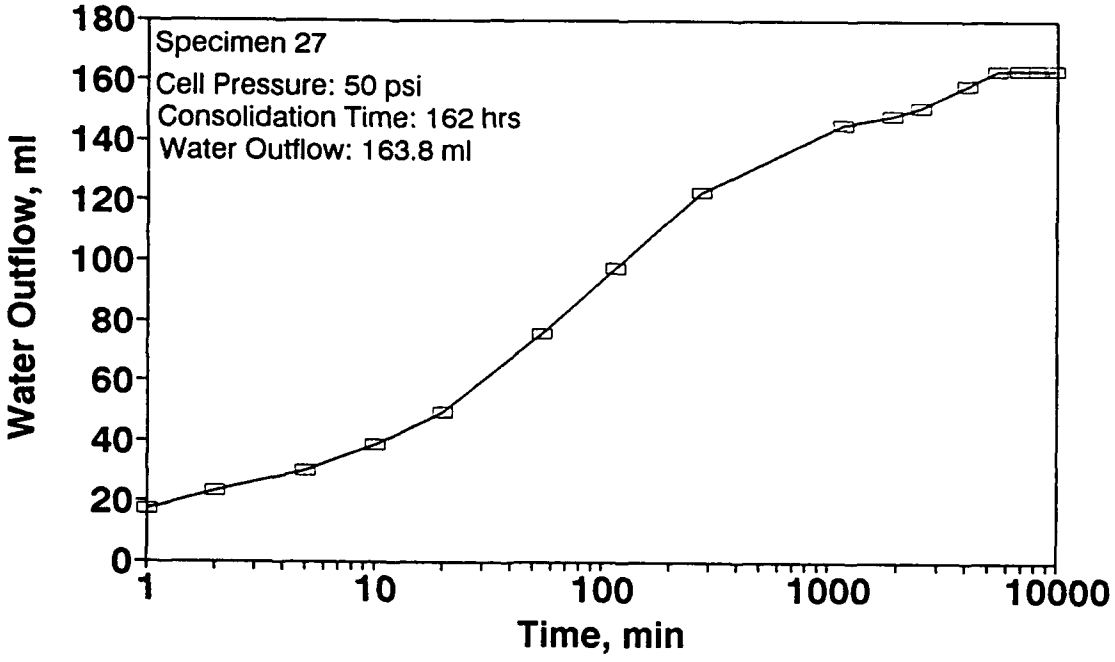
Specimen 27
Cell Pressure: 50 psi
Consolidation Time: 162 hrs
Water Outflow: 163.8 ml
Water Outflow, ml
Time, min
0
20
40
60
80
100
120
140
160
180
1
10
100
1000
10000

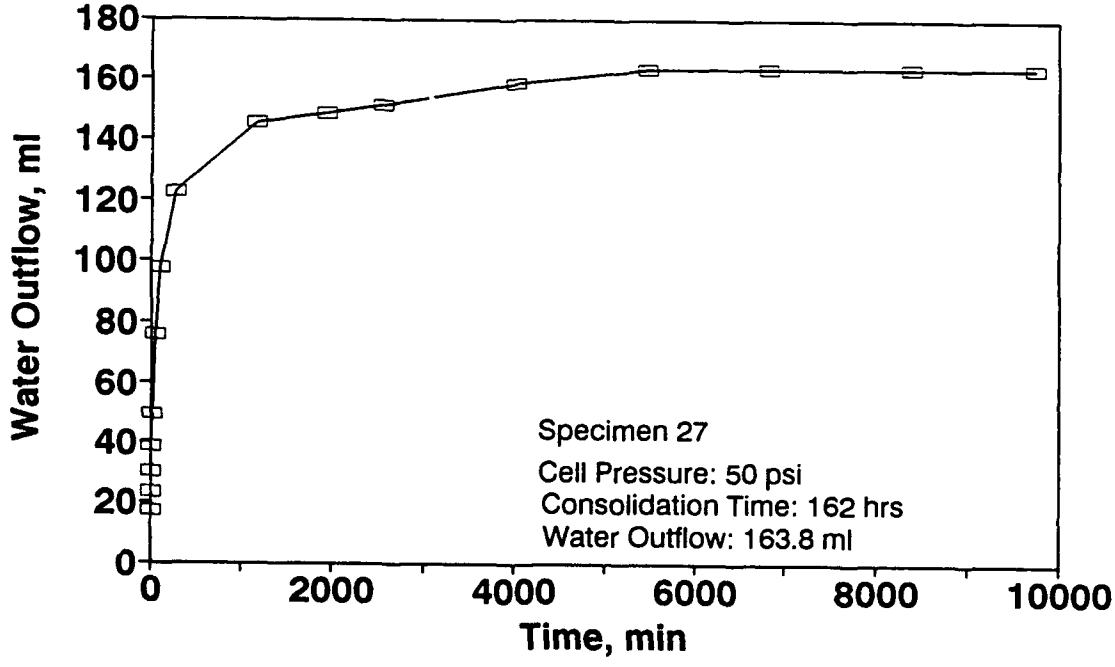
Specimen 27
Cell Pressure: 50 psi
Consolidation Time: 162 hrs
Water Outflow: 163.8 ml
Water Outflow, ml
Time, min
0
20
40
60
80
100
120
140
160
180
0
2000
4000
6000
8000
10000

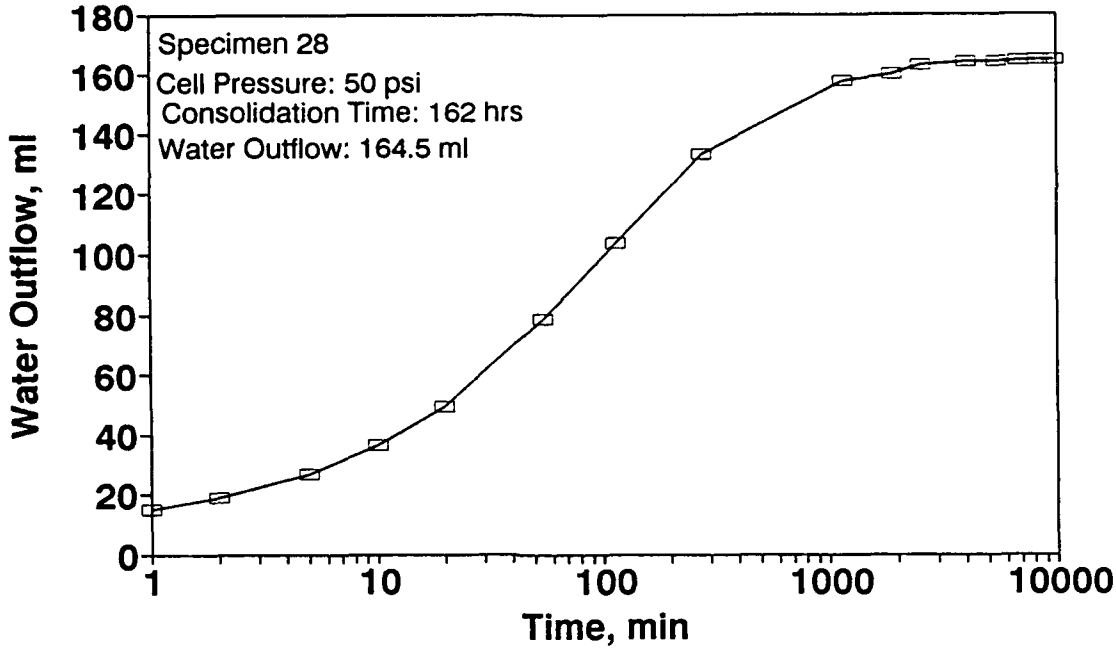
Specimen 28
Cell Pressure: 50 psi
Consolidation Time: 162 hrs
Water Outflow: 164.5 ml
Water Outflow, ml
Time, min
0
20
40
60
80
100
120
140
160
180
1
10
100
1000
10000

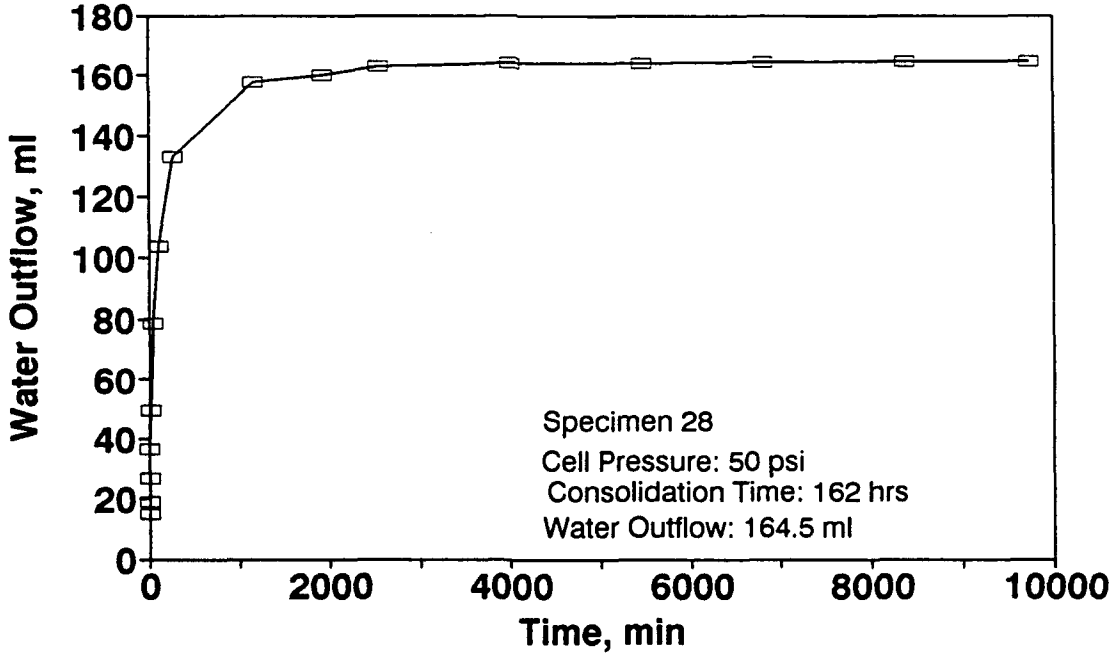
Specimen 28
Cell Pressure: 50 psi
Consolidation Time: 162 hrs
Water Outflow: 164.5 ml
Water Outflow, ml
Time, min
0
20
40
60
80
100
120
140
160
180
0
2000
4000
6000
8000
10000

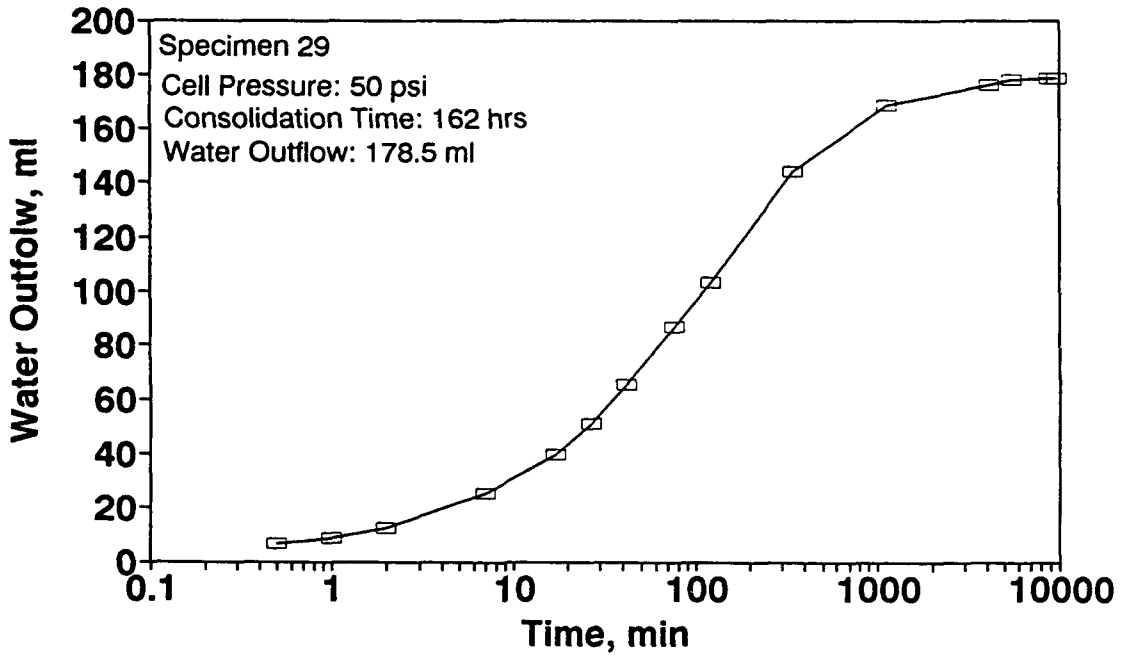
Specimen 29
Cell Pressure: 50 psi
Consolidation Time: 162 hrs
Water Outflow: 178.5 ml
Water Outfolw, ml
200
180
160
140
120
100
80
60
40
20
0
0.1
1
10
100
1000
10000
Time, min

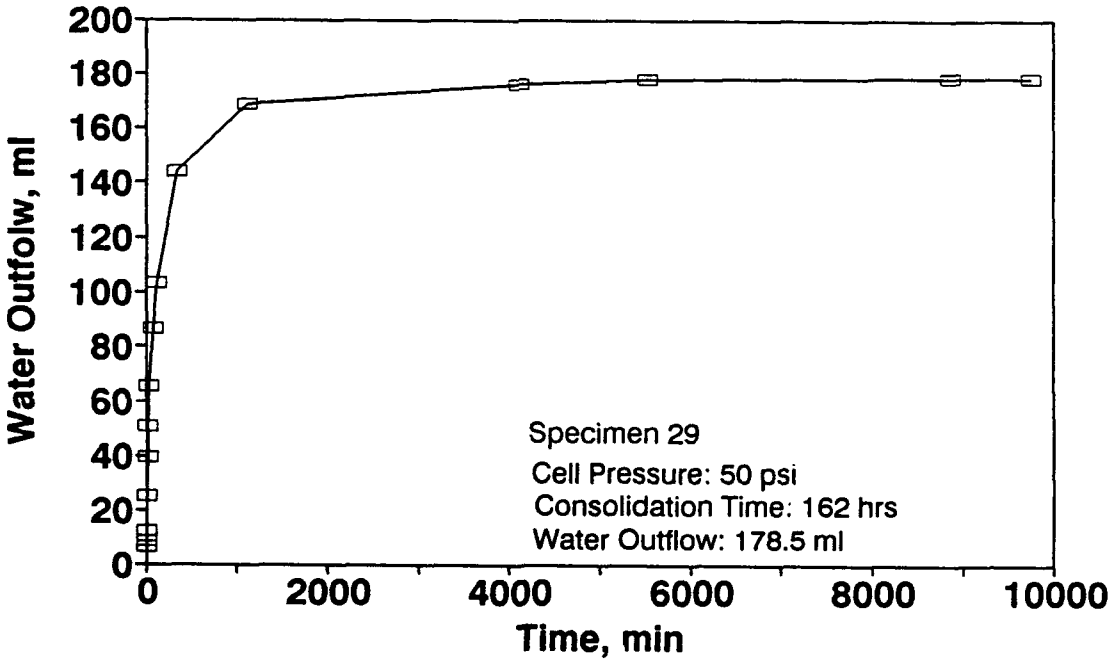
Water Outfolw, ml
200
180
160
140
120
100
80
60
40
20
0
Specimen 29
Cell Pressure: 50 psi
Consolidation Time: 162 hrs
Water Outflow: 178.5 ml
0
2000
4000
6000
8000
10000
Time, min

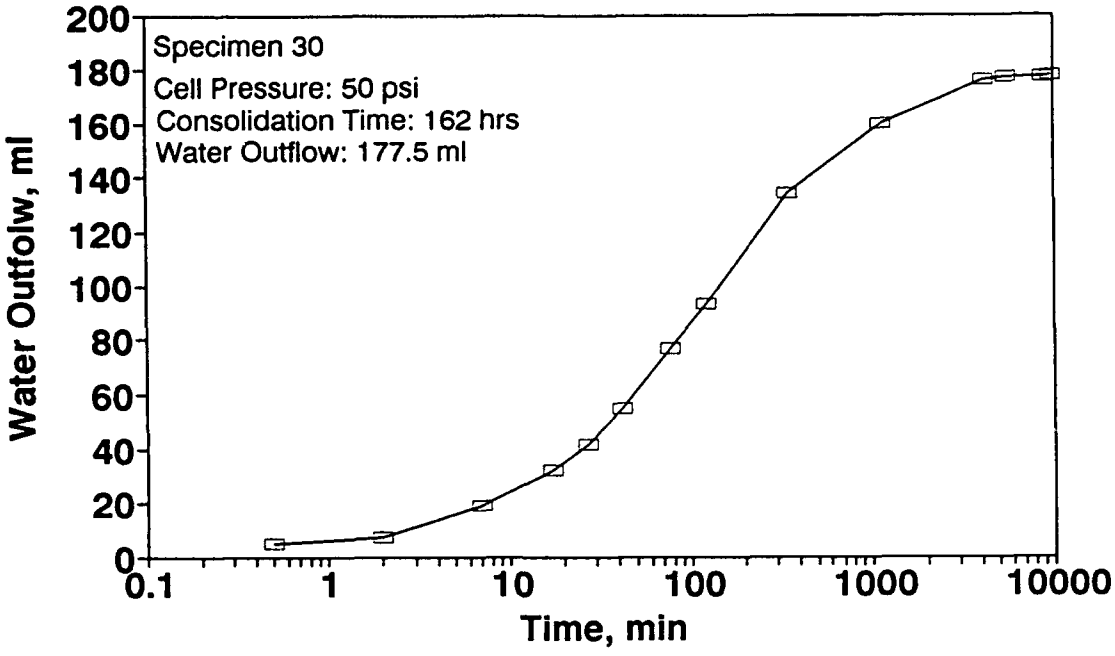
Specimen 30
Cell Pressure: 50 psi
Consolidation Time: 162 hrs
Water Outflow: 177.5 ml
Water Outfolw, ml
Time, min
0
20
40
60
80
100
120
140
160
180
200
0.1
1
10
100
1000
10000

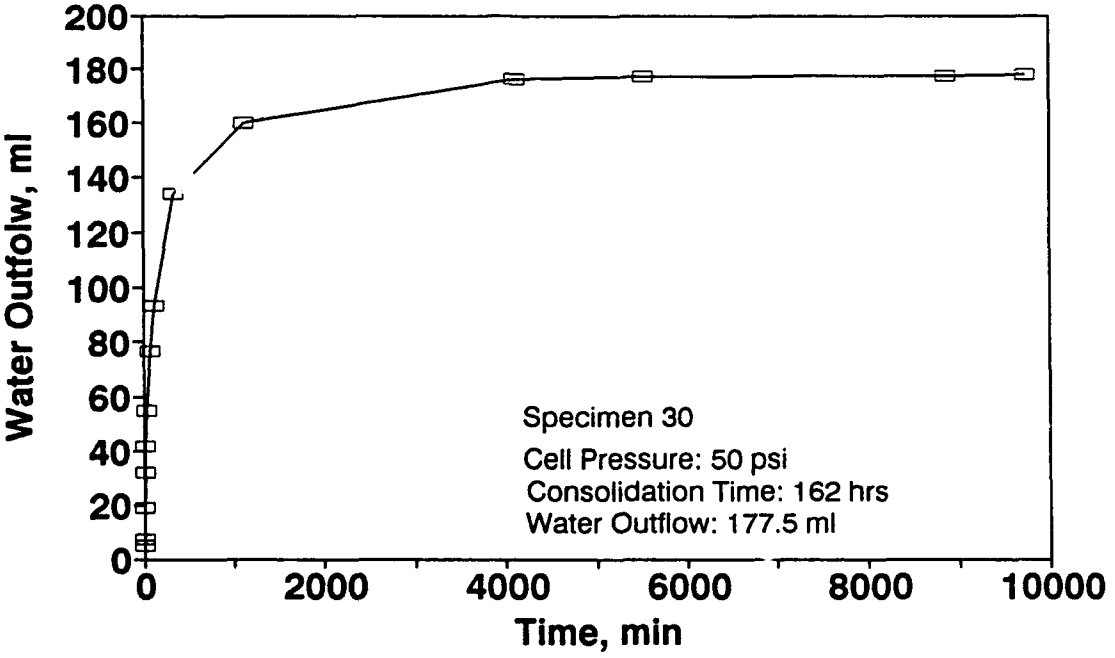
Specimen 30
Cell Pressure: 50 psi
Consolidation Time: 162 hrs
Water Outflow: 177.5 ml
Water Outfolw, ml
Time, min
0
20
40
60
80
100
120
140
160
180
200
0
2000
4000
6000
8000
10000

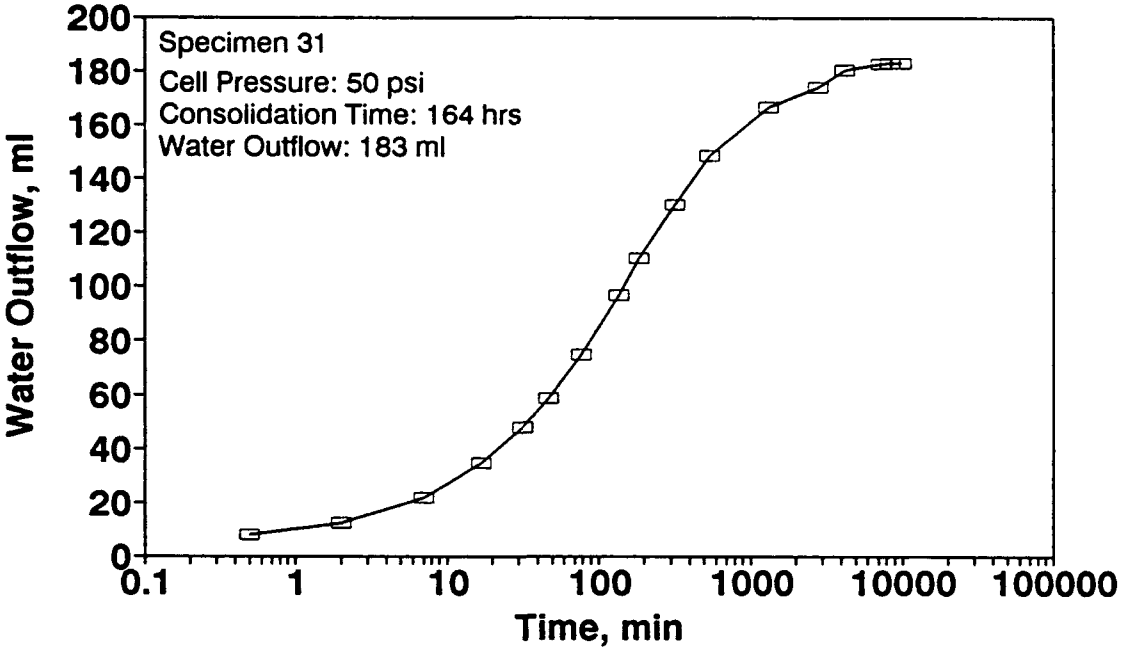
Specimen 31
Cell Pressure: 50 psi
Consolidation Time: 164 hrs
Water Outflow: 183 ml
Water Outflow, ml
Time, min
0
20
40
60
80
100
120
140
160
180
200
0.1
1
10
100
1000
10000
100000

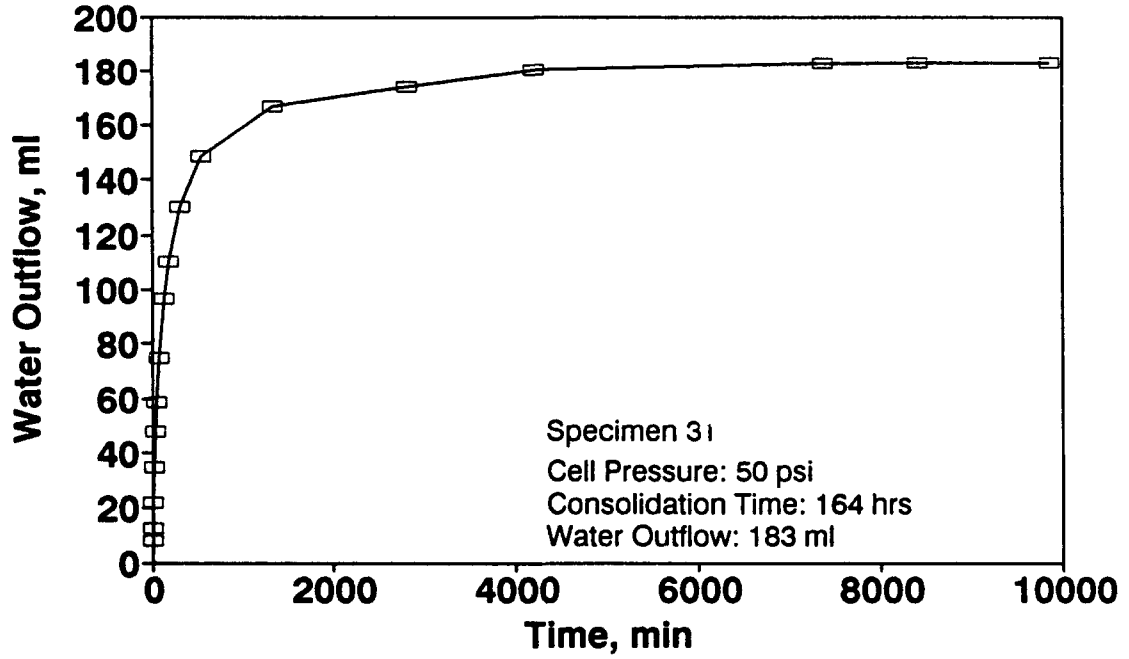
Specimen 31
Cell Pressure: 50 psi
Consolidation Time: 164 hrs
Water Outflow: 183 ml
Water Outflow, ml
Time, min
0
20
40
60
80
100
120
140
160
180
200
0
2000
4000
6000
8000
10000

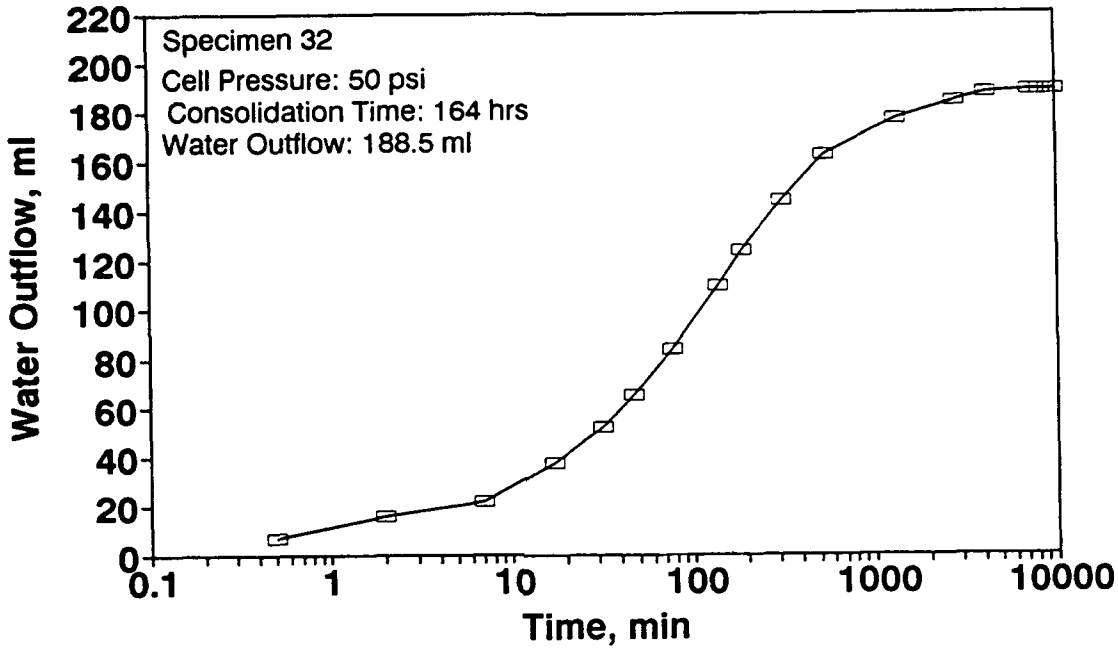
Specimen 32
Cell Pressure: 50 psi
Consolidation Time: 164 hrs
Water Outflow: 188.5 ml
Water Outflow, ml
220
200
180
160
140
120
100
80
60
40
20
0
0.1
1
10
100
1000
10000
Time, min

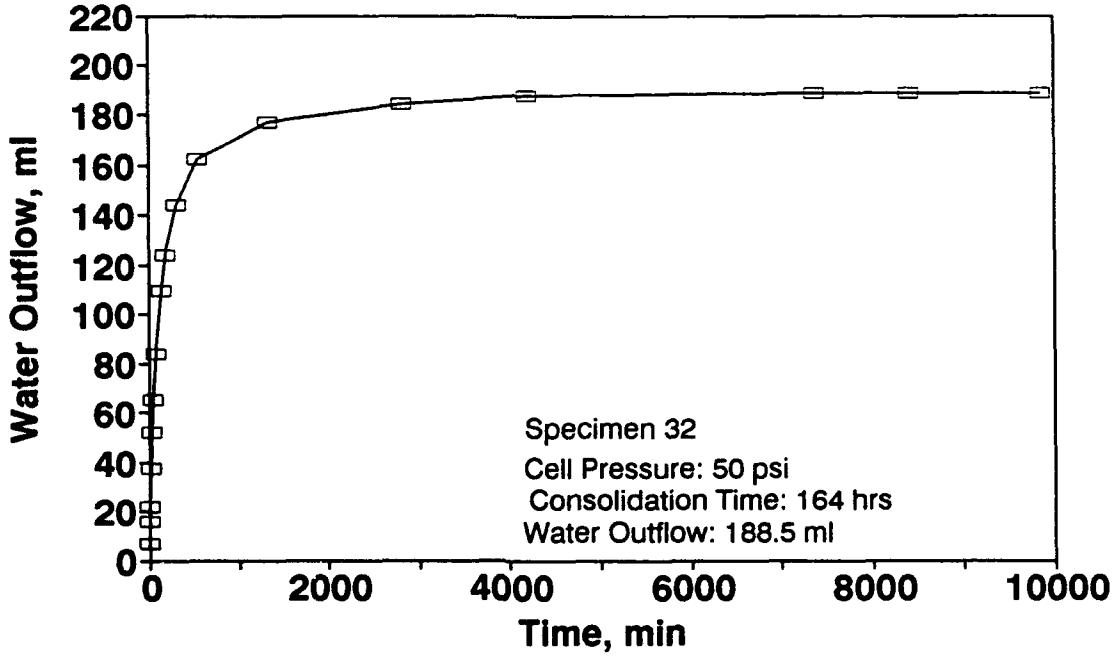
Water Outflow, ml
220
200
180
160
140
120
100
80
60
40
20
0
Specimen 32
Cell Pressure: 50 psi
Consolidation Time: 164 hrs
Water Outflow: 188.5 ml
0
2000
4000
6000
8000
10000
Time, min

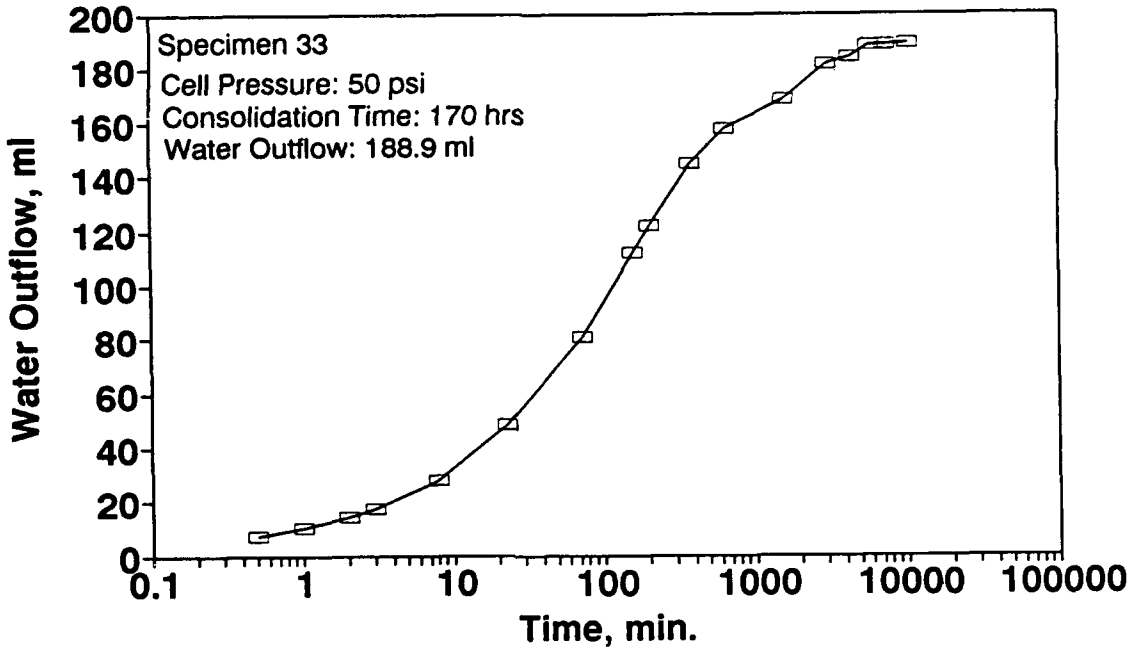
Specimen 33
Cell Pressure: 50 psi
Consolidation Time: 170 hrs
Water Outflow: 188.9 ml
Water Outflow, ml
200
180
160
140
120
100
80
60
40
20
0
0.1
1
10
100
1000
10000
100000
Time, min.

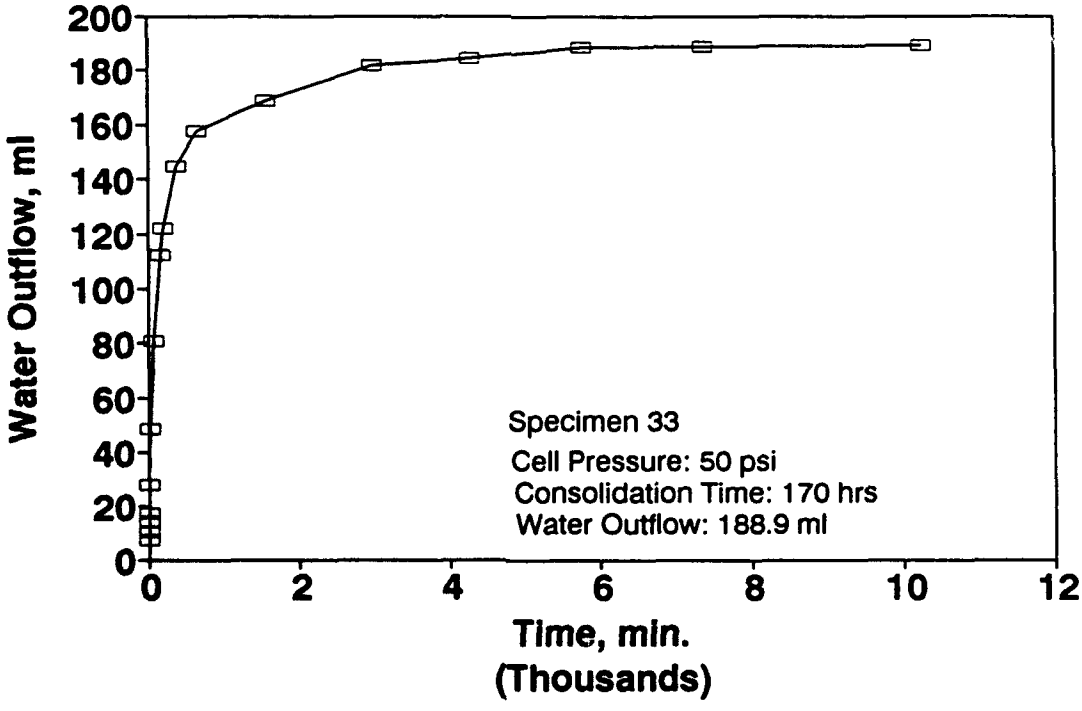
Water Outflow, ml
200
180
160
140
120
100
80
60
40
20
0
Specimen 33
Cell Pressure: 50 psi
Consolidation Time: 170 hrs
Water Outflow: 188.9 ml
0
2
4
6
8
10
12
Time, min.
(Thousands)

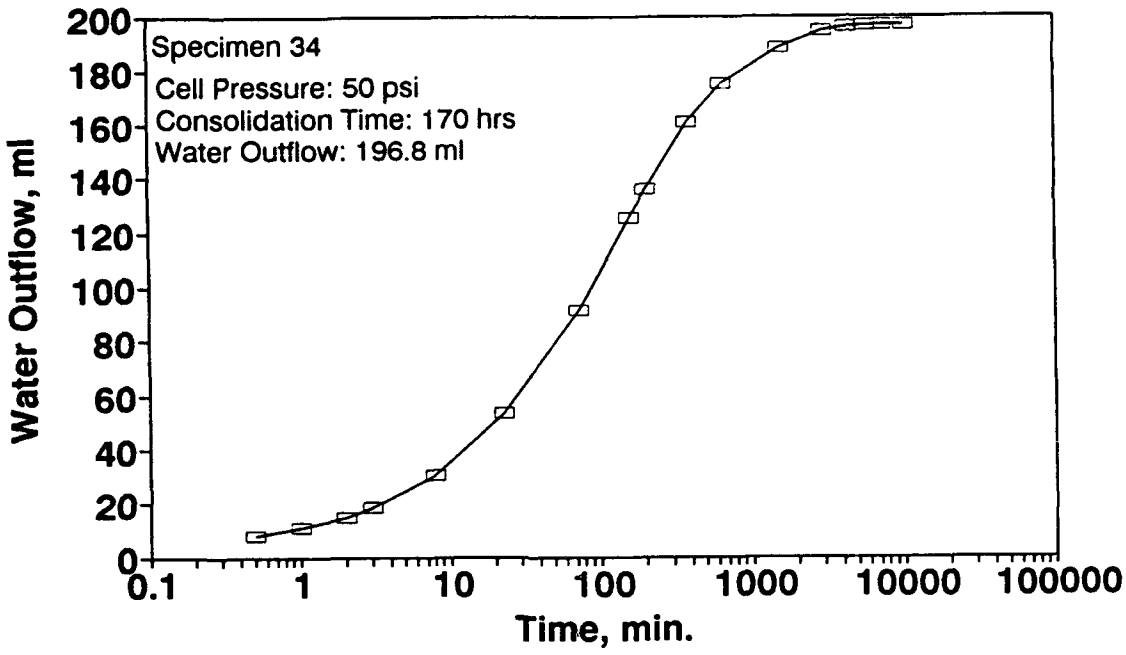
Specimen 34
Cell Pressure: 50 psi
Consolidation Time: 170 hrs
Water Outflow: 196.8 ml
Water Outflow, ml
200
180
160
140
120
100
80
60
40
20
0
0.1
1
10
100
1000
10000
100000
Time, min.

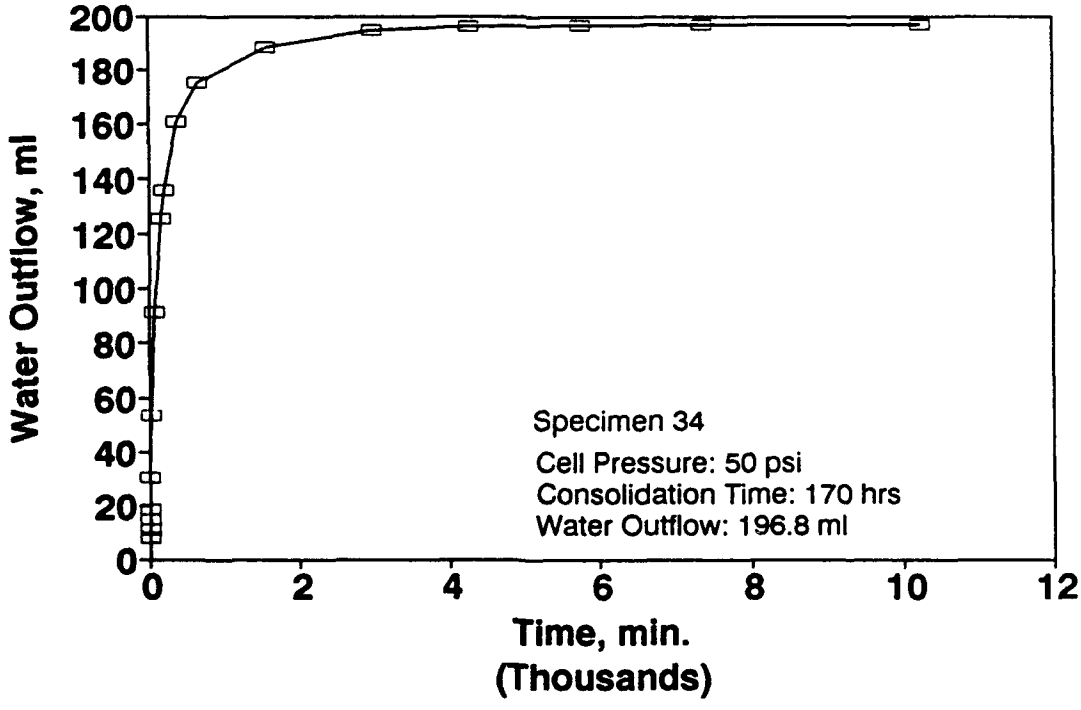
Specimen 34
Cell Pressure: 50 psi
Consolidation Time: 170 hrs
Water Outflow: 196.8 ml
Water Outflow, ml
200
180
160
140
120
100
80
60
40
20
0
0
2
4
6
8
10
12
Time, min.
(Thousands)

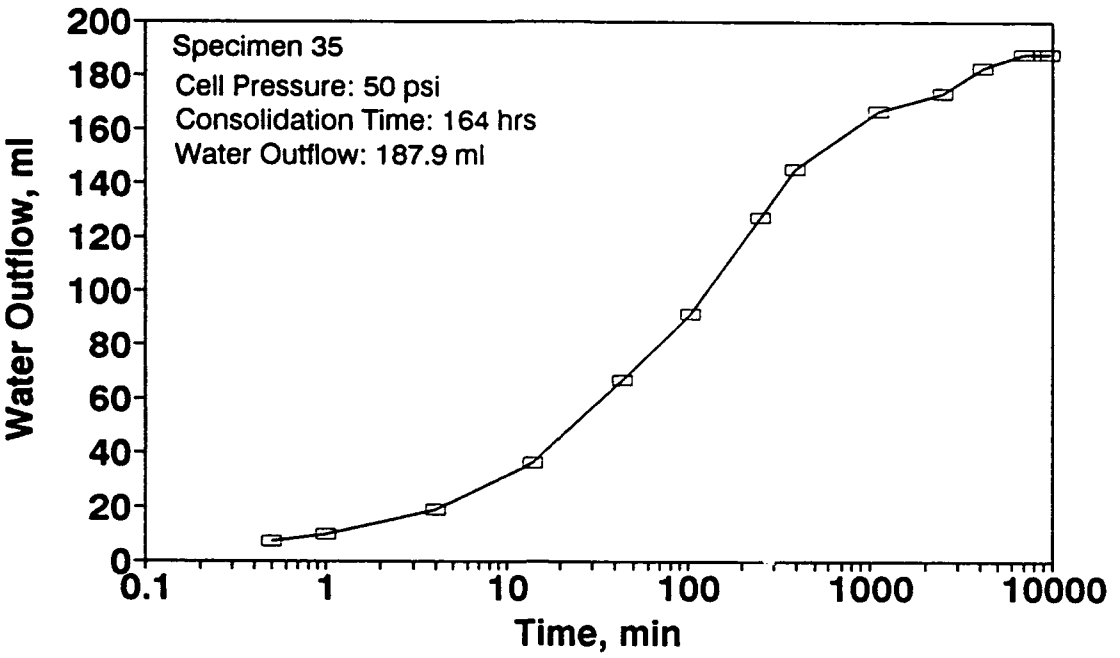
Specimen 35
Cell Pressure: 50 psi
Consolidation Time: 164 hrs
Water Outflow: 187.9 ml
Water Outflow, ml
200
180
160
140
120
100
80
60
40
20
0
0.1
1
10
100
1000
10000
Time, min

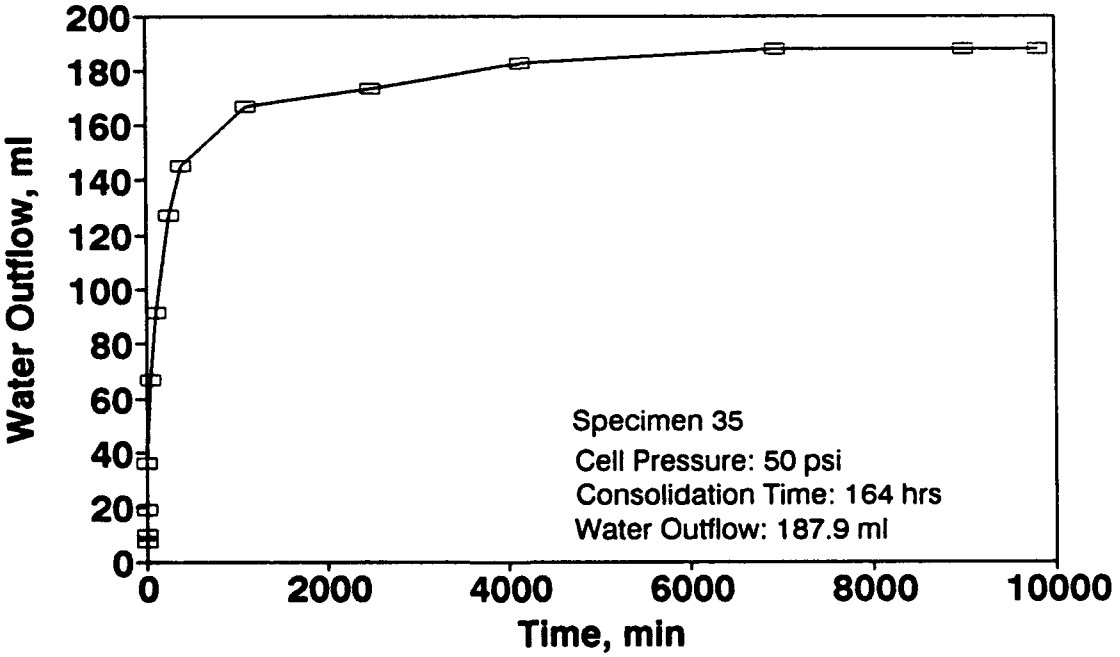
Water Outflow, ml
200
180
160
140
120
100
80
60
40
20
0
Specimen 35
Cell Pressure: 50 psi
Consolidation Time: 164 hrs
Water Outflow: 187.9 ml
0
2000
4000
6000
8000
10000
Time, min

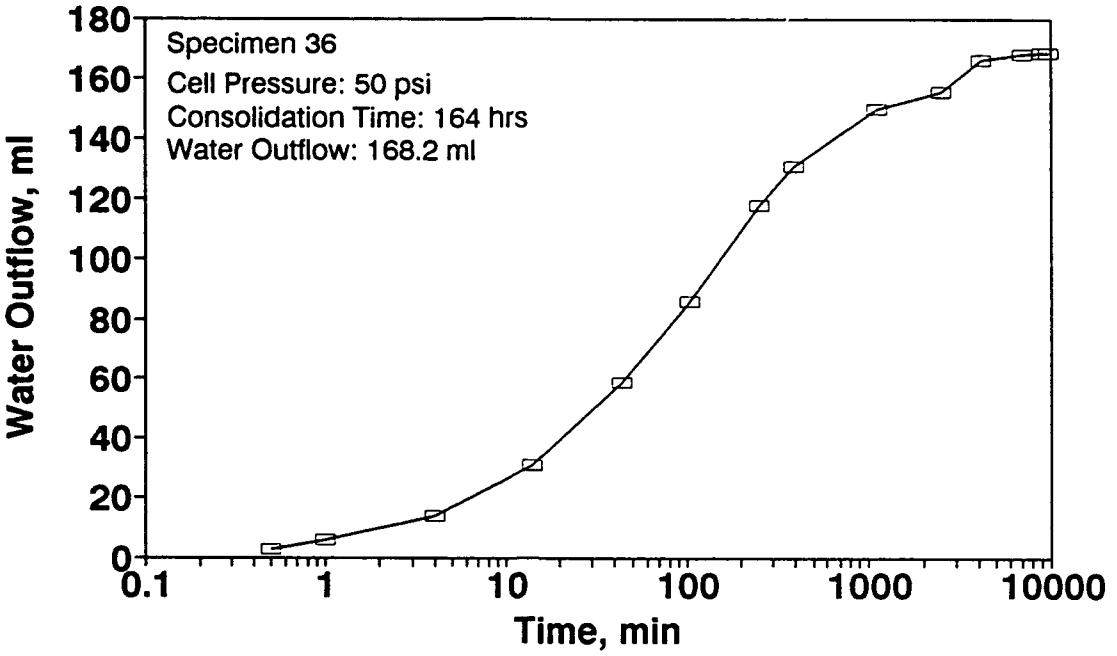
Specimen 36
Cell Pressure: 50 psi
Consolidation Time: 164 hrs
Water Outflow: 168.2 ml
Water Outflow, ml
Time, min
0
20
40
60
80
100
120
140
160
180
0.1
1
10
100
1000
10000

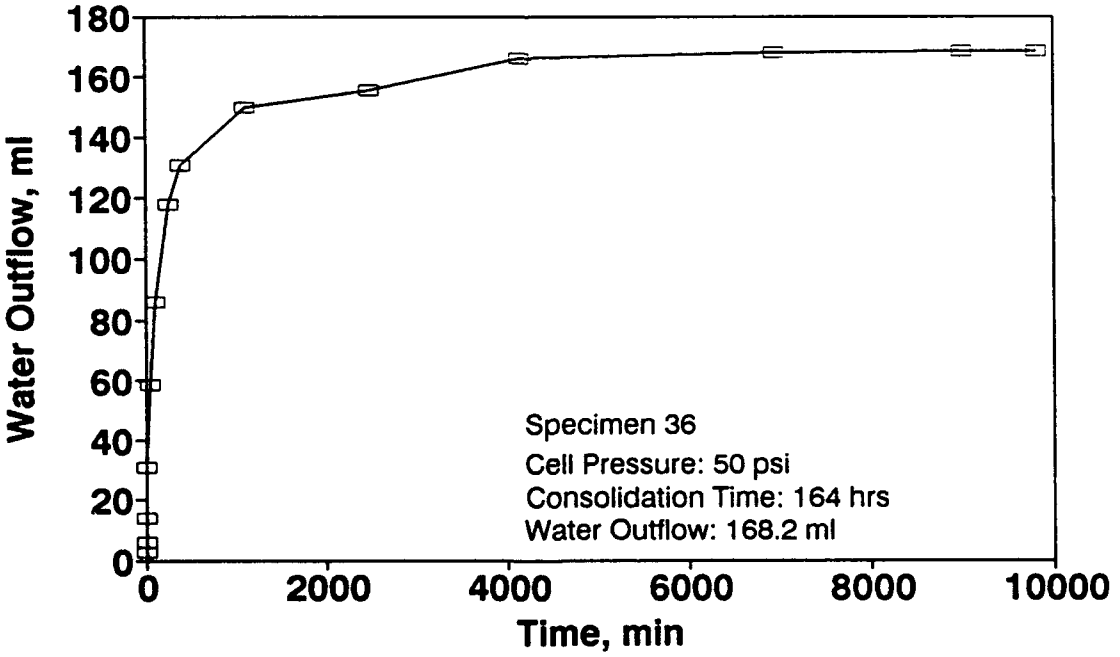
Specimen 36
Cell Pressure: 50 psi
Consolidation Time: 164 hrs
Water Outflow: 168.2 ml
Water Outflow, ml
Time, min
0
20
40
60
80
100
120
140
160
180
0
2000
4000
6000
8000
10000

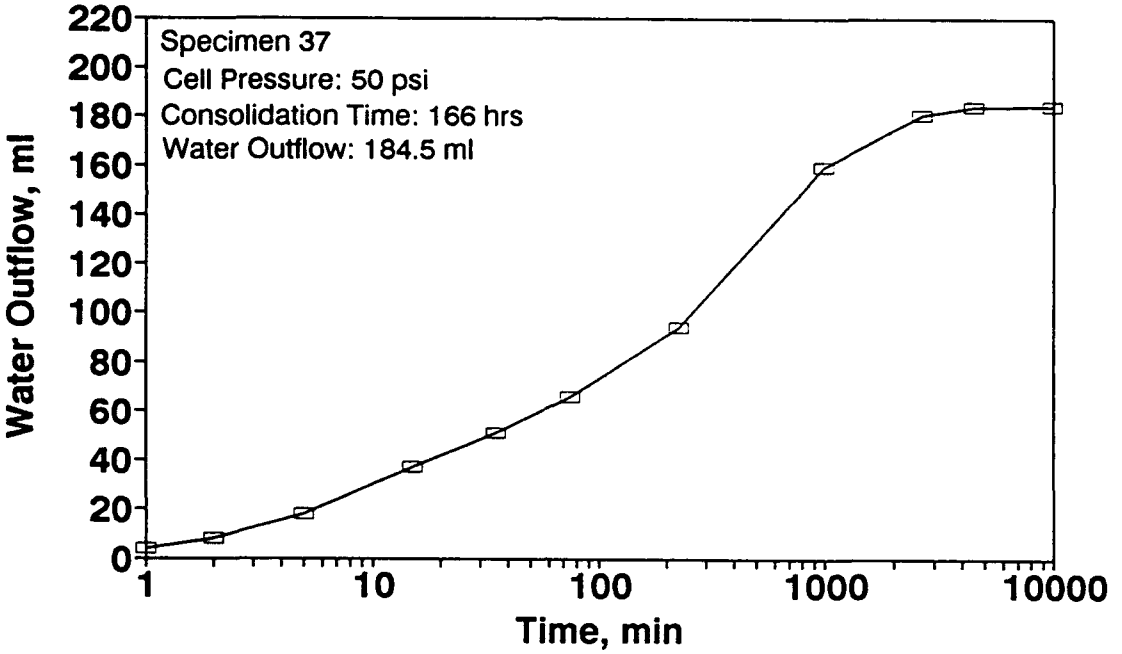
Specimen 37
Cell Pressure: 50 psi
Consolidation Time: 166 hrs
Water Outflow: 184.5 ml
Water Outflow, ml
220
200
180
160
140
120
100
80
60
40
20
0
1
10
100
1000
10000
Time, min

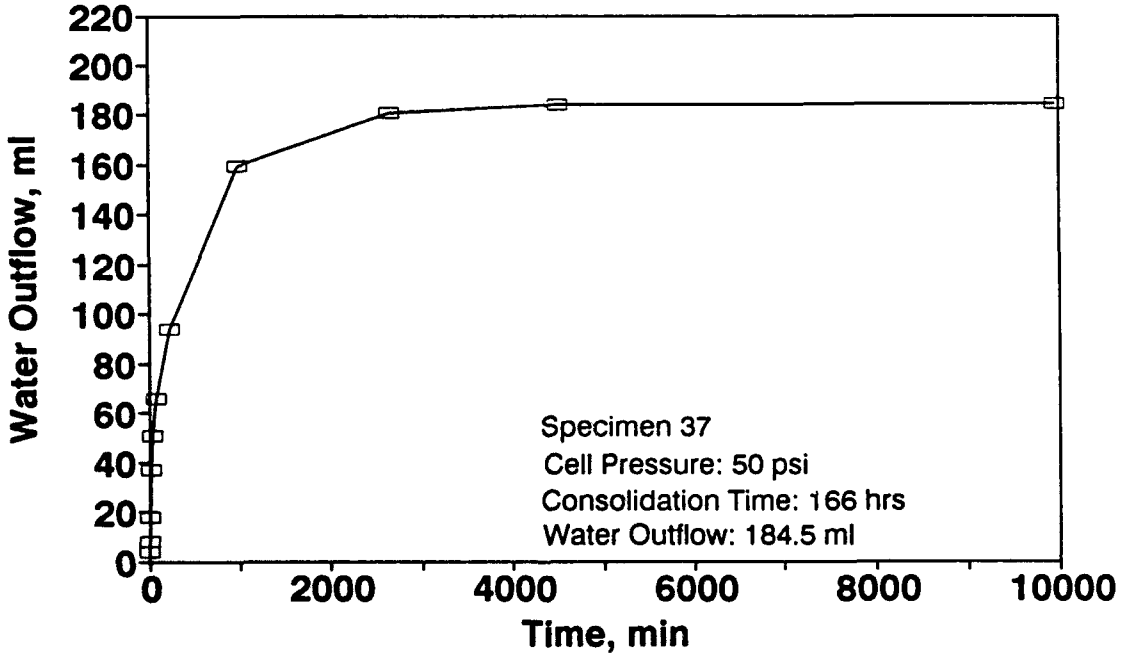
Water Outflow, ml
220
200
180
160
140
120
100
80
60
40
20
0
Specimen 37
Cell Pressure: 50 psi
Consolidation Time: 166 hrs
Water Outflow: 184.5 ml
0
2000
4000
6000
8000
10000
Time, min

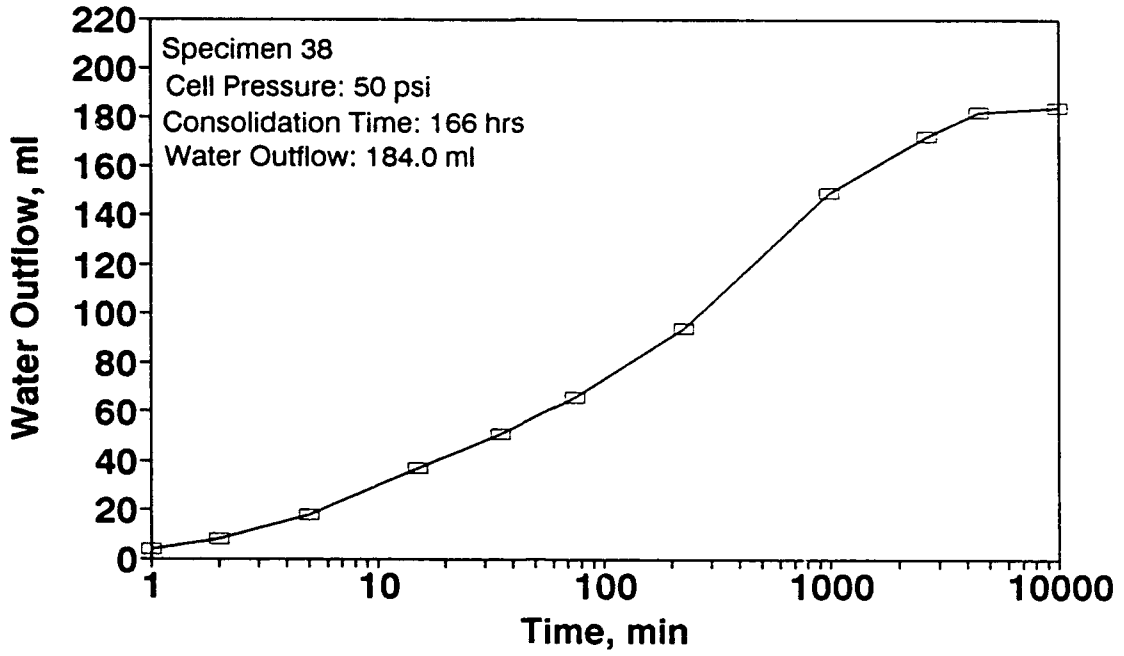
Specimen 38
Cell Pressure: 50 psi
Consolidation Time: 166 hrs
Water Outflow: 184.0 ml
Water Outflow, ml
Time, min
0
20
40
60
80
100
120
140
160
180
200
220
1
10
100
1000
10000

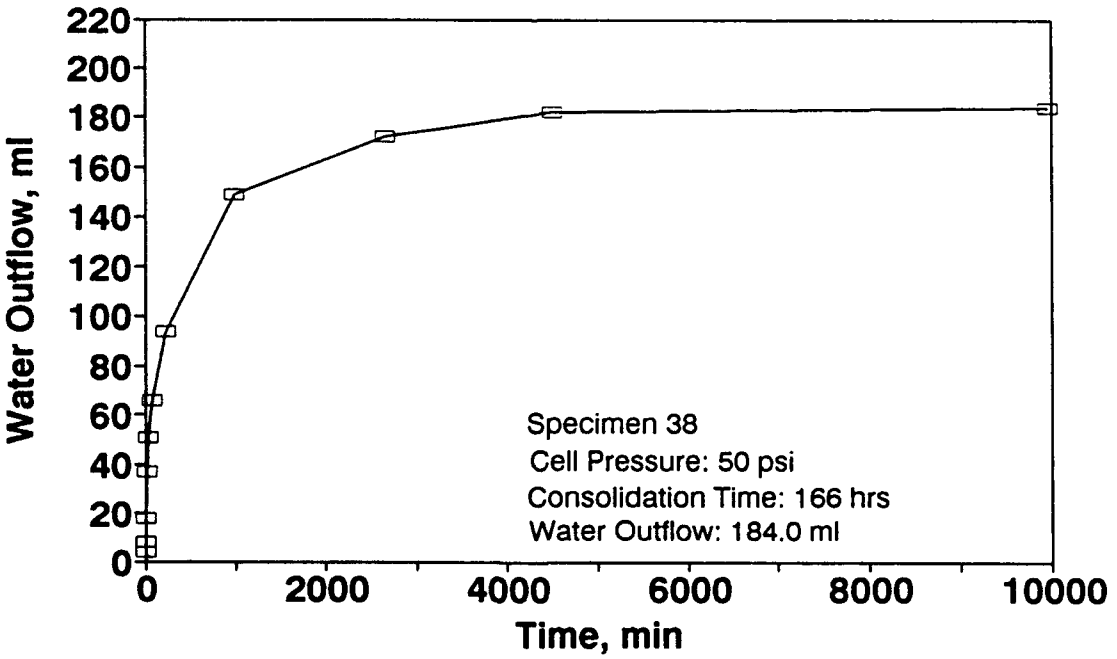
Specimen 38
Cell Pressure: 50 psi
Consolidation Time: 166 hrs
Water Outflow: 184.0 ml
Water Outflow, ml
Time, min
0
20
40
60
80
100
120
140
160
180
200
220
0
2000
4000
6000
8000
10000

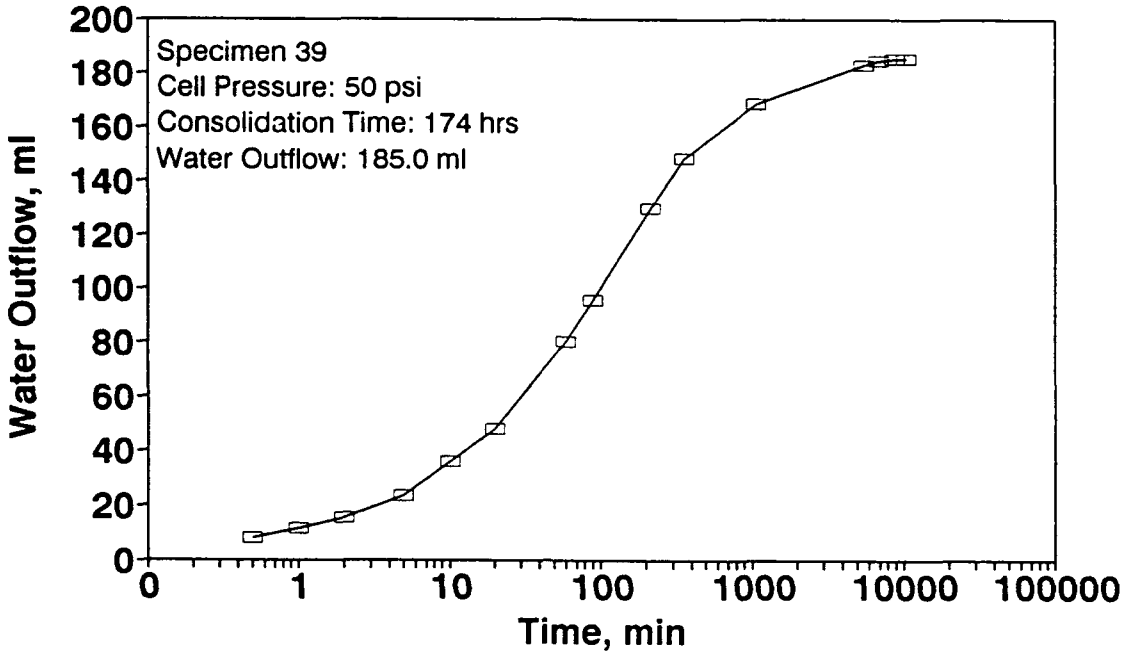
Specimen 39
Cell Pressure: 50 psi
Consolidation Time: 174 hrs
Water Outflow: 185.0 ml
Water Outflow, ml
200
180
160
140
120
100
80
60
40
20
0
0
1
10
100
1000
10000
100000
Time, min

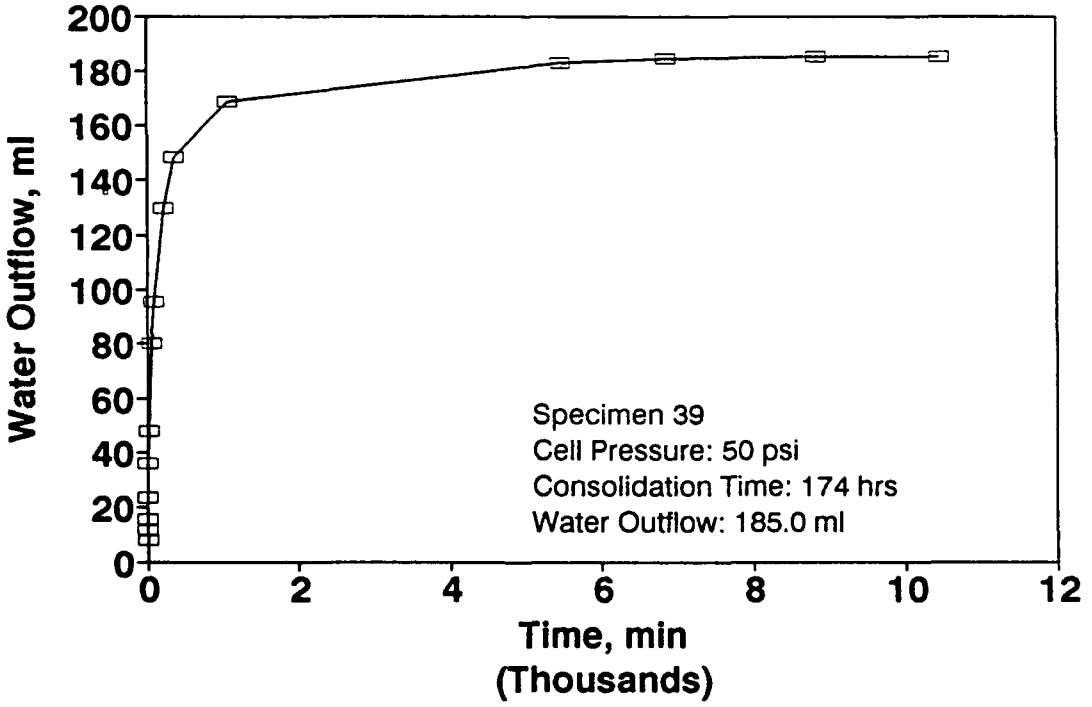
Specimen 39
Cell Pressure: 50 psi
Consolidation Time: 174 hrs
Water Outflow: 185.0 ml
Water Outflow, ml
200
180
160
140
120
100
80
60
40
20
0
0
2
4
6
8
10
12
Time, min
(Thousands)

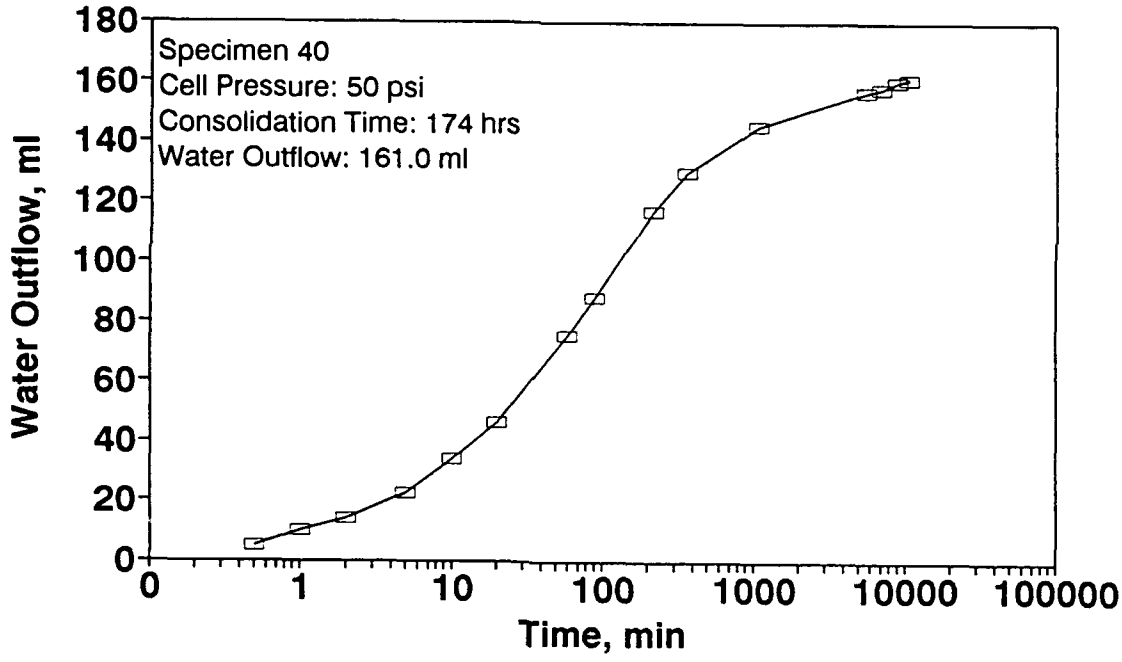
Specimen 40
Cell Pressure: 50 psi
Consolidation Time: 174 hrs
Water Outflow: 161.0 ml
Water Outflow, ml
180
160
140
120
100
80
60
40
20
0
0
1
10
100
1000
10000
100000
Time, min

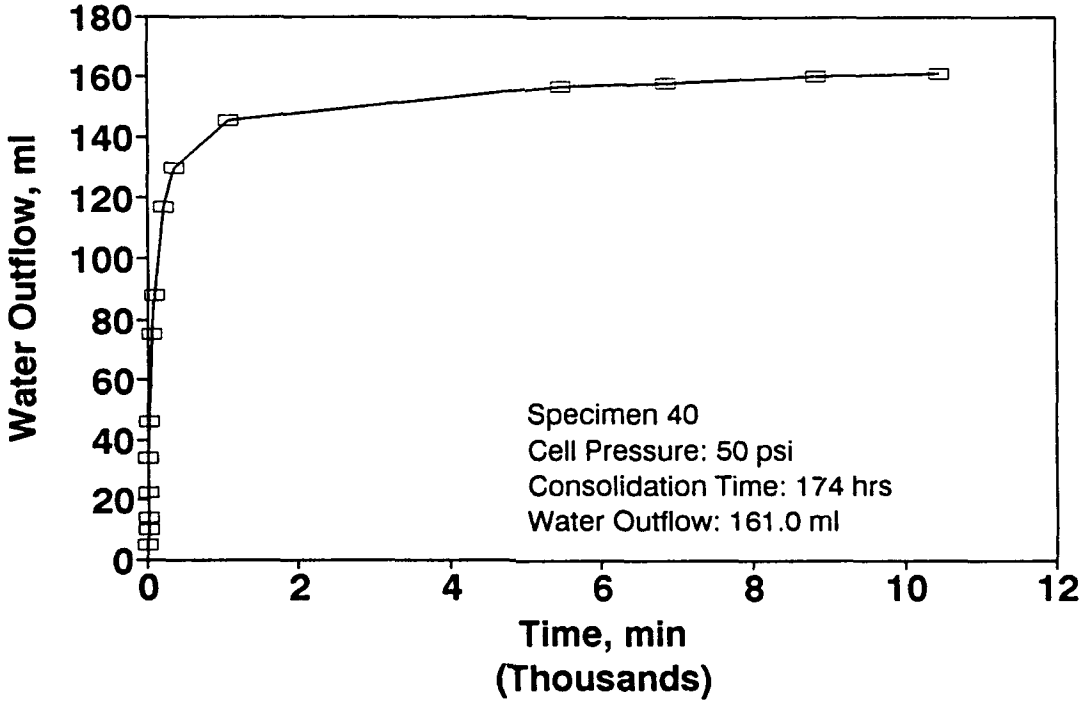
Water Outflow, ml
180
160
140
120
100
80
60
40
20
0
Specimen 40
Cell Pressure: 50 psi
Consolidation Time: 174 hrs
Water Outflow: 161.0 ml
0
2
4
6
8
10
12
Time, min
(Thousands)

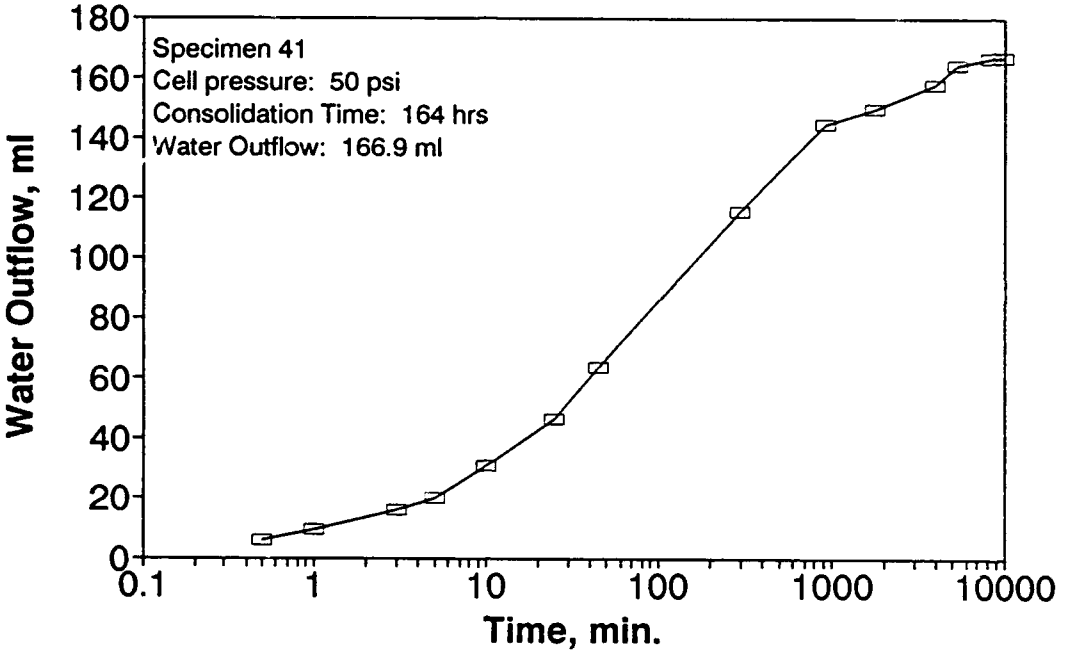
Specimen 41
Cell pressure: 50 psi
Consolidation Time: 164 hrs
Water Outflow: 166.9 ml
Water Outflow, ml
Time, min.
0
20
40
60
80
100
120
140
160
180
0.1
1
10
100
1000
10000

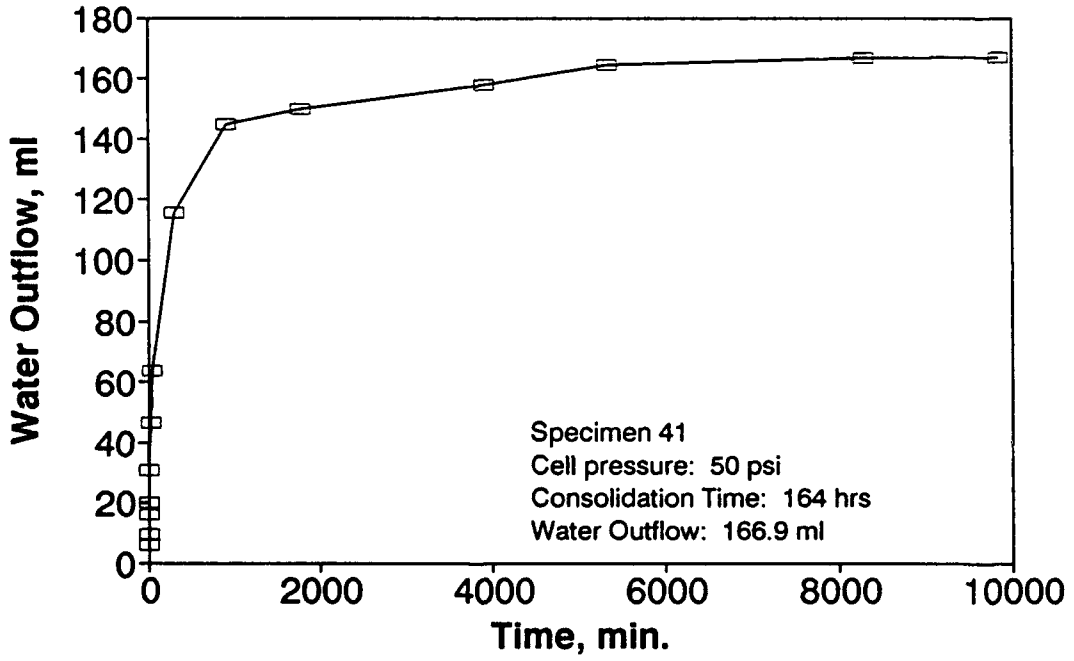
Specimen 41
Cell pressure: 50 psi
Consolidation Time: 164 hrs
Water Outflow: 166.9 ml
Water Outflow, ml
Time, min.
0
20
40
60
80
100
120
140
160
180
0
2000
4000
6000
8000
10000

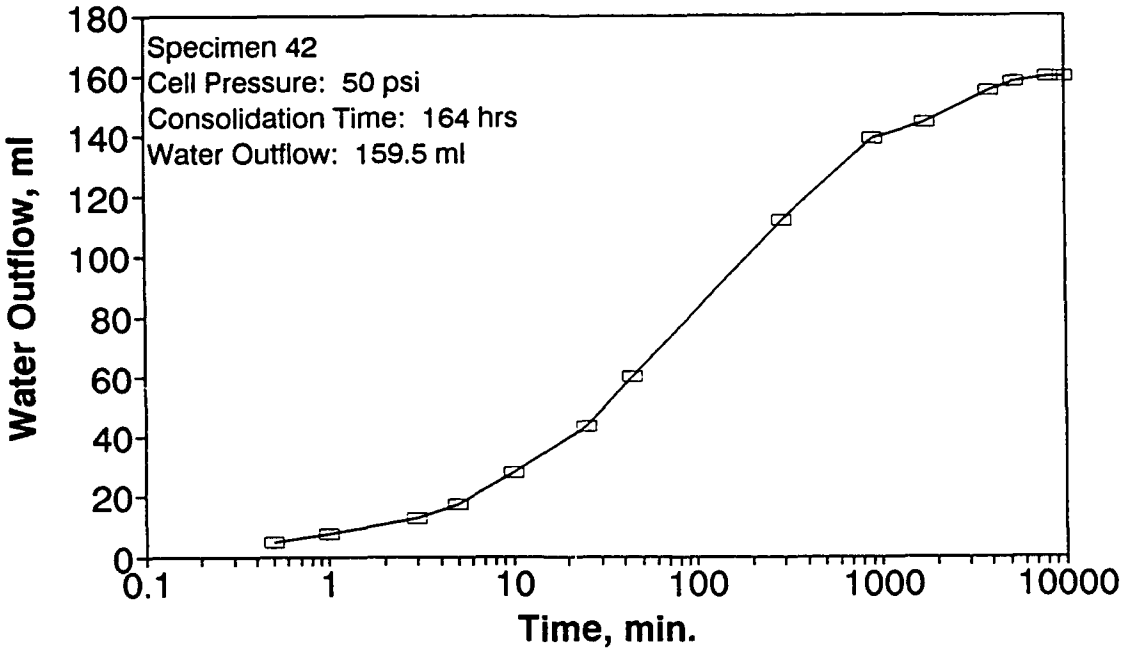
Specimen 42
Cell Pressure: 50 psi
Consolidation Time: 164 hrs
Water Outflow: 159.5 ml
Water Outflow, ml
Time, min.
0
20
40
60
80
100
120
140
160
180
0.1
1
10
100
1000
10000

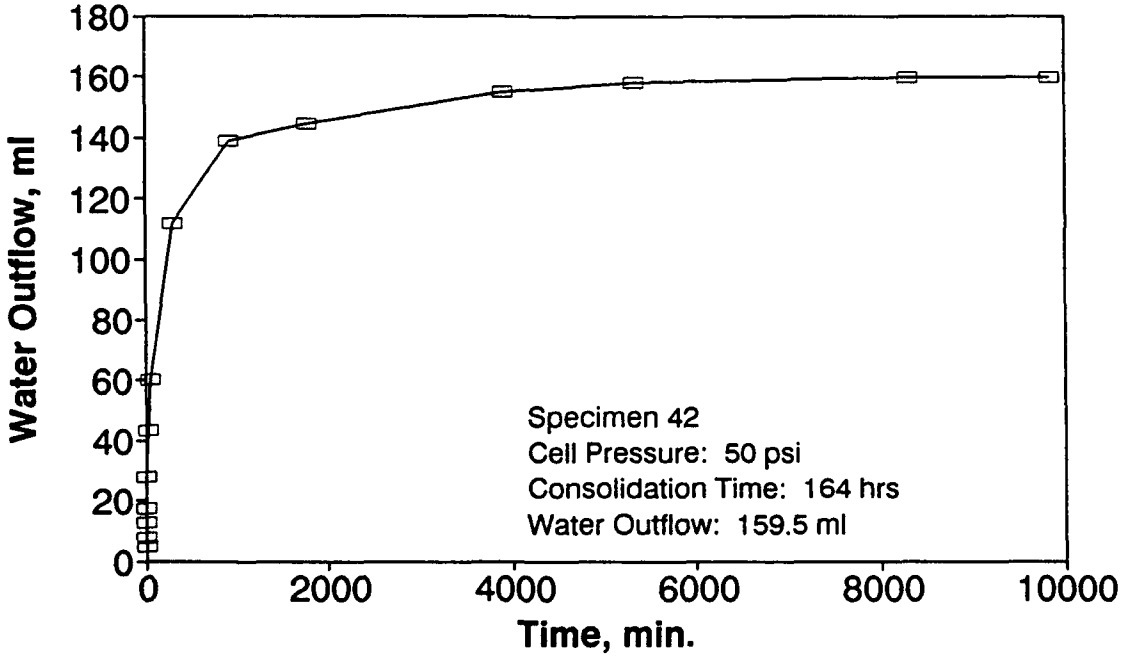
Specimen 42
Cell Pressure: 50 psi
Consolidation Time: 164 hrs
Water Outflow: 159.5 ml
Water Outflow, ml
Time, min.
0
20
40
60
80
100
120
140
160
180
0
2000
4000
6000
8000
10000

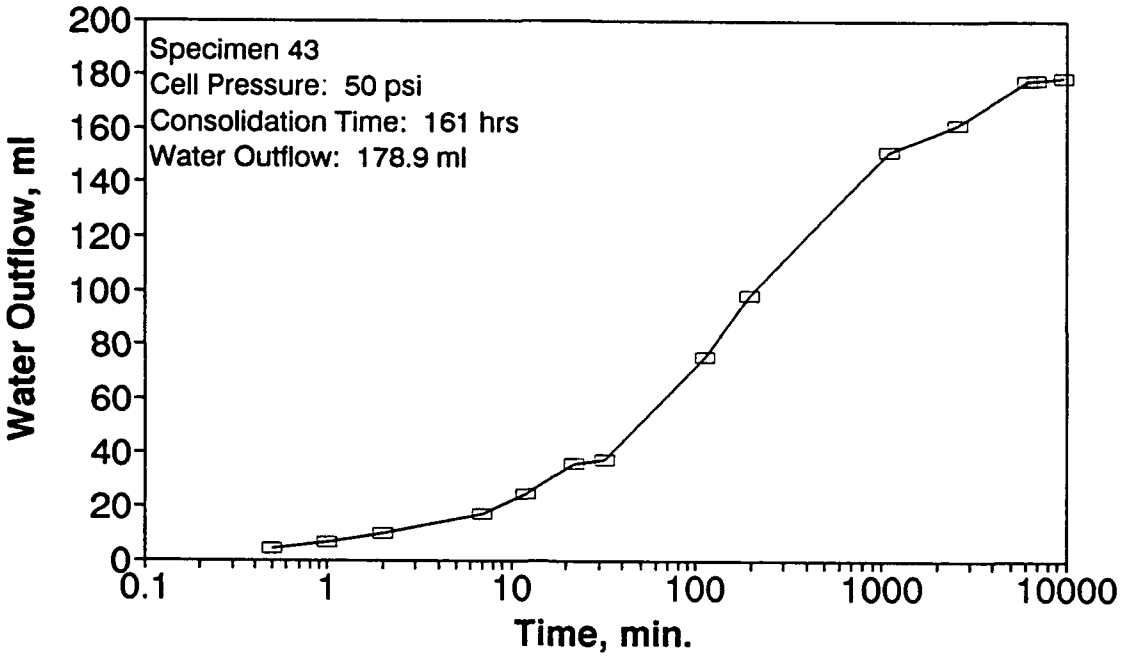
Specimen 43
Cell Pressure: 50 psi
Consolidation Time: 161 hrs
Water Outflow: 178.9 ml
Water Outflow, ml
Time, min.
0
20
40
60
80
100
120
140
160
180
200
0.1
1
10
100
1000
10000

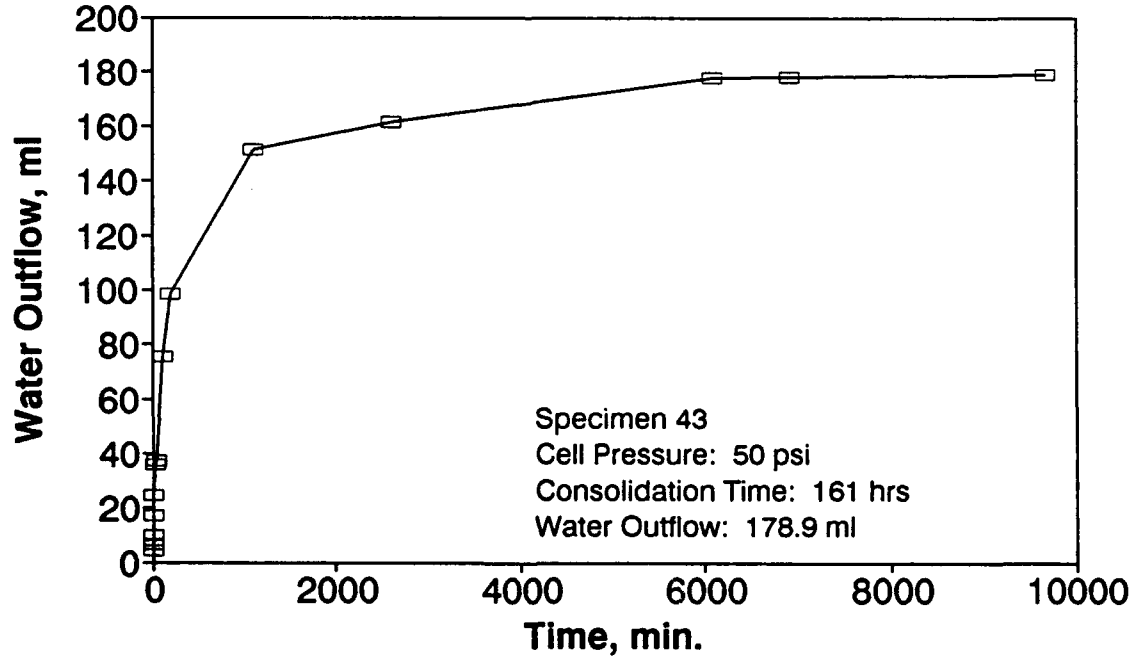
Specimen 43
Cell Pressure: 50 psi
Consolidation Time: 161 hrs
Water Outflow: 178.9 ml
Water Outflow, ml
Time, min.
0
20
40
60
80
100
120
140
160
180
200
0
2000
4000
6000
8000
10000

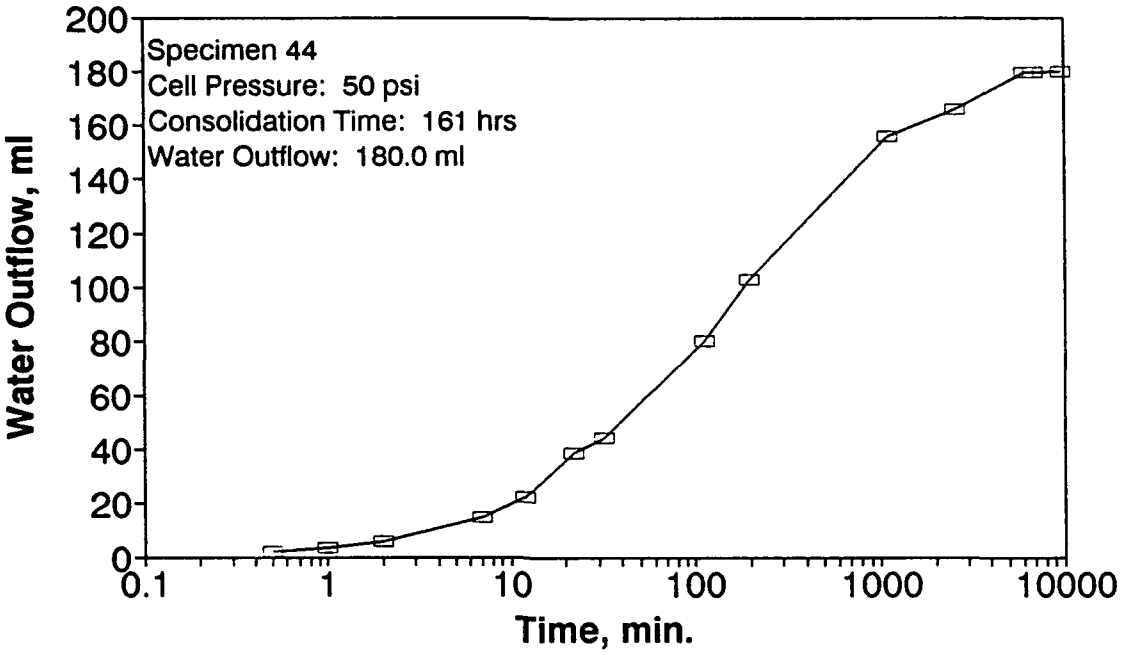
Specimen 44
Cell Pressure: 50 psi
Consolidation Time: 161 hrs
Water Outflow: 180.0 ml
Water Outflow, ml
Time, min.
0
20
40
60
80
100
120
140
160
180
200
0.1
1
10
100
1000
10000

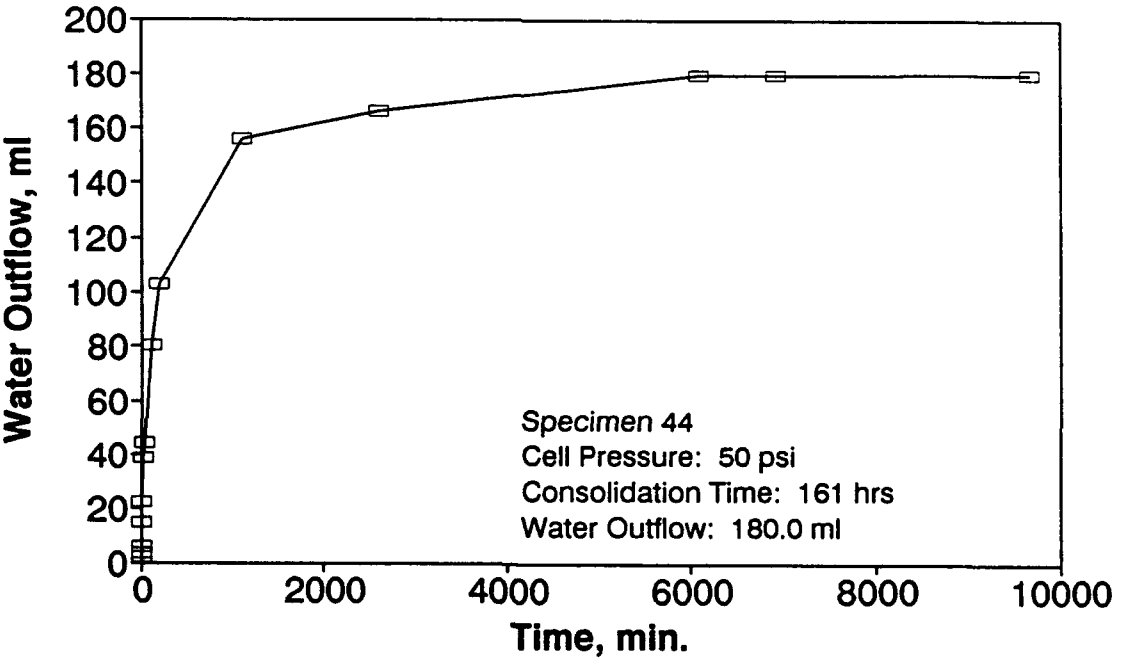
Specimen 44
Cell Pressure: 50 psi
Consolidation Time: 161 hrs
Water Outflow: 180.0 ml
Water Outflow, ml
Time, min.
0
20
40
60
80
100
120
140
160
180
200
0
2000
4000
6000
8000
10000

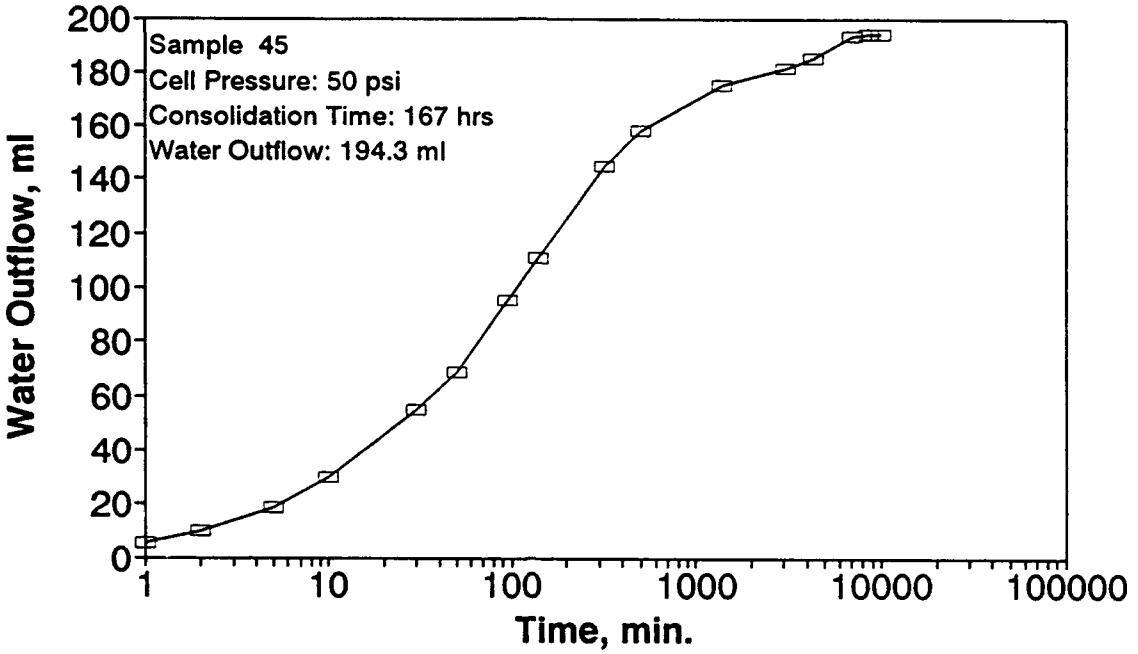
Sample 45
Cell Pressure: 50 psi
Consolidation Time: 167 hrs
Water Outflow: 194.3 ml
Water Outflow, ml
200
180
160
140
120
100
80
60
40
20
0
1
10
100
1000
10000
100000
Time, min.

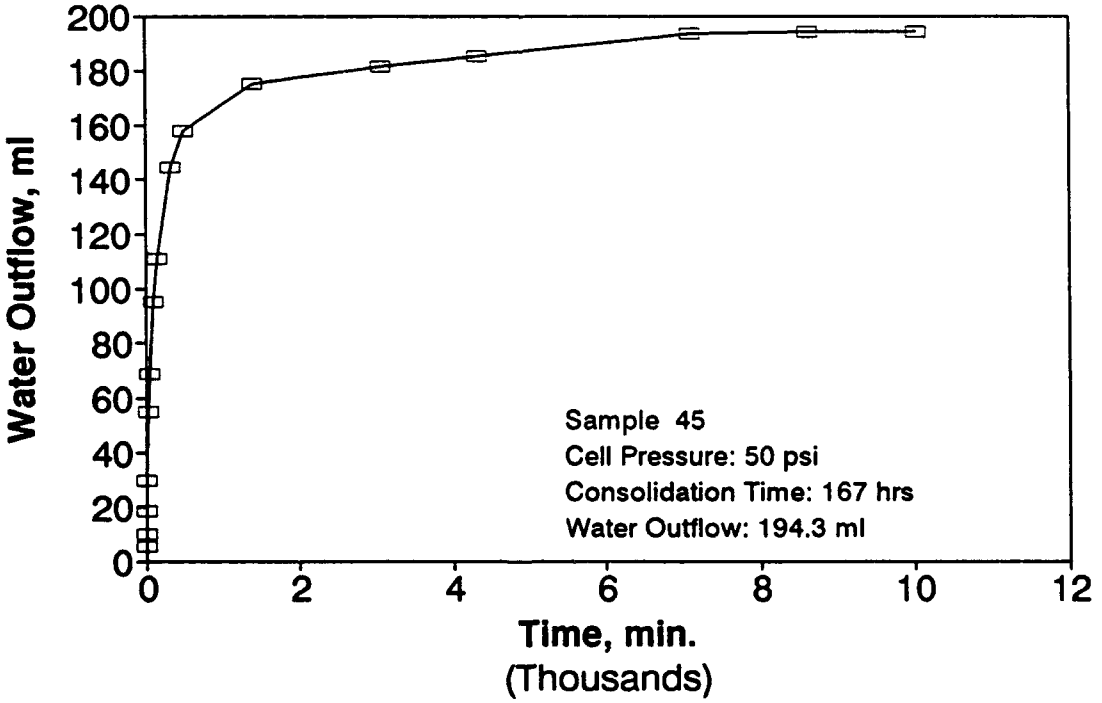
Water Outflow, ml
200
180
160
140
120
100
80
60
40
20
0
Sample 45
Cell Pressure: 50 psi
Consolidation Time: 167 hrs
Water Outflow: 194.3 ml
0
2
4
6
8
10
12
Time, min.
(Thousands)

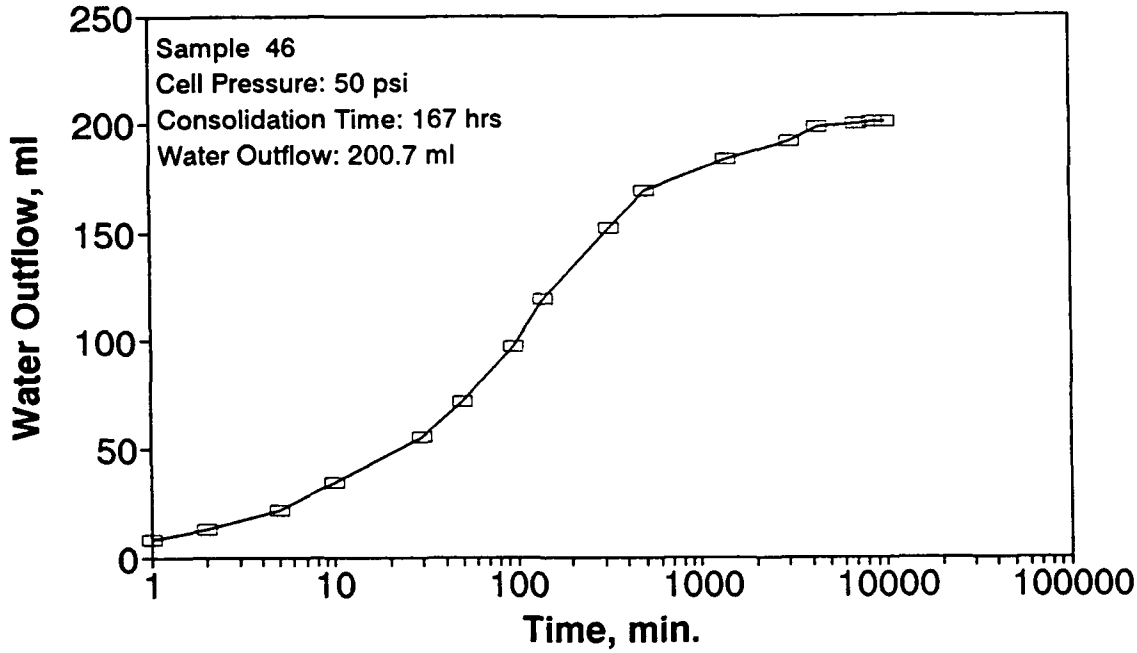
Sample 46
Cell Pressure: 50 psi
Consolidation Time: 167 hrs
Water Outflow: 200.7 ml
Water Outflow, ml
250
200
150
100
50
0
1
10
100
1000
10000
100000
Time, min.

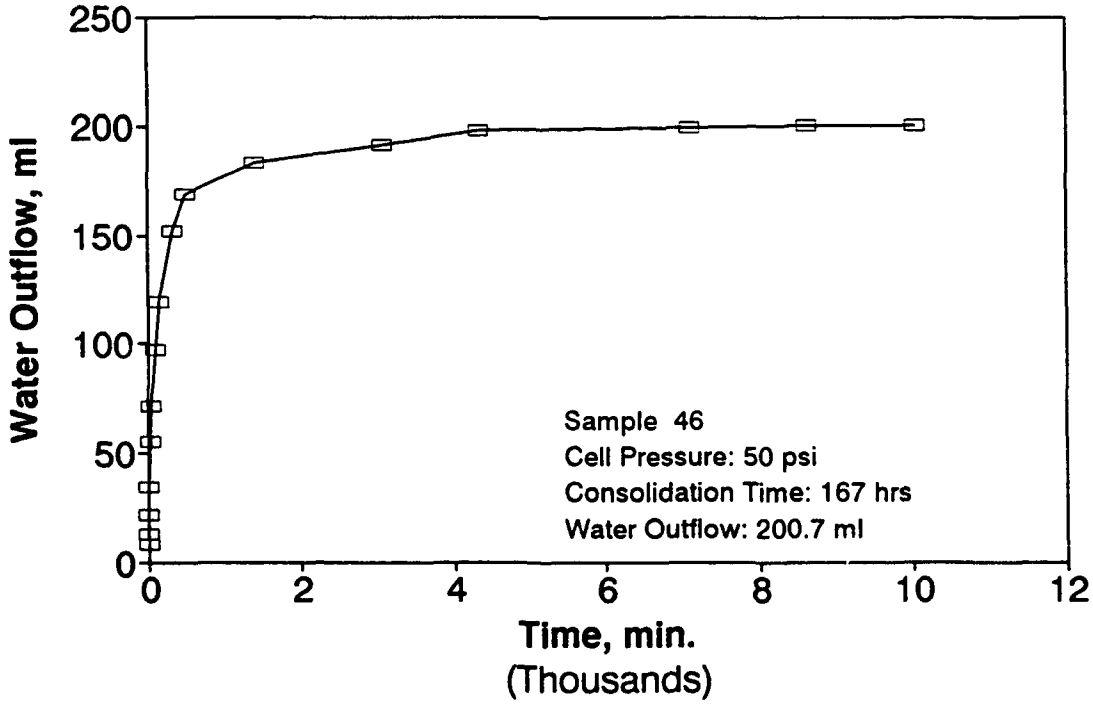
Sample 46
Cell Pressure: 50 psi
Consolidation Time: 167 hrs
Water Outflow: 200.7 ml
Water Outflow, ml
250
200
150
100
50
0
0
2
4
6
8
10
12
Time, min.
(Thousands)

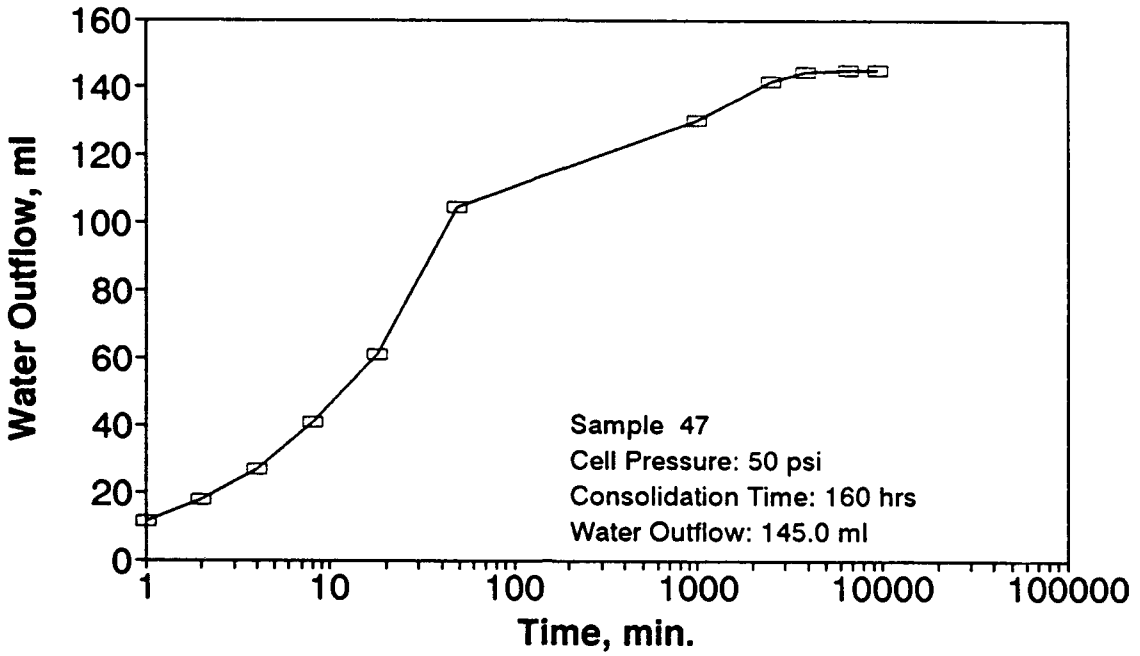
Water Outflow, ml
160
140
120
100
80
60
40
20
0
1
10
100
1000
10000
100000
Time, min.
Sample 47
Cell Pressure: 50 psi
Consolidation Time: 160 hrs
Water Outflow: 145.0 ml

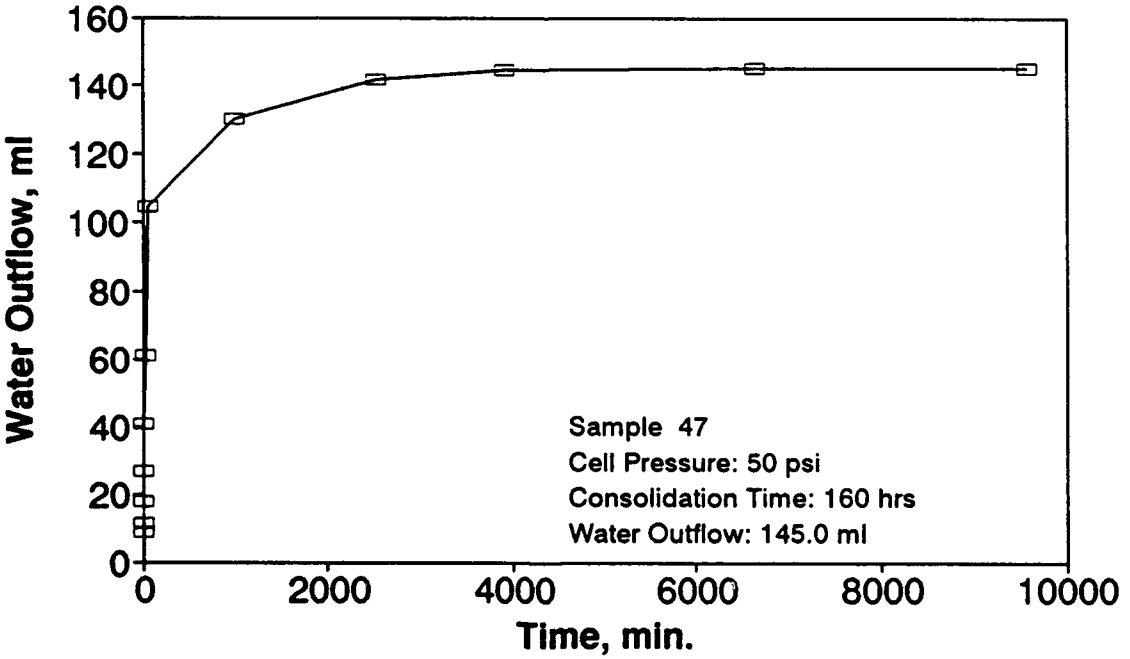
Water Outflow, ml
160
140
120
100
80
60
40
20
0
0
2000
4000
6000
8000
10000
Time, min.
Sample 47
Cell Pressure: 50 psi
Consolidation Time: 160 hrs
Water Outflow: 145.0 ml

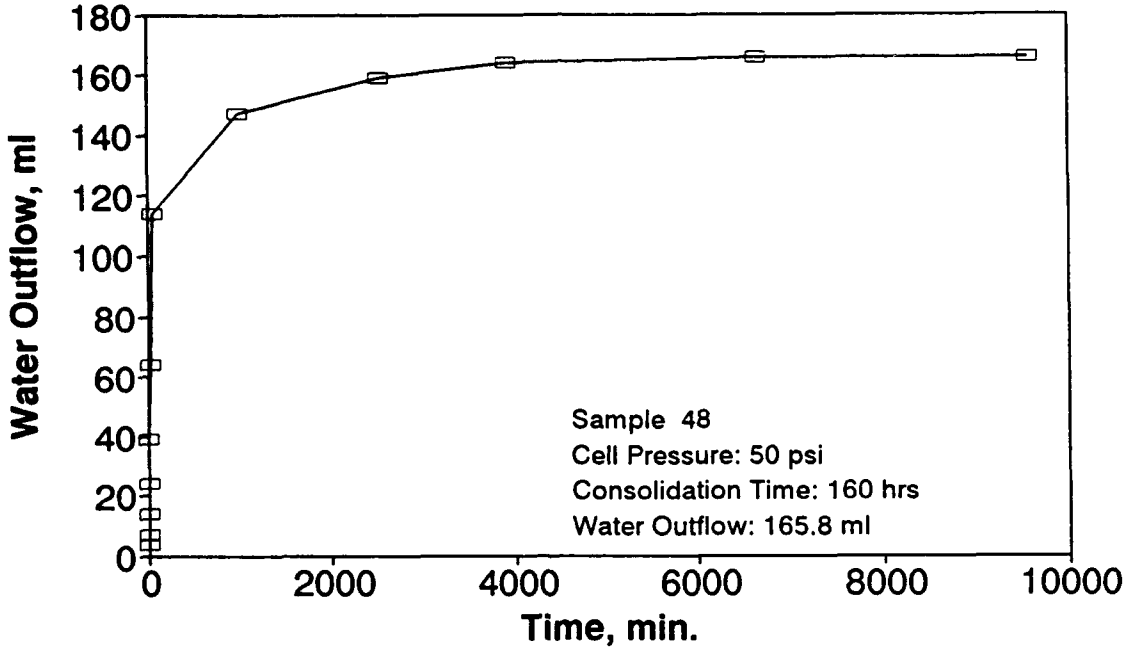
Water Outflow, ml
180
160
140
120
100
80
60
40
20
0
0
2000
4000
6000
8000
10000
Time, min.
Sample 48
Cell Pressure: 50 psi
Consolidation Time: 160 hrs
Water Outflow: 165.8 ml

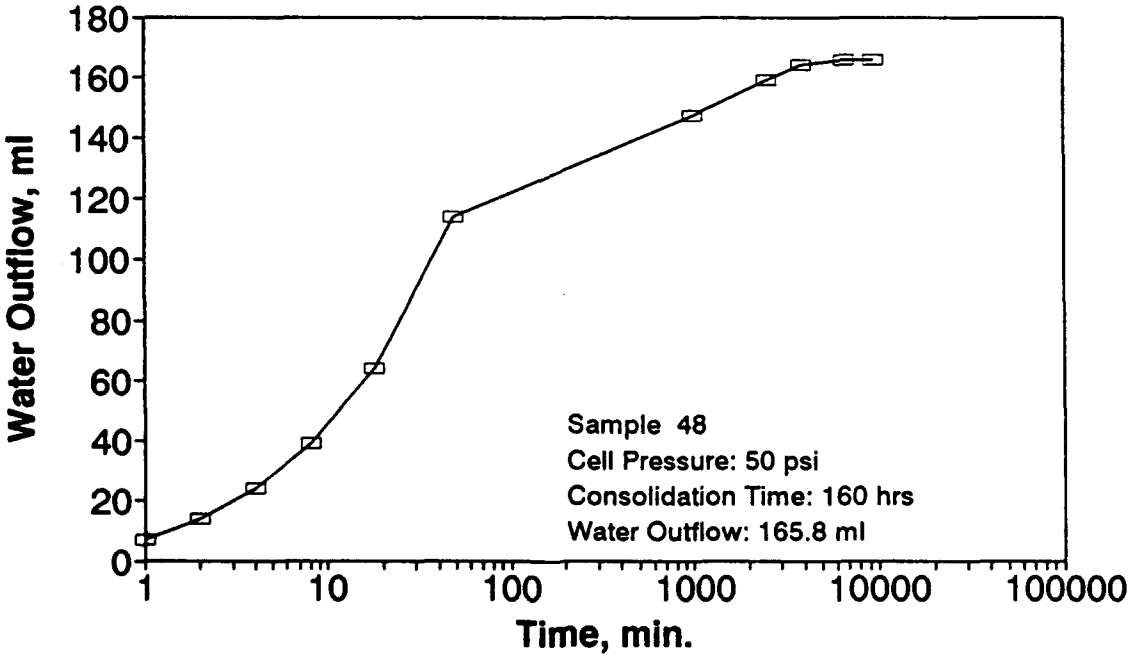
Water Outflow, ml
180
160
140
120
100
80
60
40
20
0
1
10
100
1000
10000
100000
Time, min.
Sample 48
Cell Pressure: 50 psi
Consolidation Time: 160 hrs
Water Outflow: 165.8 ml

APPENDIX B

CALIBRATION DATA OF THE LOAD TRANSMITTED TO THE SPECIMEN IN THE TRIAXIAL TEST SET UP

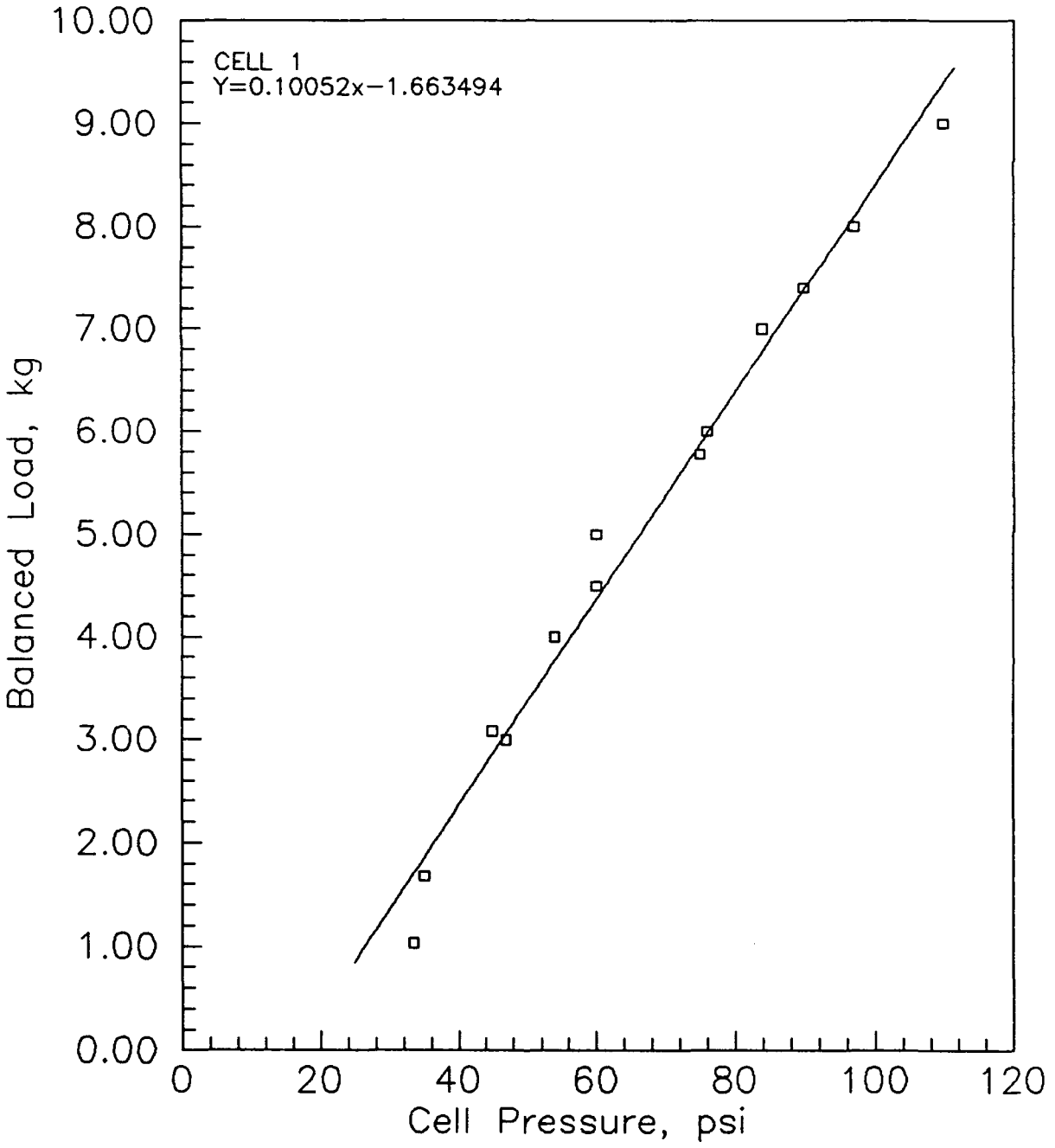
CELL 1
Y=0.10052x−1.663494
Balanced Load, kg
Cell Pressure, psi
10.00
9.00
8.00
7.00
6.00
5.00
4.00
3.00
2.00
1.00
0.00
0
20
40
60
80
100
120

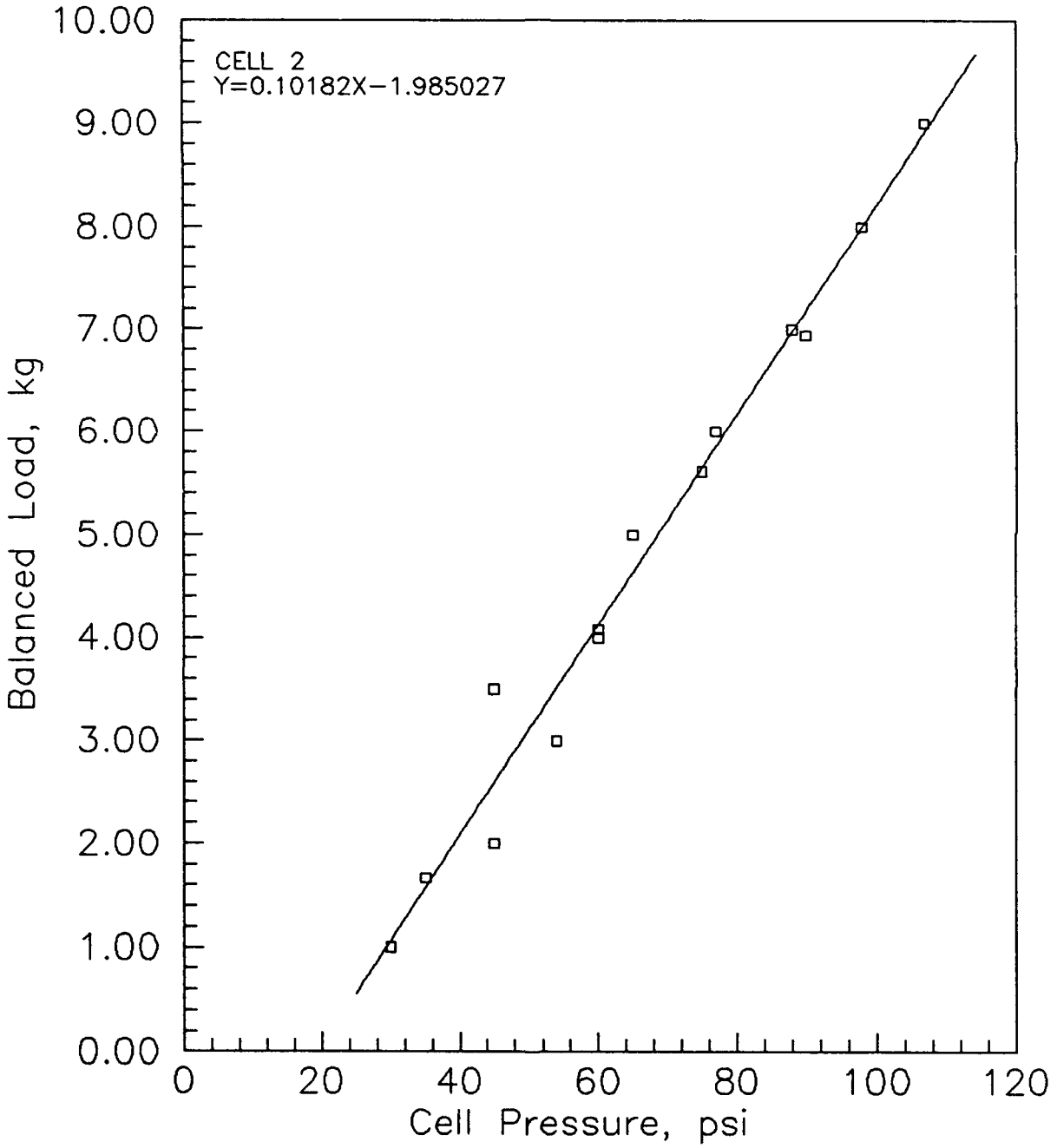
CELL 2
Y=0.10182X-1.985027
Balanced Load, kg
Cell Pressure, psi
10.00
9.00
8.00
7.00
6.00
5.00
4.00
3.00
2.00
1.00
0.00
0
20
40
60
80
100
120

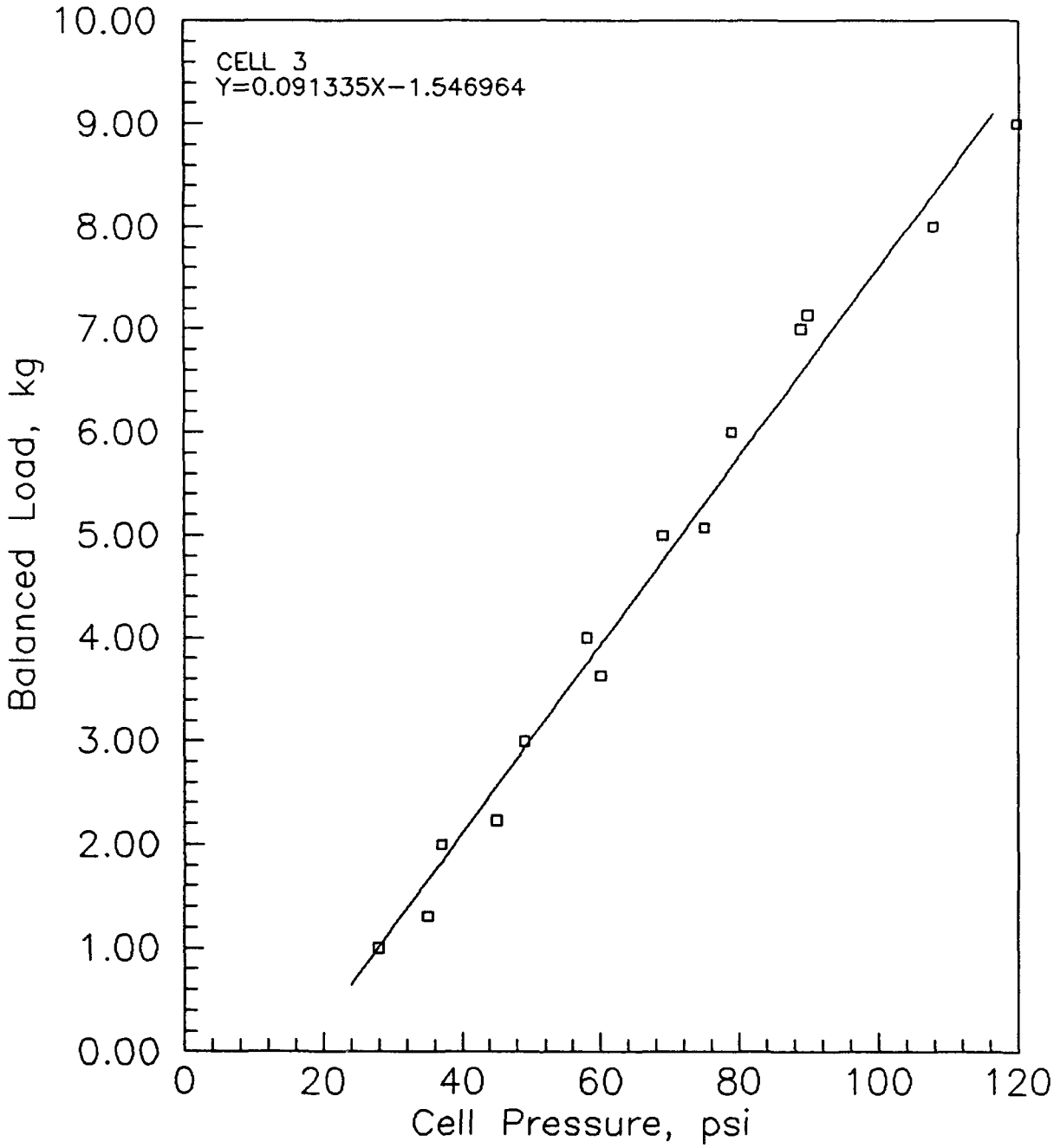
CELL 3
Y=0.091335X-1.546964
Balanced Load, kg
Cell Pressure, psi
10.00
9.00
8.00
7.00
6.00
5.00
4.00
3.00
2.00
1.00
0.00
0
20
40
60
80
100
120

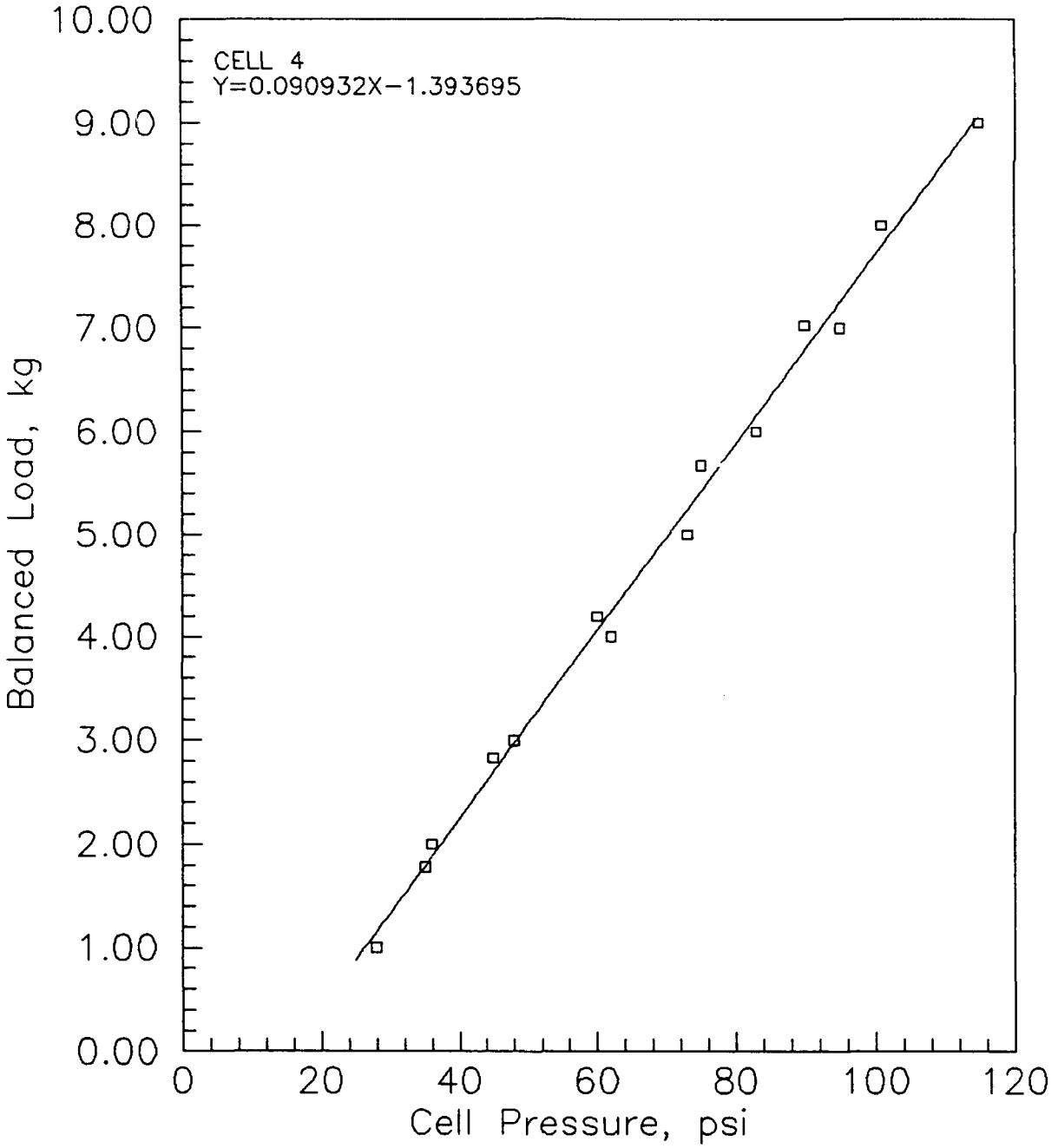
CELL 4
Y=0.090932X-1.393695
Balanced Load, kg
10.00
9.00
8.00
7.00
6.00
5.00
4.00
3.00
2.00
1.00
0.00
0
20
40
60
80
100
120
Cell Pressure, psi

APPENDIX C

RECORDS OF SPECIMEN EQUILIBRATION

TO PREDETERMINED SOIL SUCTIONS

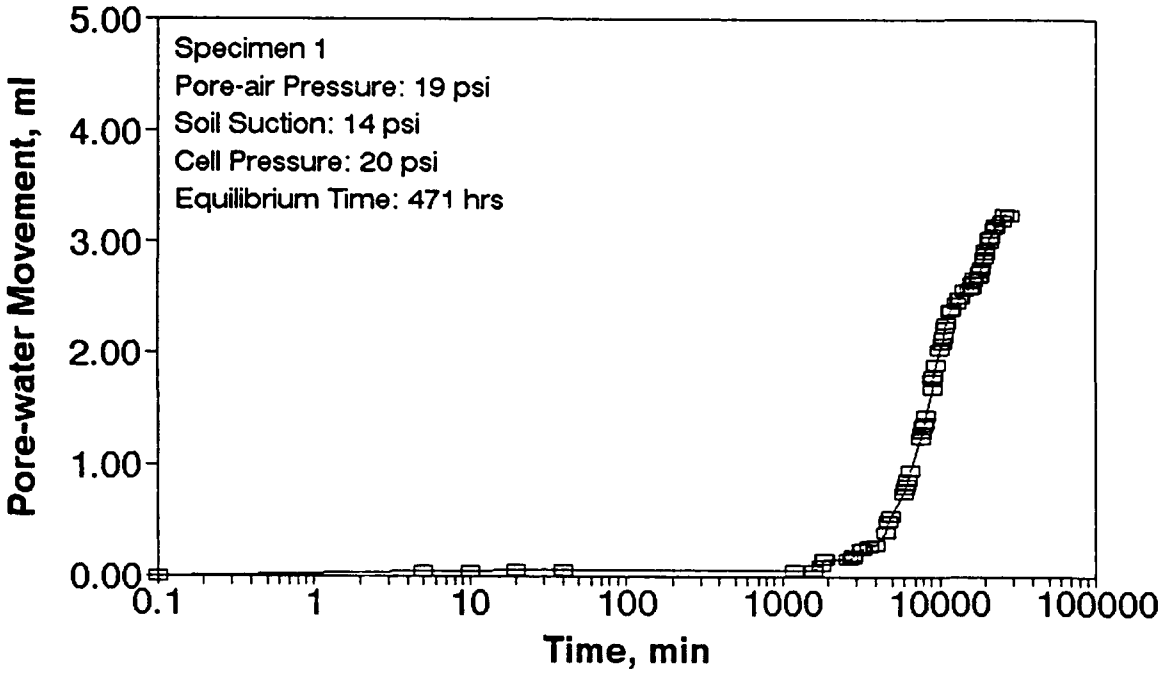
Specimen 1
Pore-air Pressure: 19 psi
Soil Suction: 14 psi
Cell Pressure: 20 psi
Equilibrium Time: 471 hrs
Pore-water Movement, ml
5.00
4.00
3.00
2.00
1.00
0.00
0.1
1
10
100
1000
10000
100000
Time, min

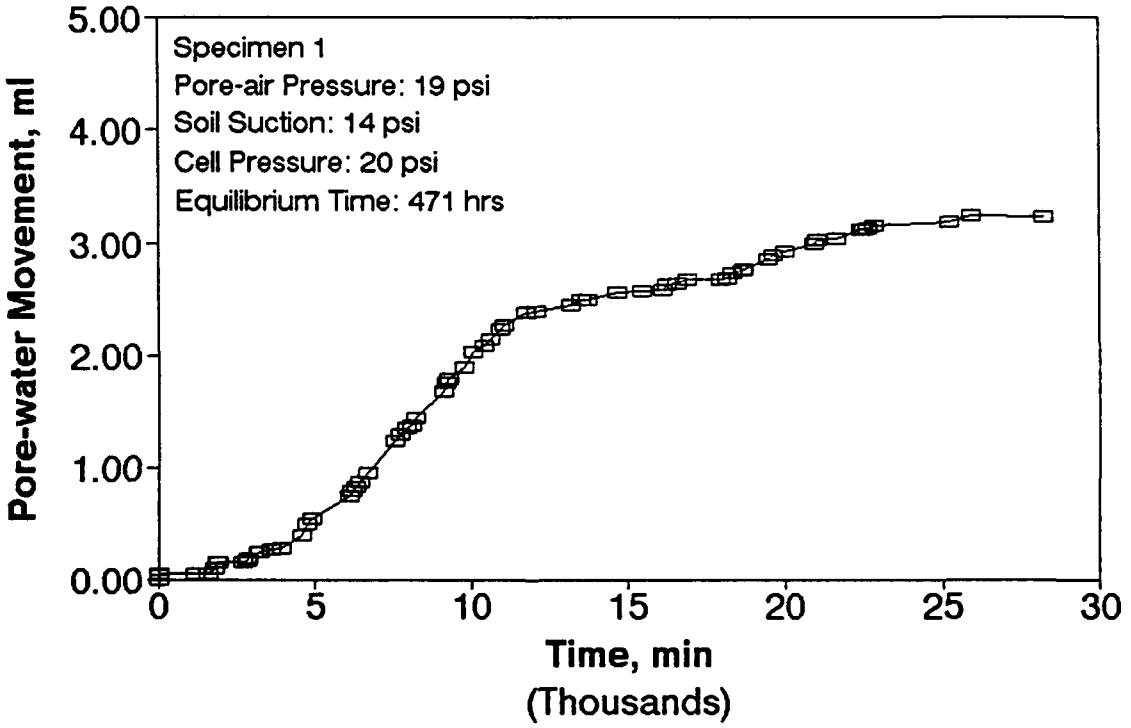
Specimen 1
Pore-air Pressure: 19 psi
Soil Suction: 14 psi
Cell Pressure: 20 psi
Equilibrium Time: 471 hrs
Pore-water Movement, ml
5.00
4.00
3.00
2.00
1.00
0.00
0
5
10
15
20
25
30
Time, min
(Thousands)

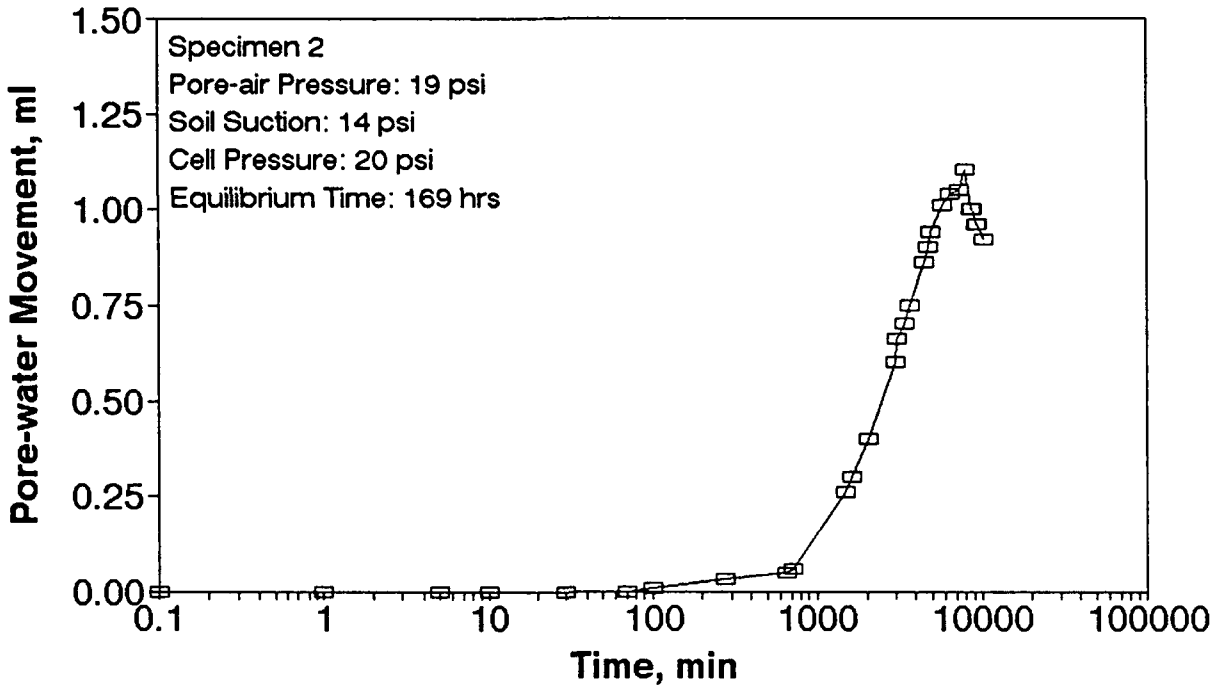
Specimen 2
Pore-air Pressure: 19 psi
Soil Suction: 14 psi
Cell Pressure: 20 psi
Equilibrium Time: 169 hrs
Pore-water Movement, ml
1.50
1.25
1.00
0.75
0.50
0.25
0.00
0.1
1
10
100
1000
10000
100000
Time, min

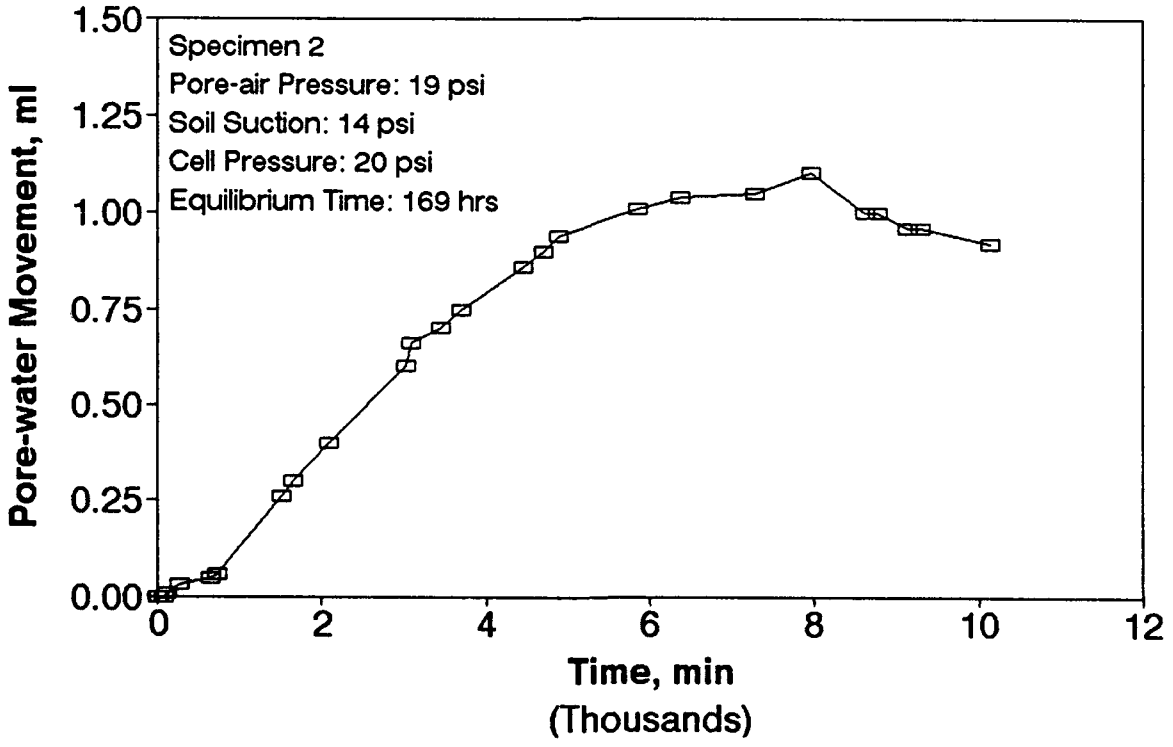
Specimen 2
Pore-air Pressure: 19 psi
Soil Suction: 14 psi
Cell Pressure: 20 psi
Equilibrium Time: 169 hrs
Pore-water Movement, ml
1.50
1.25
1.00
0.75
0.50
0.25
0.00
0
2
4
6
8
10
12
Time, min
(Thousands)

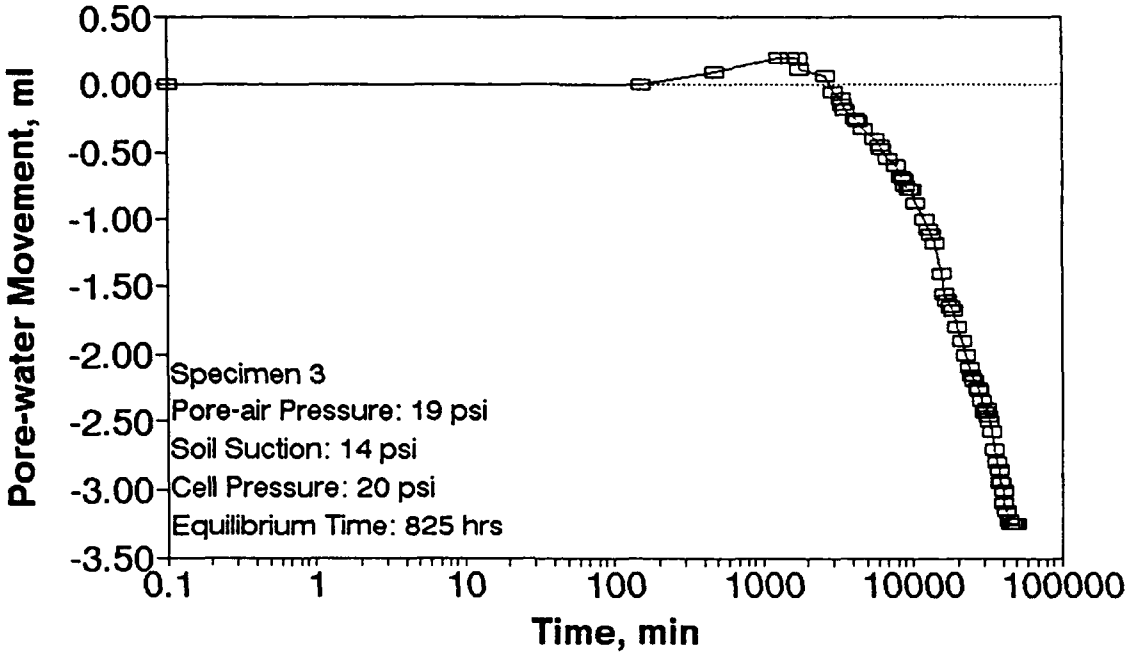
0.50
0.00
-0.50
-1.00
-1.50
-2.00
-2.50
-3.00
-3.50
Pore-water Movement, ml
Specimen 3
Pore-air Pressure: 19 psi
Soil Suction: 14 psi
Cell Pressure: 20 psi
Equilibrium Time: 825 hrs
0.1
1
10
100
1000
10000
100000
Time, min

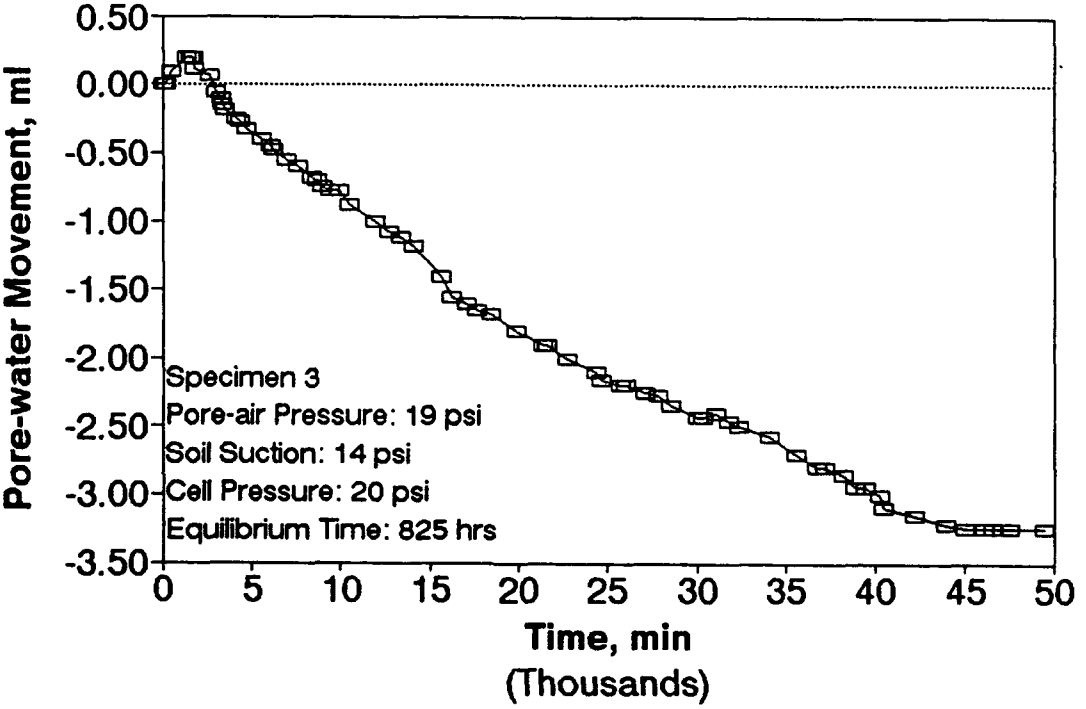
0.50
0.00
-0.50
-1.00
-1.50
-2.00
-2.50
-3.00
-3.50
Pore-water Movement, ml
Specimen 3
Pore-air Pressure: 19 psi
Soil Suction: 14 psi
Cell Pressure: 20 psi
Equilibrium Time: 825 hrs
0
5
10
15
20
25
30
35
40
45
50
Time, min
(Thousands)

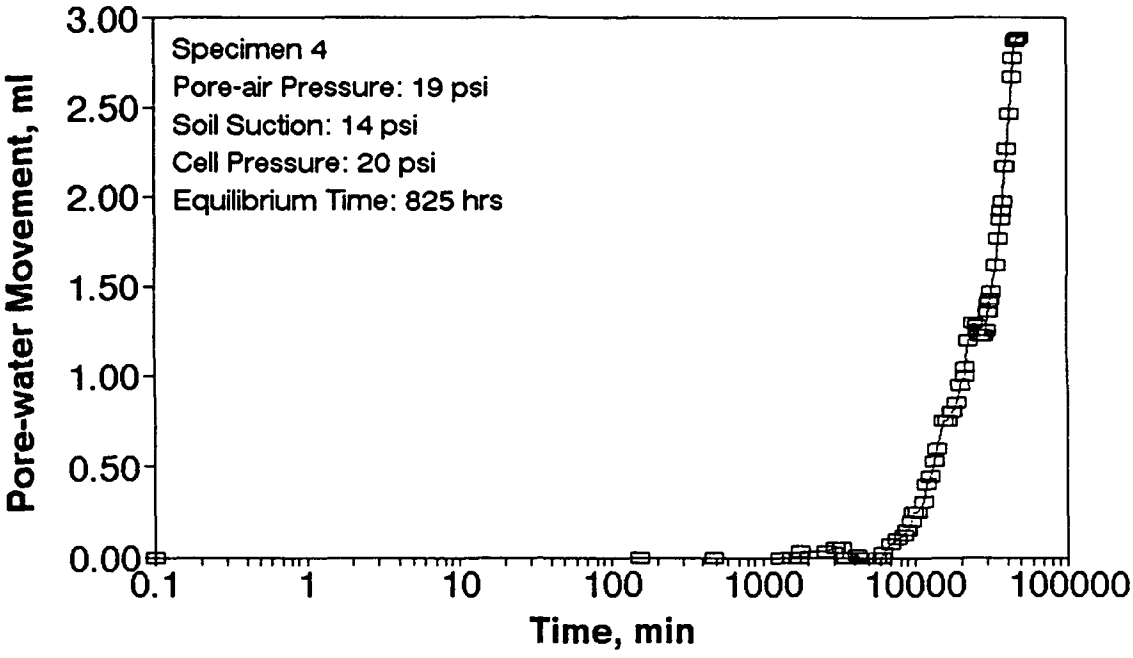
Specimen 4
Pore-air Pressure: 19 psi
Soil Suction: 14 psi
Cell Pressure: 20 psi
Equilibrium Time: 825 hrs
Pore-water Movement, ml
3.00
2.50
2.00
1.50
1.00
0.50
0.00
0.1
1
10
100
1000
10000
100000
Time, min

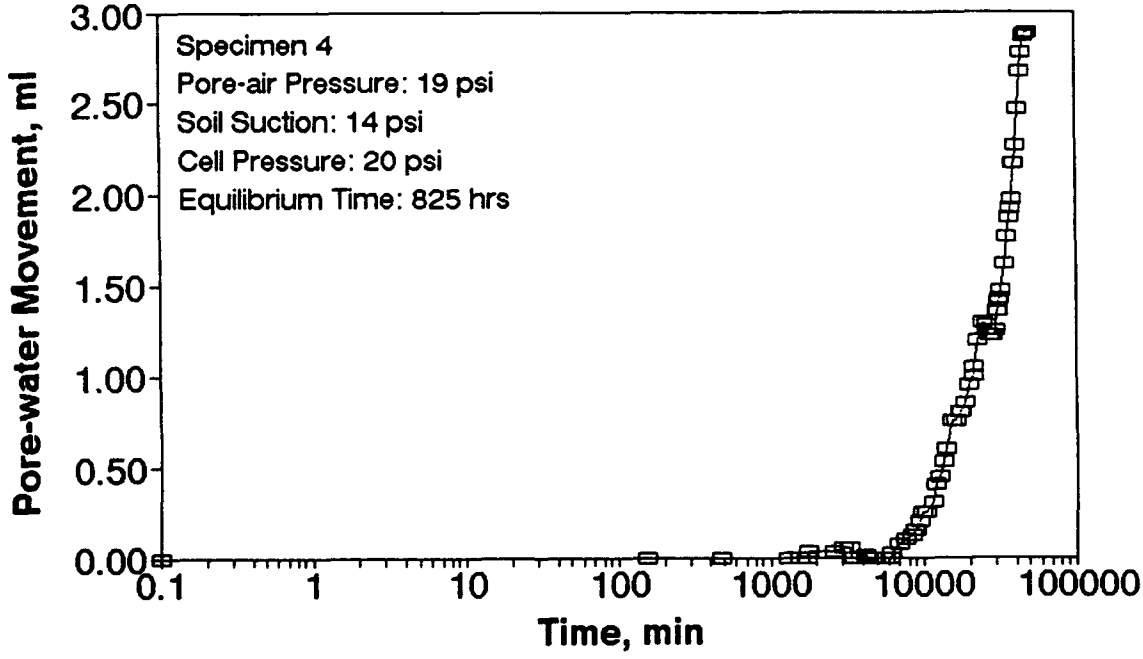
Specimen 4
Pore-air Pressure: 19 psi
Soil Suction: 14 psi
Cell Pressure: 20 psi
Equilibrium Time: 825 hrs
Pore-water Movement, ml
3.00
2.50
2.00
1.50
1.00
0.50
0.00
0.1
1
10
100
1000
10000
100000
Time, min

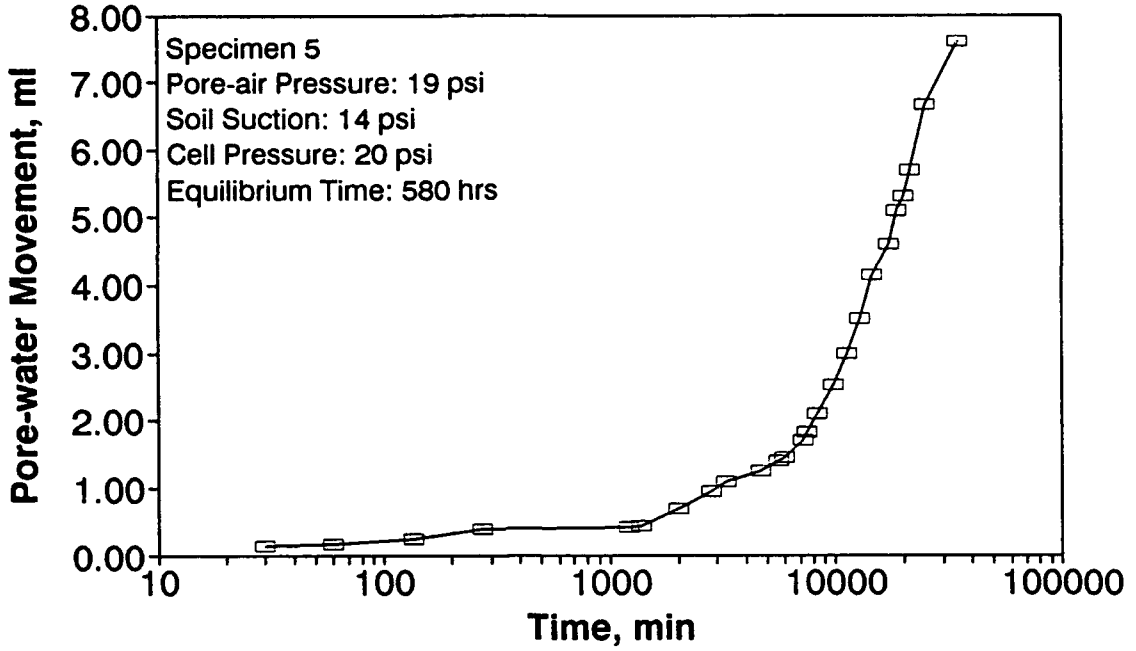
Specimen 5
Pore-air Pressure: 19 psi
Soil Suction: 14 psi
Cell Pressure: 20 psi
Equilibrium Time: 580 hrs
Pore-water Movement, ml
8.00
7.00
6.00
5.00
4.00
3.00
2.00
1.00
0.00
10
100
1000
10000
100000
Time, min

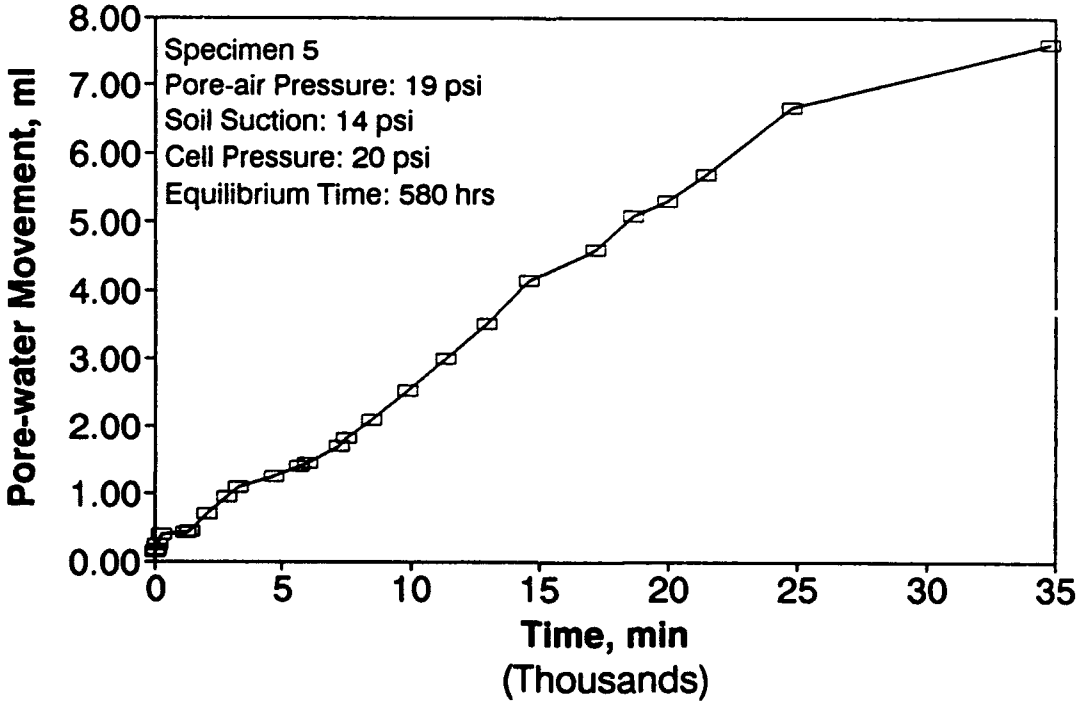
Specimen 5
Pore-air Pressure: 19 psi
Soil Suction: 14 psi
Cell Pressure: 20 psi
Equilibrium Time: 580 hrs
Pore-water Movement, ml
8.00
7.00
6.00
5.00
4.00
3.00
2.00
1.00
0.00
0
5
10
15
20
25
30
35
Time, min
(Thousands)

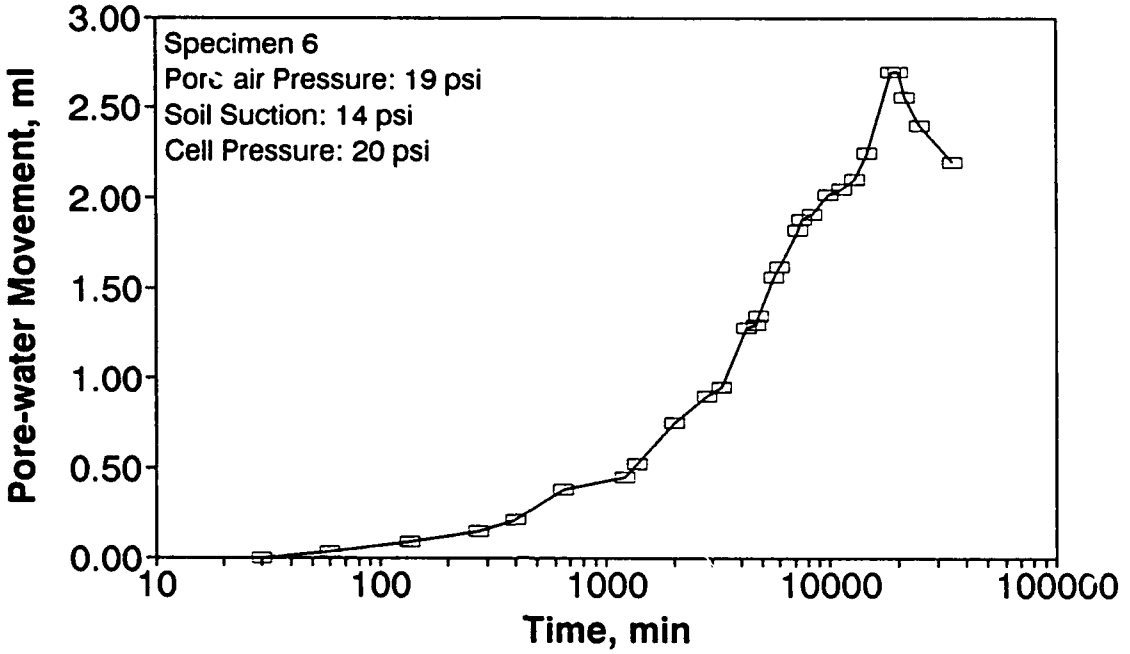
Specimen 6
Pore air Pressure: 19 psi
Soil Suction: 14 psi
Cell Pressure: 20 psi
Pore-water Movement, ml
3.00
2.50
2.00
1.50
1.00
0.50
0.00
10
100
1000
10000
100000
Time, min

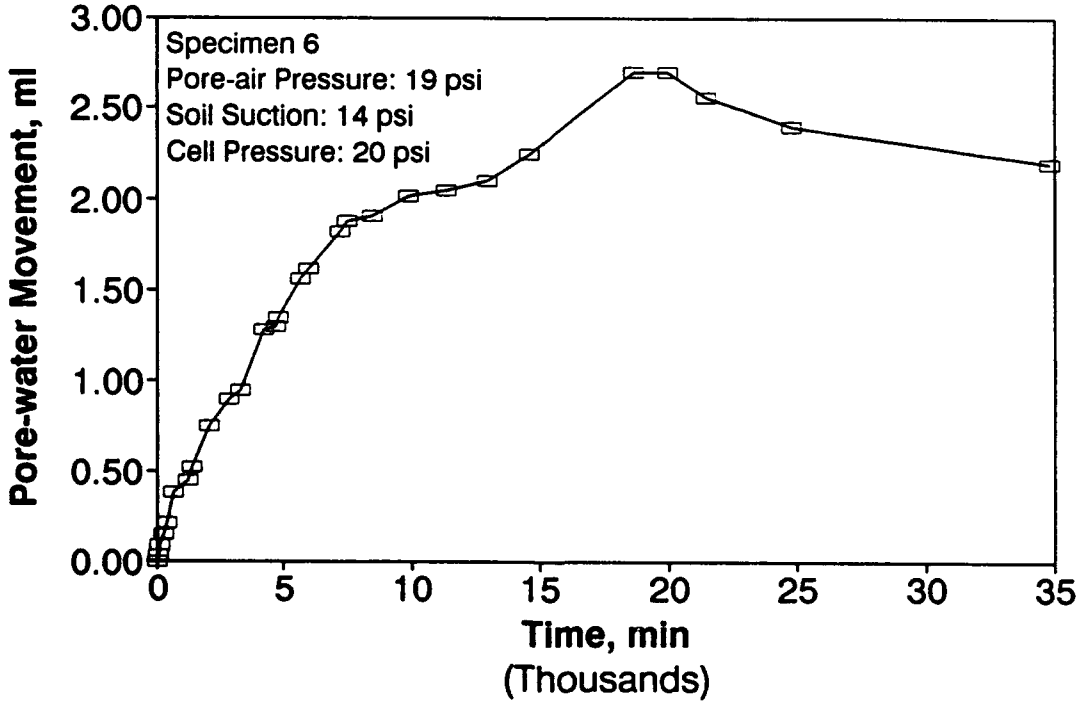
Specimen 6
Pore-air Pressure: 19 psi
Soil Suction: 14 psi
Cell Pressure: 20 psi
Pore-water Movement, ml
3.00
2.50
2.00
1.50
1.00
0.50
0.00
0
5
10
15
20
25
30
35
Time, min
(Thousands)

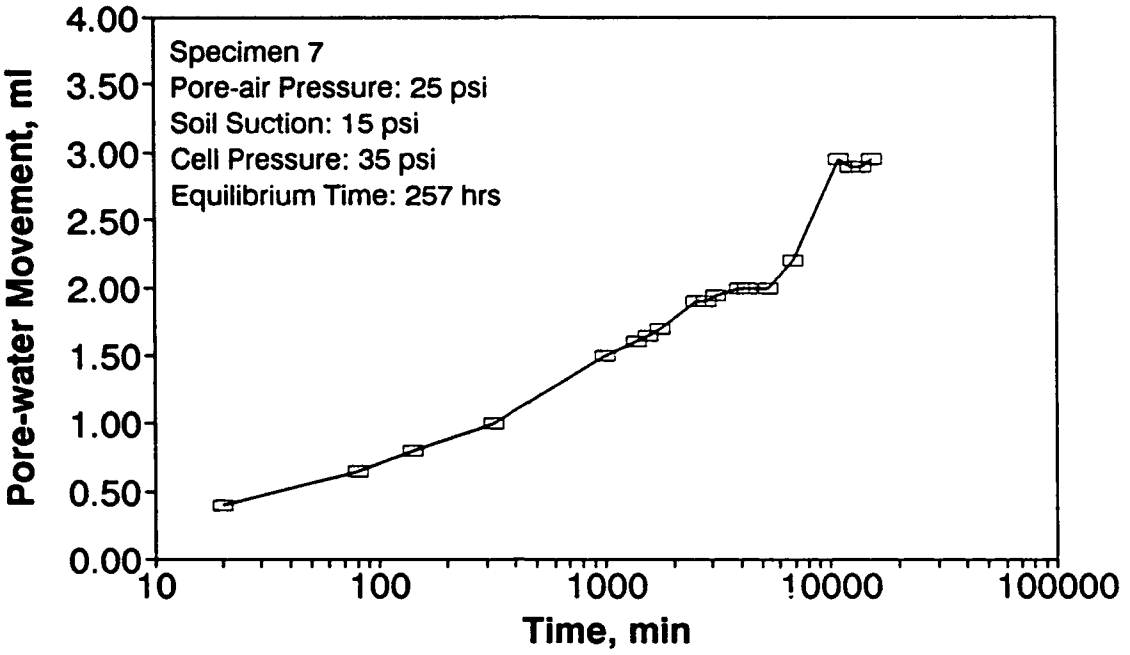
Specimen 7
Pore-air Pressure: 25 psi
Soil Suction: 15 psi
Cell Pressure: 35 psi
Equilibrium Time: 257 hrs
Pore-water Movement, ml
4.00
3.50
3.00
2.50
2.00
1.50
1.00
0.50
0.00
10
100
1000
10000
100000
Time, min

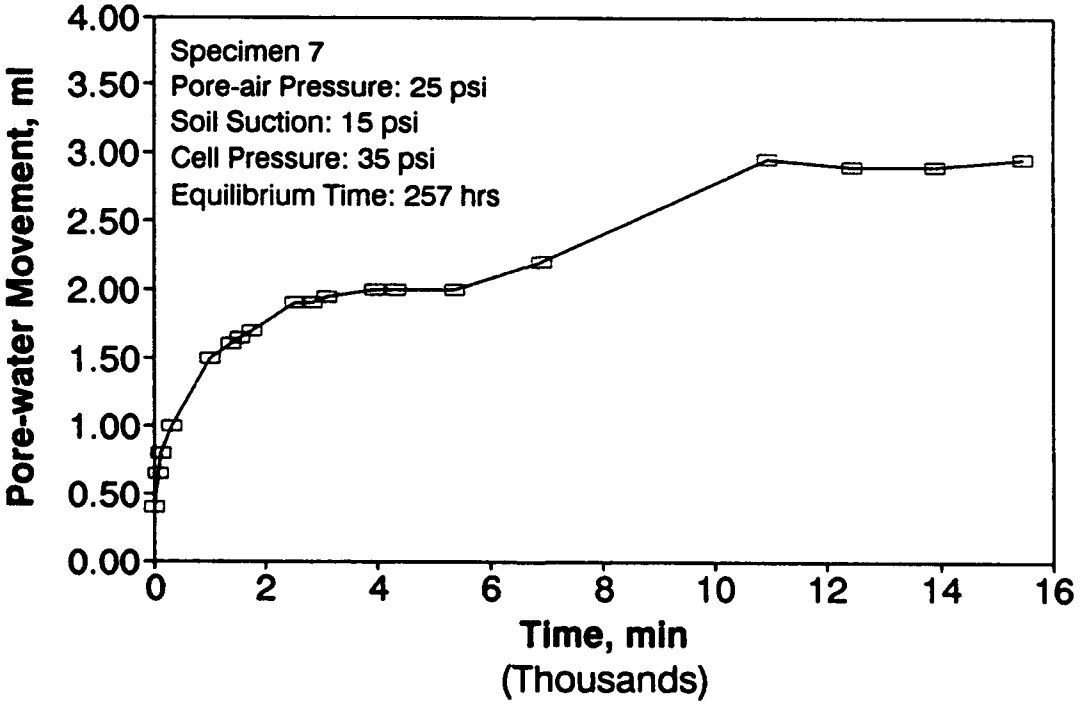
Specimen 7
Pore-air Pressure: 25 psi
Soil Suction: 15 psi
Cell Pressure: 35 psi
Equilibrium Time: 257 hrs
Pore-water Movement, ml
4.00
3.50
3.00
2.50
2.00
1.50
1.00
0.50
0.00
0
2
4
6
8
10
12
14
16
Time, min
(Thousands)

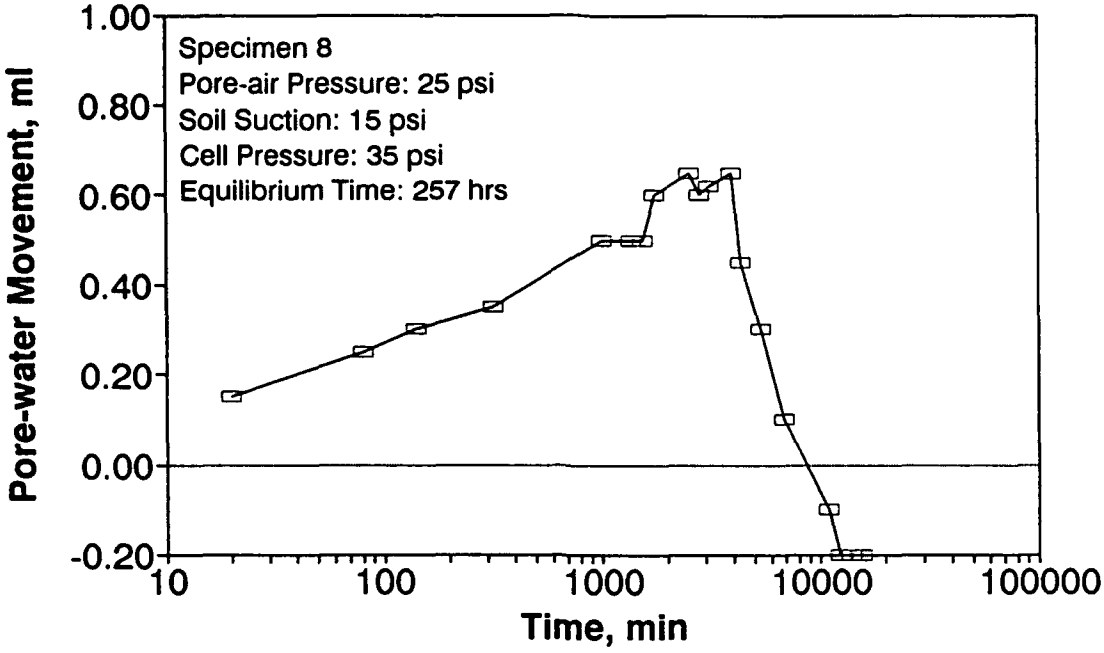
Specimen 8
Pore-air Pressure: 25 psi
Soil Suction: 15 psi
Cell Pressure: 35 psi
Equilibrium Time: 257 hrs
Pore-water Movement, ml
1.00
0.80
0.60
0.40
0.20
0.00
-0.20
10
100
1000
10000
100000
Time, min

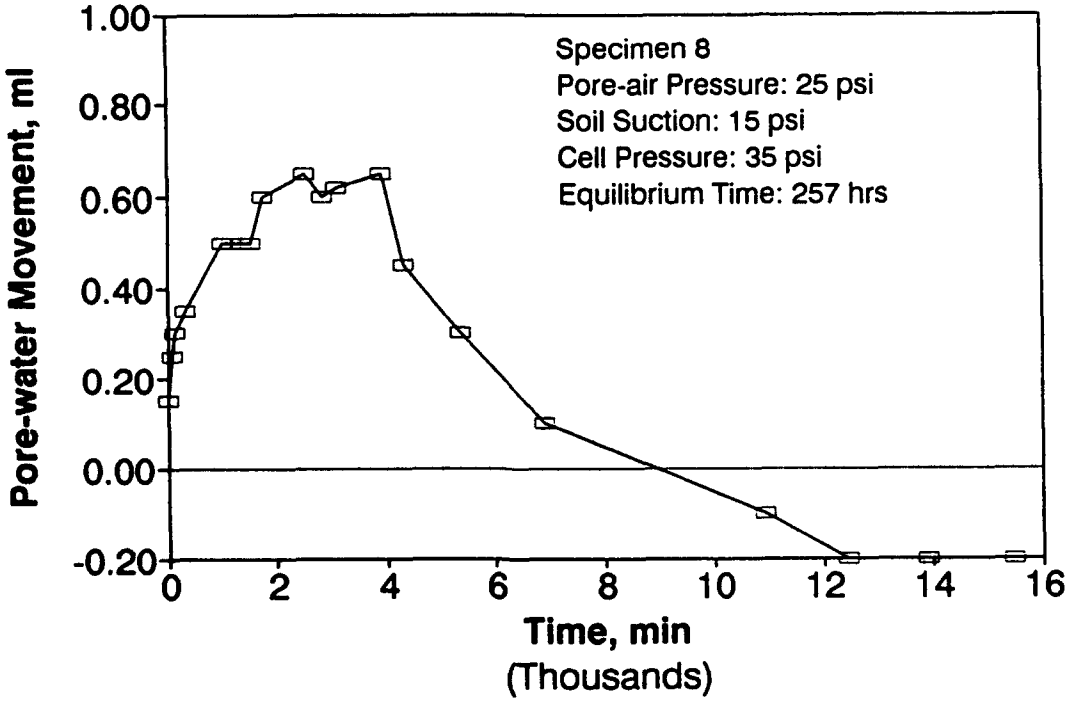
Specimen 8
Pore-air Pressure: 25 psi
Soil Suction: 15 psi
Cell Pressure: 35 psi
Equilibrium Time: 257 hrs
Pore-water Movement, ml
1.00
0.80
0.60
0.40
0.20
0.00
-0.20
0
2
4
6
8
10
12
14
16
Time, min
(Thousands)

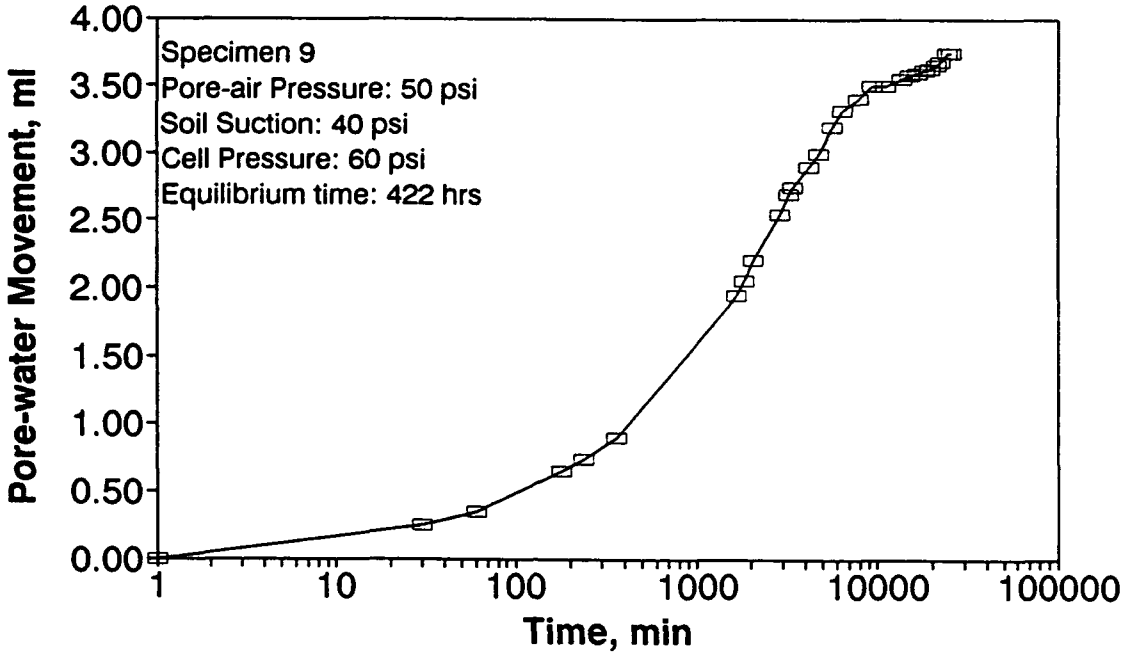
Specimen 9
Pore-air Pressure: 50 psi
Soil Suction: 40 psi
Cell Pressure: 60 psi
Equilibrium time: 422 hrs
Pore-water Movement, ml
4.00
3.50
3.00
2.50
2.00
1.50
1.00
0.50
0.00
1
10
100
1000
10000
100000
Time, min

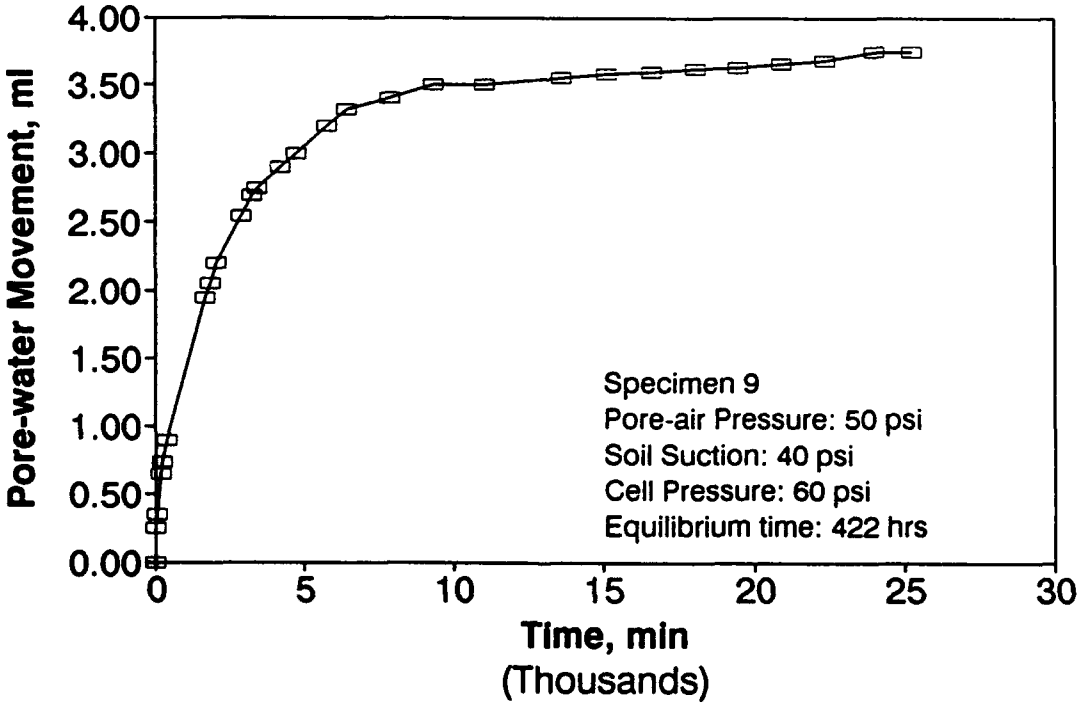
Pore-water Movement, ml
4.00
3.50
3.00
2.50
2.00
1.50
1.00
0.50
0.00
0
5
10
15
20
25
30
Time, min
(Thousands)
Specimen 9
Pore-air Pressure: 50 psi
Soil Suction: 40 psi
Cell Pressure: 60 psi
Equilibrium time: 422 hrs

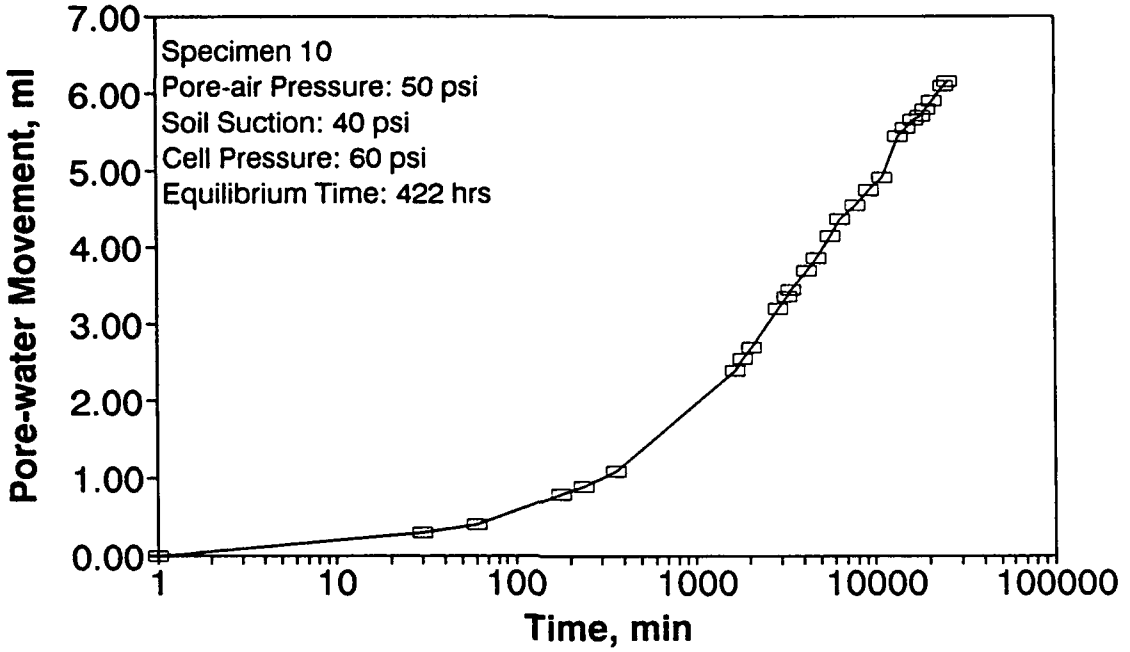
Specimen 10
Pore-air Pressure: 50 psi
Soil Suction: 40 psi
Cell Pressure: 60 psi
Equilibrium Time: 422 hrs
Pore-water Movement, ml
7.00
6.00
5.00
4.00
3.00
2.00
1.00
0.00
1
10
100
1000
10000
100000
Time, min

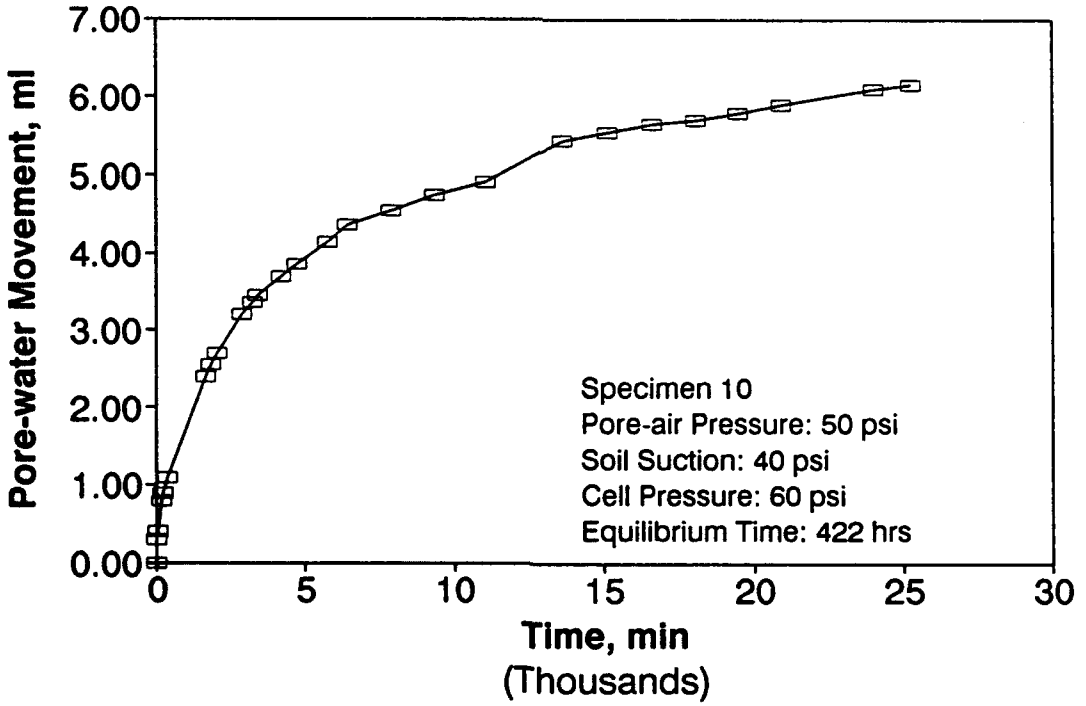
Specimen 10
Pore-air Pressure: 50 psi
Soil Suction: 40 psi
Cell Pressure: 60 psi
Equilibrium Time: 422 hrs
Pore-water Movement, ml
7.00
6.00
5.00
4.00
3.00
2.00
1.00
0.00
0
5
10
15
20
25
30
Time, min
(Thousands)

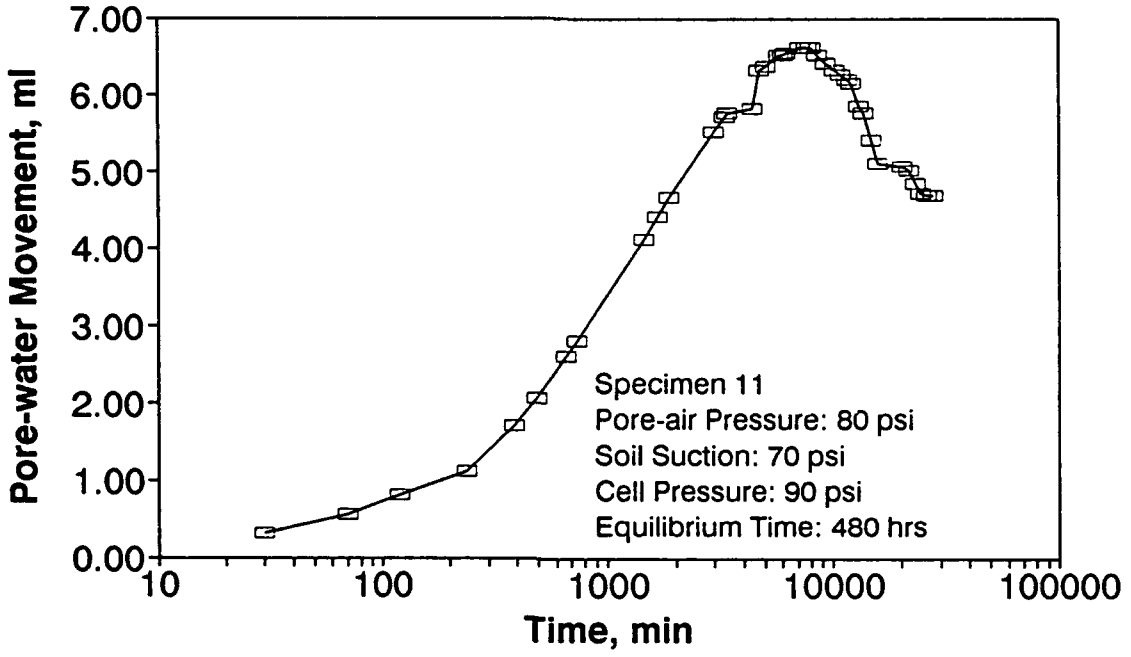
Pore-water Movement, ml
7.00
6.00
5.00
4.00
3.00
2.00
1.00
0.00
10
100
1000
10000
100000
Time, min
Specimen 11
Pore-air Pressure: 80 psi
Soil Suction: 70 psi
Cell Pressure: 90 psi
Equilibrium Time: 480 hrs

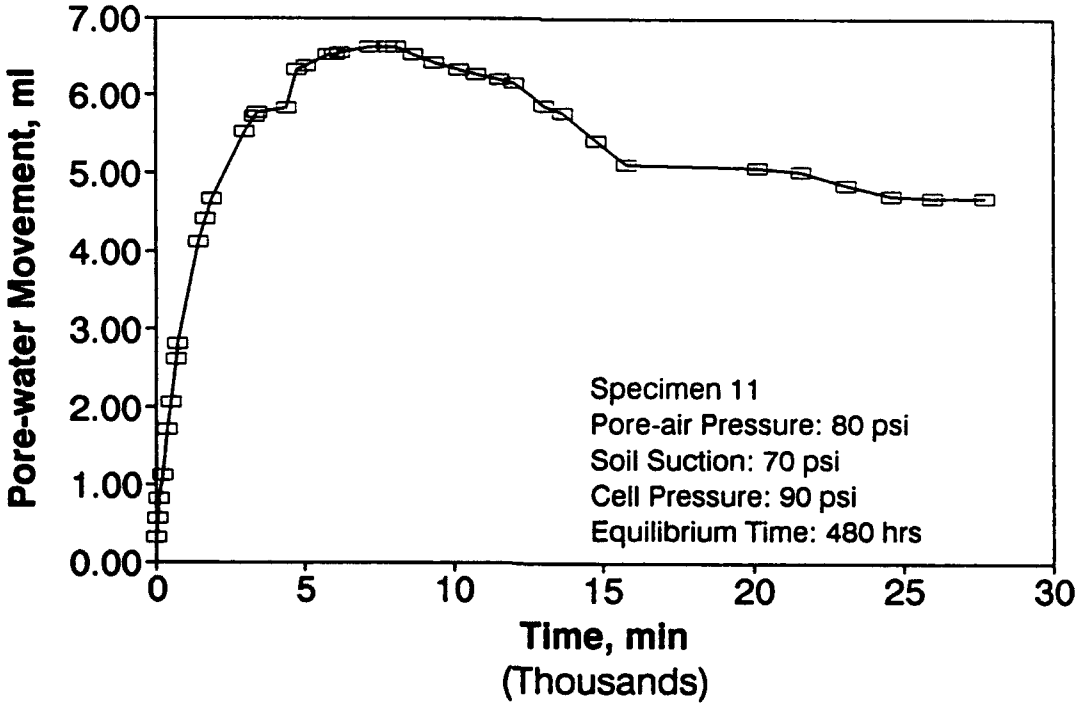
Pore-water Movement, ml
7.00
6.00
5.00
4.00
3.00
2.00
1.00
0.00
0
5
10
15
20
25
30
Time, min
(Thousands)
Specimen 11
Pore-air Pressure: 80 psi
Soil Suction: 70 psi
Cell Pressure: 90 psi
Equilibrium Time: 480 hrs

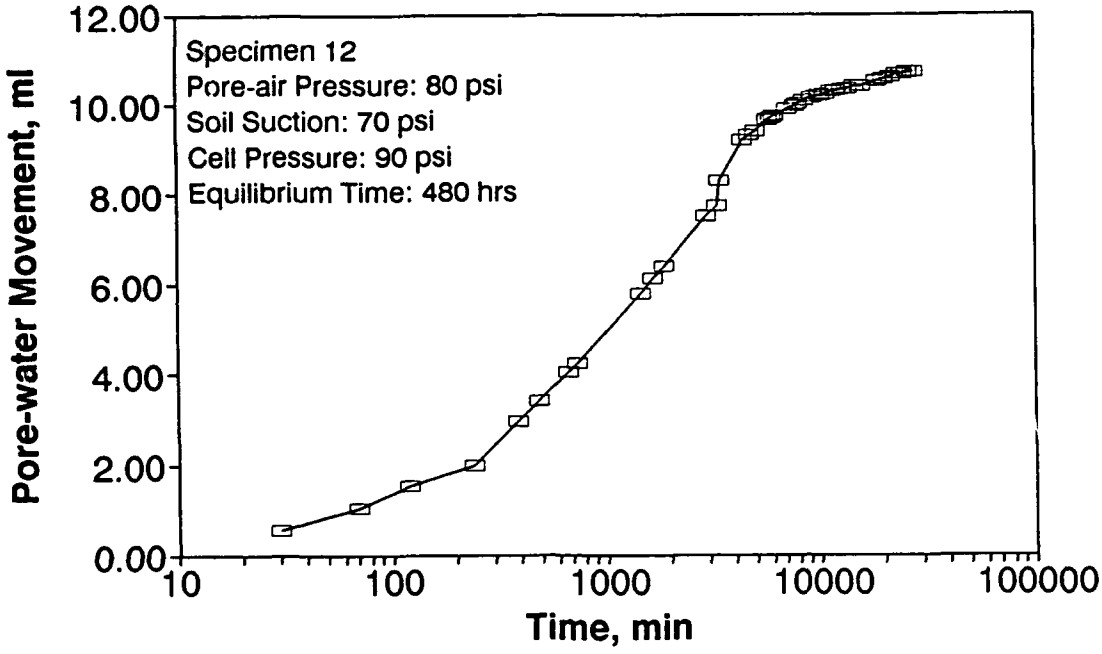
Specimen 12
Pore-air Pressure: 80 psi
Soil Suction: 70 psi
Cell Pressure: 90 psi
Equilibrium Time: 480 hrs
Pore-water Movement, ml
12.00
10.00
8.00
6.00
4.00
2.00
0.00
10
100
1000
10000
100000
Time, min

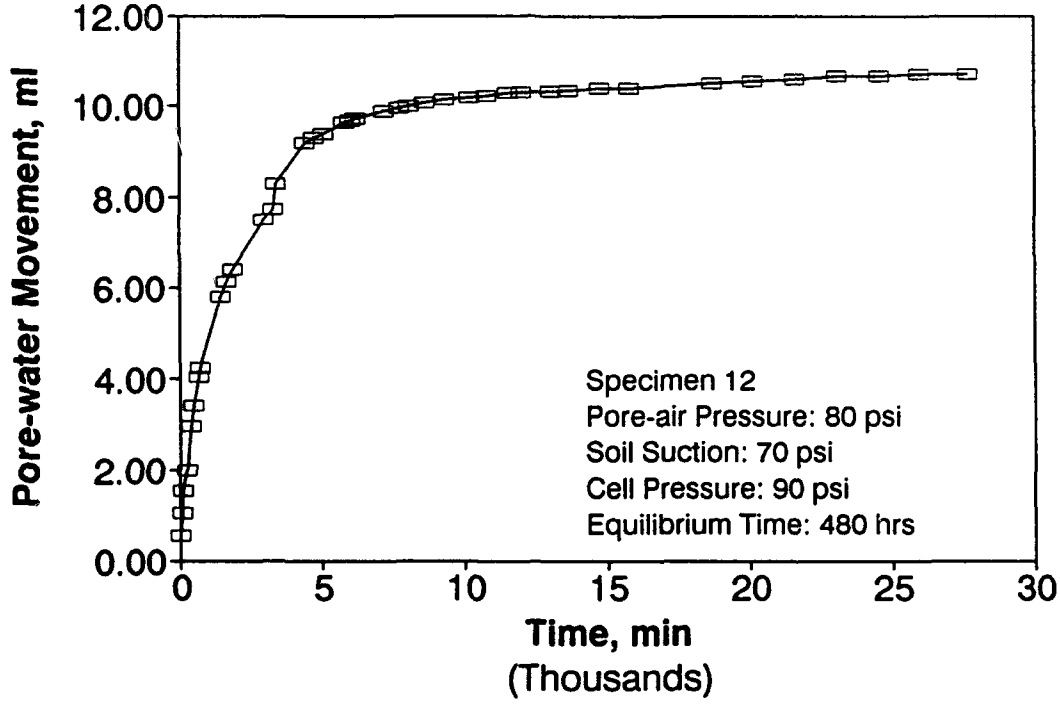
Specimen 12
Pore-air Pressure: 80 psi
Soil Suction: 70 psi
Cell Pressure: 90 psi
Equilibrium Time: 480 hrs
Pore-water Movement, ml
12.00
10.00
8.00
6.00
4.00
2.00
0.00
0
5
10
15
20
25
30
Time, min
(Thousands)

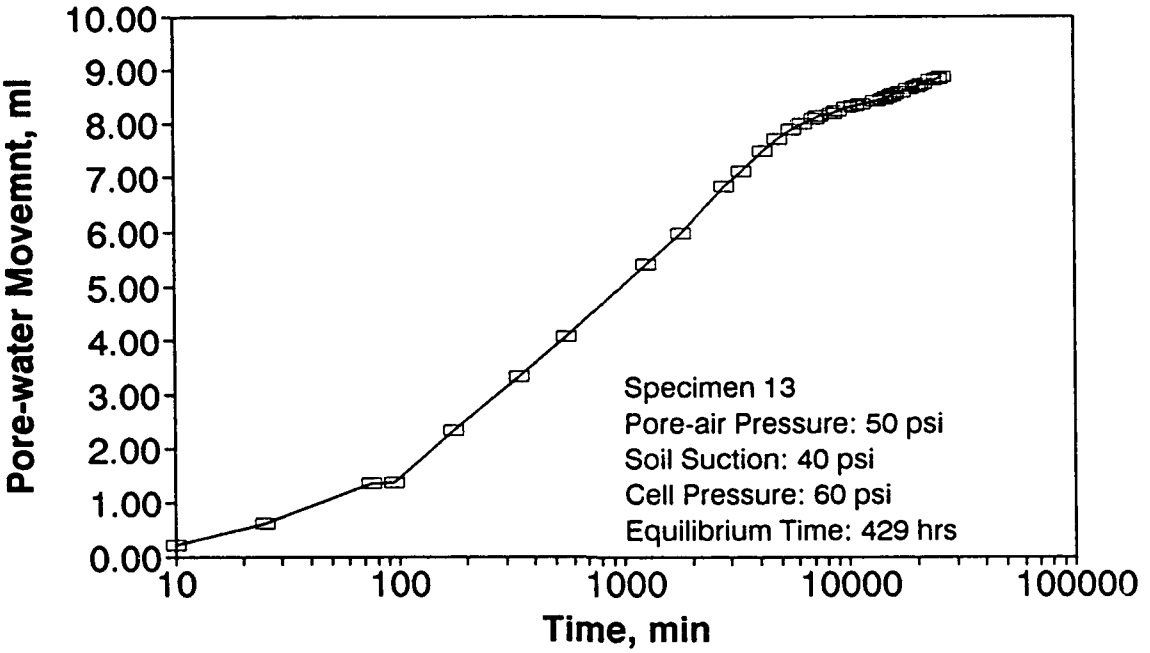
Pore-water Movemnt, ml
10.00
9.00
8.00
7.00
6.00
5.00
4.00
3.00
2.00
1.00
0.00
10
100
1000
10000
100000
Time, min
Specimen 13
Pore-air Pressure: 50 psi
Soil Suction: 40 psi
Cell Pressure: 60 psi
Equilibrium Time: 429 hrs

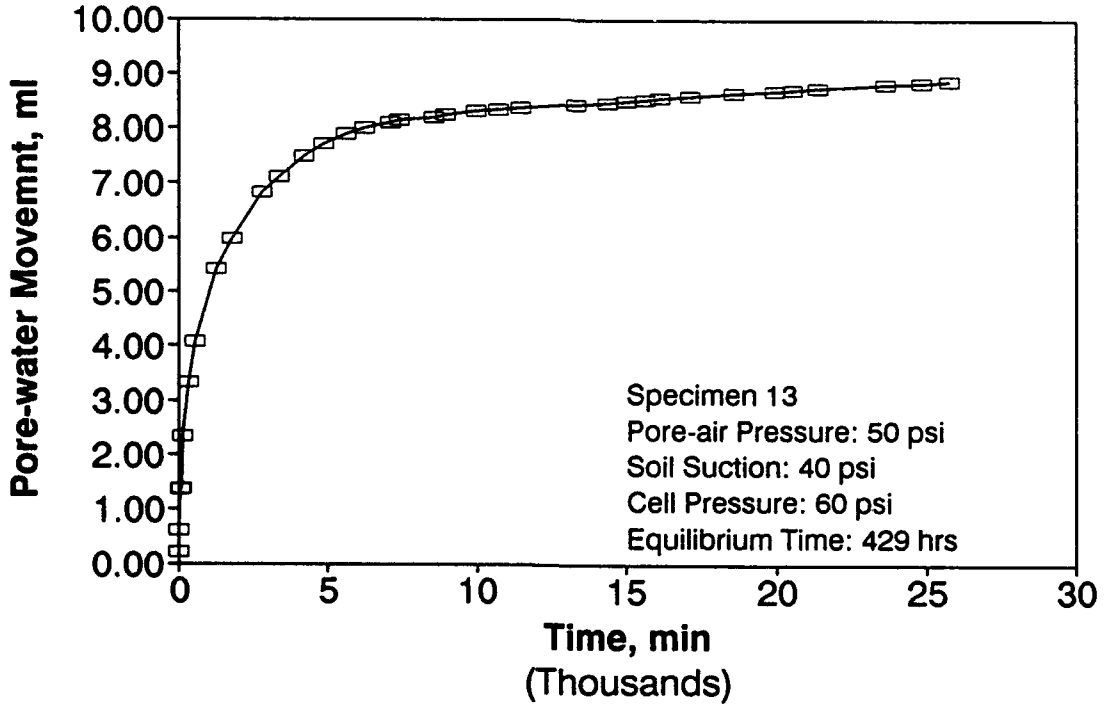
Pore-water Movemnt, ml
10.00
9.00
8.00
7.00
6.00
5.00
4.00
3.00
2.00
1.00
0.00
0
5
10
15
20
25
30
Time, min
(Thousands)
Specimen 13
Pore-air Pressure: 50 psi
Soil Suction: 40 psi
Cell Pressure: 60 psi
Equilibrium Time: 429 hrs

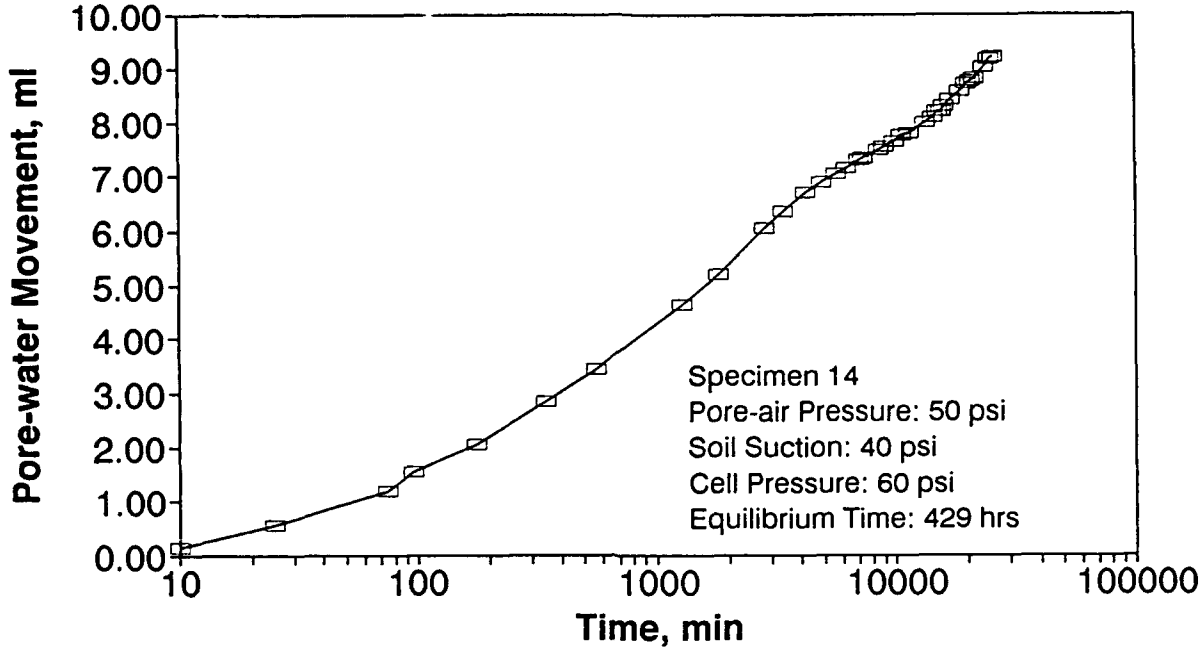
Pore-water Movement, ml
10.00
9.00
8.00
7.00
6.00
5.00
4.00
3.00
2.00
1.00
0.00
10
100
1000
10000
100000
Time, min
Specimen 14
Pore-air Pressure: 50 psi
Soil Suction: 40 psi
Cell Pressure: 60 psi
Equilibrium Time: 429 hrs

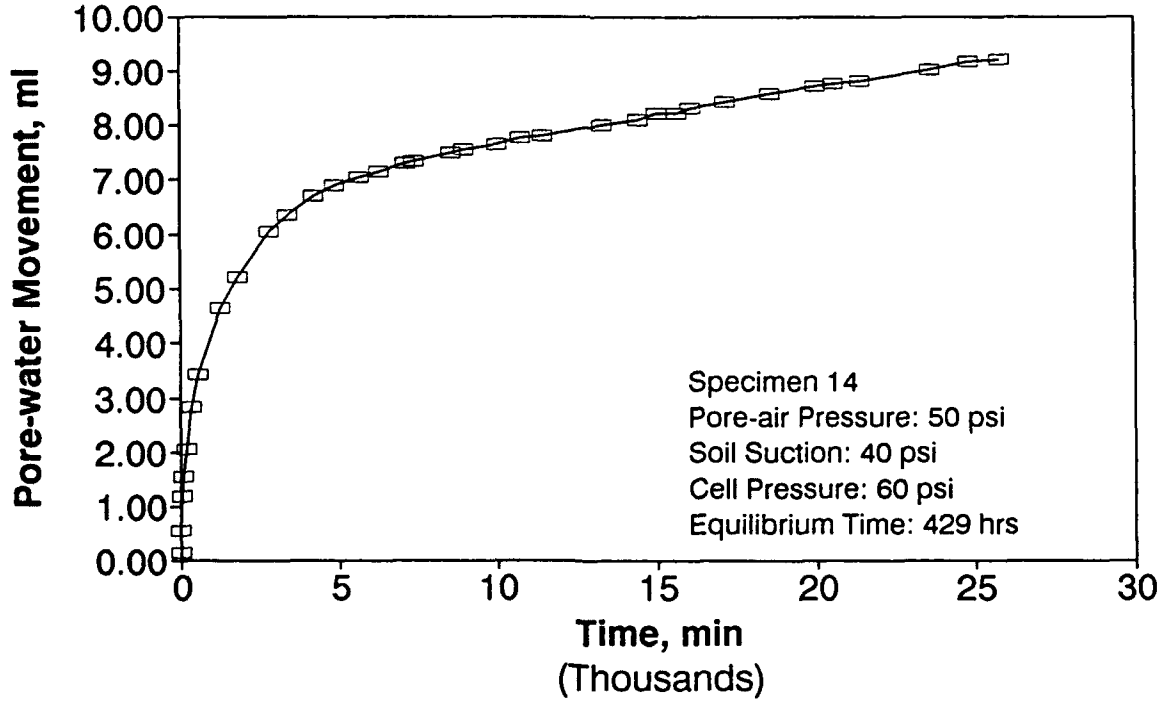
Pore-water Movement, ml
10.00
9.00
8.00
7.00
6.00
5.00
4.00
3.00
2.00
1.00
0.00
0
5
10
15
20
25
30
Time, min
(Thousands)
Specimen 14
Pore-air Pressure: 50 psi
Soil Suction: 40 psi
Cell Pressure: 60 psi
Equilibrium Time: 429 hrs

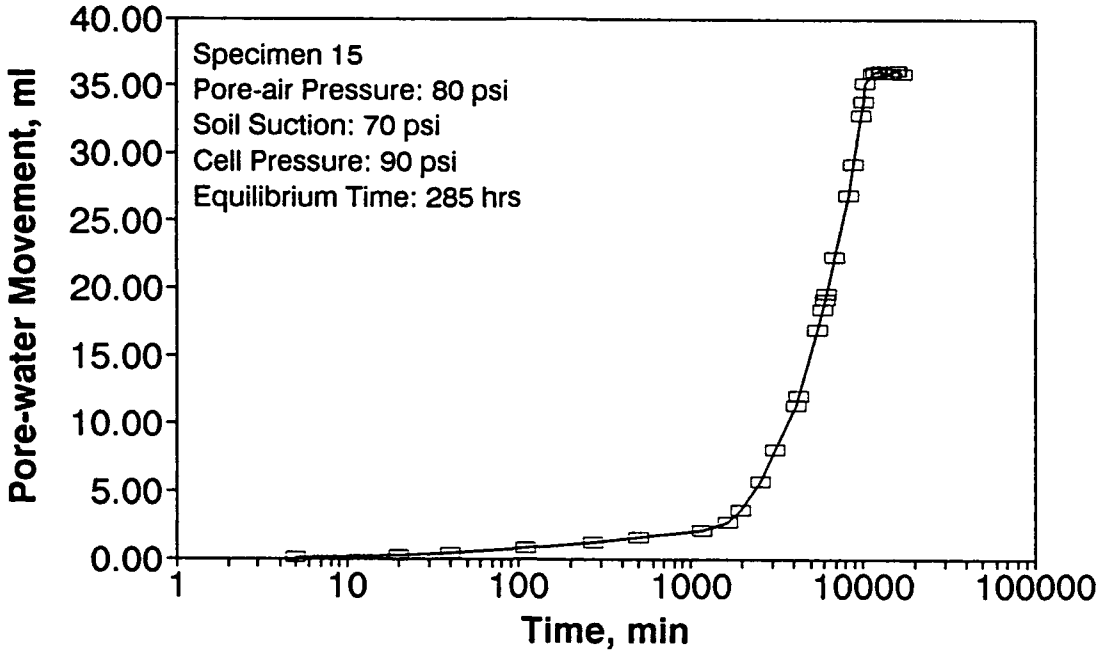
Specimen 15
Pore-air Pressure: 80 psi
Soil Suction: 70 psi
Cell Pressure: 90 psi
Equilibrium Time: 285 hrs
Pore-water Movement, ml
40.00
35.00
30.00
25.00
20.00
15.00
10.00
5.00
0.00
1
10
100
1000
10000
100000
Time, min

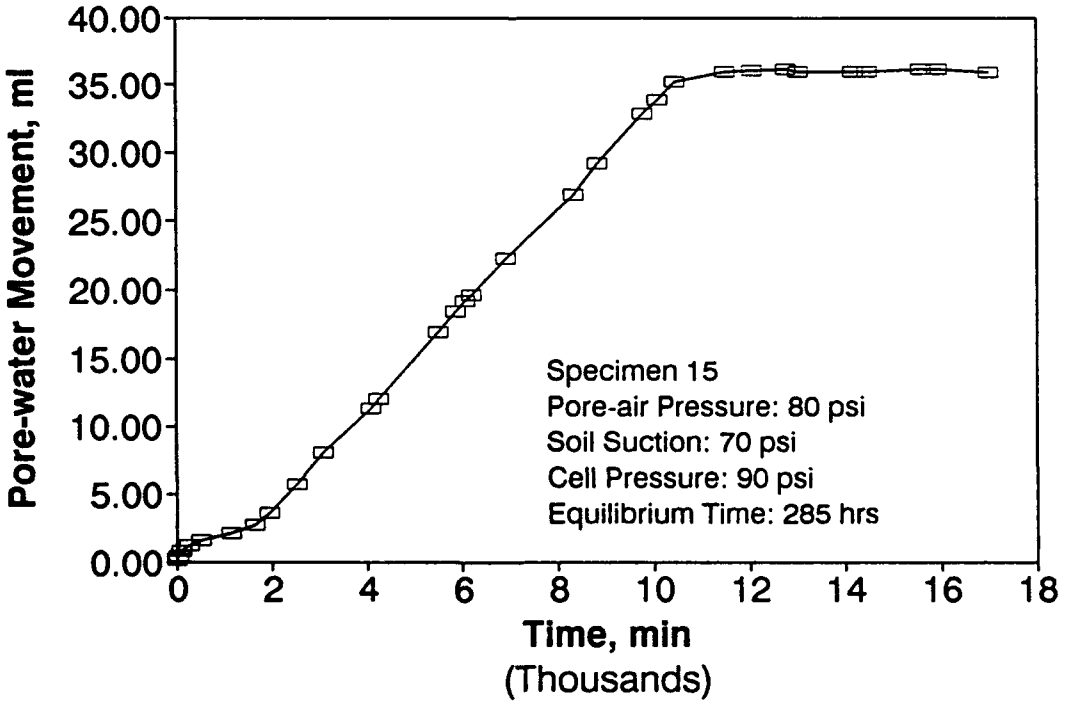
Pore-water Movement, ml
40.00
35.00
30.00
25.00
20.00
15.00
10.00
5.00
0.00
Specimen 15
Pore-air Pressure: 80 psi
Soil Suction: 70 psi
Cell Pressure: 90 psi
Equilibrium Time: 285 hrs
0
2
4
6
8
10
12
14
16
18
Time, min
(Thousands)

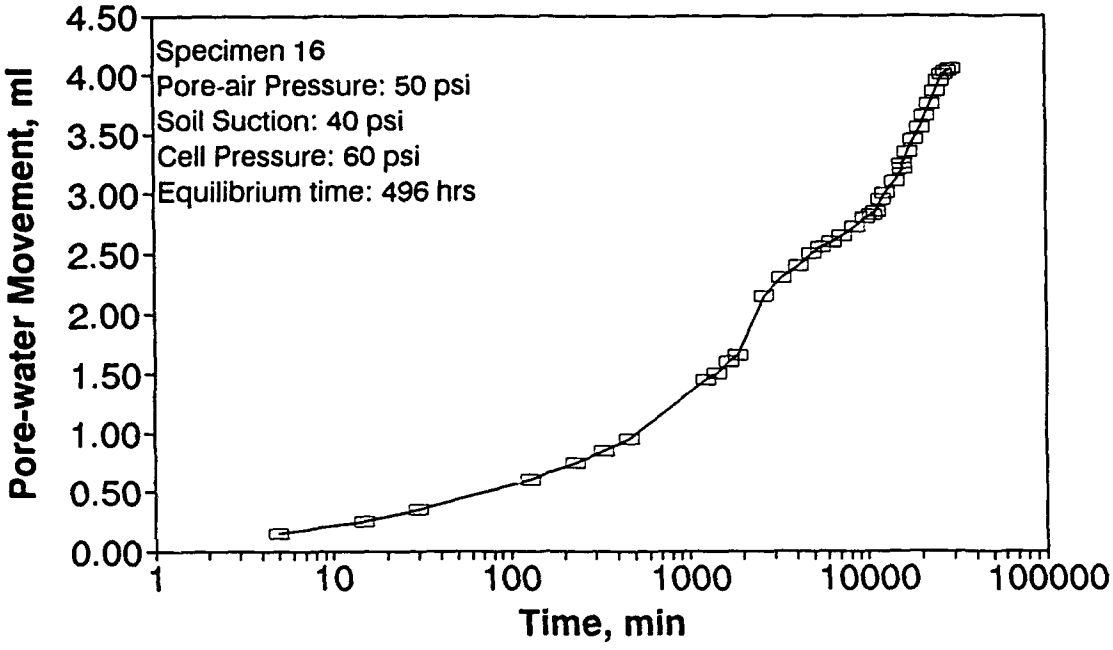
Specimen 16
Pore-air Pressure: 50 psi
Soil Suction: 40 psi
Cell Pressure: 60 psi
Equilibrium time: 496 hrs
Pore-water Movement, ml
4.50
4.00
3.50
3.00
2.50
2.00
1.50
1.00
0.50
0.00
1
10
100
1000
10000
100000
Time, min

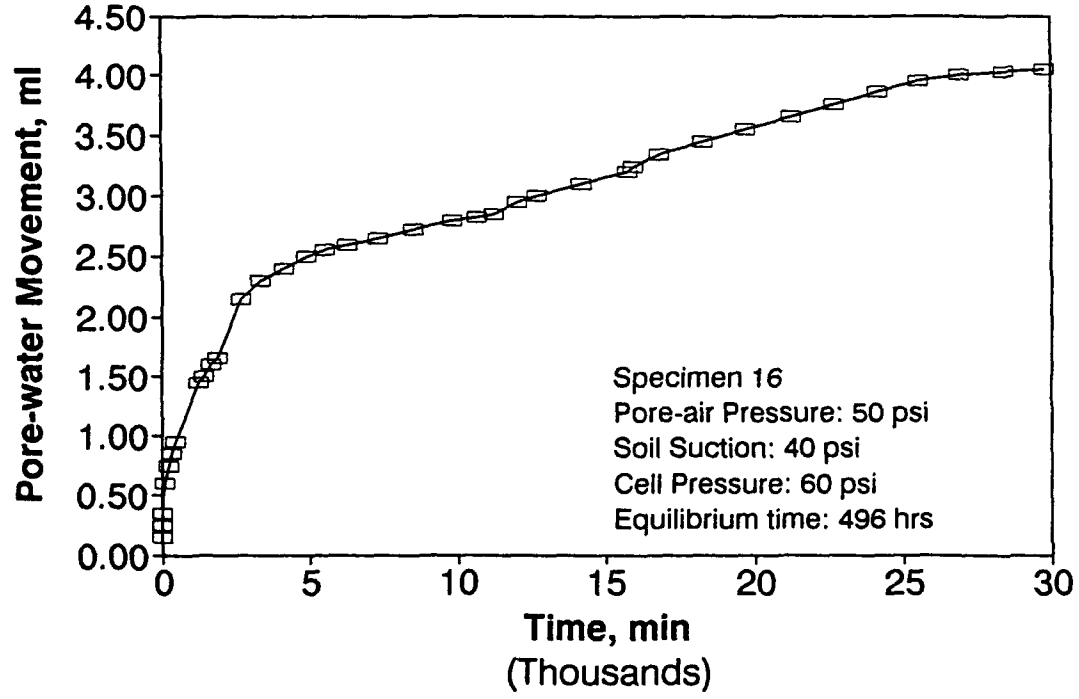
Pore-water Movement, ml
4.50
4.00
3.50
3.00
2.50
2.00
1.50
1.00
0.50
0.00
0
5
10
15
20
25
30
Specimen 16
Pore-air Pressure: 50 psi
Soil Suction: 40 psi
Cell Pressure: 60 psi
Equilibrium time: 496 hrs
Time, min
(Thousands)

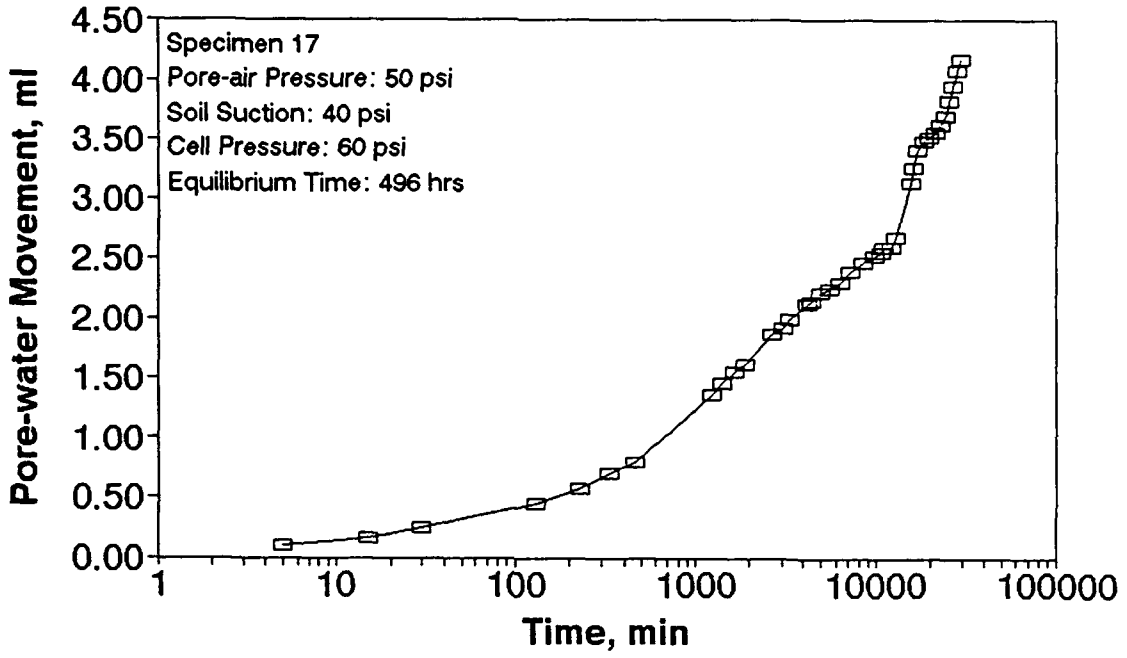
Specimen 17
Pore-air Pressure: 50 psi
Soil Suction: 40 psi
Cell Pressure: 60 psi
Equilibrium Time: 496 hrs
Pore-water Movement, ml
4.50
4.00
3.50
3.00
2.50
2.00
1.50
1.00
0.50
0.00
1
10
100
1000
10000
100000
Time, min

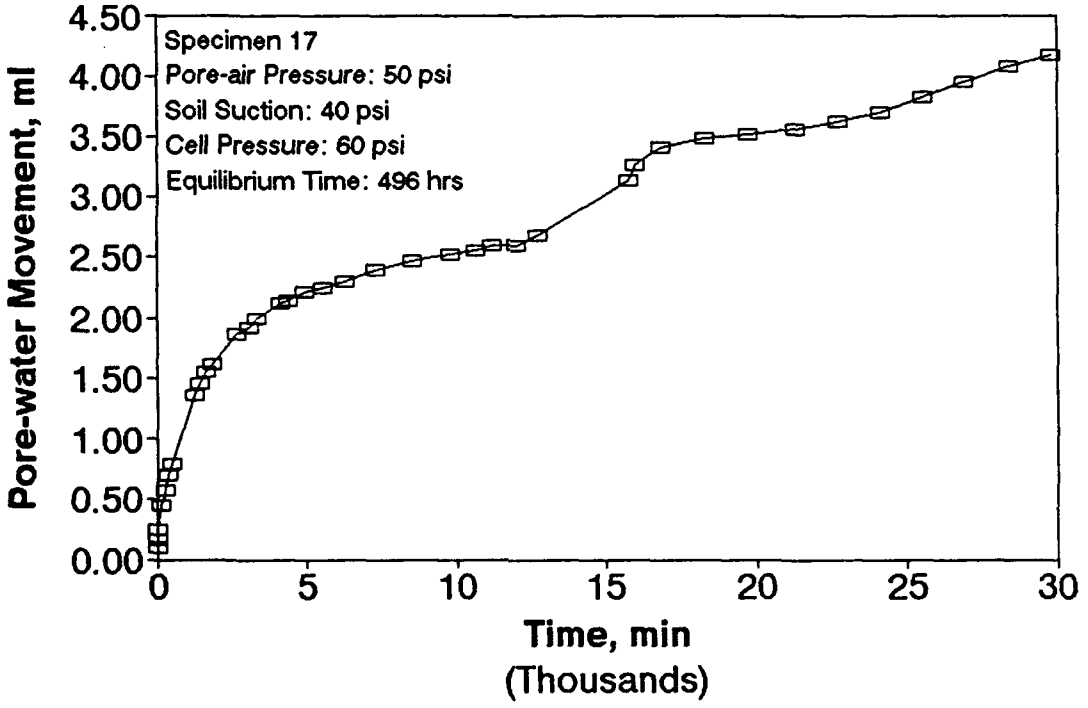
Specimen 17
Pore-air Pressure: 50 psi
Soil Suction: 40 psi
Cell Pressure: 60 psi
Equilibrium Time: 496 hrs
Pore-water Movement, ml
4.50
4.00
3.50
3.00
2.50
2.00
1.50
1.00
0.50
0.00
0
5
10
15
20
25
30
Time, min
(Thousands)

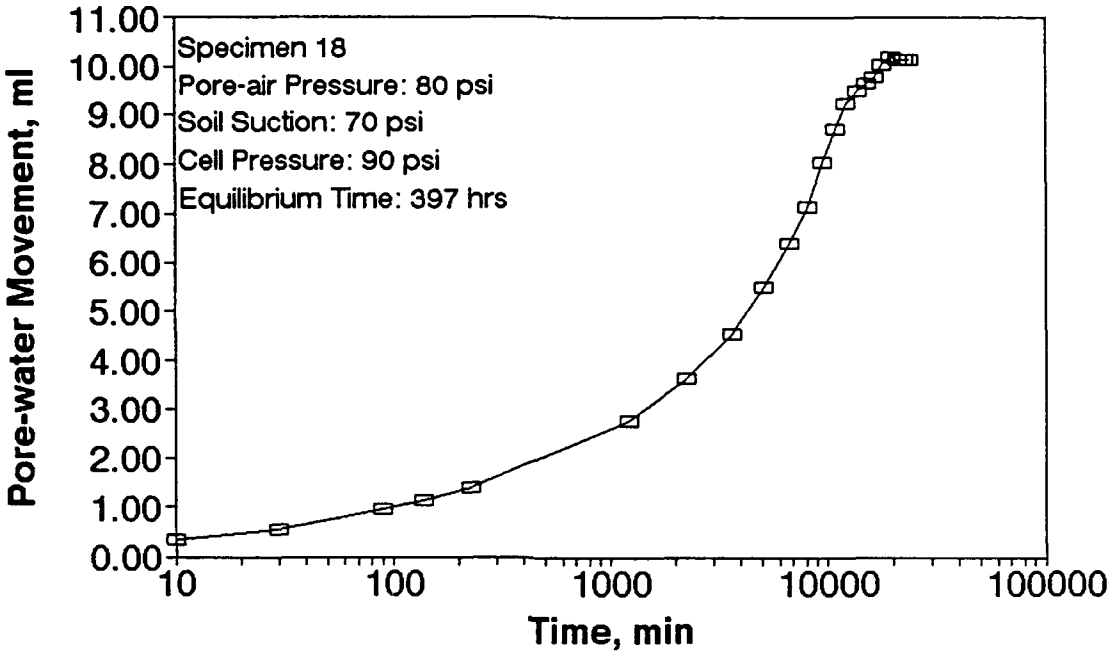
Specimen 18
Pore-air Pressure: 80 psi
Soil Suction: 70 psi
Cell Pressure: 90 psi
Equilibrium Time: 397 hrs
Pore-water Movement, ml
11.00
10.00
9.00
8.00
7.00
6.00
5.00
4.00
3.00
2.00
1.00
0.00
10
100
1000
10000
100000
Time, min

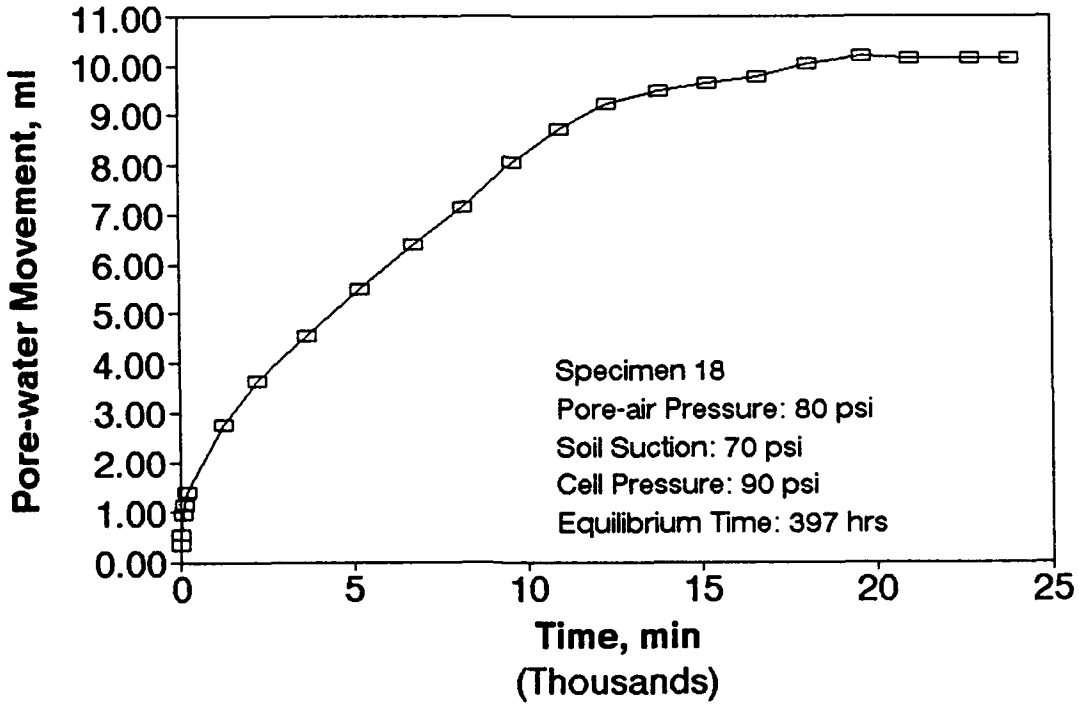
Specimen 18
Pore-air Pressure: 80 psi
Soil Suction: 70 psi
Cell Pressure: 90 psi
Equilibrium Time: 397 hrs
Pore-water Movement, ml
11.00
10.00
9.00
8.00
7.00
6.00
5.00
4.00
3.00
2.00
1.00
0.00
0
5
10
15
20
25
Time, min
(Thousands)

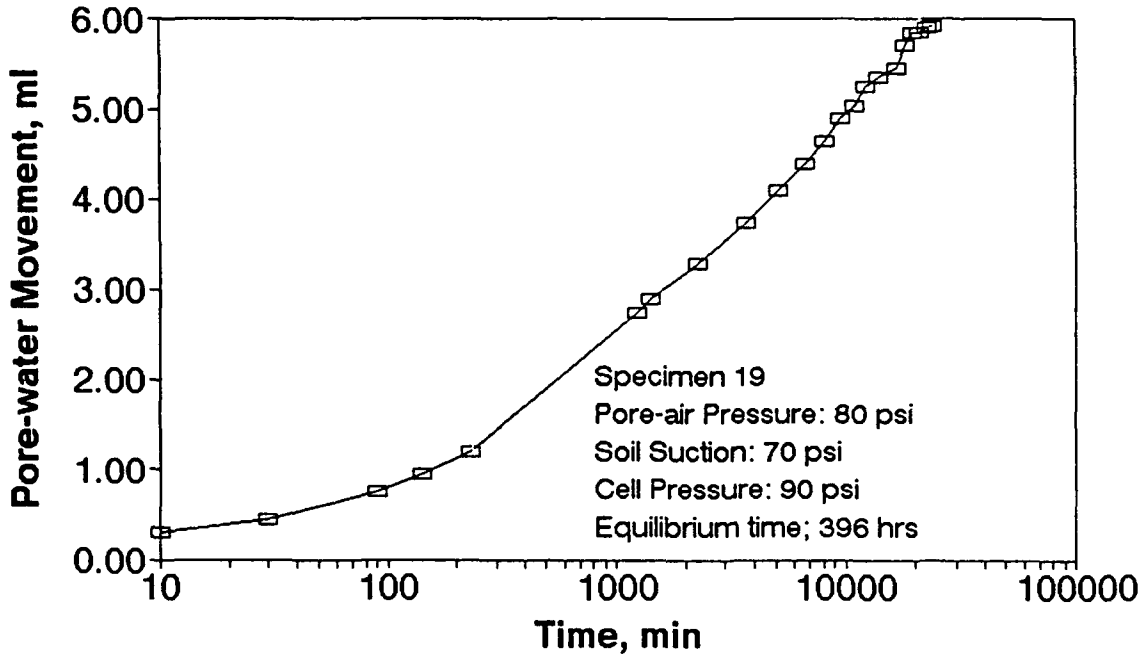
Pore-water Movement, ml
6.00
5.00
4.00
3.00
2.00
1.00
0.00
10
100
1000
10000
100000
Time, min
Specimen 19
Pore-air Pressure: 80 psi
Soil Suction: 70 psi
Cell Pressure: 90 psi
Equilibrium time; 396 hrs

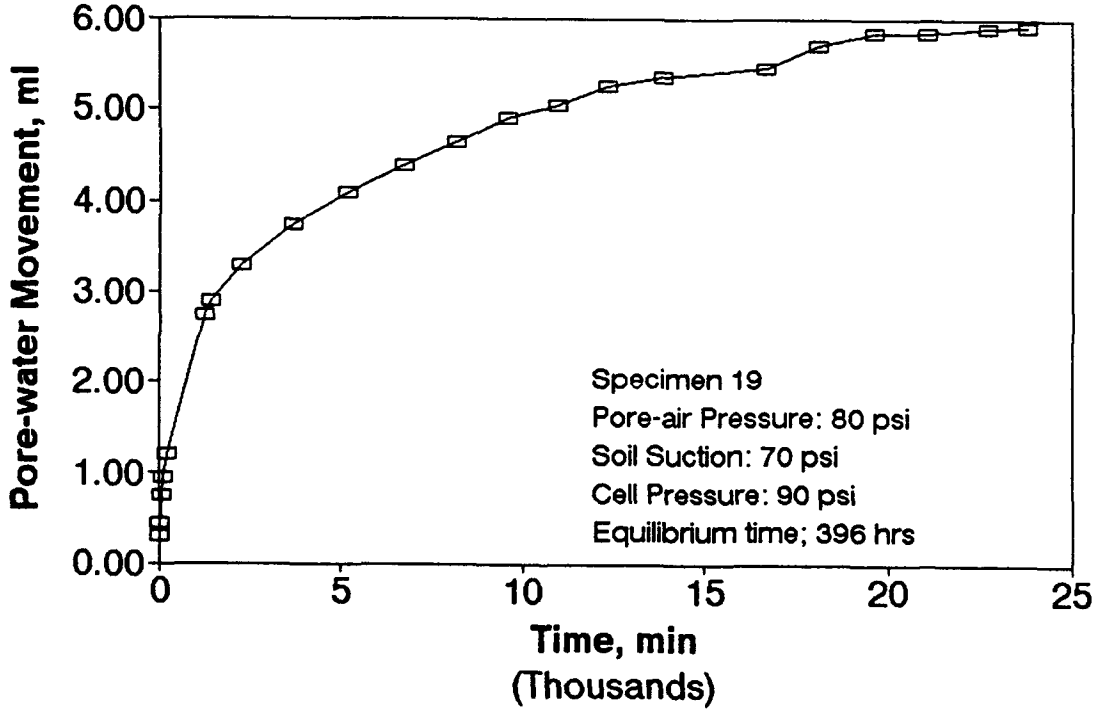
Pore-water Movement, ml
6.00
5.00
4.00
3.00
2.00
1.00
0.00
0
5
10
15
20
25
Time, min
(Thousands)
Specimen 19
Pore-air Pressure: 80 psi
Soil Suction: 70 psi
Cell Pressure: 90 psi
Equilibrium time; 396 hrs

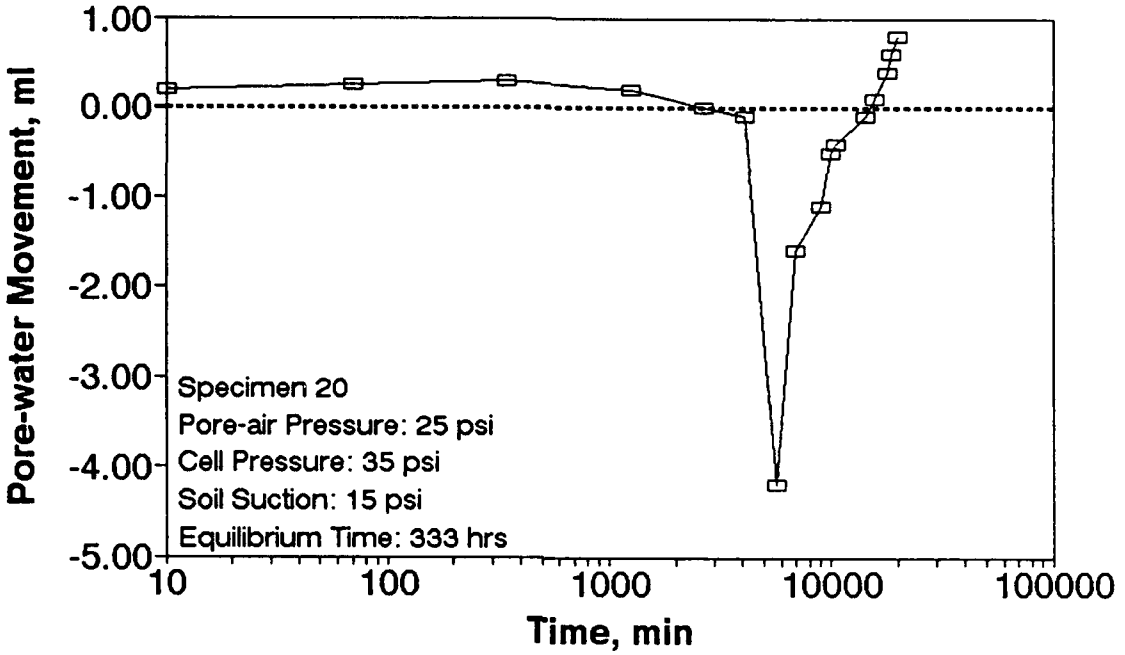
1.00
0.00
-1.00
-2.00
-3.00
-4.00
-5.00
Pore-water Movement, ml
Specimen 20
Pore-air Pressure: 25 psi
Cell Pressure: 35 psi
Soil Suction: 15 psi
Equilibrium Time: 333 hrs
10
100
1000
10000
100000
Time, min

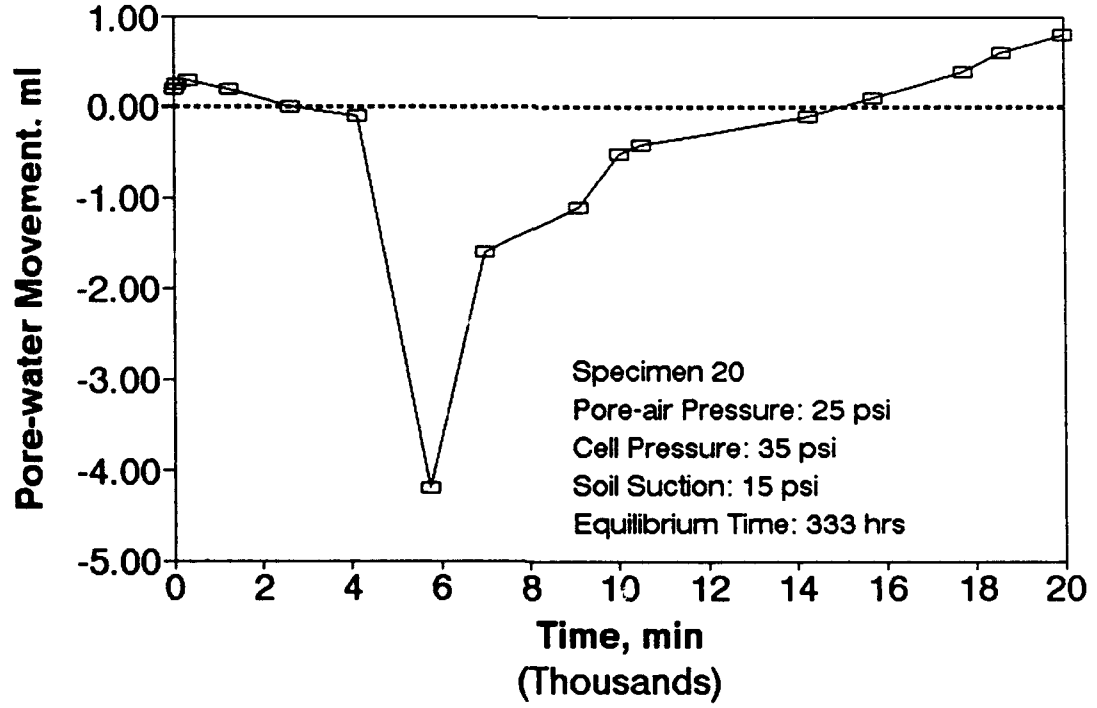
1.00
0.00
-1.00
-2.00
-3.00
-4.00
-5.00
Pore-water Movement, ml
Specimen 20
Pore-air Pressure: 25 psi
Cell Pressure: 35 psi
Soil Suction: 15 psi
Equilibrium Time: 333 hrs
0
2
4
6
8
10
12
14
16
18
20
Time, min
(Thousands)

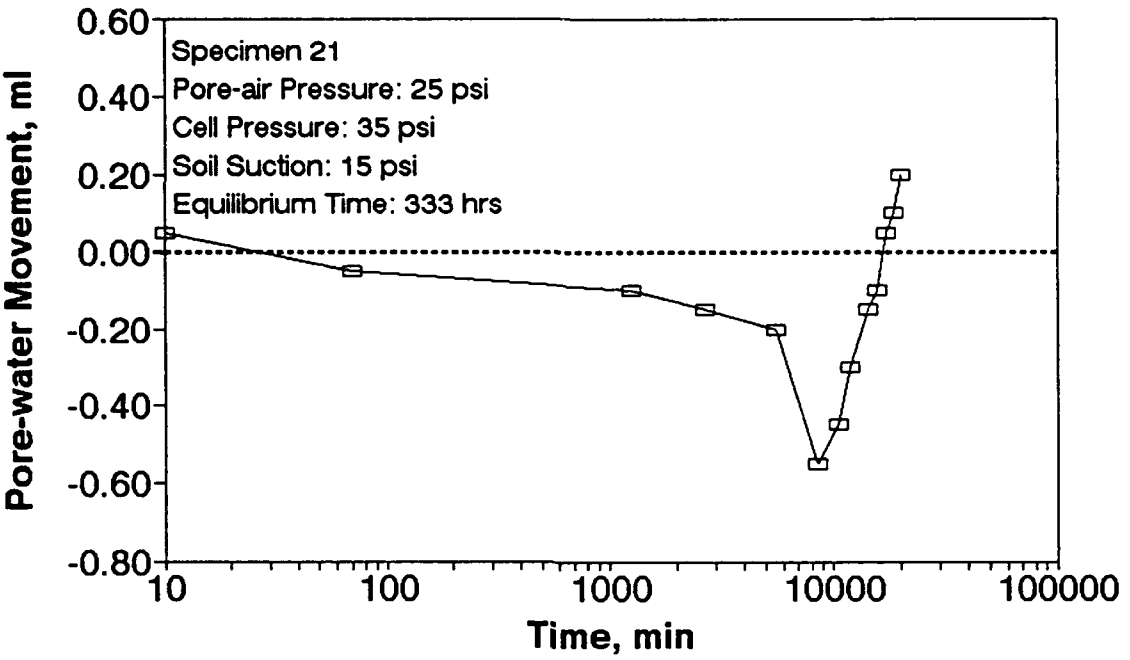
Specimen 21
Pore-air Pressure: 25 psi
Cell Pressure: 35 psi
Soil Suction: 15 psi
Equilibrium Time: 333 hrs
Pore-water Movement, ml
0.60
0.40
0.20
0.00
-0.20
-0.40
-0.60
-0.80
10
100
1000
10000
100000
Time, min

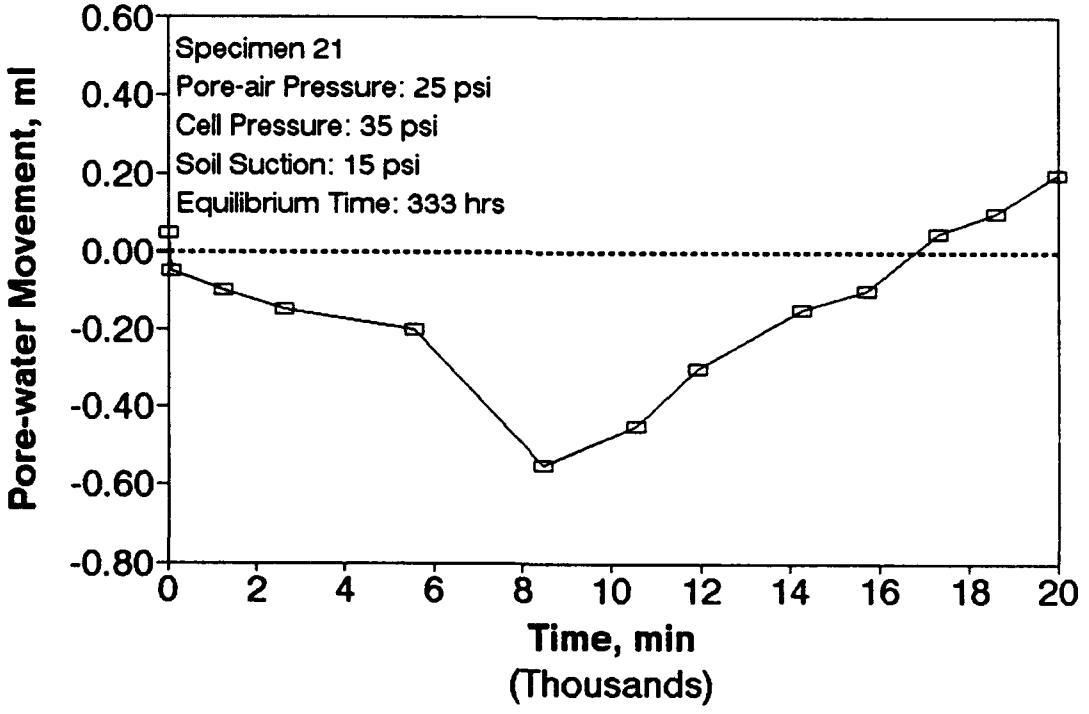
Specimen 21
Pore-air Pressure: 25 psi
Cell Pressure: 35 psi
Soil Suction: 15 psi
Equilibrium Time: 333 hrs
Pore-water Movement, ml
0.60
0.40
0.20
0.00
-0.20
-0.40
-0.60
-0.80
0
2
4
6
8
10
12
14
16
18
20
Time, min
(Thousands)

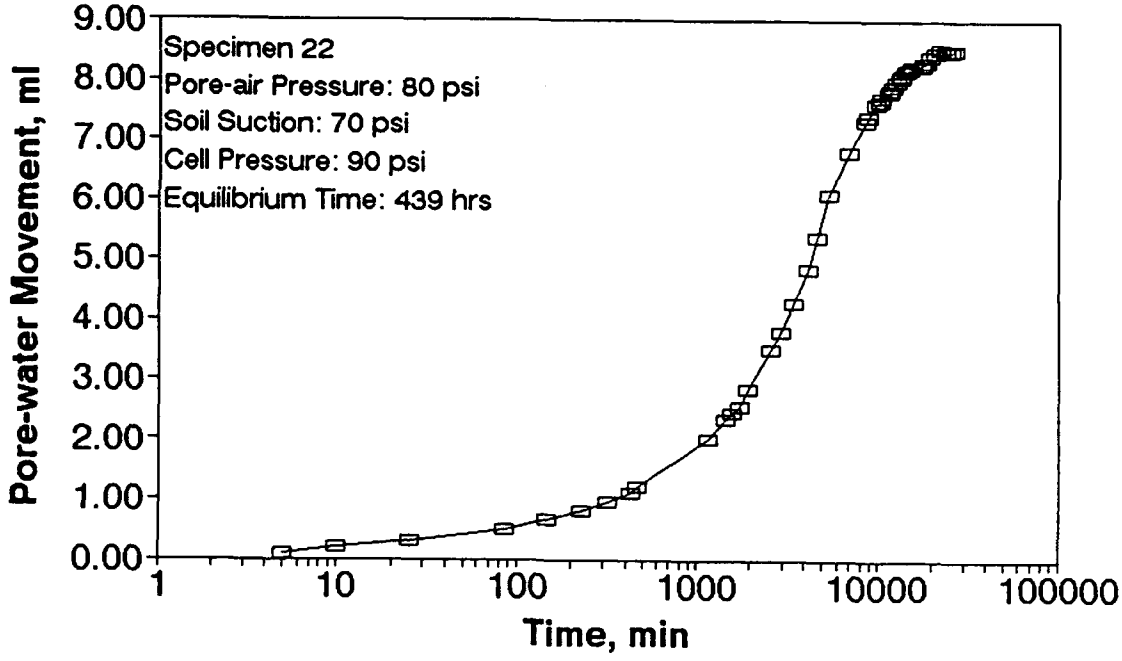
Specimen 22
Pore-air Pressure: 80 psi
Soil Suction: 70 psi
Cell Pressure: 90 psi
Equilibrium Time: 439 hrs
Pore-water Movement, ml
9.00
8.00
7.00
6.00
5.00
4.00
3.00
2.00
1.00
0.00
1
10
100
1000
10000
100000
Time, min

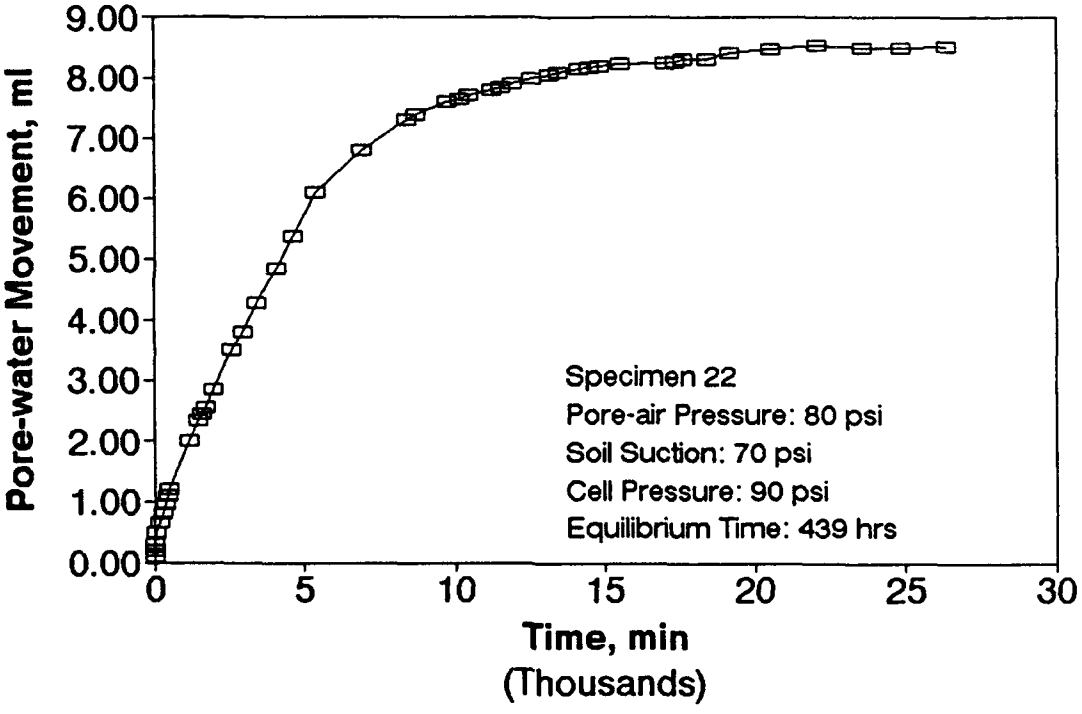
Specimen 22
Pore-air Pressure: 80 psi
Soil Suction: 70 psi
Cell Pressure: 90 psi
Equilibrium Time: 439 hrs
Pore-water Movement, ml
9.00
8.00
7.00
6.00
5.00
4.00
3.00
2.00
1.00
0.00
0
5
10
15
20
25
30
Time, min
(Thousands)

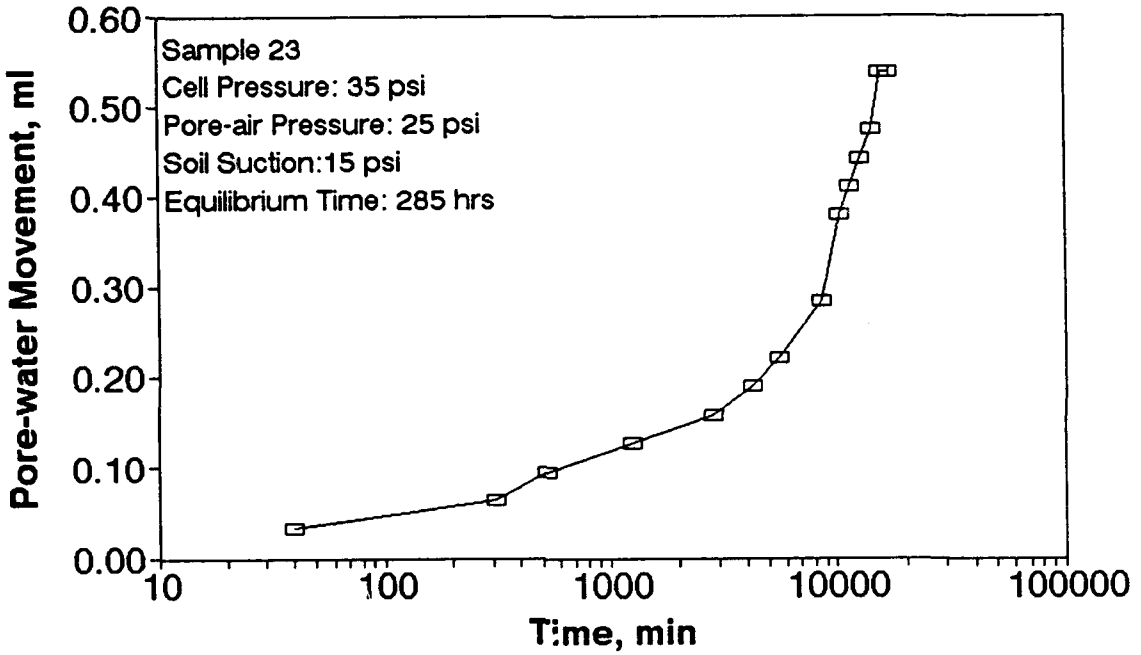
Sample 23
Cell Pressure: 35 psi
Pore-air Pressure: 25 psi
Soil Suction:15 psi
Equilibrium Time: 285 hrs
Pore-water Movement, ml
0.60
0.50
0.40
0.30
0.20
0.10
0.00
10
100
1000
10000
100000
Time, min

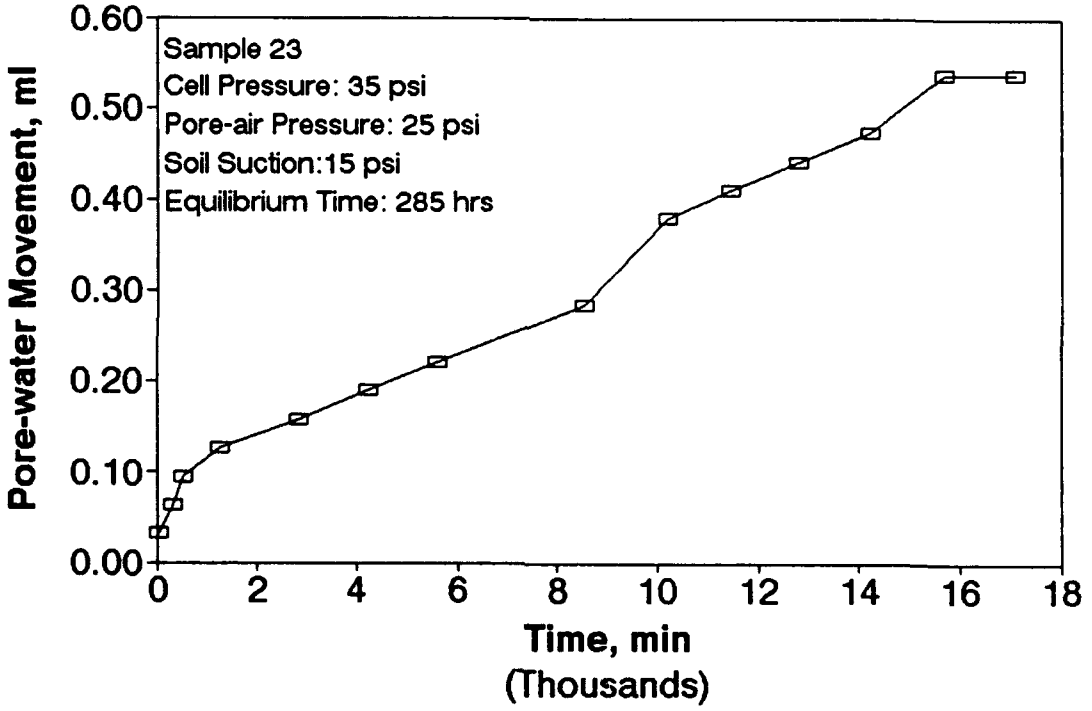
Sample 23
Cell Pressure: 35 psi
Pore-air Pressure: 25 psi
Soil Suction:15 psi
Equilibrium Time: 285 hrs
Pore-water Movement, ml
0.60
0.50
0.40
0.30
0.20
0.10
0.00
0
2
4
6
8
10
12
14
16
18
Time, min
(Thousands)

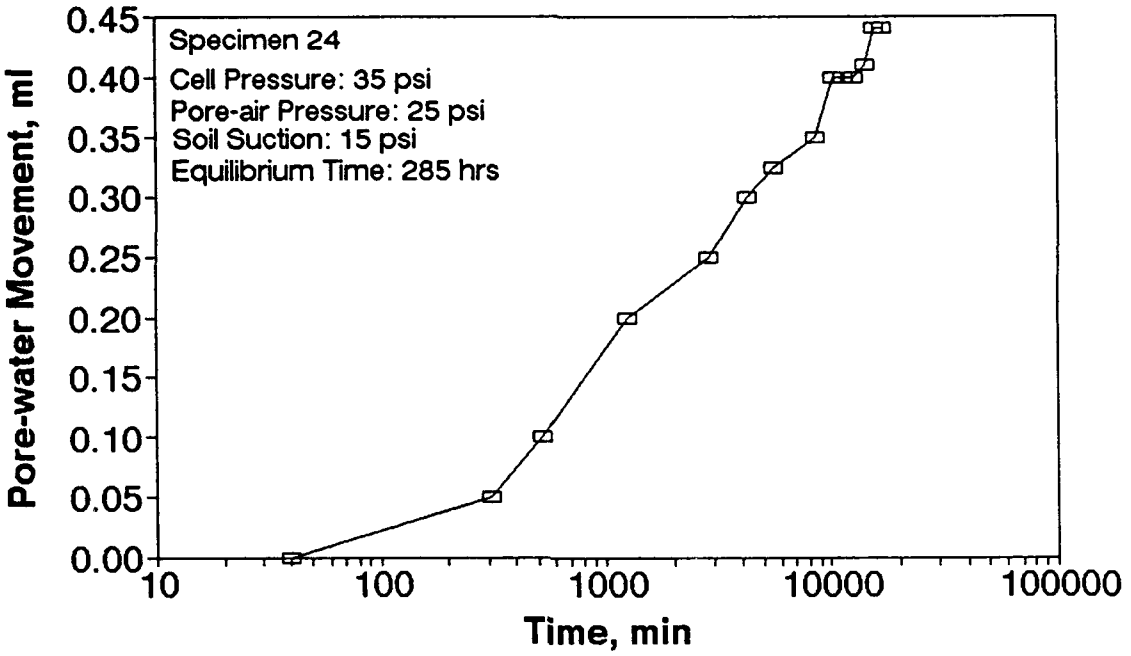
Specimen 24
Cell Pressure: 35 psi
Pore-air Pressure: 25 psi
Soil Suction: 15 psi
Equilibrium Time: 285 hrs
Pore-water Movement, ml
0.45
0.40
0.35
0.30
0.25
0.20
0.15
0.10
0.05
0.00
10
100
1000
10000
100000
Time, min

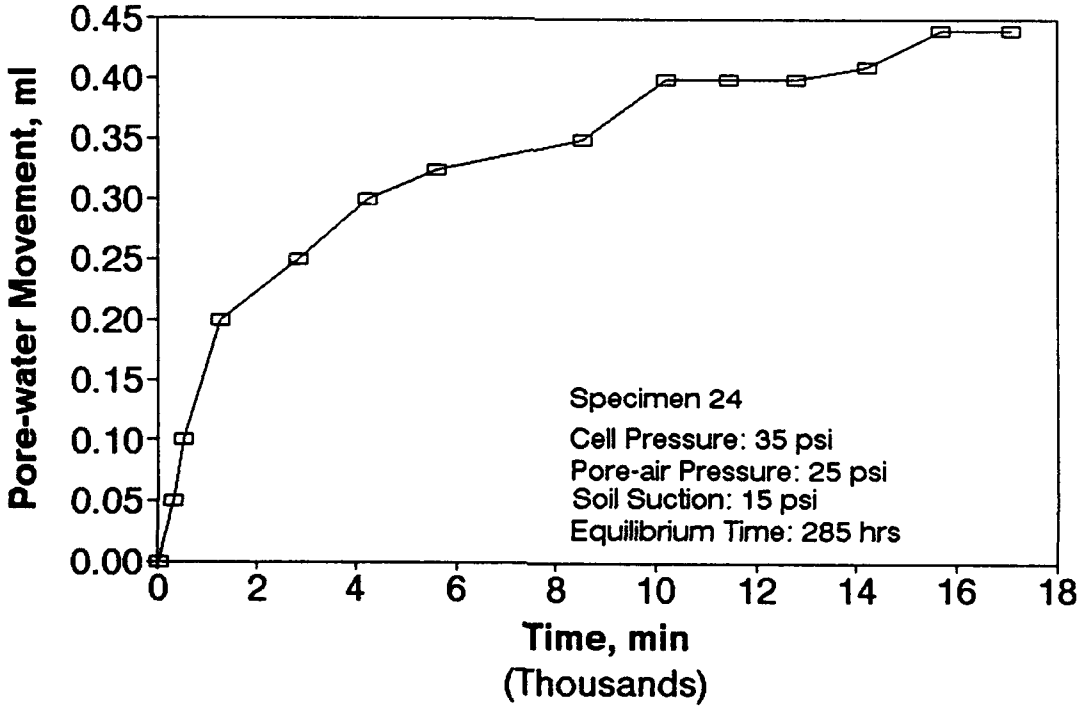
Pore-water Movement, ml
0.45
0.40
0.35
0.30
0.25
0.20
0.15
0.10
0.05
0.00
Specimen 24
Cell Pressure: 35 psi
Pore-air Pressure: 25 psi
Soil Suction: 15 psi
Equilibrium Time: 285 hrs
0
2
4
6
8
10
12
14
16
18
Time, min
(Thousands)

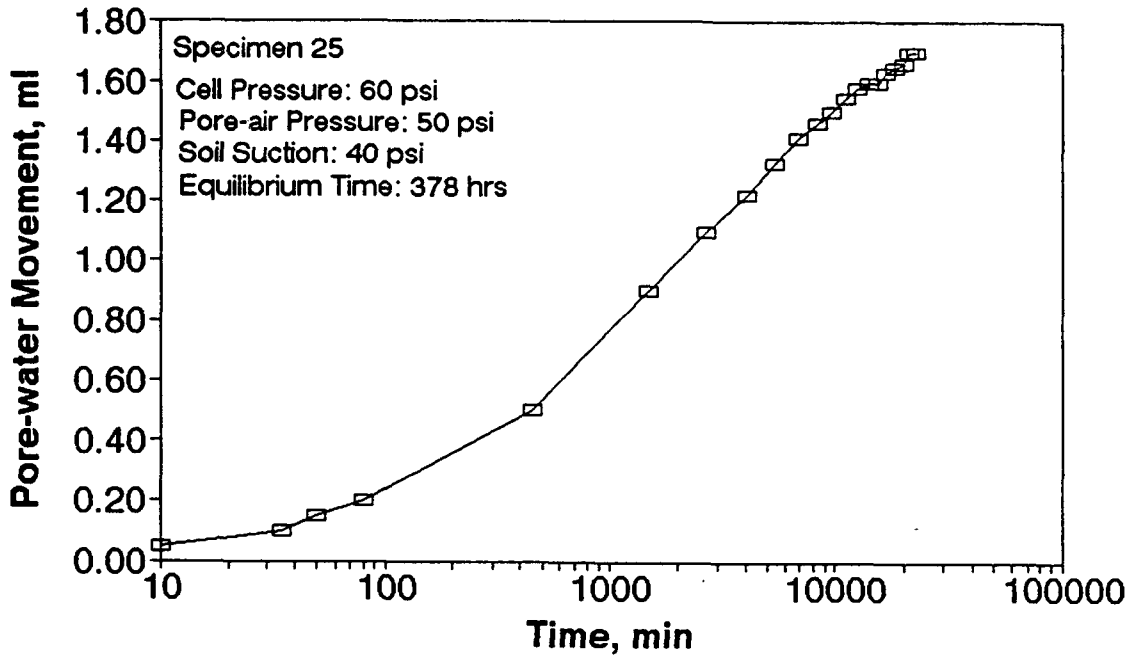
Specimen 25
Cell Pressure: 60 psi
Pore-air Pressure: 50 psi
Soil Suction: 40 psi
Equilibrium Time: 378 hrs
Pore-water Movement, ml
1.80
1.60
1.40
1.20
1.00
0.80
0.60
0.40
0.20
0.00
10
100
1000
10000
100000
Time, min

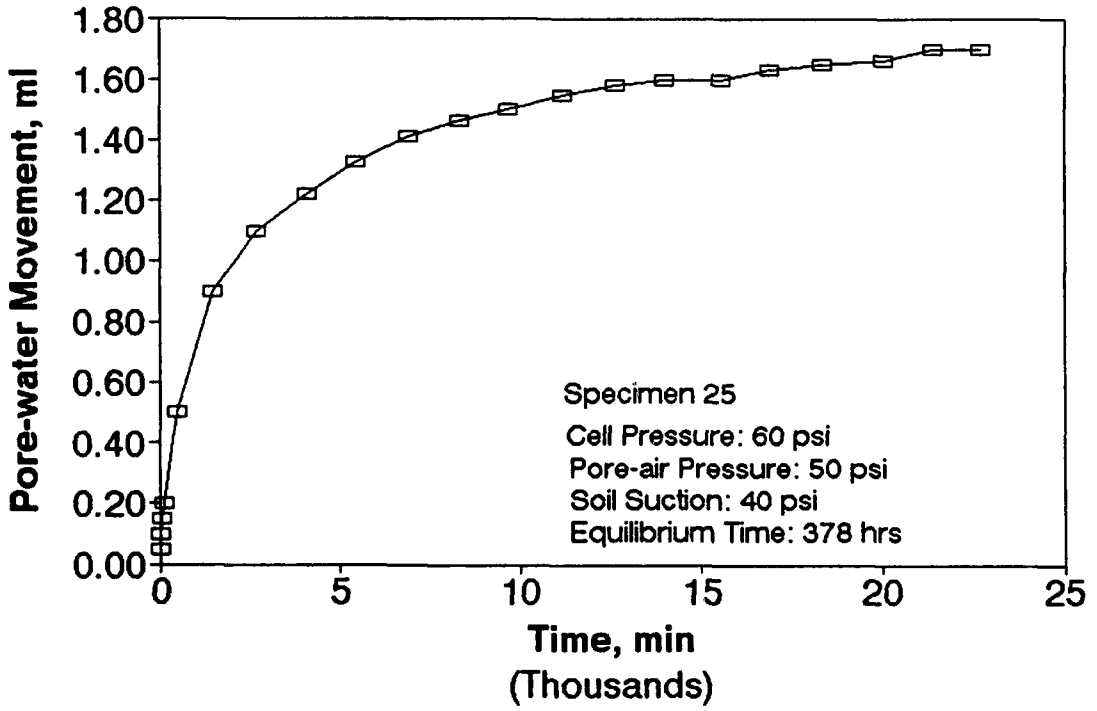
Specimen 25
Cell Pressure: 60 psi
Pore-air Pressure: 50 psi
Soil Suction: 40 psi
Equilibrium Time: 378 hrs
Pore-water Movement, ml
1.80
1.60
1.40
1.20
1.00
0.80
0.60
0.40
0.20
0.00
0
5
10
15
20
25
Time, min
(Thousands)

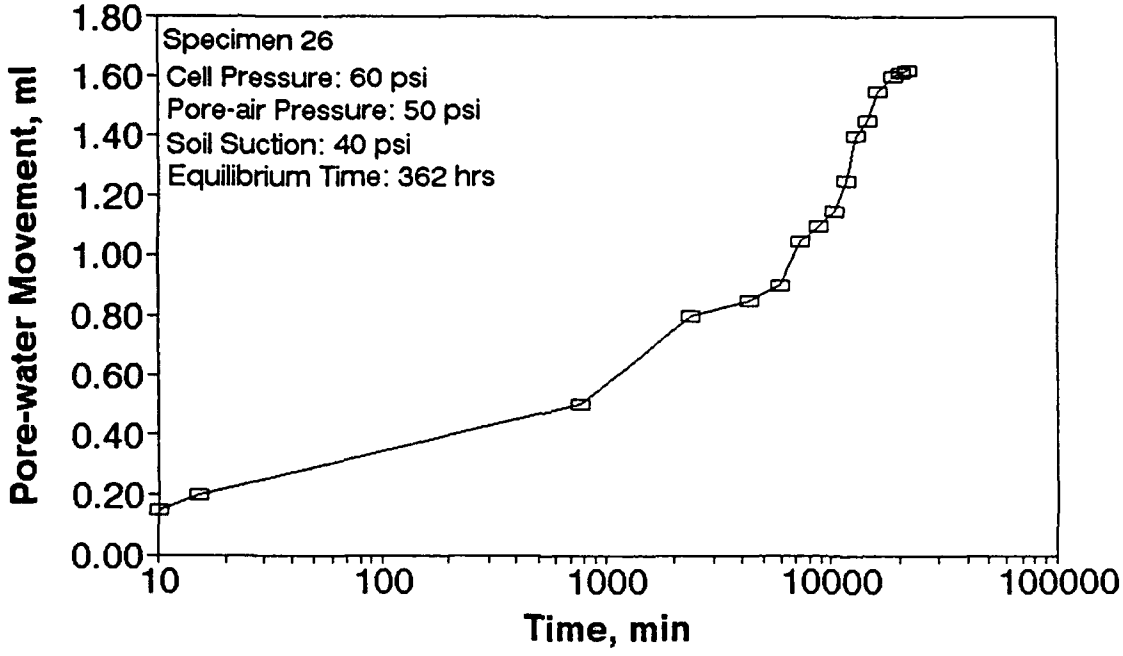
Specimen 26
Cell Pressure: 60 psi
Pore-air Pressure: 50 psi
Soil Suction: 40 psi
Equilibrium Time: 362 hrs
Pore-water Movement, ml
1.80
1.60
1.40
1.20
1.00
0.80
0.60
0.40
0.20
0.00
10
100
1000
10000
100000
Time, min

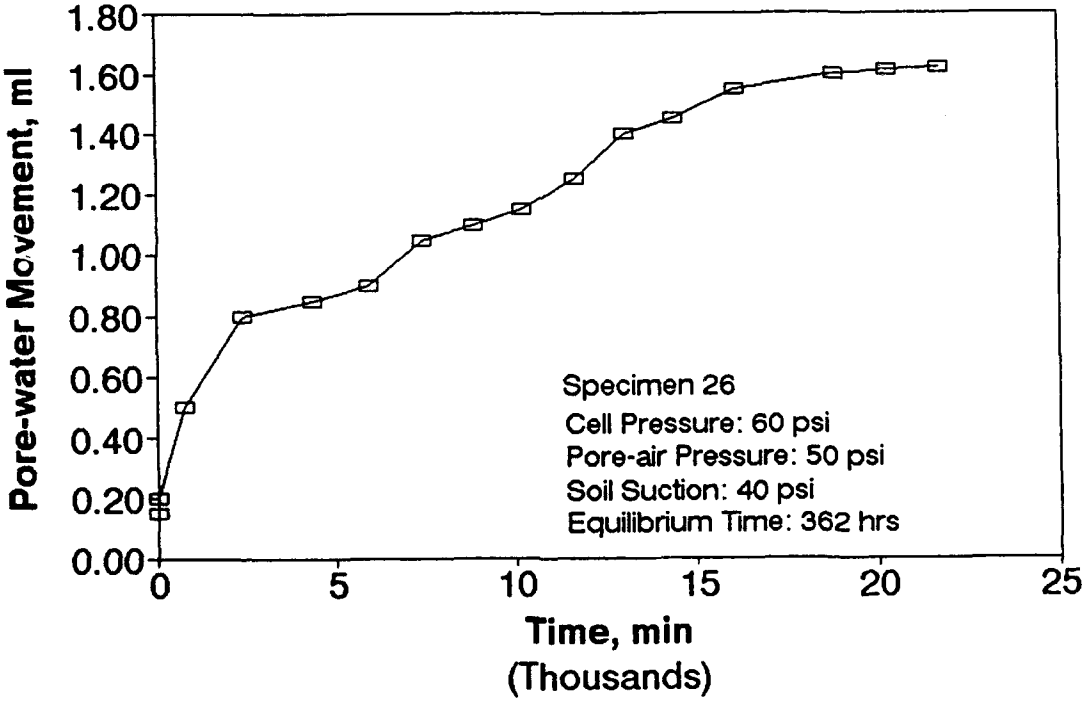
Specimen 26
Cell Pressure: 60 psi
Pore-air Pressure: 50 psi
Soil Suction: 40 psi
Equilibrium Time: 362 hrs
Pore-water Movement, ml
1.80
1.60
1.40
1.20
1.00
0.80
0.60
0.40
0.20
0.00
0
5
10
15
20
25
Time, min
(Thousands)

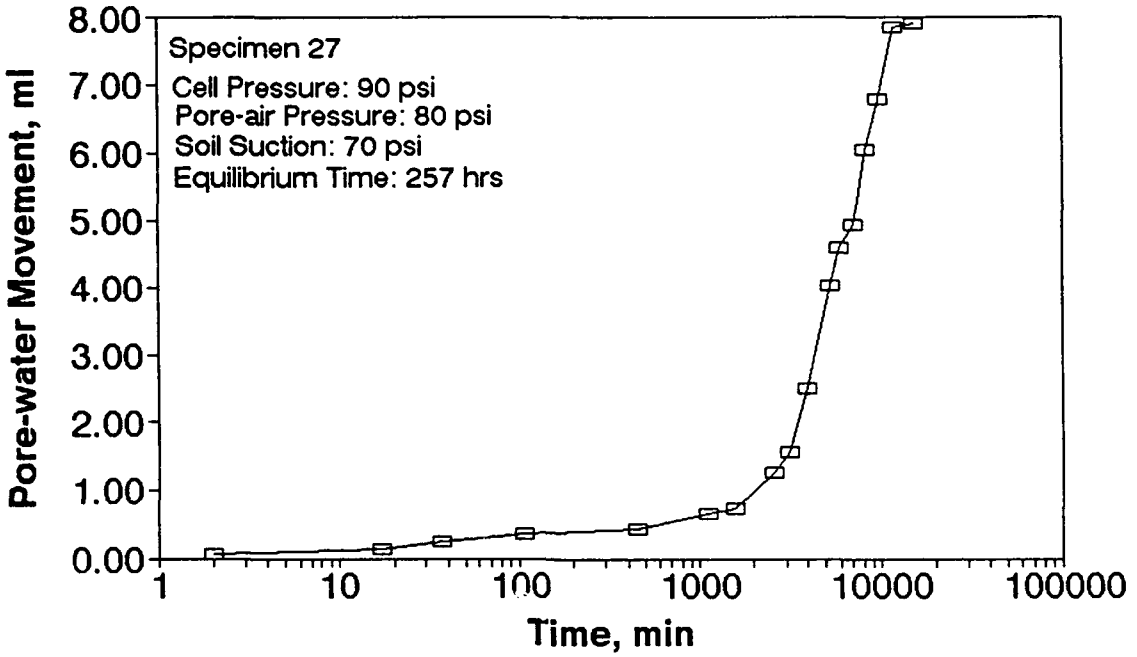
Specimen 27
Cell Pressure: 90 psi
Pore-air Pressure: 80 psi
Soil Suction: 70 psi
Equilibrium Time: 257 hrs
Pore-water Movement, ml
8.00
7.00
6.00
5.00
4.00
3.00
2.00
1.00
0.00
1
10
100
1000
10000
100000
Time, min

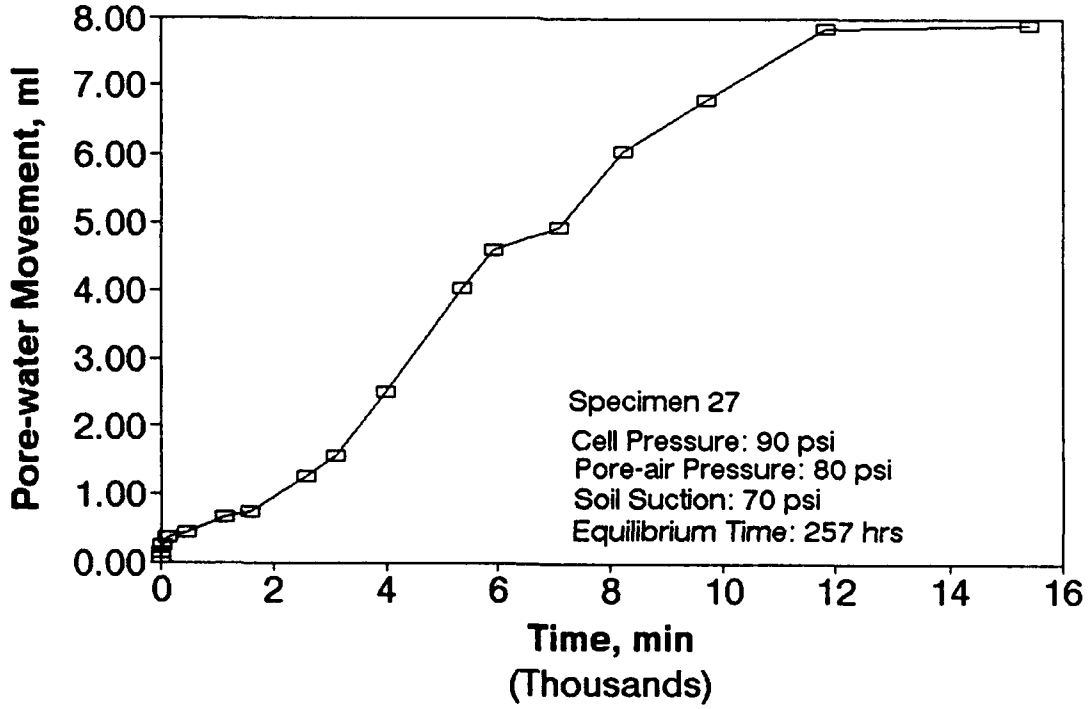
Pore-water Movement, ml
8.00
7.00
6.00
5.00
4.00
3.00
2.00
1.00
0.00
Specimen 27
Cell Pressure: 90 psi
Pore-air Pressure: 80 psi
Soil Suction: 70 psi
Equilibrium Time: 257 hrs
0
2
4
6
8
10
12
14
16
Time, min
(Thousands)

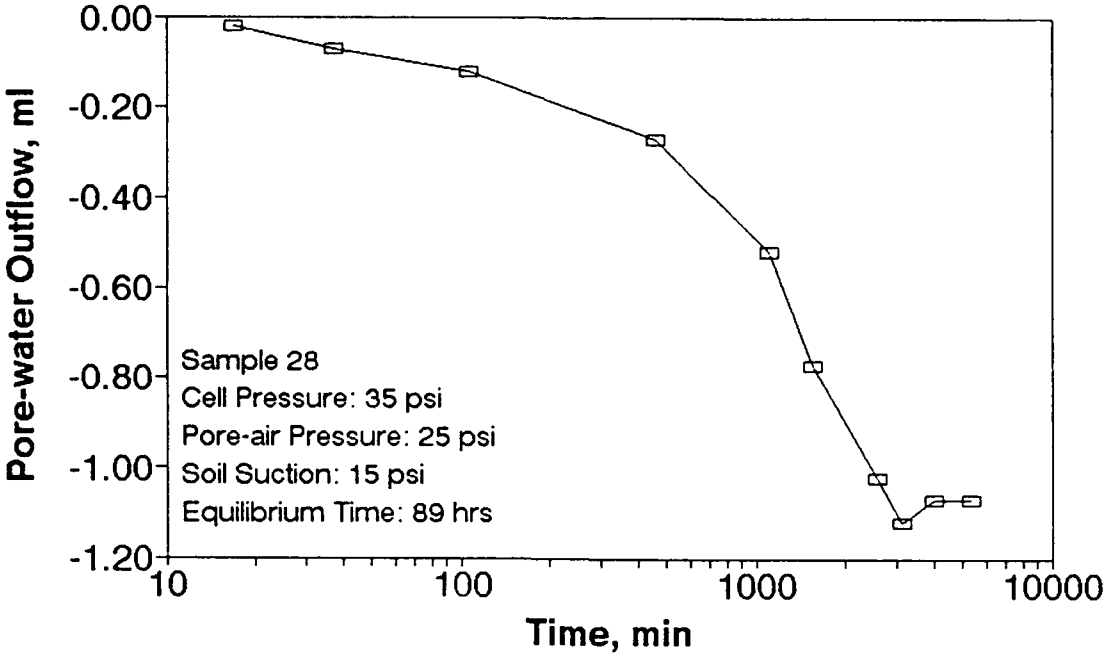
0.00
-0.20
-0.40
-0.60
-0.80
-1.00
-1.20
Pore-water Outflow, ml
Sample 28
Cell Pressure: 35 psi
Pore-air Pressure: 25 psi
Soil Suction: 15 psi
Equilibrium Time: 89 hrs
10
100
1000
10000
Time, min

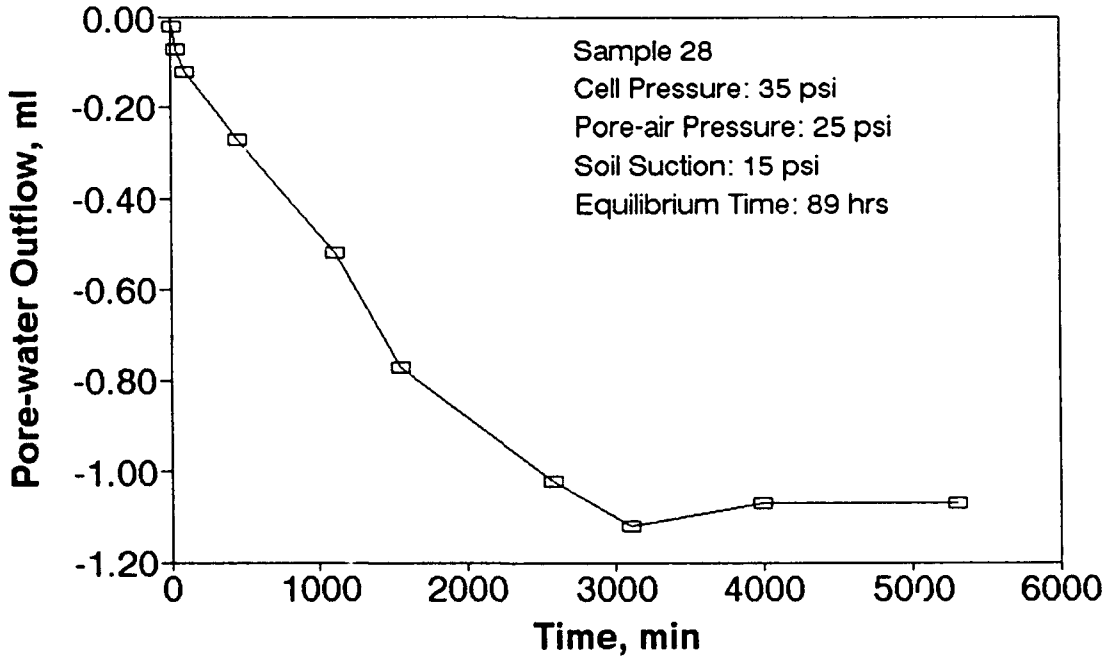
0.00
-0.20
-0.40
-0.60
-0.80
-1.00
-1.20
Pore-water Outflow, ml
Sample 28
Cell Pressure: 35 psi
Pore-air Pressure: 25 psi
Soil Suction: 15 psi
Equilibrium Time: 89 hrs
0
1000
2000
3000
4000
5000
6000
Time, min

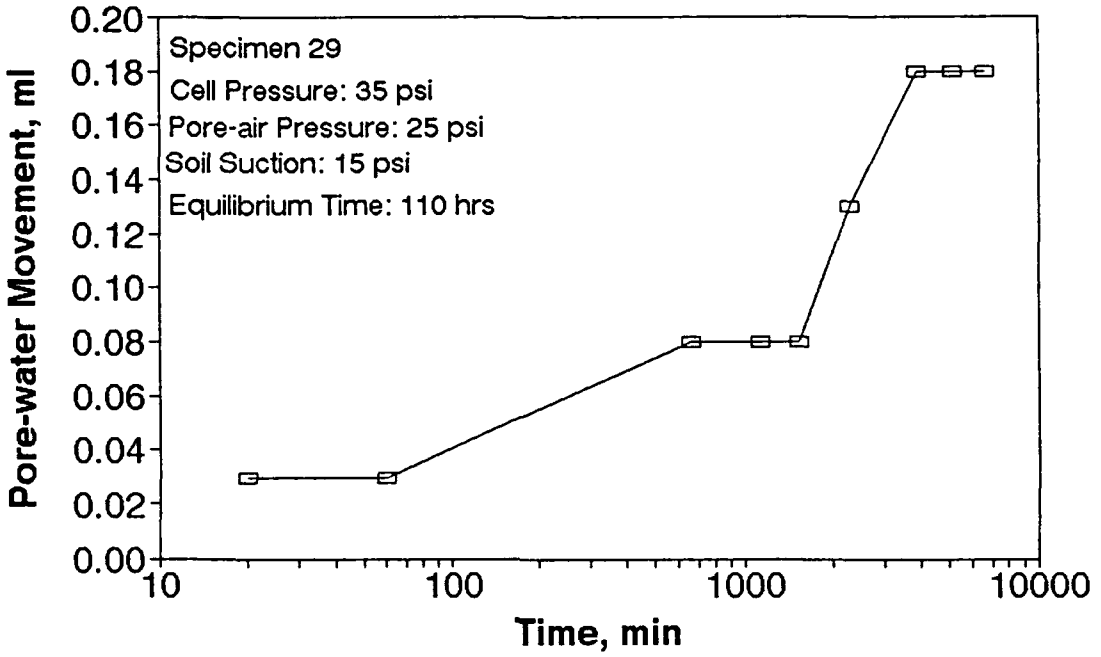
Specimen 29
Cell Pressure: 35 psi
Pore-air Pressure: 25 psi
Soil Suction: 15 psi
Equilibrium Time: 110 hrs
Pore-water Movement, ml
0.20
0.18
0.16
0.14
0.12
0.10
0.08
0.06
0.04
0.02
0.00
10
100
1000
10000
Time, min

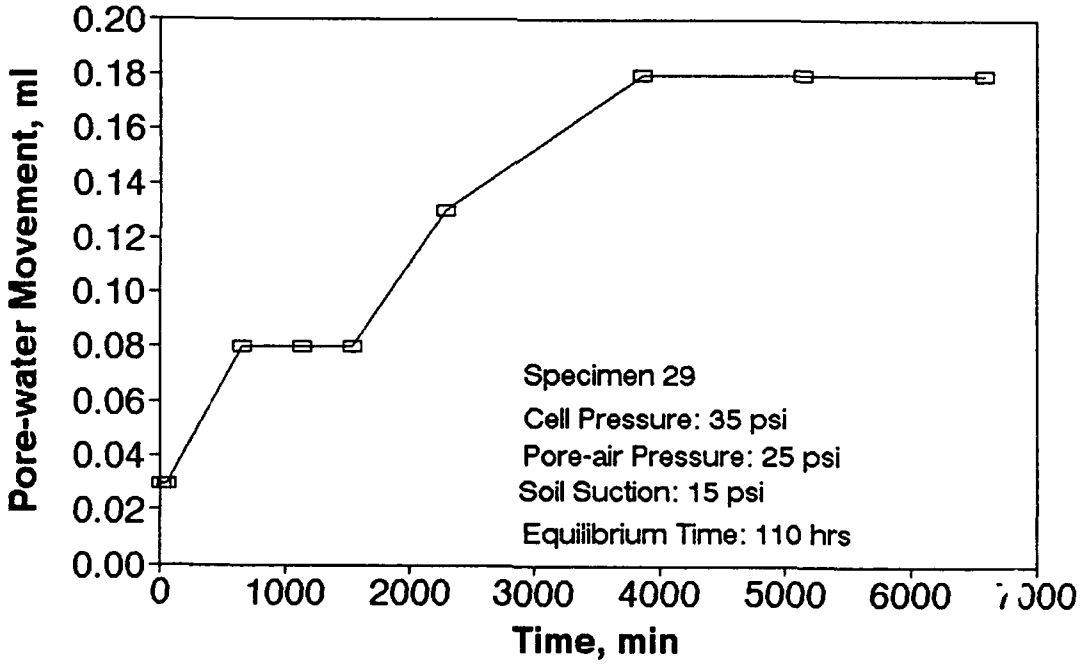
Specimen 29
Cell Pressure: 35 psi
Pore-air Pressure: 25 psi
Soil Suction: 15 psi
Equilibrium Time: 110 hrs
Pore-water Movement, ml
0.20
0.18
0.16
0.14
0.12
0.10
0.08
0.06
0.04
0.02
0.00
0
1000
2000
3000
4000
5000
6000
Time, min

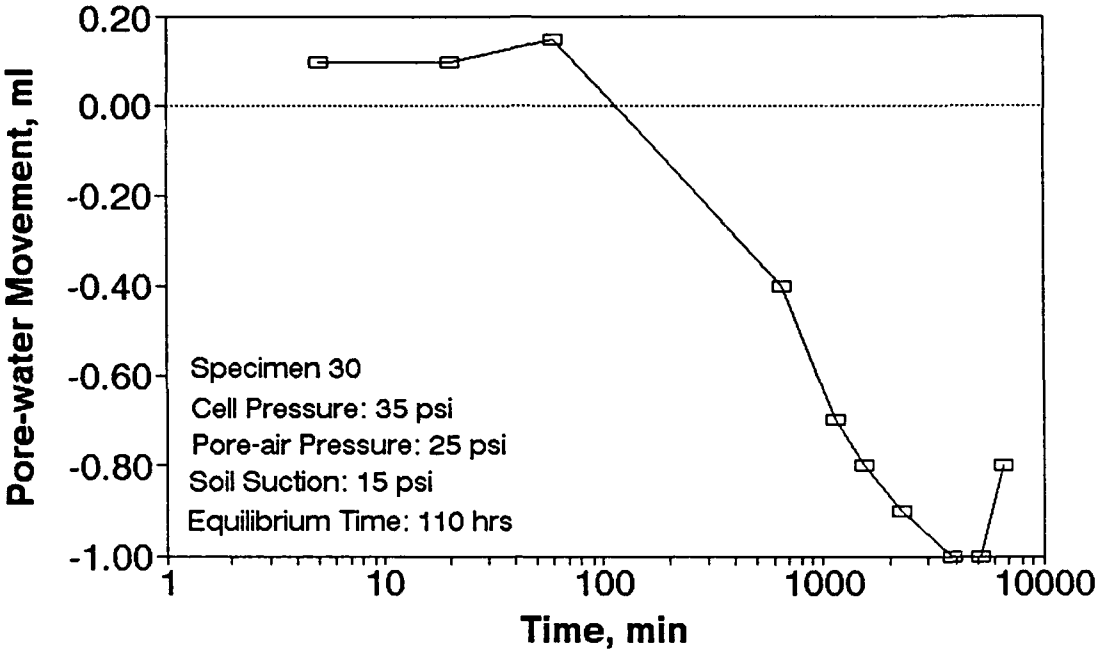
0.20
0.00
-0.20
-0.40
-0.60
-0.80
-1.00
Pore-water Movement, ml
Specimen 30
Cell Pressure: 35 psi
Pore-air Pressure: 25 psi
Soil Suction: 15 psi
Equilibrium Time: 110 hrs
1
10
100
1000
10000
Time, min

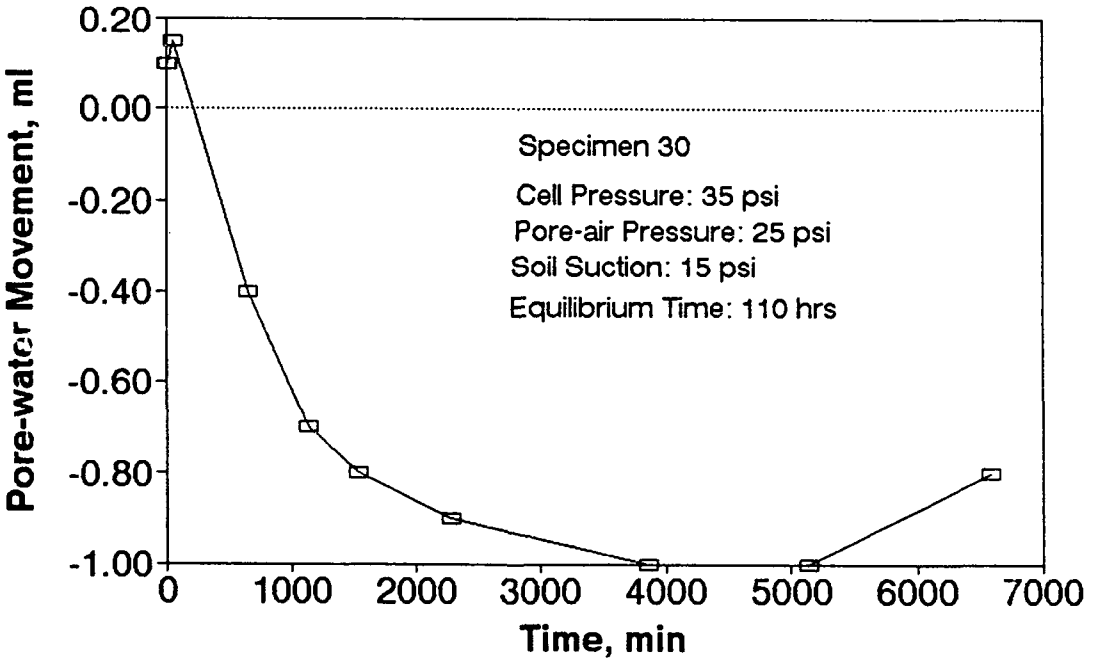
0.20
0.00
-0.20
-0.40
-0.60
-0.80
-1.00
Pore-water Movement, ml
Specimen 30
Cell Pressure: 35 psi
Pore-air Pressure: 25 psi
Soil Suction: 15 psi
Equilibrium Time: 110 hrs
0
1000
2000
3000
4000
5000
6000
7000
Time, min

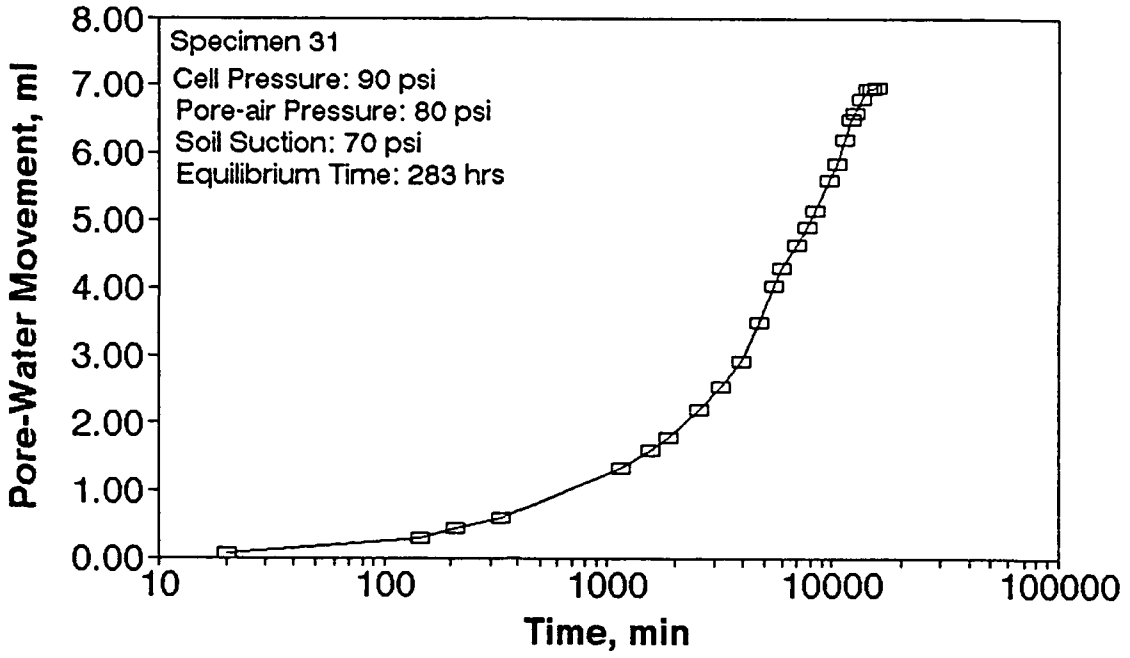
Specimen 31
Cell Pressure: 90 psi
Pore-air Pressure: 80 psi
Soil Suction: 70 psi
Equilibrium Time: 283 hrs
Pore-Water Movement, ml
8.00
7.00
6.00
5.00
4.00
3.00
2.00
1.00
0.00
10
100
1000
10000
100000
Time, min

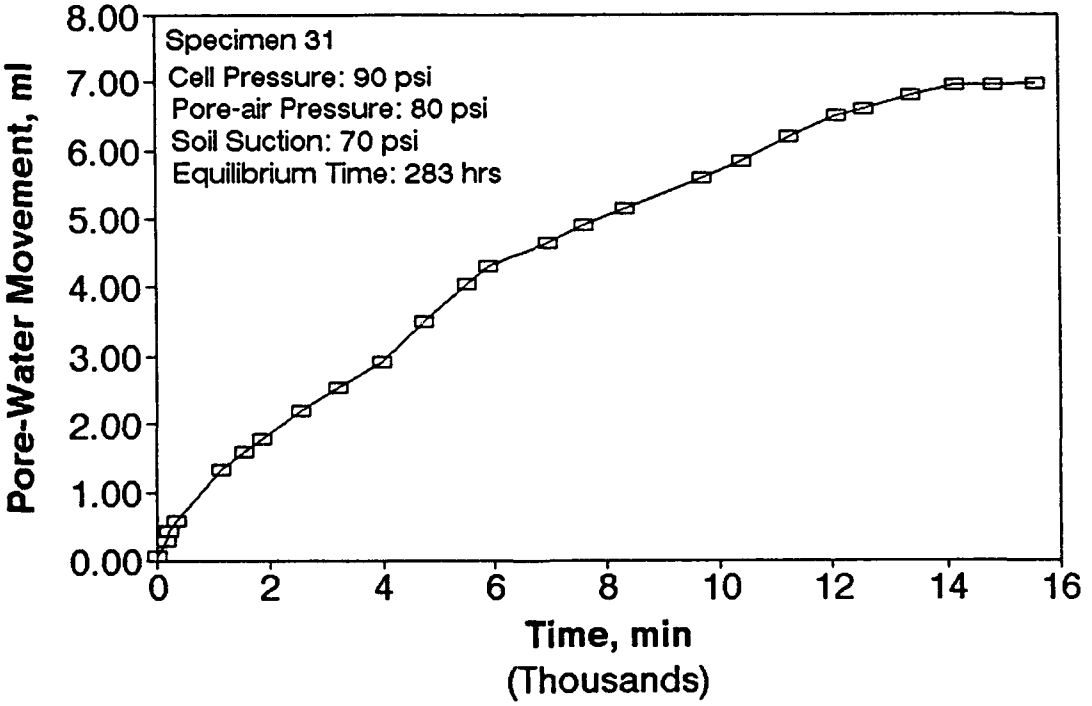
Specimen 31
Cell Pressure: 90 psi
Pore-air Pressure: 80 psi
Soil Suction: 70 psi
Equilibrium Time: 283 hrs
Pore-Water Movement, ml
8.00
7.00
6.00
5.00
4.00
3.00
2.00
1.00
0.00
0
2
4
6
8
10
12
14
16
Time, min
(Thousands)

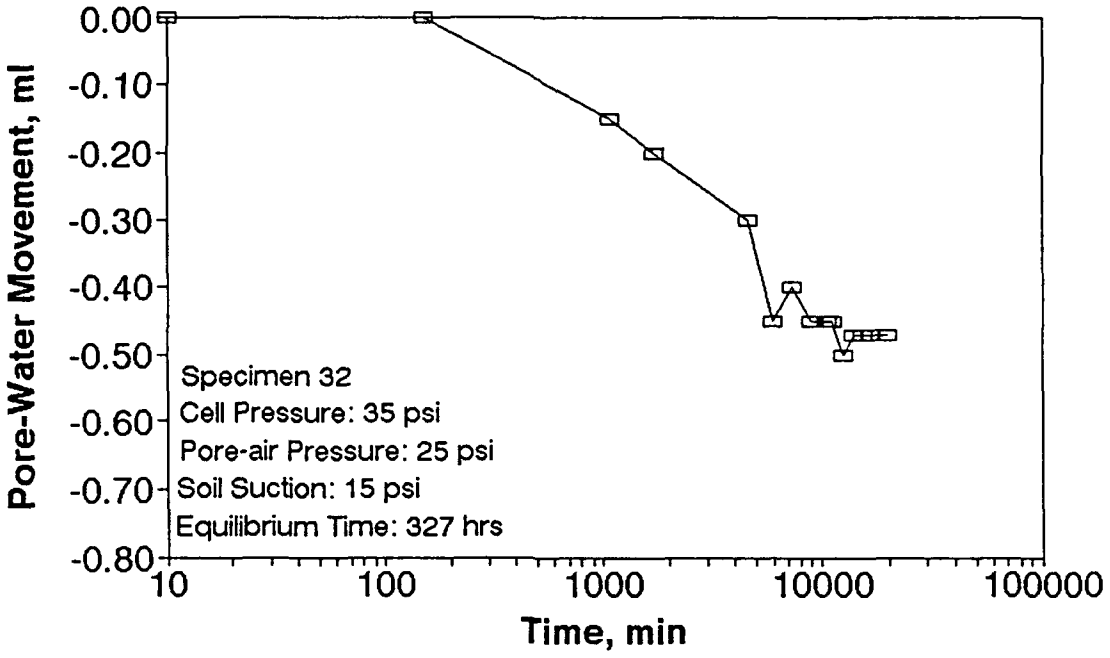
Pore-Water Movement, ml
0.00
-0.10
-0.20
-0.30
-0.40
-0.50
-0.60
-0.70
-0.80
Specimen 32
Cell Pressure: 35 psi
Pore-air Pressure: 25 psi
Soil Suction: 15 psi
Equilibrium Time: 327 hrs
10
100
1000
10000
100000
Time, min

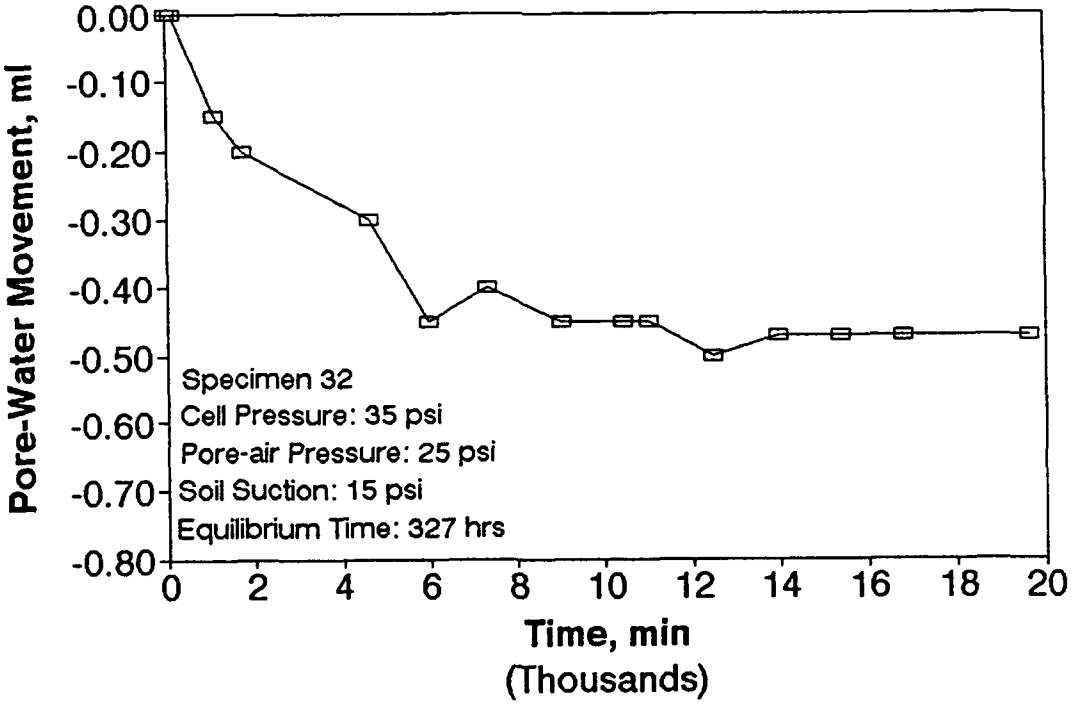
Pore-Water Movement, ml
0.00
-0.10
-0.20
-0.30
-0.40
-0.50
-0.60
-0.70
-0.80
Specimen 32
Cell Pressure: 35 psi
Pore-air Pressure: 25 psi
Soil Suction: 15 psi
Equilibrium Time: 327 hrs
0
2
4
6
8
10
12
14
16
18
20
Time, min
(Thousands)

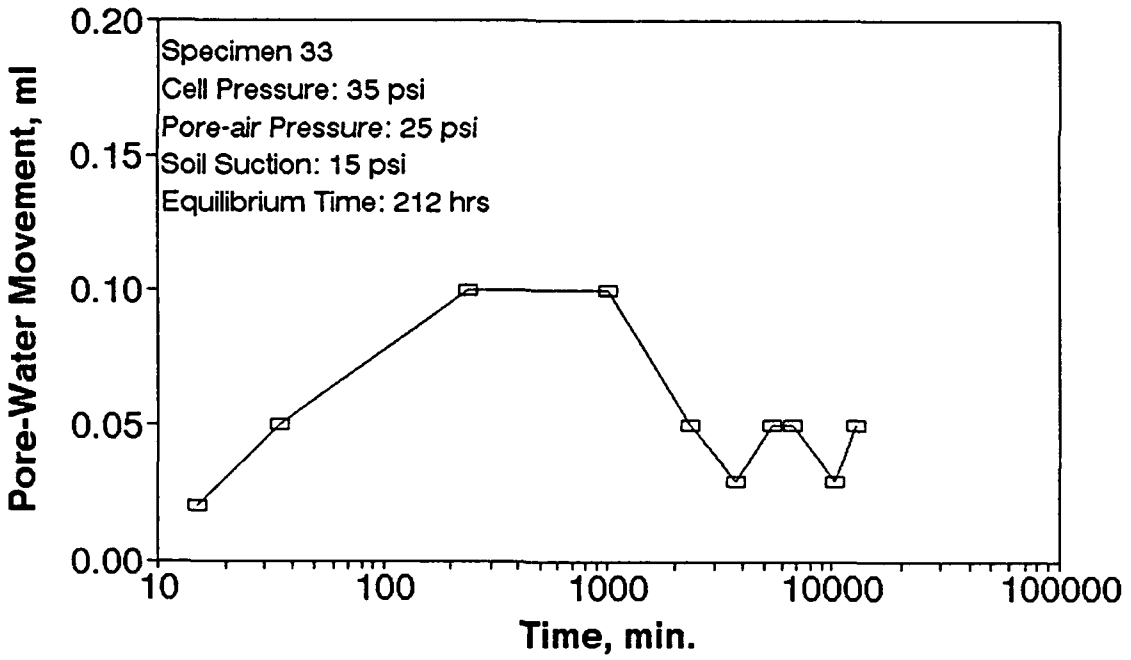
Specimen 33
Cell Pressure: 35 psi
Pore-air Pressure: 25 psi
Soil Suction: 15 psi
Equilibrium Time: 212 hrs
Pore-Water Movement, ml
0.20
0.15
0.10
0.05
0.00
10
100
1000
10000
100000
Time, min.

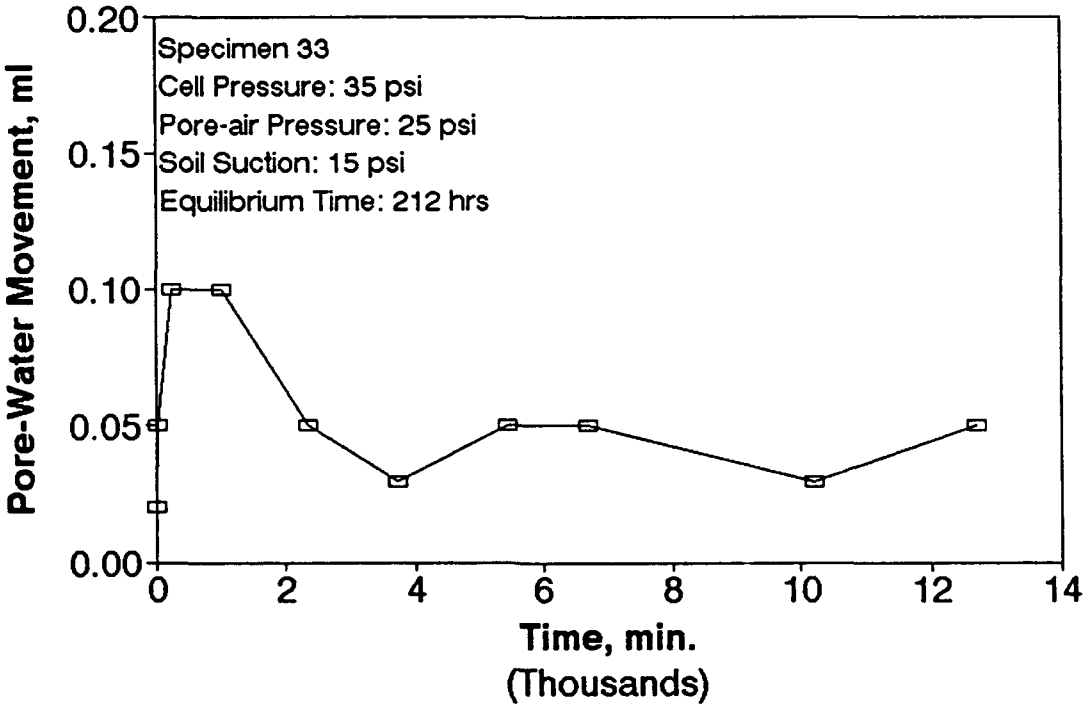
Specimen 33
Cell Pressure: 35 psi
Pore-air Pressure: 25 psi
Soil Suction: 15 psi
Equilibrium Time: 212 hrs
Pore-Water Movement, ml
0.20
0.15
0.10
0.05
0.00
0
2
4
6
8
10
12
14
Time, min.
(Thousands)

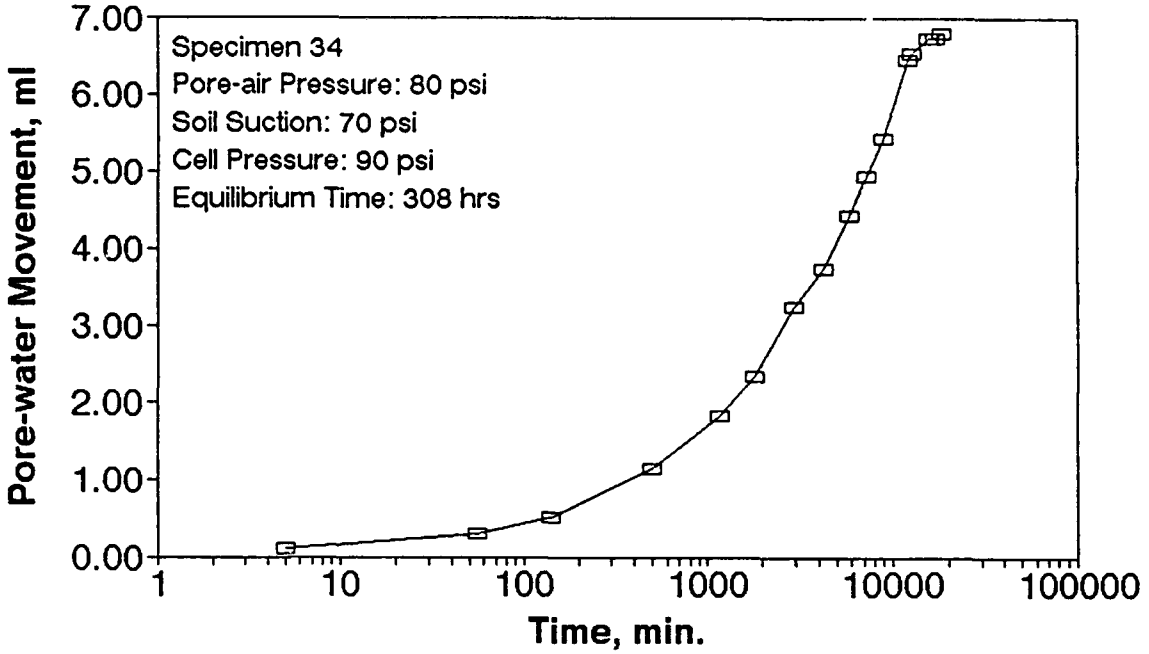
Specimen 34
Pore-air Pressure: 80 psi
Soil Suction: 70 psi
Cell Pressure: 90 psi
Equilibrium Time: 308 hrs
Pore-water Movement, ml
7.00
6.00
5.00
4.00
3.00
2.00
1.00
0.00
1
10
100
1000
10000
100000
Time, min.

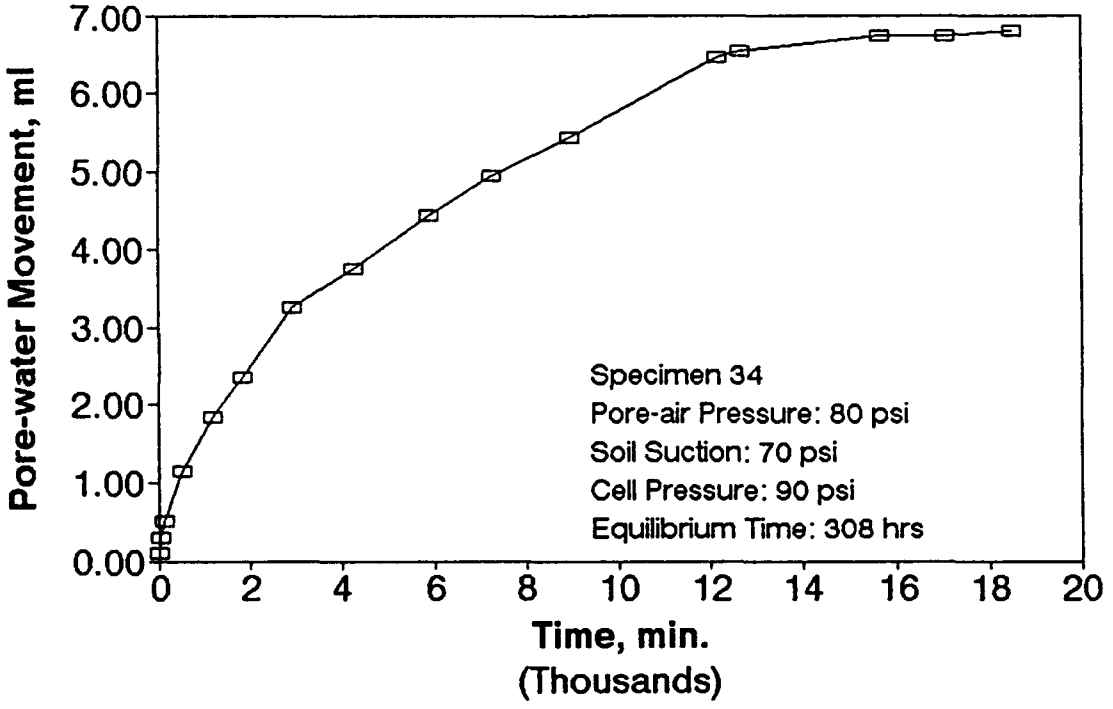
Specimen 34
Pore-air Pressure: 80 psi
Soil Suction: 70 psi
Cell Pressure: 90 psi
Equilibrium Time: 308 hrs
Pore-water Movement, ml
7.00
6.00
5.00
4.00
3.00
2.00
1.00
0.00
0
2
4
6
8
10
12
14
16
18
20
Time, min.
(Thousands)

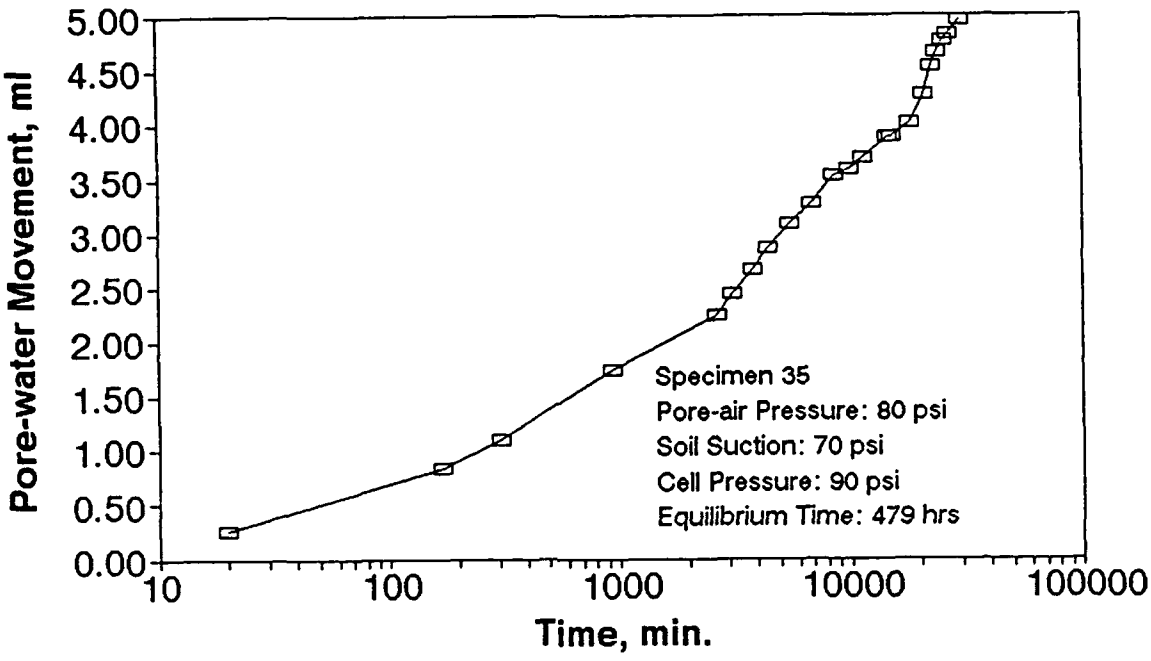
Pore-water Movement, ml
5.00
4.50
4.00
3.50
3.00
2.50
2.00
1.50
1.00
0.50
0.00
10
100
1000
10000
100000
Time, min.
Specimen 35
Pore-air Pressure: 80 psi
Soil Suction: 70 psi
Cell Pressure: 90 psi
Equilibrium Time: 479 hrs

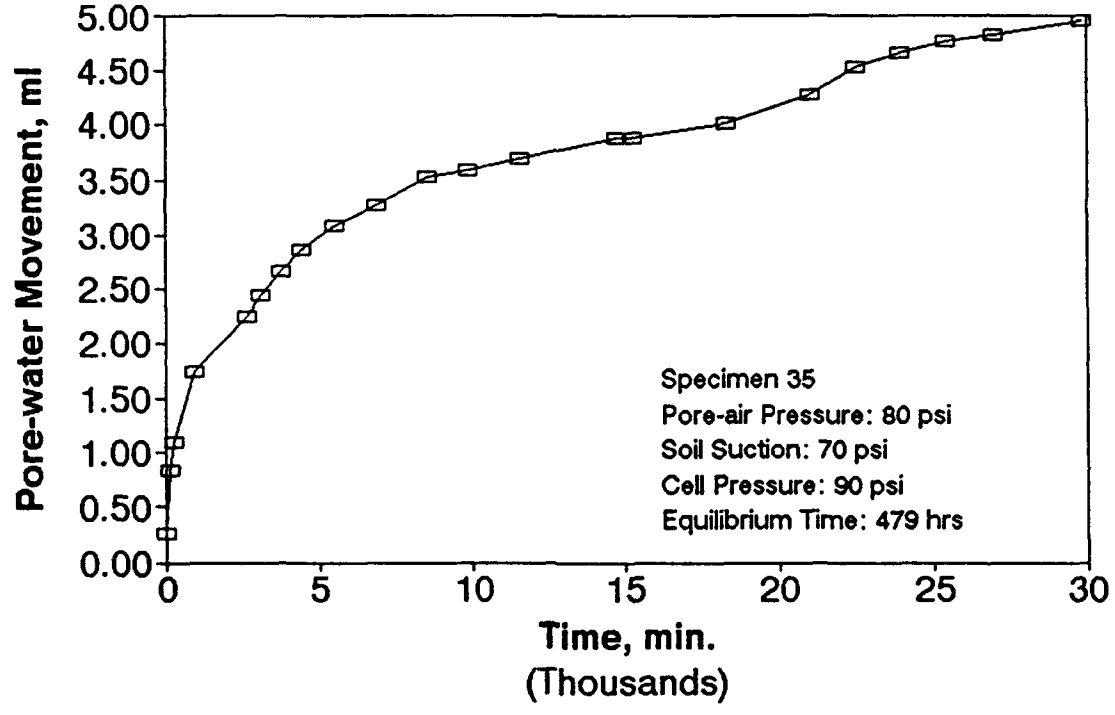
Pore-water Movement, ml
5.00
4.50
4.00
3.50
3.00
2.50
2.00
1.50
1.00
0.50
0.00
0
5
10
15
20
25
30
Time, min.
(Thousands)
Specimen 35
Pore-air Pressure: 80 psi
Soil Suction: 70 psi
Cell Pressure: 90 psi
Equilibrium Time: 479 hrs

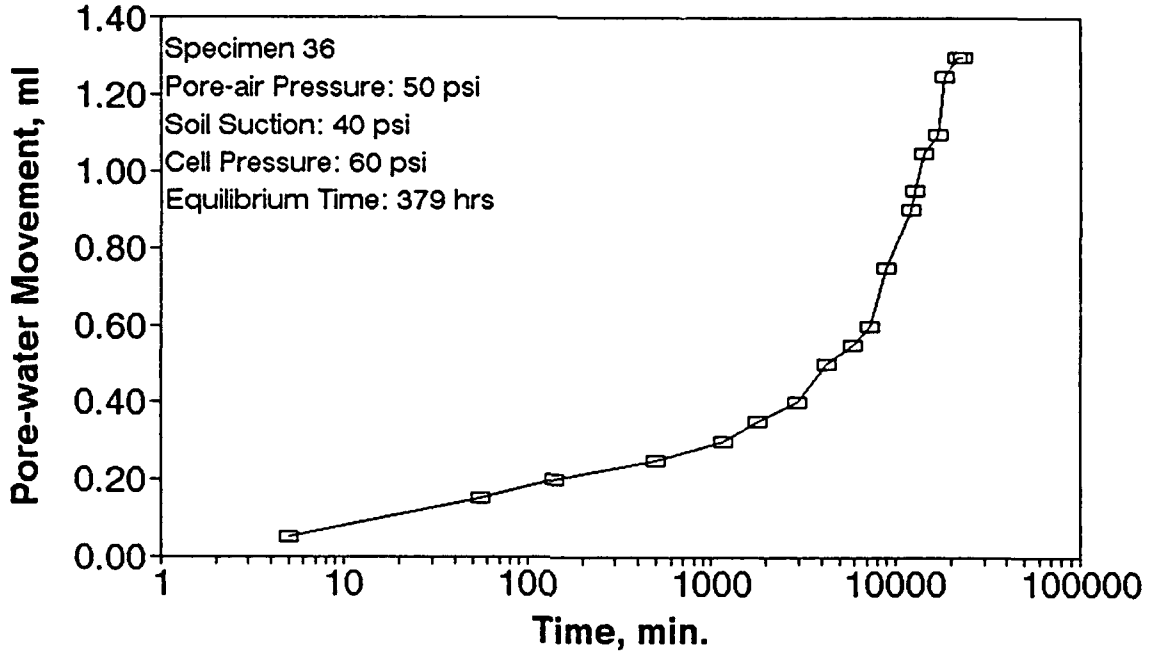
Specimen 36
Pore-air Pressure: 50 psi
Soil Suction: 40 psi
Cell Pressure: 60 psi
Equilibrium Time: 379 hrs
Pore-water Movement, ml
1.40
1.20
1.00
0.80
0.60
0.40
0.20
0.00
1
10
100
1000
10000
100000
Time, min.

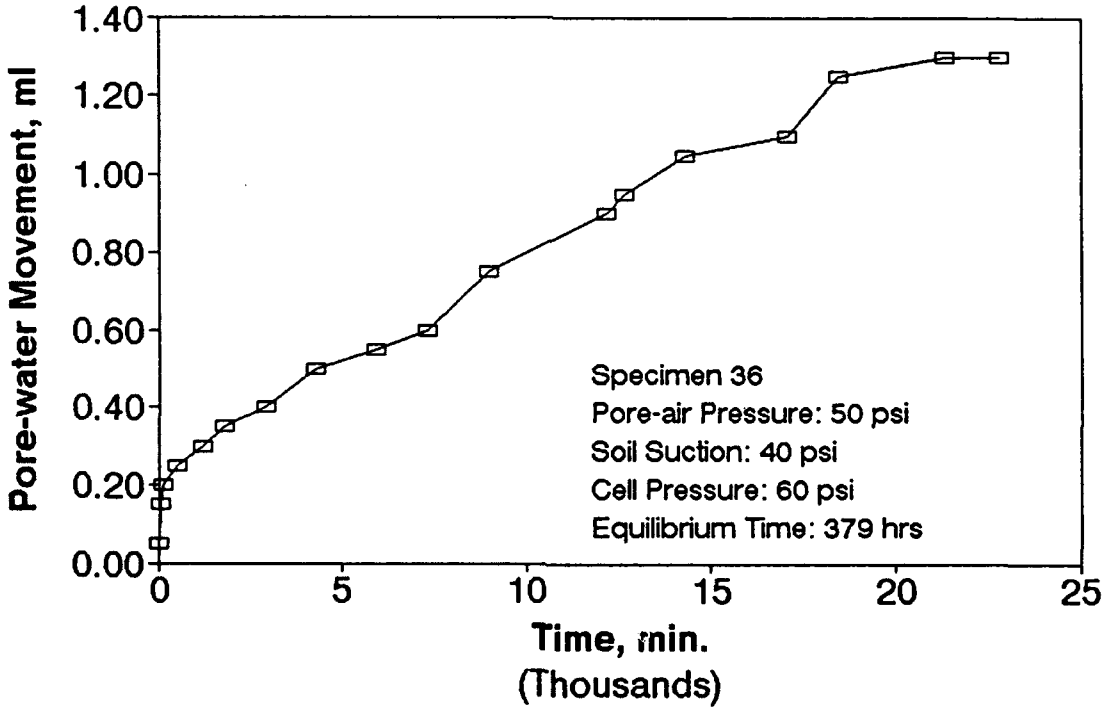
Pore-water Movement, ml
1.40
1.20
1.00
0.80
0.60
0.40
0.20
0.00
Specimen 36
Pore-air Pressure: 50 psi
Soil Suction: 40 psi
Cell Pressure: 60 psi
Equilibrium Time: 379 hrs
0
5
10
15
20
25
Time, min.
(Thousands)

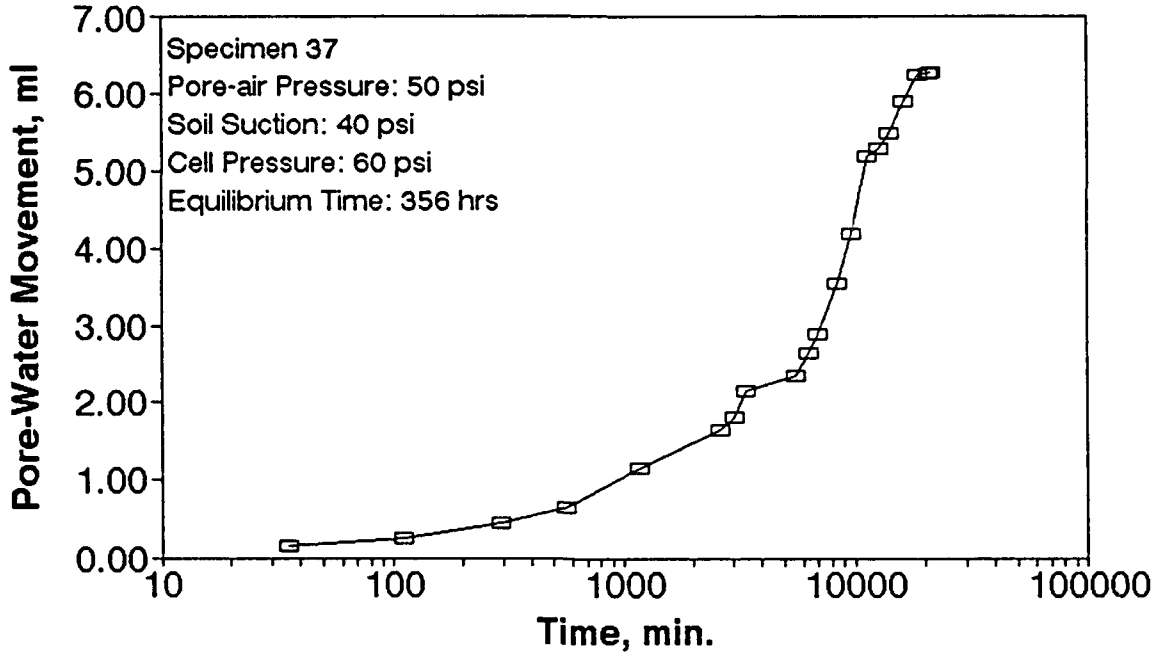
Specimen 37
Pore-air Pressure: 50 psi
Soil Suction: 40 psi
Cell Pressure: 60 psi
Equilibrium Time: 356 hrs
Pore-Water Movement, ml
7.00
6.00
5.00
4.00
3.00
2.00
1.00
0.00
10
100
1000
10000
100000
Time, min.

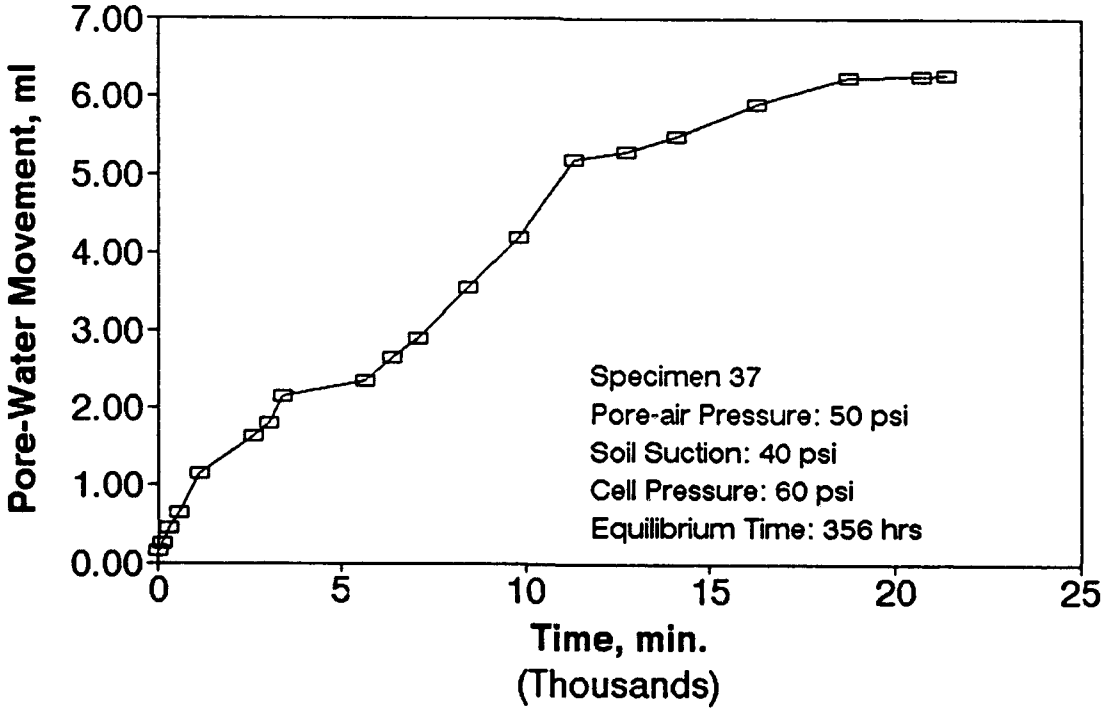
Specimen 37
Pore-air Pressure: 50 psi
Soil Suction: 40 psi
Cell Pressure: 60 psi
Equilibrium Time: 356 hrs
Pore-Water Movement, ml
7.00
6.00
5.00
4.00
3.00
2.00
1.00
0.00
0
5
10
15
20
25
Time, min.
(Thousands)

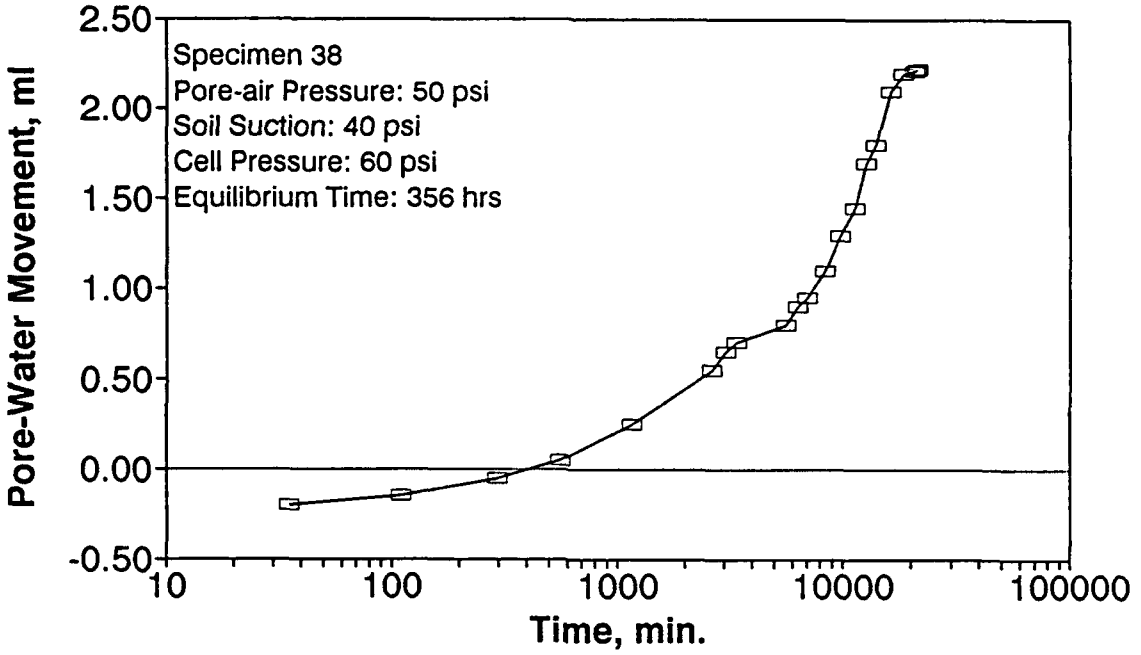
Specimen 38
Pore-air Pressure: 50 psi
Soil Suction: 40 psi
Cell Pressure: 60 psi
Equilibrium Time: 356 hrs
Pore-Water Movement, ml
2.50
2.00
1.50
1.00
0.50
0.00
-0.50
10
100
1000
10000
100000
Time, min.

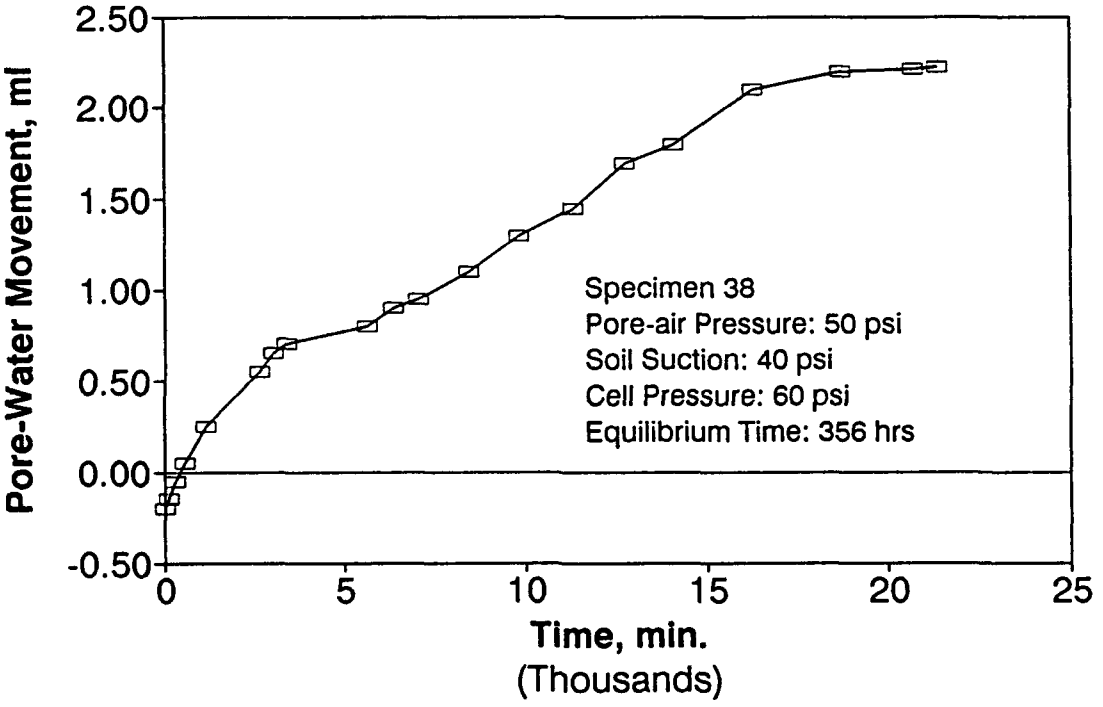
Specimen 38
Pore-air Pressure: 50 psi
Soil Suction: 40 psi
Cell Pressure: 60 psi
Equilibrium Time: 356 hrs
Pore-Water Movement, ml
2.50
2.00
1.50
1.00
0.50
0.00
-0.50
0
5
10
15
20
25
Time, min.
(Thousands)

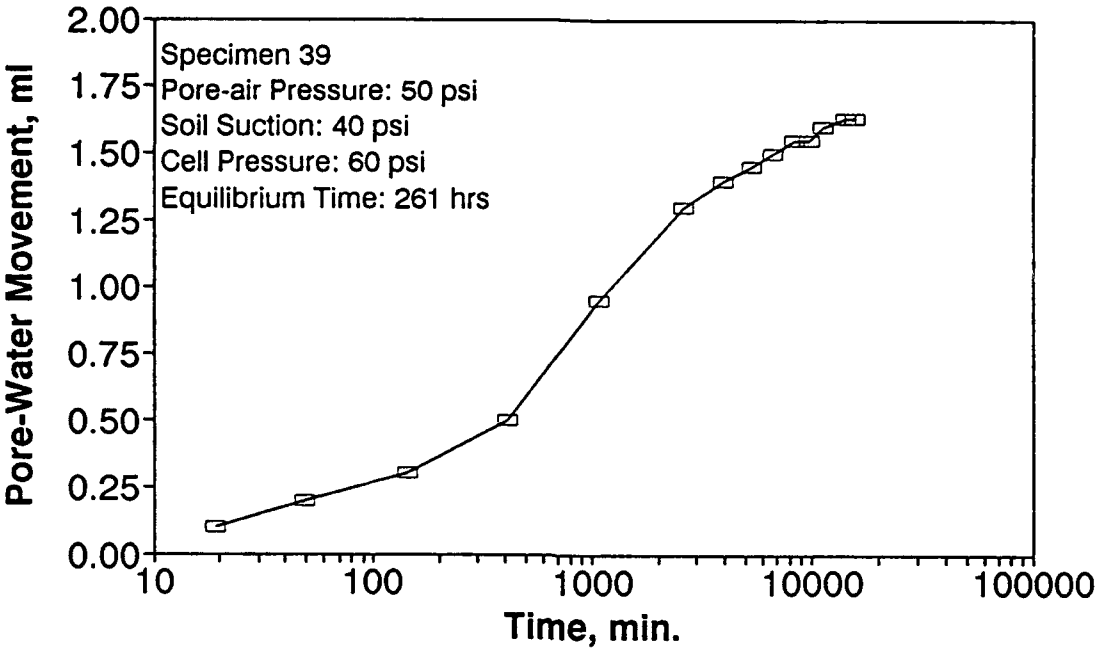
Specimen 39
Pore-air Pressure: 50 psi
Soil Suction: 40 psi
Cell Pressure: 60 psi
Equilibrium Time: 261 hrs
Pore-Water Movement, ml
2.00
1.75
1.50
1.25
1.00
0.75
0.50
0.25
0.00
10
100
1000
10000
100000
Time, min.

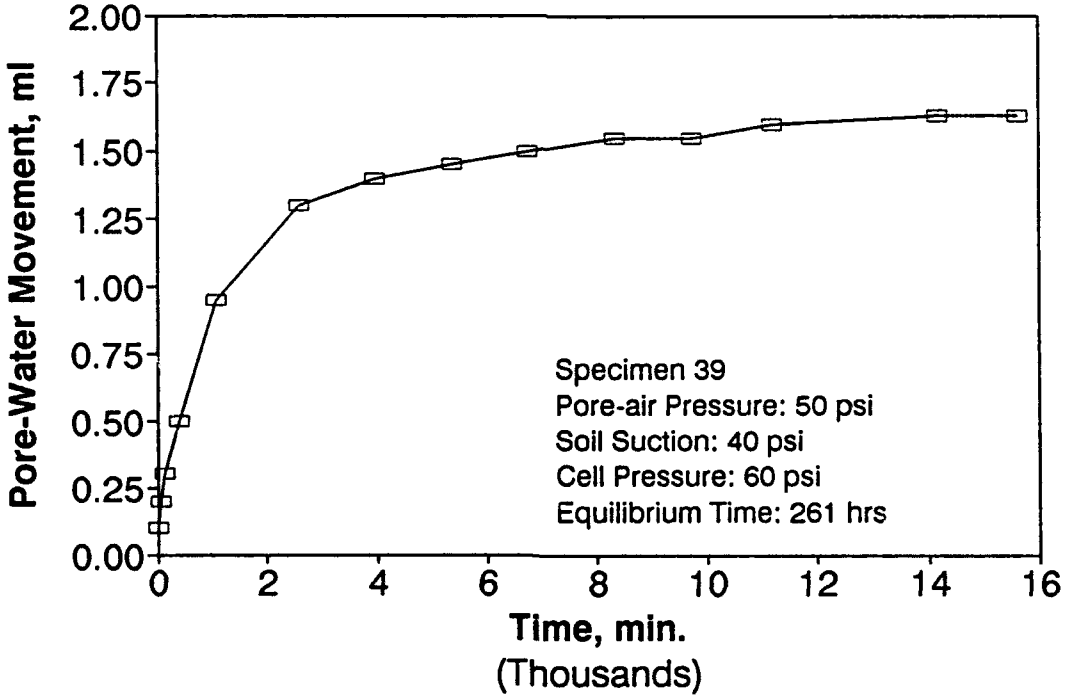
Specimen 39
Pore-air Pressure: 50 psi
Soil Suction: 40 psi
Cell Pressure: 60 psi
Equilibrium Time: 261 hrs
Pore-Water Movement, ml
2.00
1.75
1.50
1.25
1.00
0.75
0.50
0.25
0.00
0
2
4
6
8
10
12
14
16
Time, min.
(Thousands)

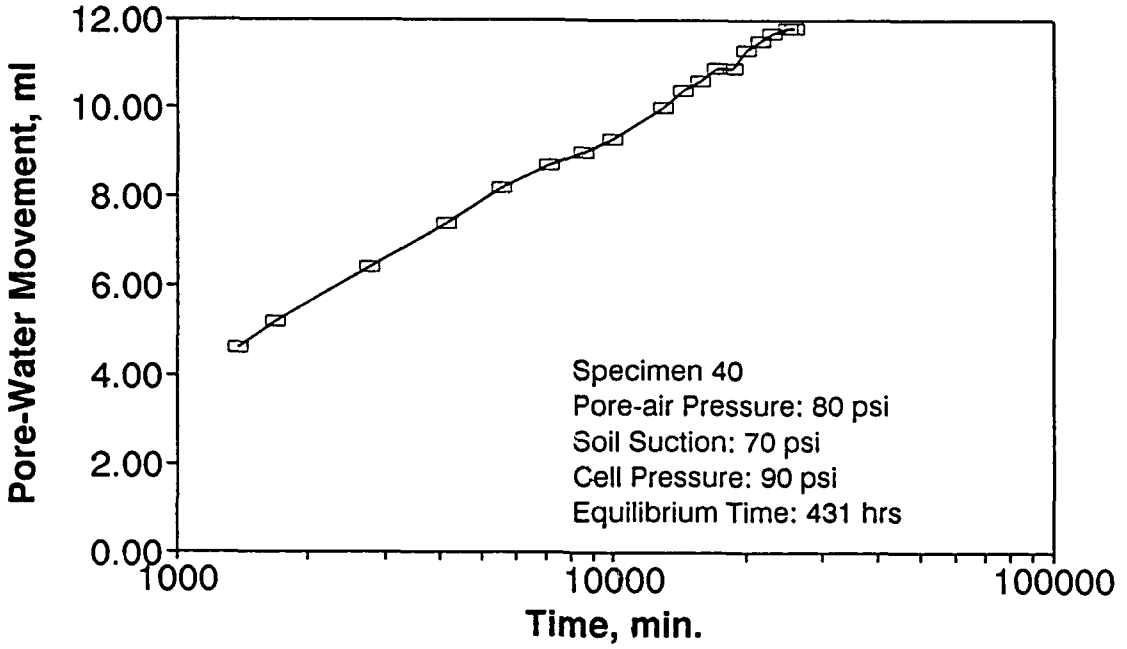
12.00
10.00
8.00
6.00
4.00
2.00
0.00
Pore-Water Movement, ml
1000
10000
100000
Time, min.
Specimen 40
Pore-air Pressure: 80 psi
Soil Suction: 70 psi
Cell Pressure: 90 psi
Equilibrium Time: 431 hrs

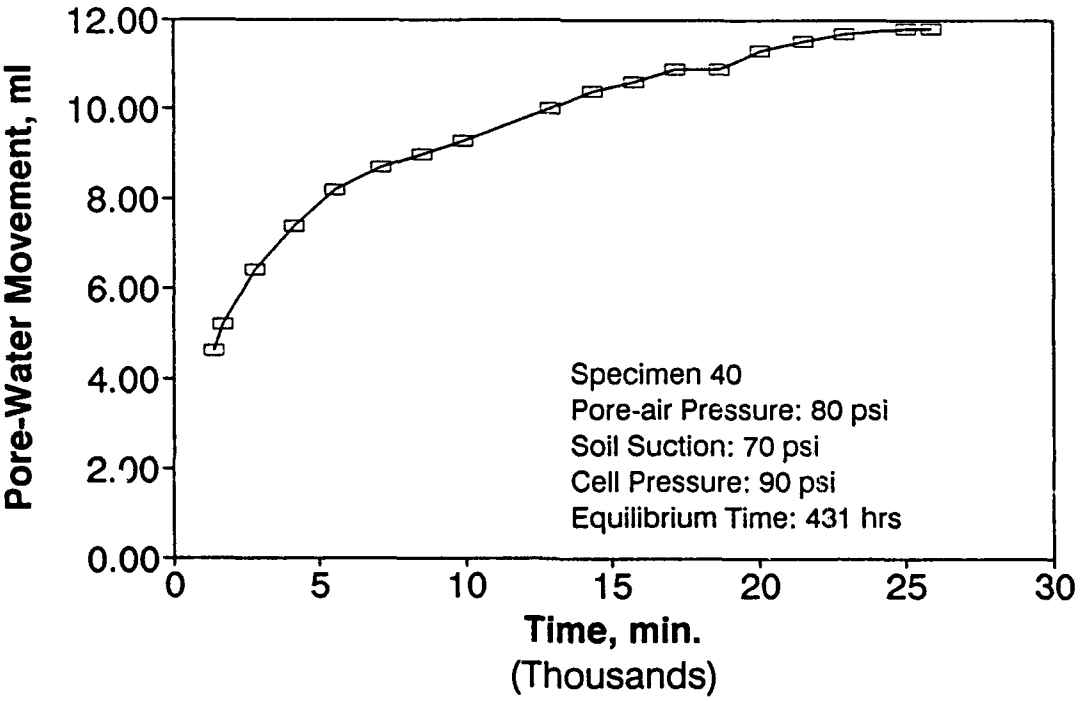
12.00
10.00
8.00
6.00
4.00
2.00
0.00
Pore-Water Movement, ml
0
5
10
15
20
25
30
Time, min.
(Thousands)
Specimen 40
Pore-air Pressure: 80 psi
Soil Suction: 70 psi
Cell Pressure: 90 psi
Equilibrium Time: 431 hrs

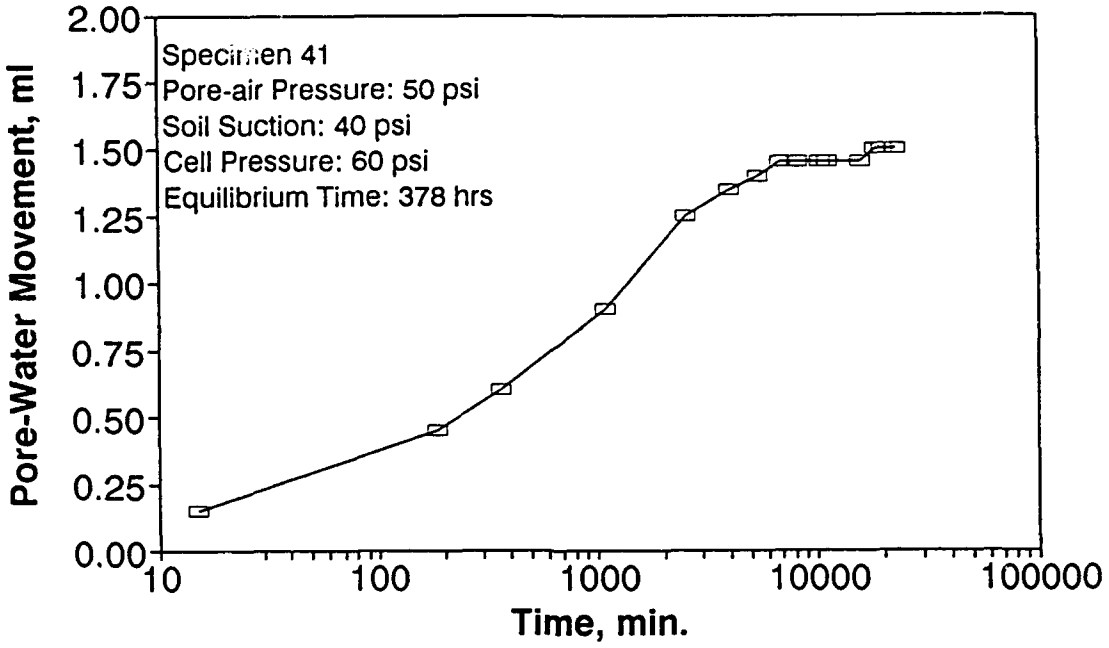
Specimen 41
Pore-air Pressure: 50 psi
Soil Suction: 40 psi
Cell Pressure: 60 psi
Equilibrium Time: 378 hrs
Pore-Water Movement, ml
2.00
1.75
1.50
1.25
1.00
0.75
0.50
0.25
0.00
10
100
1000
10000
100000
Time, min.

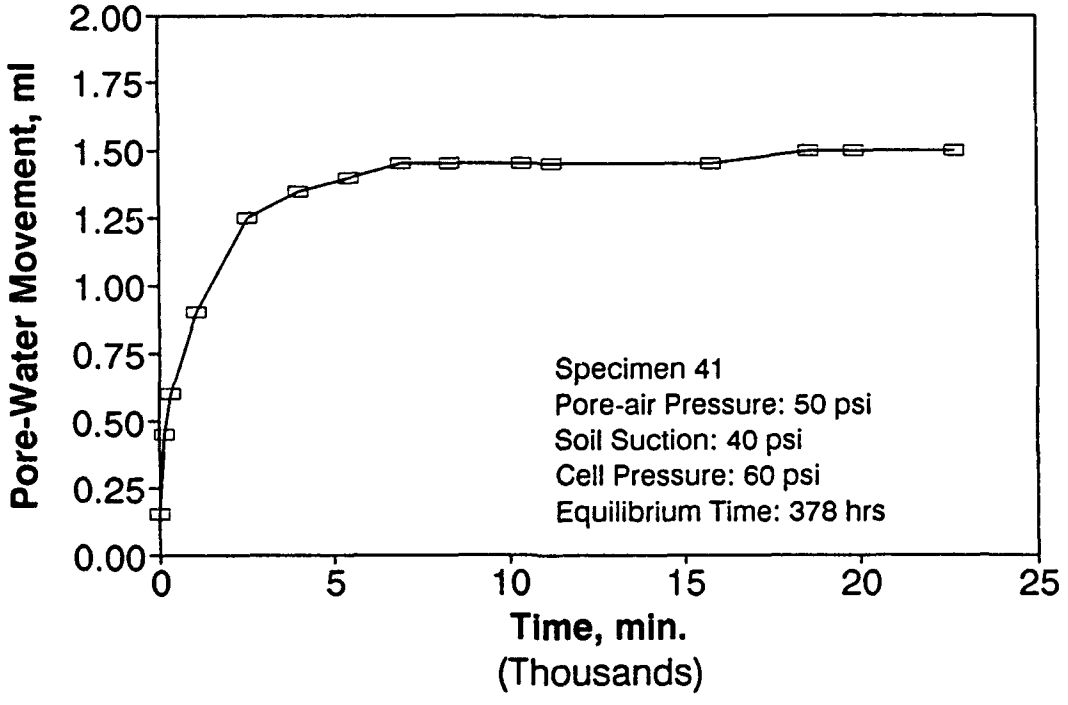
Pore-Water Movement, ml
2.00
1.75
1.50
1.25
1.00
0.75
0.50
0.25
0.00
Specimen 41
Pore-air Pressure: 50 psi
Soil Suction: 40 psi
Cell Pressure: 60 psi
Equilibrium Time: 378 hrs
0
5
10
15
20
25
Time, min.
(Thousands)

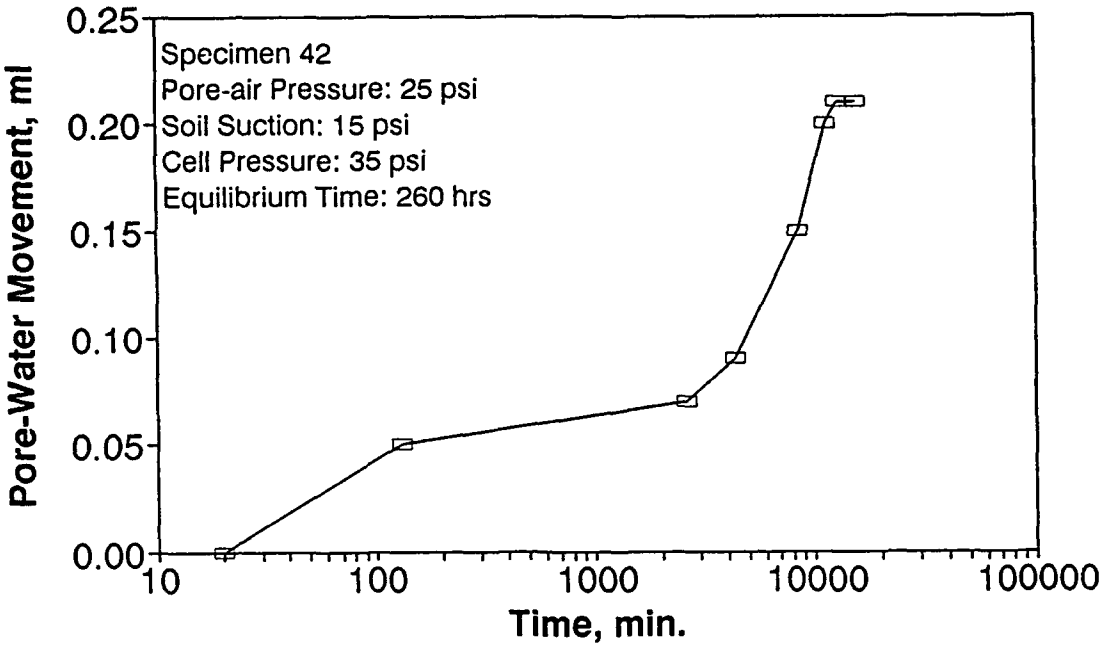
Specimen 42
Pore-air Pressure: 25 psi
Soil Suction: 15 psi
Cell Pressure: 35 psi
Equilibrium Time: 260 hrs
Pore-Water Movement, ml
0.25
0.20
0.15
0.10
0.05
0.00
10
100
1000
10000
100000
Time, min.

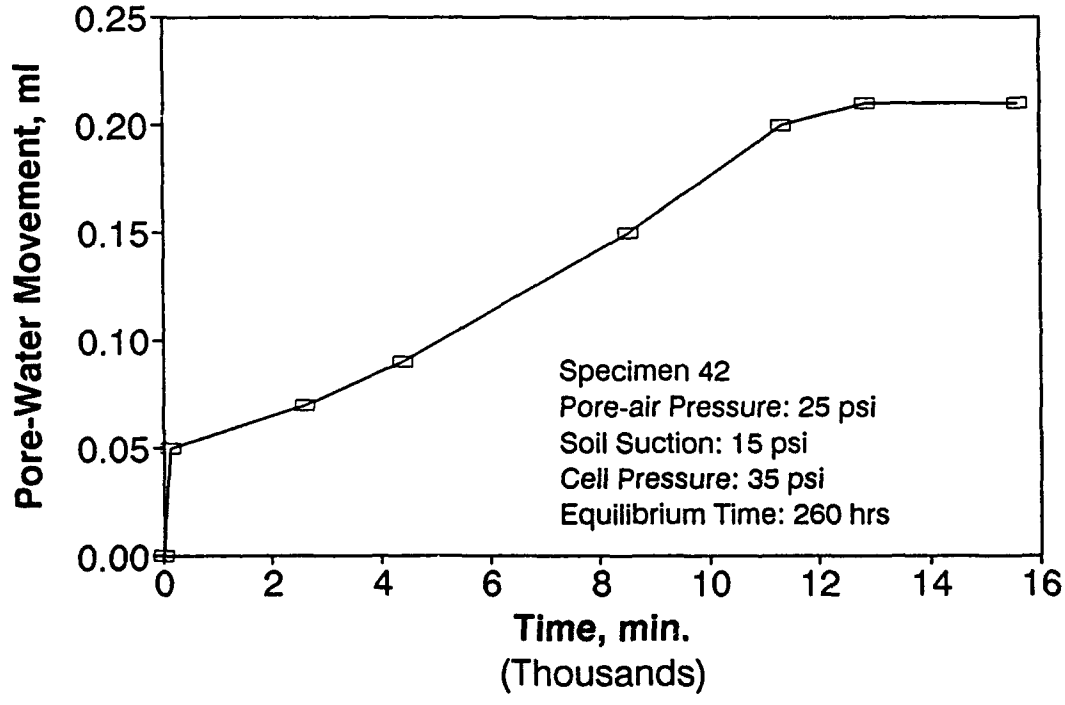
Specimen 42
Pore-air Pressure: 25 psi
Soil Suction: 15 psi
Cell Pressure: 35 psi
Equilibrium Time: 260 hrs
Pore-Water Movement, ml
0.25
0.20
0.15
0.10
0.05
0.00
0
2
4
6
8
10
12
14
16
Time, min.
(Thousands)

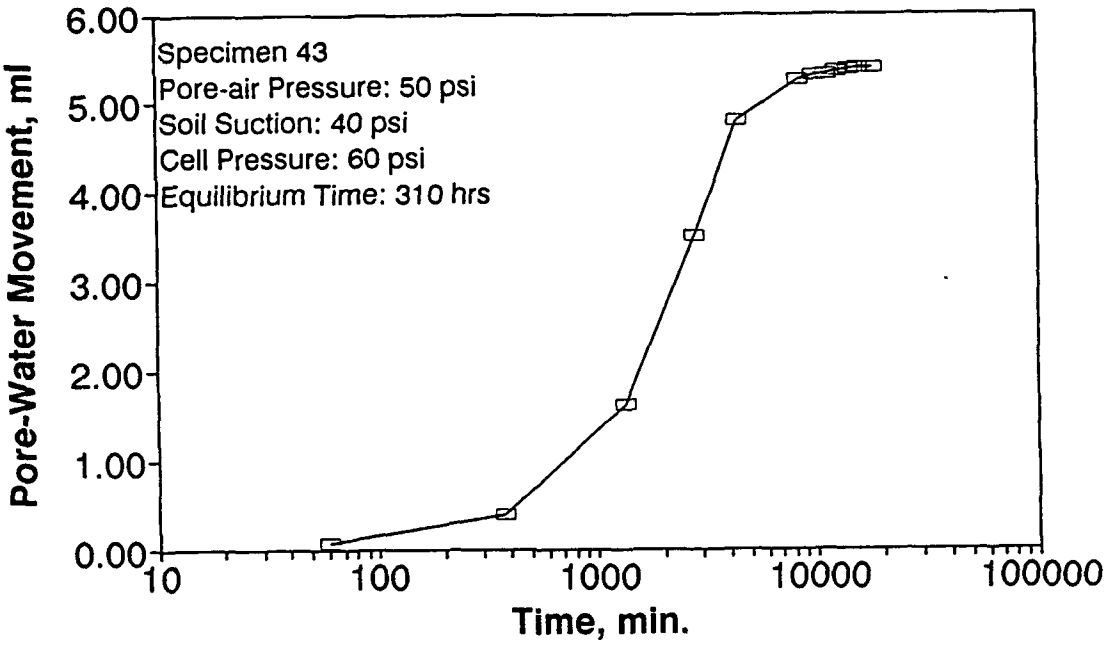
Specimen 43
Pore-air Pressure: 50 psi
Soil Suction: 40 psi
Cell Pressure: 60 psi
Equilibrium Time: 310 hrs
Pore-Water Movement, ml
6.00
5.00
4.00
3.00
2.00
1.00
0.00
10
100
1000
10000
100000
Time, min.

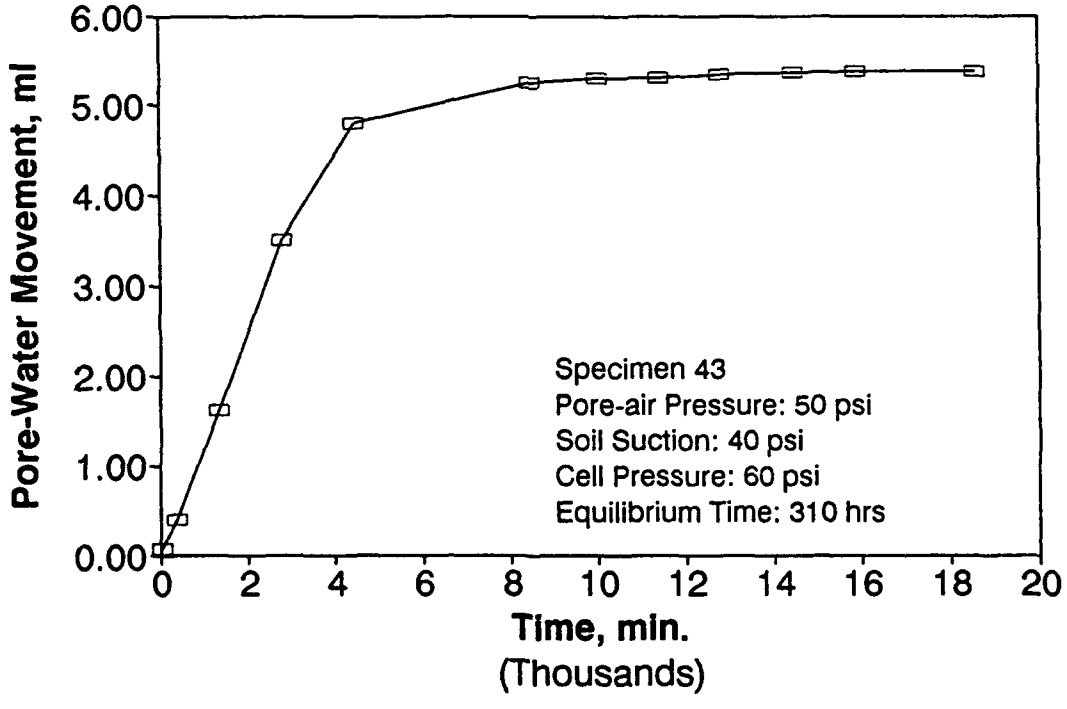
Specimen 43
Pore-air Pressure: 50 psi
Soil Suction: 40 psi
Cell Pressure: 60 psi
Equilibrium Time: 310 hrs
Pore-Water Movement, ml
6.00
5.00
4.00
3.00
2.00
1.00
0.00
0
2
4
6
8
10
12
14
16
18
20
Time, min.
(Thousands)

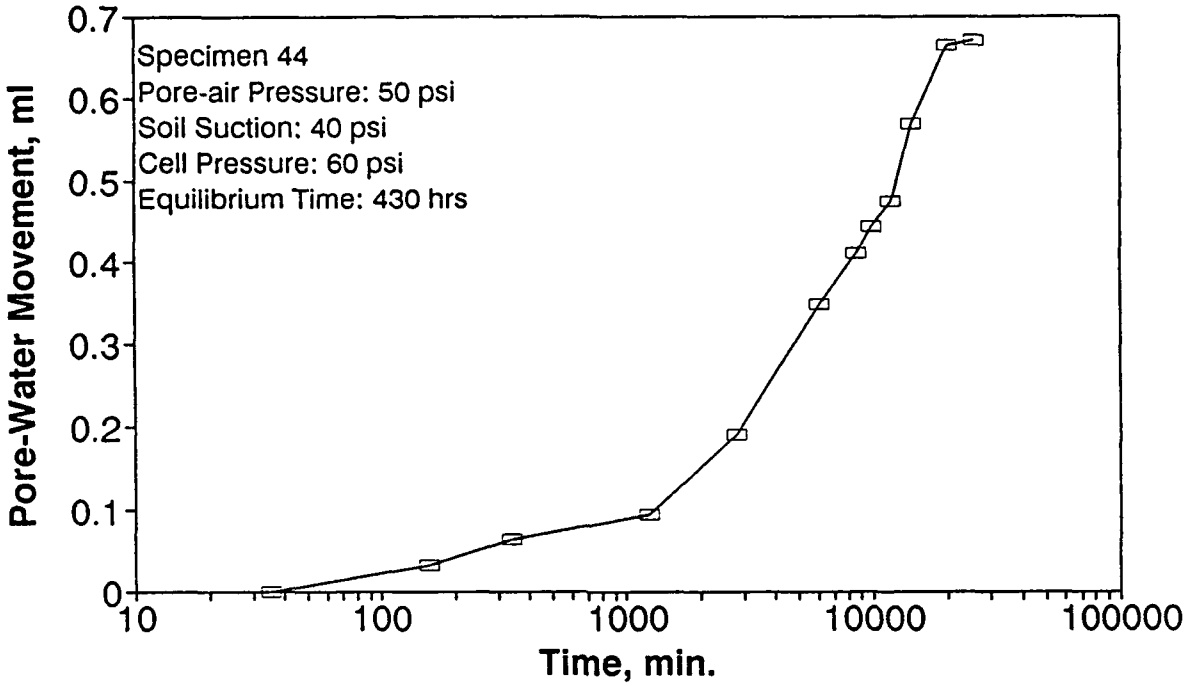
Specimen 44
Pore-air Pressure: 50 psi
Soil Suction: 40 psi
Cell Pressure: 60 psi
Equilibrium Time: 430 hrs
Pore-Water Movement, ml
0.7
0.6
0.5
0.4
0.3
0.2
0.1
0
10
100
1000
10000
100000
Time, min.

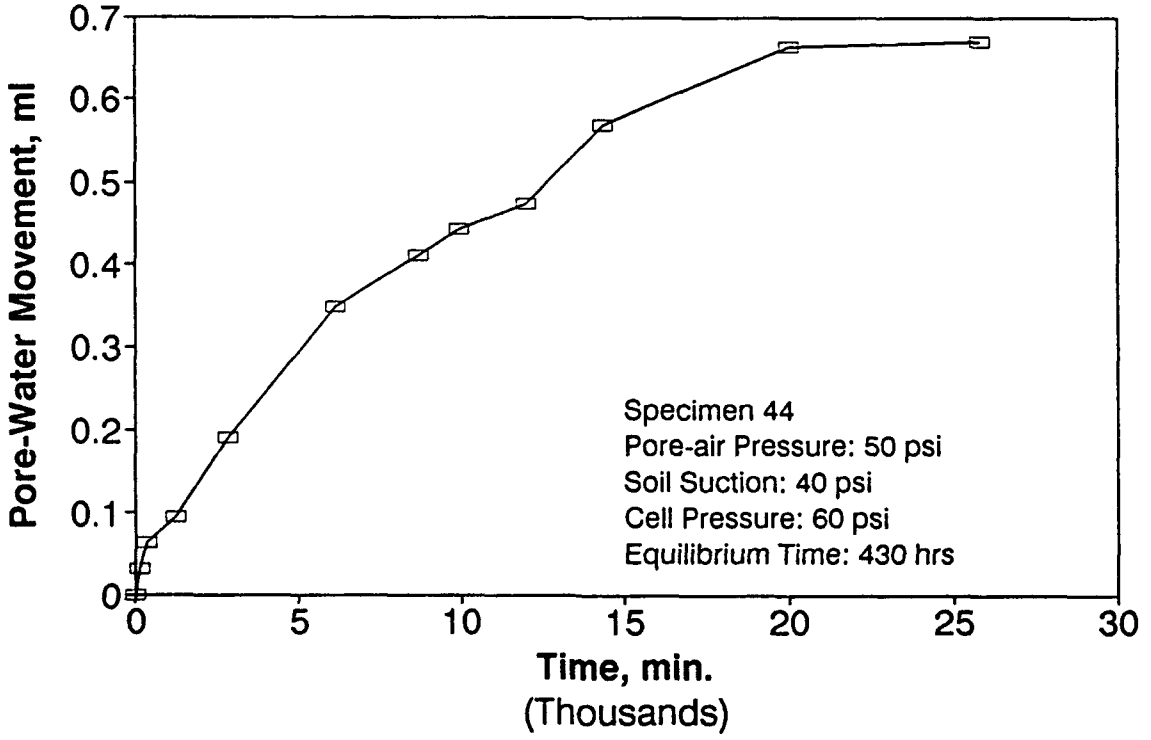
Specimen 44
Pore-air Pressure: 50 psi
Soil Suction: 40 psi
Cell Pressure: 60 psi
Equilibrium Time: 430 hrs
Pore-Water Movement, ml
0.7
0.6
0.5
0.4
0.3
0.2
0.1
0
0
5
10
15
20
25
30
Time, min.
(Thousands)

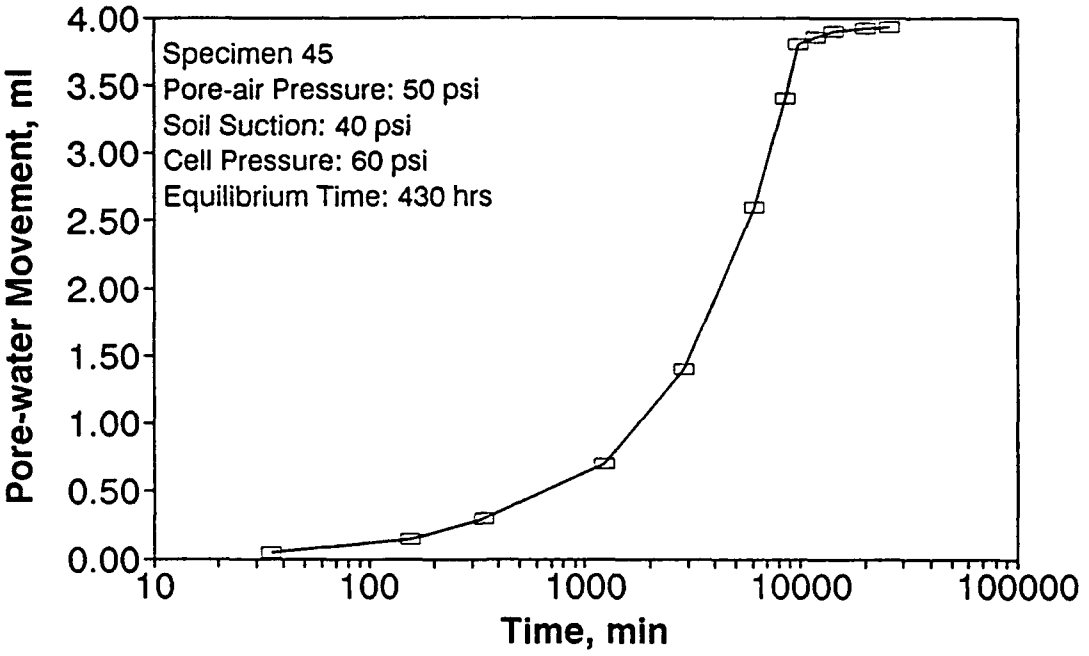
Specimen 45
Pore-air Pressure: 50 psi
Soil Suction: 40 psi
Cell Pressure: 60 psi
Equilibrium Time: 430 hrs
Pore-water Movement, ml
4.00
3.50
3.00
2.50
2.00
1.50
1.00
0.50
0.00
10
100
1000
10000
100000
Time, min

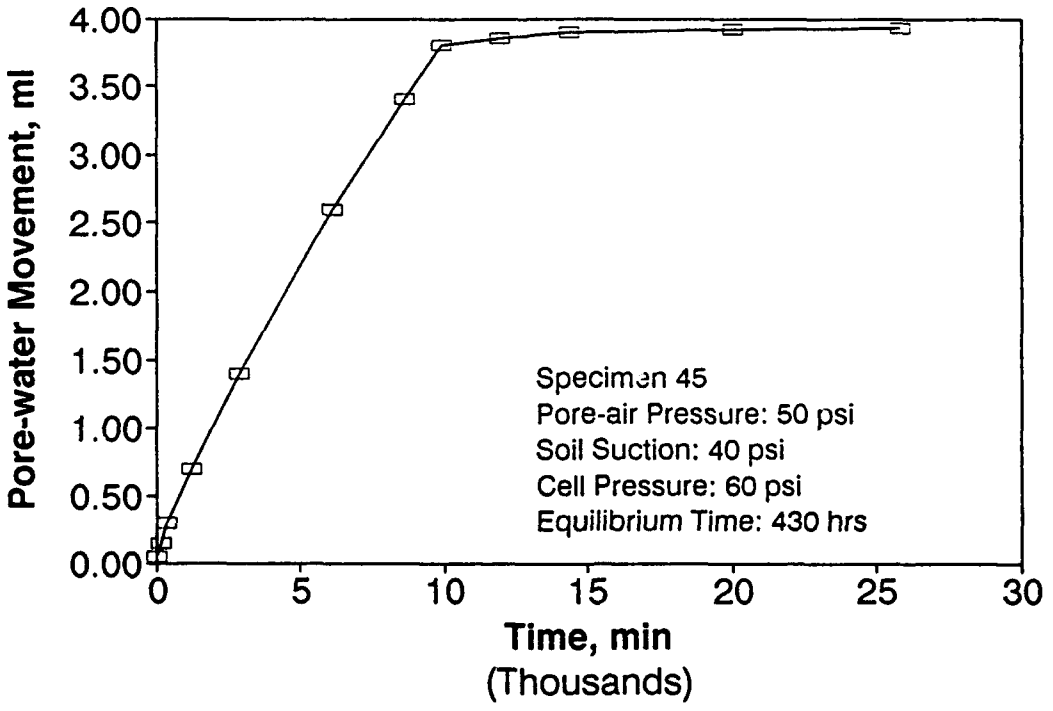
Specimen 45
Pore-air Pressure: 50 psi
Soil Suction: 40 psi
Cell Pressure: 60 psi
Equilibrium Time: 430 hrs
Pore-water Movement, ml
4.00
3.50
3.00
2.50
2.00
1.50
1.00
0.50
0.00
0
5
10
15
20
25
30
Time, min
(Thousands)

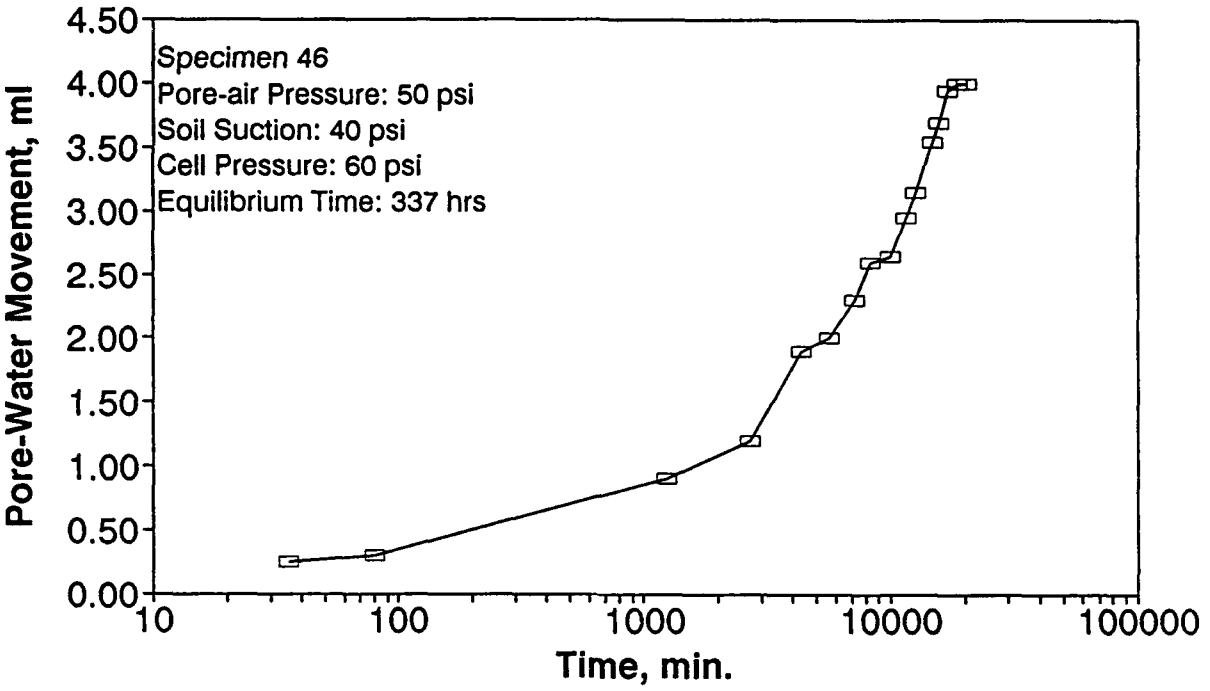
Specimen 46
Pore-air Pressure: 50 psi
Soil Suction: 40 psi
Cell Pressure: 60 psi
Equilibrium Time: 337 hrs
Pore-Water Movement, ml
4.50
4.00
3.50
3.00
2.50
2.00
1.50
1.00
0.50
0.00
10
100
1000
10000
100000
Time, min.

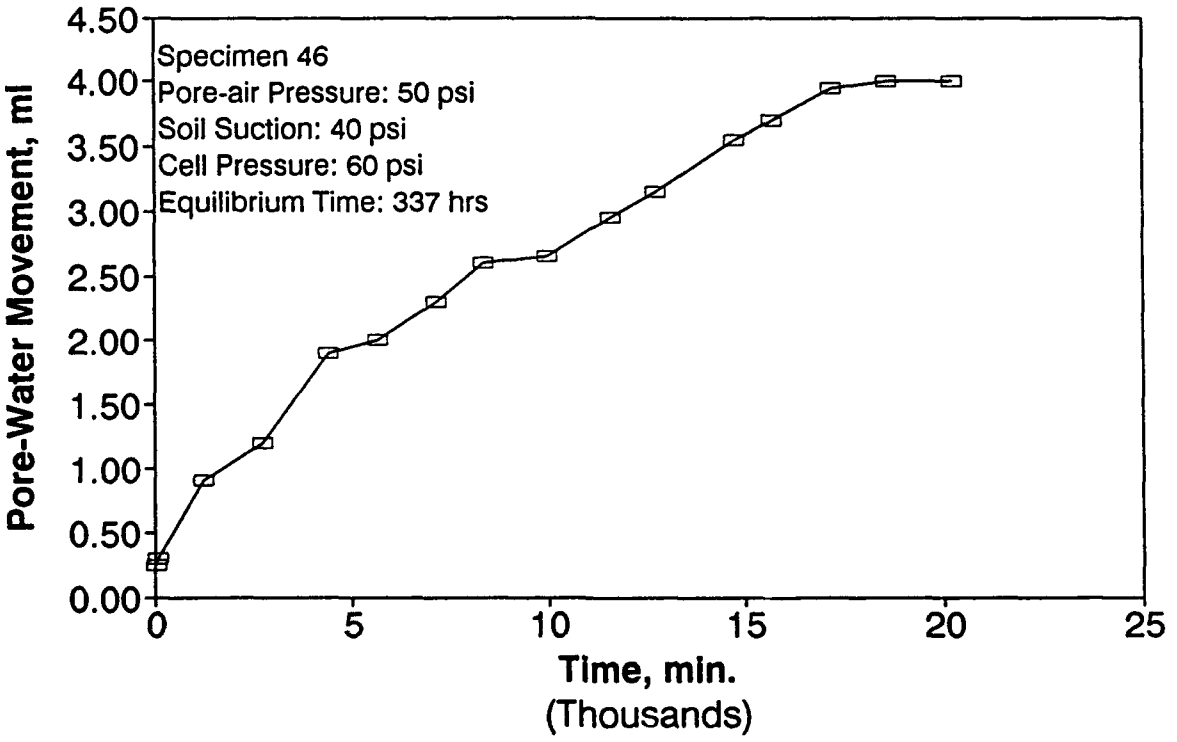
Specimen 46
Pore-air Pressure: 50 psi
Soil Suction: 40 psi
Cell Pressure: 60 psi
Equilibrium Time: 337 hrs
Pore-Water Movement, ml
4.50
4.00
3.50
3.00
2.50
2.00
1.50
1.00
0.50
0.00
0
5
10
15
20
25
Time, min.
(Thousands)

APPENDIX D

RECORDS OF CREEP AND RECOVERY TESTS

AT CONSTANT SOIL SUCTION

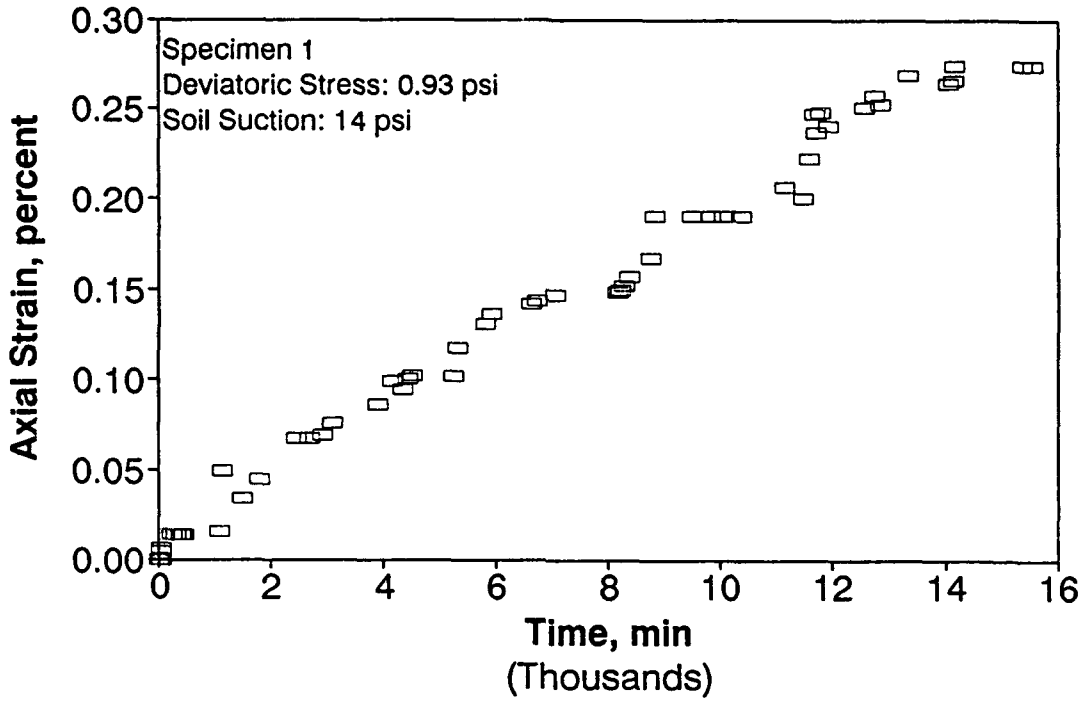
Specimen 1
Deviatoric Stress: 0.93 psi
Soil Suction: 14 psi
Axial Strain, percent
0.30
0.25
0.20
0.15
0.10
0.05
0.00
0
2
4
6
8
10
12
14
16
Time, min
(Thousands)

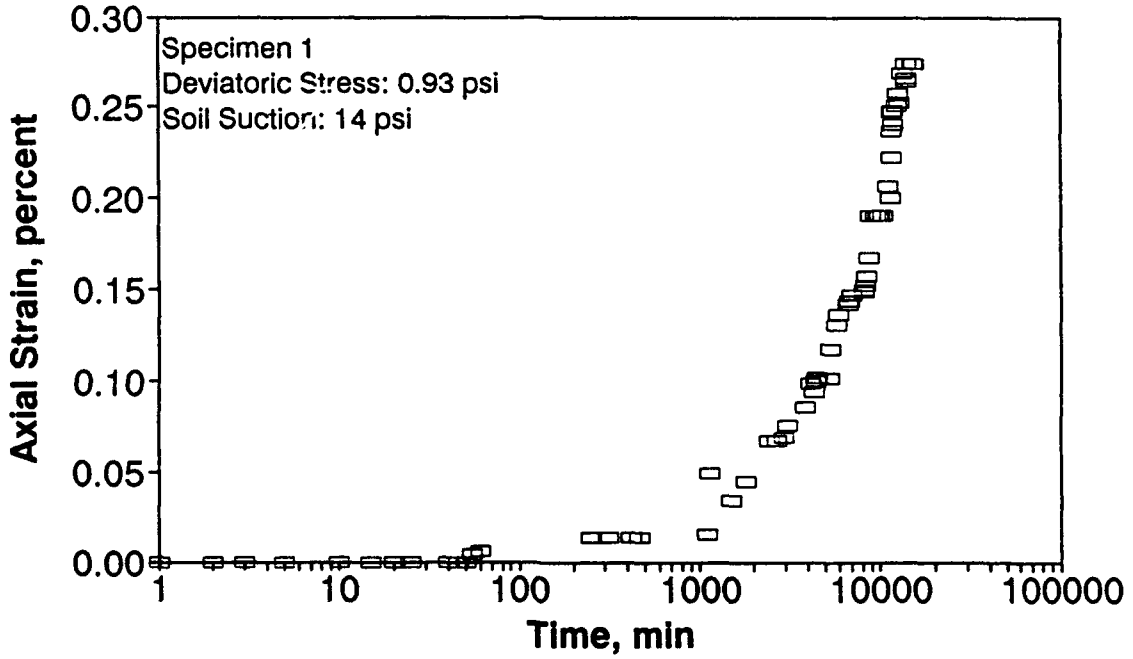
Specimen 1
Deviatoric Stress: 0.93 psi
Soil Suction: 14 psi
Axial Strain, percent
0.30
0.25
0.20
0.15
0.10
0.05
0.00
1
10
100
1000
10000
100000
Time, min

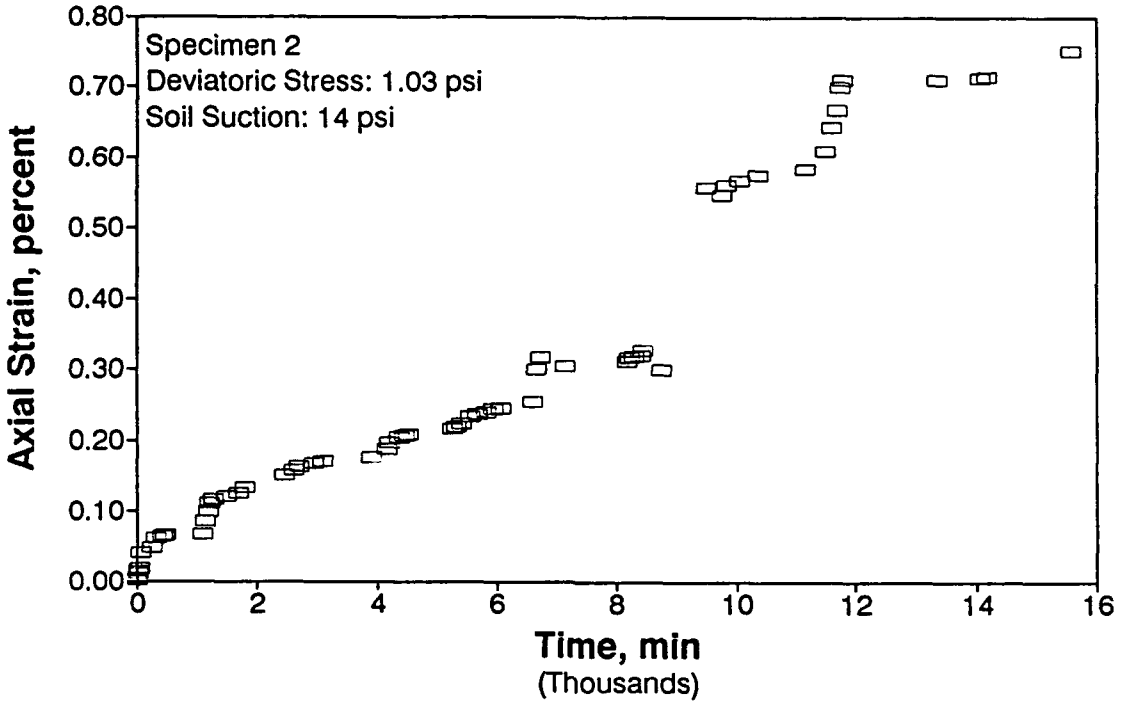
Specimen 2
Deviatoric Stress: 1.03 psi
Soil Suction: 14 psi
Axial Strain, percent
0.80
0.70
0.60
0.50
0.40
0.30
0.20
0.10
0.00
0
2
4
6
8
10
12
14
16
Time, min
(Thousands)

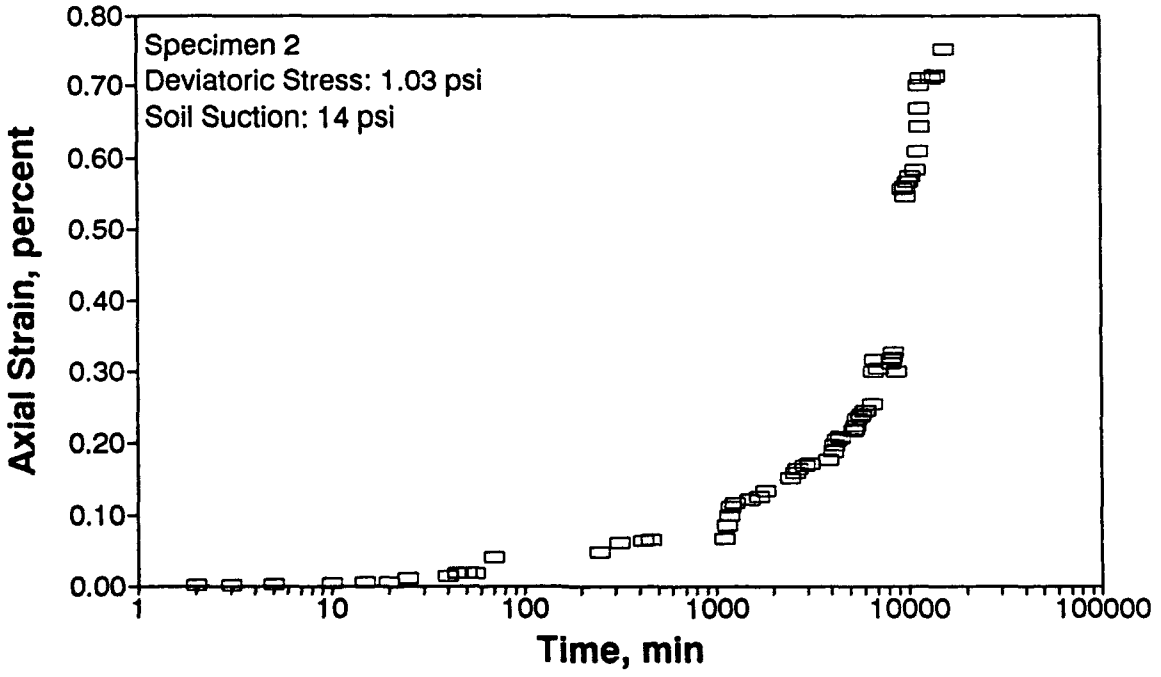
Specimen 2
Deviatoric Stress: 1.03 psi
Soil Suction: 14 psi
Axial Strain, percent
0.80
0.70
0.60
0.50
0.40
0.30
0.20
0.10
0.00
1
10
100
1000
10000
100000
Time, min

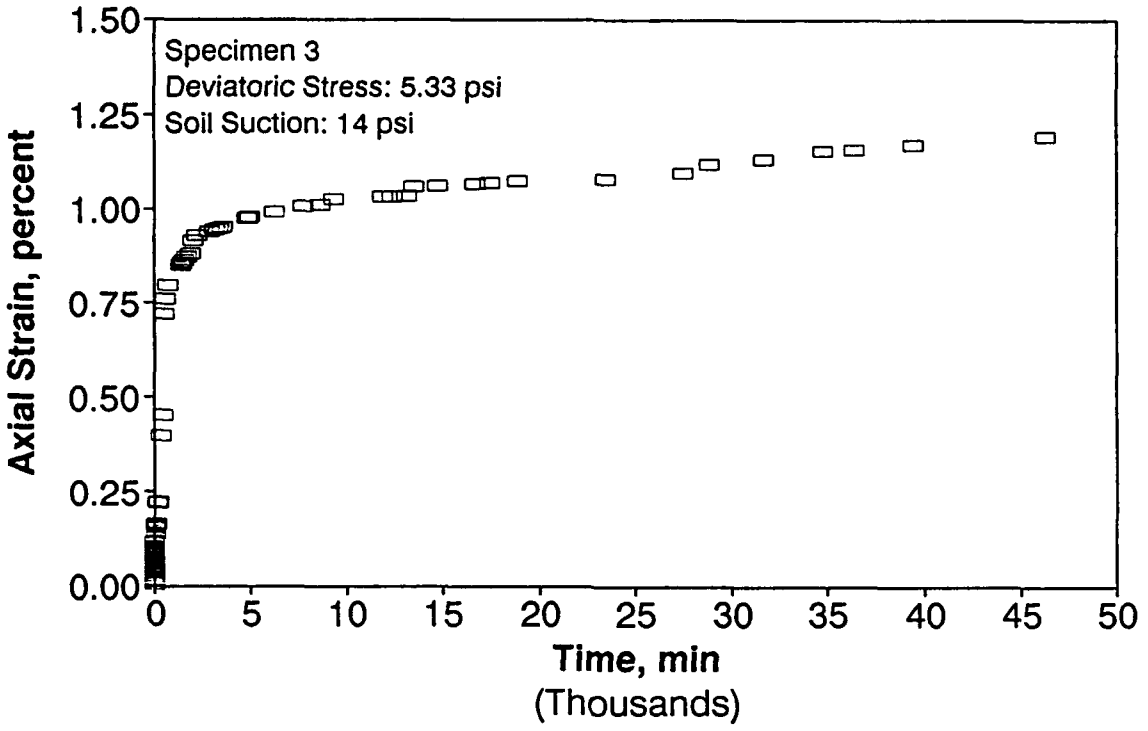
Specimen 3
Deviatoric Stress: 5.33 psi
Soil Suction: 14 psi
Axial Strain, percent
1.50
1.25
1.00
0.75
0.50
0.25
0.00
0
5
10
15
20
25
30
35
40
45
50
Time, min
(Thousands)

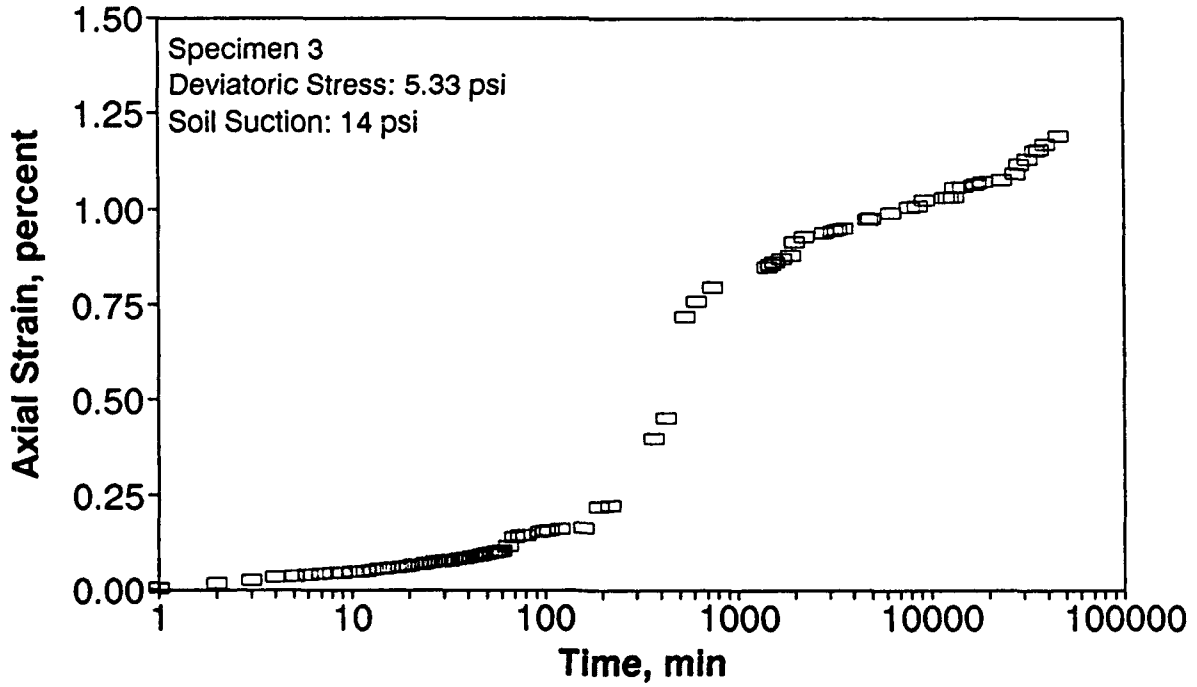
Specimen 3
Deviatoric Stress: 5.33 psi
Soil Suction: 14 psi
Axial Strain, percent
1.50
1.25
1.00
0.75
0.50
0.25
0.00
1
10
100
1000
10000
100000
Time, min

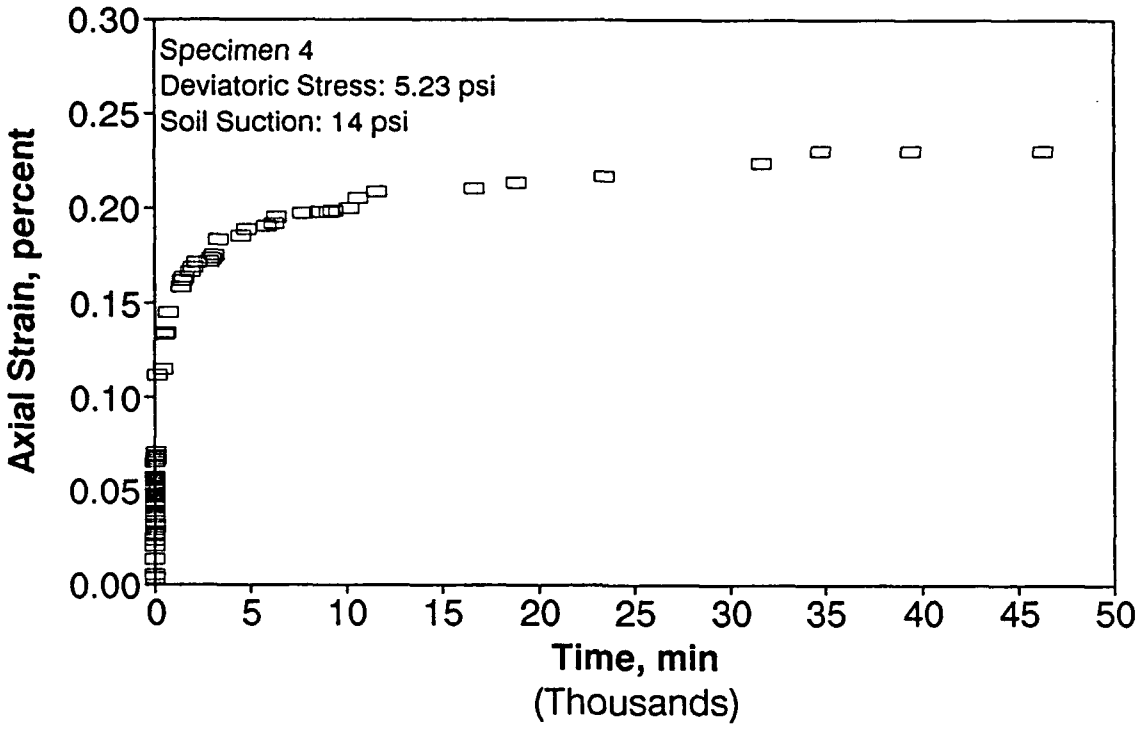
Specimen 4
Deviatoric Stress: 5.23 psi
Soil Suction: 14 psi
Axial Strain, percent
0.30
0.25
0.20
0.15
0.10
0.05
0.00
0
5
10
15
20
25
30
35
40
45
50
Time, min
(Thousands)

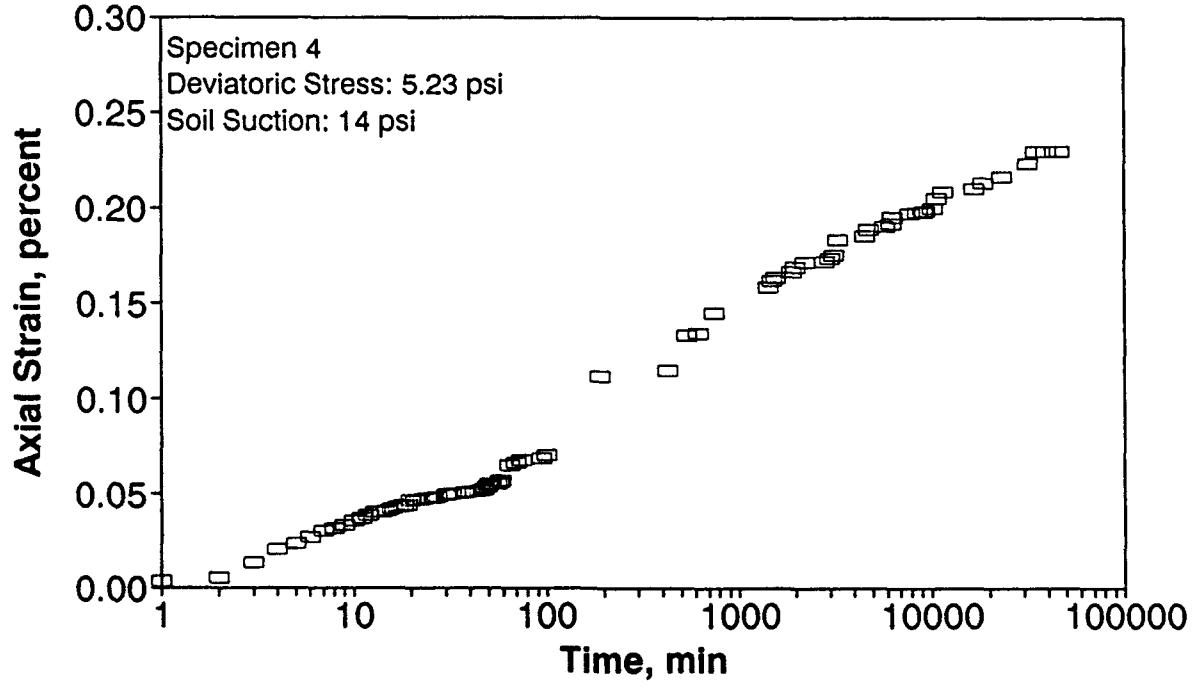
Specimen 4
Deviatoric Stress: 5.23 psi
Soil Suction: 14 psi
Axial Strain, percent
0.30
0.25
0.20
0.15
0.10
0.05
0.00
1
10
100
1000
10000
100000
Time, min

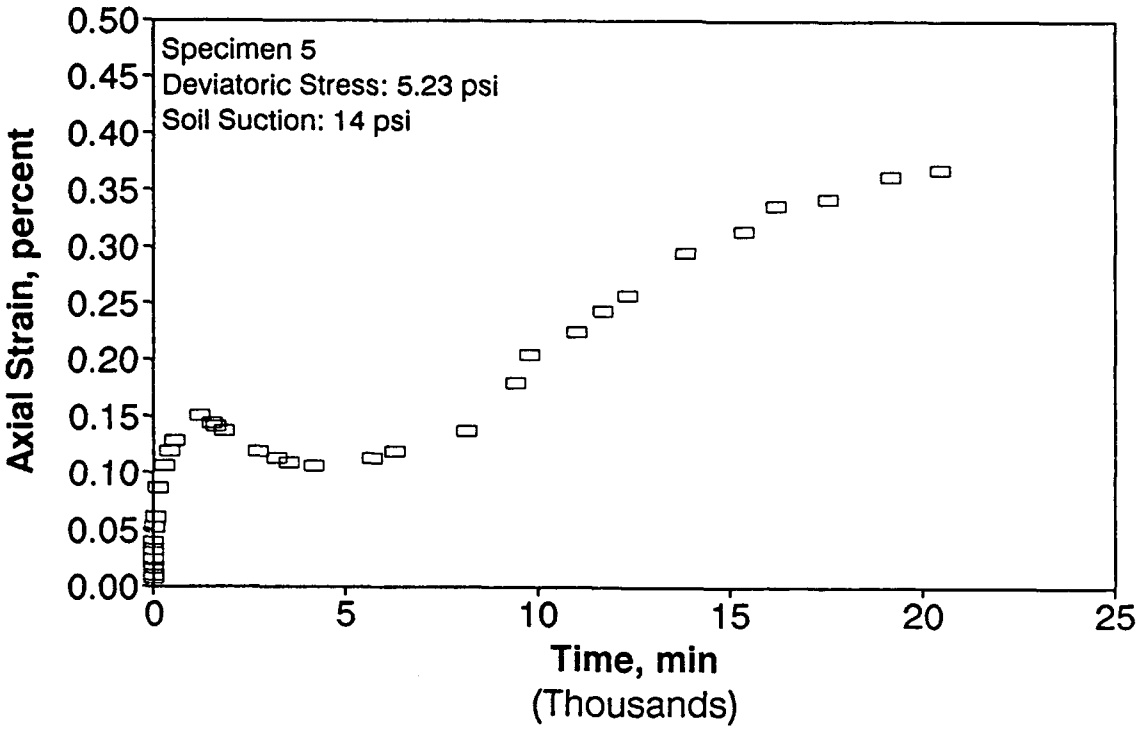
Specimen 5
Deviatoric Stress: 5.23 psi
Soil Suction: 14 psi
Axial Strain, percent
0.50
0.45
0.40
0.35
0.30
0.25
0.20
0.15
0.10
0.05
0.00
0
5
10
15
20
25
Time, min
(Thousands)

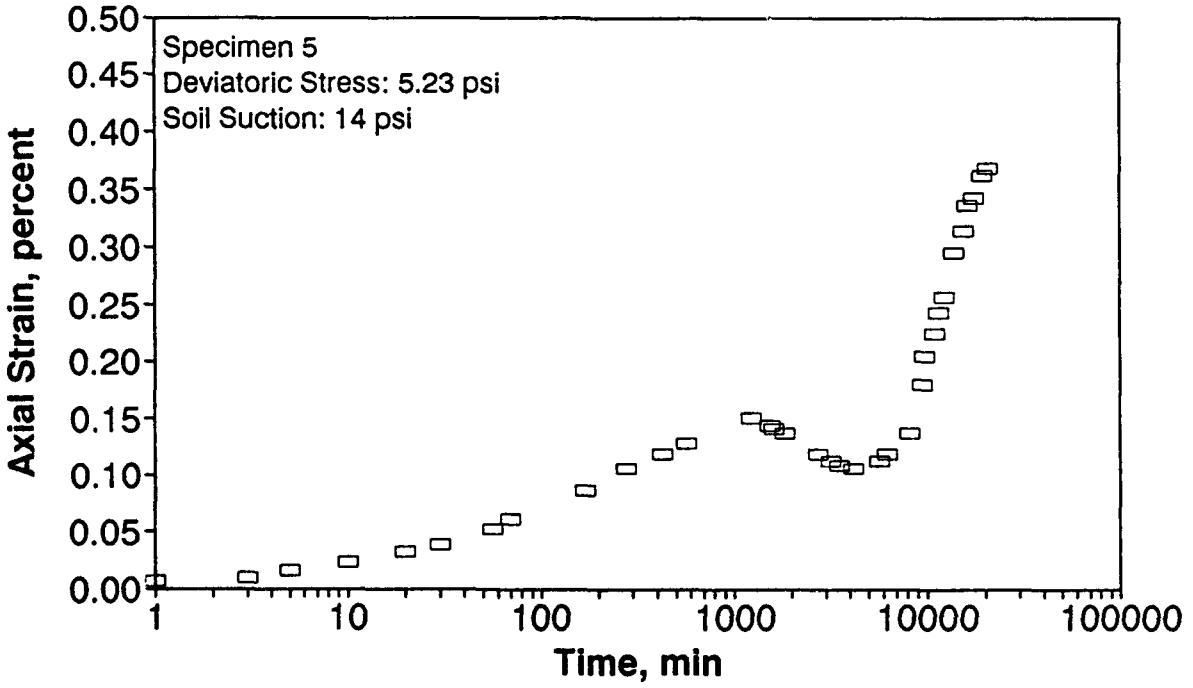
Specimen 5
Deviatoric Stress: 5.23 psi
Soil Suction: 14 psi
Axial Strain, percent
0.50
0.45
0.40
0.35
0.30
0.25
0.20
0.15
0.10
0.05
0.00
1
10
100
1000
10000
100000
Time, min

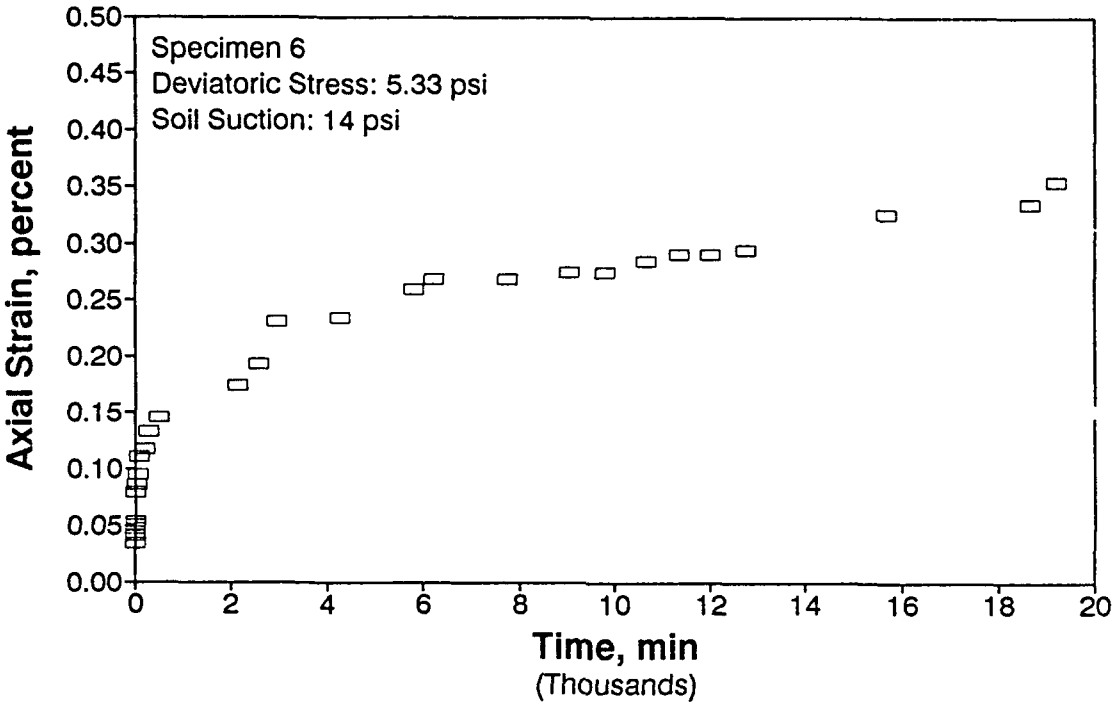
Specimen 6
Deviatoric Stress: 5.33 psi
Soil Suction: 14 psi
Axial Strain, percent
0.50
0.45
0.40
0.35
0.30
0.25
0.20
0.15
0.10
0.05
0.00
0
2
4
6
8
10
12
14
16
18
20
Time, min
(Thousands)

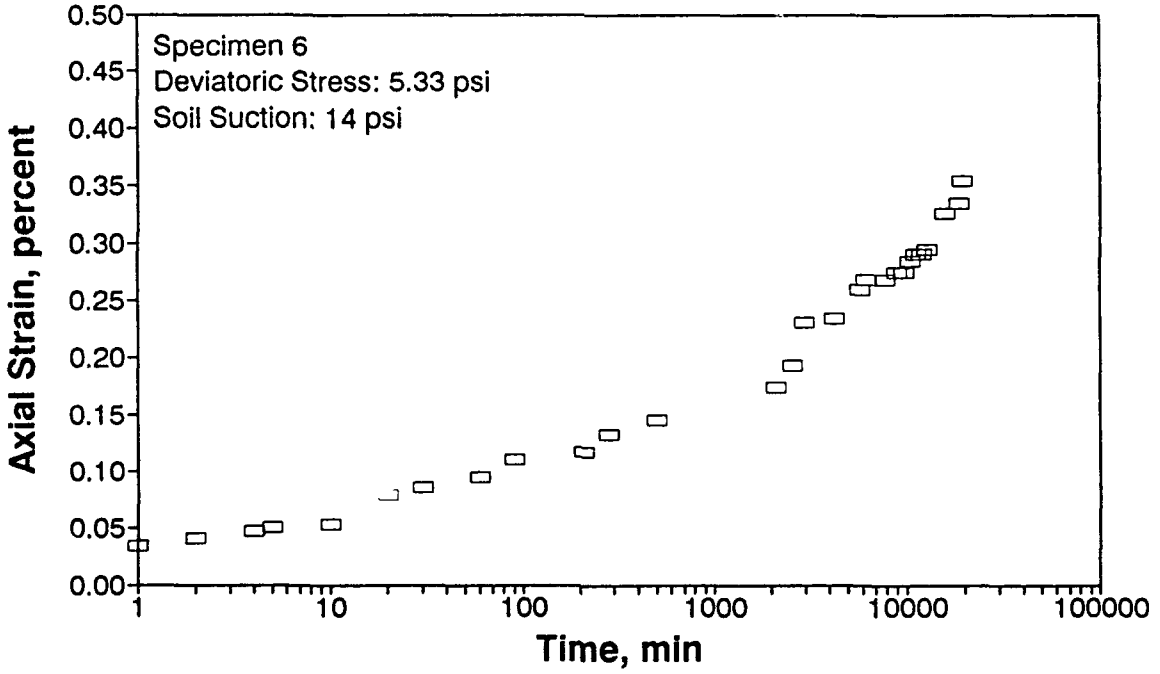
Specimen 6
Deviatoric Stress: 5.33 psi
Soil Suction: 14 psi
Axial Strain, percent
0.50
0.45
0.40
0.35
0.30
0.25
0.20
0.15
0.10
0.05
0.00
1
10
100
1000
10000
100000
Time, min

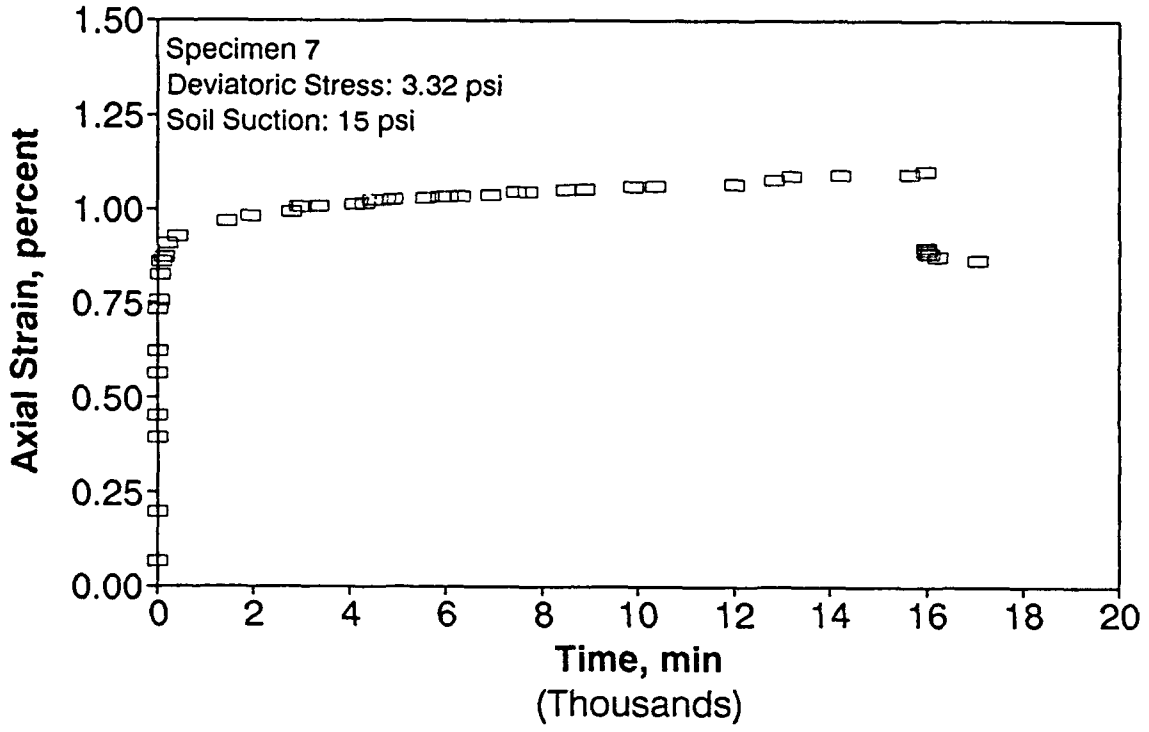
Specimen 7
Deviatoric Stress: 3.32 psi
Soil Suction: 15 psi
Axial Strain, percent
1.50
1.25
1.00
0.75
0.50
0.25
0.00
0
2
4
6
8
10
12
14
16
18
20
Time, min
(Thousands)

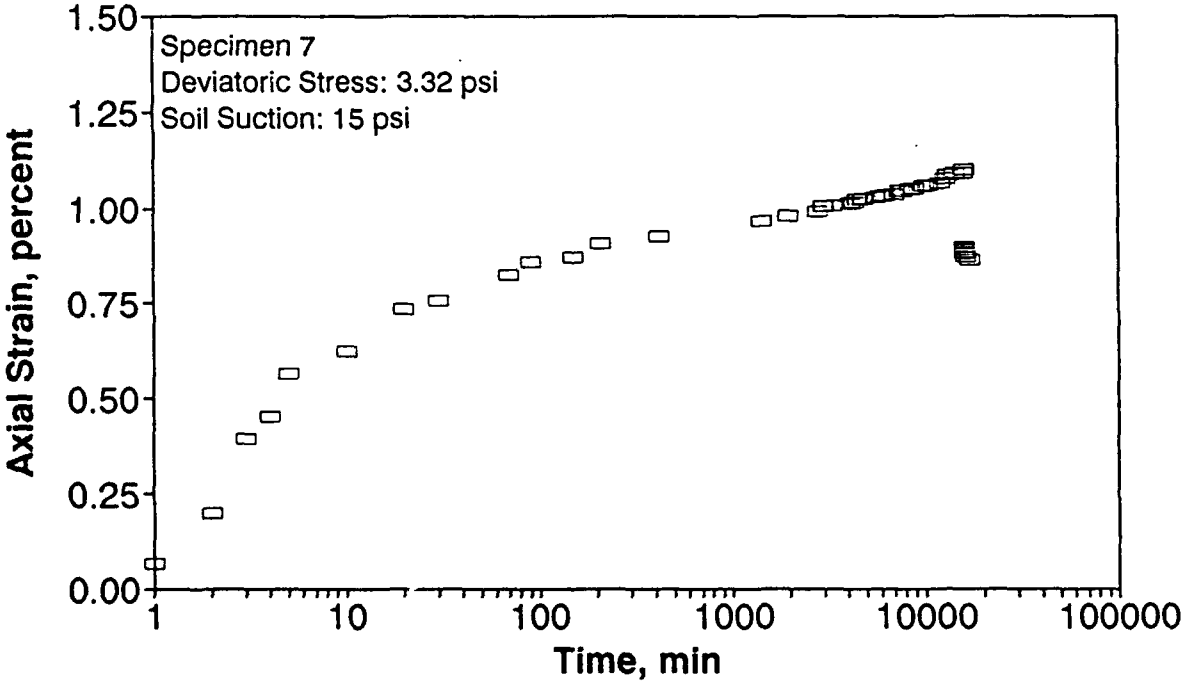
Specimen 7
Deviatoric Stress: 3.32 psi
Soil Suction: 15 psi
Axial Strain, percent
1.50
1.25
1.00
0.75
0.50
0.25
0.00
1
10
100
1000
10000
100000
Time, min

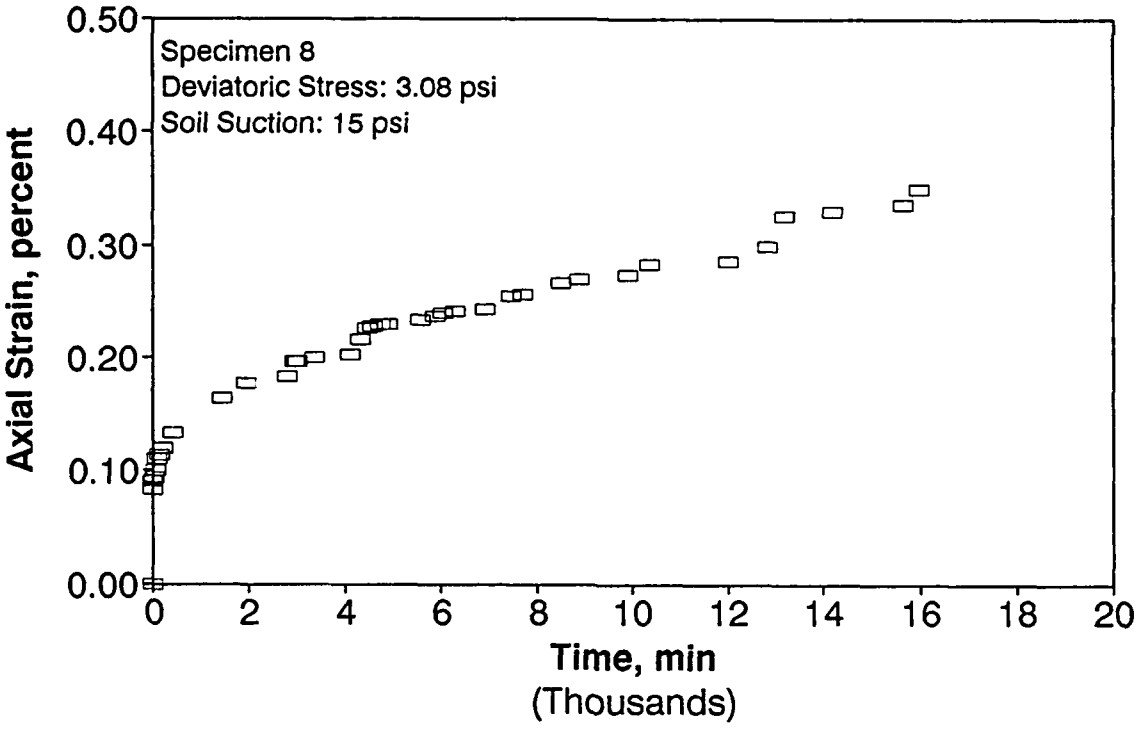
Specimen 8
Deviatoric Stress: 3.08 psi
Soil Suction: 15 psi
Axial Strain, percent
0.50
0.40
0.30
0.20
0.10
0.00
0
2
4
6
8
10
12
14
16
18
20
Time, min
(Thousands)

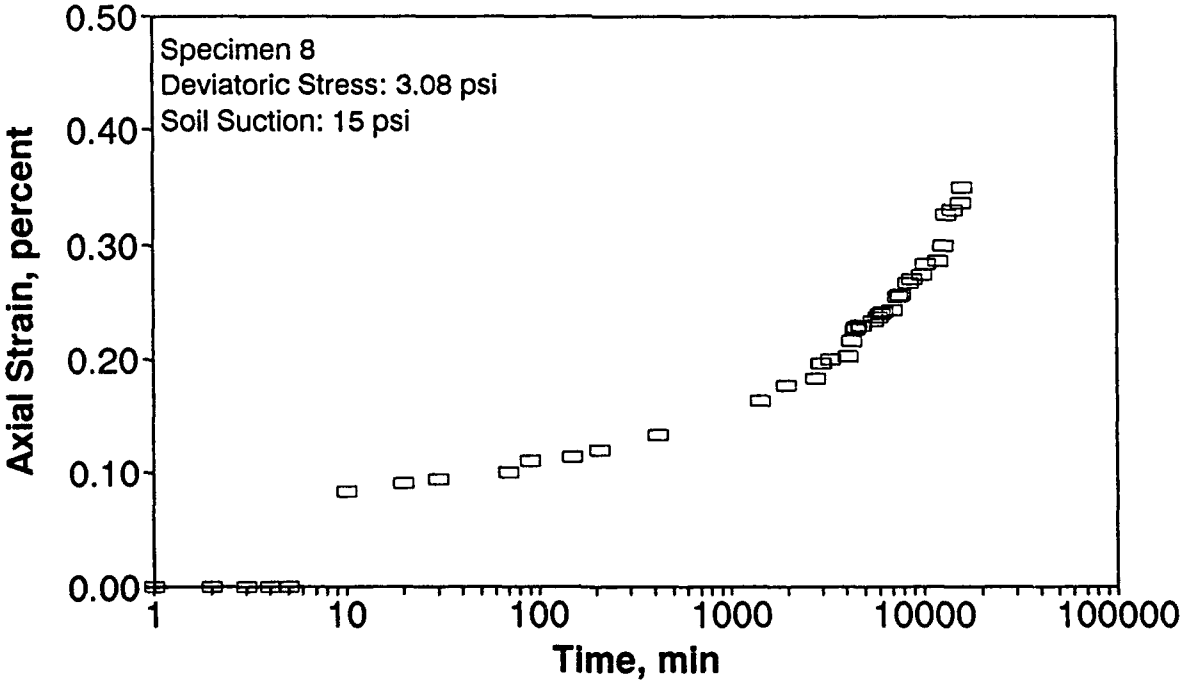
Specimen 8
Deviatoric Stress: 3.08 psi
Soil Suction: 15 psi
Axial Strain, percent
0.50
0.40
0.30
0.20
0.10
0.00
1
10
100
1000
10000
100000
Time, min

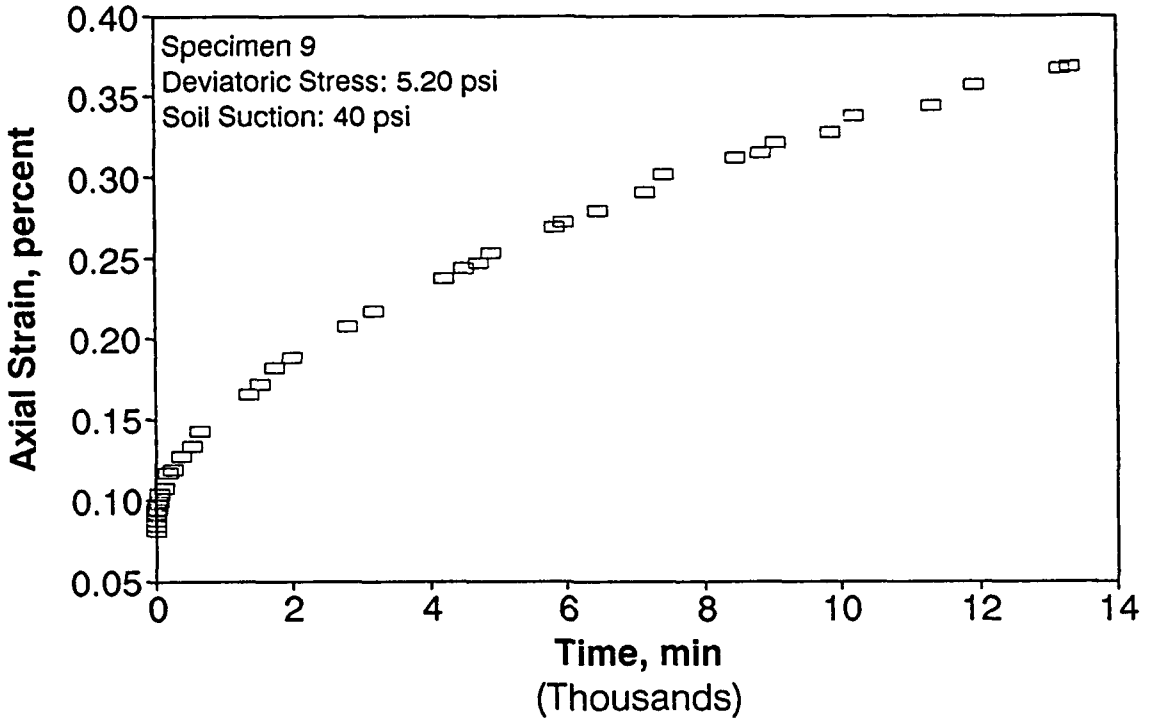
Specimen 9
Deviatoric Stress: 5.20 psi
Soil Suction: 40 psi
Axial Strain, percent
0.40
0.35
0.30
0.25
0.20
0.15
0.10
0.05
0
2
4
6
8
10
12
14
Time, min
(Thousands)

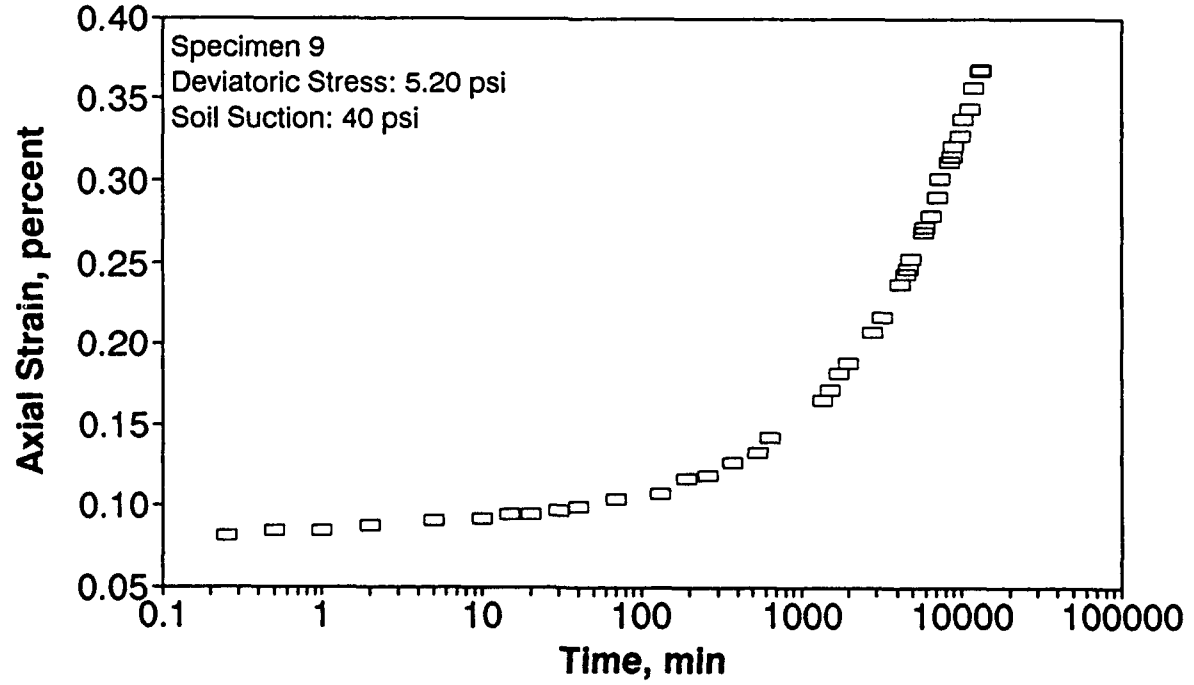
Specimen 9
Deviatoric Stress: 5.20 psi
Soil Suction: 40 psi
Axial Strain, percent
0.40
0.35
0.30
0.25
0.20
0.15
0.10
0.05
0.1
1
10
100
1000
10000
100000
Time, min

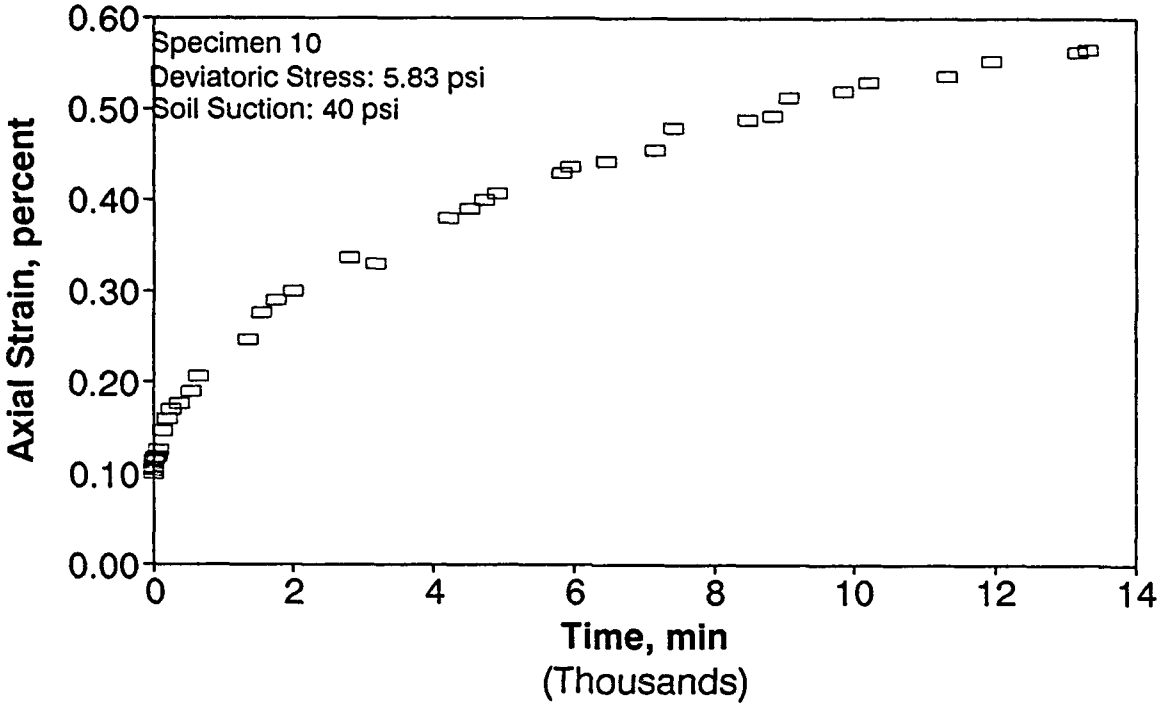
Specimen 10
Deviatoric Stress: 5.83 psi
Soil Suction: 40 psi
Axial Strain, percent
0.60
0.50
0.40
0.30
0.20
0.10
0.00
0
2
4
6
8
10
12
14
Time, min
(Thousands)

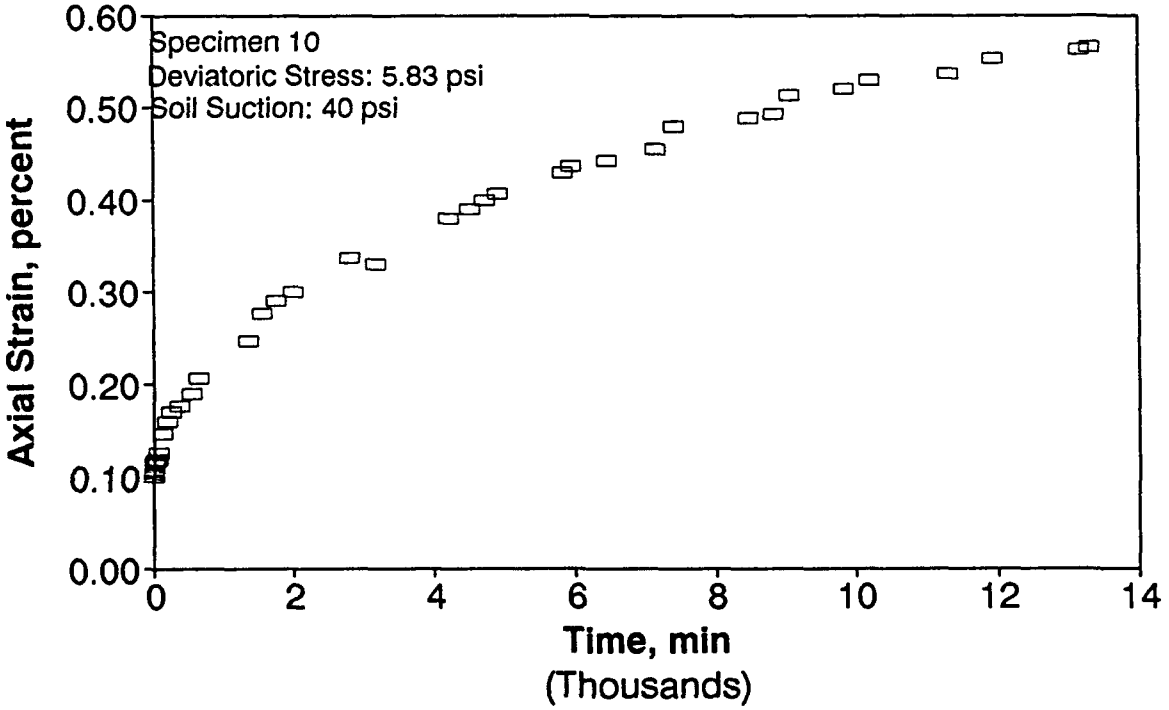
Specimen 10
Deviatoric Stress: 5.83 psi
Soil Suction: 40 psi
Axial Strain, percent
0.60
0.50
0.40
0.30
0.20
0.10
0.00
0
2
4
6
8
10
12
14
Time, min
(Thousands)

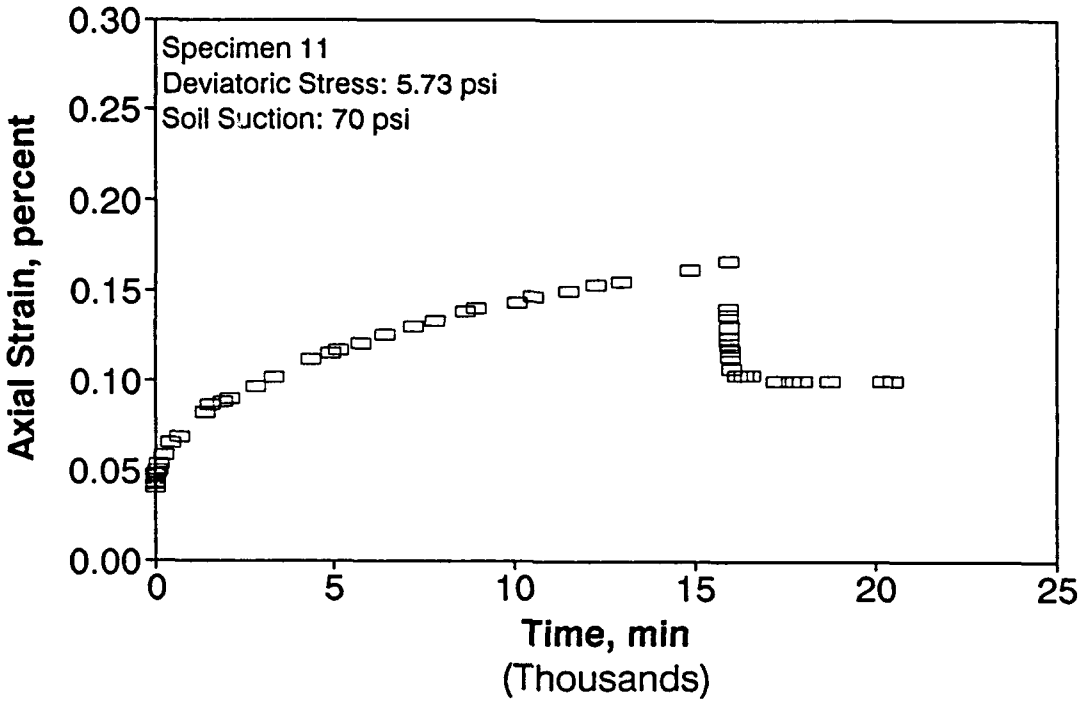
Specimen 11
Deviatoric Stress: 5.73 psi
Soil Suction: 70 psi
Axial Strain, percent
0.30
0.25
0.20
0.15
0.10
0.05
0.00
0
5
10
15
20
25
Time, min
(Thousands)

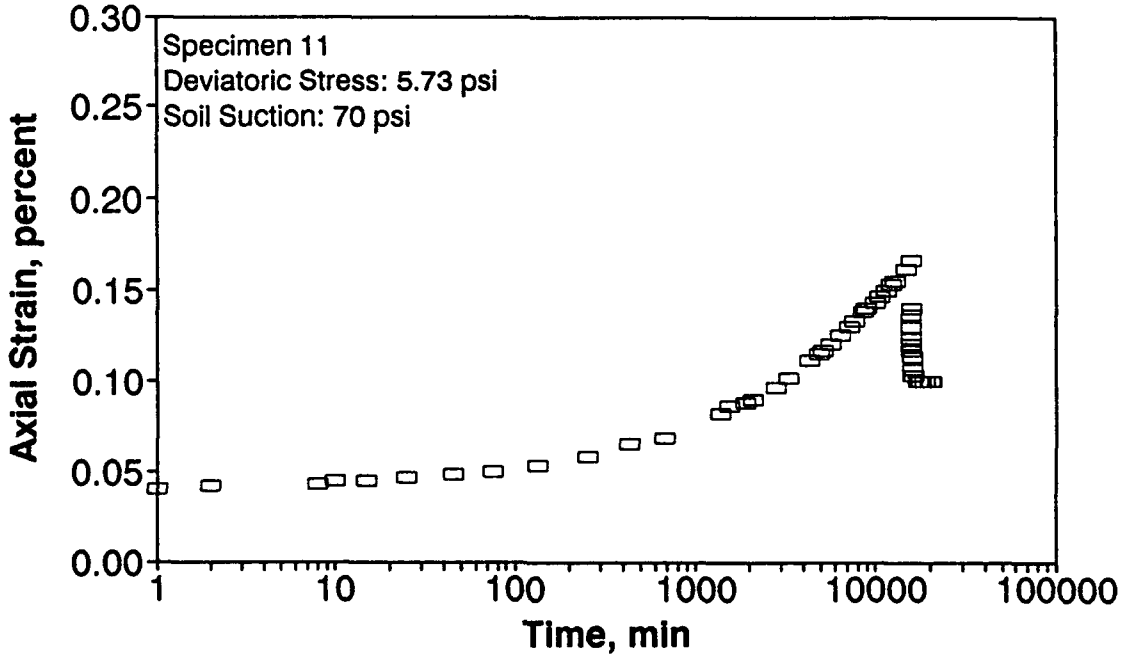
Specimen 11
Deviatoric Stress: 5.73 psi
Soil Suction: 70 psi
Axial Strain, percent
0.30
0.25
0.20
0.15
0.10
0.05
0.00
1
10
100
1000
10000
100000
Time, min

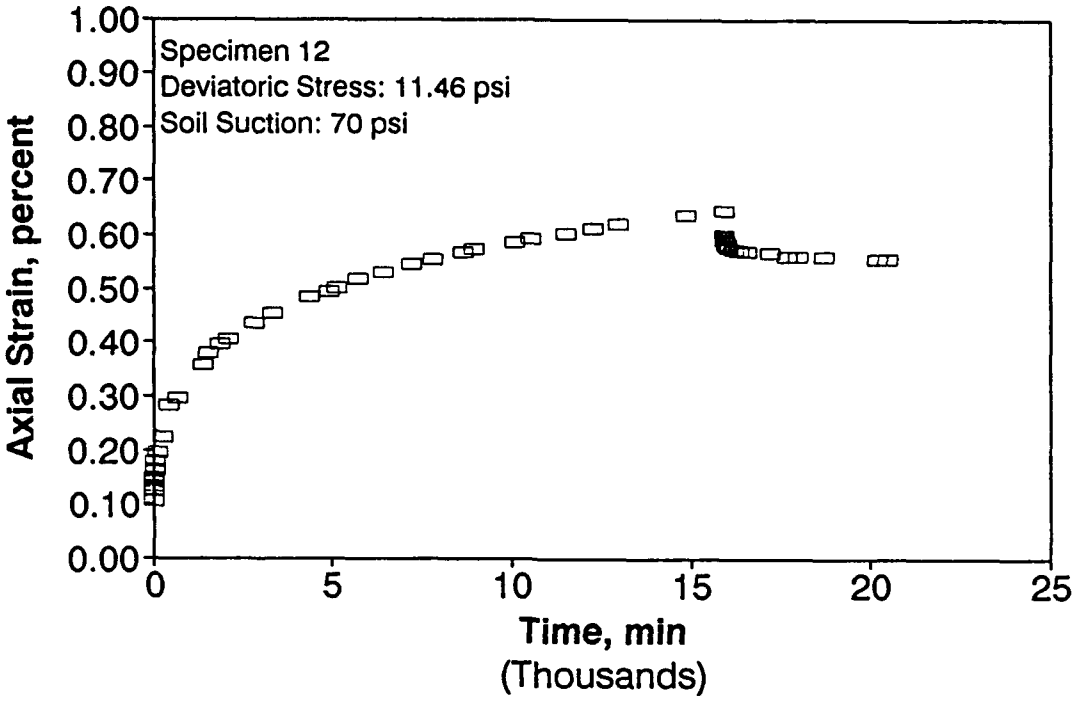
Specimen 12
Deviatoric Stress: 11.46 psi
Soil Suction: 70 psi
Axial Strain, percent
1.00
0.90
0.80
0.70
0.60
0.50
0.40
0.30
0.20
0.10
0.00
0
5
10
15
20
25
Time, min
(Thousands)

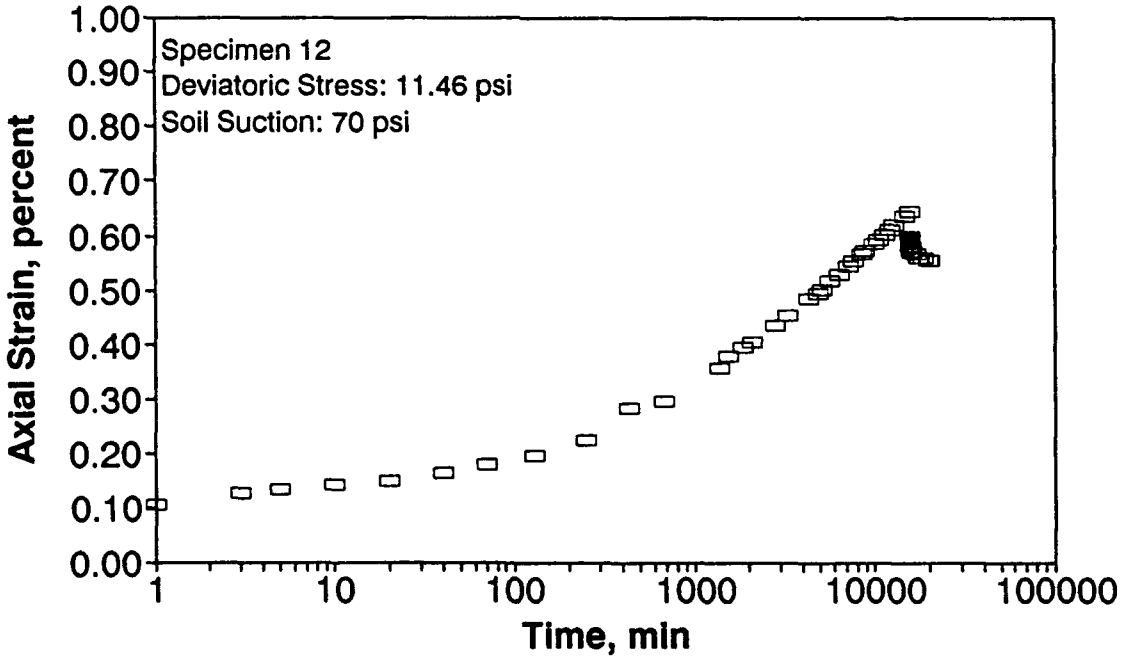
Specimen 12
Deviatoric Stress: 11.46 psi
Soil Suction: 70 psi
Axial Strain, percent
1.00
0.90
0.80
0.70
0.60
0.50
0.40
0.30
0.20
0.10
0.00
1
10
100
1000
10000
100000
Time, min

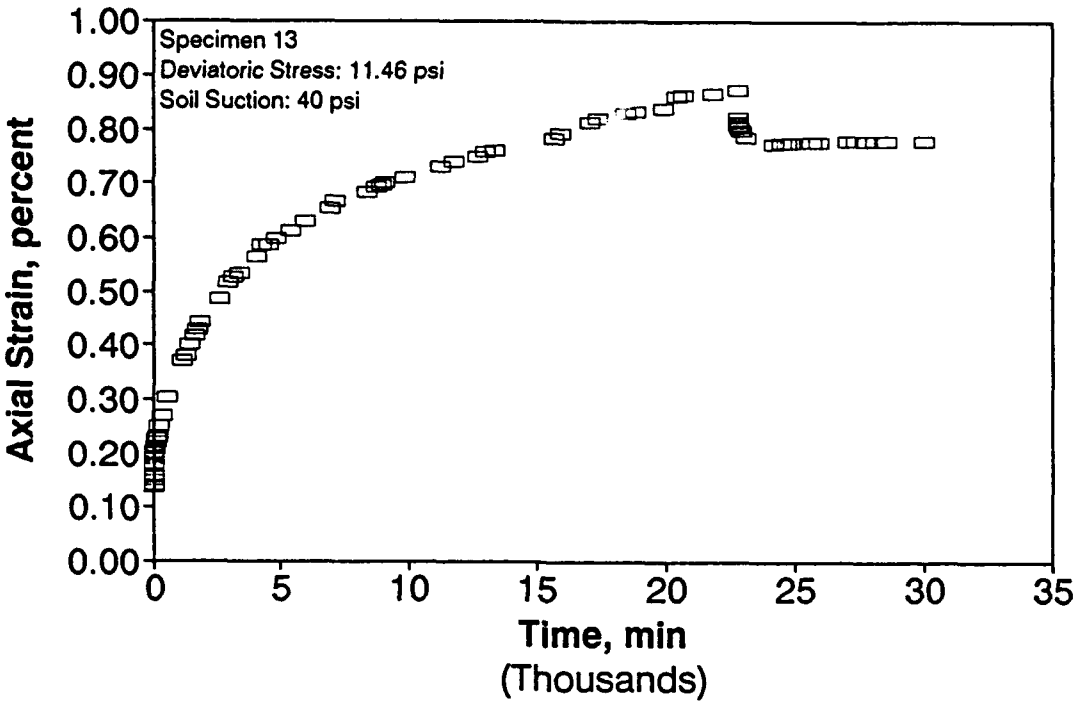
Specimen 13
Deviatoric Stress: 11.46 psi
Soil Suction: 40 psi
Axial Strain, percent
1.00
0.90
0.80
0.70
0.60
0.50
0.40
0.30
0.20
0.10
0.00
0
5
10
15
20
25
30
35
Time, min
(Thousands)

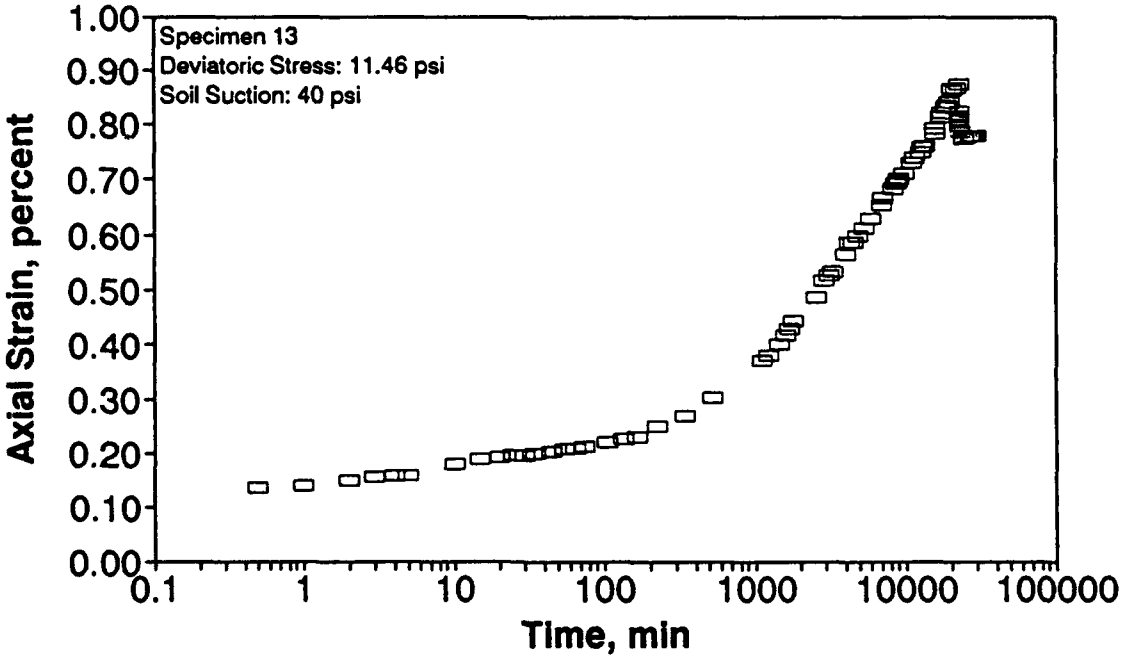
Specimen 13
Deviatoric Stress: 11.46 psi
Soil Suction: 40 psi
Axial Strain, percent
1.00
0.90
0.80
0.70
0.60
0.50
0.40
0.30
0.20
0.10
0.00
0.1
1
10
100
1000
10000
100000
Time, min

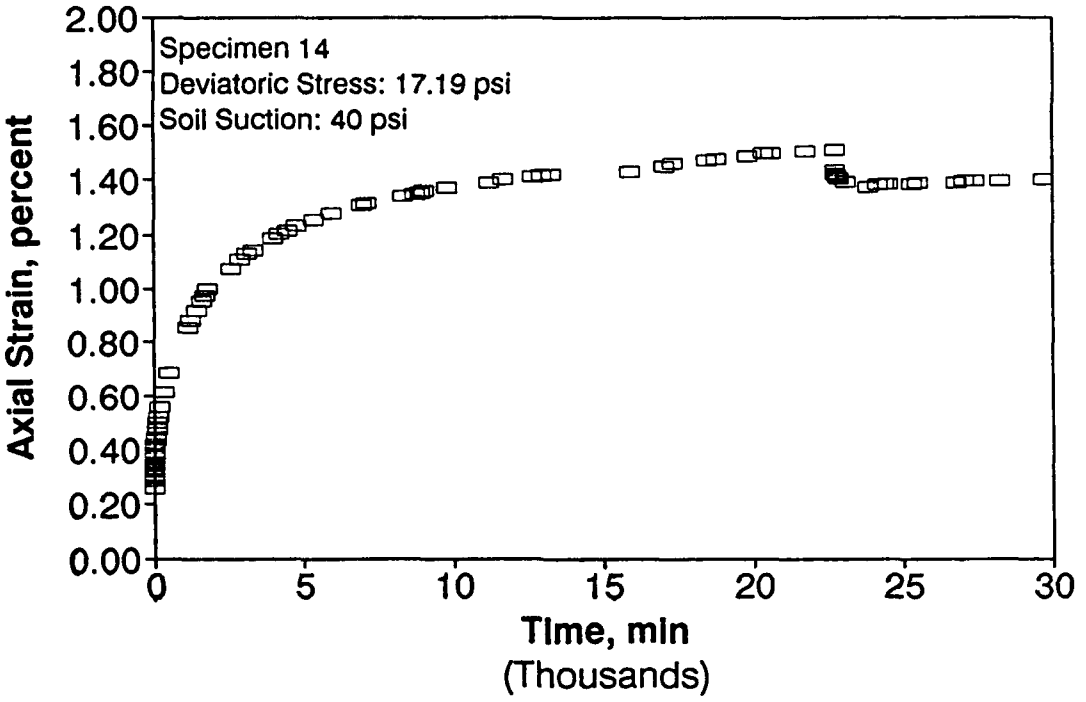
Specimen 14
Deviatoric Stress: 17.19 psi
Soil Suction: 40 psi
Axial Strain, percent
2.00
1.80
1.60
1.40
1.20
1.00
0.80
0.60
0.40
0.20
0.00
0
5
10
15
20
25
30
Time, min
(Thousands)

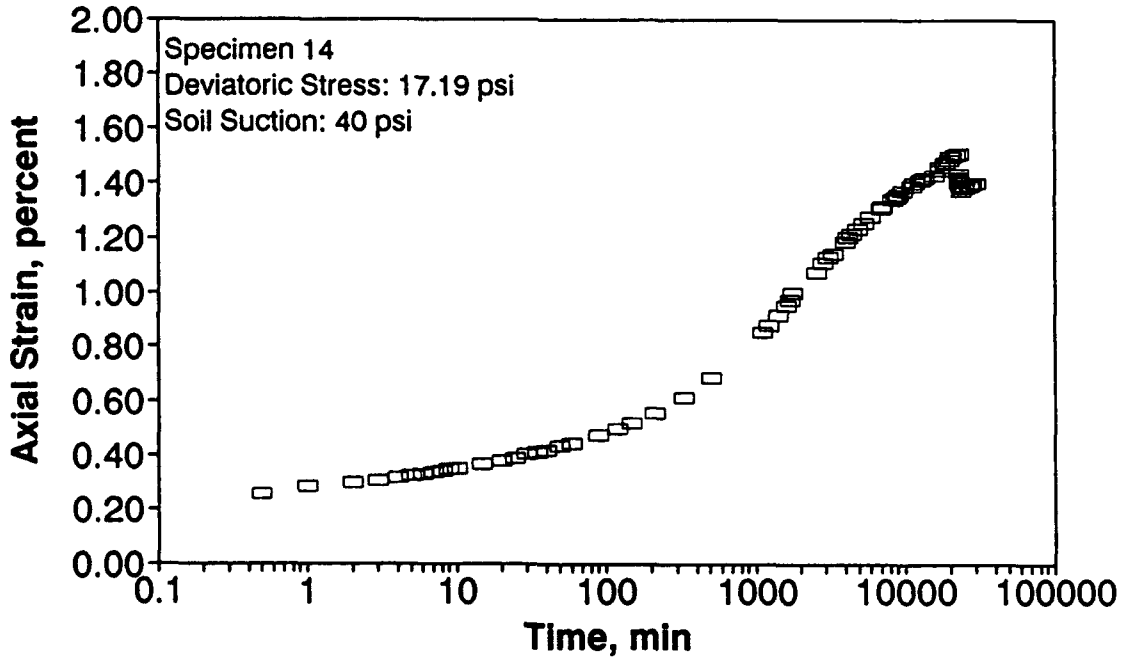
Specimen 14
Deviatoric Stress: 17.19 psi
Soil Suction: 40 psi
Axial Strain, percent
2.00
1.80
1.60
1.40
1.20
1.00
0.80
0.60
0.40
0.20
0.00
0.1
1
10
100
1000
10000
100000
Time, min

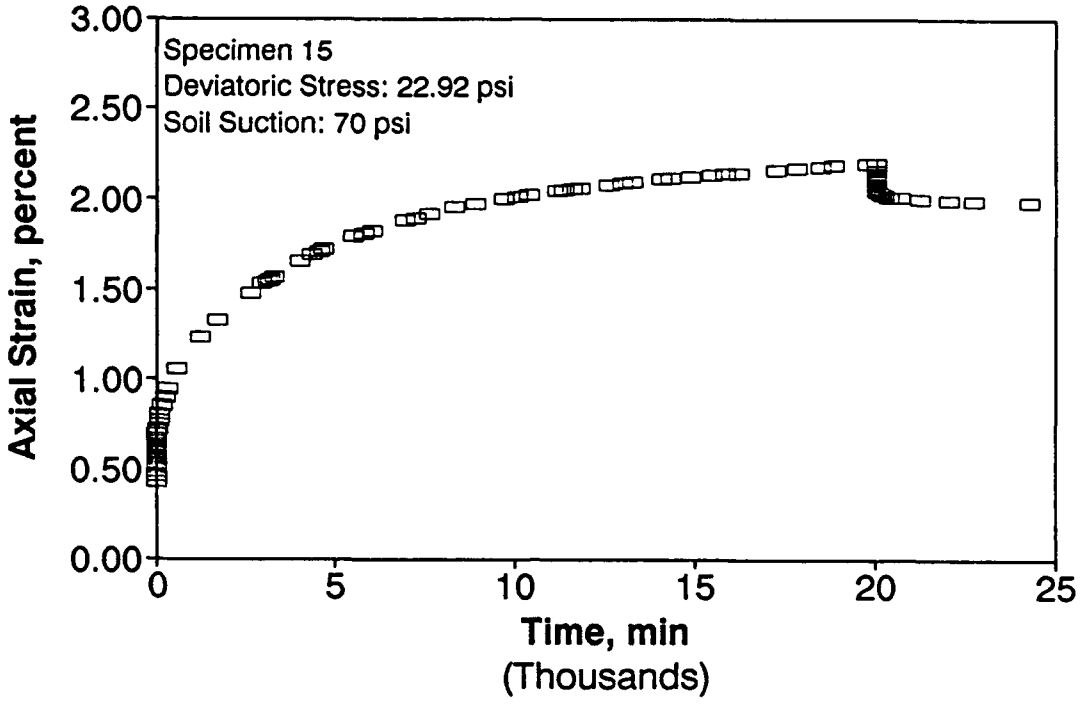
Specimen 15
Deviatoric Stress: 22.92 psi
Soil Suction: 70 psi
Axial Strain, percent
3.00
2.50
2.00
1.50
1.00
0.50
0.00
0
5
10
15
20
25
Time, min
(Thousands)

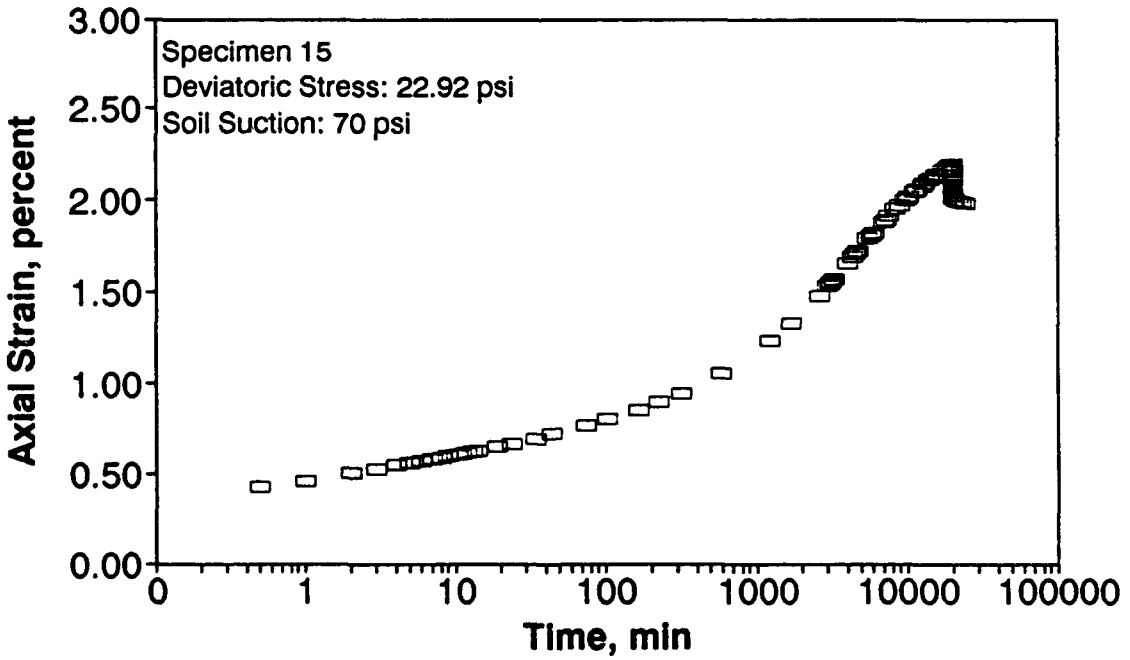
Specimen 15
Deviatoric Stress: 22.92 psi
Soil Suction: 70 psi
Axial Strain, percent
3.00
2.50
2.00
1.50
1.00
0.50
0.00
0
1
10
100
1000
10000
100000
Time, min

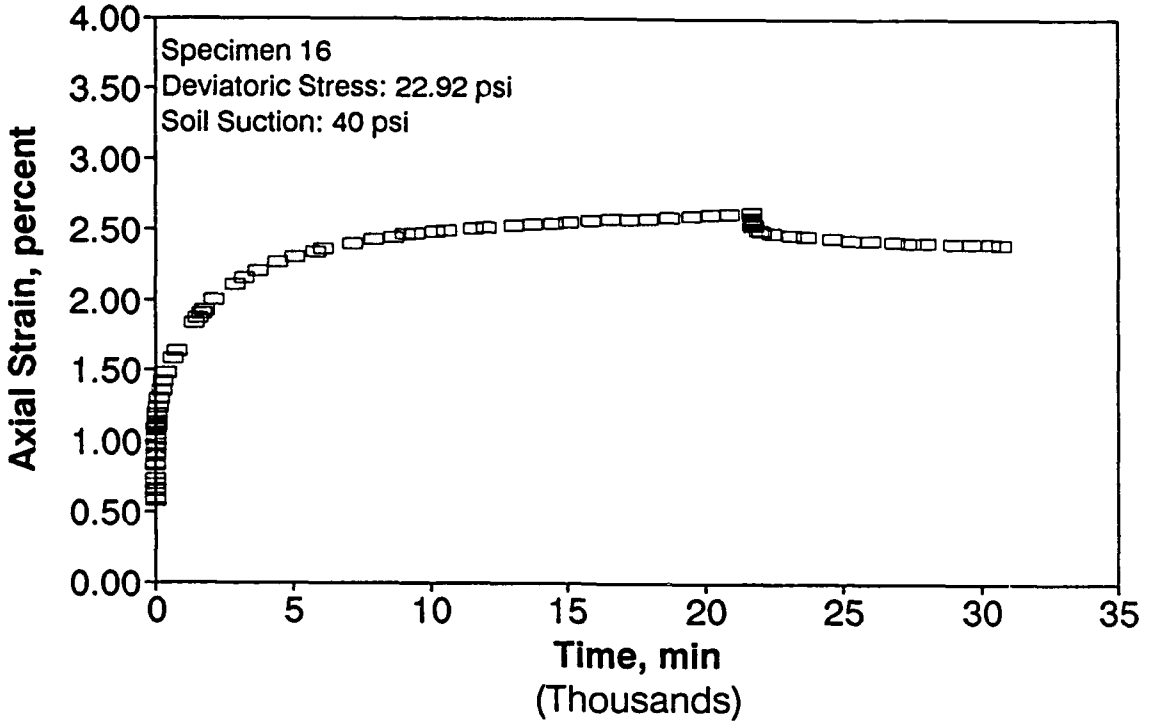
Specimen 16
Deviatoric Stress: 22.92 psi
Soil Suction: 40 psi
Axial Strain, percent
4.00
3.50
3.00
2.50
2.00
1.50
1.00
0.50
0.00
0
5
10
15
20
25
30
35
Time, min
(Thousands)

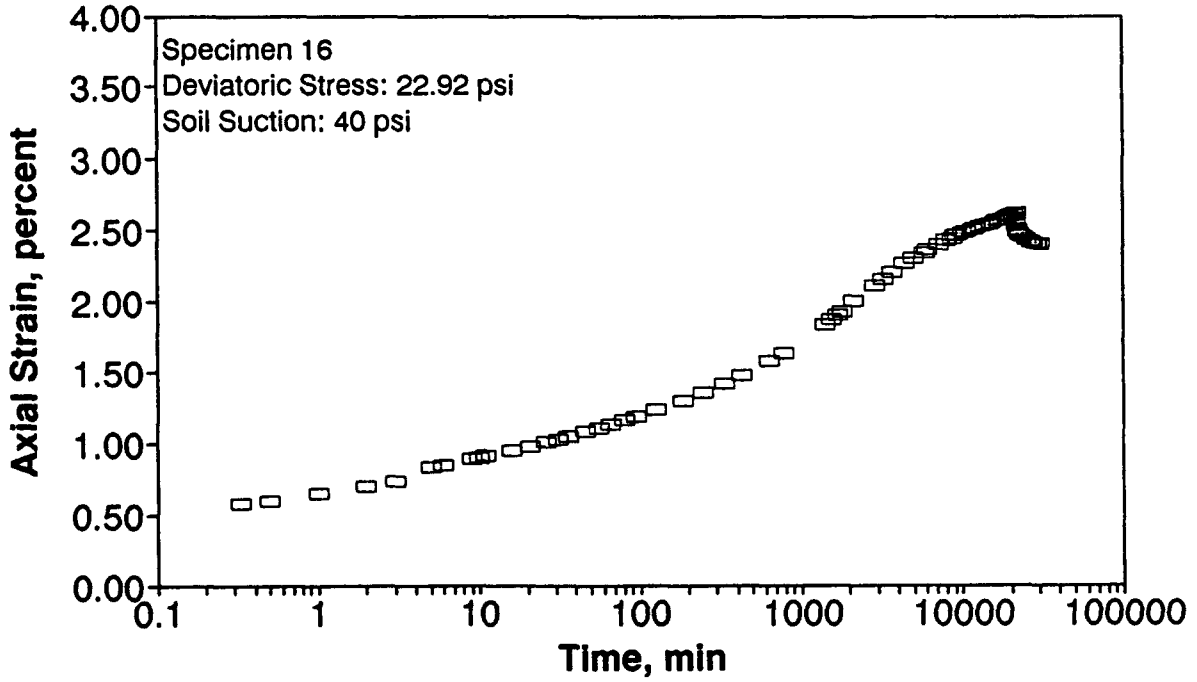
Specimen 16
Deviatoric Stress: 22.92 psi
Soil Suction: 40 psi
Axial Strain, percent
4.00
3.50
3.00
2.50
2.00
1.50
1.00
0.50
0.00
0.1
1
10
100
1000
10000
100000
Time, min

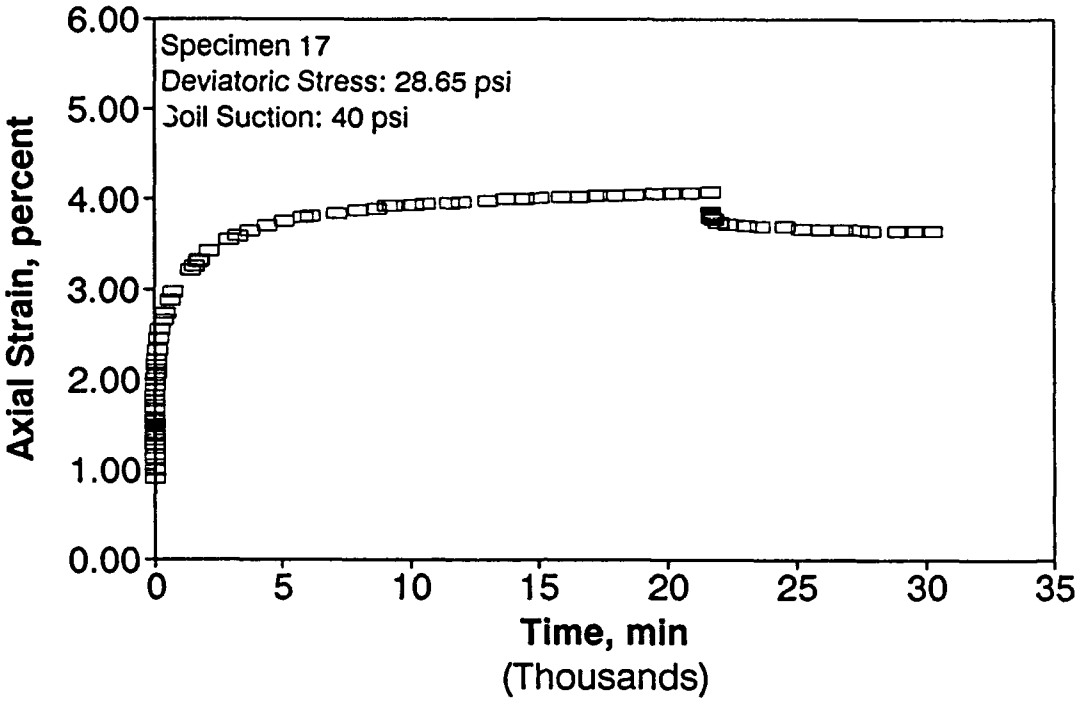
Specimen 17
Deviatoric Stress: 28.65 psi
Soil Suction: 40 psi
Axial Strain, percent
6.00
5.00
4.00
3.00
2.00
1.00
0.00
0
5
10
15
20
25
30
35
Time, min
(Thousands)

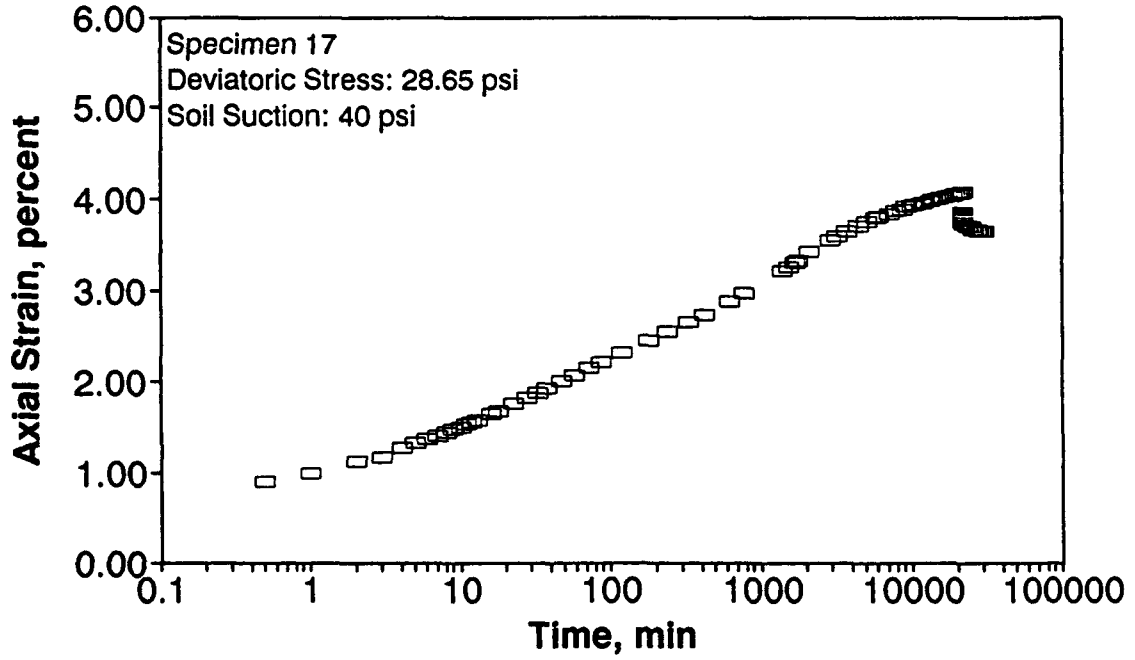
Specimen 17
Deviatoric Stress: 28.65 psi
Soil Suction: 40 psi
Axial Strain, percent
6.00
5.00
4.00
3.00
2.00
1.00
0.00
0.1
1
10
100
1000
10000
100000
Time, min

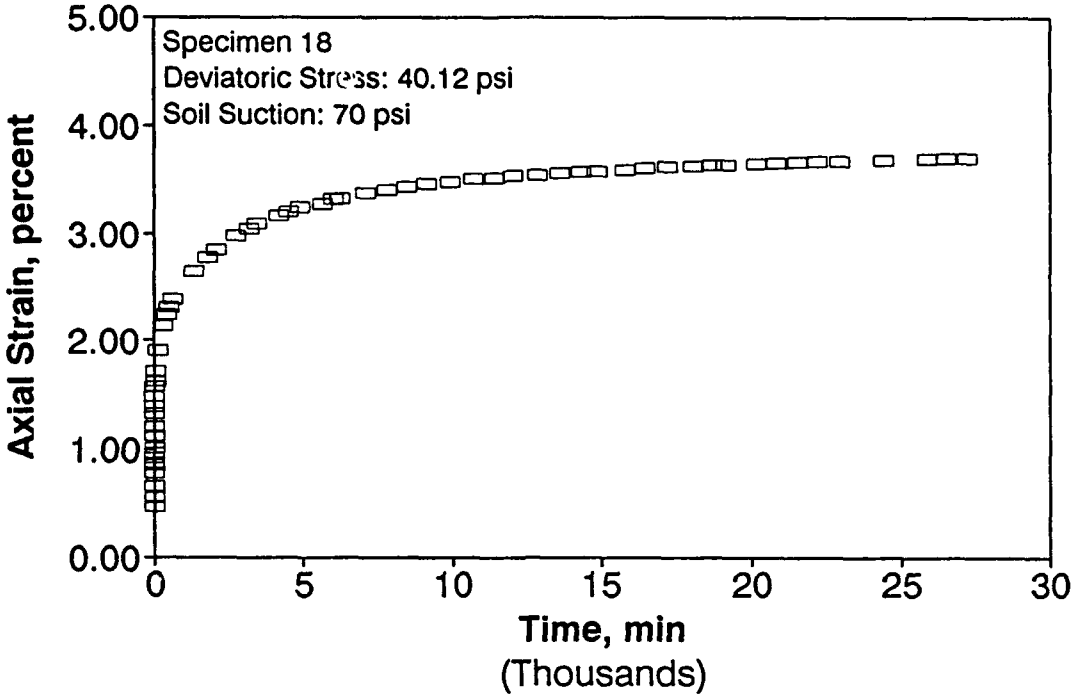
Specimen 18
Deviatoric Stress: 40.12 psi
Soil Suction: 70 psi
Axial Strain, percent
5.00
4.00
3.00
2.00
1.00
0.00
0
5
10
15
20
25
30
Time, min
(Thousands)

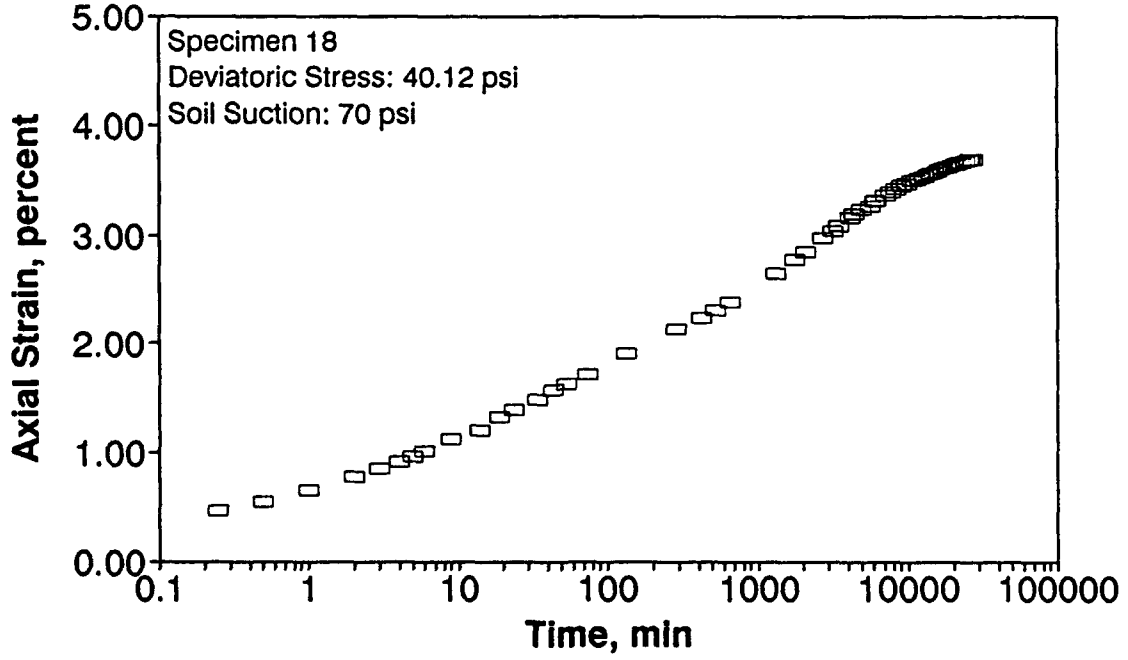
Specimen 18
Deviatoric Stress: 40.12 psi
Soil Suction: 70 psi
Axial Strain, percent
5.00
4.00
3.00
2.00
1.00
0.00
0.1
1
10
100
1000
10000
100000
Time, min

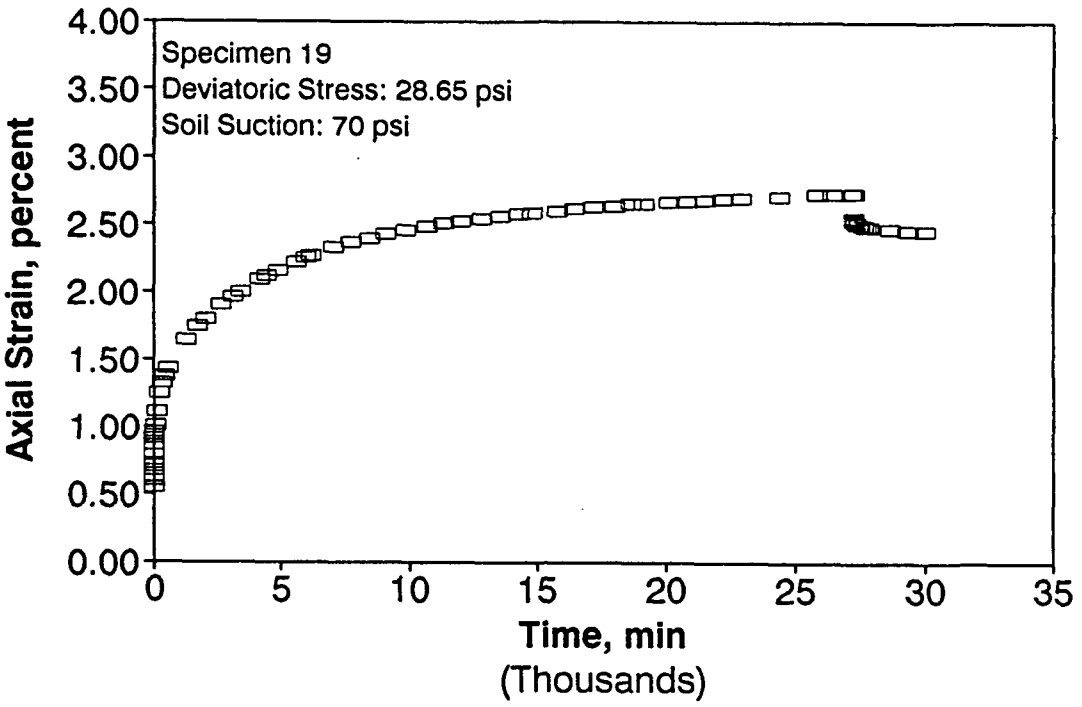
Specimen 19
Deviatoric Stress: 28.65 psi
Soil Suction: 70 psi
Axial Strain, percent
4.00
3.50
3.00
2.50
2.00
1.50
1.00
0.50
0.00
0
5
10
15
20
25
30
35
Time, min
(Thousands)

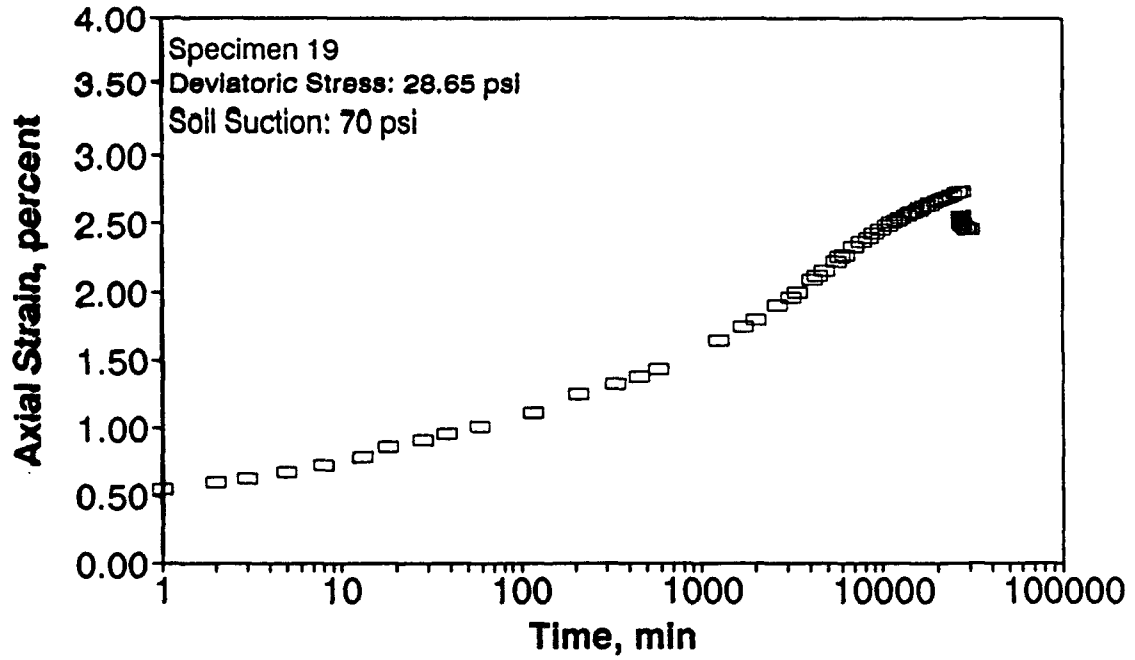
Specimen 19
Deviatoric Stress: 28.65 psi
Soil Suction: 70 psi
Axial Strain, percent
4.00
3.50
3.00
2.50
2.00
1.50
1.00
0.50
0.00
1
10
100
1000
10000
100000
Time, min

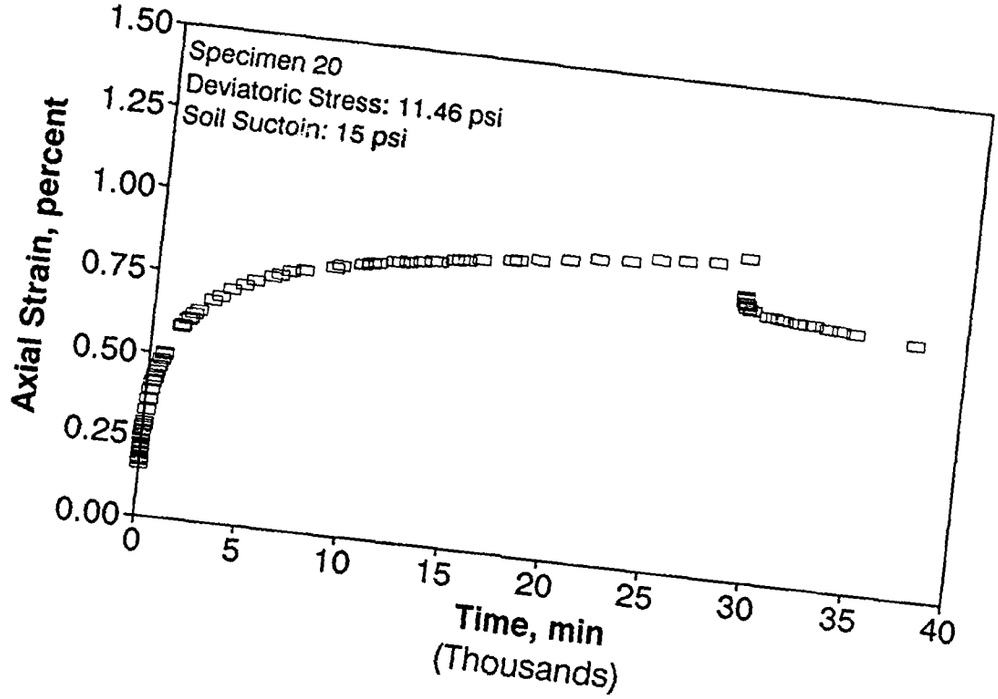
Specimen 20
Deviatoric Stress: 11.46 psi
Soil Suctoin: 15 psi
Axial Strain, percent
1.50
1.25
1.00
0.75
0.50
0.25
0.00
0
5
10
15
20
25
30
35
40
Time, min
(Thousands)

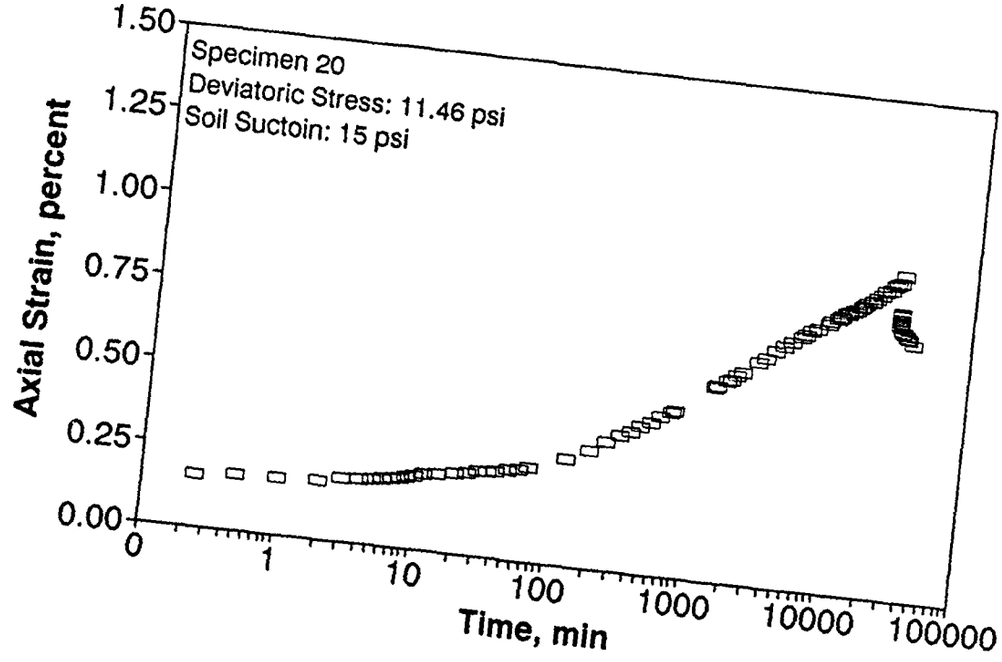
Specimen 20
Deviatoric Stress: 11.46 psi
Soil Suctoin: 15 psi
Axial Strain, percent
1.50
1.25
1.00
0.75
0.50
0.25
0.00
0
1
10
100
1000
10000
100000
Time, min

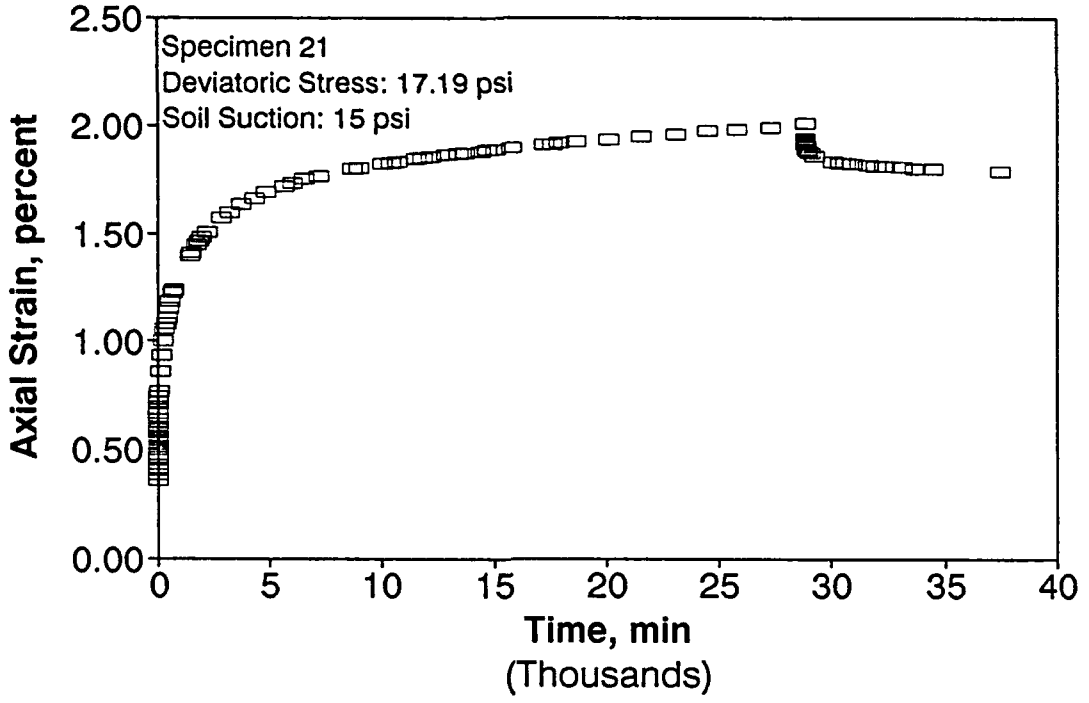
Specimen 21
Deviatoric Stress: 17.19 psi
Soil Suction: 15 psi
Axial Strain, percent
2.50
2.00
1.50
1.00
0.50
0.00
0
5
10
15
20
25
30
35
40
Time, min
(Thousands)

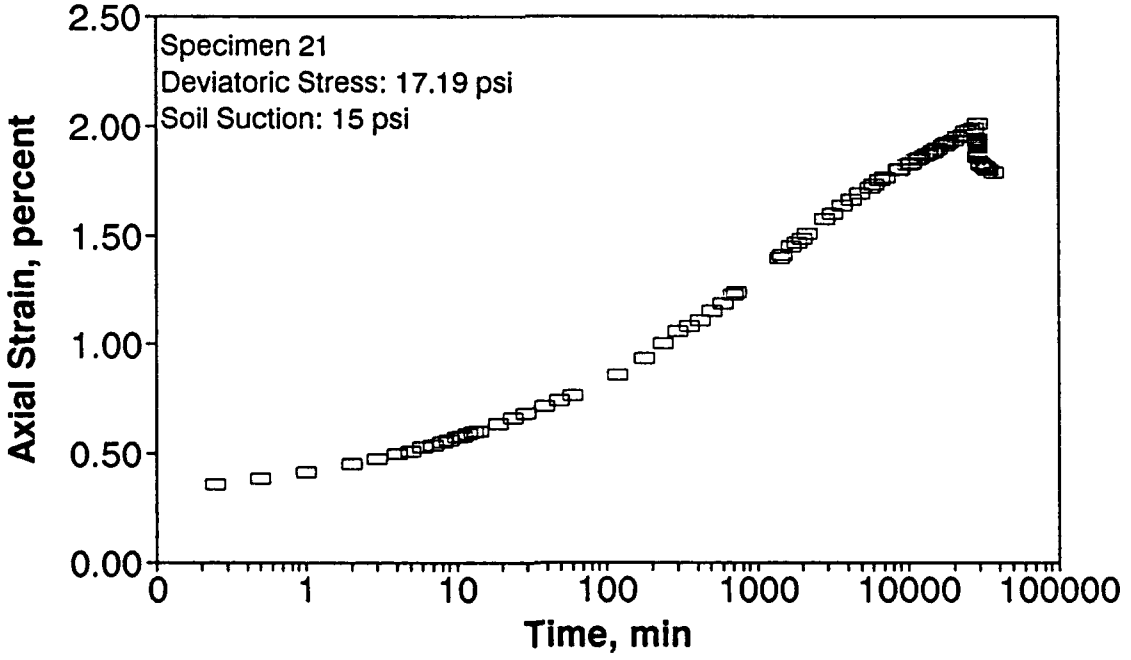
Specimen 21
Deviatoric Stress: 17.19 psi
Soil Suction: 15 psi
Axial Strain, percent
2.50
2.00
1.50
1.00
0.50
0.00
0
1
10
100
1000
10000
100000
Time, min

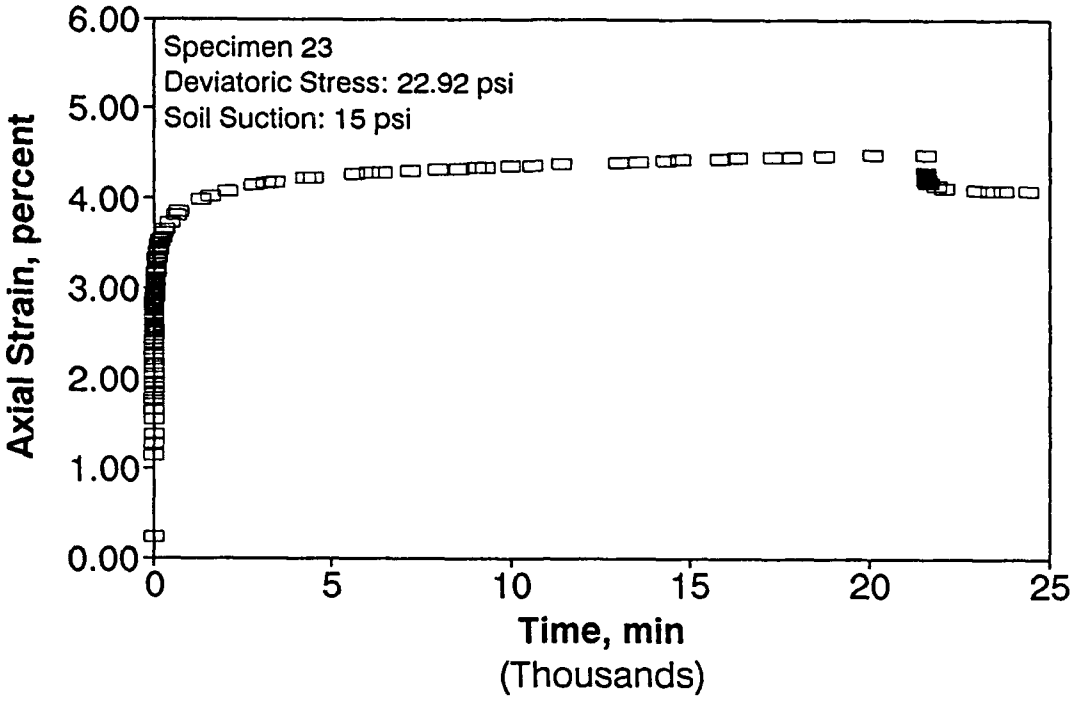
Specimen 23
Deviatoric Stress: 22.92 psi
Soil Suction: 15 psi
Axial Strain, percent
6.00
5.00
4.00
3.00
2.00
1.00
0.00
0
5
10
15
20
25
Time, min
(Thousands)

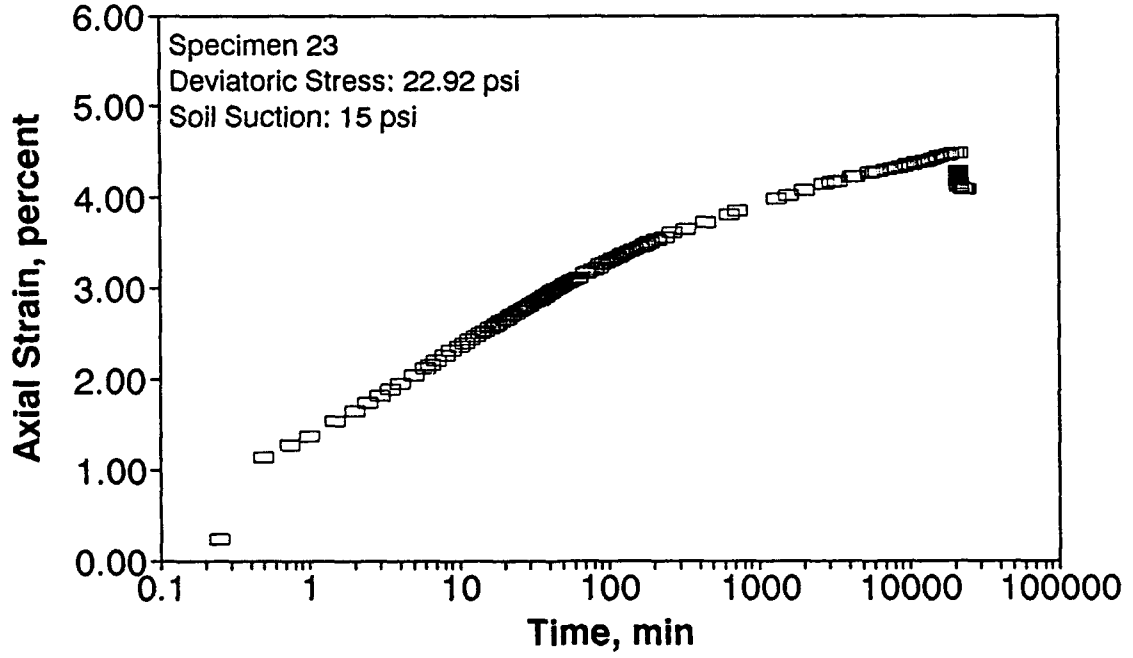
Specimen 23
Deviatoric Stress: 22.92 psi
Soil Suction: 15 psi
Axial Strain, percent
6.00
5.00
4.00
3.00
2.00
1.00
0.00
0.1
1
10
100
1000
10000
100000
Time, min

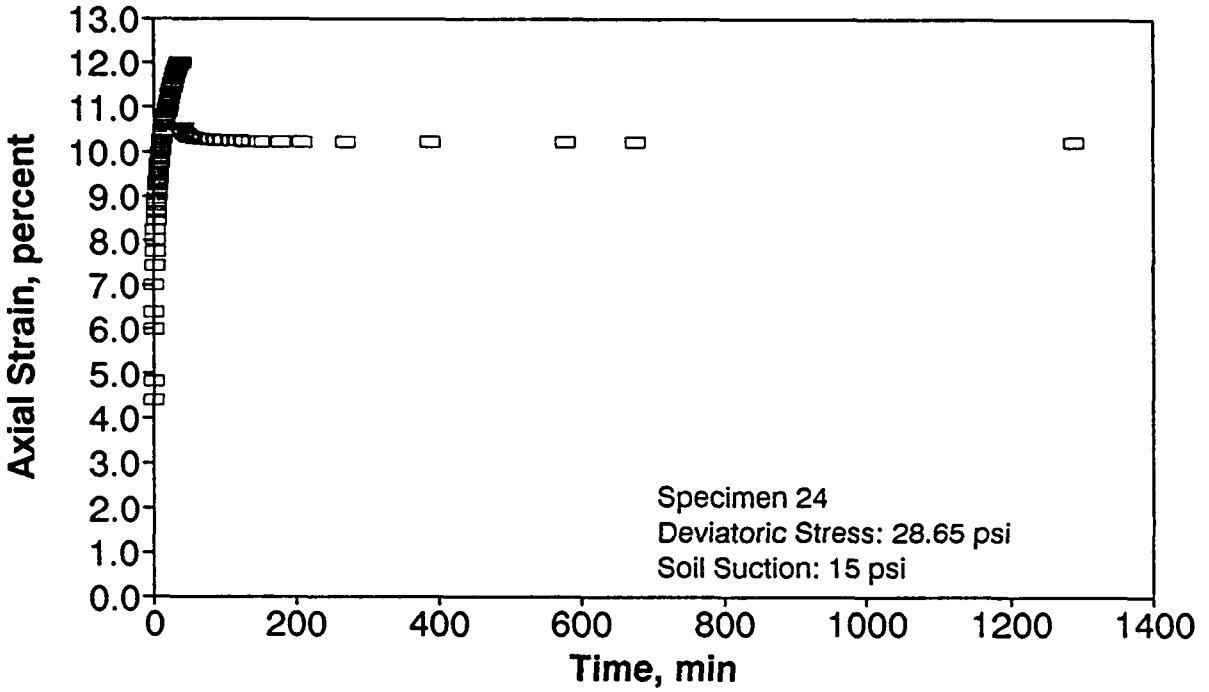
Axial Strain, percent
13.0
12.0
11.0
10.0
9.0
8.0
7.0
6.0
5.0
4.0
3.0
2.0
1.0
0.0
0
200
400
600
800
1000
1200
1400
Time, min
Specimen 24
Deviatoric Stress: 28.65 psi
Soil Suction: 15 psi

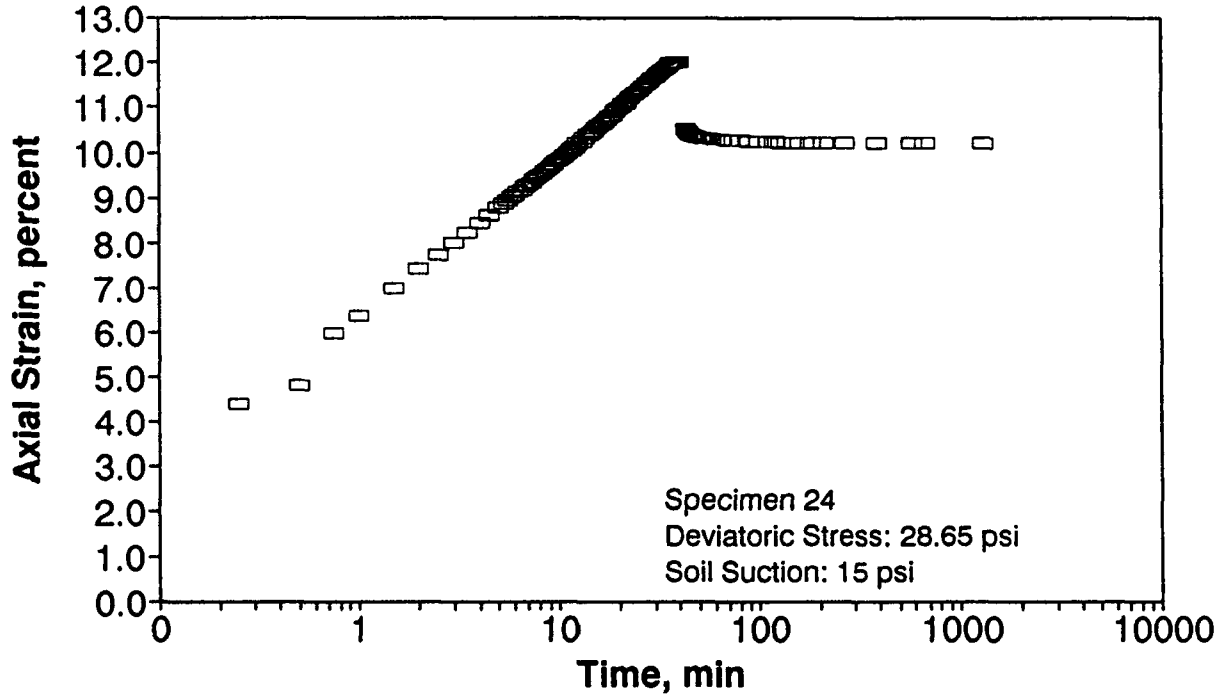
Axial Strain, percent
13.0
12.0
11.0
10.0
9.0
8.0
7.0
6.0
5.0
4.0
3.0
2.0
1.0
0.0
0
1
10
100
1000
10000
Time, min
Specimen 24
Deviatoric Stress: 28.65 psi
Soil Suction: 15 psi

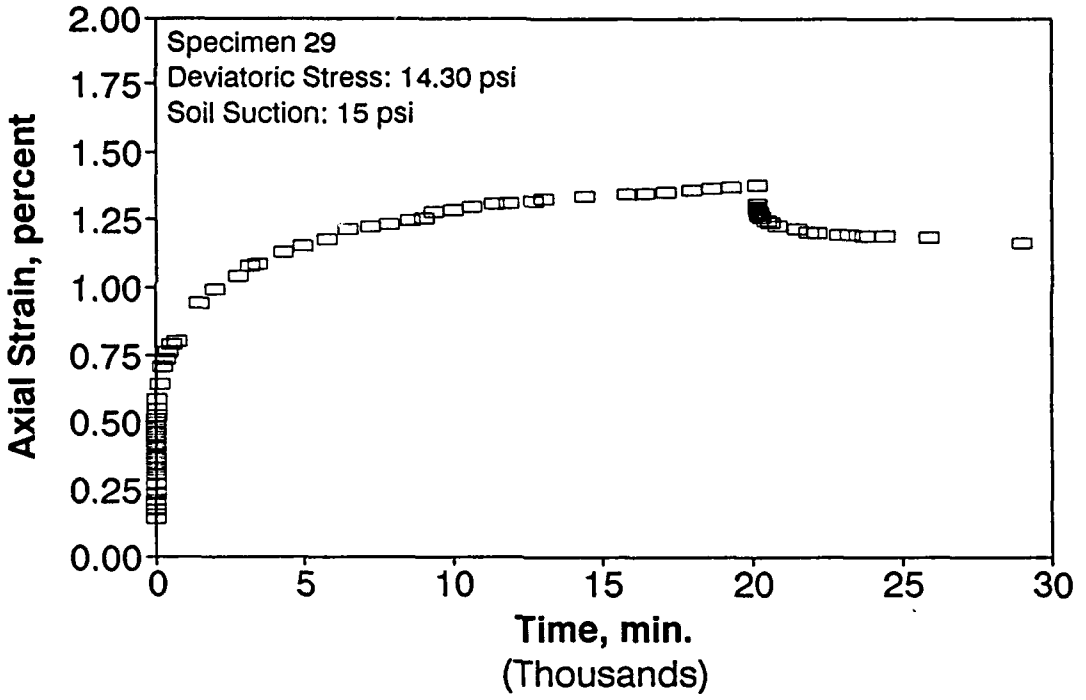
Specimen 29
Deviatoric Stress: 14.30 psi
Soil Suction: 15 psi
Axial Strain, percent
2.00
1.75
1.50
1.25
1.00
0.75
0.50
0.25
0.00
0
5
10
15
20
25
30
Time, min.
(Thousands)

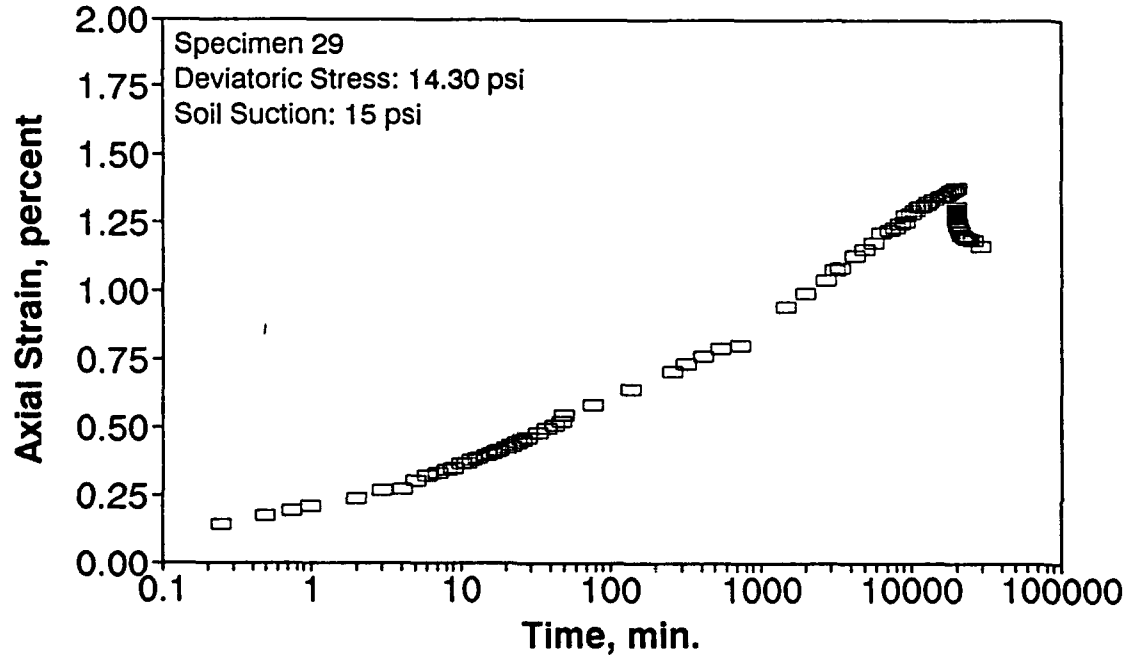
Specimen 29
Deviatoric Stress: 14.30 psi
Soil Suction: 15 psi
Axial Strain, percent
2.00
1.75
1.50
1.25
1.00
0.75
0.50
0.25
0.00
0.1
1
10
100
1000
10000
100000
Time, min.

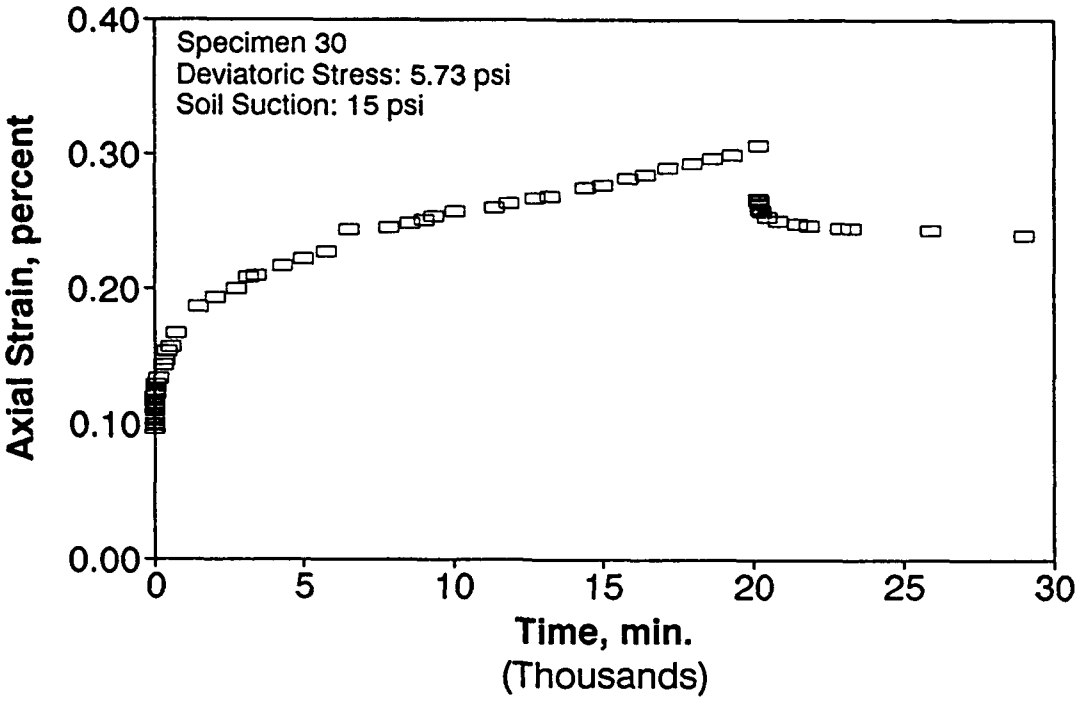
Specimen 30
Deviatoric Stress: 5.73 psi
Soil Suction: 15 psi
Axial Strain, percent
0.40
0.30
0.20
0.10
0.00
0
5
10
15
20
25
30
Time, min.
(Thousands)

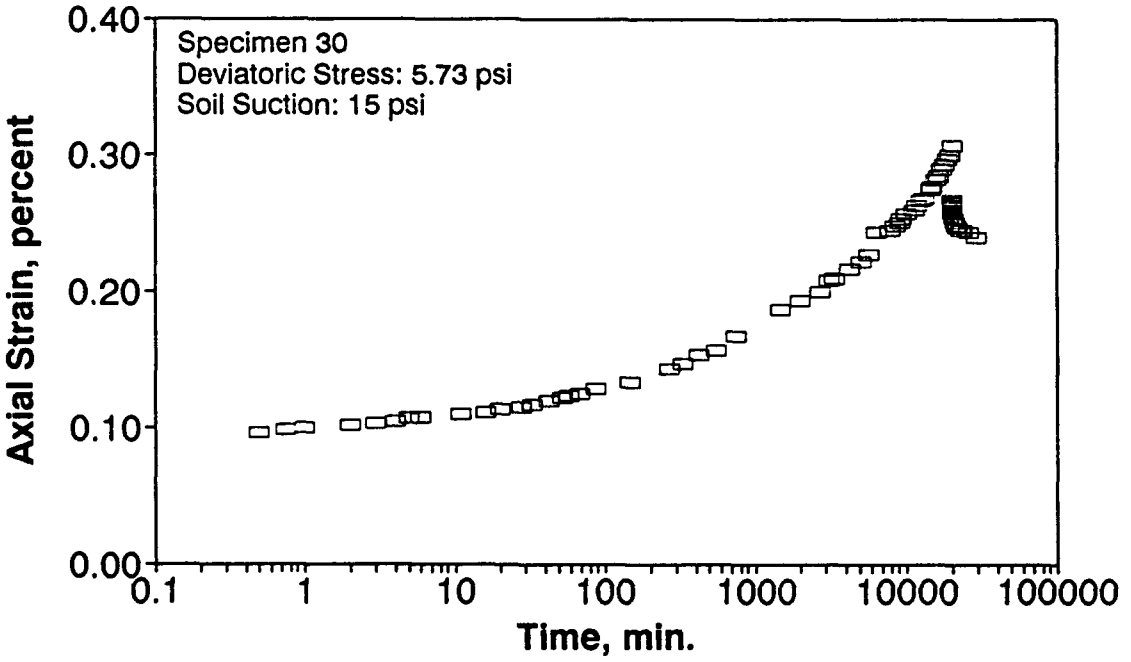
Specimen 30
Deviatoric Stress: 5.73 psi
Soil Suction: 15 psi
Axial Strain, percent
0.40
0.30
0.20
0.10
0.00
0.1
1
10
100
1000
10000
100000
Time, min.

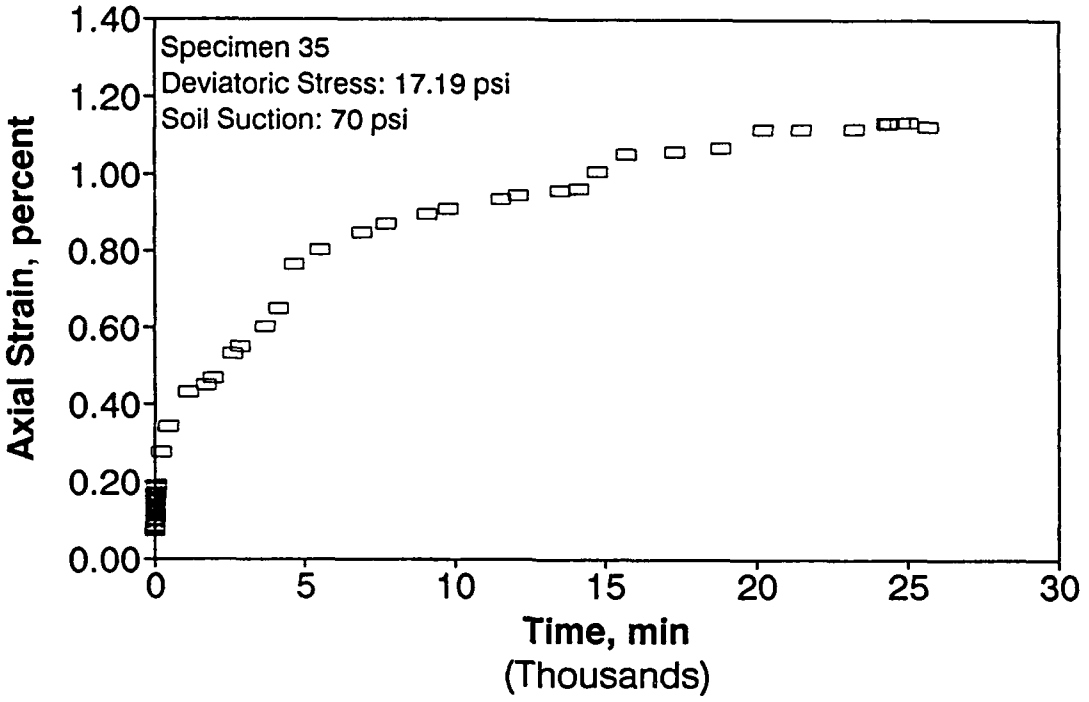
Specimen 35
Deviatoric Stress: 17.19 psi
Soil Suction: 70 psi
Axial Strain, percent
1.40
1.20
1.00
0.80
0.60
0.40
0.20
0.00
0
5
10
15
20
25
30
Time, min
(Thousands)

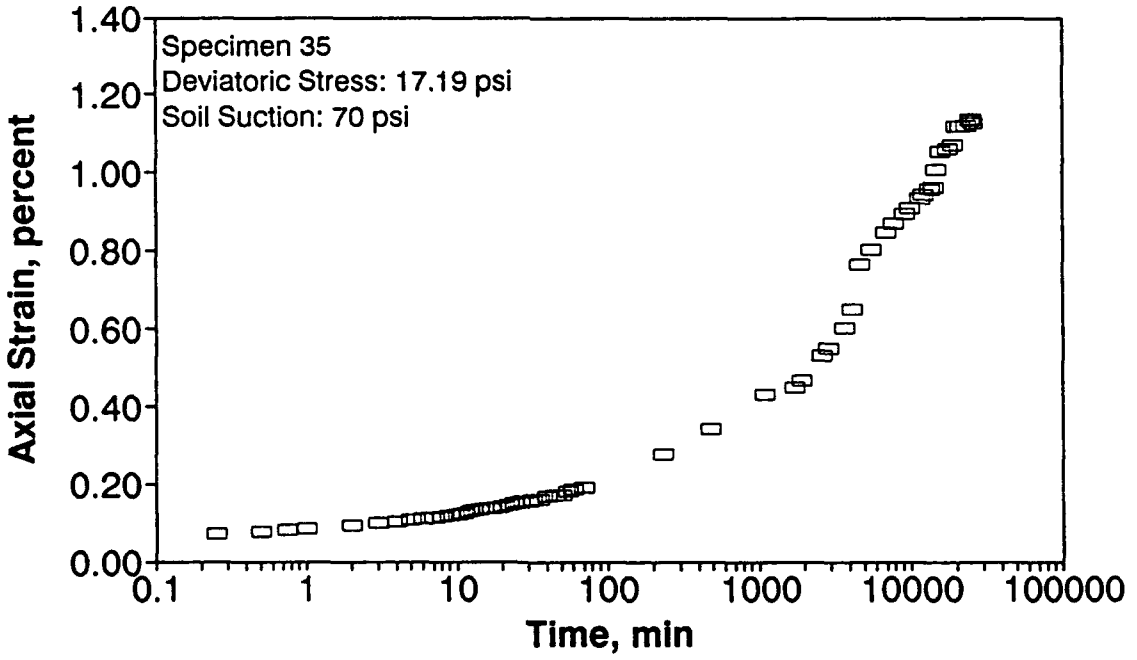
Specimen 35
Deviatoric Stress: 17.19 psi
Soil Suction: 70 psi
Axial Strain, percent
1.40
1.20
1.00
0.80
0.60
0.40
0.20
0.00
0.1
1
10
100
1000
10000
100000
Time, min

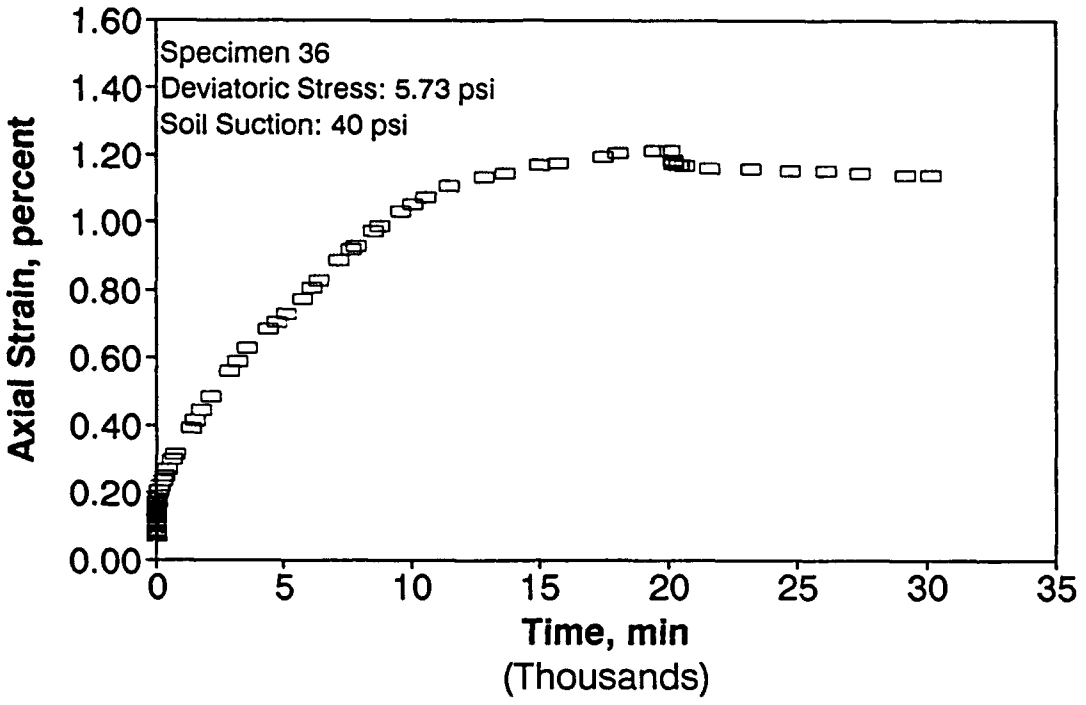
Specimen 36
Deviatoric Stress: 5.73 psi
Soil Suction: 40 psi
Axial Strain, percent
1.60
1.40
1.20
1.00
0.80
0.60
0.40
0.20
0.00
0
5
10
15
20
25
30
35
Time, min
(Thousands)

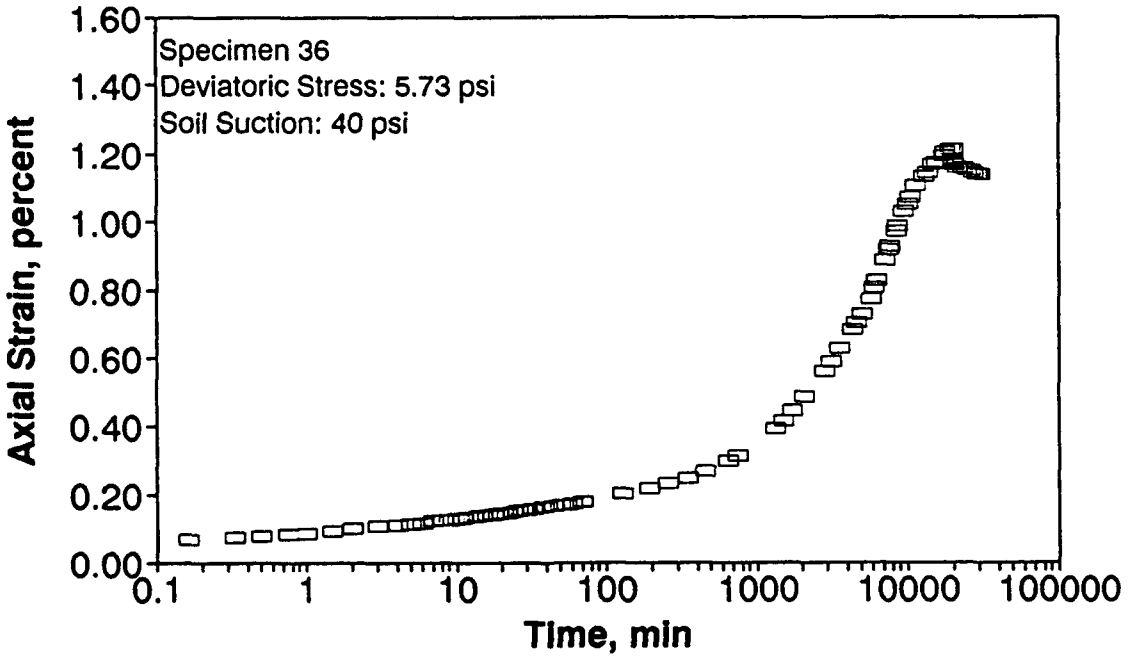
Specimen 36
Deviatoric Stress: 5.73 psi
Soil Suction: 40 psi
Axial Strain, percent
1.60
1.40
1.20
1.00
0.80
0.60
0.40
0.20
0.00
0.1
1
10
100
1000
10000
100000
Time, min

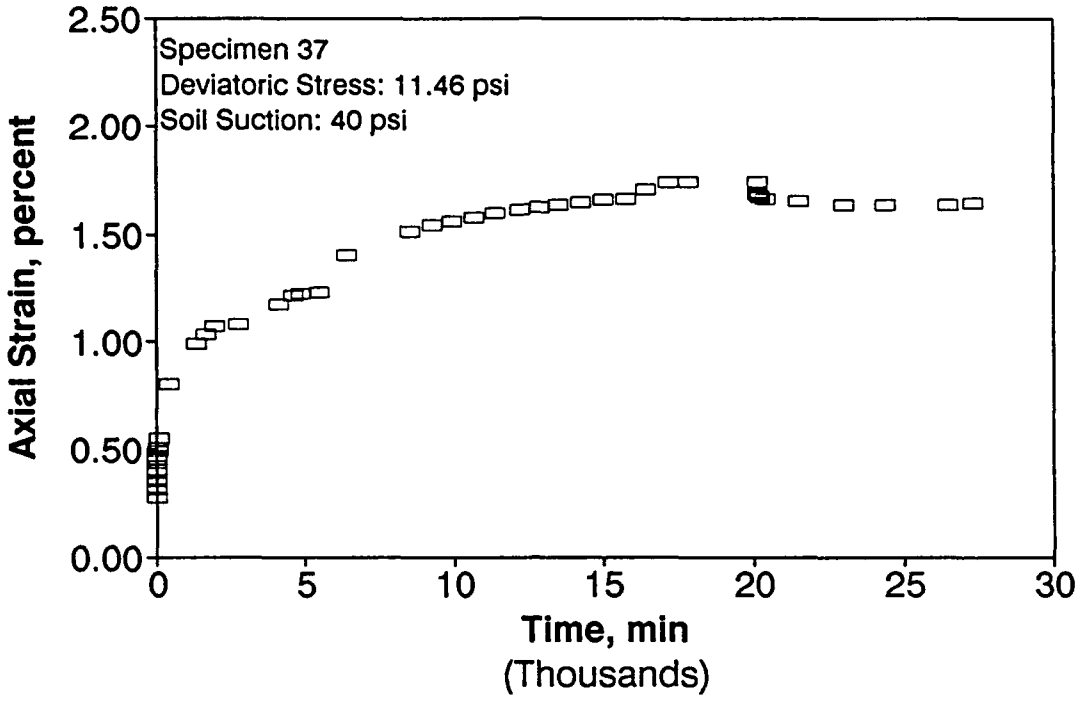
Specimen 37
Deviatoric Stress: 11.46 psi
Soil Suction: 40 psi
Axial Strain, percent
2.50
2.00
1.50
1.00
0.50
0.00
0
5
10
15
20
25
30
Time, min
(Thousands)

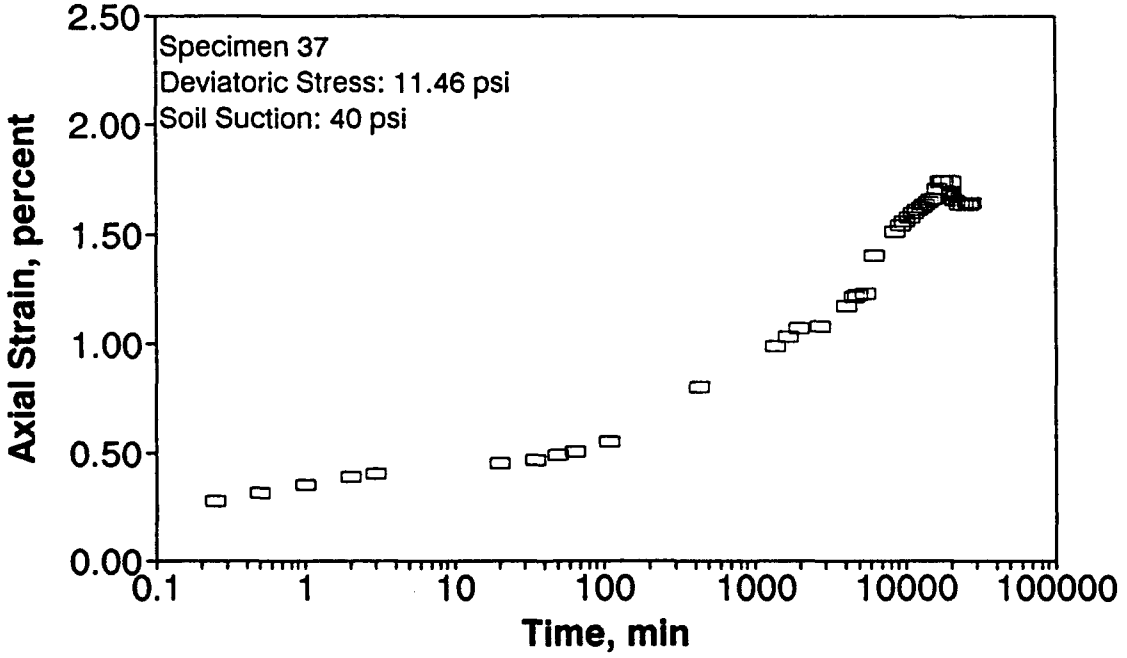
Specimen 37
Deviatoric Stress: 11.46 psi
Soil Suction: 40 psi
Axial Strain, percent
2.50
2.00
1.50
1.00
0.50
0.00
0.1
1
10
100
1000
10000
100000
Time, min

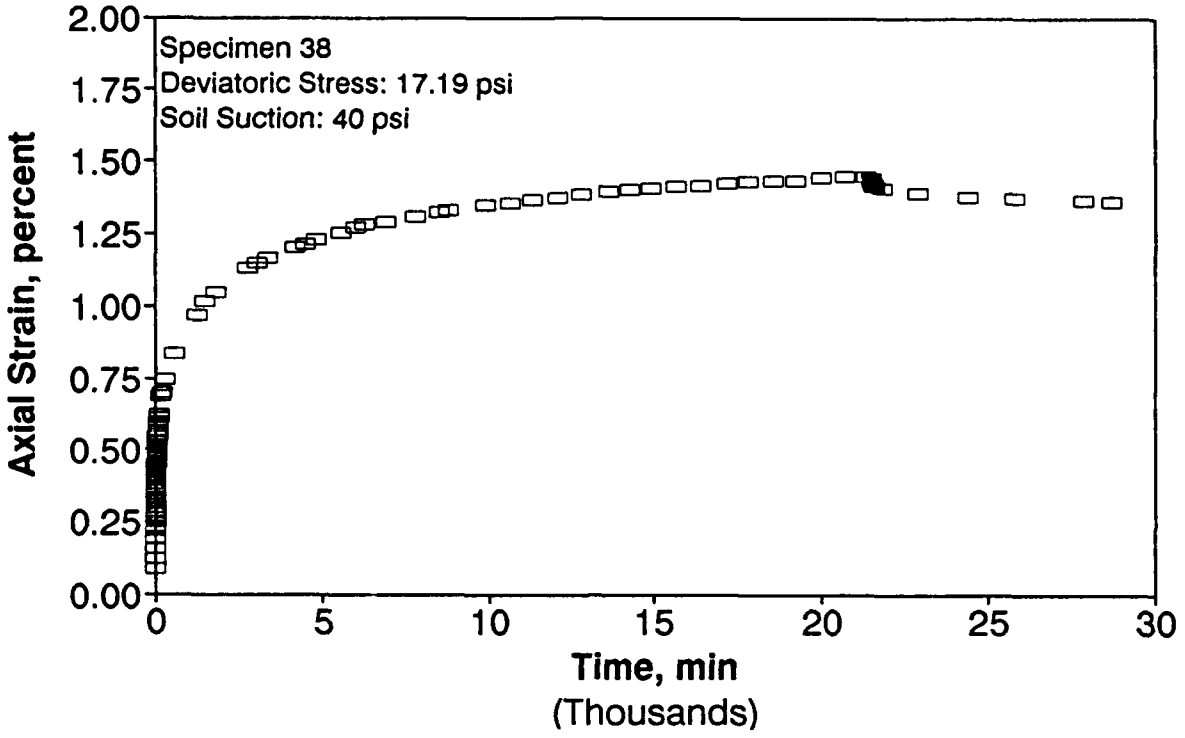
Specimen 38
Deviatoric Stress: 17.19 psi
Soil Suction: 40 psi
Axial Strain, percent
2.00
1.75
1.50
1.25
1.00
0.75
0.50
0.25
0.00
0
5
10
15
20
25
30
Time, min
(Thousands)

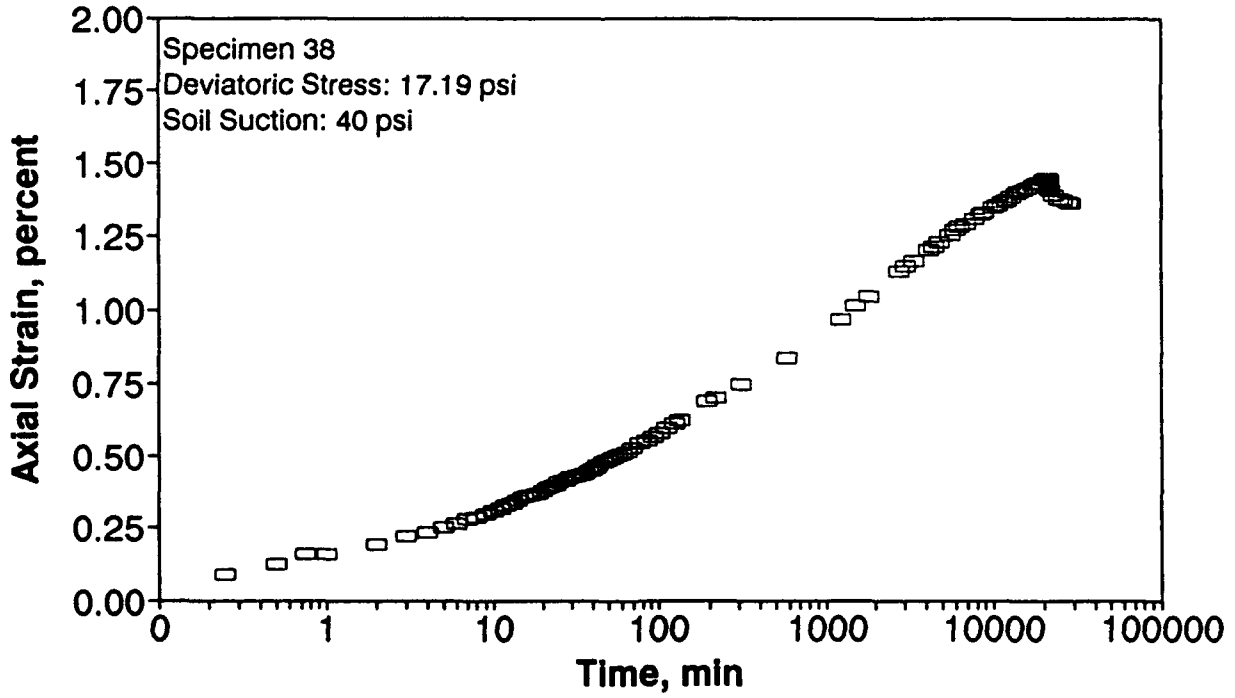
Specimen 38
Deviatoric Stress: 17.19 psi
Soil Suction: 40 psi
Axial Strain, percent
2.00
1.75
1.50
1.25
1.00
0.75
0.50
0.25
0.00
0
1
10
100
1000
10000
100000
Time, min

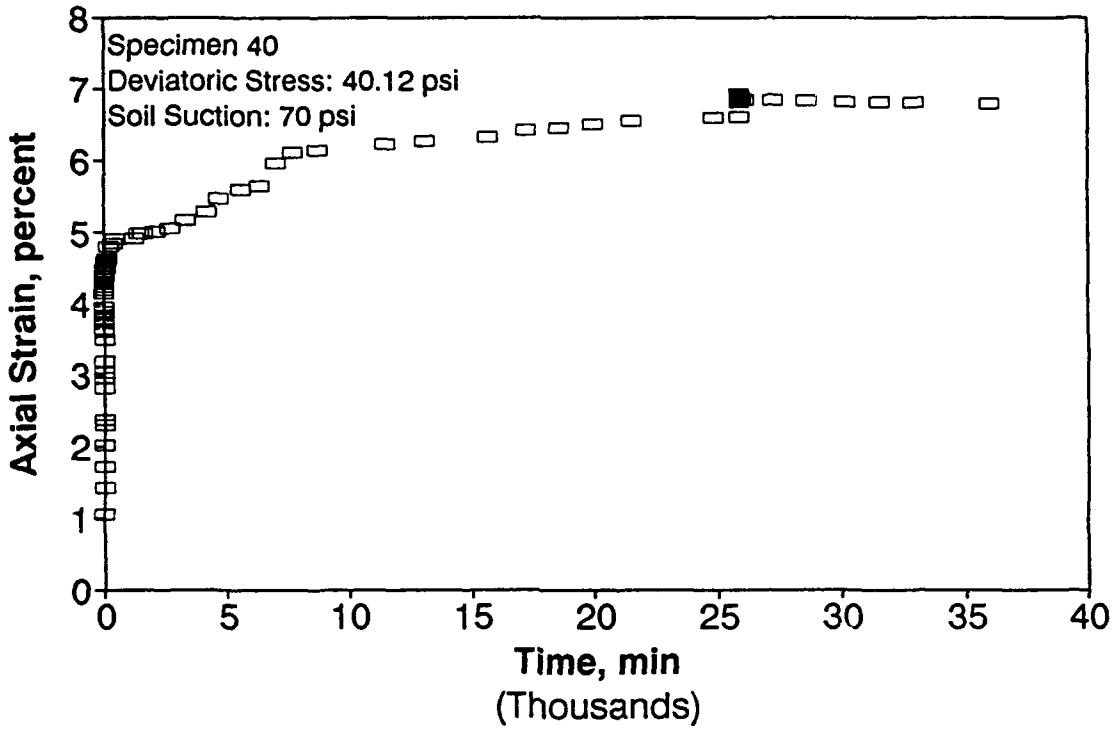
Specimen 40
Deviatoric Stress: 40.12 psi
Soil Suction: 70 psi
Axial Strain, percent
0
1
2
3
4
5
6
7
8
0
5
10
15
20
25
30
35
40
Time, min
(Thousands)

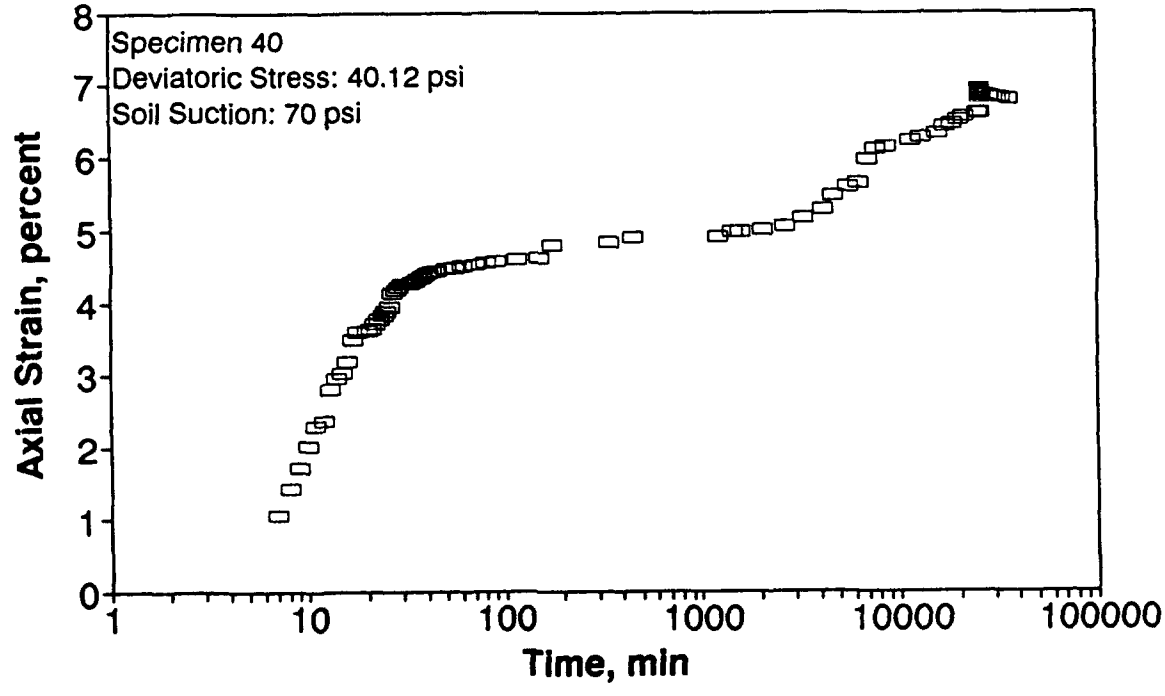
Specimen 40
Deviatoric Stress: 40.12 psi
Soil Suction: 70 psi
Axial Strain, percent
0
1
2
3
4
5
6
7
8
1
10
100
1000
10000
100000
Time, min

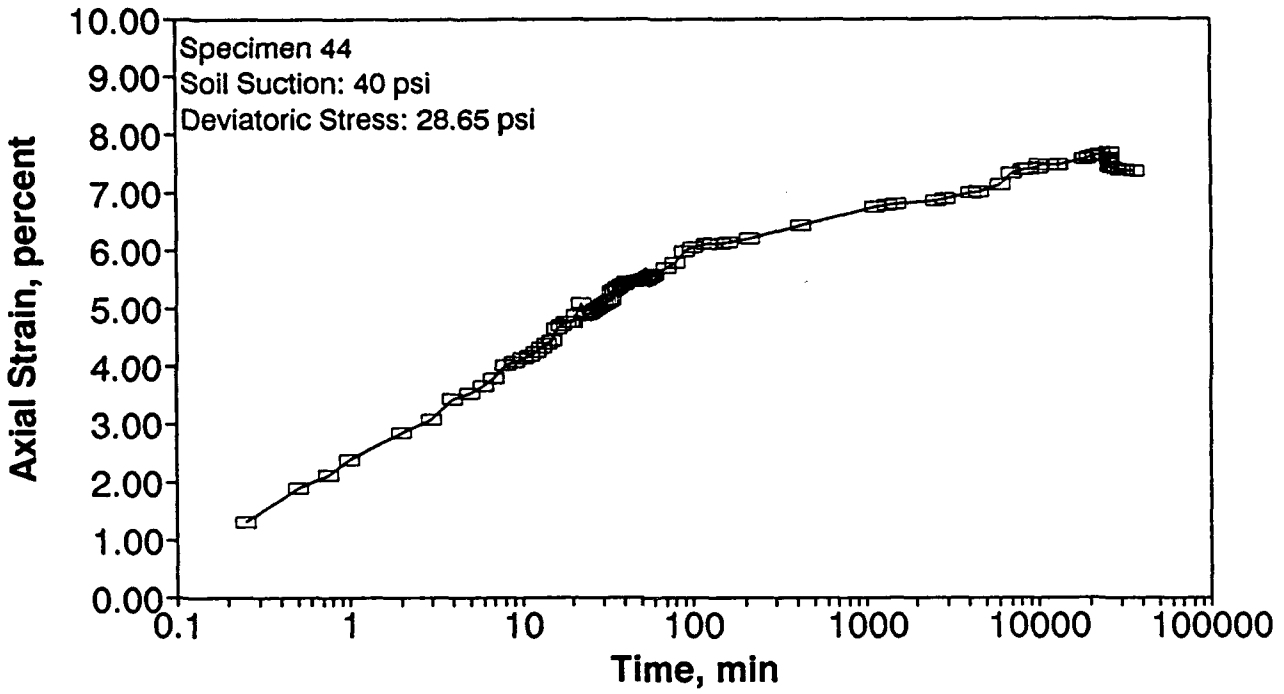
Specimen 44
Soil Suction: 40 psi
Deviatoric Stress: 28.65 psi
Axial Strain, percent
10.00
9.00
8.00
7.00
6.00
5.00
4.00
3.00
2.00
1.00
0.00
0.1
1
10
100
1000
10000
100000
Time, min

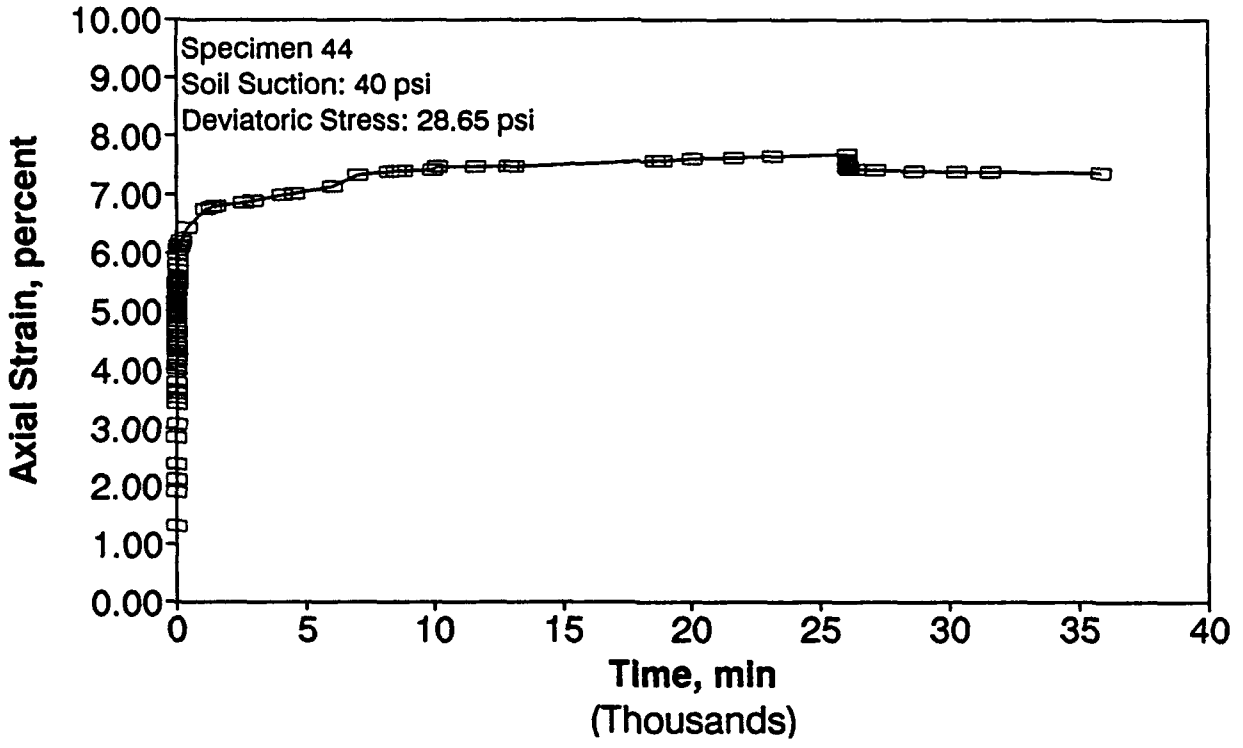
Specimen 44
Soil Suction: 40 psi
Deviatoric Stress: 28.65 psi
Axial Strain, percent
10.00
9.00
8.00
7.00
6.00
5.00
4.00
3.00
2.00
1.00
0.00
0
5
10
15
20
25
30
35
40
Time, min
(Thousands)

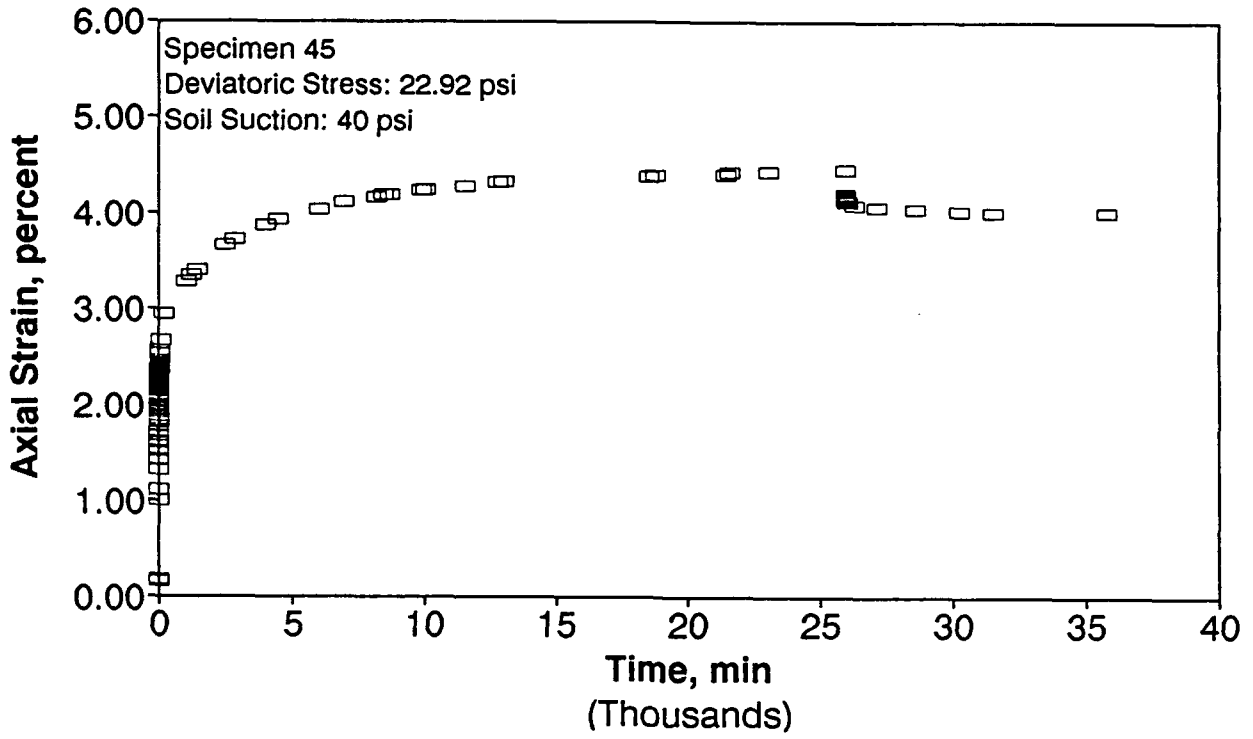
Specimen 45
Deviatoric Stress: 22.92 psi
Soil Suction: 40 psi
Axial Strain, percent
6.00
5.00
4.00
3.00
2.00
1.00
0.00
0
5
10
15
20
25
30
35
40
Time, min
(Thousands)

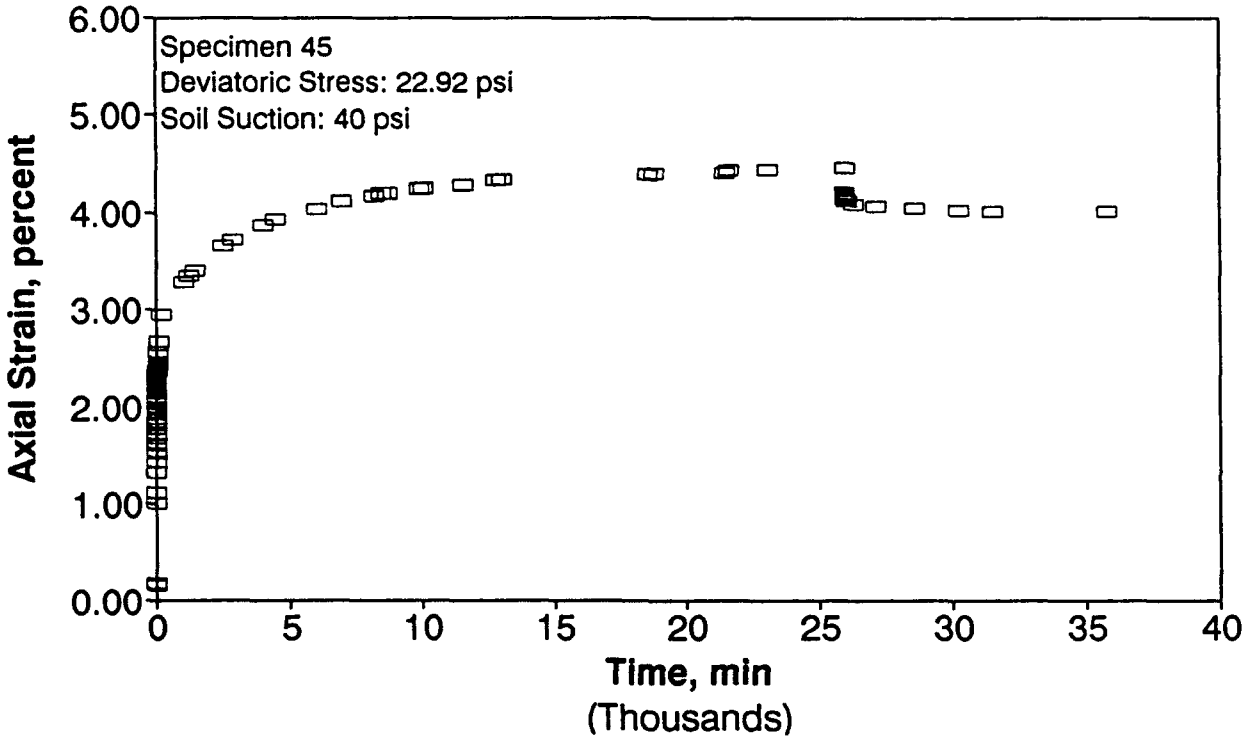
Specimen 45
Deviatoric Stress: 22.92 psi
Soil Suction: 40 psi
Axial Strain, percent
6.00
5.00
4.00
3.00
2.00
1.00
0.00
0
5
10
15
20
25
30
35
40
Time, min
(Thousands)

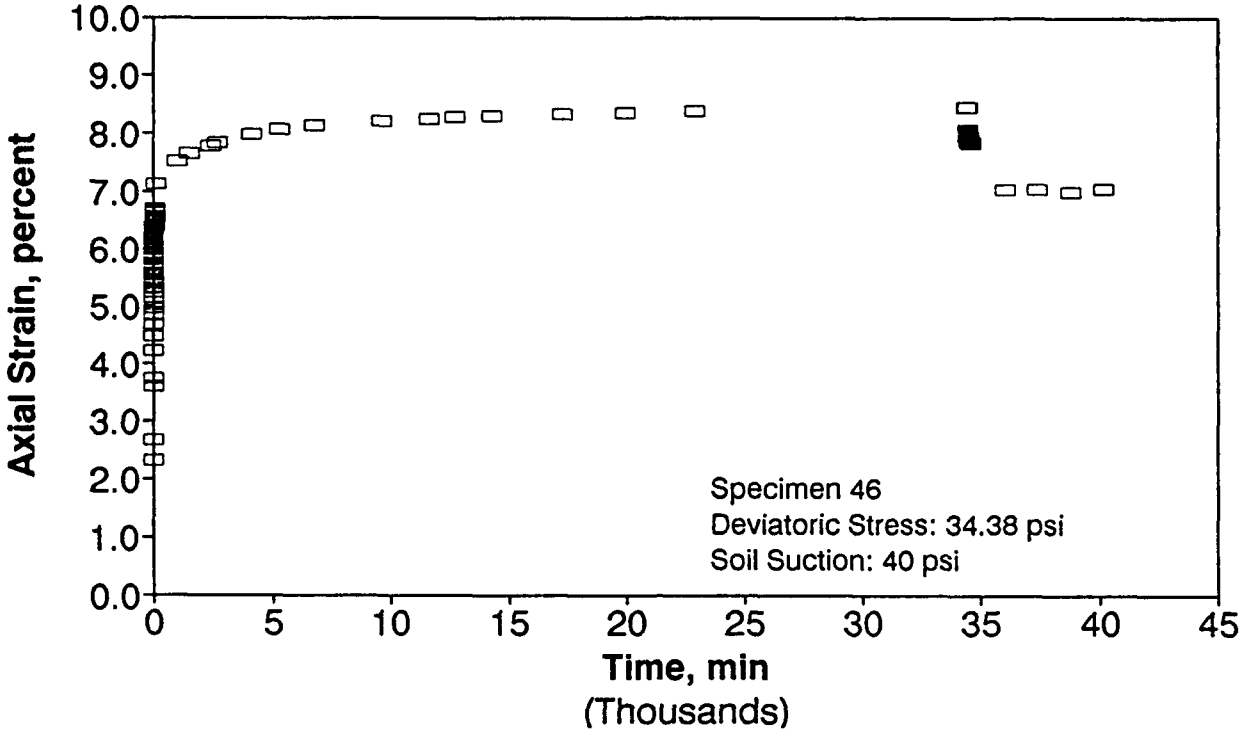
Axial Strain, percent
10.0
9.0
8.0
7.0
6.0
5.0
4.0
3.0
2.0
1.0
0.0
0
5
10
15
20
25
30
35
40
45
Time, min
(Thousands)
Specimen 46
Deviatoric Stress: 34.38 psi
Soil Suction: 40 psi

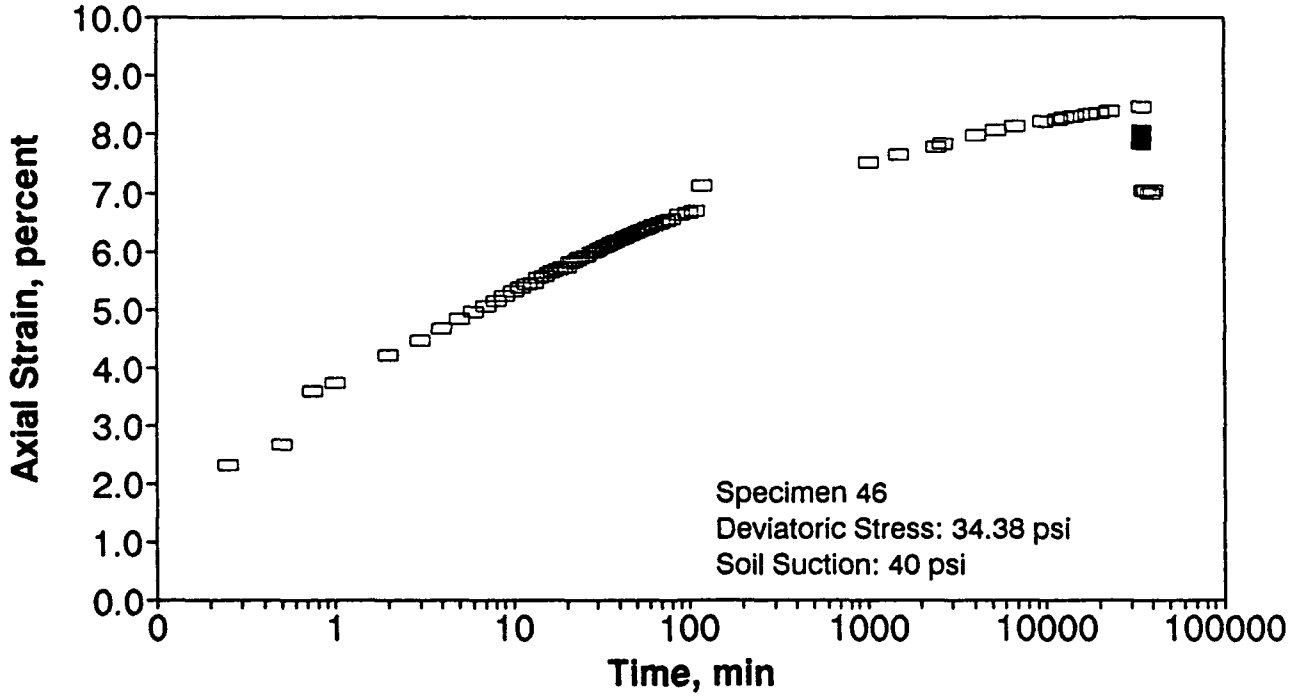
Axial Strain, percent
10.0
9.0
8.0
7.0
6.0
5.0
4.0
3.0
2.0
1.0
0.0
0
1
10
100
1000
10000
100000
Time, min
Specimen 46
Deviatoric Stress: 34.38 psi
Soil Suction: 40 psi

APPENDIX E

RESULTS OF GRAIN SIZE ANALYSES

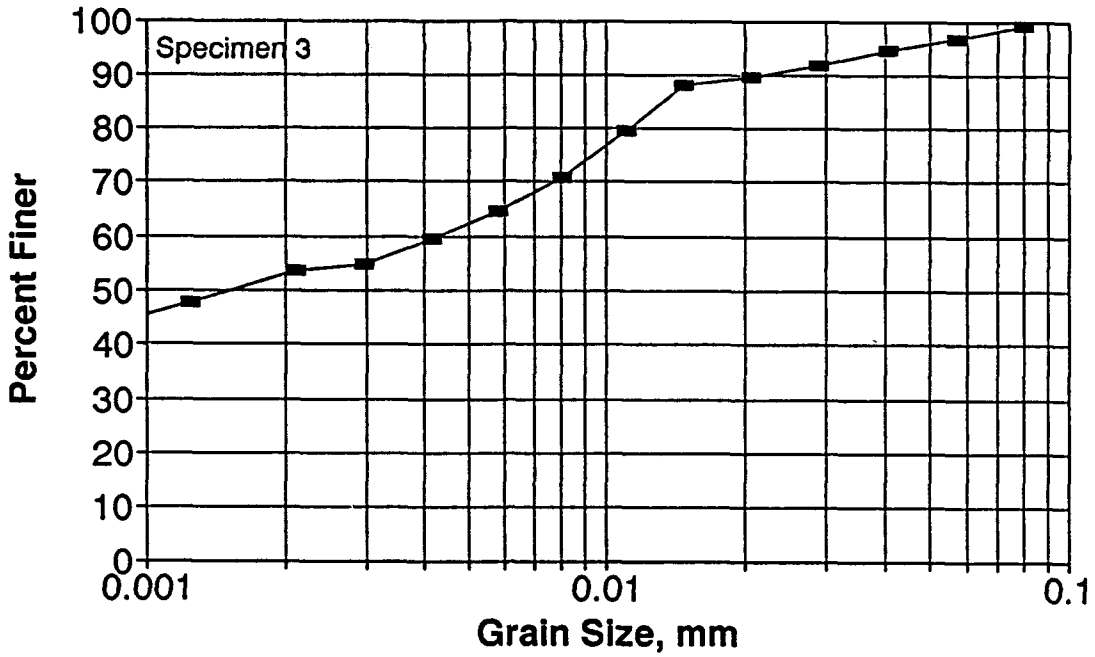
Specimen 3
Percent Finer
100
90
80
70
60
50
40
30
20
10
0
0.001
0.01
0.1
Grain Size, mm

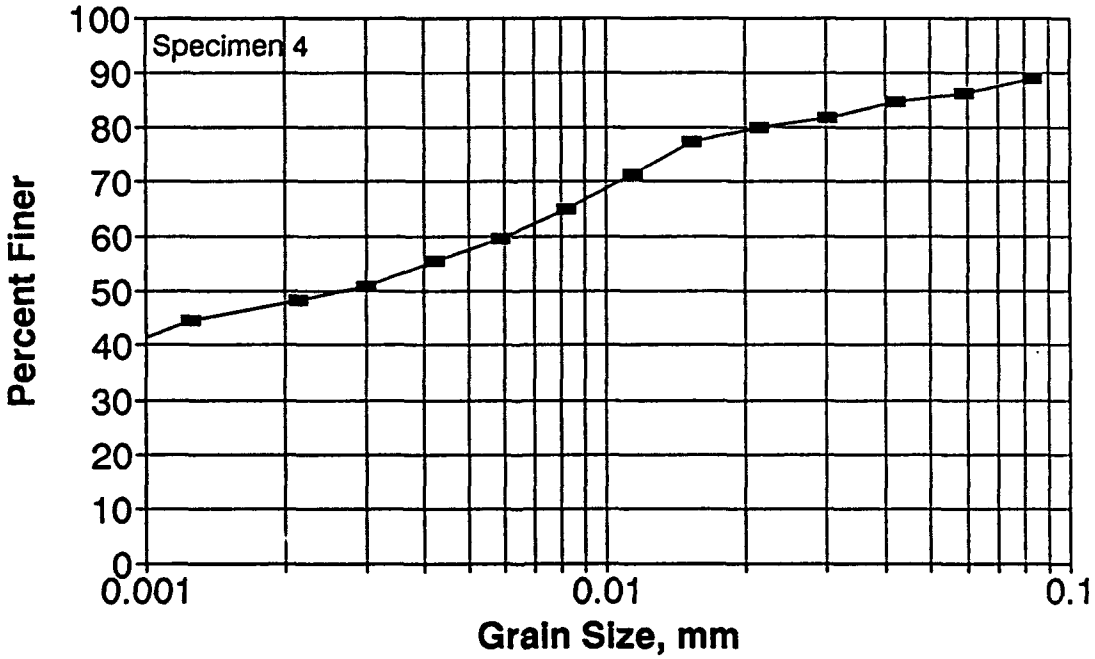
Specimen 4
Percent Finer
100
90
80
70
60
50
40
30
20
10
0
0.001
0.01
0.1
Grain Size, mm

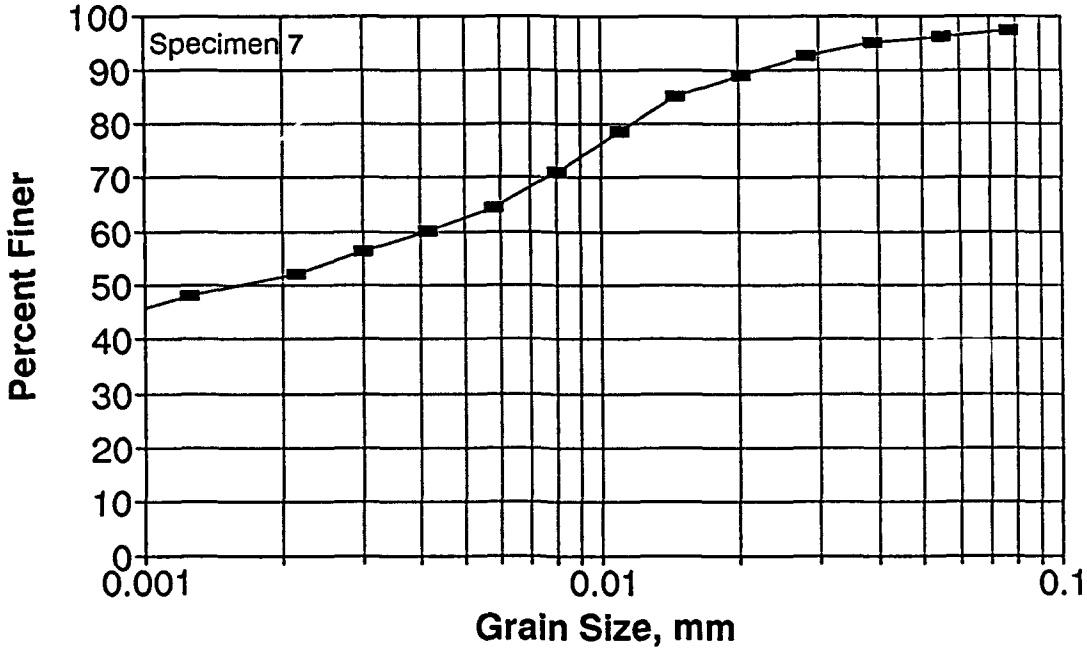
Specimen 7
Percent Finer
100
90
80
70
60
50
40
30
20
10
0
0.001
0.01
0.1
Grain Size, mm

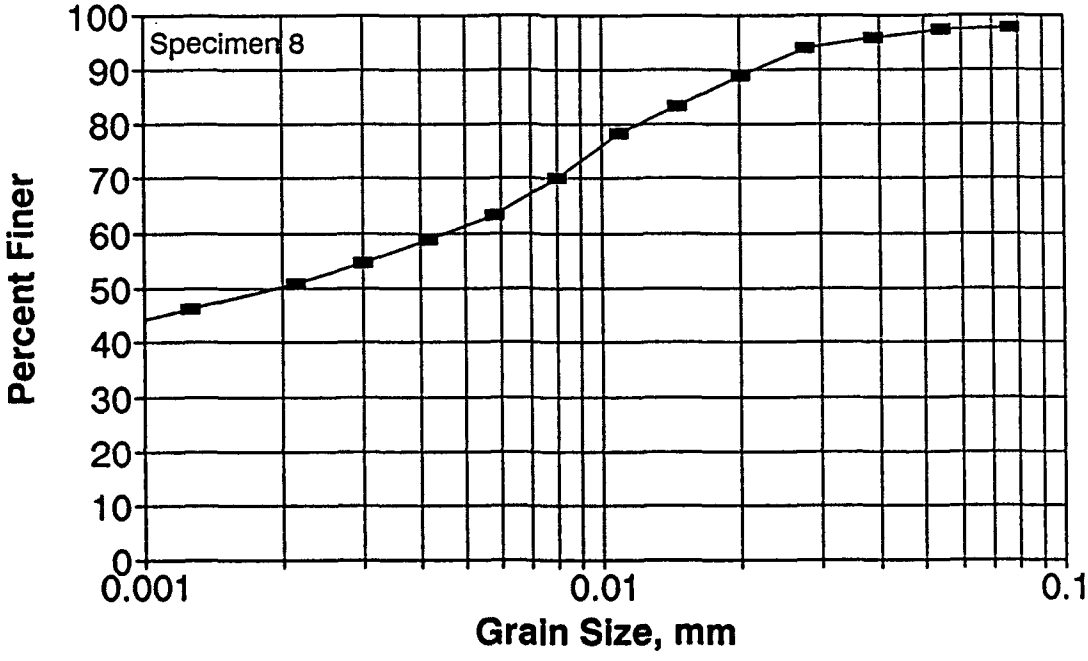
Specimen 8
Percent Finer
100
90
80
70
60
50
40
30
20
10
0
0.001
0.01
0.1
Grain Size, mm

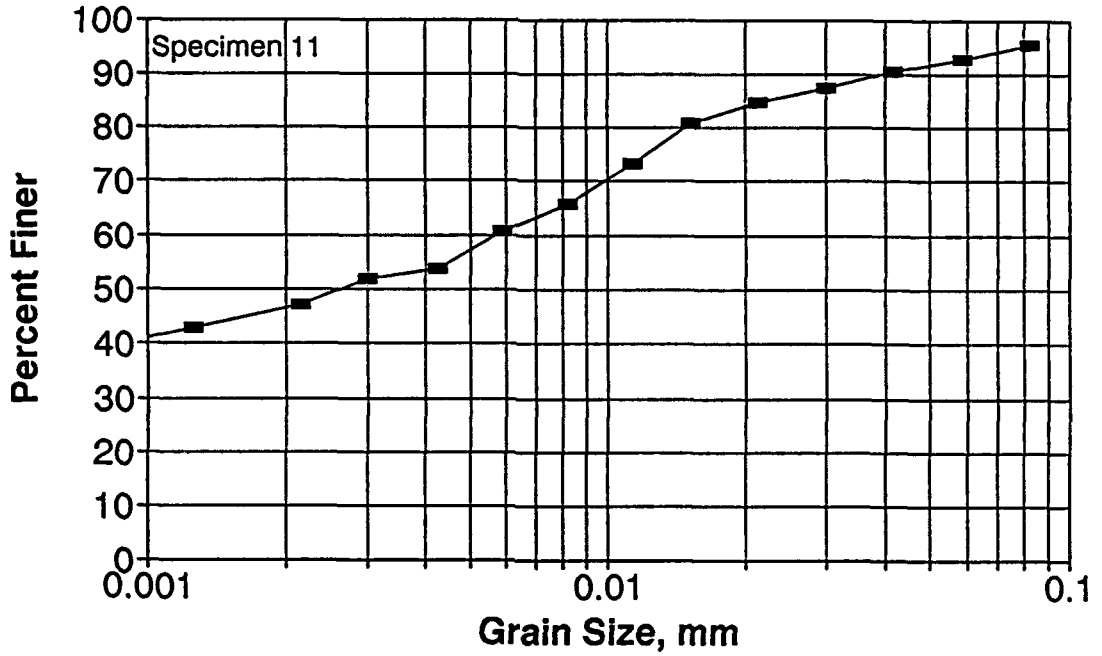
Specimen 11
Percent Finer
100
90
80
70
60
50
40
30
20
10
0
0.001
0.01
0.1
Grain Size, mm

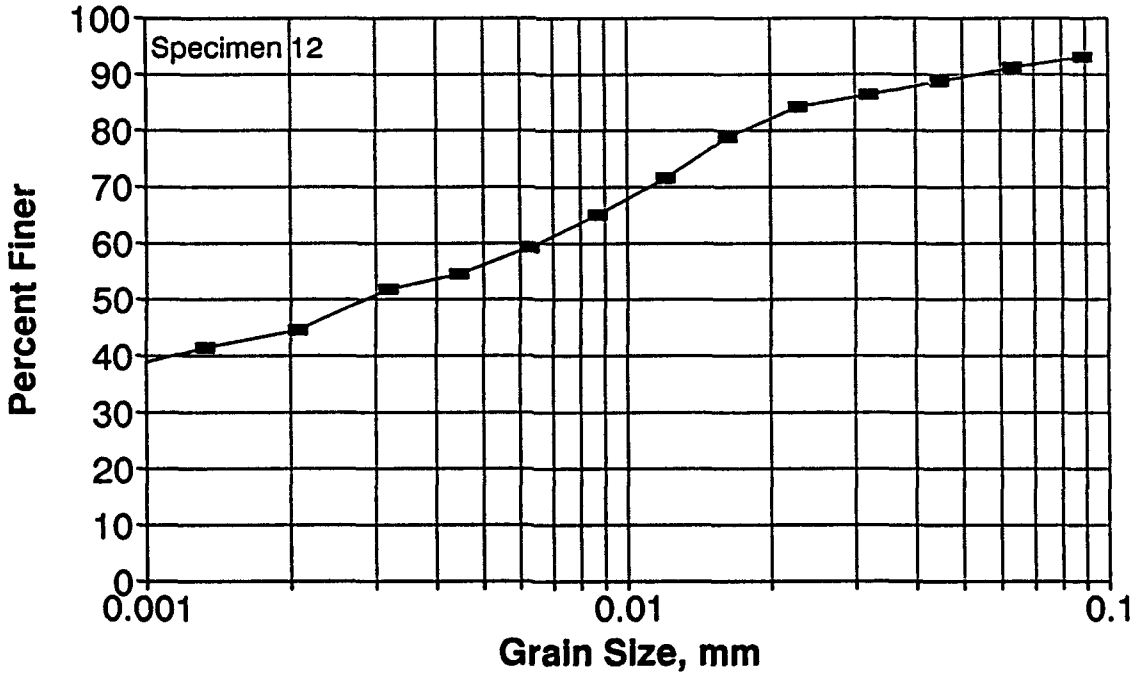
Specimen 12
Percent Finer
100
90
80
70
60
50
40
30
20
10
0
0.001
0.01
0.1
Grain Size, mm

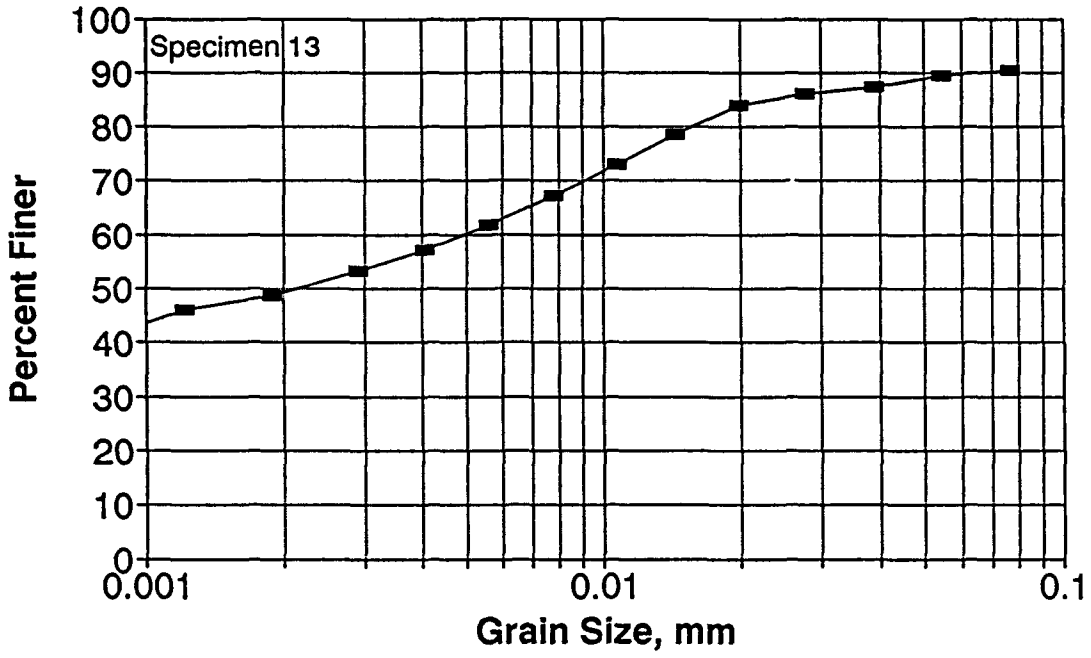
Specimen 13
100
90
80
70
60
50
40
30
20
10
0
Percent Finer
0.001
0.01
0.1
Grain Size, mm

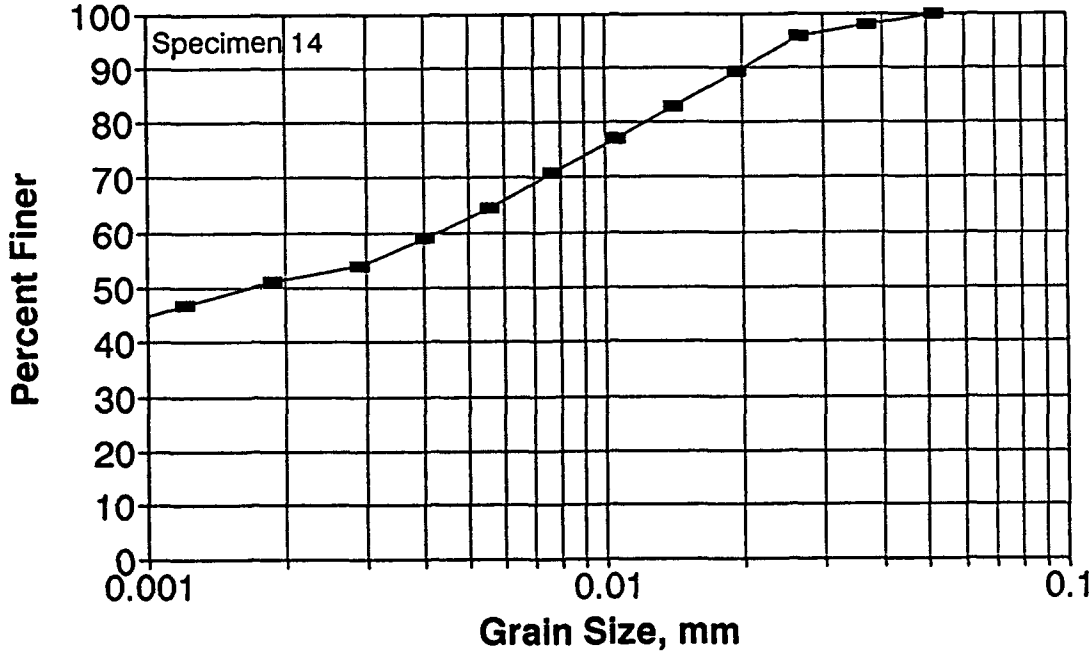
Specimen 14
100
90
80
70
60
50
40
30
20
10
0
Percent Finer
0.001
0.01
0.1
Grain Size, mm

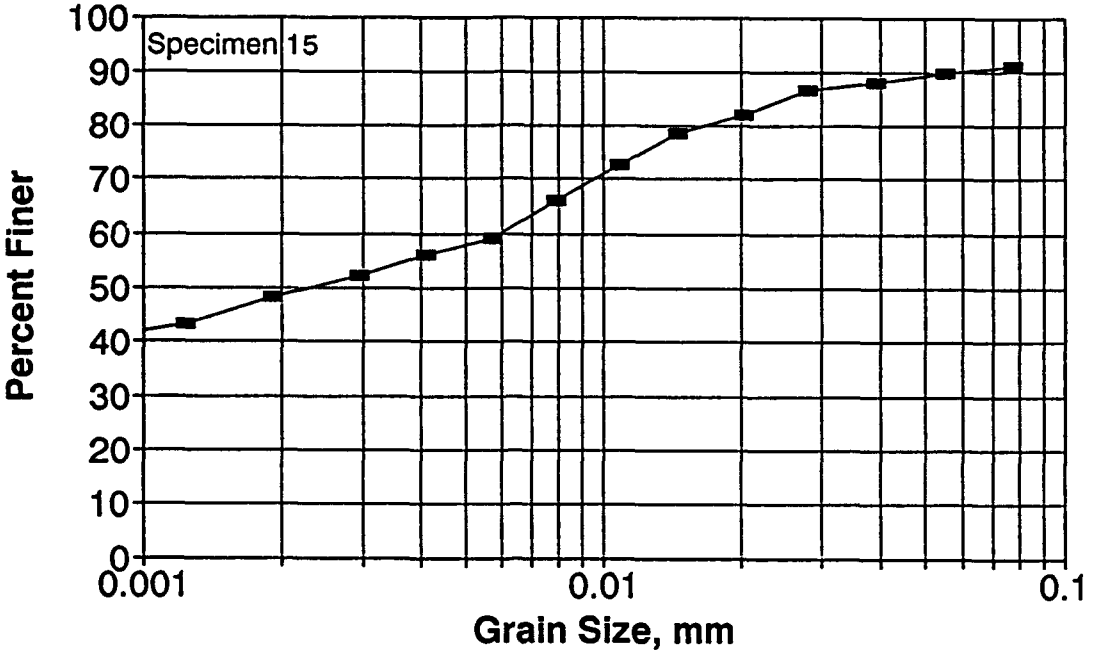
Specimen 15
Percent Finer
100
90
80
70
60
50
40
30
20
10
0
0.001
0.01
0.1
Grain Size, mm

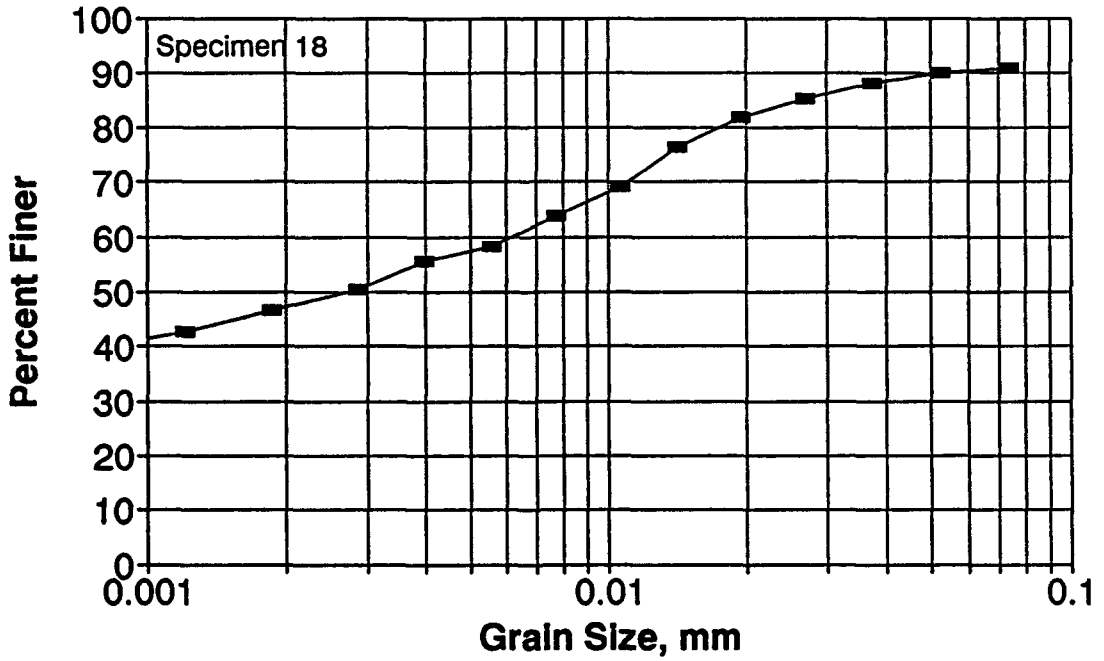
Specimen 18
Percent Finer
100
90
80
70
60
50
40
30
20
10
0
0.001
0.01
0.1
Grain Size, mm

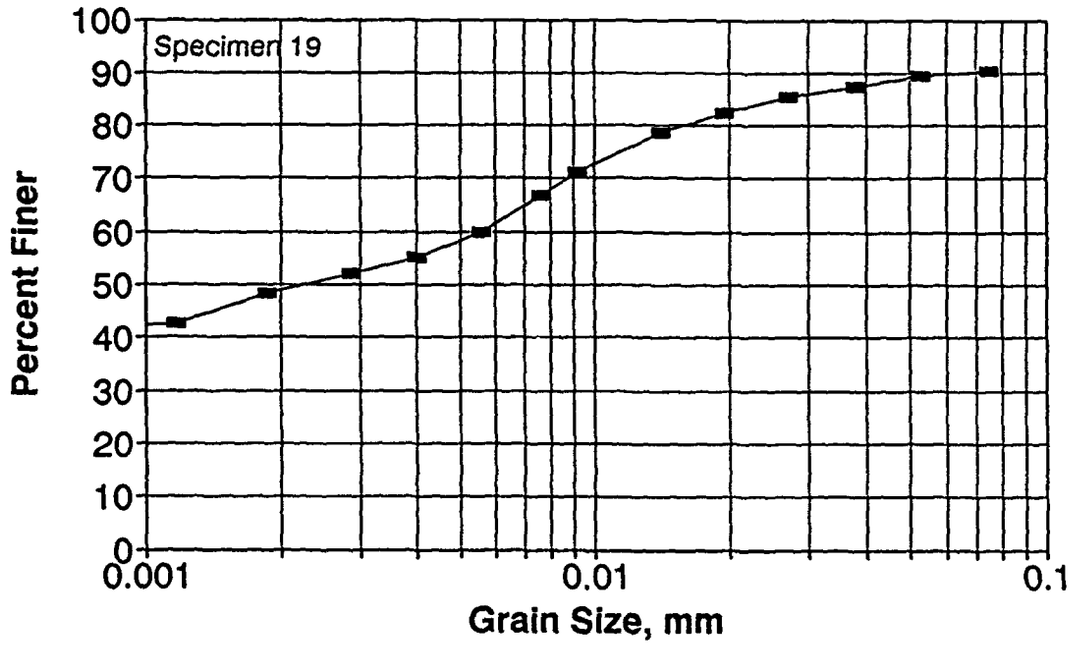
Specimen 19
100
90
80
70
60
50
40
30
20
10
0
Percent Finer
0.001
0.01
0.1
Grain Size, mm

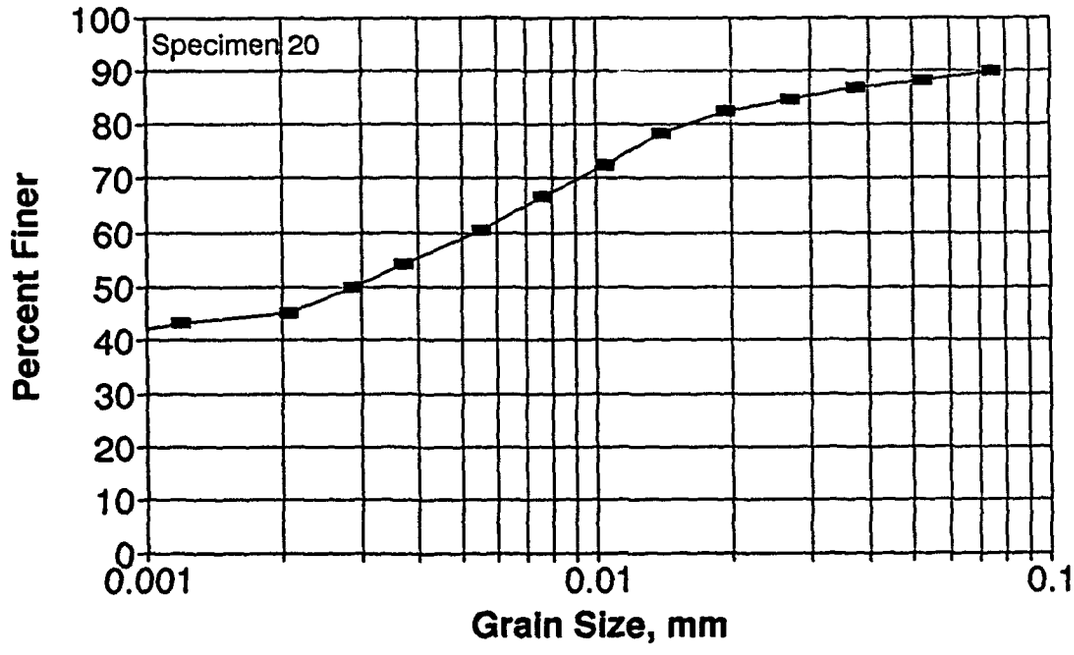
Specimen 20
100
90
80
70
60
50
40
30
20
10
0
Percent Finer
0.001
0.01
0.1
Grain Size, mm

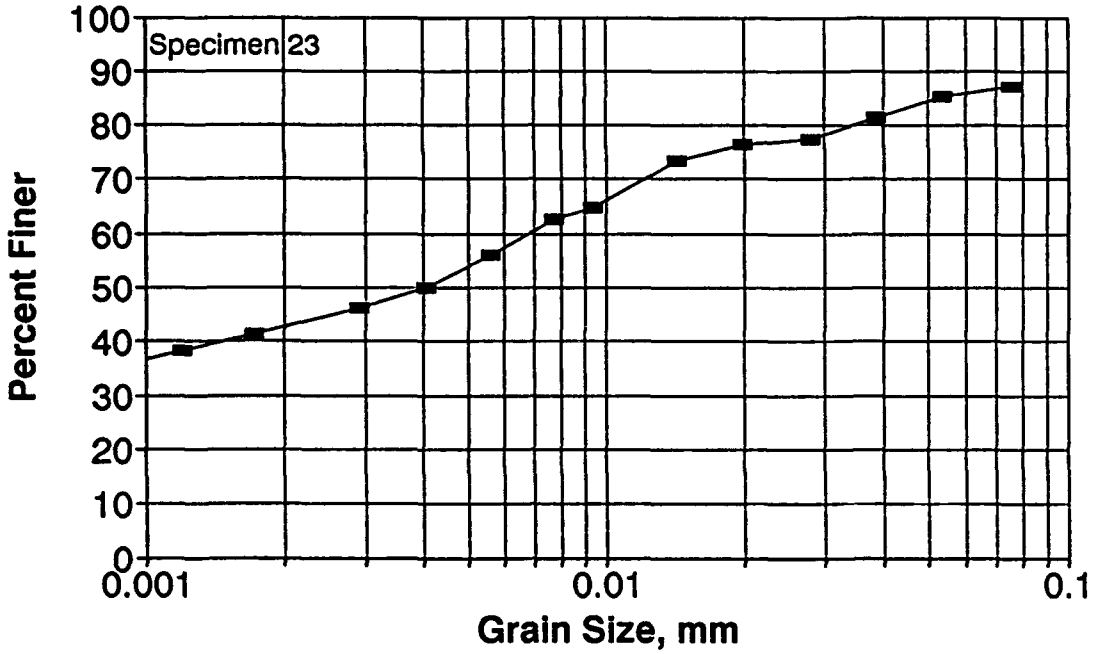
Specimen 23
Percent Finer
100
90
80
70
60
50
40
30
20
10
0
0.001
0.01
0.1
Grain Size, mm

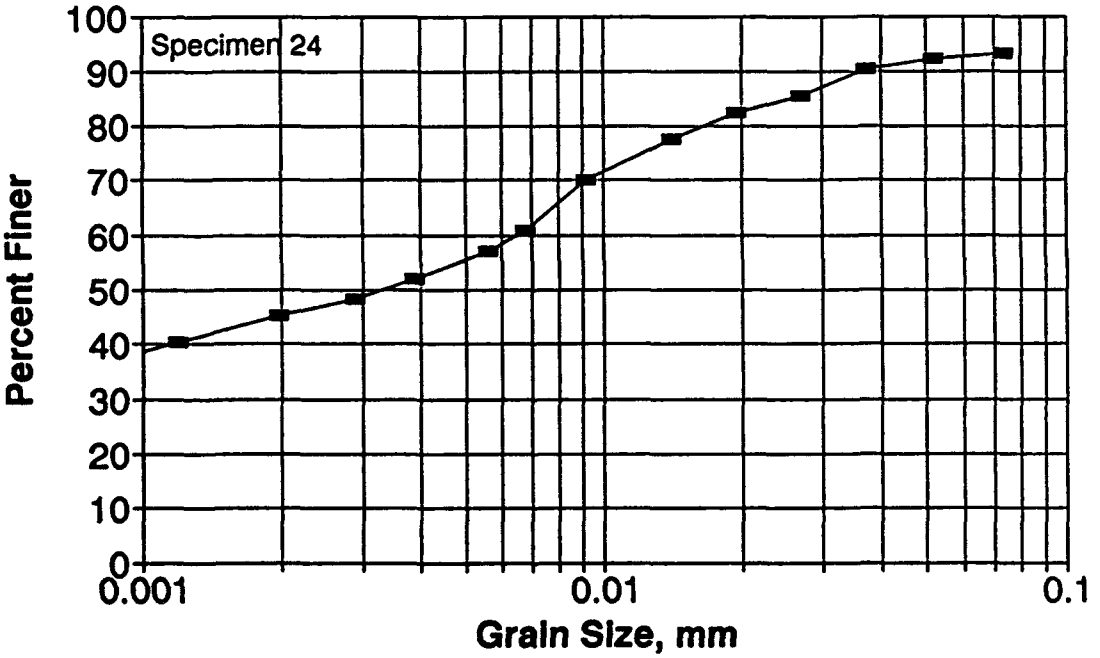
Specimen 24
Percent Finer
100
90
80
70
60
50
40
30
20
10
0
0.001
0.01
0.1
Grain Size, mm

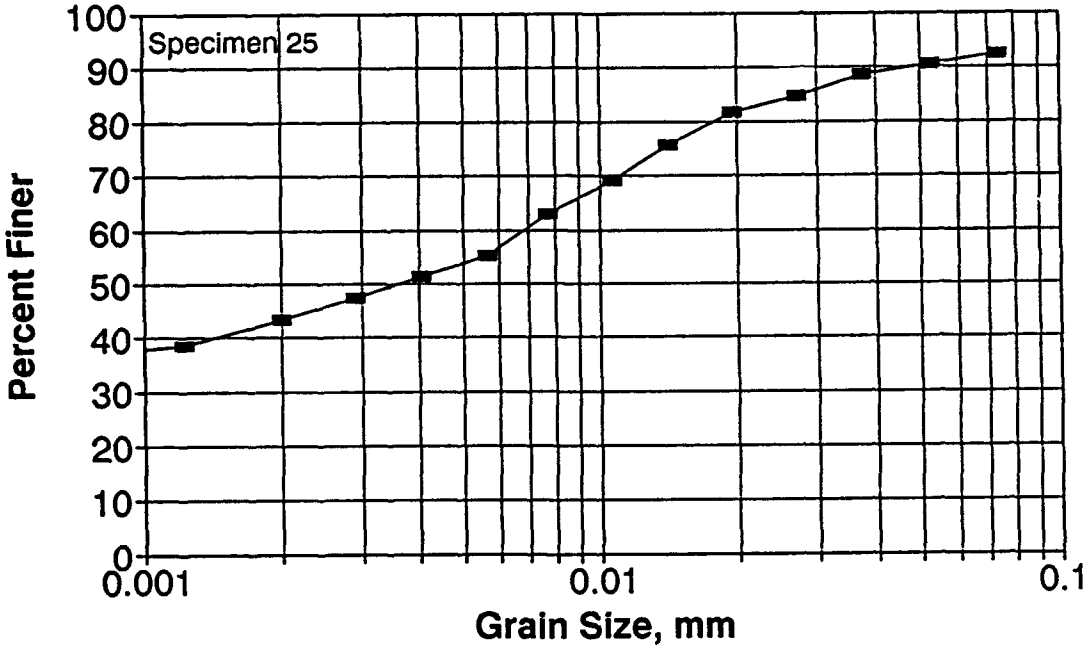
Specimen 25
Percent Finer
100
90
80
70
60
50
40
30
20
10
0
0.001
0.01
0.1
Grain Size, mm

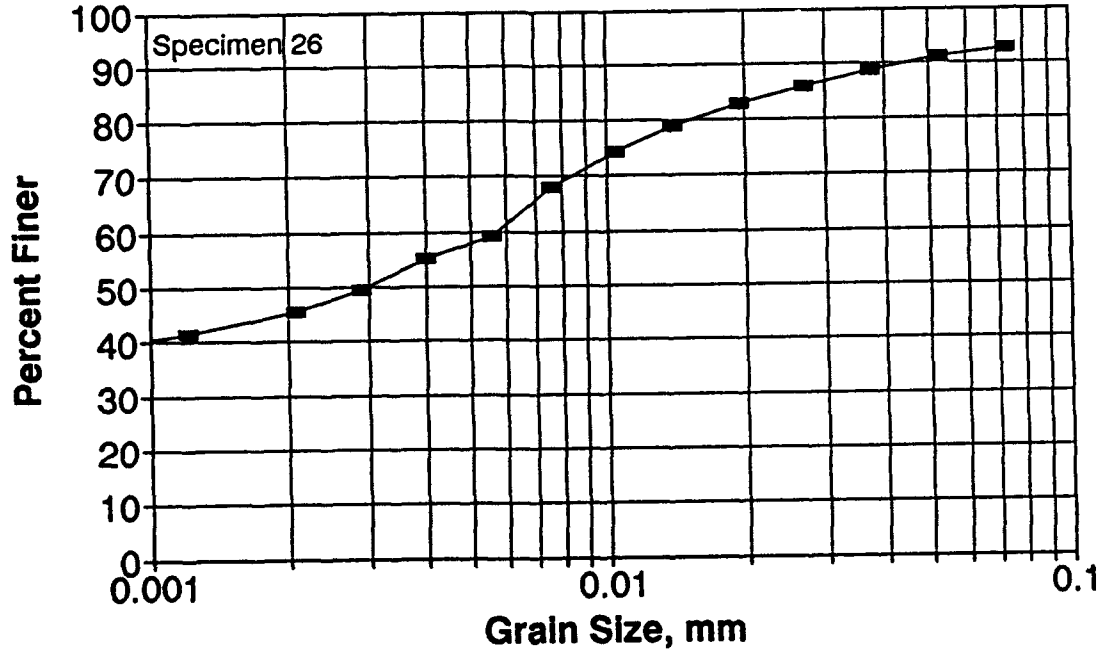
Specimen 26
Percent Finer
100
90
80
70
60
50
40
30
20
10
0
0.001
0.01
0.1
Grain Size, mm

APPENDIX F

X-RAY DIFFRACTION PATTERNS FOR CLAY MINERAL IDENTIFICATION

X-Ray Diffraction Patterns for Specimen 1 (Fine Clay)

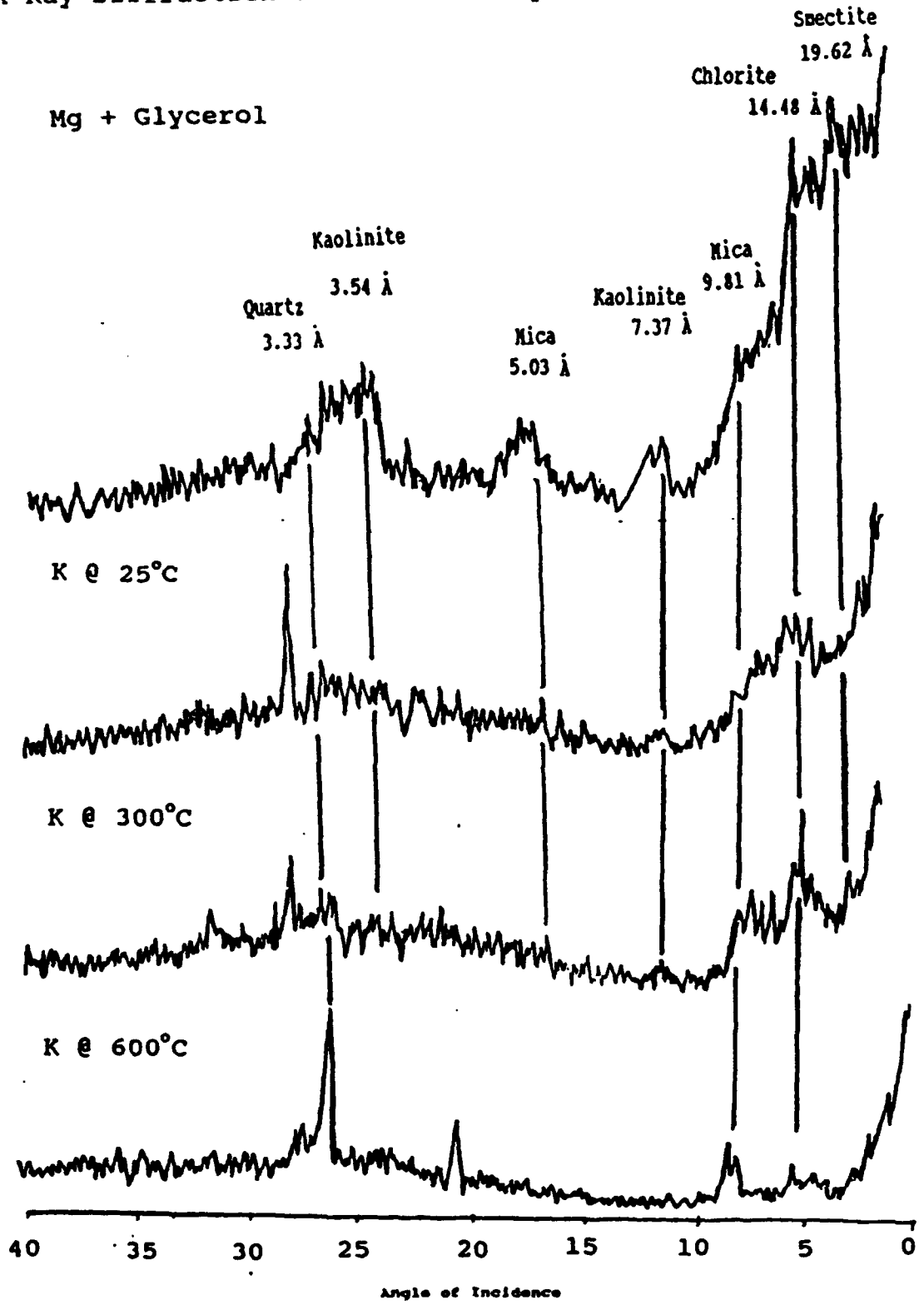

X-Ray Diffraction Patterns for Specimen 1 (Coarse Clay)

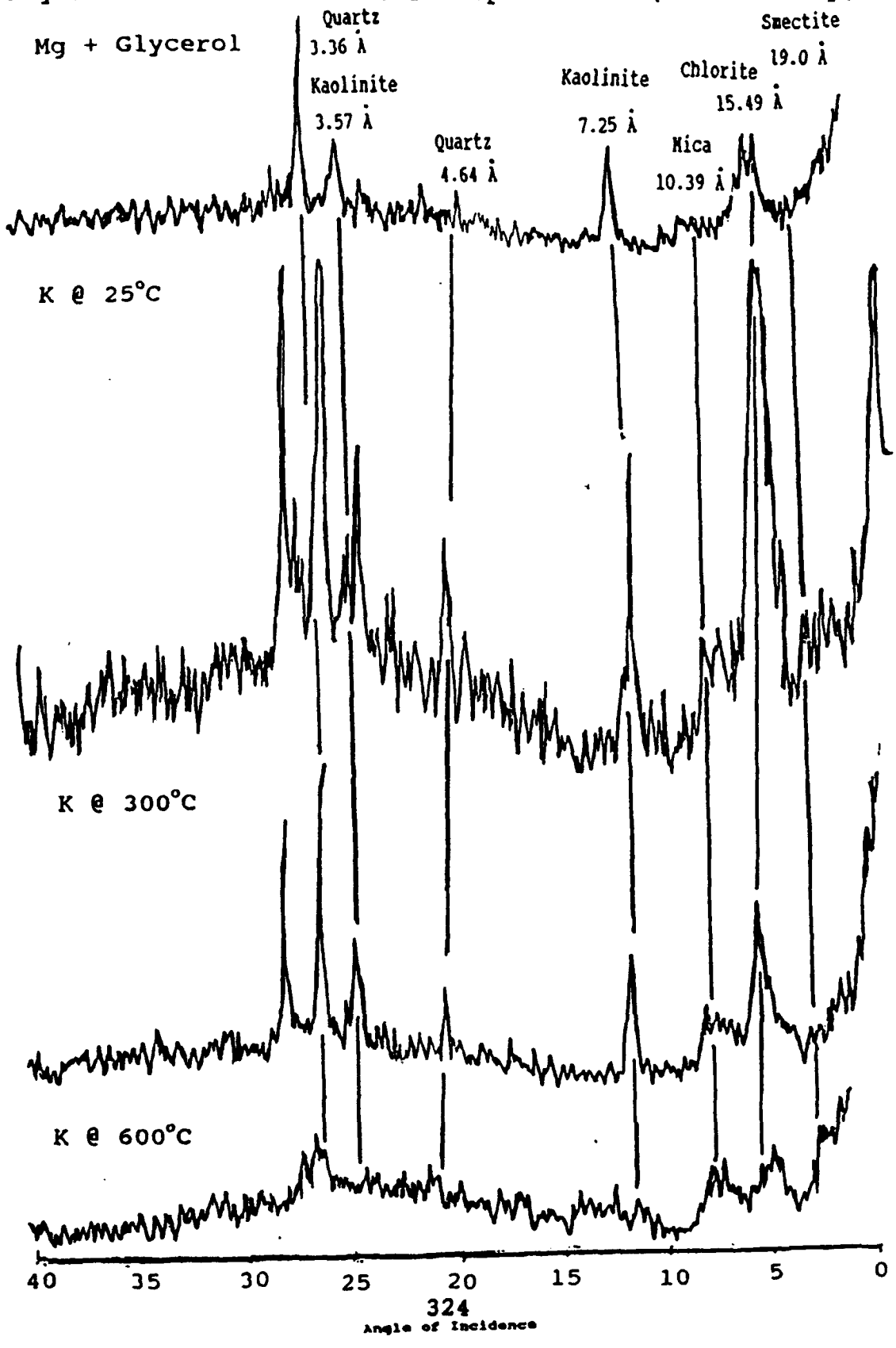

X-Ray Diffraction Patterns for Specimen 2 (Fine Clay)

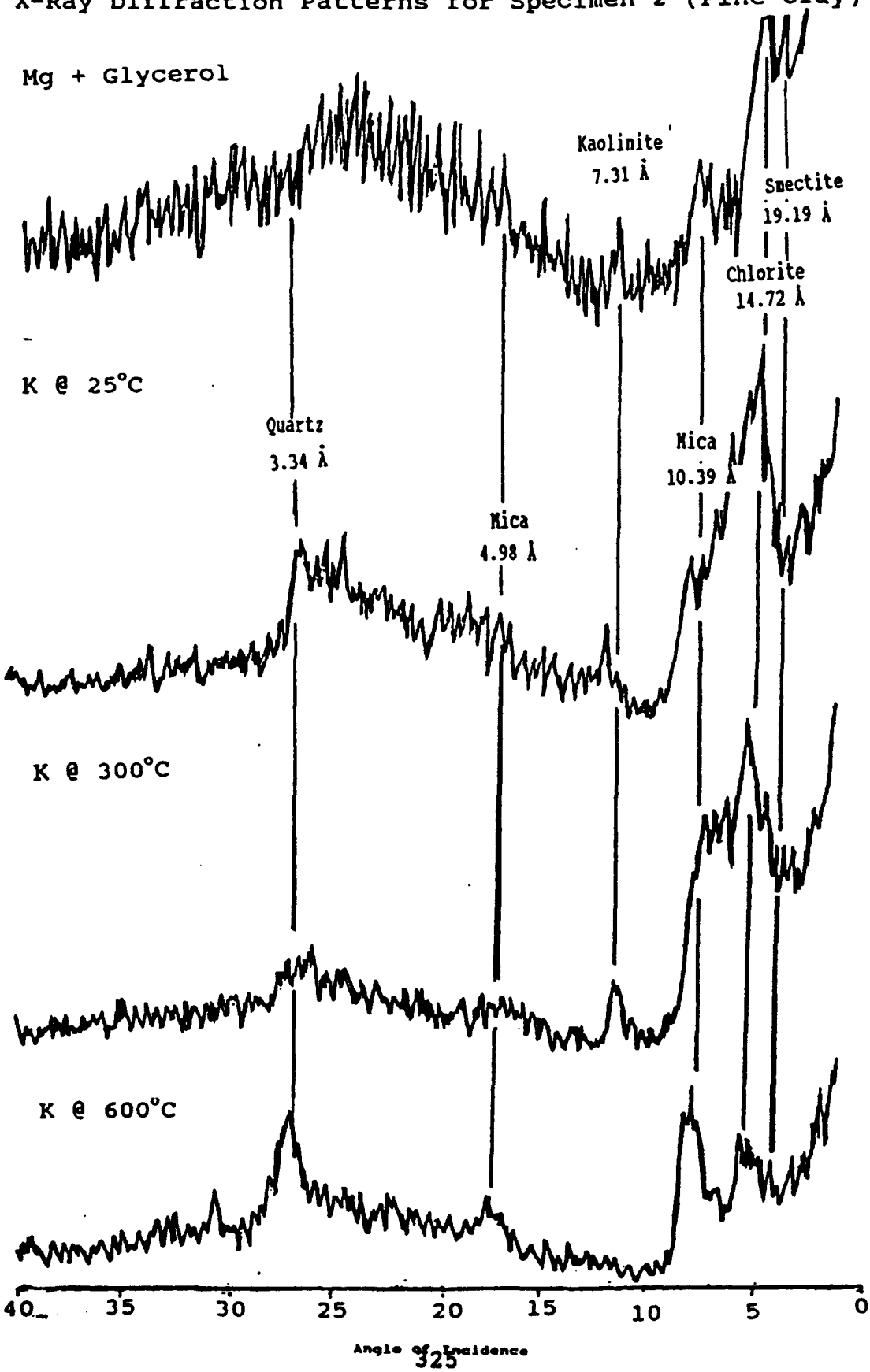

X-Ray Diffraction Patterns for Specimen 2 (Coarse Clay)

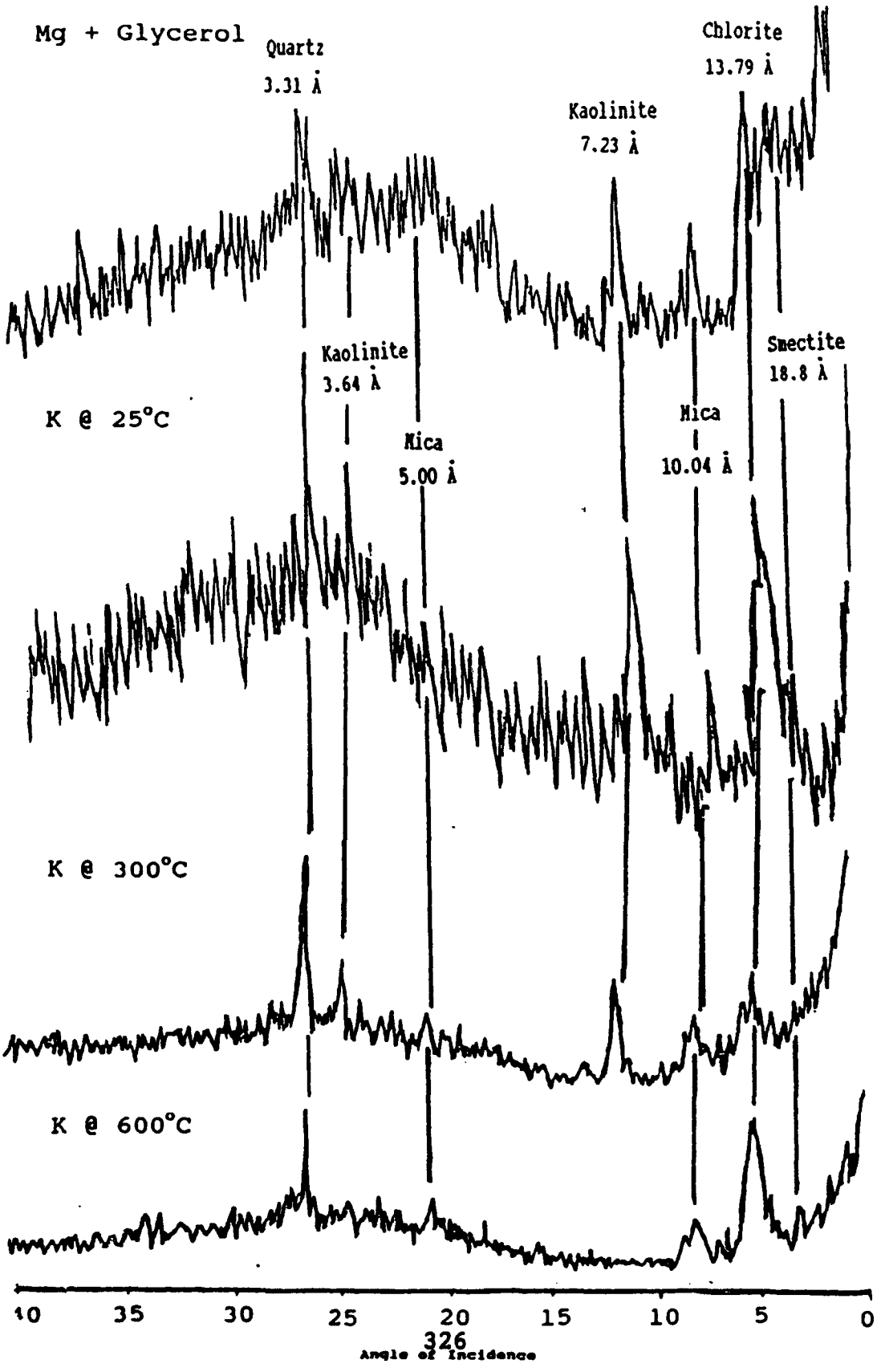

X-Ray Diffraction Patterns for Specimen 3 (Fine Clay)

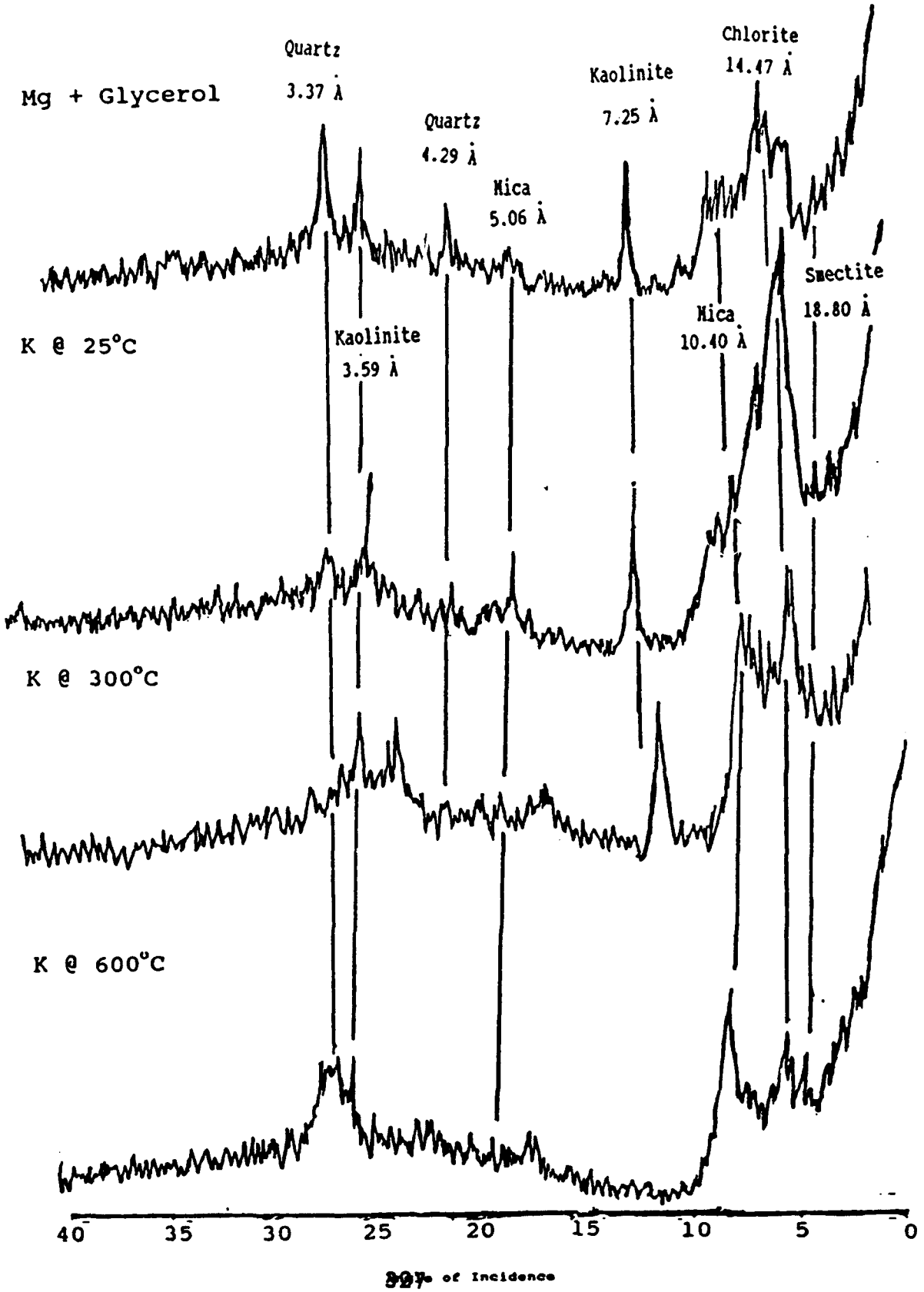

X-Ray Diffraction Patterns for Specimen 3 (Coarse Clay)

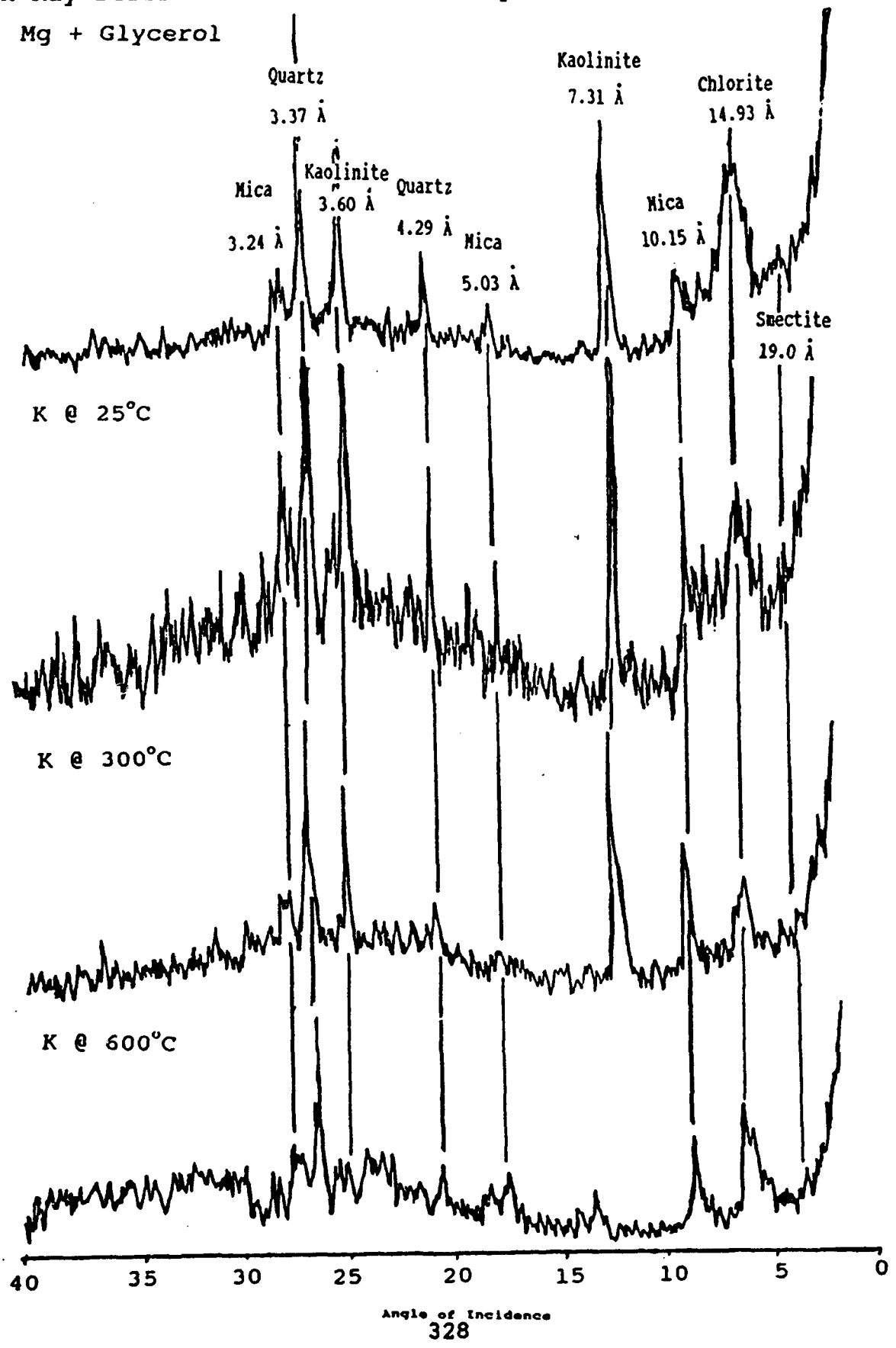

X-Ray Diffraction Patterns for Specimen 4 (Fine Clay)

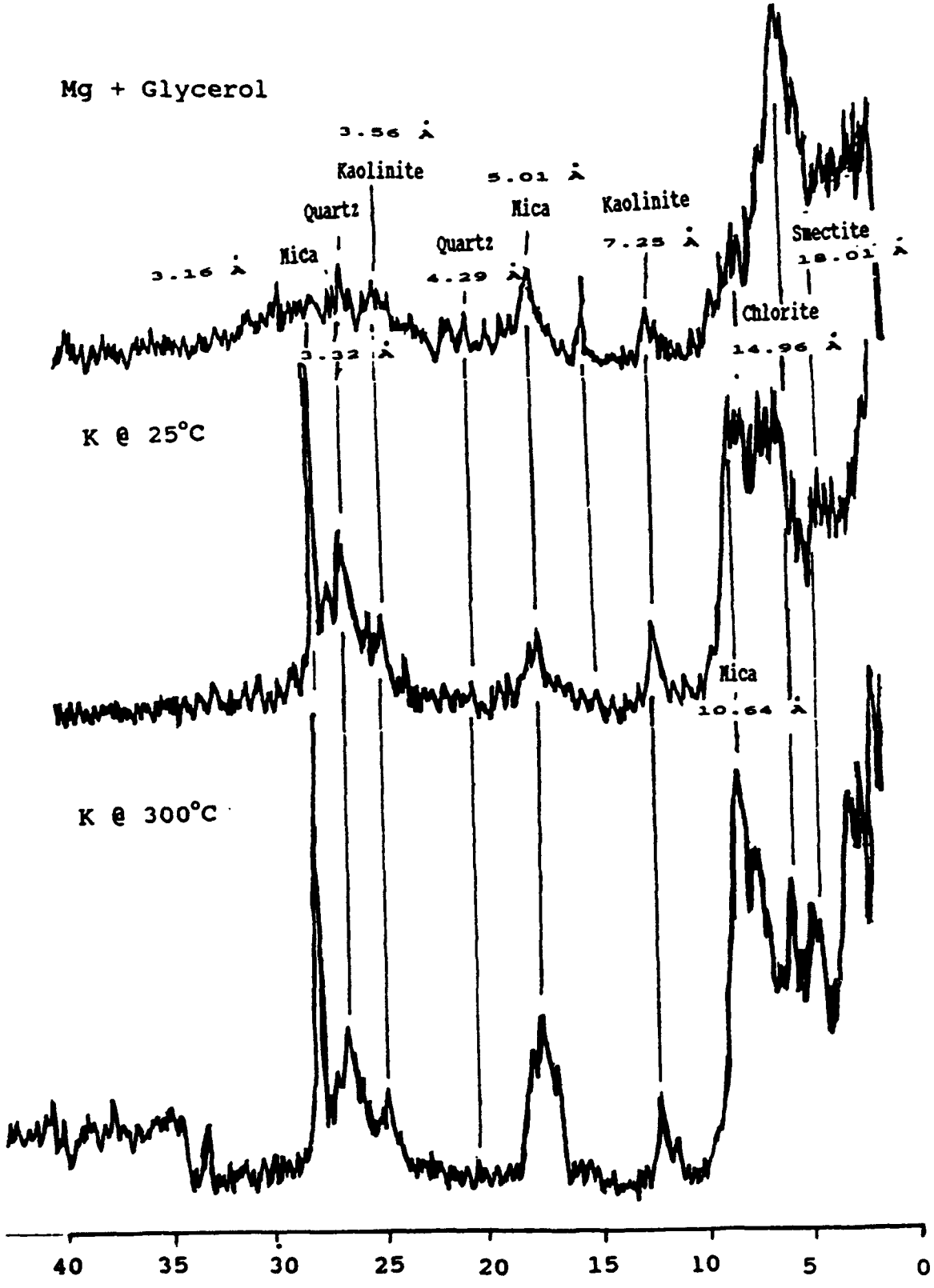

X-Ray Diffraction Patterns for Specimen 4 (Coarse Clay)

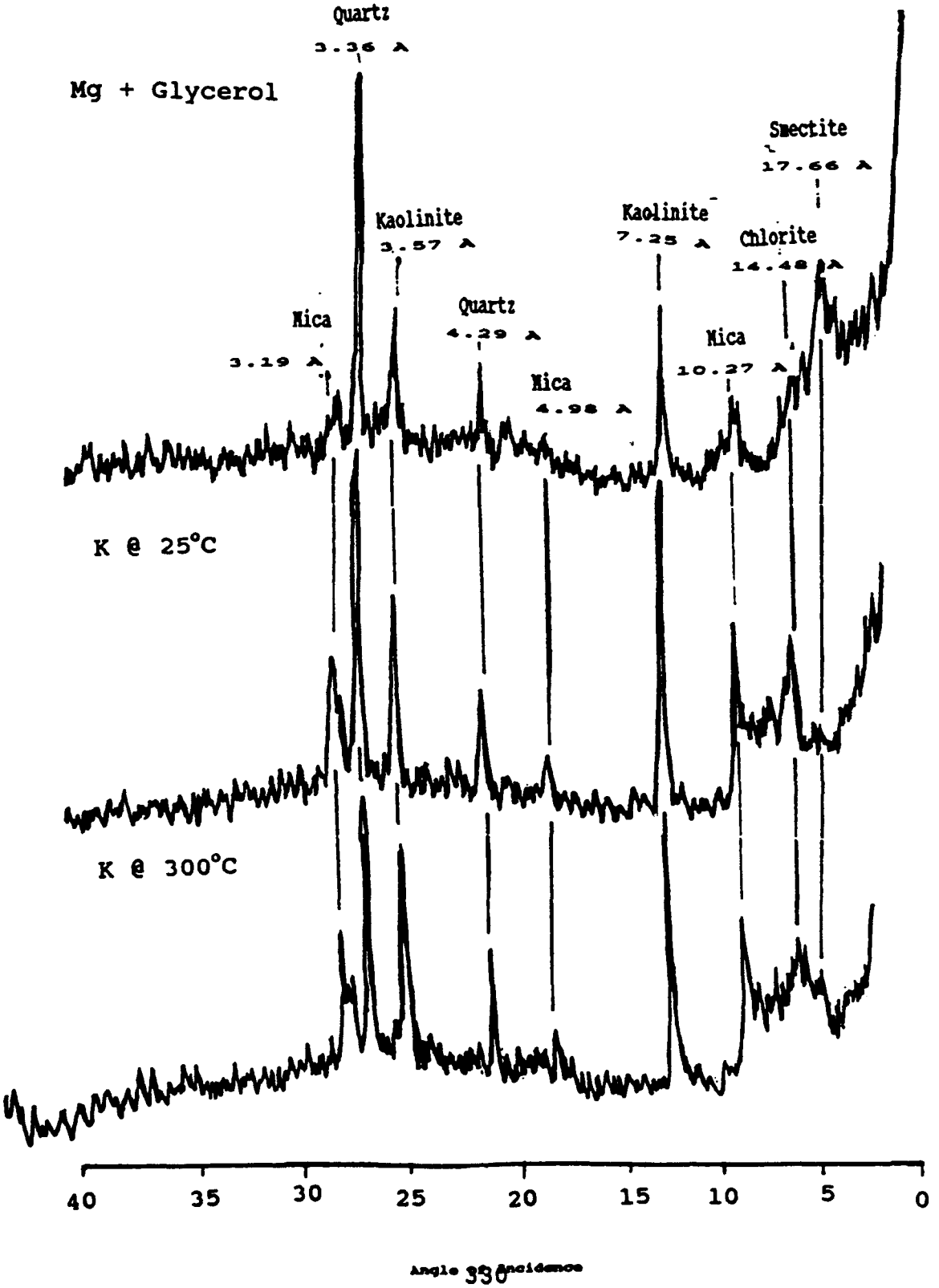

X-Ray Diffraction Patterns for Specimen 1 and 2 (Silt)

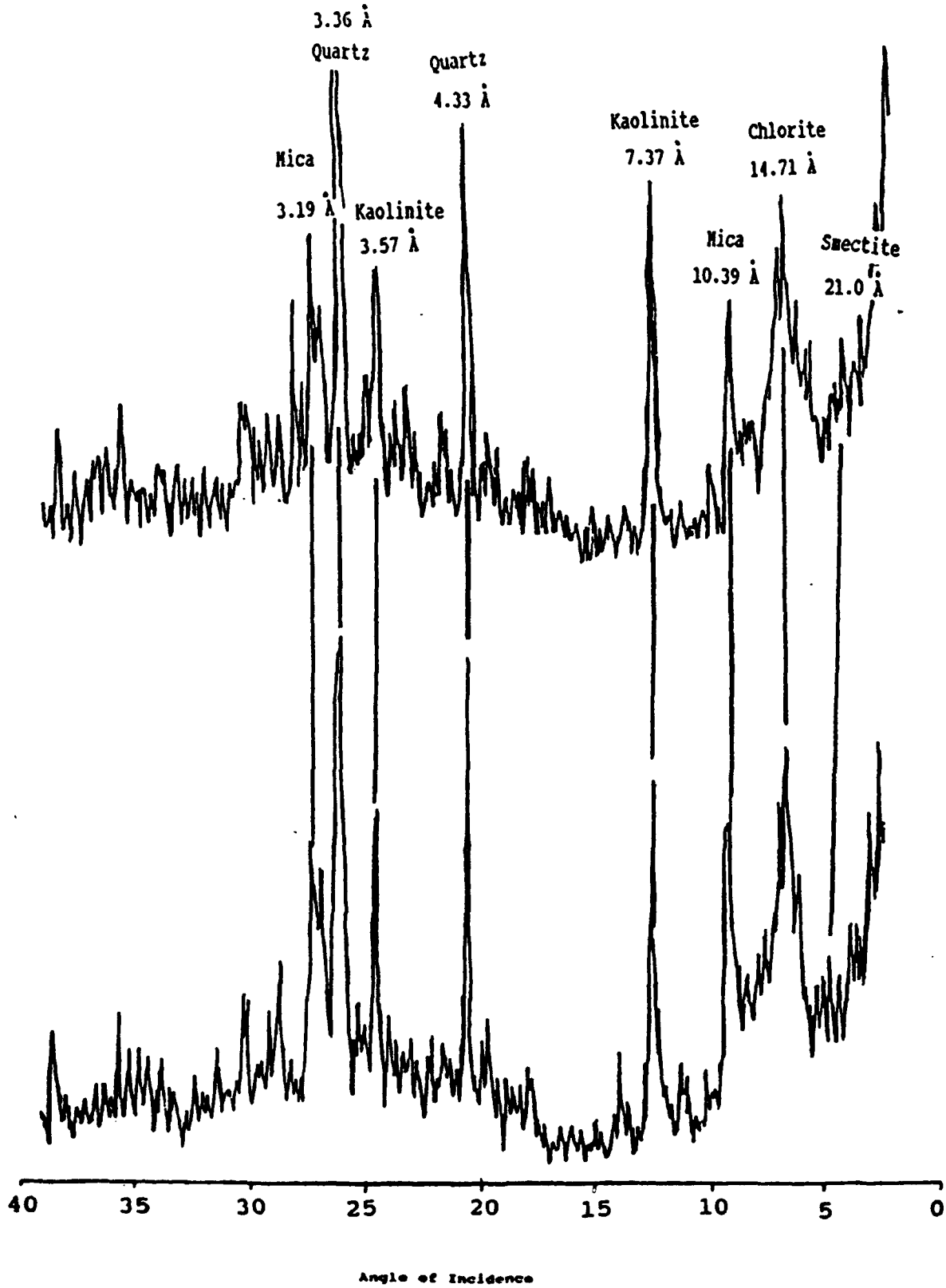

APPENDIX G

PREDICTION OF CREEP

WITH THE FOUR PARAMETER EXPONENTIAL MODEL

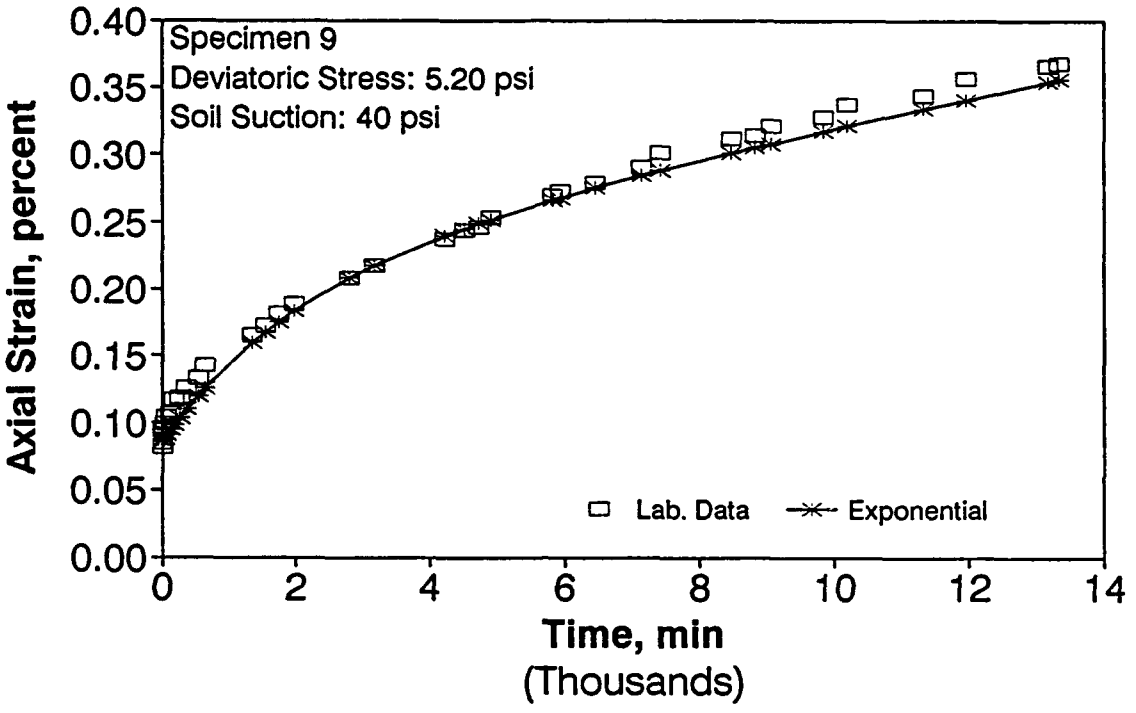
Specimen 9
Deviatoric Stress: 5.20 psi
Soil Suction: 40 psi
Axial Strain, percent
0.40
0.35
0.30
0.25
0.20
0.15
0.10
0.05
0.00
0
2
4
6
8
10
12
14
Lab. Data
Exponential
Time, min
(Thousands)

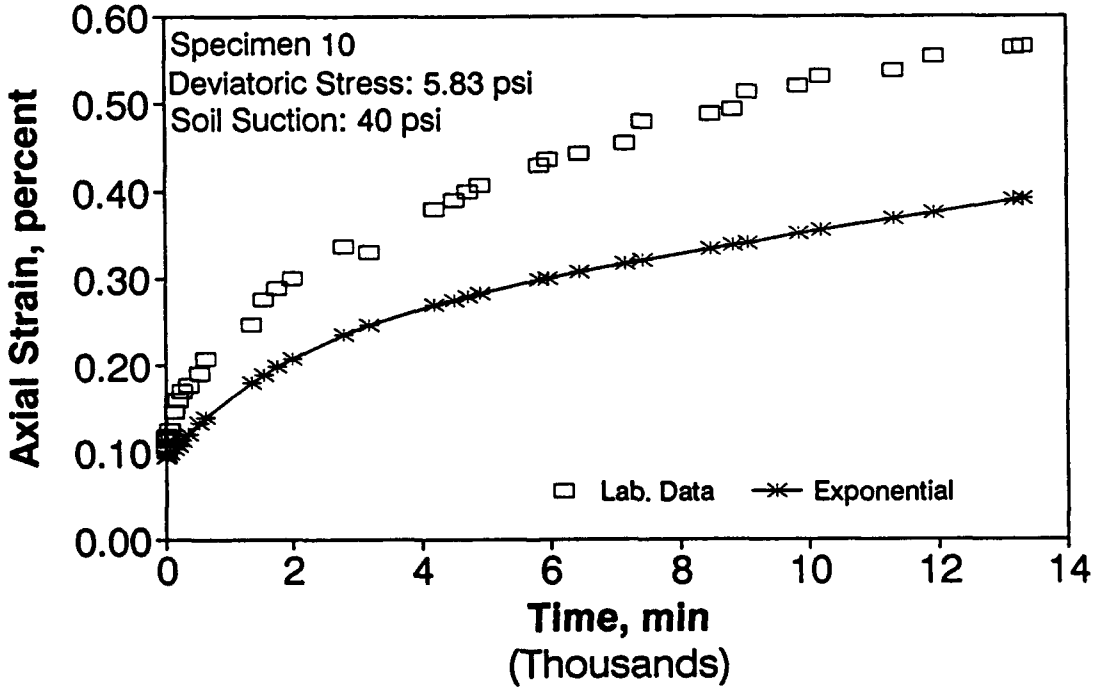
Specimen 10
Deviatoric Stress: 5.83 psi
Soil Suction: 40 psi
Axial Strain, percent
0.60
0.50
0.40
0.30
0.20
0.10
0.00
0
2
4
6
8
10
12
14
Lab. Data
Exponential
Time, min
(Thousands)

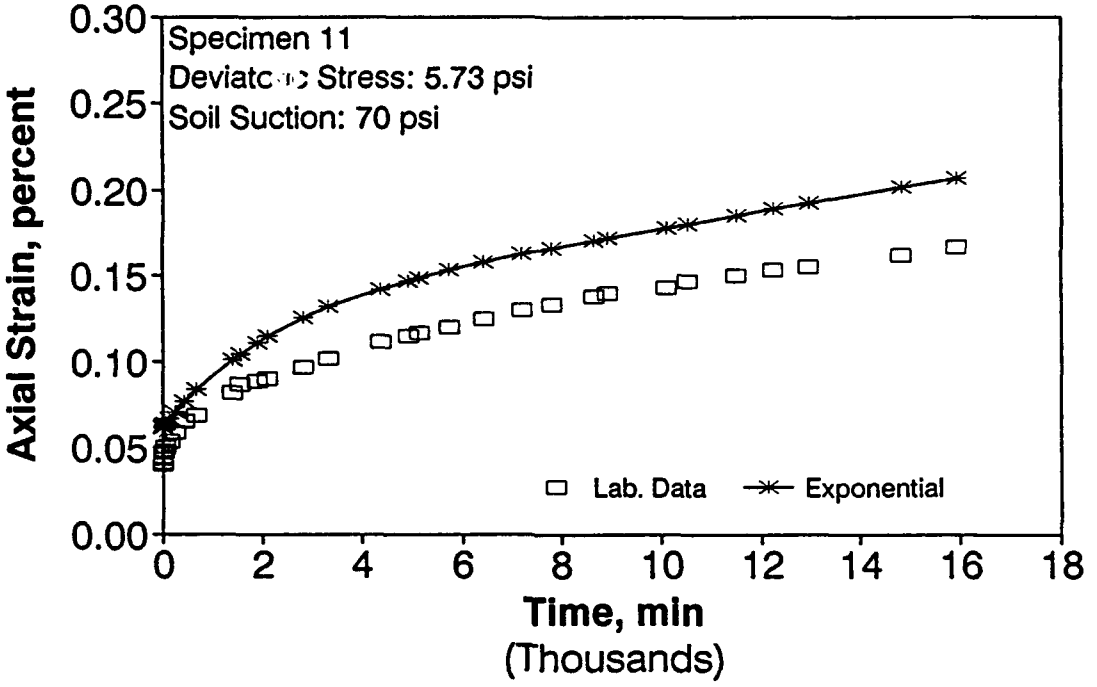
Specimen 11
Deviatoric Stress: 5.73 psi
Soil Suction: 70 psi
Axial Strain, percent
0.30
0.25
0.20
0.15
0.10
0.05
0.00
0
2
4
6
8
10
12
14
16
18
Lab. Data
Exponential
Time, min
(Thousands)

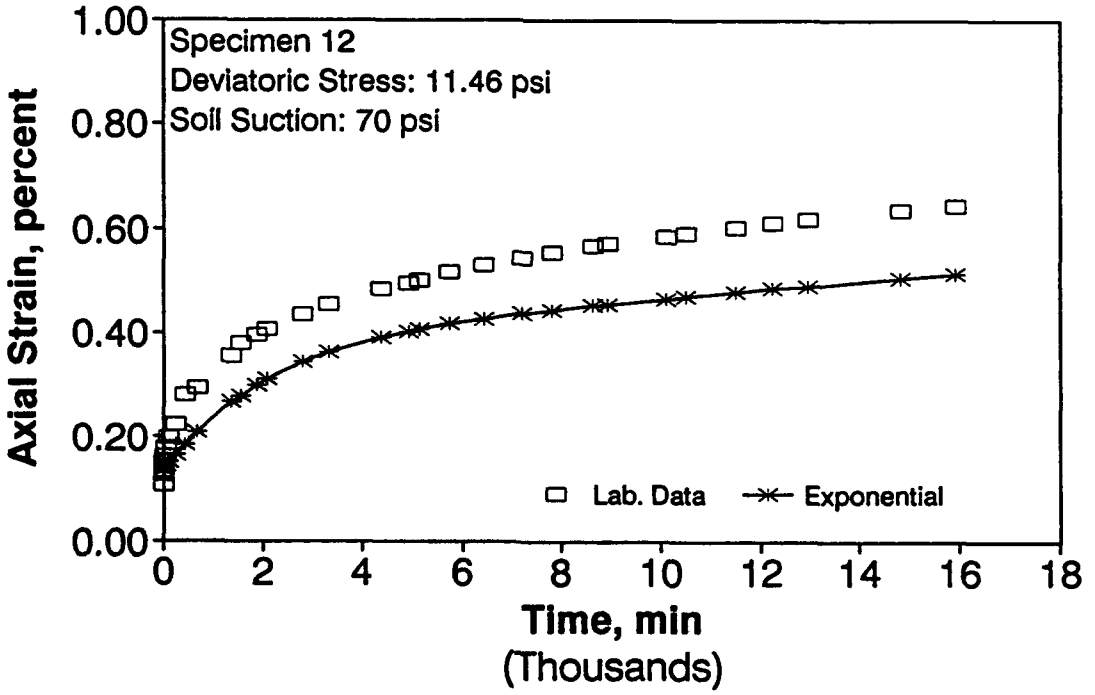
Specimen 12
Deviatoric Stress: 11.46 psi
Soil Suction: 70 psi
Axial Strain, percent
1.00
0.80
0.60
0.40
0.20
0.00
0
2
4
6
8
10
12
14
16
18
Lab. Data
Exponential
Time, min
(Thousands)

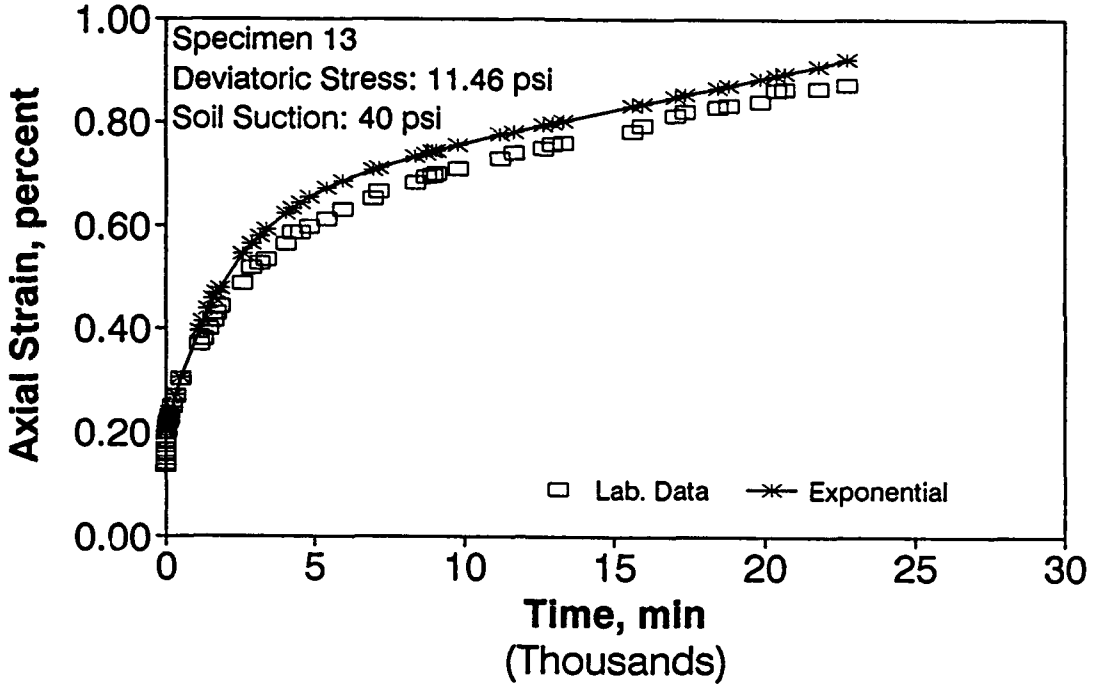
Specimen 13
Deviatoric Stress: 11.46 psi
Soil Suction: 40 psi
Axial Strain, percent
1.00
0.80
0.60
0.40
0.20
0.00
0
5
10
15
20
25
30
Time, min
(Thousands)
Lab. Data
Exponential

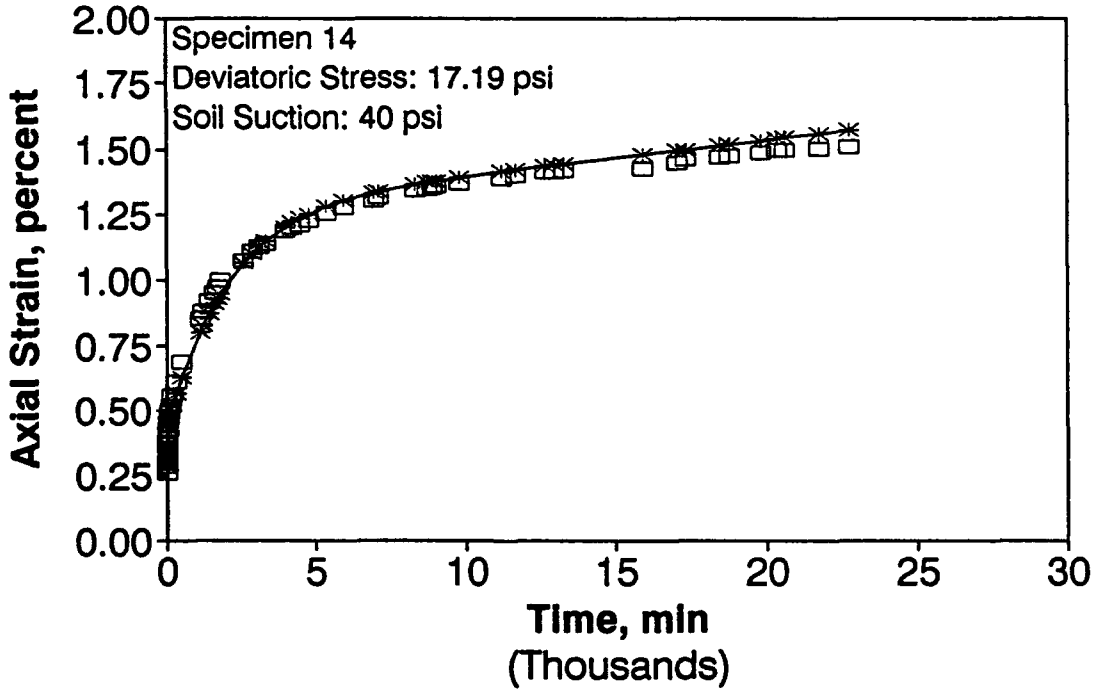
Specimen 14
Deviatoric Stress: 17.19 psi
Soil Suction: 40 psi
Axial Strain, percent
2.00
1.75
1.50
1.25
1.00
0.75
0.50
0.25
0.00
0
5
10
15
20
25
30
Time, min
(Thousands)
Lab. Data
Exponential

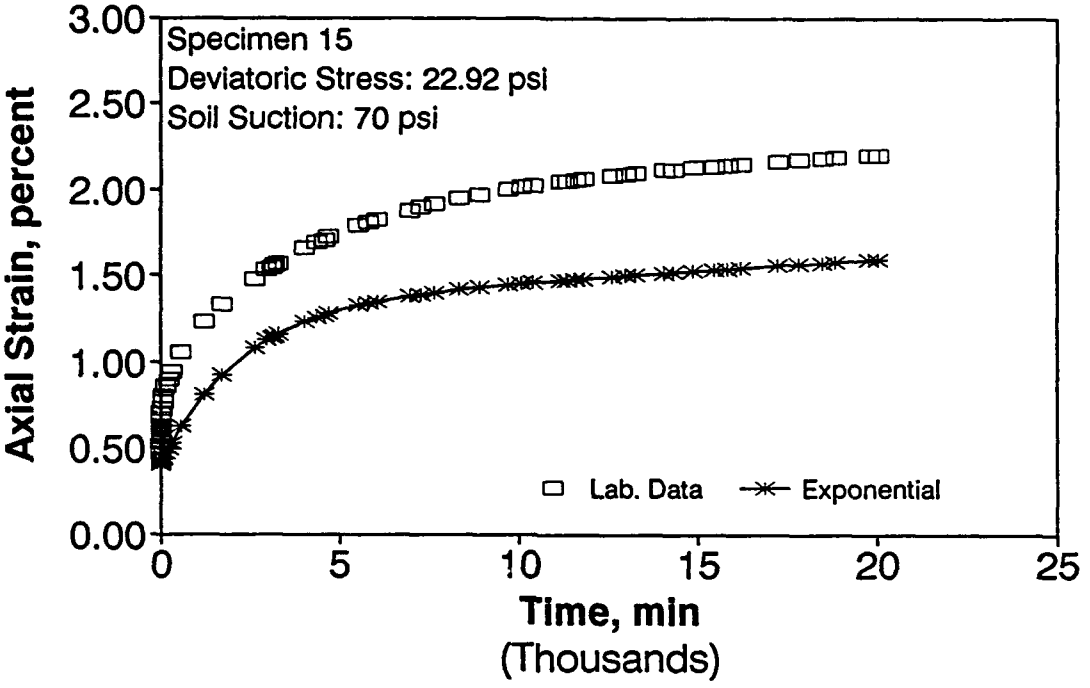
Specimen 15
Deviatoric Stress: 22.92 psi
Soil Suction: 70 psi
Axial Strain, percent
3.00
2.50
2.00
1.50
1.00
0.50
0.00
0
5
10
15
20
25
Time, min
(Thousands)
Lab. Data
Exponential

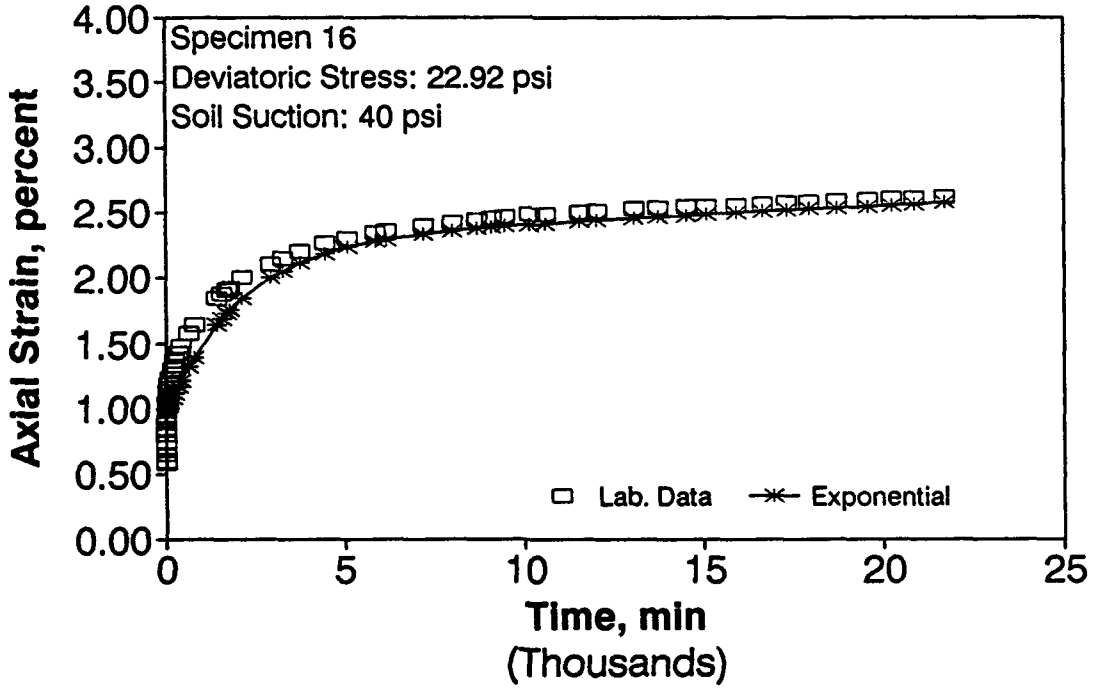
Specimen 16
Deviatoric Stress: 22.92 psi
Soil Suction: 40 psi
Axial Strain, percent
4.00
3.50
3.00
2.50
2.00
1.50
1.00
0.50
0.00
0
5
10
15
20
25
Time, min
(Thousands)
Lab. Data
Exponential

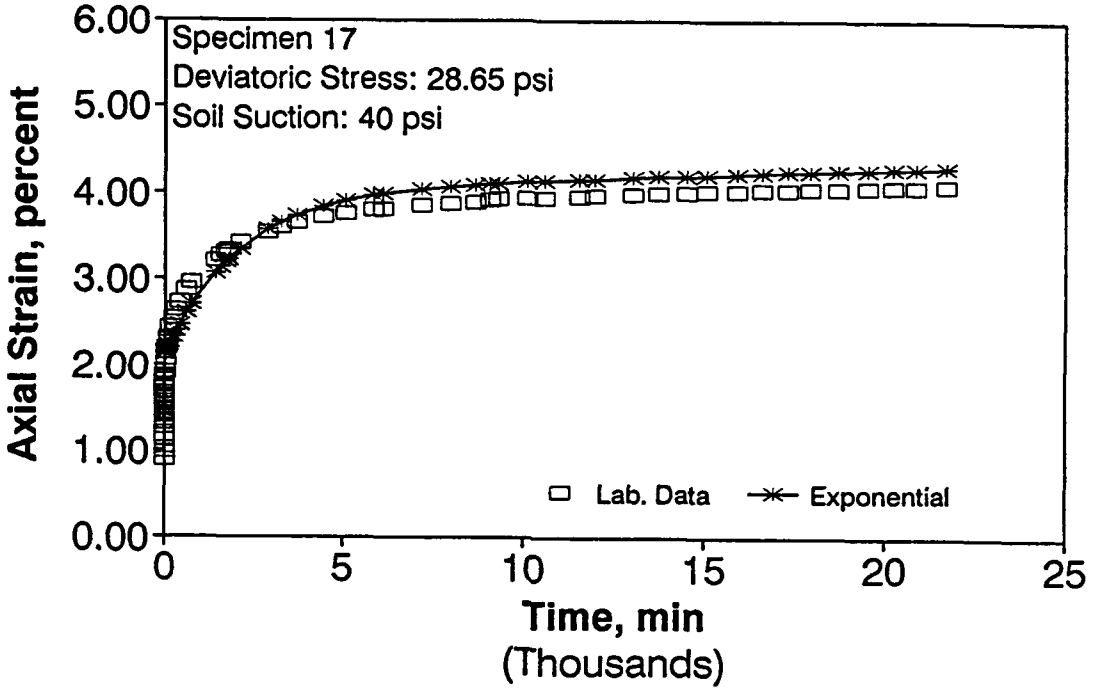
Specimen 17
Deviatoric Stress: 28.65 psi
Soil Suction: 40 psi
Axial Strain, percent
6.00
5.00
4.00
3.00
2.00
1.00
0.00
0
5
10
15
20
25
Lab. Data
Exponential
Time, min
(Thousands)

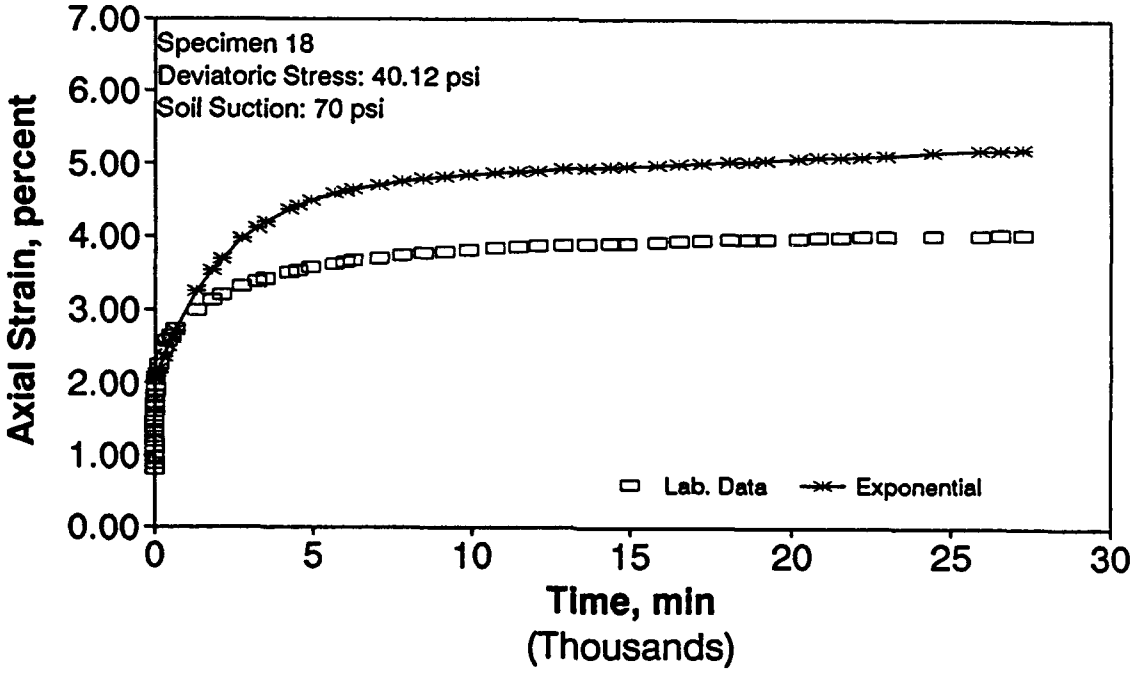
Specimen 18
Deviatoric Stress: 40.12 psi
Soil Suction: 70 psi
Axial Strain, percent
7.00
6.00
5.00
4.00
3.00
2.00
1.00
0.00
0
5
10
15
20
25
30
Lab. Data
Exponential
Time, min
(Thousands)

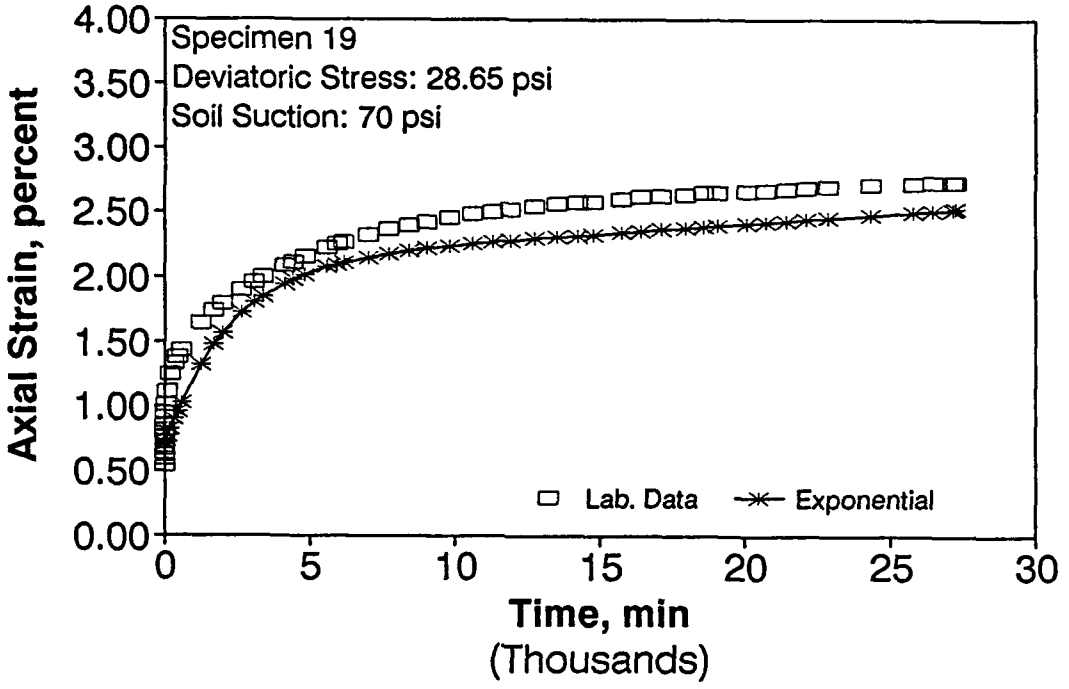
Specimen 19
Deviatoric Stress: 28.65 psi
Soil Suction: 70 psi
Axial Strain, percent
4.00
3.50
3.00
2.50
2.00
1.50
1.00
0.50
0.00
0
5
10
15
20
25
30
Time, min
(Thousands)
Lab. Data
Exponential

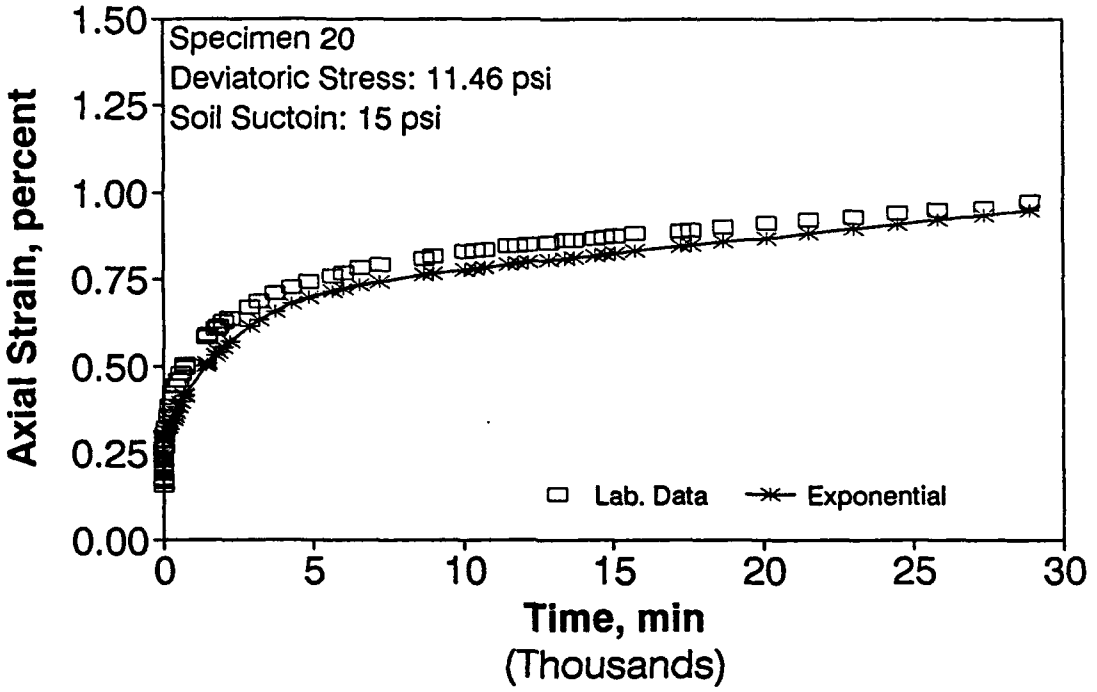
Specimen 20
Deviatoric Stress: 11.46 psi
Soil Suctoin: 15 psi
Axial Strain, percent
1.50
1.25
1.00
0.75
0.50
0.25
0.00
0
5
10
15
20
25
30
Time, min
(Thousands)
Lab. Data
Exponential

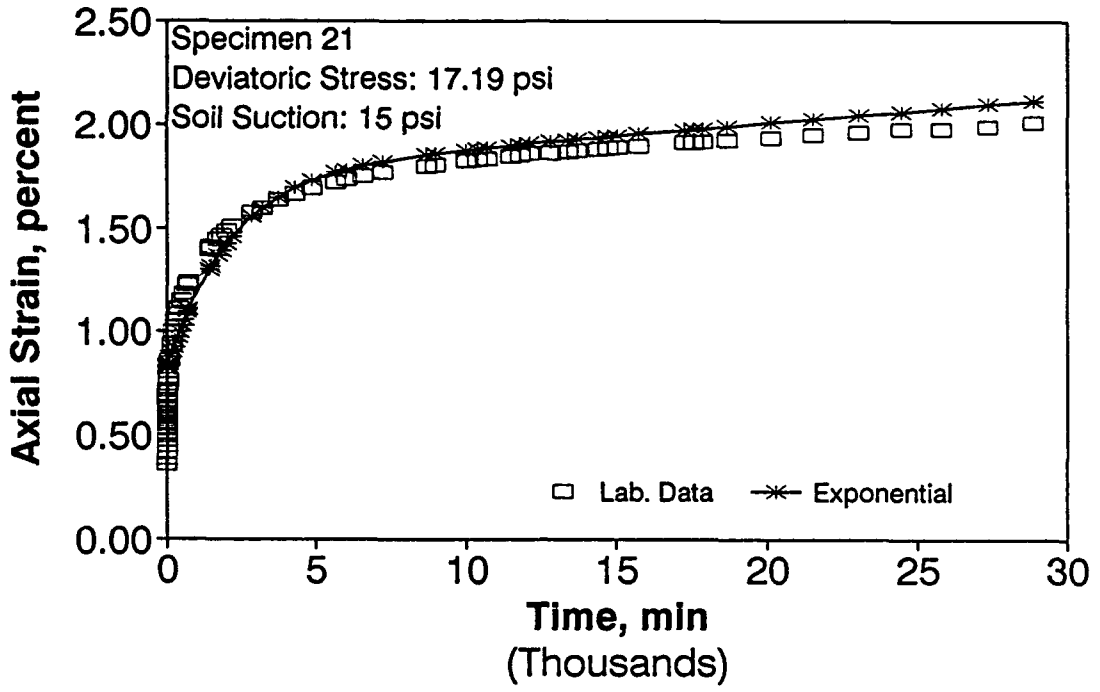
Specimen 21
Deviatoric Stress: 17.19 psi
Soil Suction: 15 psi
Axial Strain, percent
2.50
2.00
1.50
1.00
0.50
0.00
0
5
10
15
20
25
30
Lab. Data
Exponential
Time, min
(Thousands)

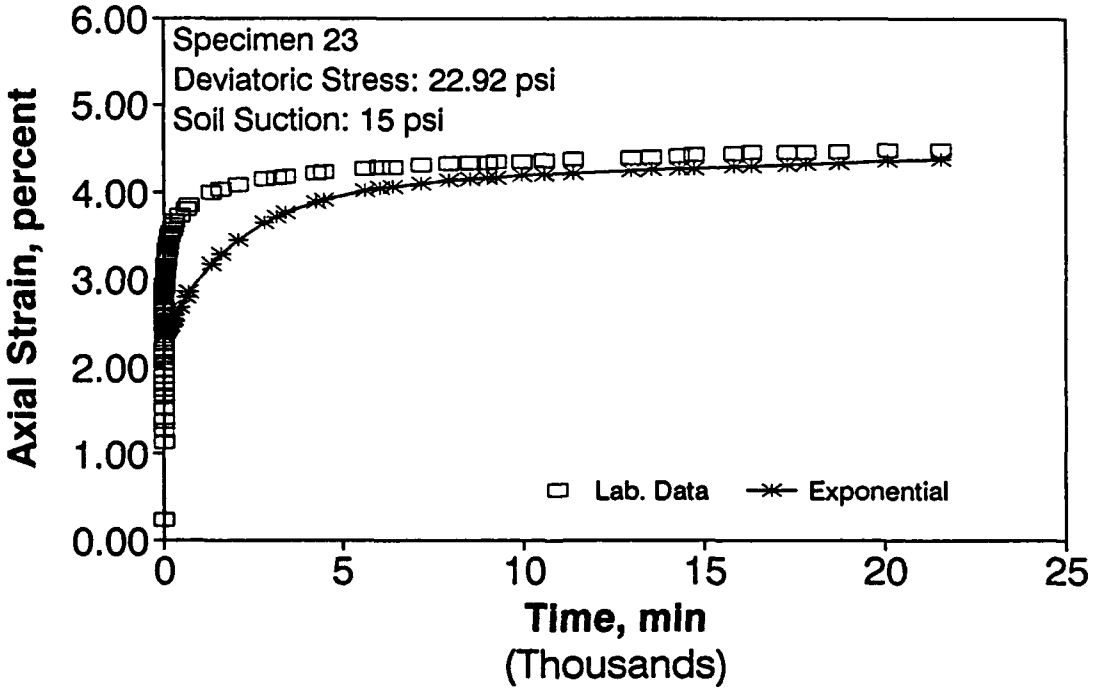
Specimen 23
Deviatoric Stress: 22.92 psi
Soil Suction: 15 psi
Axial Strain, percent
6.00
5.00
4.00
3.00
2.00
1.00
0.00
0
5
10
15
20
25
Lab. Data
Exponential
Time, min
(Thousands)

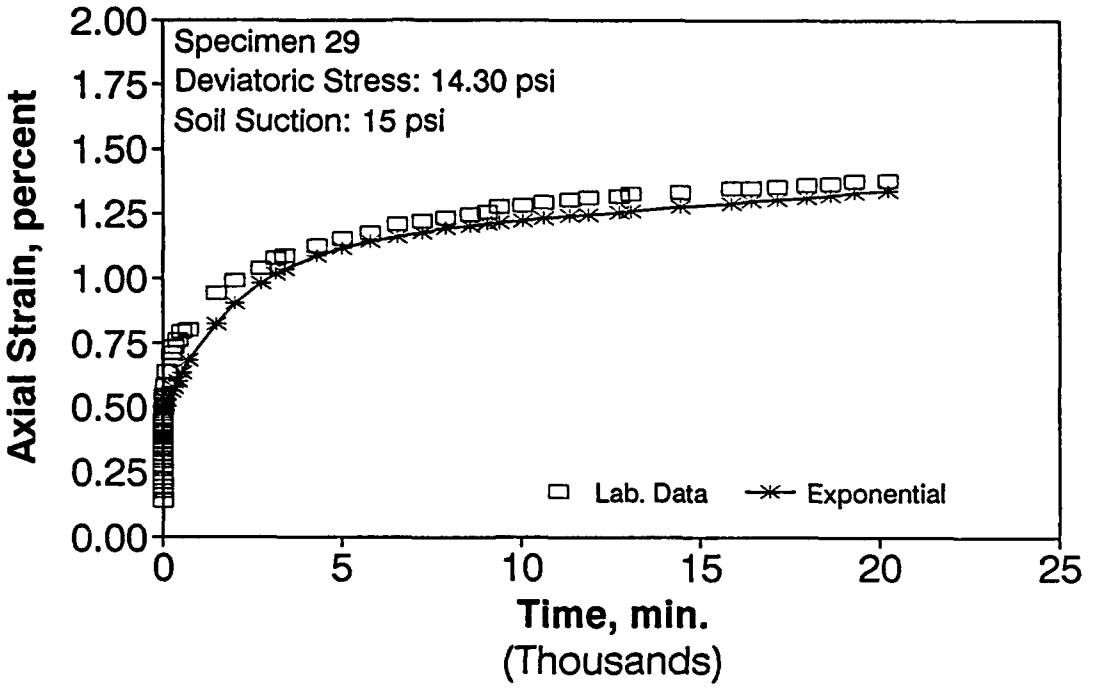
Specimen 29
Deviatoric Stress: 14.30 psi
Soil Suction: 15 psi
Axial Strain, percent
2.00
1.75
1.50
1.25
1.00
0.75
0.50
0.25
0.00
0
5
10
15
20
25
Time, min.
(Thousands)
Lab. Data
Exponential

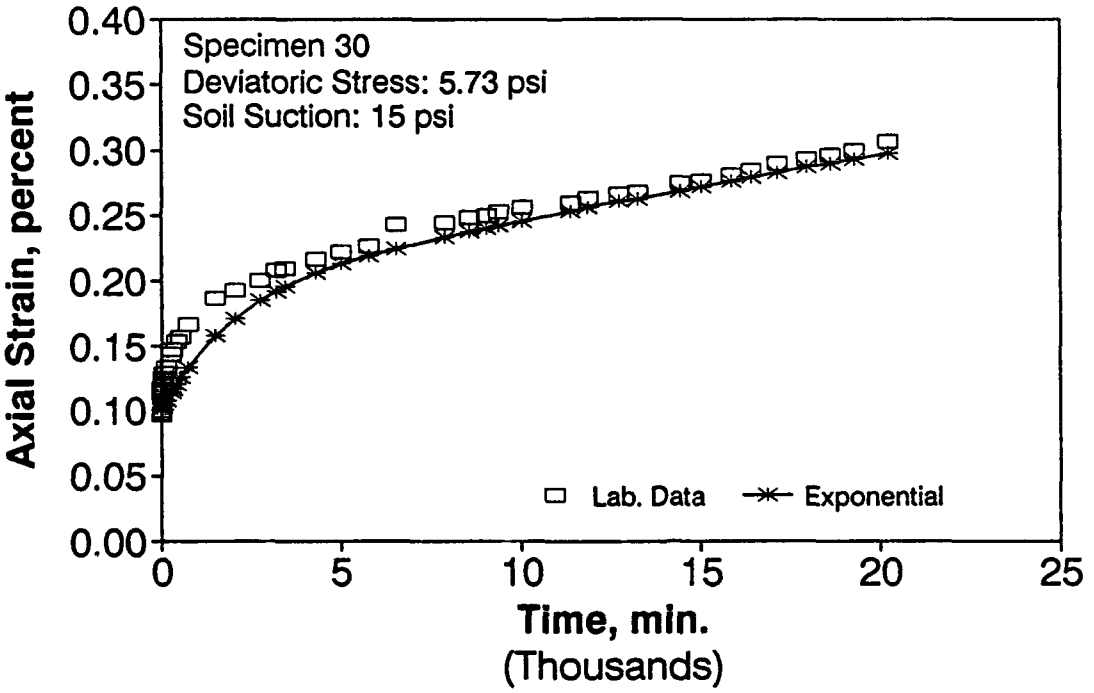
Specimen 30
Deviatoric Stress: 5.73 psi
Soil Suction: 15 psi
Axial Strain, percent
0.40
0.35
0.30
0.25
0.20
0.15
0.10
0.05
0.00
0
5
10
15
20
25
Time, min.
(Thousands)
Lab. Data
Exponential

APPENDIX H

PREDICTION OF CREEP WITH THE INITIAL POWER LAW

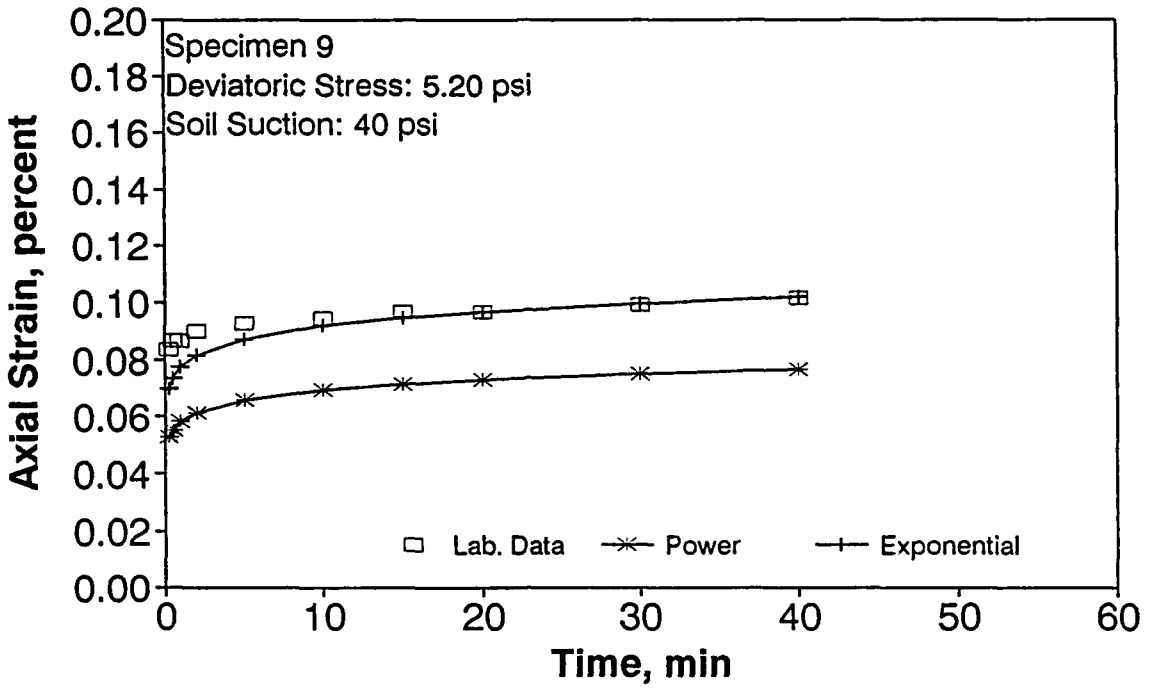
Specimen 9
Deviatoric Stress: 5.20 psi
Soil Suction: 40 psi
Axial Strain, percent
0.20
0.18
0.16
0.14
0.12
0.10
0.08
0.06
0.04
0.02
0.00
0
10
20
30
40
50
60
Time, min
Lab. Data
Power
Exponential

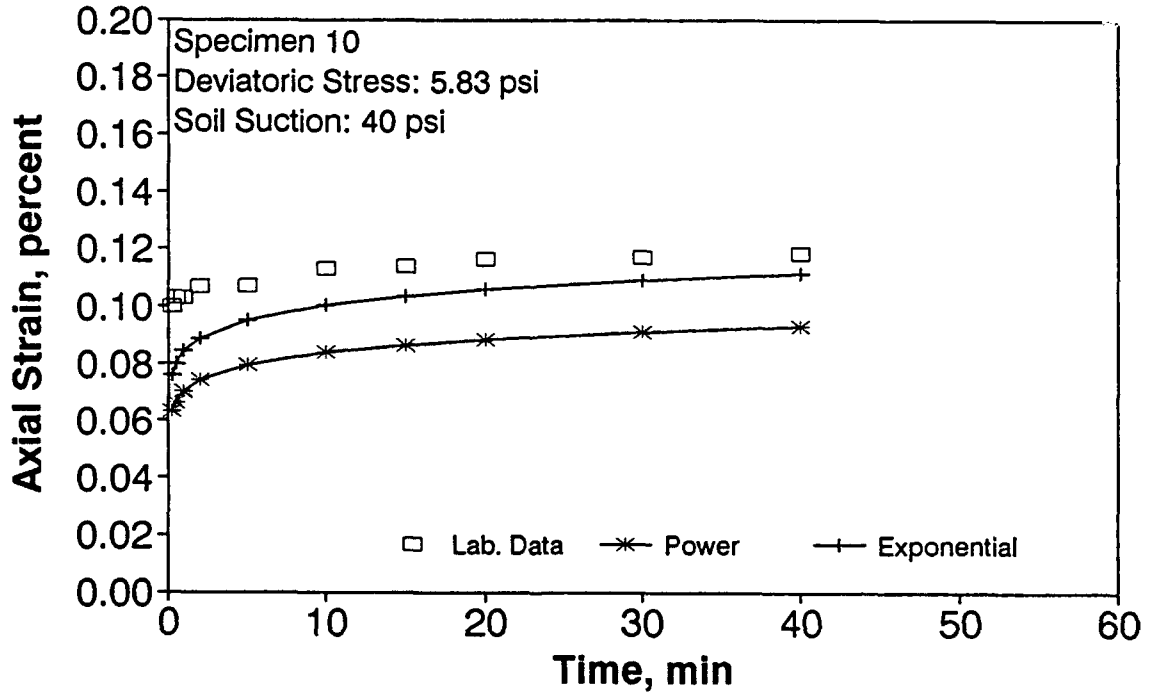
Specimen 10
Deviatoric Stress: 5.83 psi
Soil Suction: 40 psi
Axial Strain, percent
0.20
0.18
0.16
0.14
0.12
0.10
0.08
0.06
0.04
0.02
0.00
0
10
20
30
40
50
60
Time, min
Lab. Data
Power
Exponential

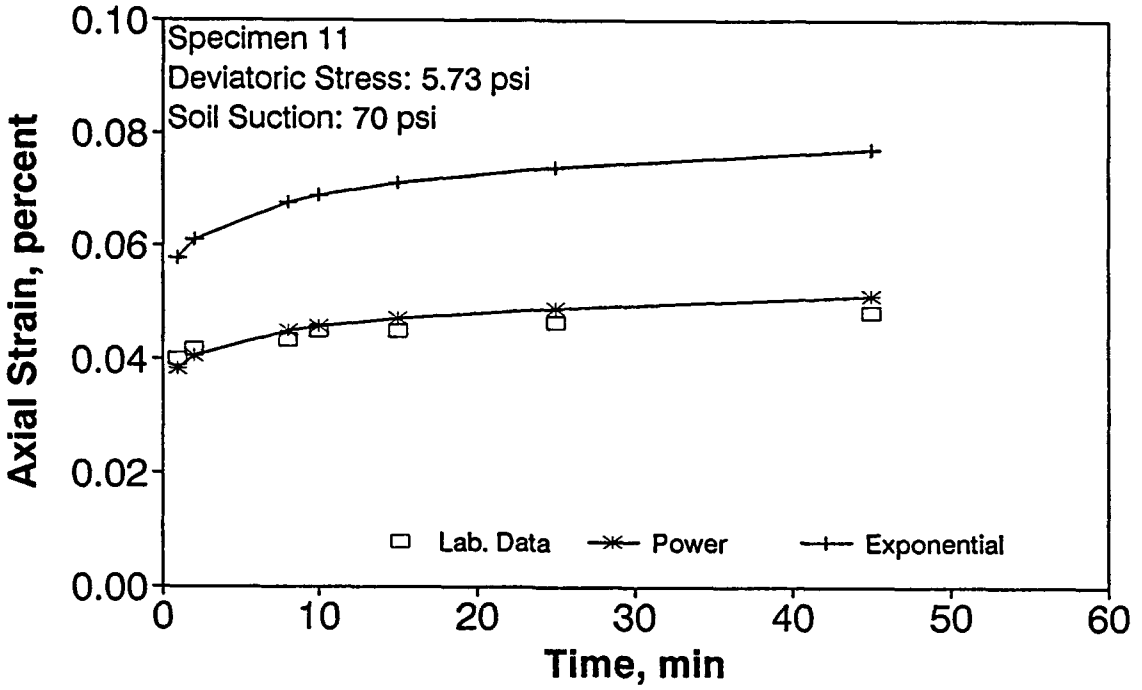
Specimen 11
Deviatoric Stress: 5.73 psi
Soil Suction: 70 psi
Axial Strain, percent
0.10
0.08
0.06
0.04
0.02
0.00
0
10
20
30
40
50
60
Time, min
Lab. Data
Power
Exponential

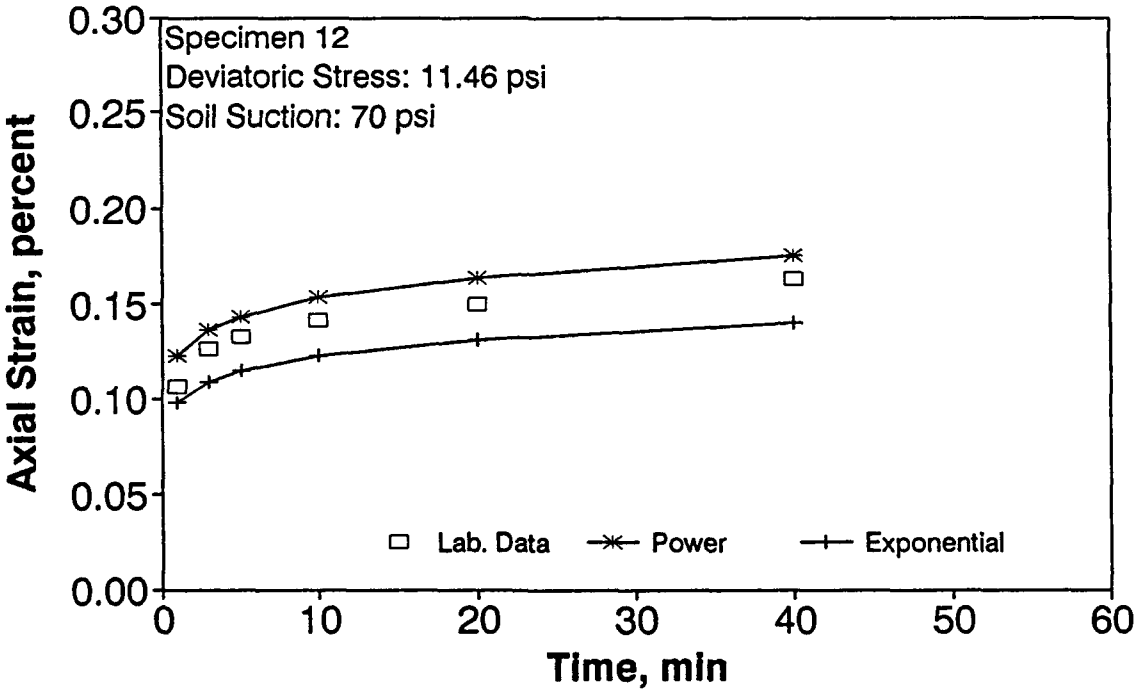
Specimen 12
Deviatoric Stress: 11.46 psi
Soil Suction: 70 psi
Axial Strain, percent
0.30
0.25
0.20
0.15
0.10
0.05
0.00
0
10
20
30
40
50
60
Time, min
Lab. Data
Power
Exponential

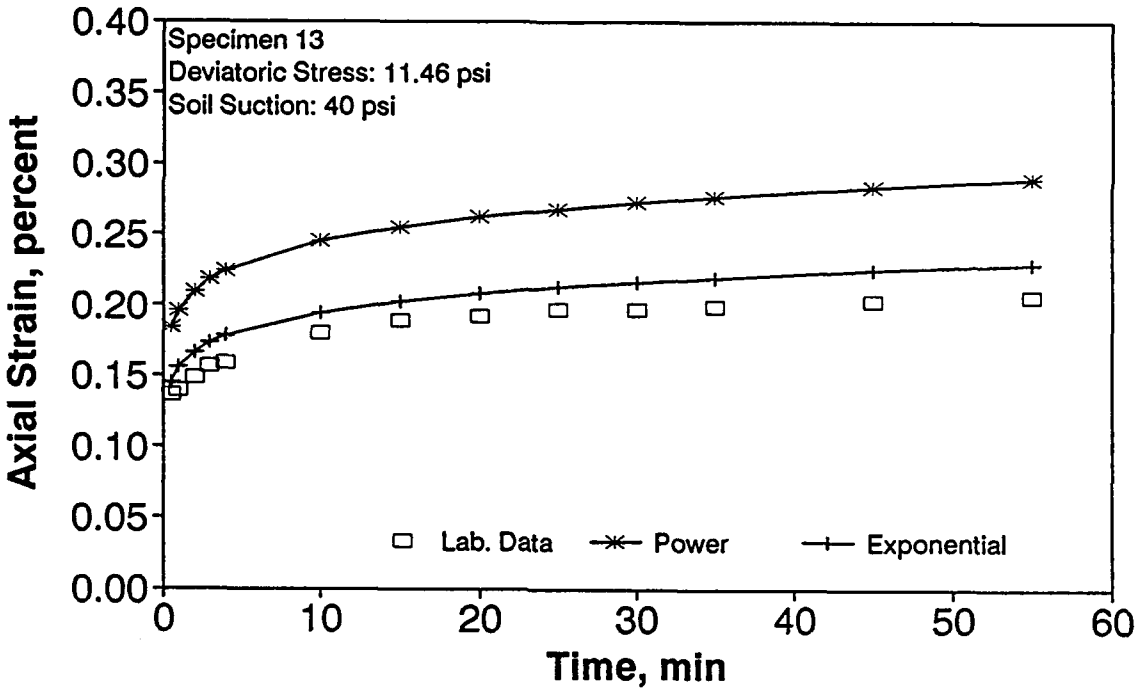
Specimen 13
Deviatoric Stress: 11.46 psi
Soil Suction: 40 psi
Axial Strain, percent
0.40
0.35
0.30
0.25
0.20
0.15
0.10
0.05
0.00
0
10
20
30
40
50
60
Time, min
Lab. Data
Power
Exponential

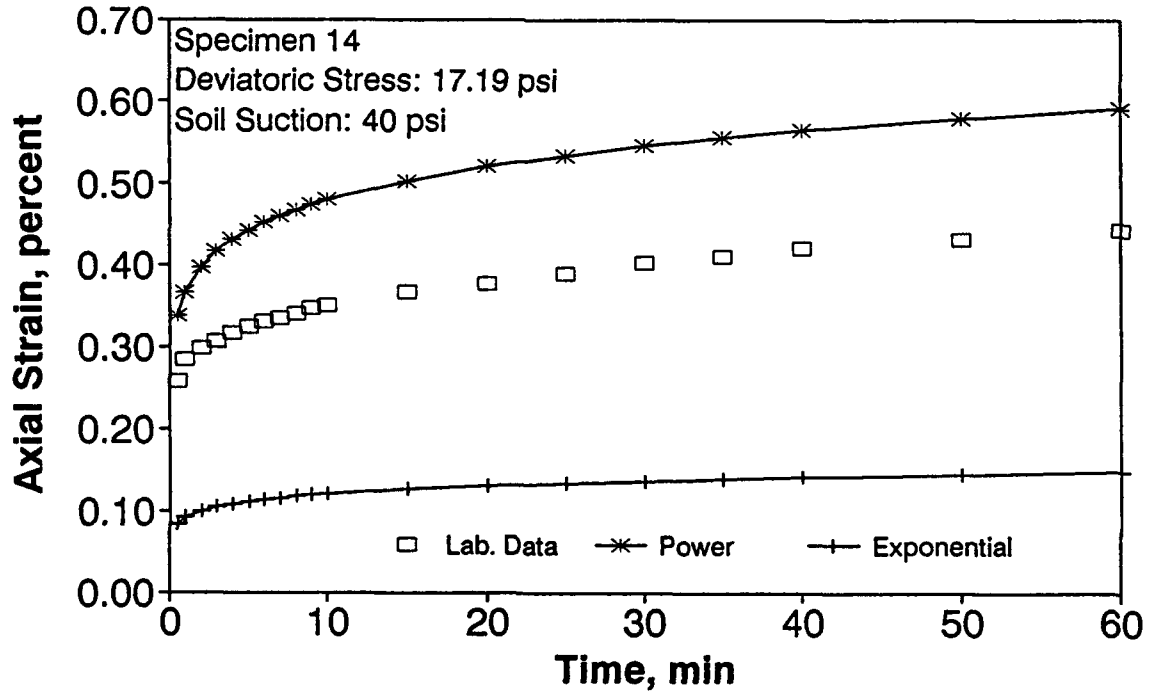
Specimen 14
Deviatoric Stress: 17.19 psi
Soil Suction: 40 psi
Axial Strain, percent
0.70
0.60
0.50
0.40
0.30
0.20
0.10
0.00
0
10
20
30
40
50
60
Time, min
Lab. Data
Power
Exponential

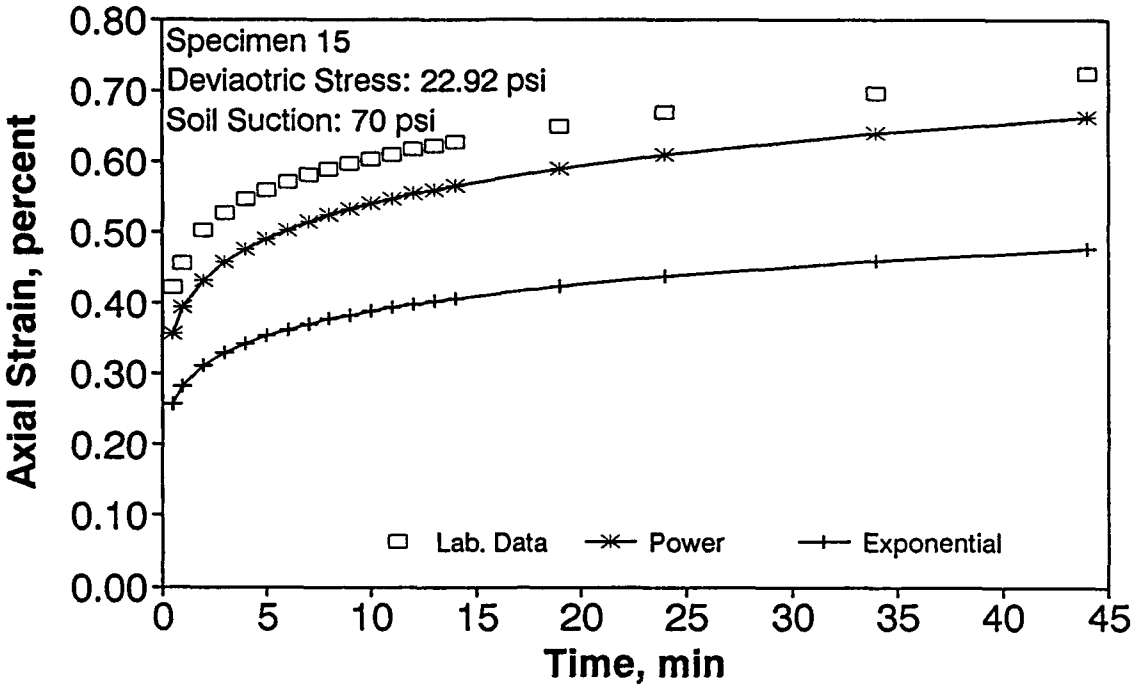
Specimen 15
Deviaotric Stress: 22.92 psi
Soil Suction: 70 psi
Axial Strain, percent
0.80
0.70
0.60
0.50
0.40
0.30
0.20
0.10
0.00
0
5
10
15
20
25
30
35
40
45
Time, min
Lab. Data
Power
Exponential

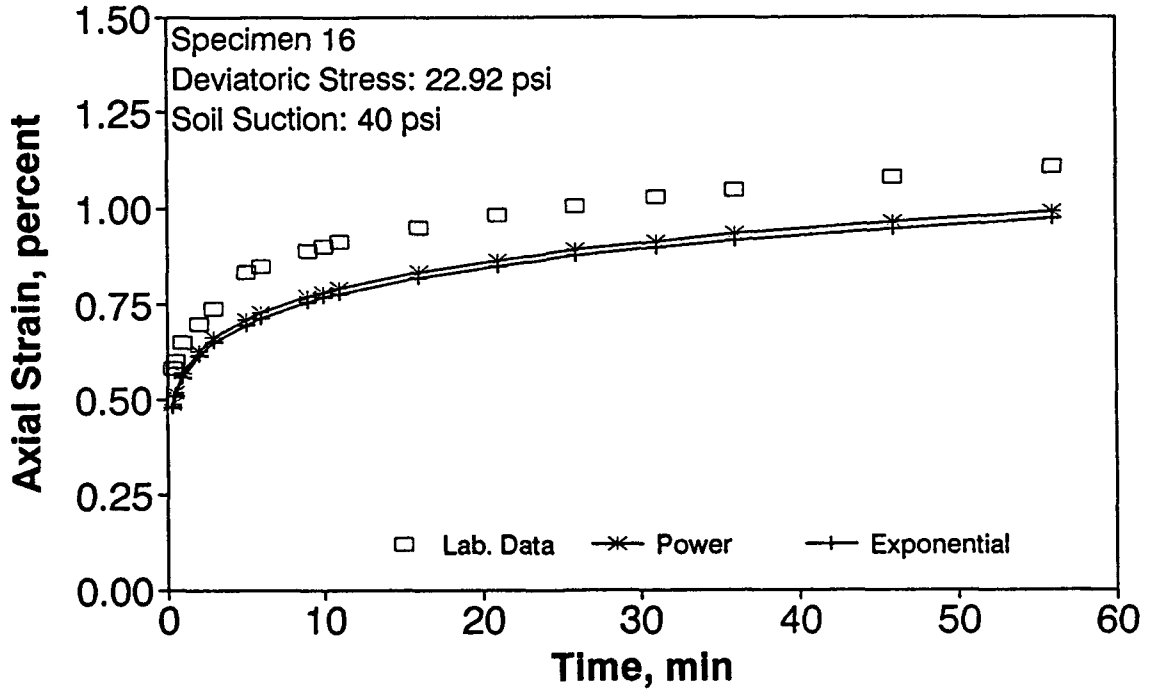
Specimen 16
Deviatoric Stress: 22.92 psi
Soil Suction: 40 psi
Axial Strain, percent
1.50
1.25
1.00
0.75
0.50
0.25
0.00
0
10
20
30
40
50
60
Time, min
Lab. Data
Power
Exponential

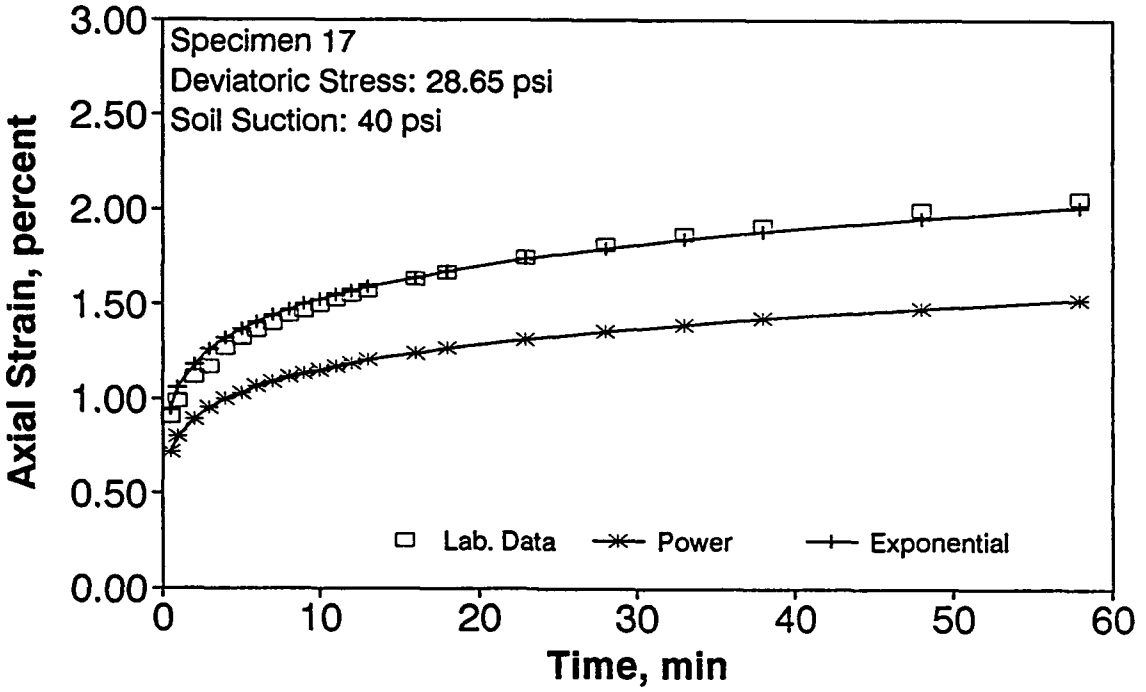
Specimen 17
Deviatoric Stress: 28.65 psi
Soil Suction: 40 psi
Axial Strain, percent
3.00
2.50
2.00
1.50
1.00
0.50
0.00
0
10
20
30
40
50
60
Time, min
Lab. Data
Power
Exponential

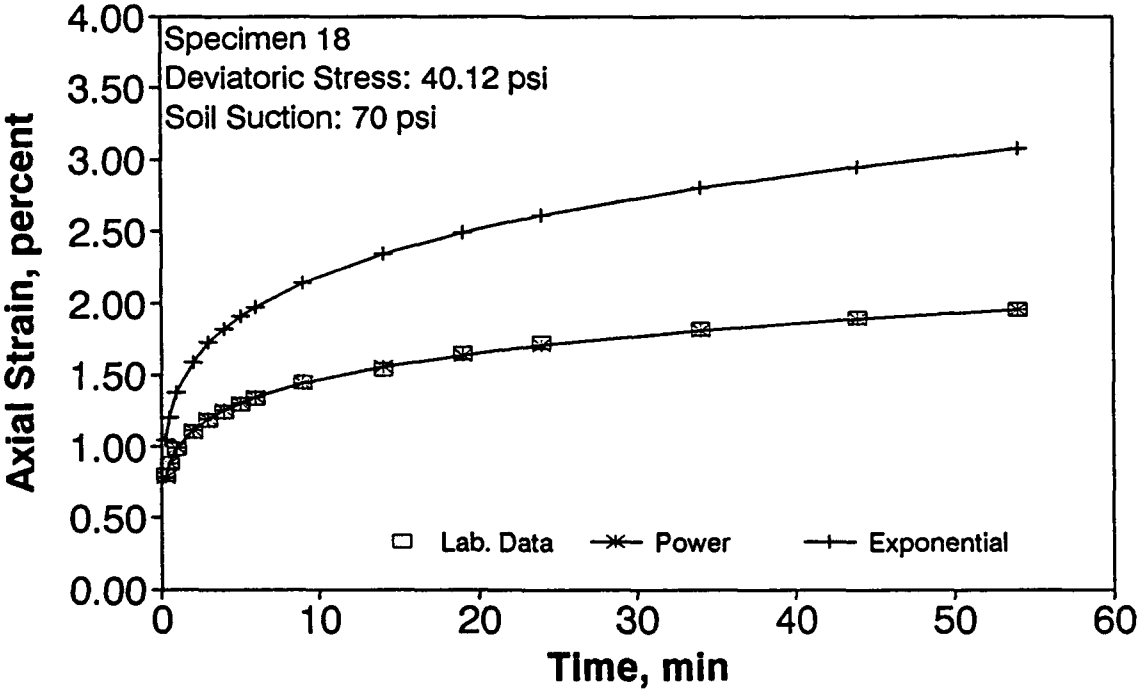
Specimen 18
Deviatoric Stress: 40.12 psi
Soil Suction: 70 psi
Axial Strain, percent
4.00
3.50
3.00
2.50
2.00
1.50
1.00
0.50
0.00
0
10
20
30
40
50
60
Time, min
Lab. Data
Power
Exponential

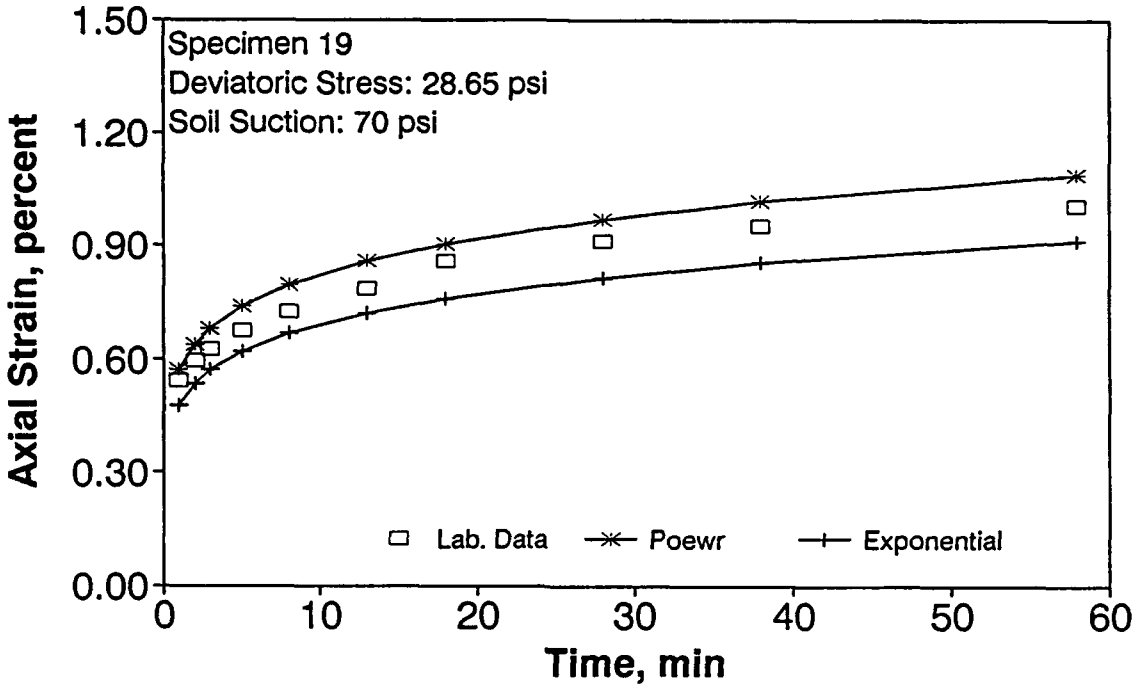
Specimen 19
Deviatoric Stress: 28.65 psi
Soil Suction: 70 psi
Axial Strain, percent
1.50
1.20
0.90
0.60
0.30
0.00
0
10
20
30
40
50
60
Time, min
Lab. Data
Poewr
Exponential

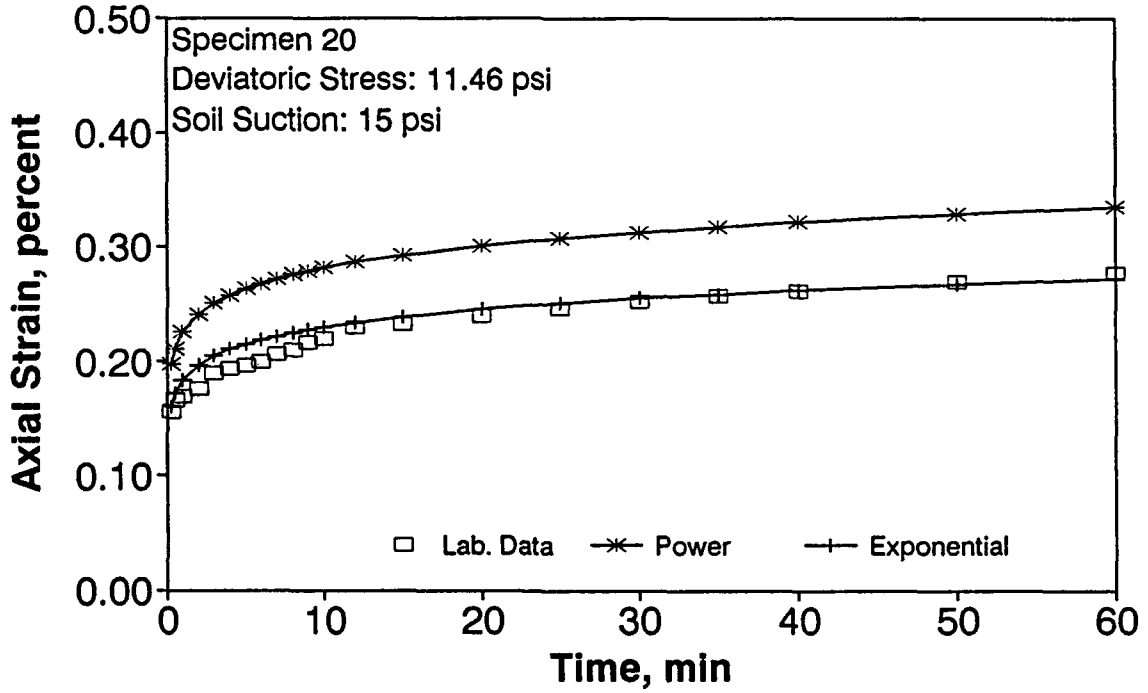
Specimen 20
Deviatoric Stress: 11.46 psi
Soil Suction: 15 psi
Axial Strain, percent
0.50
0.40
0.30
0.20
0.10
0.00
0
10
20
30
40
50
60
Time, min
Lab. Data
Power
Exponential

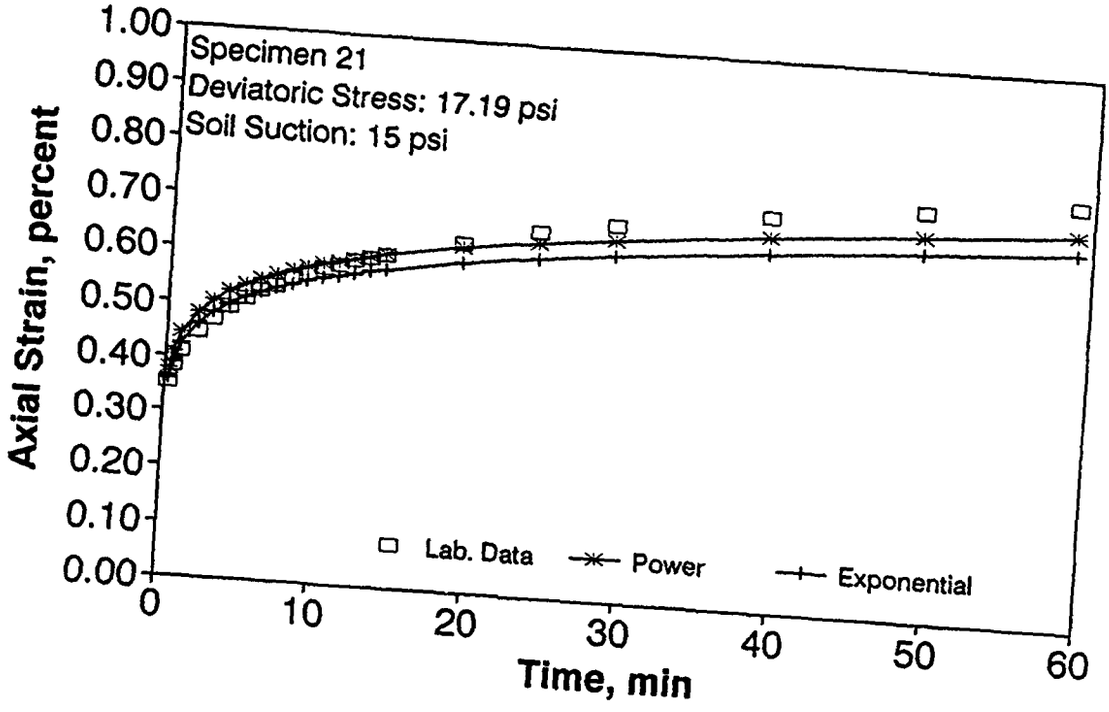
Specimen 21
Deviatoric Stress: 17.19 psi
Soil Suction: 15 psi
Axial Strain, percent
1.00
0.90
0.80
0.70
0.60
0.50
0.40
0.30
0.20
0.10
0.00
0
10
20
30
40
50
60
Time, min
Lab. Data
Power
Exponential

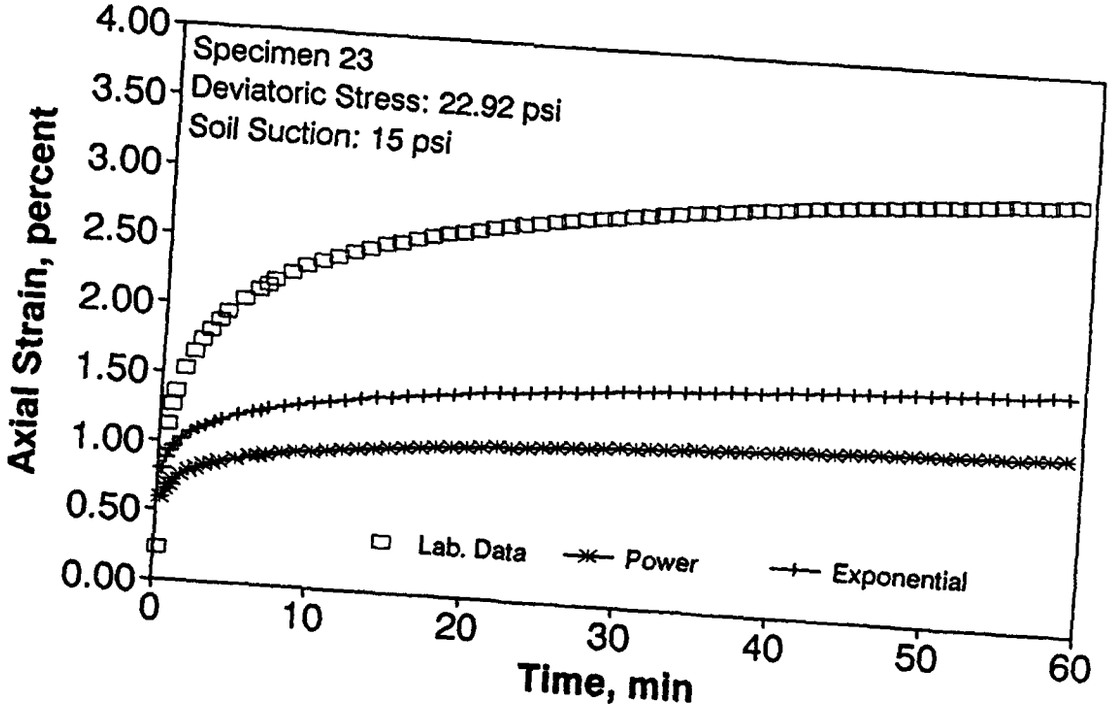
Specimen 23
Deviatoric Stress: 22.92 psi
Soil Suction: 15 psi
Axial Strain, percent
4.00
3.50
3.00
2.50
2.00
1.50
1.00
0.50
0.00
0
10
20
30
40
50
60
Time, min
Lab. Data
Power
Exponential

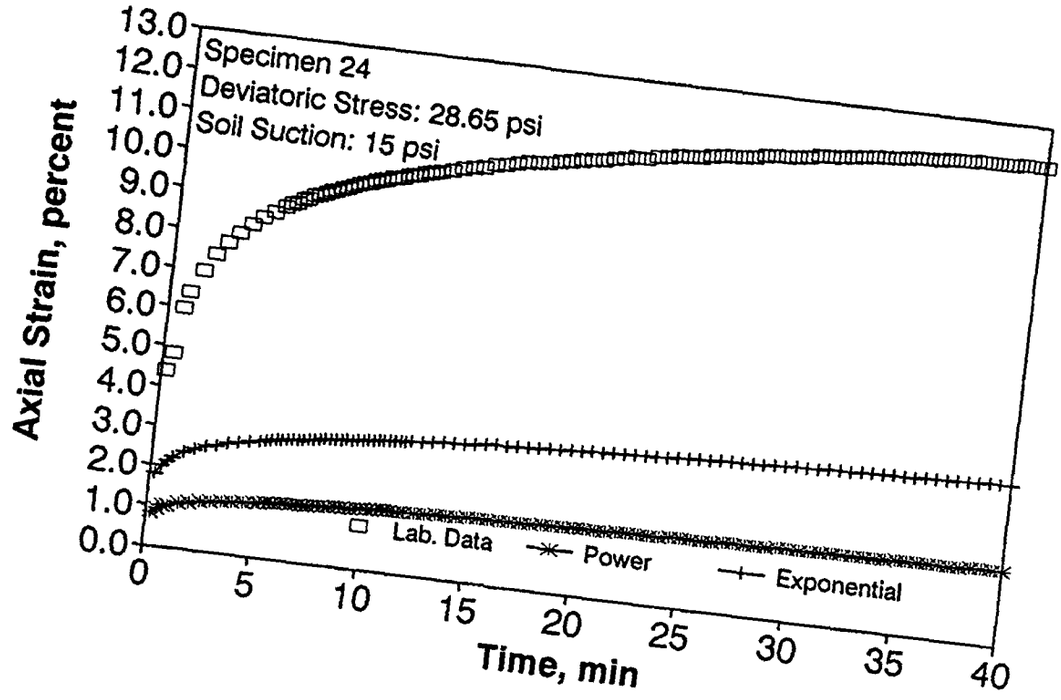
Specimen 24
Deviatoric Stress: 28.65 psi
Soil Suction: 15 psi
Axial Strain, percent
13.0
12.0
11.0
10.0
9.0
8.0
7.0
6.0
5.0
4.0
3.0
2.0
1.0
0.0
0
5
10
15
20
25
30
35
40
Time, min
Lab. Data
Power
Exponential

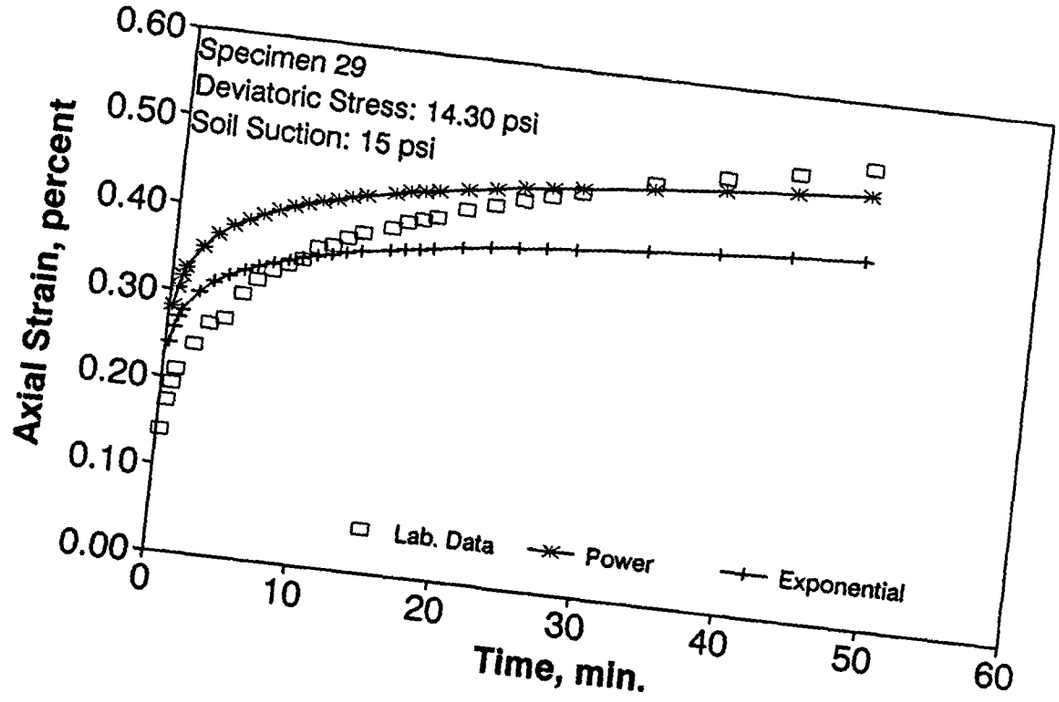
Specimen 29
Deviatoric Stress: 14.30 psi
Soil Suction: 15 psi
Axial Strain, percent
0.60
0.50
0.40
0.30
0.20
0.10
0.00
0
10
20
30
40
50
60
Time, min.
Lab. Data
Power
Exponential

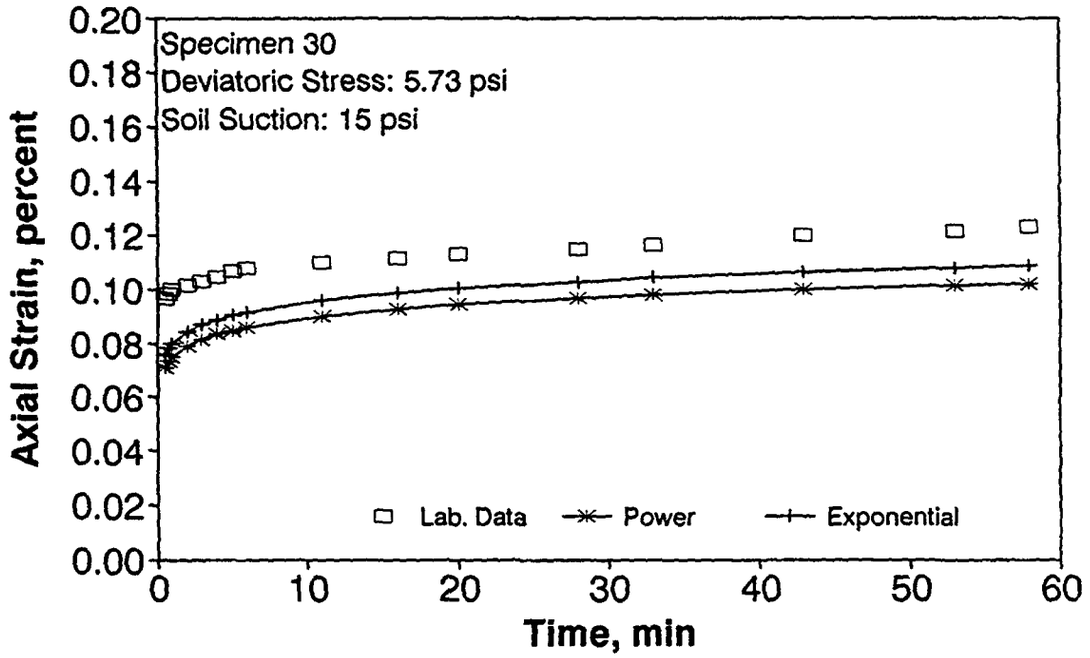
Specimen 30
Deviatoric Stress: 5.73 psi
Soil Suction: 15 psi
Axial Strain, percent
0.20
0.18
0.16
0.14
0.12
0.10
0.08
0.06
0.04
0.02
0.00
0
10
20
30
40
50
60
Time, min
Lab. Data
Power
Exponential

APPENDIX I

PREDICTION OF RECOVERY WITH THE UNLOADING POWER LAW

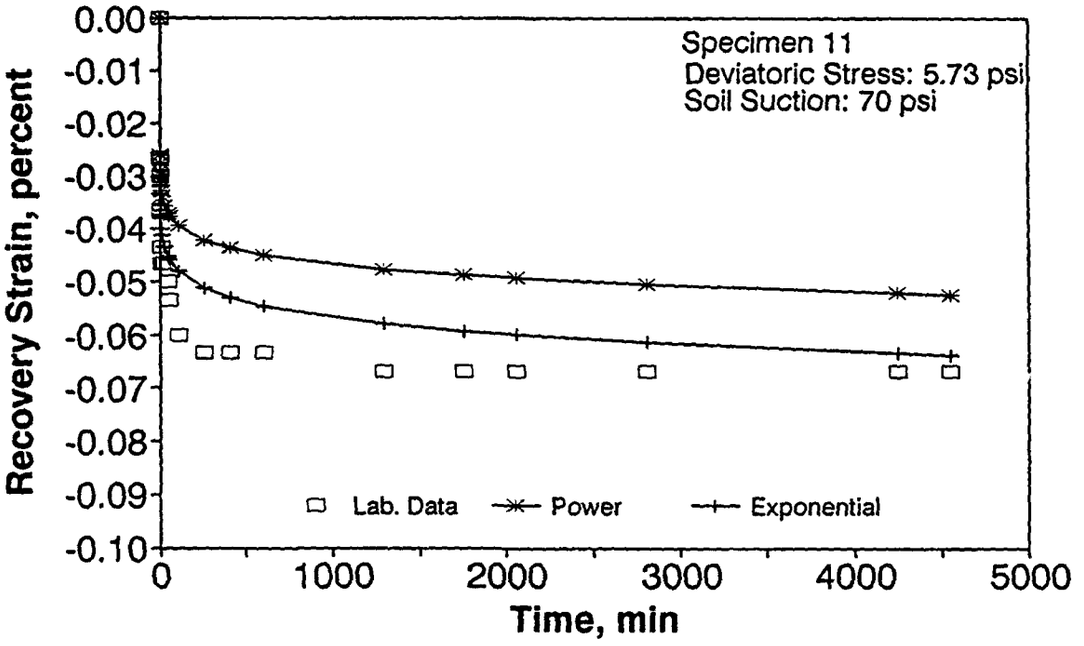
Specimen 11
Deviatoric Stress: 5.73 psi
Soil Suction: 70 psi
Recovery Strain, percent
0.00
-0.01
-0.02
-0.03
-0.04
-0.05
-0.06
-0.07
-0.08
-0.09
-0.10
0
1000
2000
3000
4000
5000
Time, min
Lab. Data
Power
Exponential

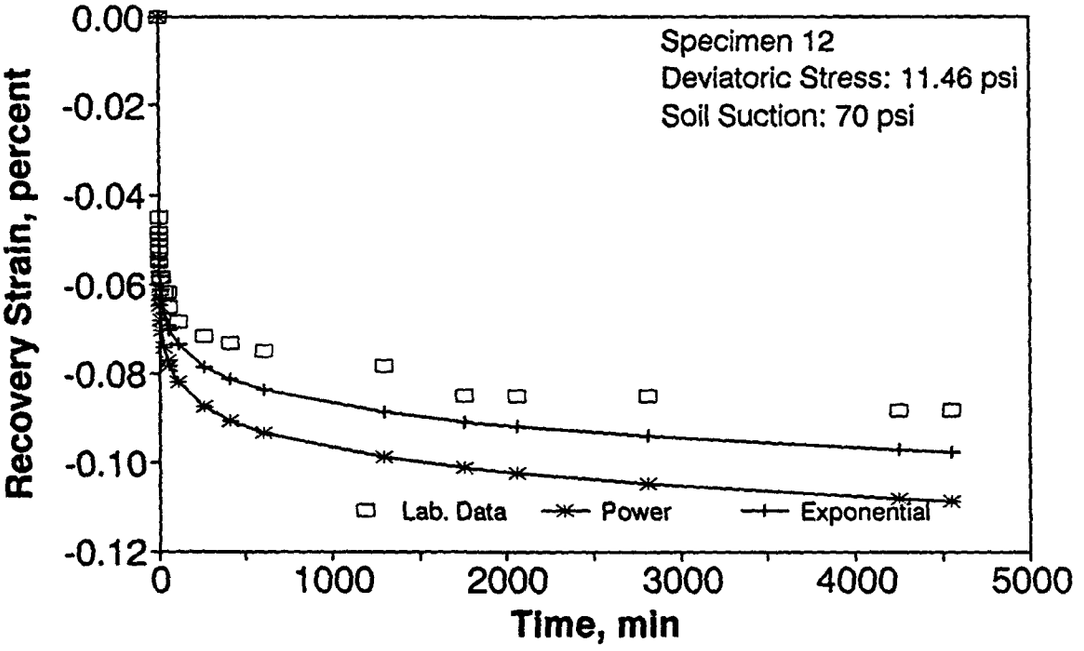
Specimen 12
Deviatoric Stress: 11.46 psi
Soil Suction: 70 psi
Recovery Strain, percent
0.00
-0.02
-0.04
-0.06
-0.08
-0.10
-0.12
0
1000
2000
3000
4000
5000
Time, min
Lab. Data
Power
Exponential

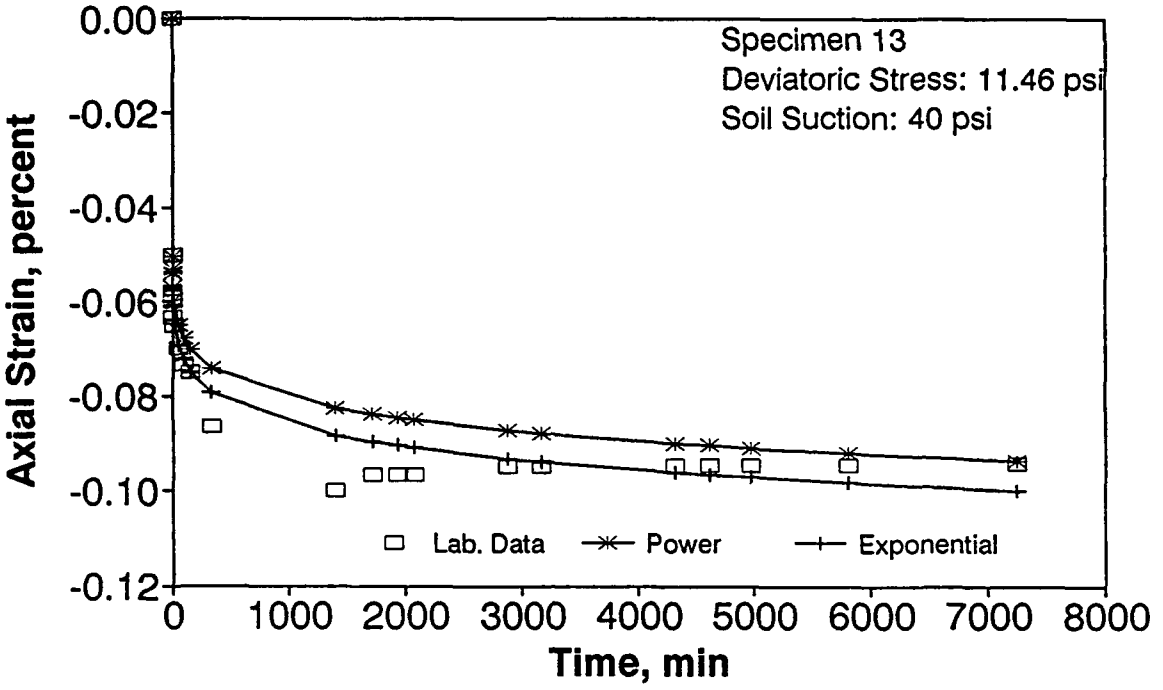
Specimen 13
Deviatoric Stress: 11.46 psi
Soil Suction: 40 psi
Axial Strain, percent
0.00
-0.02
-0.04
-0.06
-0.08
-0.10
-0.12
0
1000
2000
3000
4000
5000
6000
7000
8000
Time, min
Lab. Data
Power
Exponential

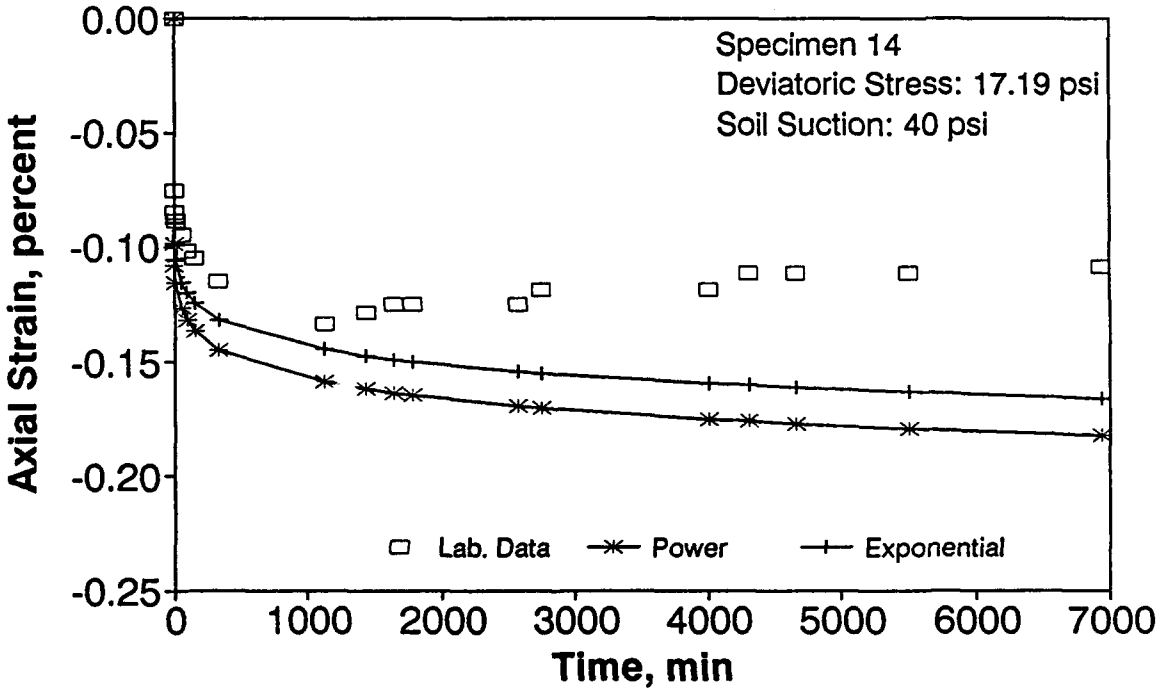
Specimen 14
Deviatoric Stress: 17.19 psi
Soil Suction: 40 psi
Axial Strain, percent
0.00
-0.05
-0.10
-0.15
-0.20
-0.25
0
1000
2000
3000
4000
5000
6000
7000
Time, min
Lab. Data
Power
Exponential

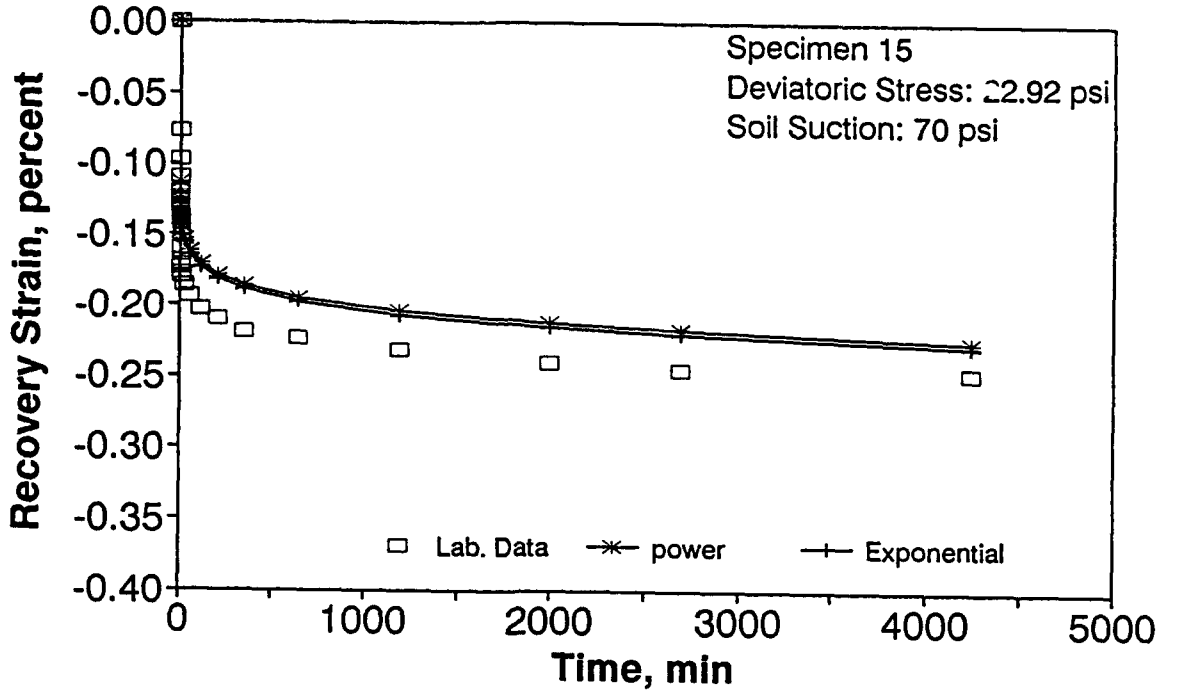
Specimen 15
Deviatoric Stress: 22.92 psi
Soil Suction: 70 psi
Recovery Strain, percent
0.00
-0.05
-0.10
-0.15
-0.20
-0.25
-0.30
-0.35
-0.40
0
1000
2000
3000
4000
5000
Time, min
Lab. Data
power
Exponential

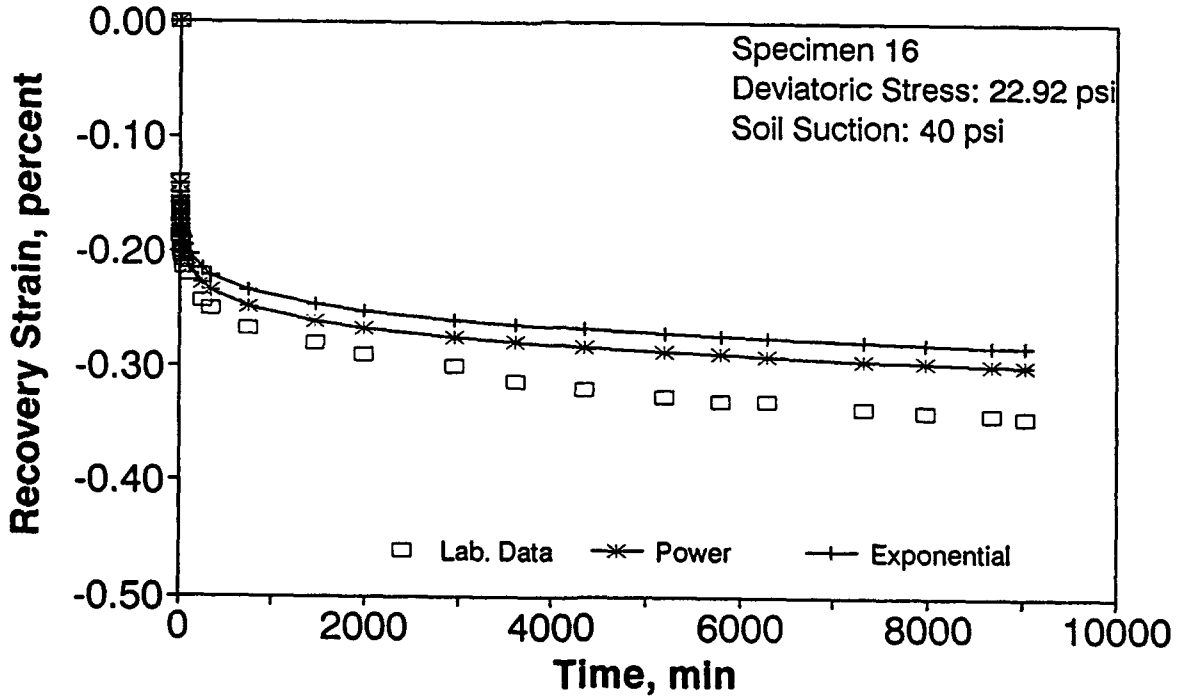
Specimen 16
Deviatoric Stress: 22.92 psi
Soil Suction: 40 psi
Recovery Strain, percent
0.00
-0.10
-0.20
-0.30
-0.40
-0.50
0
2000
4000
6000
8000
10000
Time, min
Lab. Data
Power
Exponential

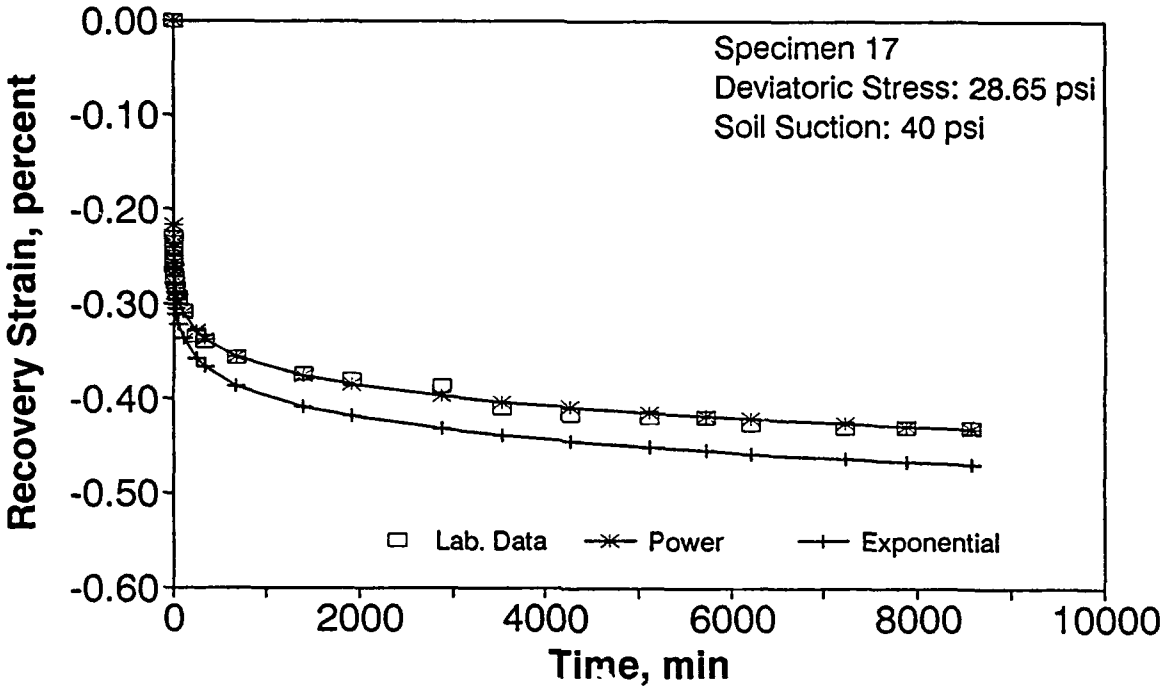
Specimen 17
Deviatoric Stress: 28.65 psi
Soil Suction: 40 psi
Recovery Strain, percent
0.00
-0.10
-0.20
-0.30
-0.40
-0.50
-0.60
0
2000
4000
6000
8000
10000
Time, min
Lab. Data
Power
Exponential

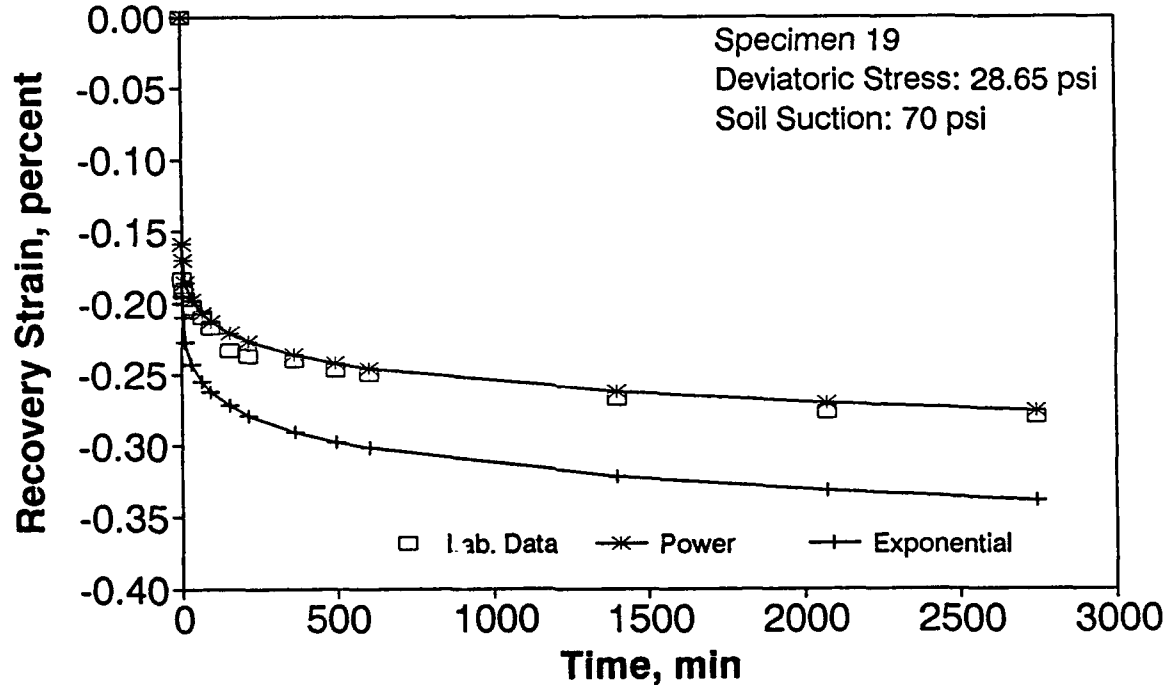
Specimen 19
Deviatoric Stress: 28.65 psi
Soil Suction: 70 psi
Recovery Strain, percent
0.00
-0.05
-0.10
-0.15
-0.20
-0.25
-0.30
-0.35
-0.40
0
500
1000
1500
2000
2500
3000
Time, min
Lab. Data
Power
Exponential

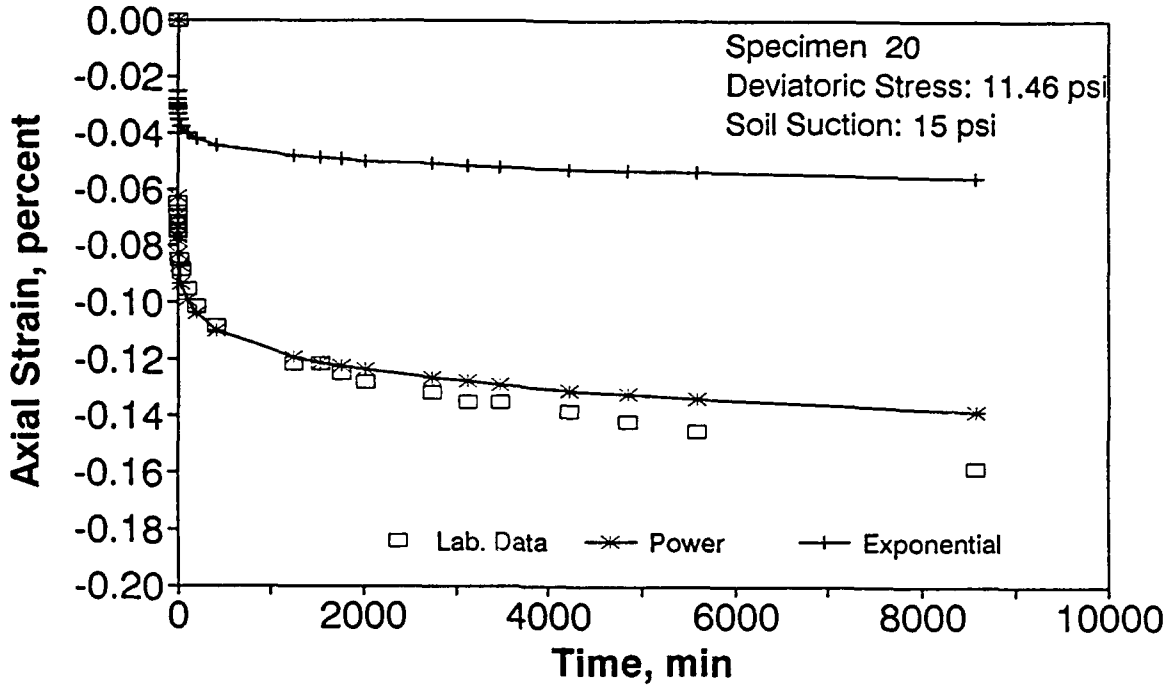
Specimen 20
Deviatoric Stress: 11.46 psi
Soil Suction: 15 psi
Axial Strain, percent
0.00
-0.02
-0.04
-0.06
-0.08
-0.10
-0.12
-0.14
-0.16
-0.18
-0.20
0
2000
4000
6000
8000
10000
Time, min
Lab. Data
Power
Exponential

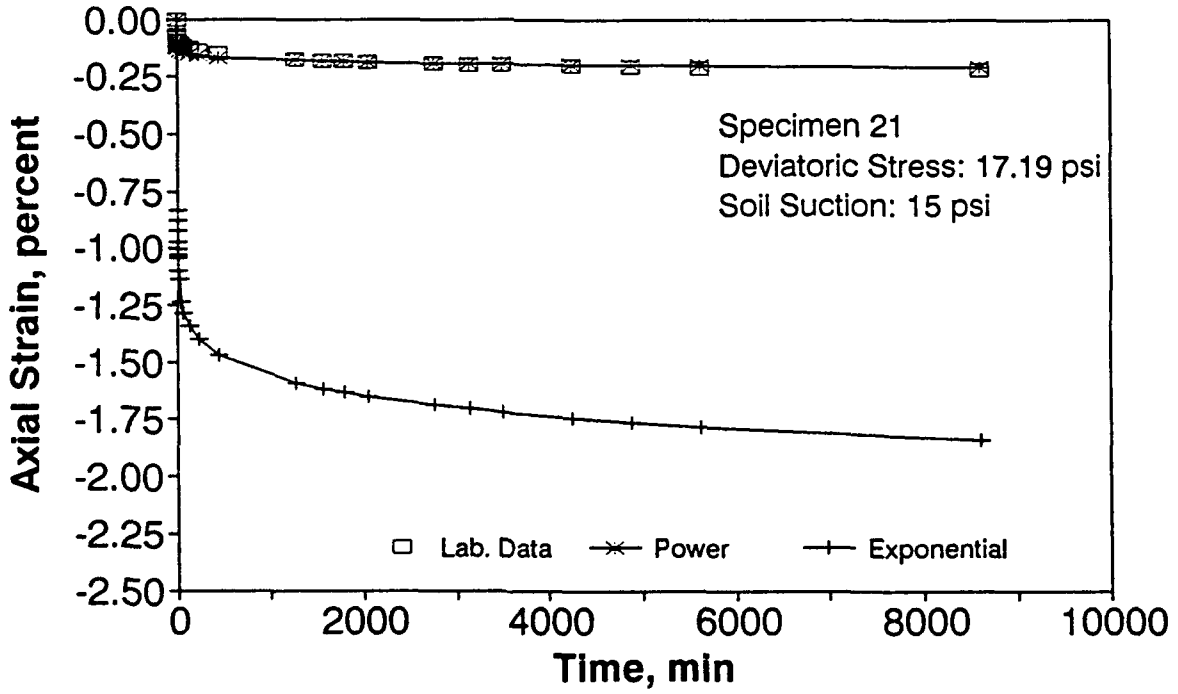
Specimen 21
Deviatoric Stress: 17.19 psi
Soil Suction: 15 psi
Axial Strain, percent
0.00
-0.25
-0.50
-0.75
-1.00
-1.25
-1.50
-1.75
-2.00
-2.25
-2.50
0
2000
4000
6000
8000
10000
Time, min
Lab. Data
Power
Exponential

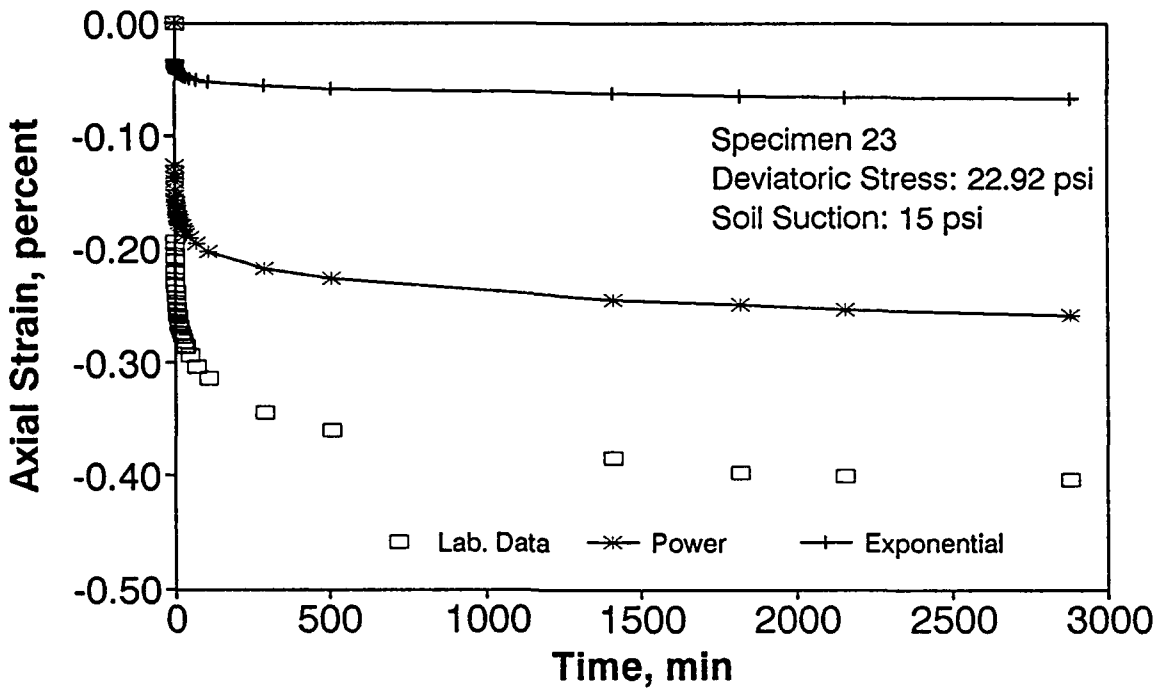
0.00
-0.10
-0.20
-0.30
-0.40
-0.50
Axial Strain, percent
Specimen 23
Deviatoric Stress: 22.92 psi
Soil Suction: 15 psi
Lab. Data
Power
Exponential
0
500
1000
1500
2000
2500
3000
Time, min

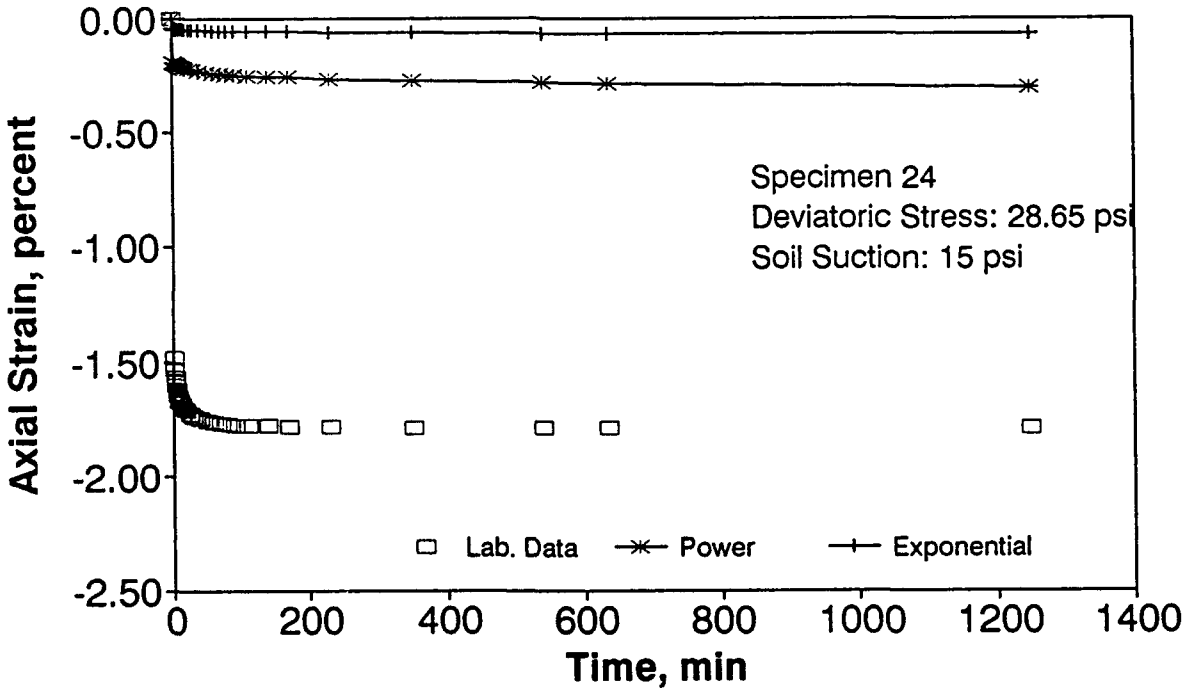
0.00
-0.50
-1.00
-1.50
-2.00
-2.50
Axial Strain, percent
Specimen 24
Deviatoric Stress: 28.65 psi
Soil Suction: 15 psi
Lab. Data
Power
Exponential
0
200
400
600
800
1000
1200
1400
Time, min

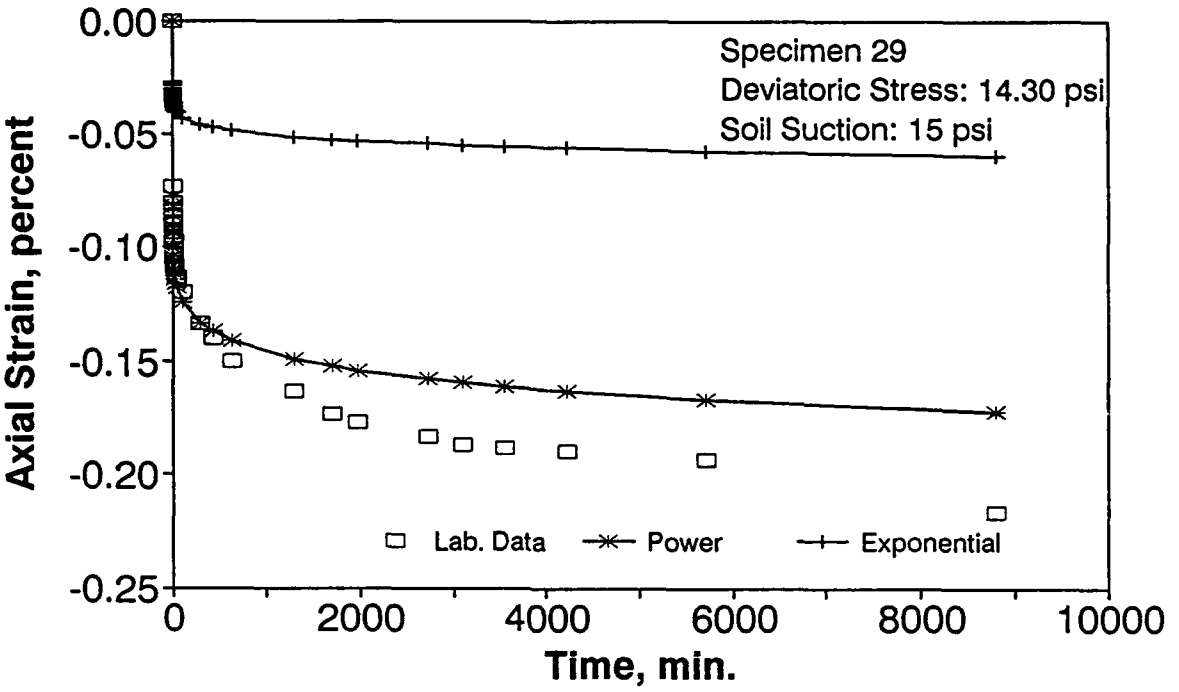
Specimen 29
Deviatoric Stress: 14.30 psi
Soil Suction: 15 psi
Axial Strain, percent
0.00
-0.05
-0.10
-0.15
-0.20
-0.25
0
2000
4000
6000
8000
10000
Time, min.
Lab. Data
Power
Exponential

APPENDIX J

FORTRAN LISTING OF PROGRAM "HSTRAIN"

```
$LARGE
$NOTRUNCATE
C**********************************************************************
C
C                          PROGRAM HSTRAIN.FOR
C
C  THIS PROGRAM REDUCES THE COLLECTED DATA BY 2063 FOURIER ANALYSER
C  FOR THE PROJECT 'UNSATURATED CLAYEY SOILS BEHAVIOR UNDER HIGH
C  STRAIN RATES'. THE TESTS ARE PERFORMED ON STRESS CONTRAL USING MTS
C  FACILITY. THREE CHANNLE DATA WERE COLLECTED.
C
C  IFILE--INPUT DATA FILE NAME;
C  FILELOAD--OUTPUT DATA FILE NAME FOR STRESS-TIME RELATION;
C  FILEDIS--OUTPUT DATA FILE NAME FOR STRAIN-TIME RELATION;
C  STRESS--DIMENSION FOR STRESS DATA;
C  STRAIN--DIMENSION FOR STRAIN DATA;
C  VOLT--DIMENSION FOR MICROPROFILE WAVEFORM DATA;
C  TSTRESS--DIMENSION FOR TIME DATA WITH STRESS;
C  TSTRAIN--DIMENSION FOR TIME DATA WITH STRAIN;
C  BEGINVOLT--BEGINING POINT OF UP-RAMP CURVE FOR MICROPROFILE
C            WAVEFORM;
C  BEGINSTRESS--BEGINING POINT OF UP-RAMP CURVE COLLECTED BY
C              LOAD CELL;
C  BEGINSTRAIN--BEGINING POINT OF STRAIN-TIME CURVE;
C**********************************************************************
      CHARACTER IFILE*20,FILELOAD*20,FILEDIS*20,IFILE1*20,FILELOAD1*20
     &          FILEDIS1*20
      COMMON /STRAIN1/ STRAIN
      COMMON /STRESS1/ STRESS
      COMMON /VOIT1/ VOLT
      COMMON /TSTRESS1/TSTRESS
      COMMON /TSTRAIN1/TSTRAIN
      INTEGER BEGINVOLT,BEGINSTRESS,BEGINSTRAIN
      DIMENSION STRAIN(4100),STRESS(4100),VOLT(4100),TSTRESS(4100),
     &          TSTRAIN(4100)
C
C     BEGIN TO READ DATA FROM SCREEN
      WRITE(*,*)'ENTER THE DATA POINTS FOR EACH CHANNEL'
      READ(*,*)NUMPTS
      WRITE(*,*)'ENTER THE TIME LENTH OF COLLECTING DATA (milisec.)'
      READ(*,*)TIMELEN
      WRITE(*,*)'ENTER THE VALUE OF DISPLACEMENT CARTRIDGE (in)'
      READ(*,*)CAR1
      WRITE(*,*)'ENTER THE VALUE OF LOAD CARTRIDGE (Ib)'
      READ(*,*)CAR2
      WRITE(*,*)'ENTER THE FIRST FILE NUMBER IN THE SET'
      READ(*,*)NSTART
      WRITE(*,*)'ENTER THE NUMBER OF FILE IN THE SET'
      READ(*,*)NFILES
      WRITE(*,*)'ENTER THE INPUT DATA FILE NAME IN THE SET'
      READ(*,10)IFILE
      WRITE(*,*)'ENTER THE OUTPUT STRESS DATA FILE NAME IN THE SET'
      READ(*,10)FILELOAD
      WRITE(*,*)'ENTER THE OUTPUT STRAIN DATA FILE NAME IN THE SET'
      READ(*,10)FILEDIS
10    FORMAT(A20)
C
C
      OPEN(UNIT=41,FILE='POINT.OUT',STATUS='NEW')
C
```

```
      DO 2000 IT=NSTART,(NSTART+NFILES-1)
      WRITE(*,*)'FILE NUMBER=',IT
      KK=IT*4
      WRITE(41,*)'*****************************************************
     &***********'
      WRITE(41,*)'FILE NUMBER=',IT,'     APPLIED LOAD(kg)=',KK
      WRITE(41,*)'*****************************************************
     &***********'
C
      WRITE(*,*)'CALLING SUBROUTINE GET_FILE_NAME'
      CALL GET_FILE_NAME(IFILE,FILELOAD,FILEDIS,IFILE1,FILELOAD1,
     &     FILEDIS1,IT)
      IFILE1=IFILE1
      FILELOAD1=FILELOAD1
      FILEDIS1=FILEDIS1
C
C
      WRITE(*,*)'CALLING SUBROUTINE READ_DATA_FILE'
      CALL READ_DATA_FILE(IFILE1,NUMPTS,CAR1,CAR2)
C
C
      WRITE(*,*)'CALLING SUBROUTINE SMOOTH_DATA'
      CALL SMOOTH_DATA(NUMPTS)
C
C
      WRITE(*,*)'CALLING SUBROUTINE FIND_BEGIN_POINTS'
      CALL FIND_BEGIN_POINTS(NUMPTS,BEGINVOLT,BEGINSTRESS,
     &     BEGINSTRAIN)
      BEGINVOLT=BEGINVOLT
      BEGINSTRESS=BEGINSTRESS
      BEGINSTRAIN=BEGINSTRAIN
C
C
      WRITE(*,*)'CALLING SUBROUTINE INITIALIZE_DATA'
      CALL INITIALIZE_DATA(BEGINVOLT,BEGINSTRESS,BEGINSTRAIN,NUMPTS)
C
C
      WRITE(*,*)'CALL SUBROUTINE VARIATION_WITH_TIME'
      CALL VARIATION_WITH_TIME(NUMPTS,BEGINSTRESS,BEGINSTRAIN,
     &     TIMELEN,FILELOAD1,FILEDIS1)
C
C
      WRITE(*,*)'CALLING SUBROUTINE FIND_MAXIMUM_POINTS'
      CALL FIND_MAXIMUM_POINTS(NUMPTS,TIMELEN,BEGINVOLT,BEGINSTRESS,
     &BEGINSTRAIN)
C
C
2000  CONTINUE
      STOP
      END
C
C*********************************************************************
C                        THE SUBROUTINE FOLLOWED
C*********************************************************************
C
C*********************************************************************
C                        SUBROUTINE GET_FILE_NAME
C     THIS SUBROUTINE GENERATES THE INPUT AND OUTPUT DATA FILE NAMES
C*********************************************************************
C
```

```
      SUBROUTINE GET_FILE_NAME(IFILE,FILELOAD,FILEDIS,IFILE1,FILELOAD1
     &           FILEDIS1,IT)
      CHARACTER IFILE*20,IFILE1*20,FILELOAD*20,FILELOAD1*20,
     &          FILEDIS*20,FILEDIS1*20
      CHARACTER A*2
      CHARACTER*8 ALL(1:30)
C
      DATA ALL/'01','02','03','04','05','06','07','08','09','10',
     &         '11','12','13','14','15','16','17','18','19','20',
     &         '21','22','23','24','25','26','27','28','29','30'/
C
      A=ALL(IT)
      IFILE1=IFILE(1:LENTH(IFILE,20))//A//'.DAT'
      FILEDIS1=FILEDIS(1:LENTH(FILEDIS,20))//A//'.DAT'
      FILELOAD1=FILELOAD(1:LENTH(FILELOAD,20))//A//'.DAT'
      RETURN
      END
C
      INTEGER FUNCTION LENTH(STRING,MAXLEN)
      CHARACTER STRING*20
      DO 100 I=MAXLEN,1,-1
      IF(STRING(I:I).NE.' ')THEN
      LENTH=I
      RETURN
      ENDIF
100   CONTINUE
      END
C>>>>>>>>>>>>>>>>>>>>>>>>>>>>>>>>>>>>>>>>>>>>>>>>>>>>>>>>>>>>>>>>>>>>>>>
C
C
C*************************************************************************
C                        SUBROUTINE READ_DATA_FILE
C     THIS SUBROUTINE READS THE DATA OF THREE CHANNELS TRANSFERED
C     BY "TRANS2.EXE". ALSO, CONVERTS STRAIN, STRESS DATA FORM VOLTS
C     INTO ENGINEERING UNITS.
C*************************************************************************
C
      SUBROUTINE READ_DATA_FILE(IFILE1,NUMPTS,CAR1,CAR2)
      CHARACTER IFILE1*20,JUNK*80
      COMMON /STRAIN1/ STRAIN
      COMMON /STRESS1/ STRESS
      COMMON /VOLT1/ VOLT
      DIMENSION STRAIN(4100),STRESS(4100),VOLT(4100)
C
      OPEN(UNIT=21,FILE=IFILE1,STATUS='OLD')
C
      DO 200 I=1,4
      READ(21,12)JUNK
200   CONTINUE
C
C>>>>>READ STRAIN VOLTS
      DO 210 I=1,NUMPTS
      READ(21,*)STRAIN(I)
210   CONTINUE
C
      DO 220 I=1,4
      READ(21,12)JUNK
220   CONTINUE
C
C>>>>>READ STRESS VOLTS
```

```
      DO 230 I=1,NUMPTS
      READ(21,*)STRESS(I)
230   CONTINUE
C
      READ(21,12)JUNK
C
C>>>>>READ WAVEFORM VOLTS FROM MICROPROFILE
      DO 250 I=1,NUMPTS
      READ(21,*)VOLT(I)
250   CONTINUE
C
C>>>>>CONVERT THE STRAIN AND STRESS IN VOLT INTO ENGINEERING UNITS
      DO 260 I=1,NUMPTS
      STRAIN(I)=STRAIN(I)*CAR1/10.0
      STRAIN(I)=STRAIN(I)*100.0/3.0
      STRESS(I)=STRESS(I)*CAR2/10.0
      STRESS(I)=STRESS(I)/1.5393808
      VOLT(I)=VOLT(I)*CAR2/10.0
      VOLT(I)=VOLT(I)/1.5393808
260   CONTINUE
12    FORMAT(A80)
      CLOSE(UNIT=21,STATUS='DELETE')
      RETURN
      END
C>>>>>>>>>>>>>>>>>>>>>>>>>>>>>>>>>>>>>>>>>>>>>>>>>>>>>>>>>>>>>>>>>>>>>>>>
C
C*************************************************************************
C                        SUBROUTINE SMOOTH_DATA
C     THIS SUBROUTINE SMOOTHS THE DATA OF STRAIN, STRESS AND VOLT
C*************************************************************************
C
      SUBROUTINE SMOOTH_DATA(NUMPTS)
      COMMON /STRAIN1/ STRAIN
      COMMON /STRESS1/ STRESS
      COMMON /VOLT1/ VOLT
      DIMENSION STRAIN(4100),STRESS(4100),VOLT(4100)
C
      DO 300 I=1,(NUMPTS-1)
      SUM1=0.0
      SUM2=0.0
      SUM3=0.0
      DO 301 J=0,1
      K=I+J
      SUM1=SUM1+STRAIN(K)
      SUM2=SUM2+STRESS(K)
      SUM3=SUM3+VOLT(K)
301   CONTINUE
      STRAIN(I)=SUM1/2.0
      STRESS(I)=SUM2/2.0
      VOLT(I)=SUM3/2.0
300   CONTINUE
      RETURN
      END
C>>>>>>>>>>>>>>>>>>>>>>>>>>>>>>>>>>>>>>>>>>>>>>>>>>>>>>>>>>>>>>>>>>>>>>>>
C
C*************************************************************************
C                    SUBROUTINE FINE_BEGIN_POINTS
C     THIS SUBROUTINE FINDS THE BEGINING POINTD OF TRIANGLE WAVEFORM
C     FOR VOLT, STRAIN, STRESS.
C*************************************************************************
```

```
C
      SUBROUTINE FIND_BEGIN_POINTS(NUMPTS,BEGINVOLT,BEGINSTRESS,
     &           BEGINSTRAIN)
      INTEGER BEGINVOLT,BEGINSTRESS,BEGINSTRAIN
      COMMON /VOLT1/VOLT
      COMMON /STRESS1/STRESS
      COMMON /STRAIN1/STRAIN
      DIMENSION VOLT(4100),STRESS(4100),STRAIN(4100)
C
      BEGINVOLT=0
      TEMP=0.0
C>>>>>FIND THE INITIAL AVERAGE VALUE FROM FIRST 200 POINTS
      DO 400 I=1,200
      TEMP=TEMP+VOLT(I)
400   CONTINUE
      BEGINAVG=TEMP/200.0
C>>>>>FIND THE BEGINING POINT OF UP-RAMP WAVEFORM
      DO 410 I=1,NUMPTS
      IF(VOLT(I).GE.BEGINAVG)THEN
      IF((VOLT(I+1)-BEGINAVG).GE.(VOLT(I)-BEGINAVG))THEN
      INDEX1=I
      DO 420 J=(INDEX1+1),(INDEX1+550)
      IF((VOLT(J)-BEGINAVG).LT.0.0)THEN
      GO TO 410
      ENDIF
420   CONTINUE
      BEGINVOLT=I
      WRITE(*,*)'BEGINVOLT=',BEGINVOLT
      GO TO 430
      ENDIF
      ENDIF
410   CONTINUE
430   CONTINUE
C>>>>>FIND THE BEGINING POINT OF UP-RAMP LOAD CUTVE
      DO 440 K=BEGINVOLT+1,NUMPTS
      IF(STRESS(K).GE.STRESS(BEGINVOLT))THEN
      IF(STRESS(K+1).GE.STRESS(K))THEN
      INDEX2=K
      DO 450 KK=INDEX2+1,INDEX2+550
      IF(STRESS(KK).LE.STRESS(INDEX2))THEN
      GO TO 440
      ENDIF
450   CONTINUE
      BEGINSTRESS=K
      WRITE(*,*)'BEGINSTRESS=',BEGINSTRESS
      GO TO 460
      ENDIF
      ENDIF
440   CONTINUE
460   CONTINUE
C>>>>>FIND THE BEGIN POINT OF STRAIN
      DO 470 J=BEGINSTRESS+1,NUMPTS
      IF(STRAIN(J).GE.STRAIN(BEGINSTRESS))THEN
      IF(STRAIN(J+1).GE.STRAIN(J))THEN
      INDEX3=J
      DO 480 JJ=INDEX3+1,INDEX3+550
      IF(STRAIN(JJ).LE.STRAIN(INDEX3))THEN
      GO TO 470
      ENDIF
480   CONTINUE
```

```
      BEGINSTRAIN=J
      WRITE(*,*)'BEGINSTRAIN=',BEGINSTRAIN
      GO TO 490
      ENDIF
      ENDIF
470   CONTINUE
490   RETURN
      END
C>>>>>>>>>>>>>>>>>>>>>>>>>>>>>>>>>>>>>>>>>>>>>>>>>>>>>>>>>>>>>>>>>>>>>>>>>>>
C
C*************************************************************************
C                          SUBROUTINE INITIALIZE_DATA
C     THIS SUBROUTINE INITIALIZE DATA OF STRAIN, STRESS AND VOLT
C*************************************************************************
C
      SUBROUTINE INITIALIZE_DATA(BEGINVOLT,BEGINSTRESS,BEGINSTRAIN,
     &           NUMPTS)
      COMMON /STRAIN1/ STRAIN
      COMMON /STRESS1/ STRESS
      COMMON /VOLT1/ VOLT
      INTEGER BEGINVOLT,BEGINSTRESS,BEGINSTRAIN
      DIMENSION STRAIN(4100),STRESS(4100),VOLT(4100)
C
      AVGSTRAIN=0.0
      AVGSTRESS=0.0
      AVGVOLT=0.0
C
      DO 500 I=1,BEGINVOLT
      AVGVOLT=AVGVOLT+VOLT(I)
500   CONTINUE
      AVGVOLT=AVGVOLT/FLOAT(BEGINVOLT)
C
      DO 501 I=1,BEGINSTRESS
      AVGSTRESS=AVGSTRESS+STRESS(I)
501   CONTINUE
      AVGSTRESS=AVGSTRESS/FLOAT(BEGINSTRESS)
C
      DO 502 I=1,BEGINSTRAIN
      AVGSTRAIN=AVGSTRAIN+STRAIN(I)
502   CONTINUE
      AVGSTRAIN=AVGSTRAIN/FLOAT(BEGINSTRAIN)
C
C>>>>>INITIALIZE STRAIN DATA
      IF(AVGSTRAIN.GE.0.0)THEN
      DO 510 I=1,NUMPTS
      STRAIN(I)=STRAIN(I)-AVGSTRAIN
510   CONTINUE
      ELSE
      DO 520 J=1,NUMPTS
      STRAIN(J)=STRAIN(J)+ABS(AVGSTRAIN)
520   CONTINUE
      ENDIF
C
C>>>>>INITIALIZE STRESS DATA
      IF(AVGSTRESS.GE.0.0)THEN
      DO 530 I=1,NUMPTS
      STRESS(I)=STRESS(I)-AVGSTRESS
530   CONTINUE
      ELSE
      DO 540 J=1,NUMPTS
```

```
      STRESS(J)=STRESS(J)+ABS(AVGSTRESS)
540   CONTINUE
      ENDIF
C
C>>>>>INITIALIZE VOLT DATA
      IF(AVGVOLT.GE.0.0)THEN
      DO 550 I=1,NUMPTS
      VOLT(I)=VOLT(I)-AVGVOLT
550   CONTINUE
      ELSE
      DO 560 J=1,NUMPTS
      VOLT(I)=VOLT(I)+ABS(AVGVOLT)
560   CONTINUE
      ENDIF
      RETURN
      END
C>>>>>>>>>>>>>>>>>>>>>>>>>>>>>>>>>>>>>>>>>>>>>>>>>>>>>>>>>>>>>>>>>>>>>>>>>>>
C
C*************************************************************************
C                  SUBROUTINE VARIATION_WITH_TIME
C*************************************************************************
C
      SUBROUTINE VARIATION_WITH_TIME(NUMPTS,BEGINSTRESS,BEGINSTRAIN,
     &           TIMELEN,FILELOAD1,FILEDIS1)
      CHARACTER FILELOAD1*20
      CHARACTER FILEDIS1*20
      INTEGER BEGINSTRESS,BEGINSTRAIN
      COMMON /STRAIN1/ STRAIN
      COMMON /STRESS1/ STRESS
      COMMON /TSTRESS1/ TSTRESS
      COMMON /TSTRAIN1/ TSTRAIN
      DIMENSION STRAIN(4100),STRESS(4100),TSTRAIN(4100),TSTRESS(4100)
C
      OPEN(UNIT=35,FILE=FILELOAD1,STATUS='NEW')
      OPEN(UNIT=36,FILE=FILEDIS1,STATUS='NEW')
C
      TIMESTEP=TIMELEN/NUMPTS
C>>>>>FIND RELATION OF STRESS WITH TIME
      DO 600 I=BEGINSTRESS,NUMPTS
      MLOAD=I-BEGINSTRESS+1
      TSTRESS(I)=TIMESTEP*FLOAT(MLOAD)
      WRITE(35,*)TSTRESS(I),STRESS(I)
600   CONTINUE
      CLOSE(UNIT=35)
C>>>>>FIND RELATION OF STRAIN WITH TIME
      DO 601 J=BEGINSTRAIN,NUMPTS
      MSTRAIN=J-BEGINSTRAIN+1
      TSTRAIN(J)=TIMESTEP*FLOAT(MSTRAIN)
      STRAIN(J)=ABS(STRAIN(J))
      WRITE(36,*)TSTRAIN(J),STRAIN(J)
601   CONTINUE
      CLOSE(UNIT=36)
      RETURN
      END
C>>>>>>>>>>>>>>>>>>>>>>>>>>>>>>>>>>>>>>>>>>>>>>>>>>>>>>>>>>>>>>>>>>>>>>>>>>>
C
C*************************************************************************
C                        SUBROUTINE FIND_MAXIMUM_POINTS
C     THIS SUBROUTINE FINDS THE MAXIMUM POINTS OF TRANGLE WAVEFORM
C     FOR STRAIN, STRESS AND VOLT.
```

```
C*********************************************************************
C
      SUBROUTINE FIND_MAXIMUM_POINTS(NUMPTS,TIMELEN,BEGINVOLT,
     &BEGINSTRESS,BEGINSTRAIN)
      INTEGER BEGINVOLT,BEGINSTRESS,BEGINSTRAIN
      COMMON /STRAIN1/ STRAIN
      COMMON /STRESS1/ STRESS
      COMMON /VOLT1/ VOLT
      DIMENSION STRAIN(4100),STRESS(4100),VOLT(4100)
C
C>>>>>FIND MAXIMUM VALUE OF STRAIN CURVE
      MAXSTRAIN=0
      STRAINMAX=0.0
      DO 710 I1=BEGINSTRAIN,2500
      IF(STRAIN(I1).GE.STRAINMAX)THEN
      STRAINMAX=STRAIN(I1)
      MAXSTRAIN=I1
      ENDIF
710   CONTINUE
C
C>>>>>FIND MAXIMUM VALUE OF STRESS CURVE
      MAXSTRESS=0
      STRESSMAX=0.0
      DO 720 I2=BEGINSTRESS,2500
      IF(STRESS(I2).GE.STRESSMAX)THEN
      STRESSMAX=STRESS(I2)
      MAXSTRESS=I2
      ENDIF
720   CONTINUE
C
C>>>>>FIND MAXIMUM VALUE OF VOLT CURVE
      MAXVOLT=0
      VOLTMAX=0.0
      DO 730 I3=BEGINVOLT,2500
      IF(VOLT(I3).GE.VOLTMAX)THEN
      VOLTMAX=VOLT(I3)
      MAXVOLT=I3
      ENDIF
730   CONTINUE
C
      STRAINMAXTIME=(MAXSTRAIN-BEGINSTRAIN)*(TIMELEN/FLOAT(NUMPTS))
      STRESSMAXTIME=(MAXSTRESS-BEGINSTRESS)*(TIMELEN/FLOAT(NUMPTS))
      VOLTMAXTIME=(MAXVOLT-BEGINVOLT)*(TIMELEN/FLOAT(NUMPTS))
C
C>>>>>WRITE OUTPUT DATA
      WRITE(41,*)'                    MAX. TIME, milisec.'
      WRITE(41,*)'                    -------------------'
      WRITE(41,*)STRAINMAXTIME,STRESSMAXTIME,VOLTMAXTIME
      WRITE(41,*)' '
      WRITE(41,*)'                        MAX. VALUES'
      WRITE(41,*)'                    -------------------'
      WRITE(41,*)STRAINMAX,STRESSMAX,VOLTMAX
      WRITE(41,*)' '
      WRITE(41,*)' '
      RETURN
      END
```

APPENDIX K

SELECTED RESULTS OF DYNAMIC TESTS

ON

SPECIMENS AT 15 PSI SOIL SUCTION

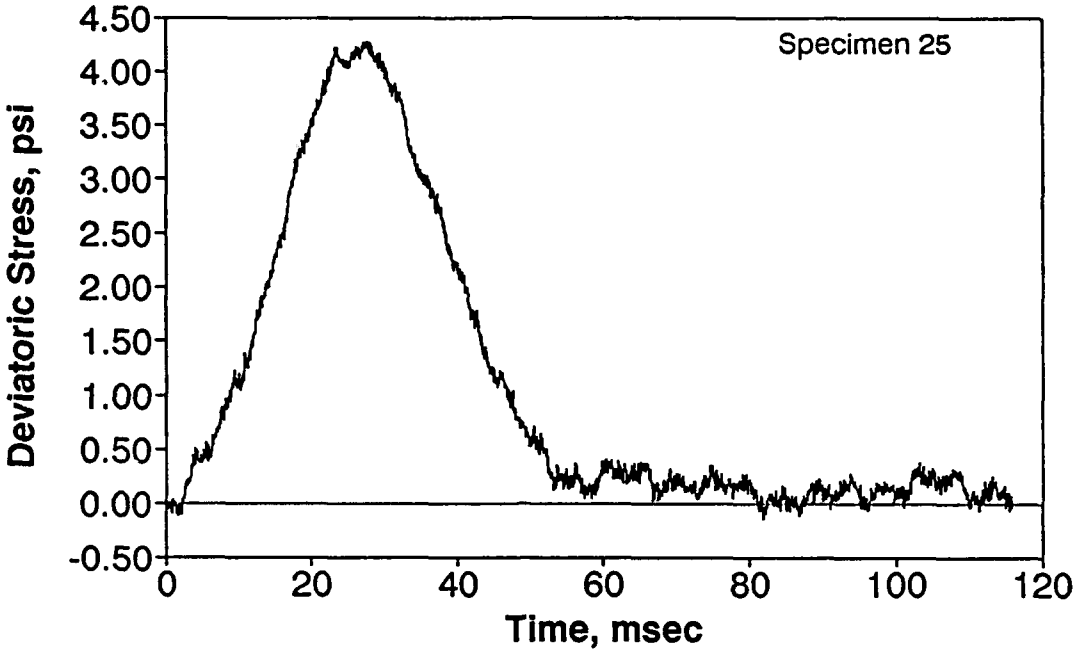
Specimen 25
Deviatoric Stress, psi
4.50
4.00
3.50
3.00
2.50
2.00
1.50
1.00
0.50
0.00
-0.50
0
20
40
60
80
100
120
Time, msec

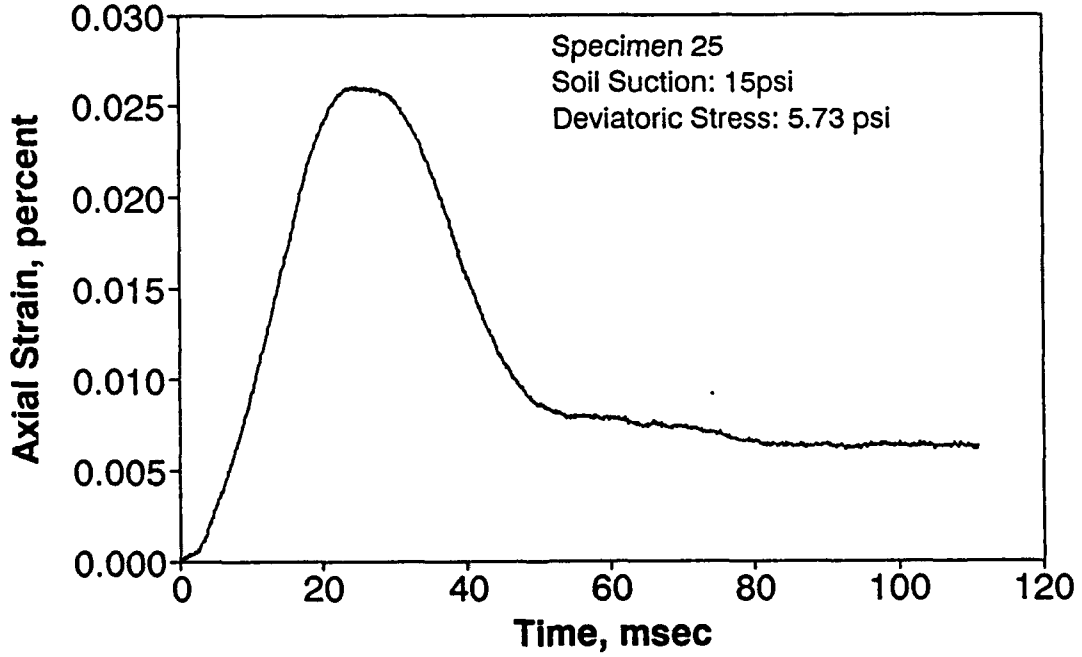
Specimen 25
Soil Suction: 15psi
Deviatoric Stress: 5.73 psi
Axial Strain, percent
0.030
0.025
0.020
0.015
0.010
0.005
0.000
0
20
40
60
80
100
120
Time, msec

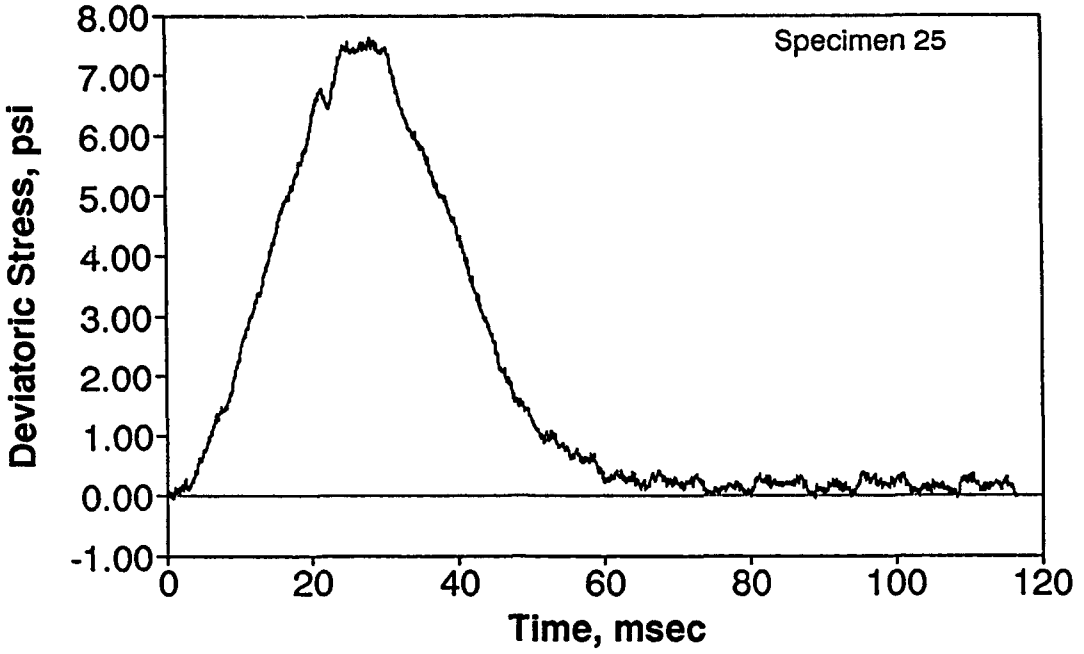
Specimen 25
Deviatoric Stress, psi
8.00
7.00
6.00
5.00
4.00
3.00
2.00
1.00
0.00
-1.00
0
20
40
60
80
100
120
Time, msec

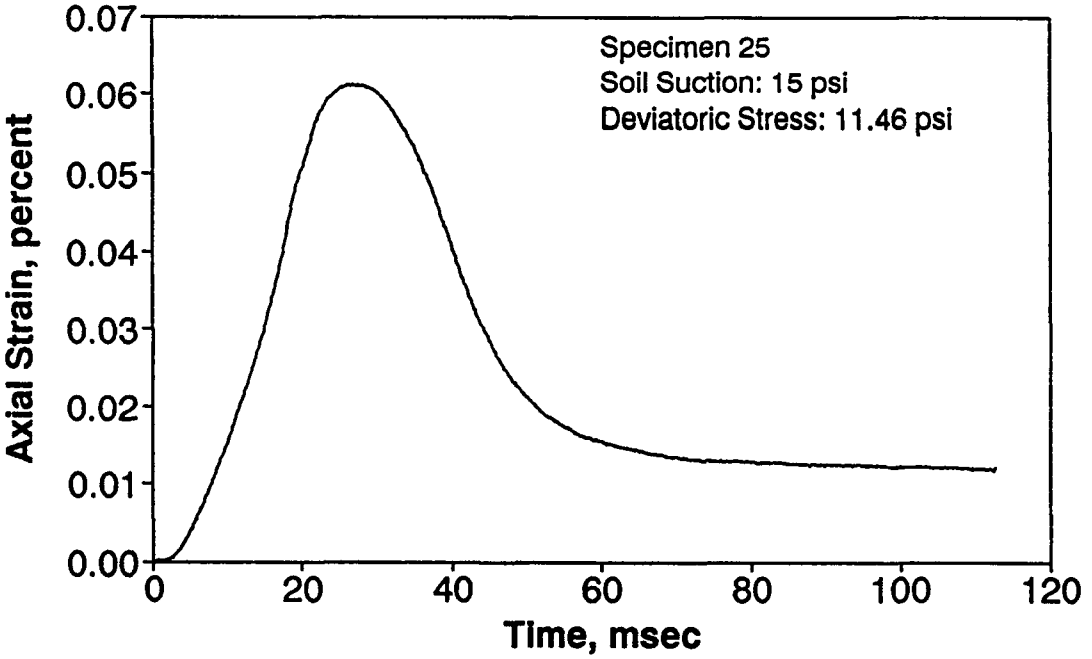
Specimen 25
Soil Suction: 15 psi
Deviatoric Stress: 11.46 psi
Axial Strain, percent
0.07
0.06
0.05
0.04
0.03
0.02
0.01
0.00
0
20
40
60
80
100
120
Time, msec

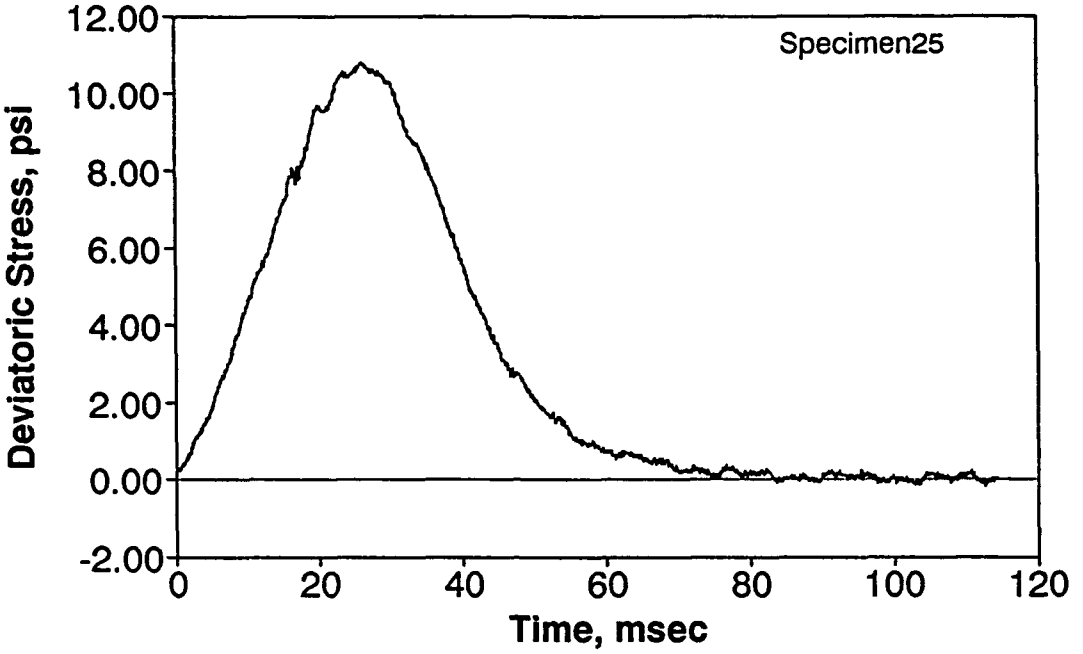
Specimen25
Deviatoric Stress, psi
12.00
10.00
8.00
6.00
4.00
2.00
0.00
-2.00
0
20
40
60
80
100
120
Time, msec

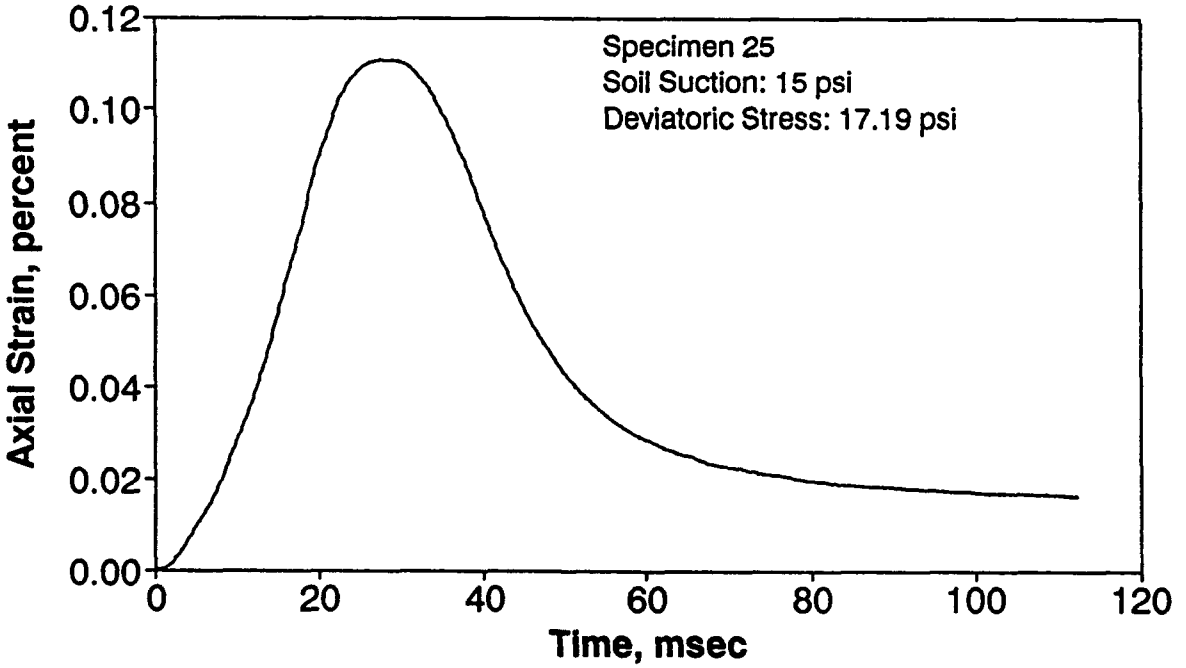
Specimen 25
Soil Suction: 15 psi
Deviatoric Stress: 17.19 psi
Axial Strain, percent
0.12
0.10
0.08
0.06
0.04
0.02
0.00
0
20
40
60
80
100
120
Time, msec

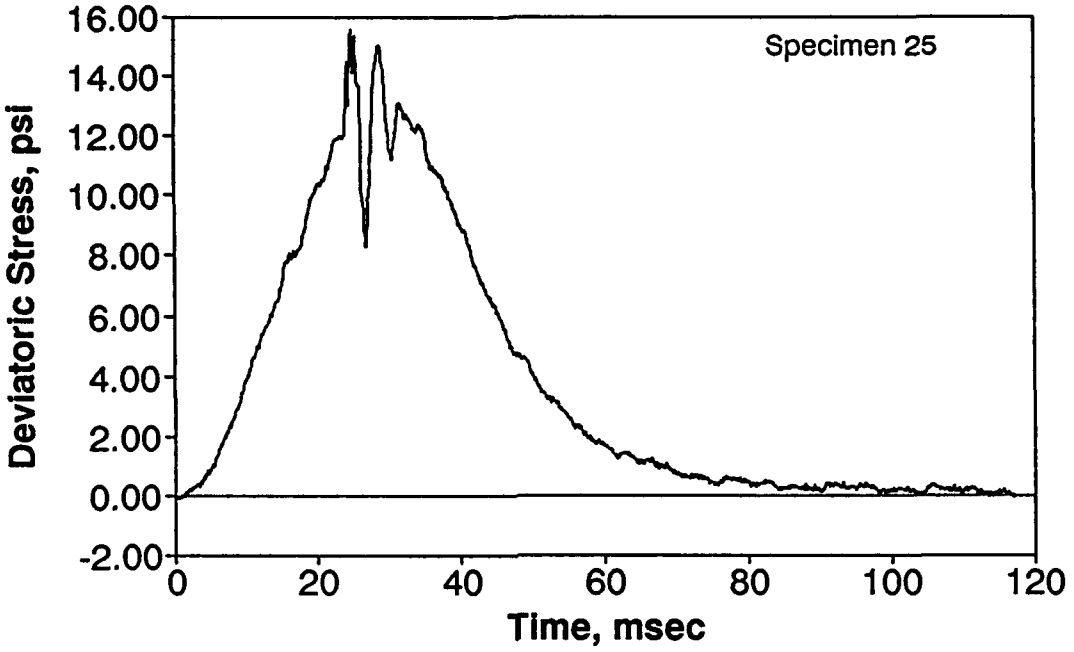
Specimen 25
Deviatoric Stress, psi
16.00
14.00
12.00
10.00
8.00
6.00
4.00
2.00
0.00
-2.00
0
20
40
60
80
100
120
Time, msec

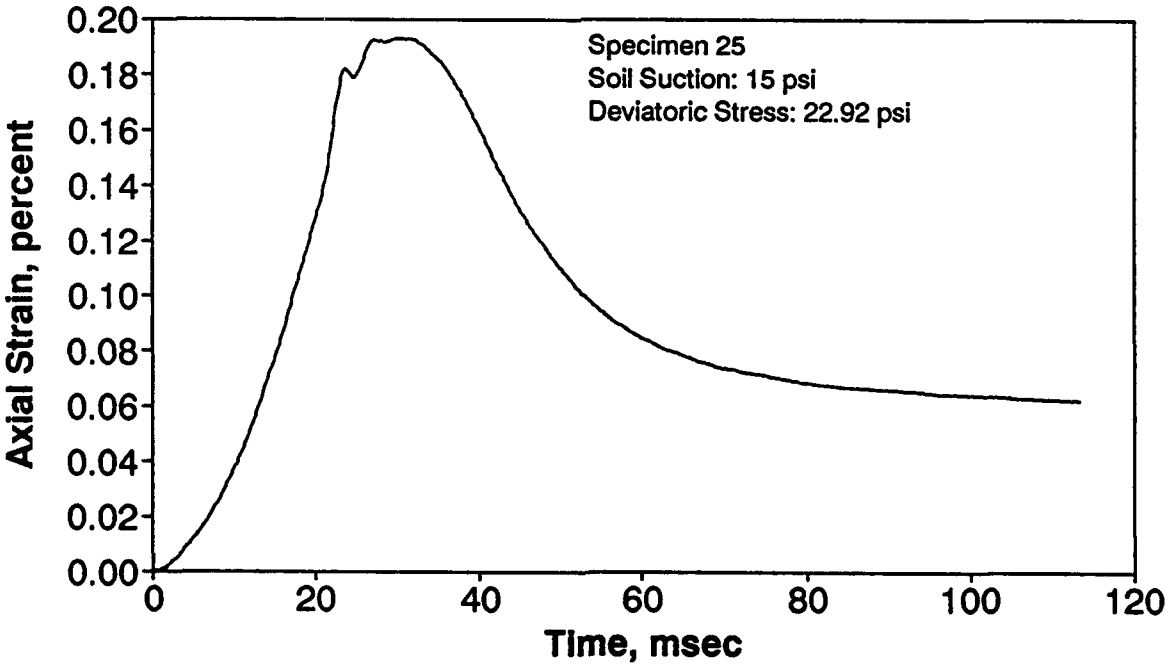
Specimen 25
Soil Suction: 15 psi
Deviatoric Stress: 22.92 psi
Axial Strain, percent
0.20
0.18
0.16
0.14
0.12
0.10
0.08
0.06
0.04
0.02
0.00
0
20
40
60
80
100
120
Time, msec

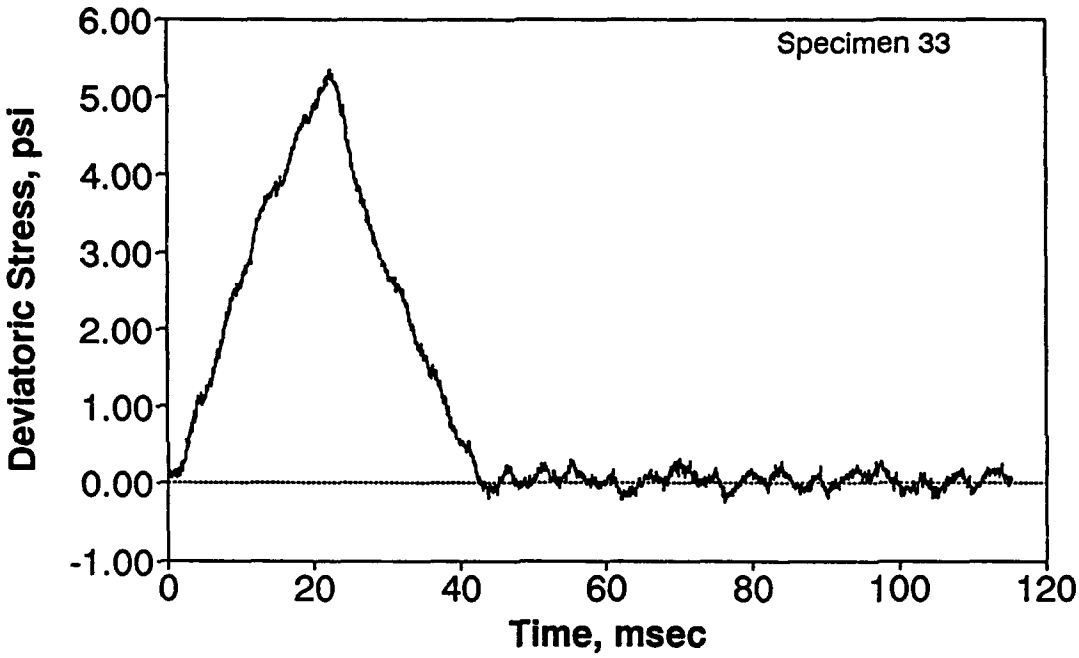
Specimen 33
Deviatoric Stress, psi
6.00
5.00
4.00
3.00
2.00
1.00
0.00
-1.00
0
20
40
60
80
100
120
Time, msec

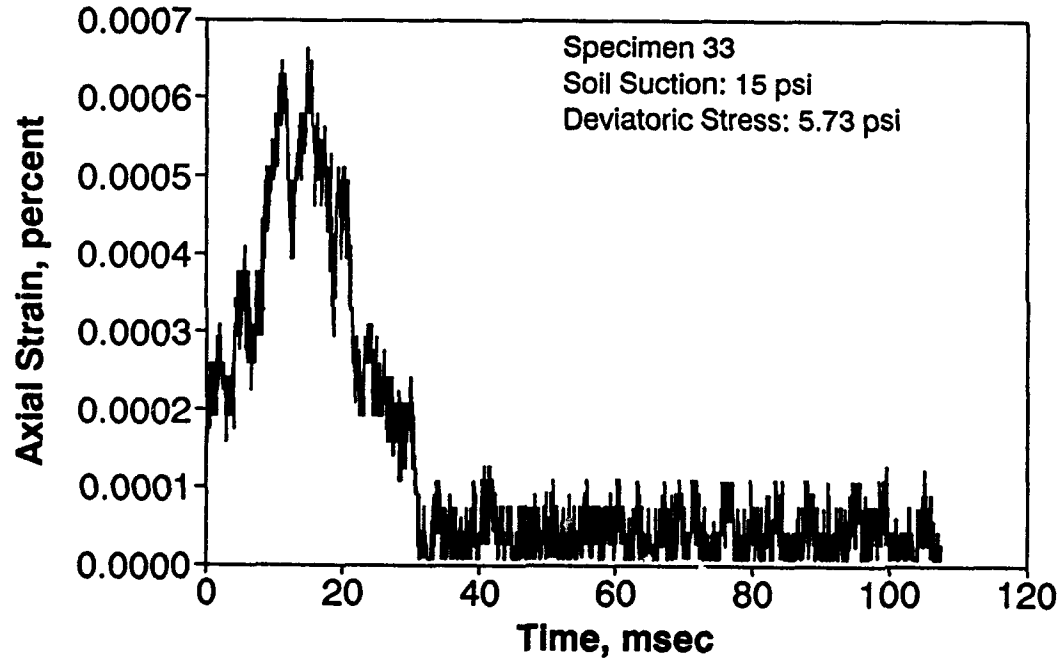
Specimen 33
Soil Suction: 15 psi
Deviatoric Stress: 5.73 psi
Axial Strain, percent
0.0007
0.0006
0.0005
0.0004
0.0003
0.0002
0.0001
0.0000
0
20
40
60
80
100
120
Time, msec

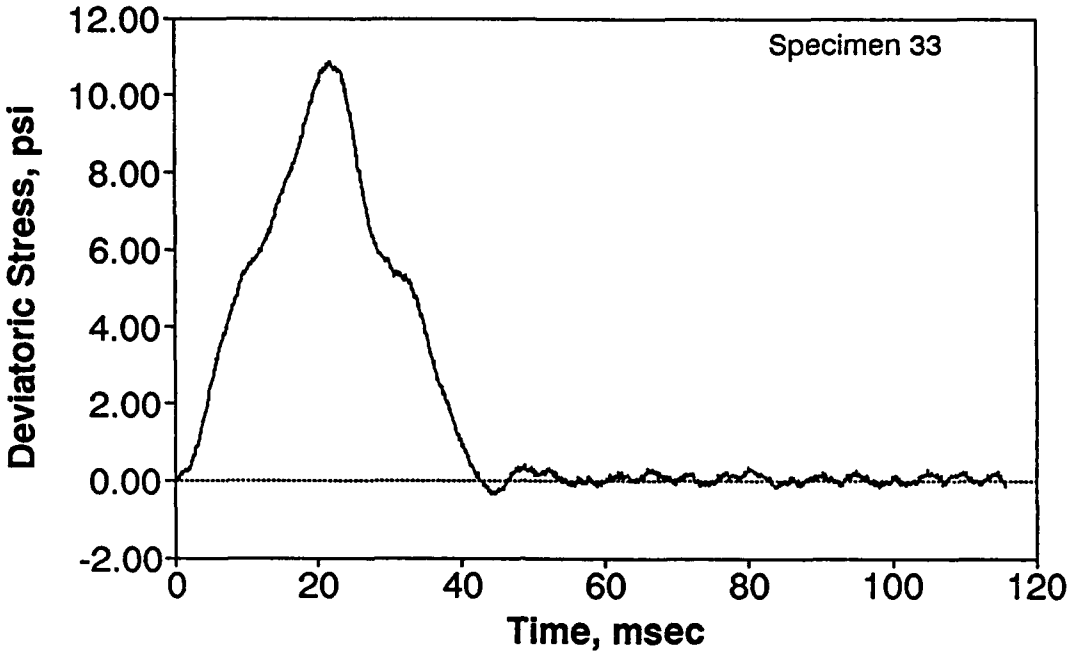
Specimen 33
Deviatoric Stress, psi
12.00
10.00
8.00
6.00
4.00
2.00
0.00
-2.00
0
20
40
60
80
100
120
Time, msec

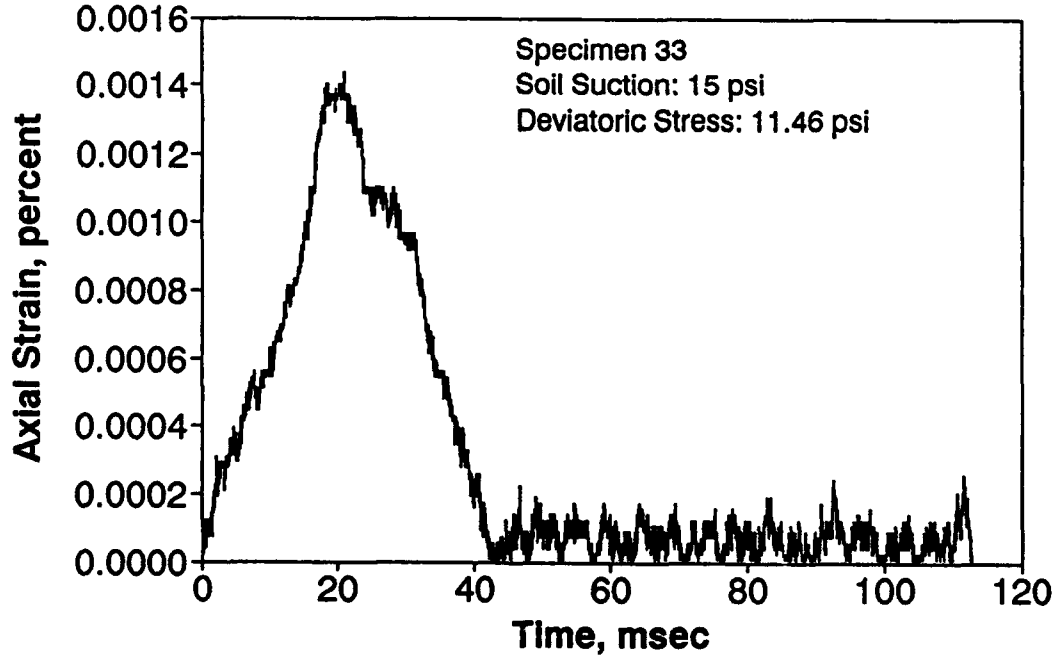
Specimen 33
Soil Suction: 15 psi
Deviatoric Stress: 11.46 psi
Axial Strain, percent
0.0016
0.0014
0.0012
0.0010
0.0008
0.0006
0.0004
0.0002
0.0000
0
20
40
60
80
100
120
Time, msec

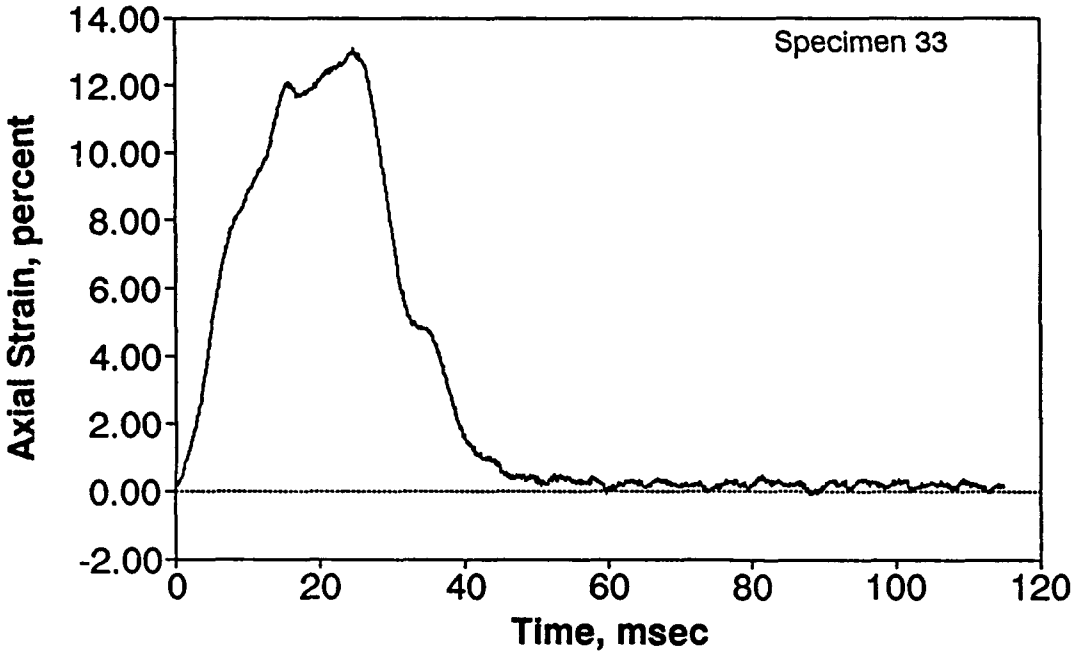
Specimen 33
Axial Strain, percent
14.00
12.00
10.00
8.00
6.00
4.00
2.00
0.00
-2.00
0
20
40
60
80
100
120
Time, msec

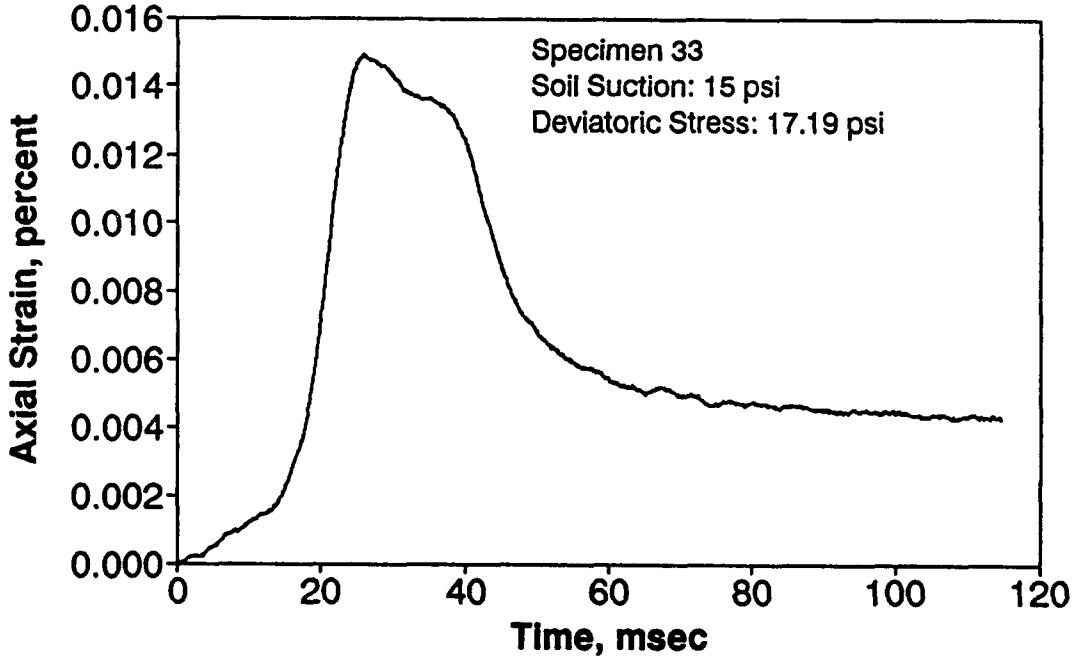
Specimen 33
Soil Suction: 15 psi
Deviatoric Stress: 17.19 psi
Axial Strain, percent
0.016
0.014
0.012
0.010
0.008
0.006
0.004
0.002
0.000
0
20
40
60
80
100
120
Time, msec

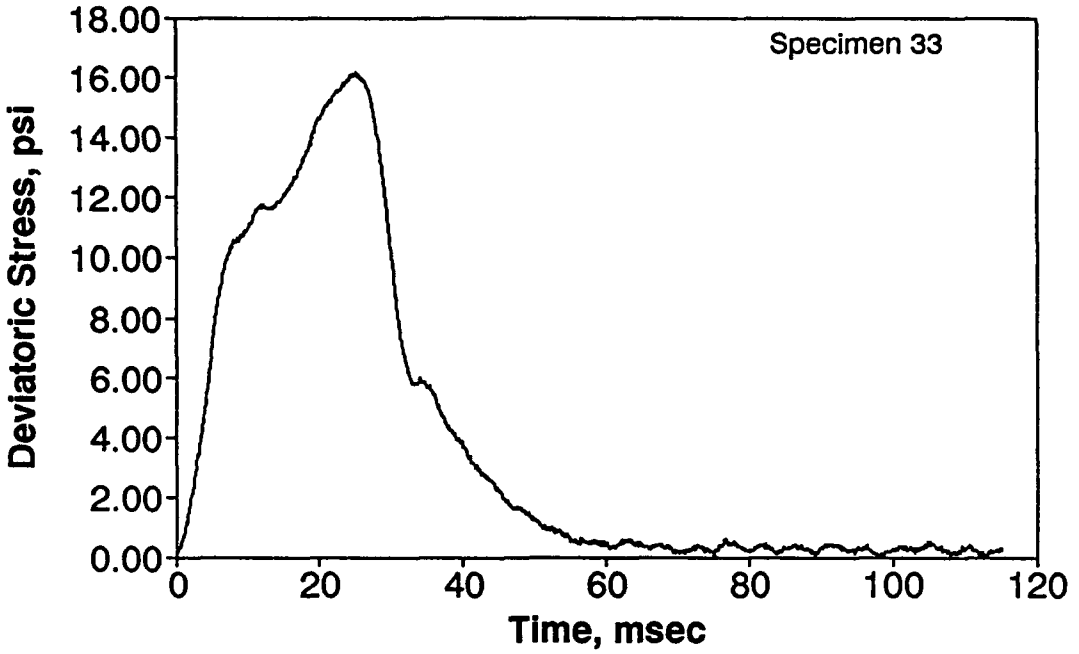
Specimen 33
Deviatoric Stress, psi
18.00
16.00
14.00
12.00
10.00
8.00
6.00
4.00
2.00
0.00
0
20
40
60
80
100
120
Time, msec

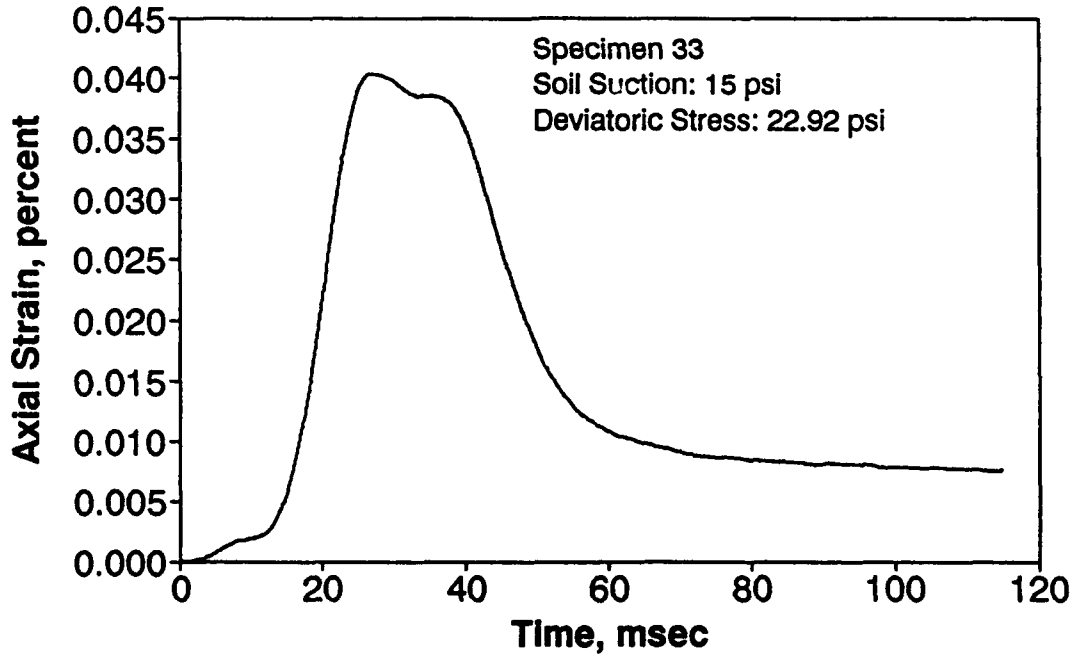
Specimen 33
Soil Suction: 15 psi
Deviatoric Stress: 22.92 psi
Axial Strain, percent
0.045
0.040
0.035
0.030
0.025
0.020
0.015
0.010
0.005
0.000
0
20
40
60
80
100
120
Time, msec

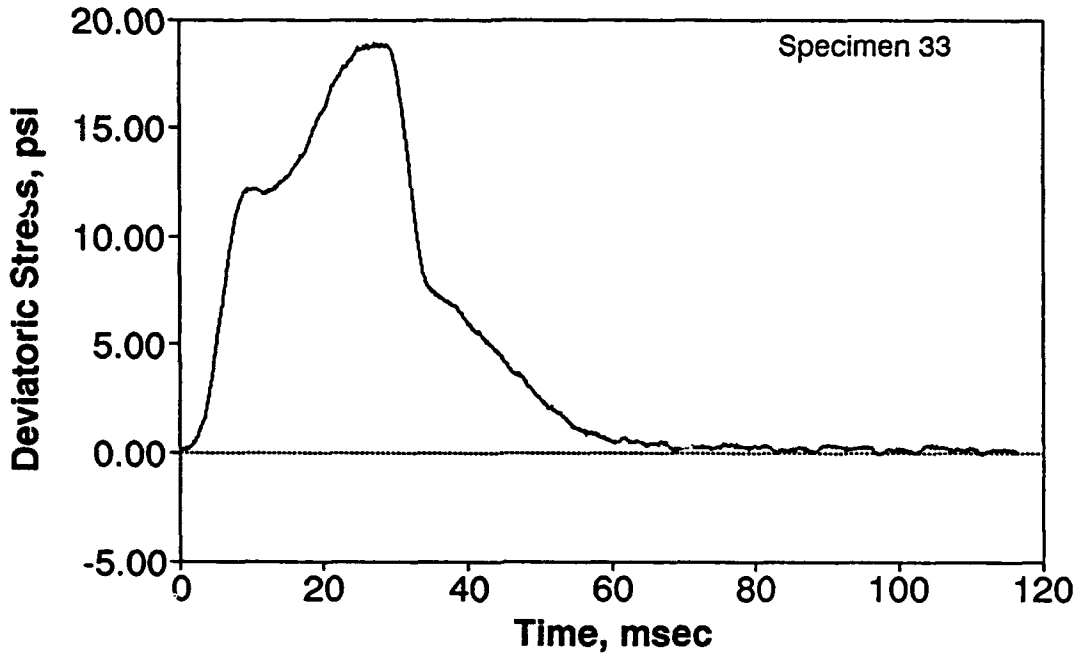
Specimen 33
Deviatoric Stress, psi
20.00
15.00
10.00
5.00
0.00
-5.00
0
20
40
60
80
100
120
Time, msec

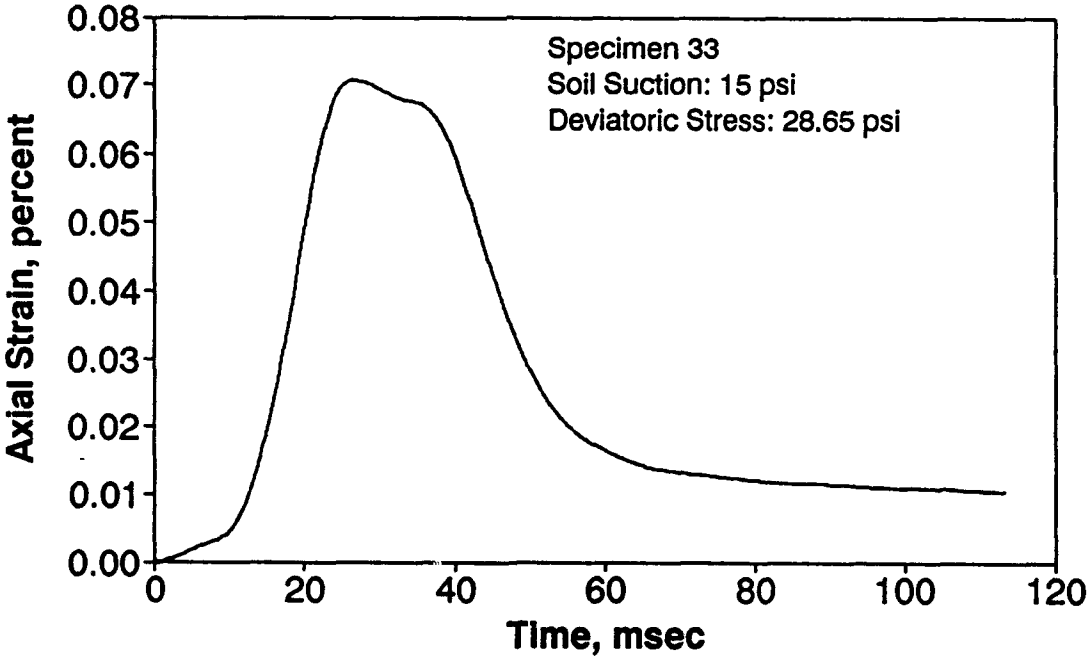
Specimen 33
Soil Suction: 15 psi
Deviatoric Stress: 28.65 psi
Axial Strain, percent
0.08
0.07
0.06
0.05
0.04
0.03
0.02
0.01
0.00
0
20
40
60
80
100
120
Time, msec

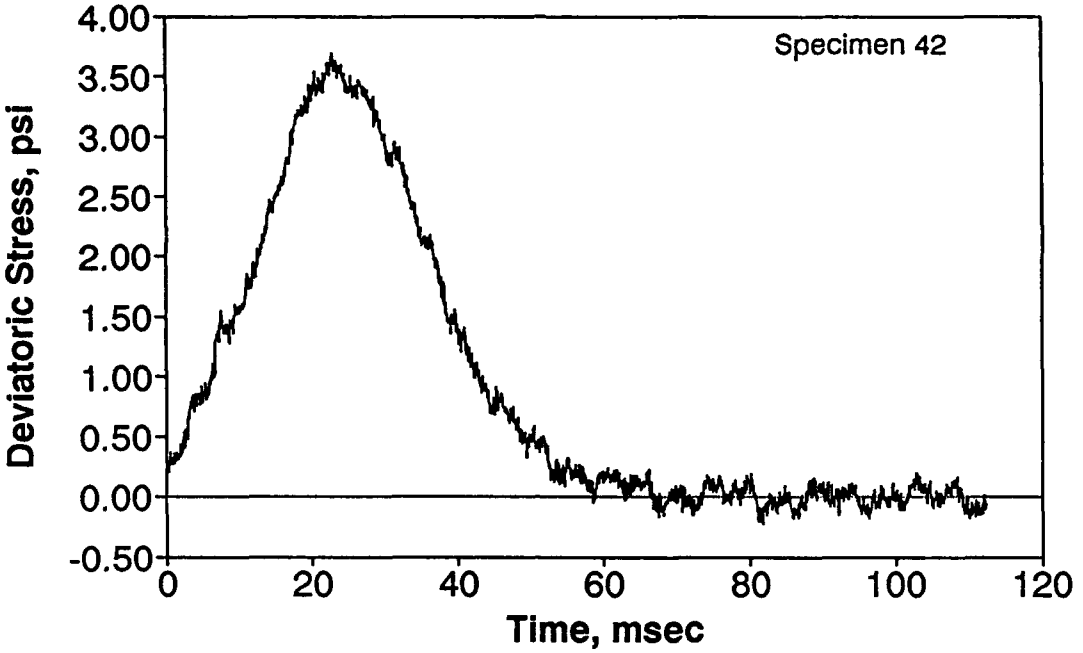
Specimen 42
Deviatoric Stress, psi
4.00
3.50
3.00
2.50
2.00
1.50
1.00
0.50
0.00
-0.50
0
20
40
60
80
100
120
Time, msec

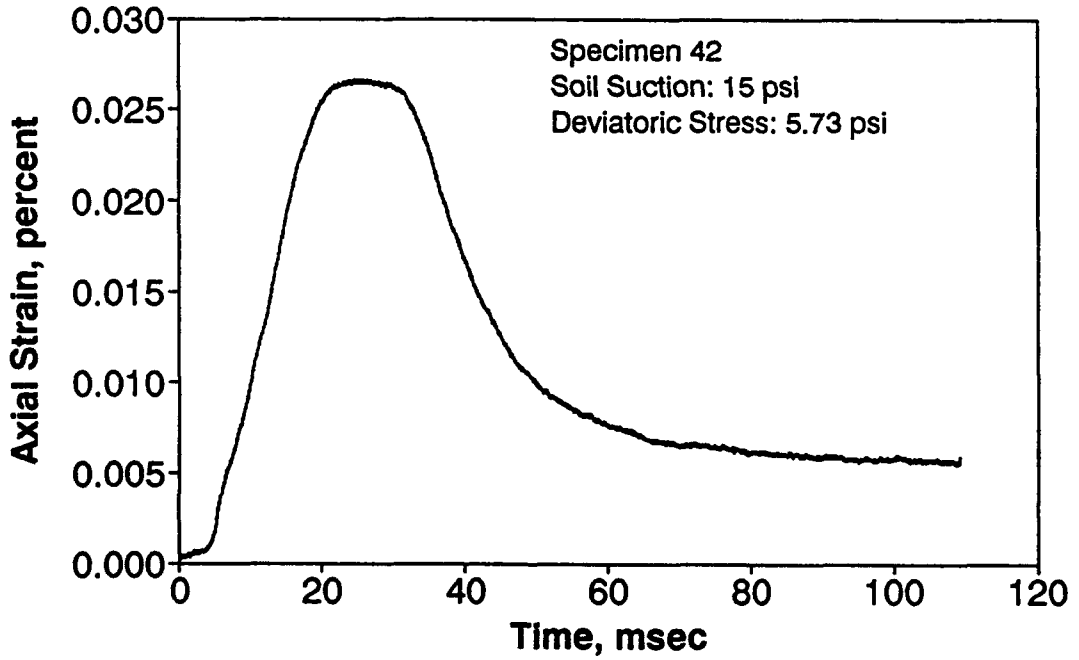
Specimen 42
Soil Suction: 15 psi
Deviatoric Stress: 5.73 psi
Axial Strain, percent
0.030
0.025
0.020
0.015
0.010
0.005
0.000
0
20
40
60
80
100
120
Time, msec

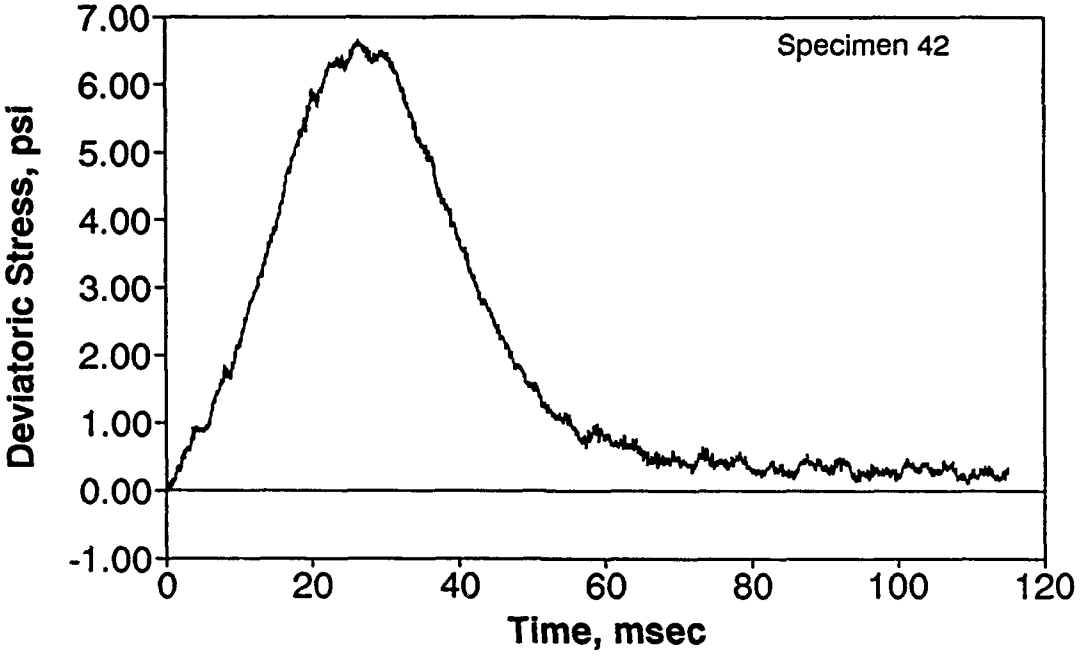
Specimen 42
Deviatoric Stress, psi
7.00
6.00
5.00
4.00
3.00
2.00
1.00
0.00
-1.00
0
20
40
60
80
100
120
Time, msec

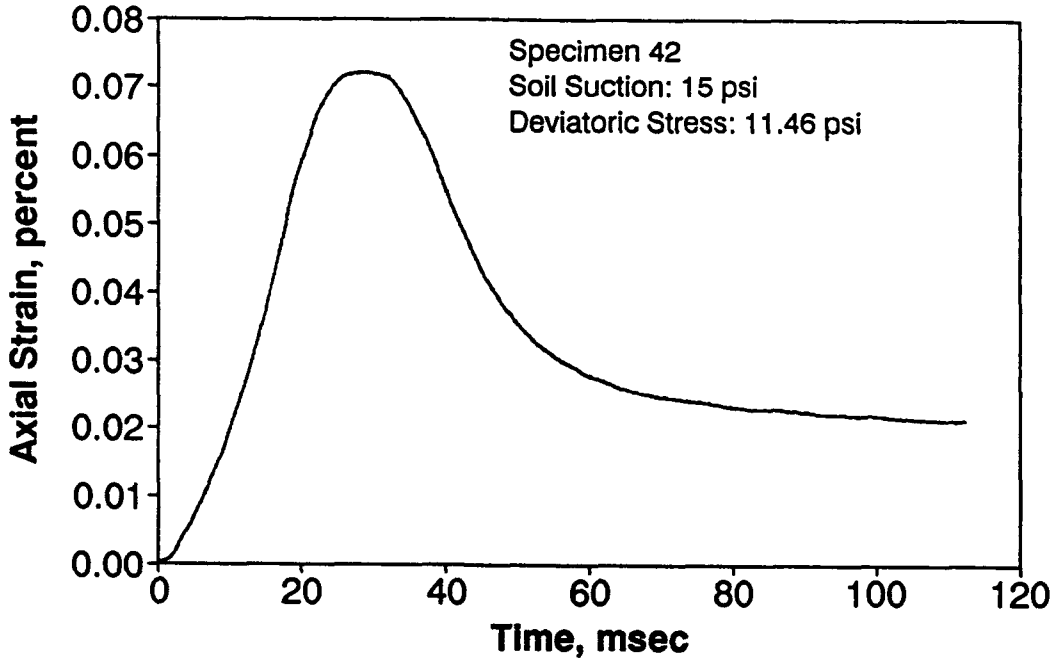
Specimen 42
Soil Suction: 15 psi
Deviatoric Stress: 11.46 psi
Axial Strain, percent
0.08
0.07
0.06
0.05
0.04
0.03
0.02
0.01
0.00
0
20
40
60
80
100
120
Time, msec

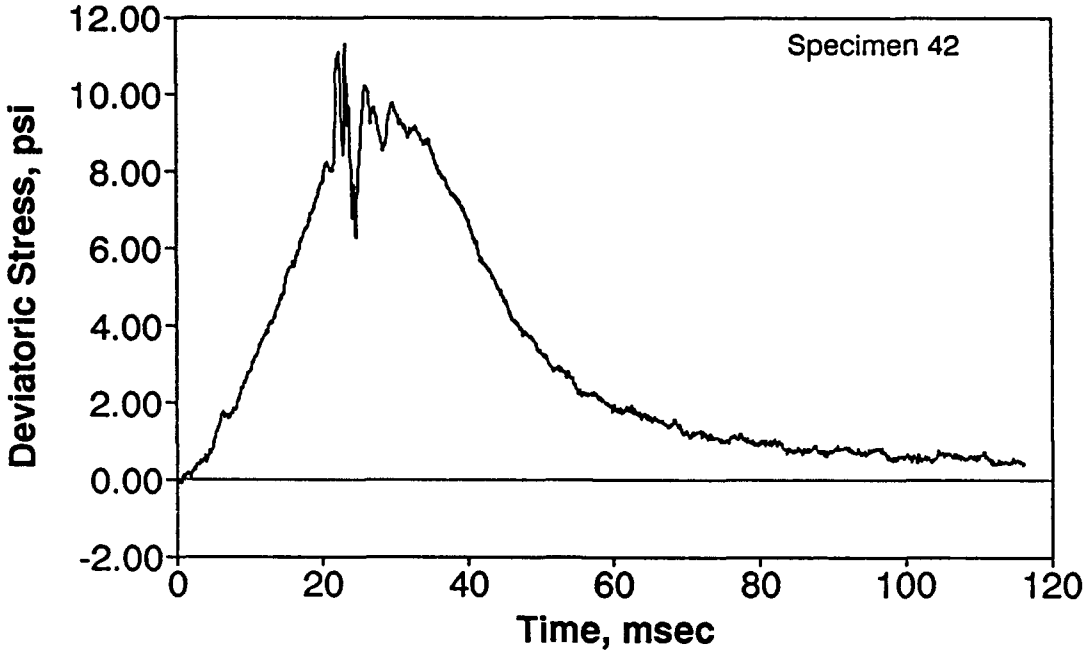
Specimen 42
Deviatoric Stress, psi
12.00
10.00
8.00
6.00
4.00
2.00
0.00
-2.00
0
20
40
60
80
100
120
Time, msec

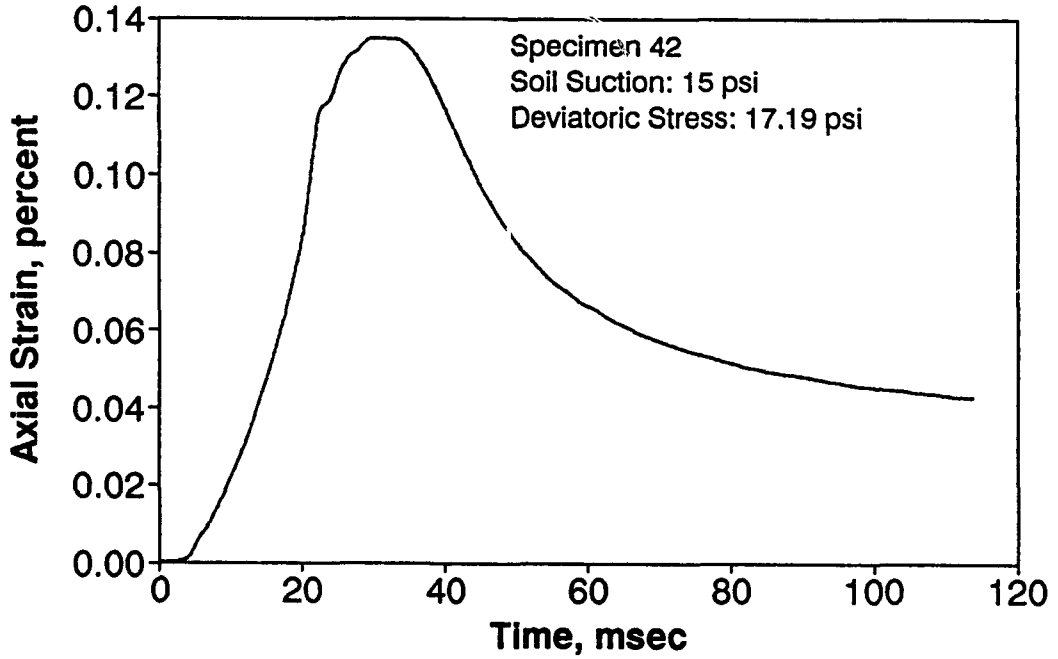
Specimen 42
Soil Suction: 15 psi
Deviatoric Stress: 17.19 psi
Axial Strain, percent
0.14
0.12
0.10
0.08
0.06
0.04
0.02
0.00
0
20
40
60
80
100
120
Time, msec

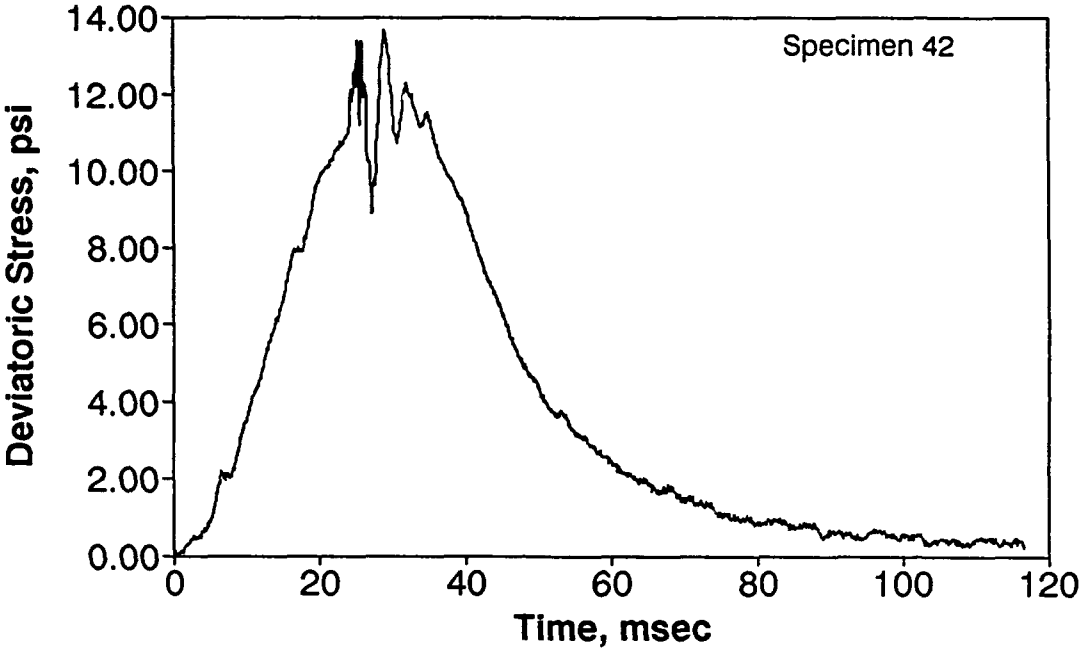
Specimen 42
Deviatoric Stress, psi
14.00
12.00
10.00
8.00
6.00
4.00
2.00
0.00
0
20
40
60
80
100
120
Time, msec

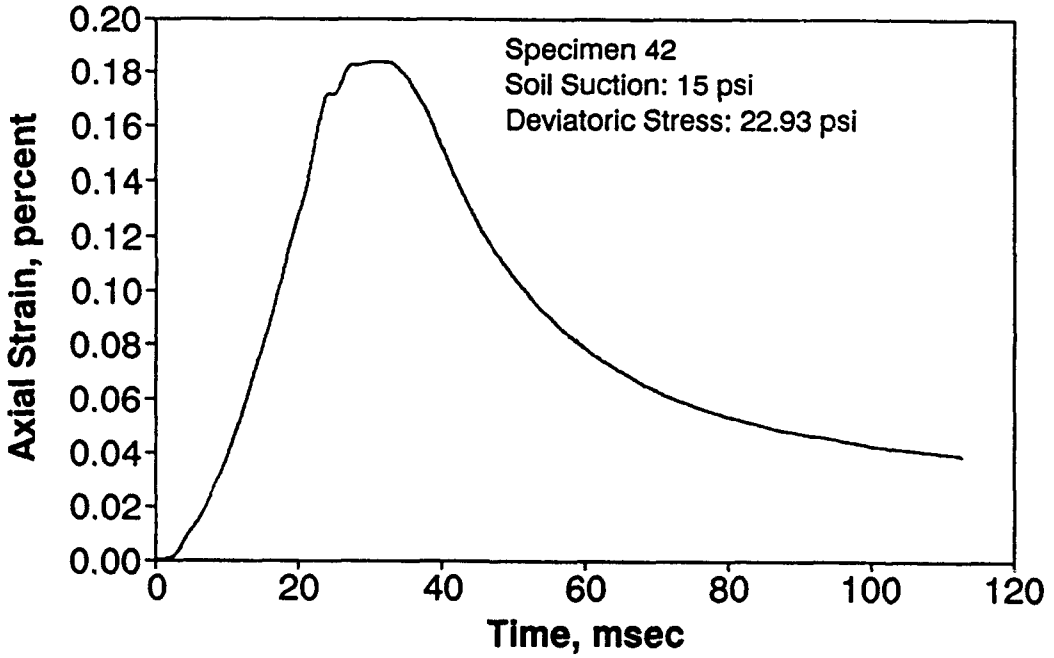
Specimen 42
Soil Suction: 15 psi
Deviatoric Stress: 22.93 psi
Axial Strain, percent
0.20
0.18
0.16
0.14
0.12
0.10
0.08
0.06
0.04
0.02
0.00
0
20
40
60
80
100
120
Time, msec

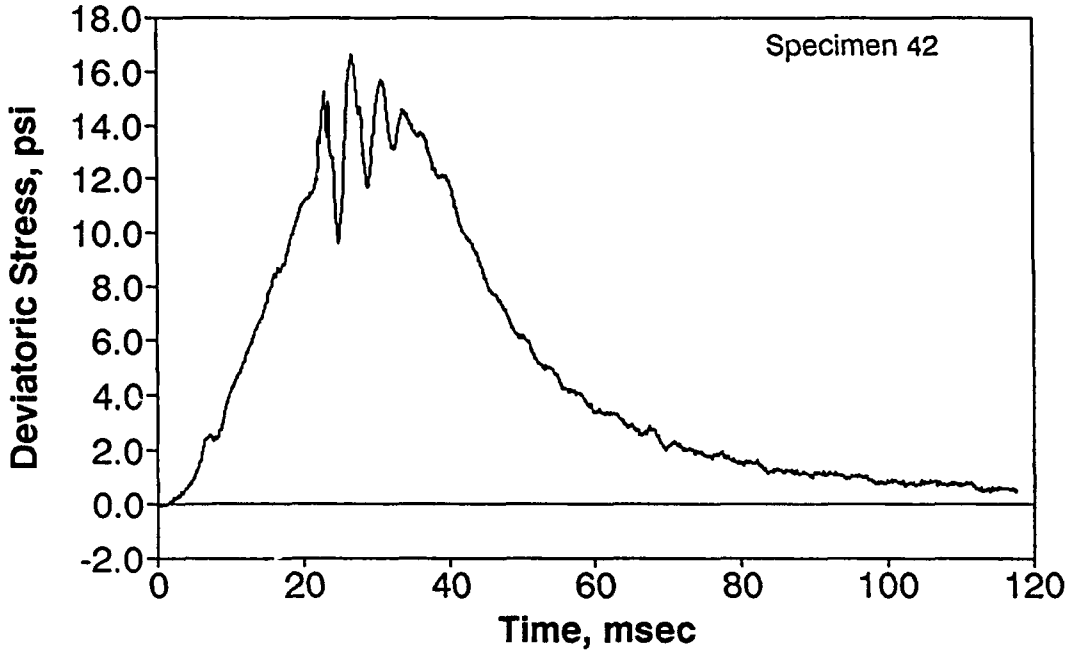
Specimen 42
Deviatoric Stress, psi
18.0
16.0
14.0
12.0
10.0
8.0
6.0
4.0
2.0
0.0
-2.0
0
20
40
60
80
100
120
Time, msec

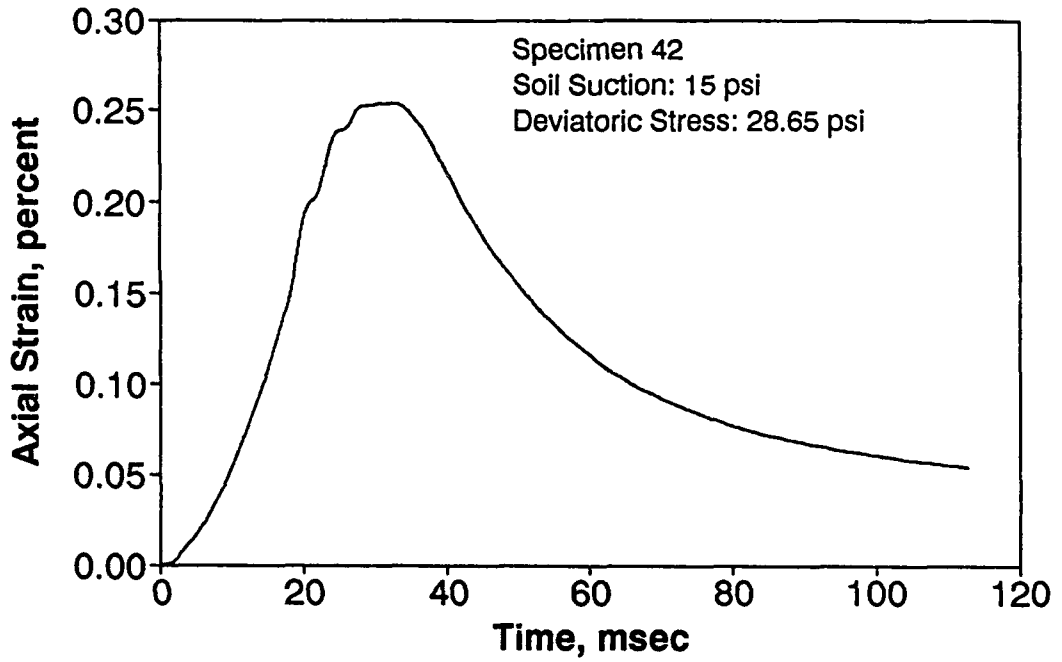
Specimen 42
Soil Suction: 15 psi
Deviatoric Stress: 28.65 psi
Axial Strain, percent
0.30
0.25
0.20
0.15
0.10
0.05
0.00
0
20
40
60
80
100
120
Time, msec

APPENDIX L

SELECTED RESULTS OF DYNAMIC TESTS

ON

SPECIMENS AT 40 PSI SOIL SUCTION

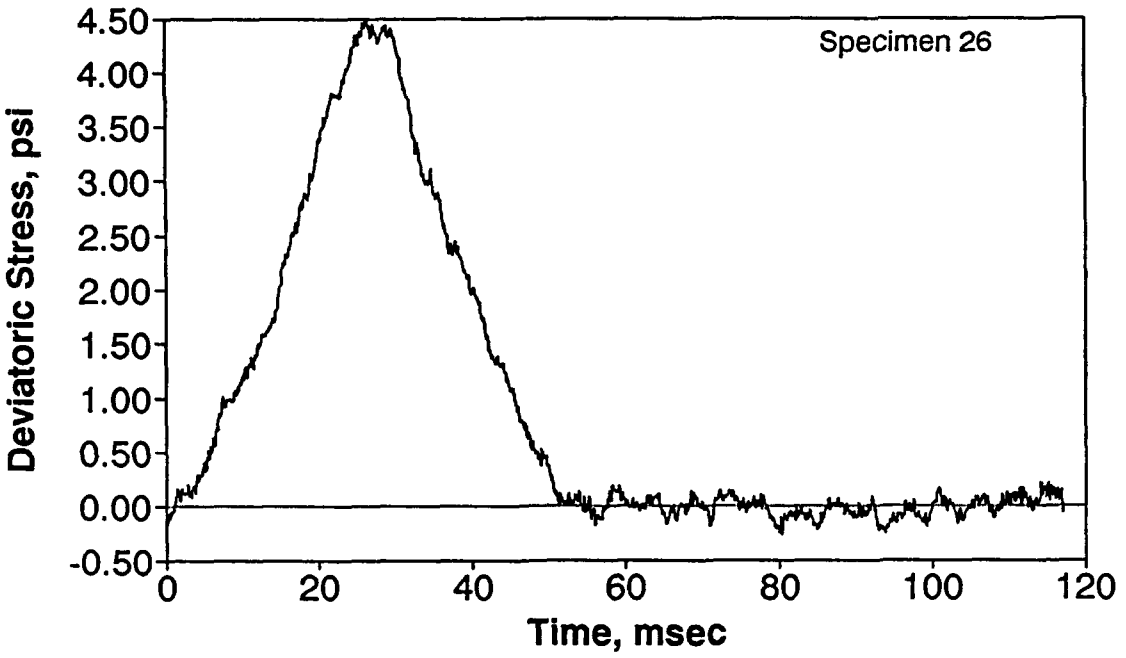
Specimen 26
Deviatoric Stress, psi
4.50
4.00
3.50
3.00
2.50
2.00
1.50
1.00
0.50
0.00
-0.50
0
20
40
60
80
100
120
Time, msec

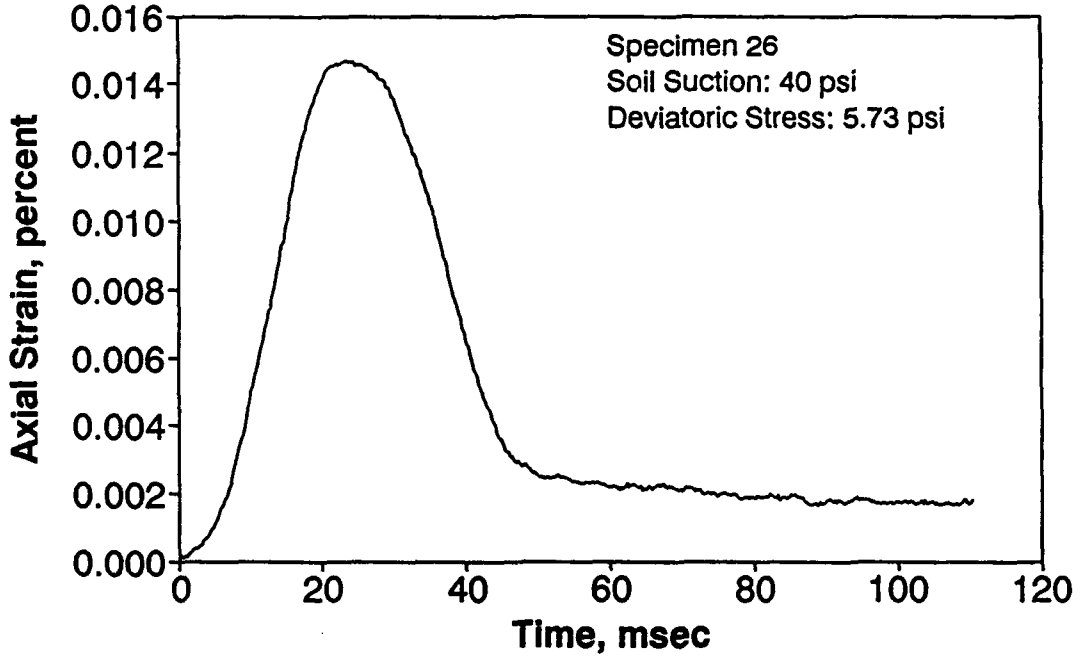
Specimen 26
Soil Suction: 40 psi
Deviatoric Stress: 5.73 psi
Axial Strain, percent
0.016
0.014
0.012
0.010
0.008
0.006
0.004
0.002
0.000
0
20
40
60
80
100
120
Time, msec

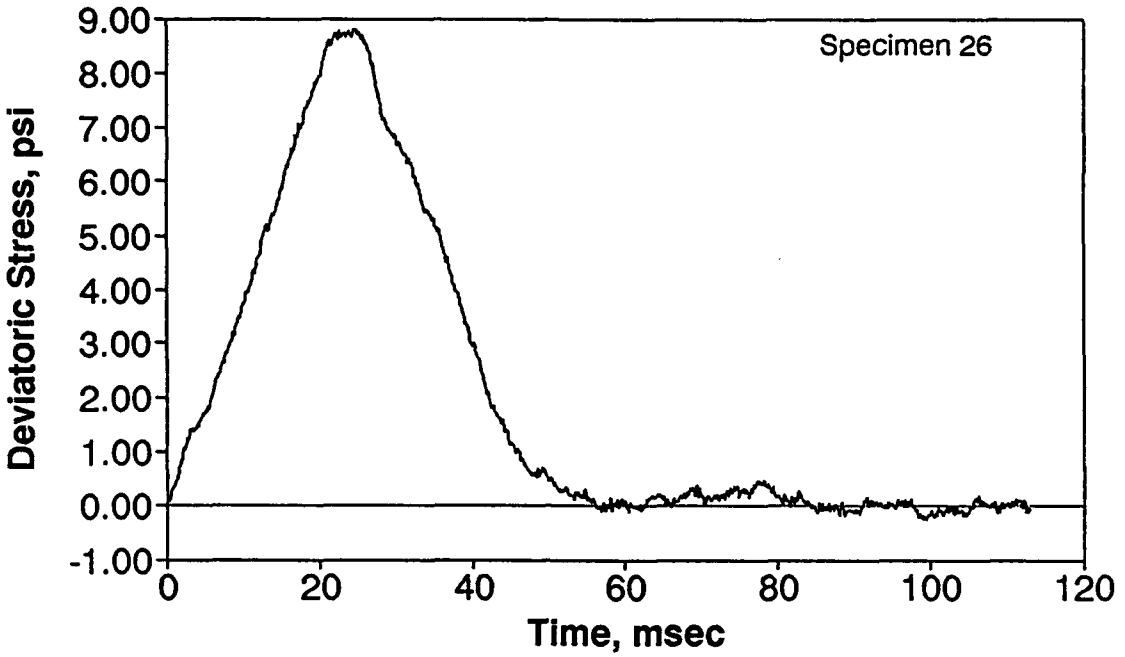
Specimen 26
Deviatoric Stress, psi
9.00
8.00
7.00
6.00
5.00
4.00
3.00
2.00
1.00
0.00
-1.00
0
20
40
60
80
100
120
Time, msec

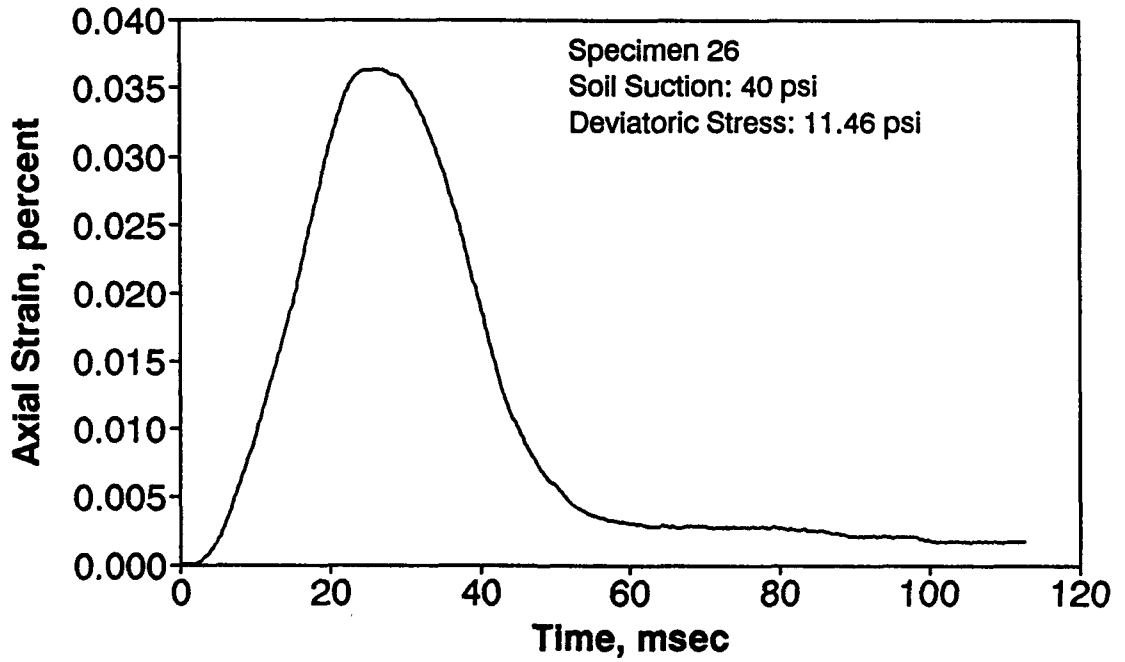
Specimen 26
Soil Suction: 40 psi
Deviatoric Stress: 11.46 psi
Axial Strain, percent
0.040
0.035
0.030
0.025
0.020
0.015
0.010
0.005
0.000
0
20
40
60
80
100
120
Time, msec

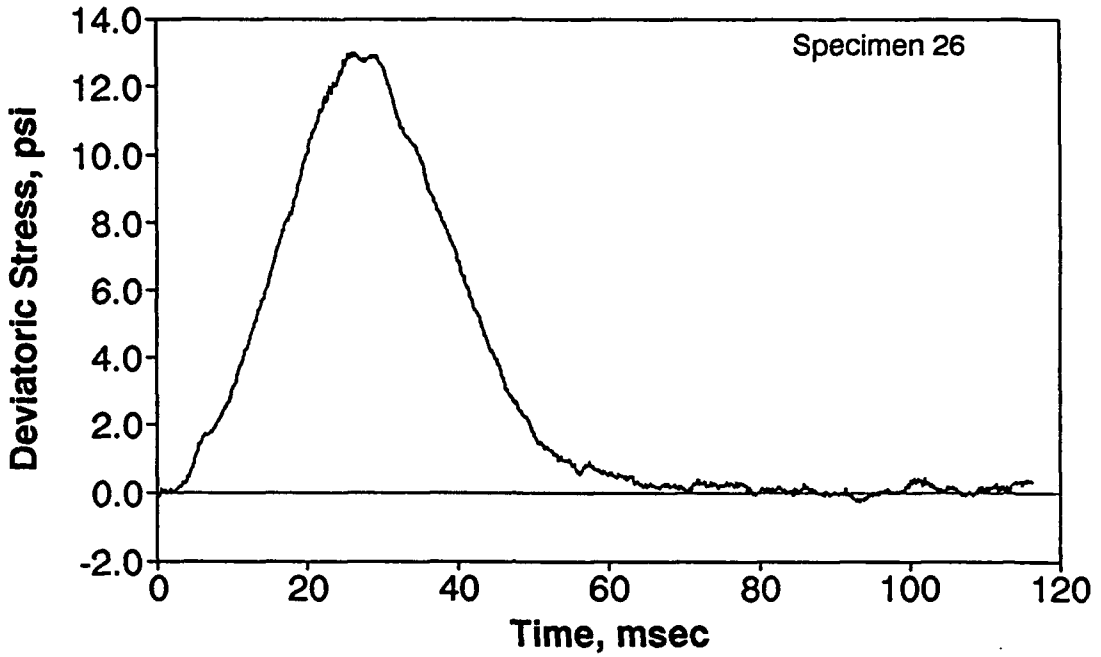
Specimen 26
Deviatoric Stress, psi
14.0
12.0
10.0
8.0
6.0
4.0
2.0
0.0
-2.0
0
20
40
60
80
100
120
Time, msec

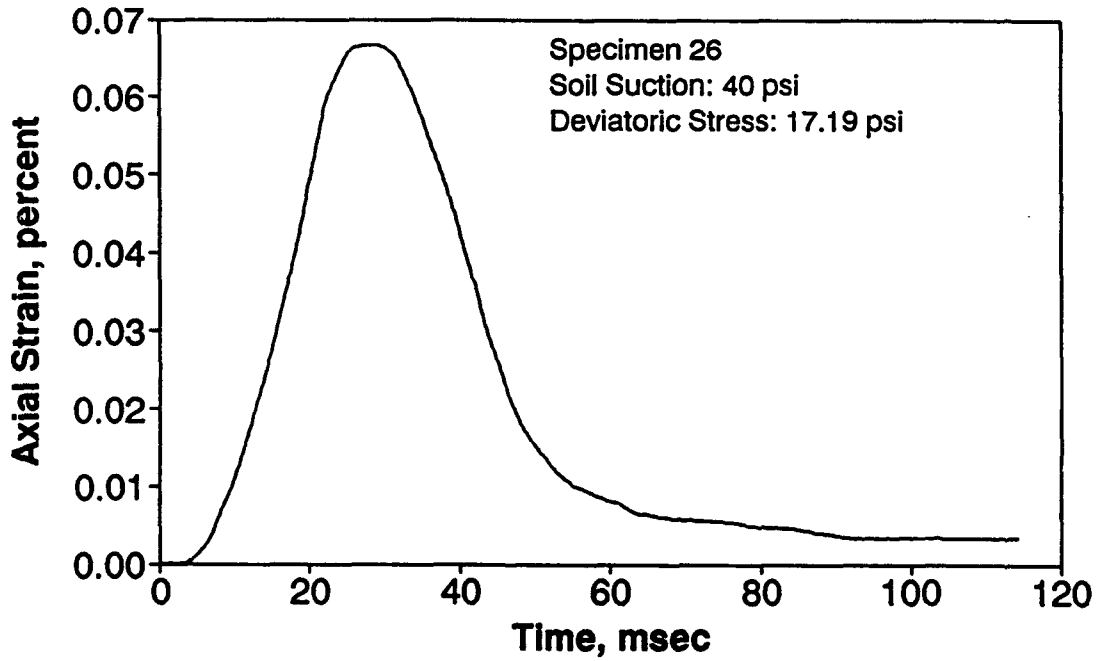
Specimen 26
Soil Suction: 40 psi
Deviatoric Stress: 17.19 psi
Axial Strain, percent
0.07
0.06
0.05
0.04
0.03
0.02
0.01
0.00
0
20
40
60
80
100
120
Time, msec

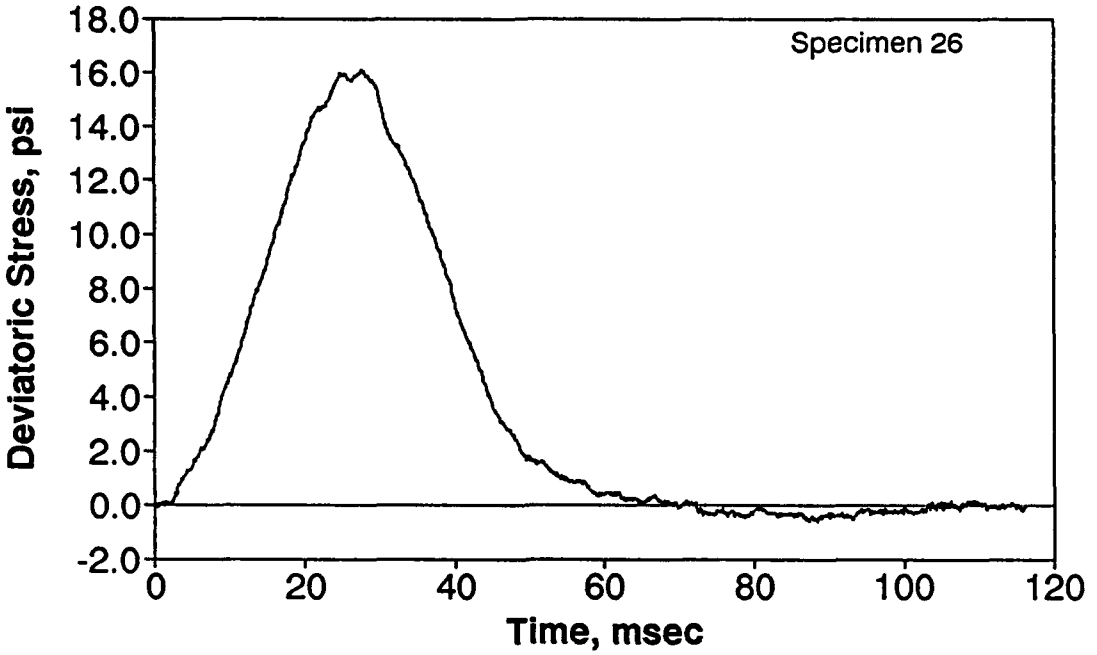
Specimen 26
Deviatoric Stress, psi
18.0
16.0
14.0
12.0
10.0
8.0
6.0
4.0
2.0
0.0
-2.0
0
20
40
60
80
100
120
Time, msec

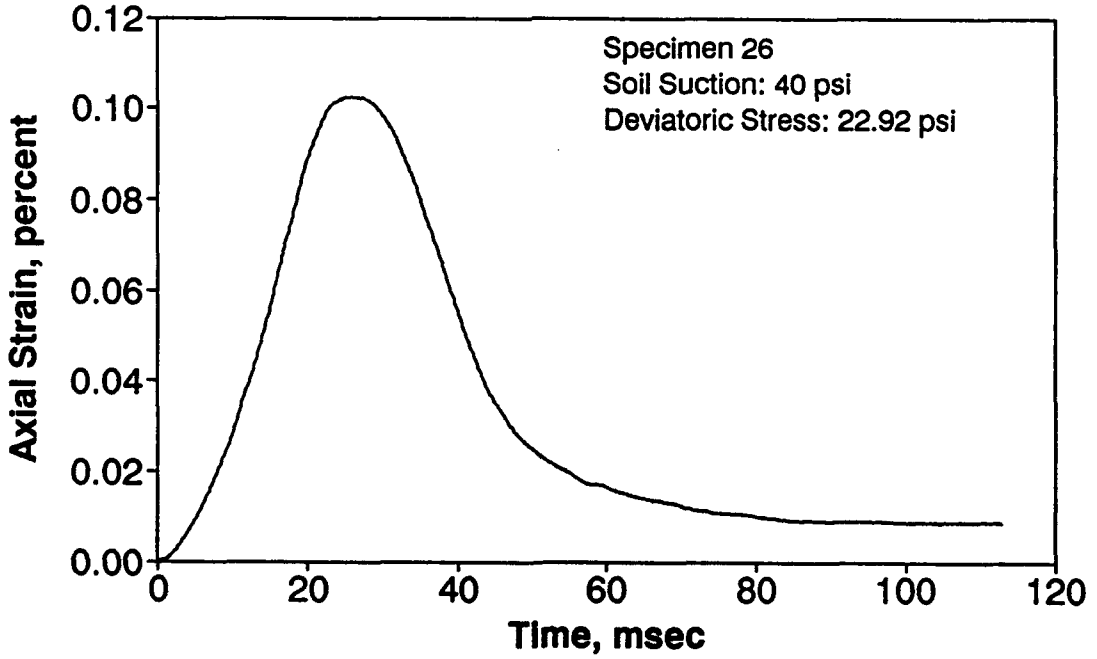
Specimen 26
Soil Suction: 40 psi
Deviatoric Stress: 22.92 psi
Axial Strain, percent
0.12
0.10
0.08
0.06
0.04
0.02
0.00
0
20
40
60
80
100
120
Time, msec

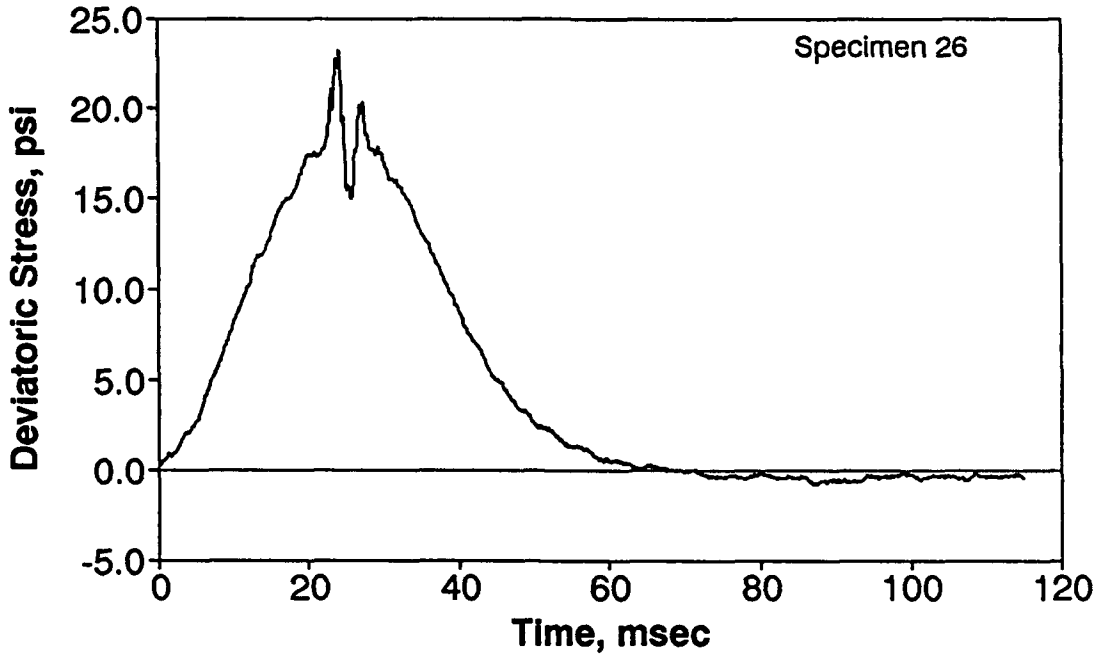
Specimen 26
Deviatoric Stress, psi
25.0
20.0
15.0
10.0
5.0
0.0
-5.0
0
20
40
60
80
100
120
Time, msec

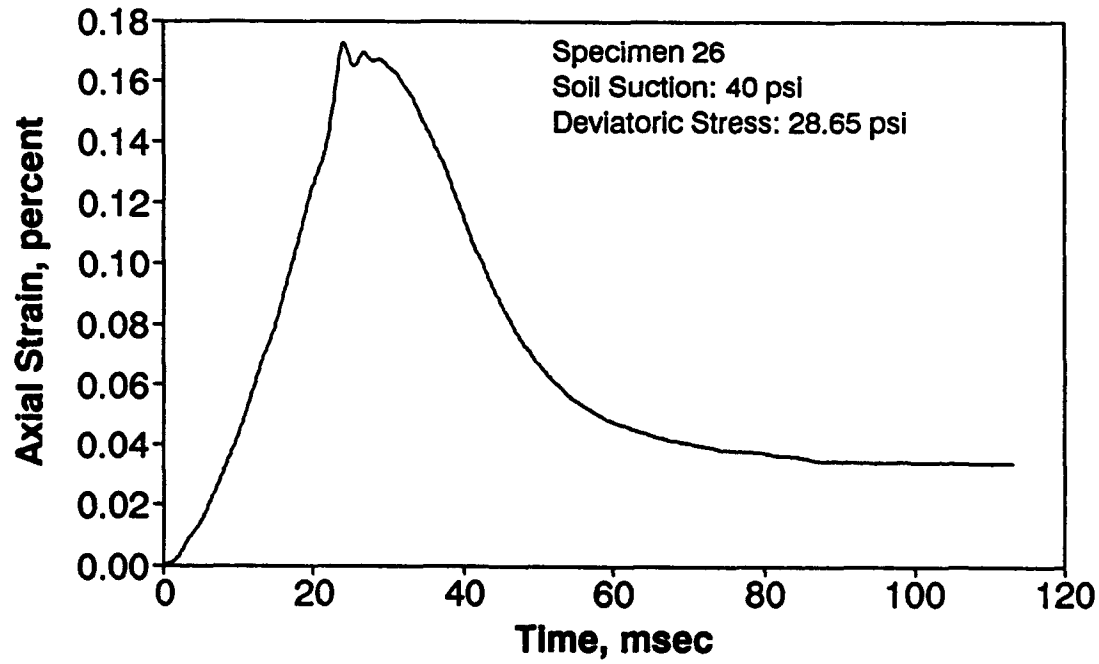
Specimen 26
Soil Suction: 40 psi
Deviatoric Stress: 28.65 psi
Axial Strain, percent
0.18
0.16
0.14
0.12
0.10
0.08
0.06
0.04
0.02
0.00
0
20
40
60
80
100
120
Time, msec

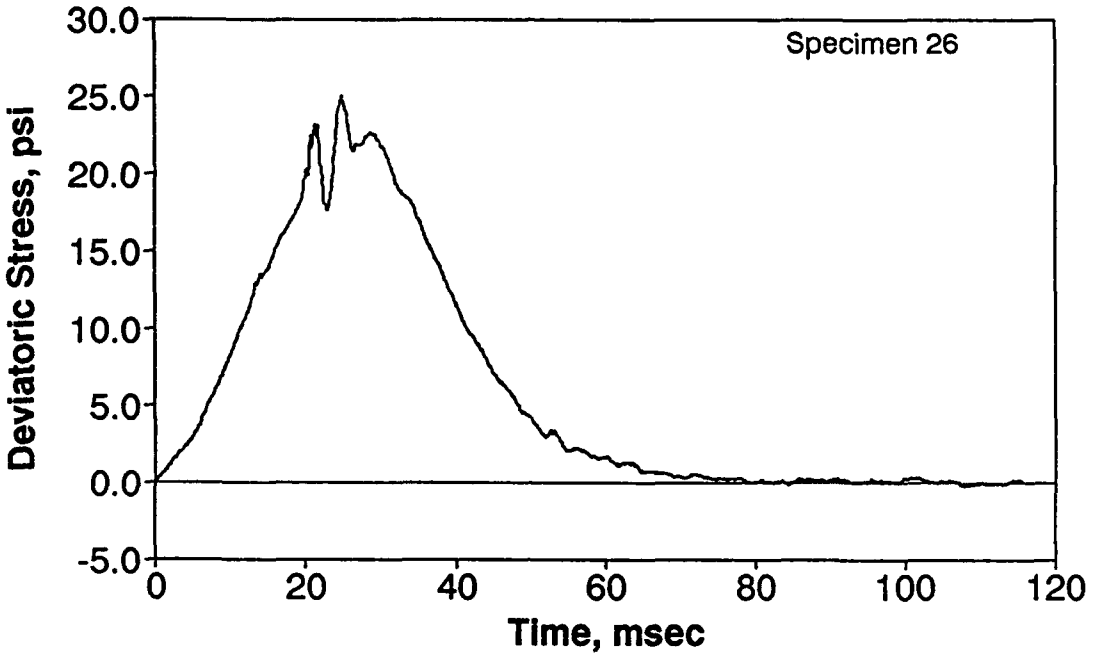
Specimen 26
Deviatoric Stress, psi
30.0
25.0
20.0
15.0
10.0
5.0
0.0
-5.0
0
20
40
60
80
100
120
Time, msec

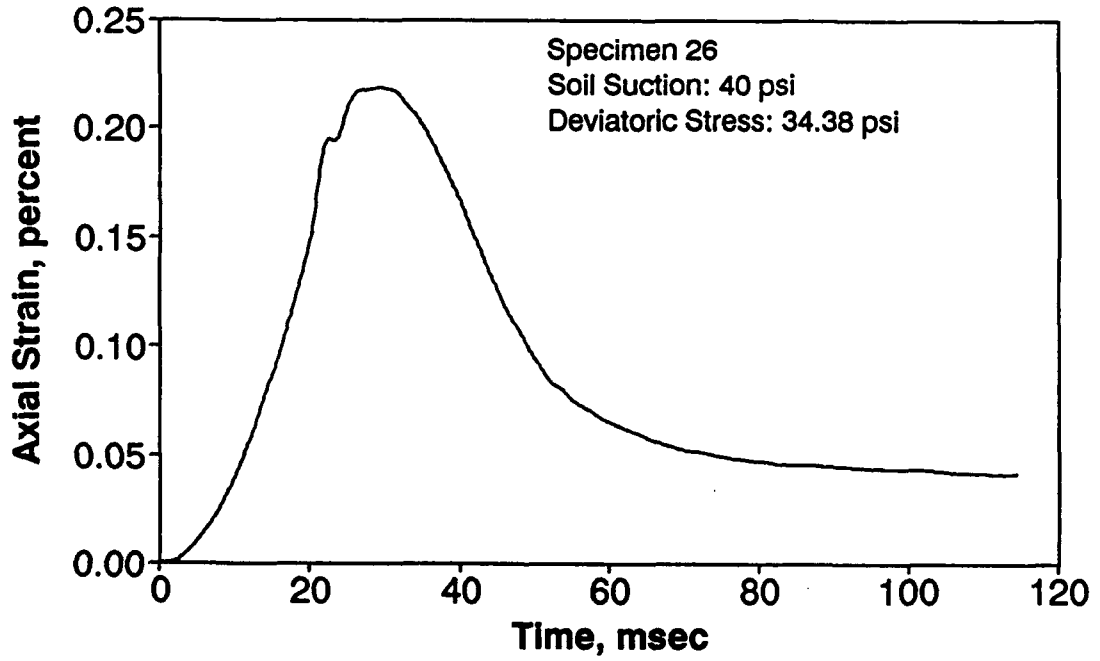
Specimen 26
Soil Suction: 40 psi
Deviatoric Stress: 34.38 psi
Axial Strain, percent
0.25
0.20
0.15
0.10
0.05
0.00
0
20
40
60
80
100
120
Time, msec

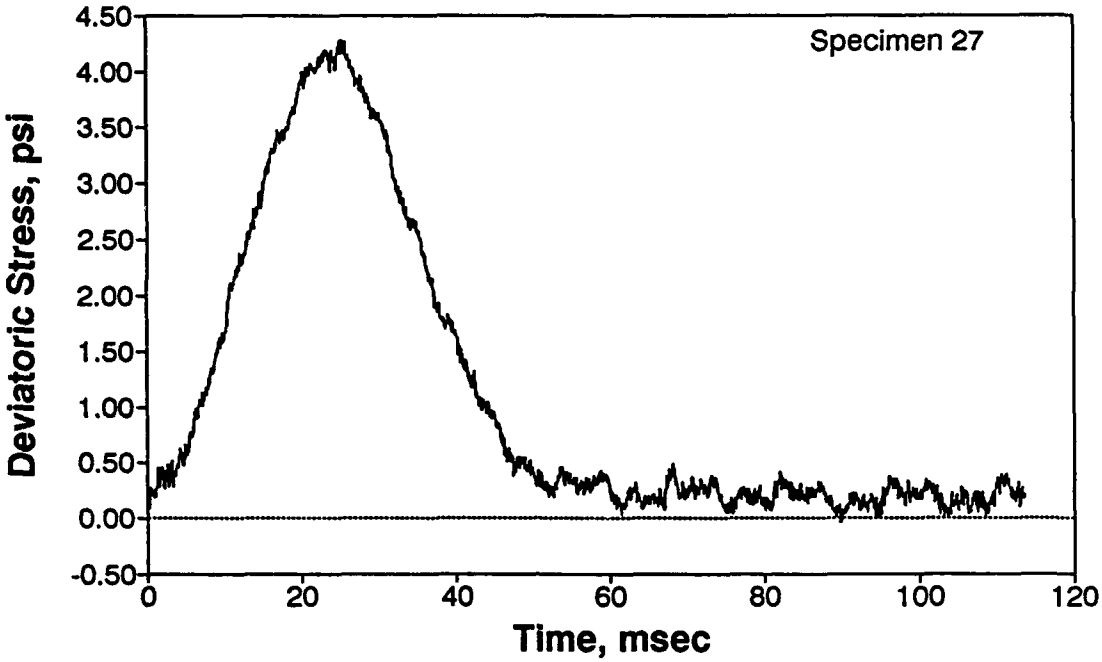
Specimen 27
Deviatoric Stress, psi
4.50
4.00
3.50
3.00
2.50
2.00
1.50
1.00
0.50
0.00
-0.50
0
20
40
60
80
100
120
Time, msec

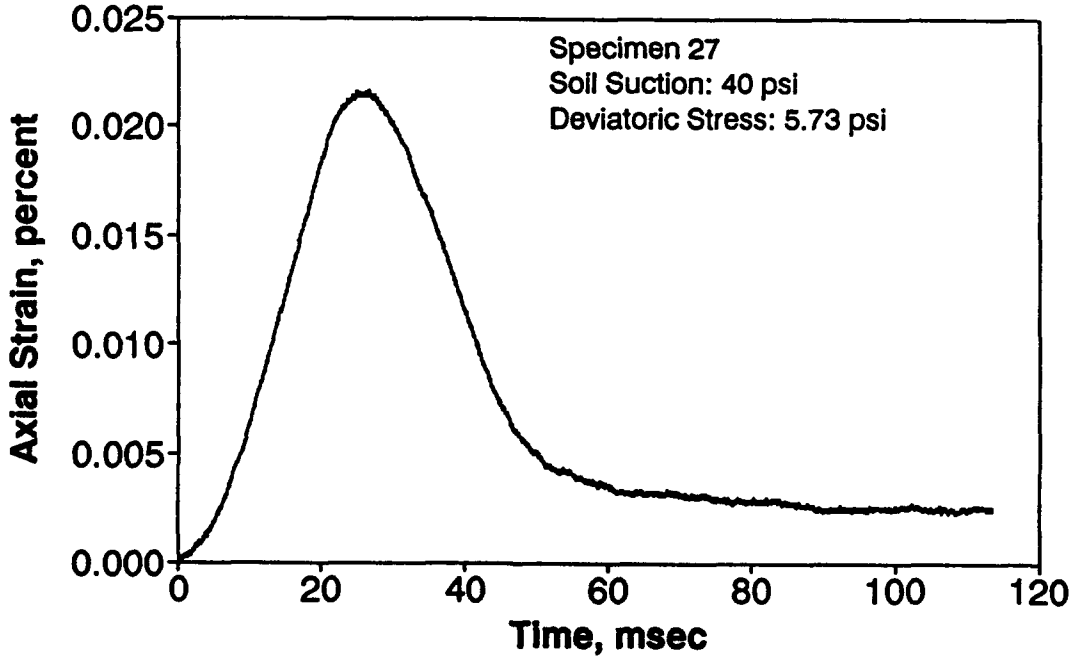
Specimen 27
Soil Suction: 40 psi
Deviatoric Stress: 5.73 psi
Axial Strain, percent
0.025
0.020
0.015
0.010
0.005
0.000
0
20
40
60
80
100
120
Time, msec

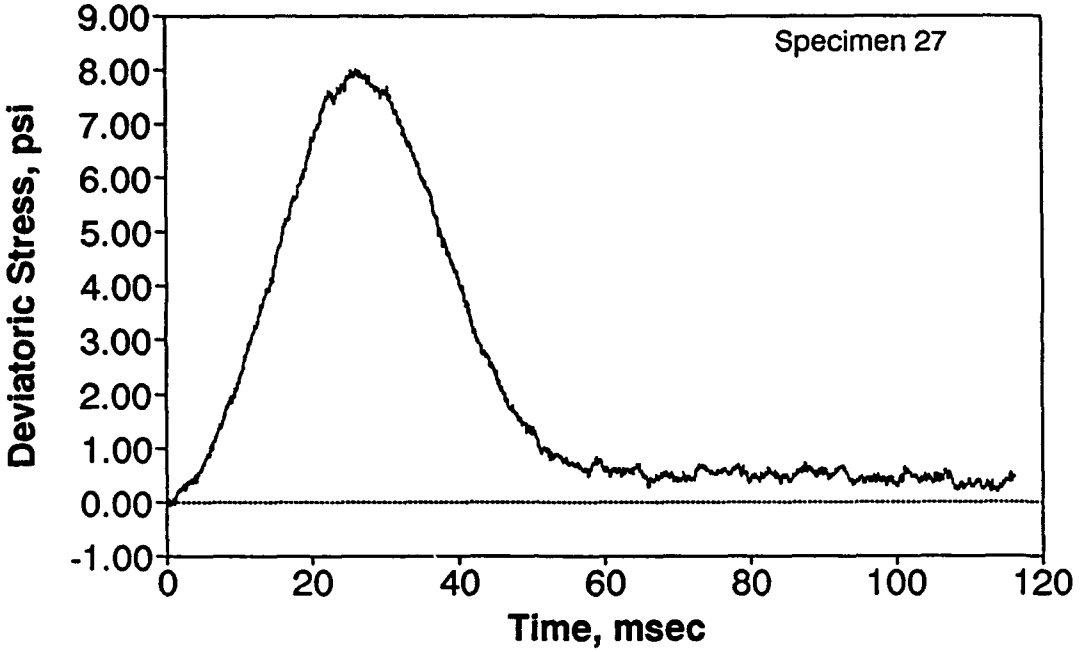
Specimen 27
Deviatoric Stress, psi
9.00
8.00
7.00
6.00
5.00
4.00
3.00
2.00
1.00
0.00
-1.00
0
20
40
60
80
100
120
Time, msec

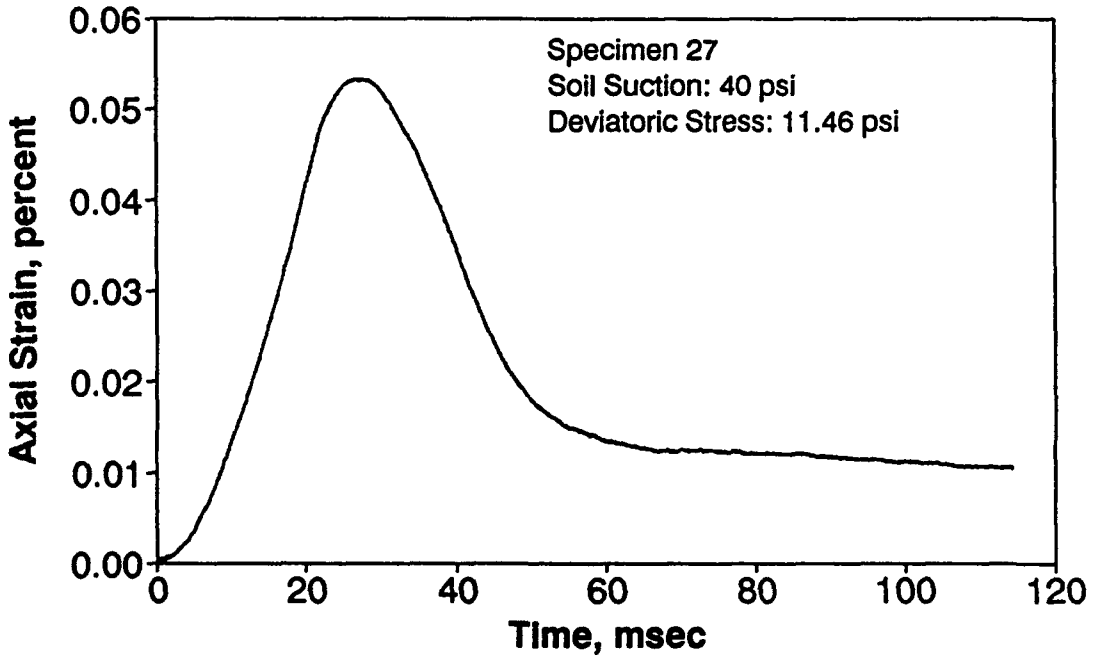
Specimen 27
Soil Suction: 40 psi
Deviatoric Stress: 11.46 psi
Axial Strain, percent
0.06
0.05
0.04
0.03
0.02
0.01
0.00
0
20
40
60
80
100
120
Time, msec

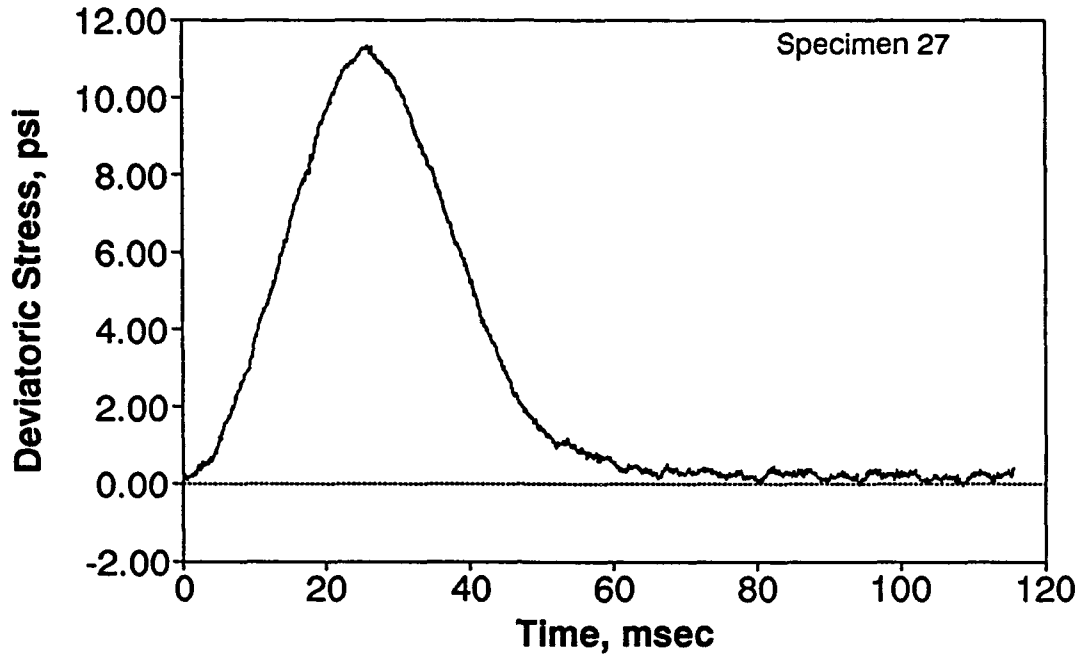
Specimen 27
Deviatoric Stress, psi
12.00
10.00
8.00
6.00
4.00
2.00
0.00
-2.00
0
20
40
60
80
100
120
Time, msec

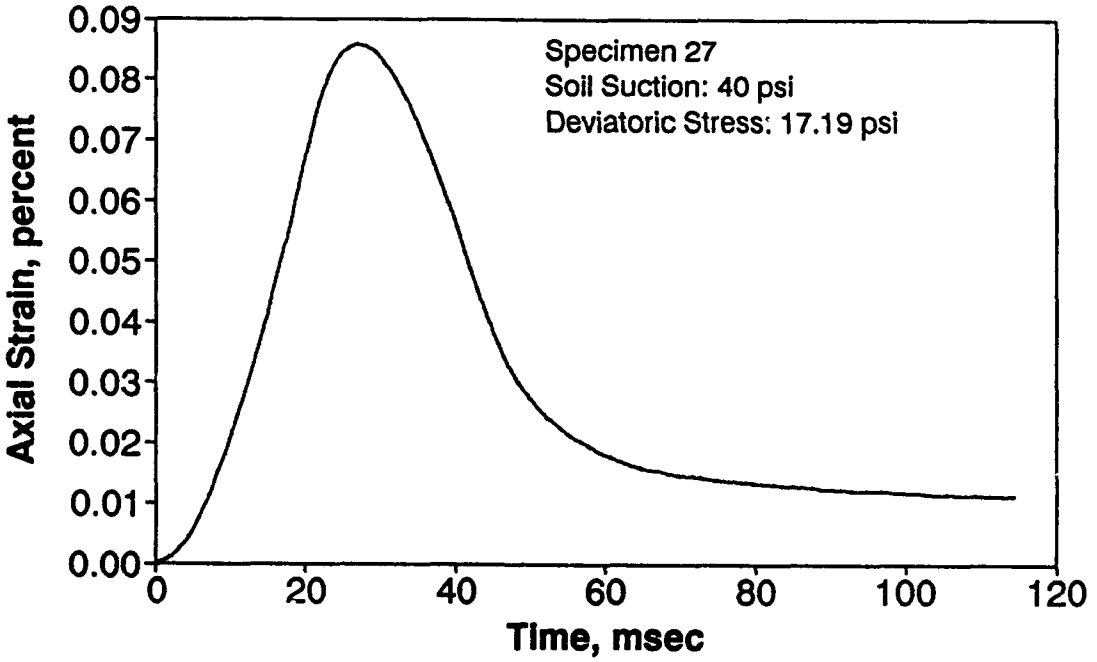
Specimen 27
Soil Suction: 40 psi
Deviatoric Stress: 17.19 psi
Axial Strain, percent
0.09
0.08
0.07
0.06
0.05
0.04
0.03
0.02
0.01
0.00
0
20
40
60
80
100
120
Time, msec

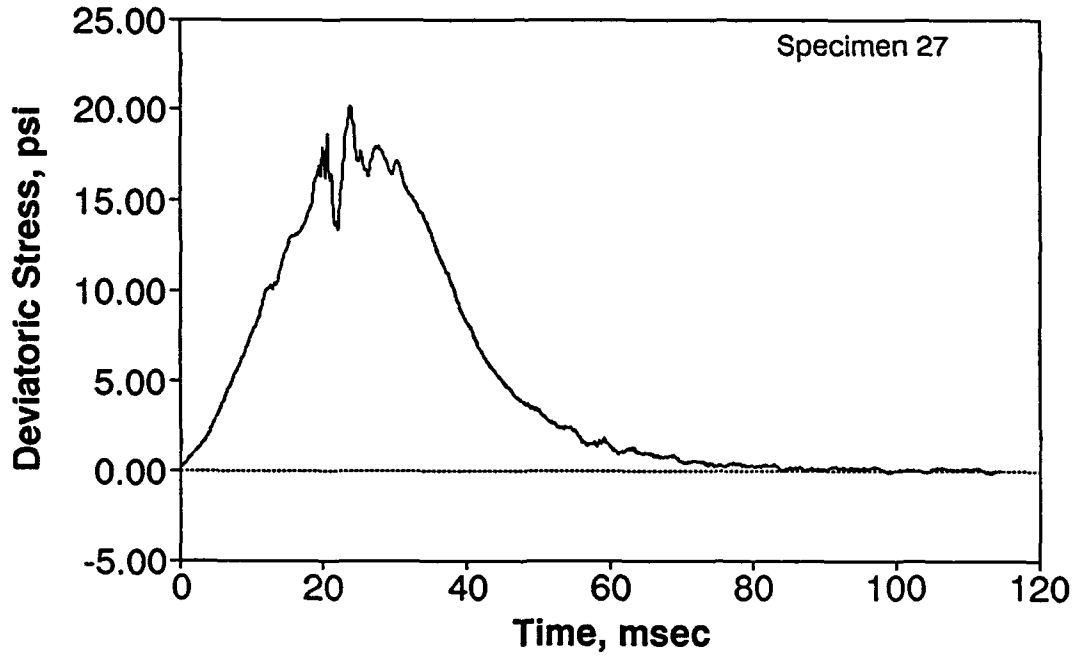
Specimen 27
Deviatoric Stress, psi
25.00
20.00
15.00
10.00
5.00
0.00
-5.00
0
20
40
60
80
100
120
Time, msec

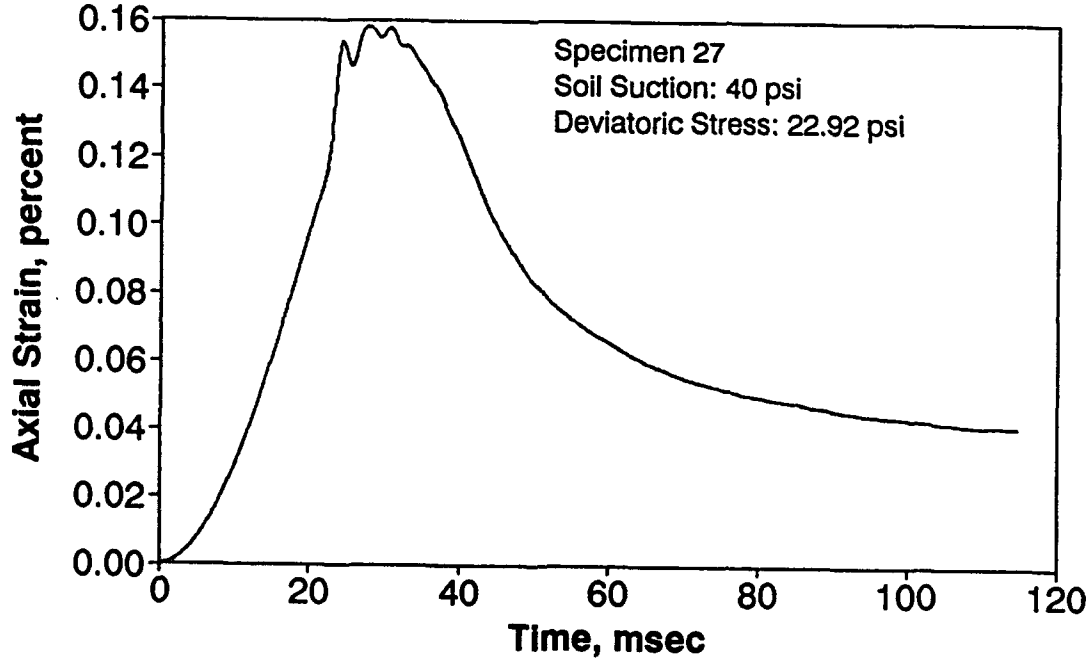
Specimen 27
Soil Suction: 40 psi
Deviatoric Stress: 22.92 psi
Axial Strain, percent
0.16
0.14
0.12
0.10
0.08
0.06
0.04
0.02
0.00
0
20
40
60
80
100
120
Time, msec

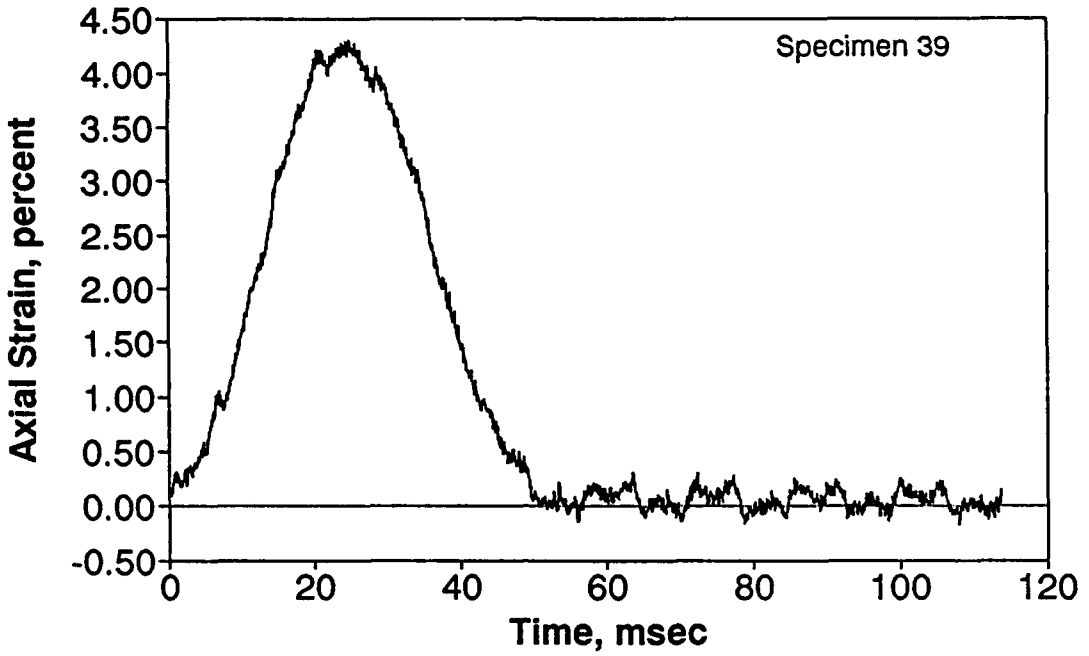
Specimen 39
Axial Strain, percent
4.50
4.00
3.50
3.00
2.50
2.00
1.50
1.00
0.50
0.00
-0.50
0
20
40
60
80
100
120
Time, msec

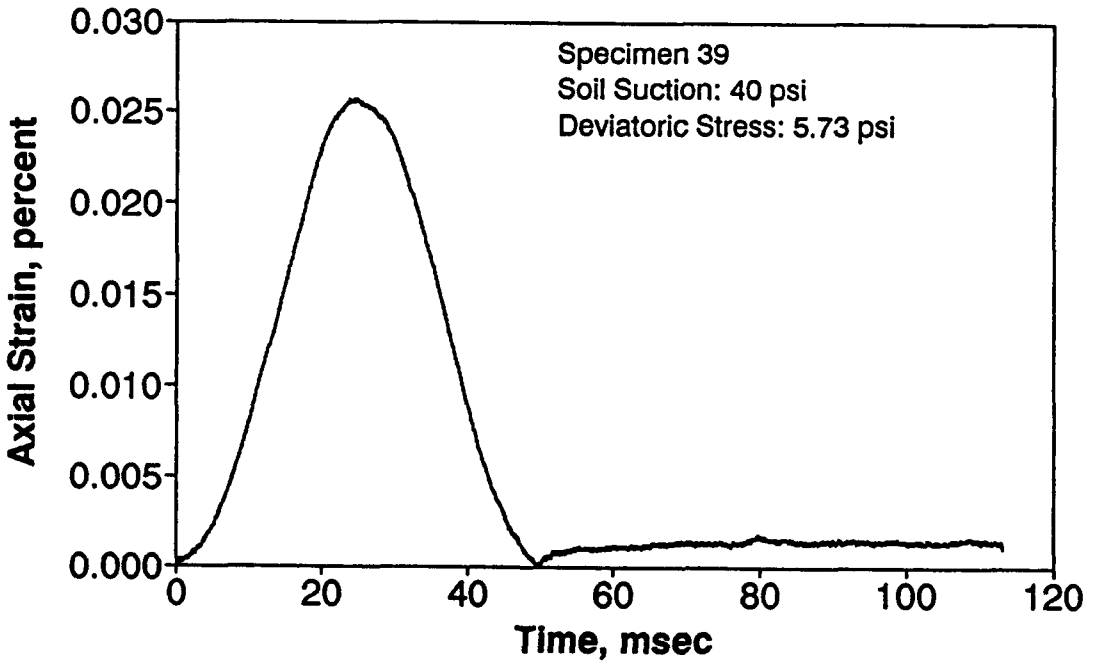
Specimen 39
Soil Suction: 40 psi
Deviatoric Stress: 5.73 psi
Axial Strain, percent
0.030
0.025
0.020
0.015
0.010
0.005
0.000
0
20
40
60
80
100
120
Time, msec

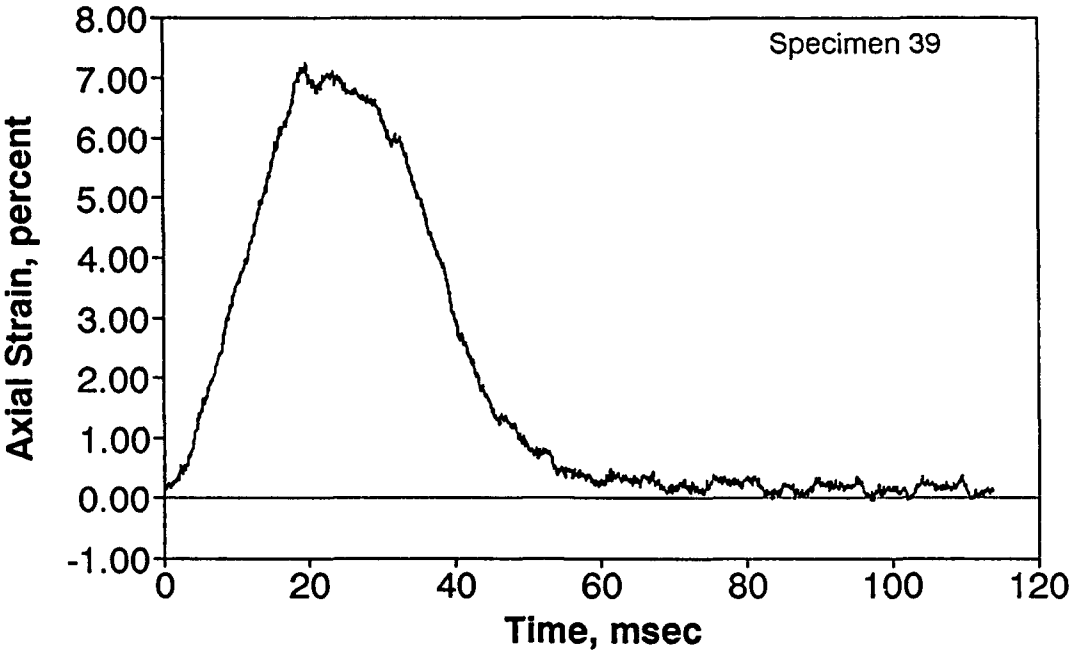
Specimen 39
Axial Strain, percent
8.00
7.00
6.00
5.00
4.00
3.00
2.00
1.00
0.00
-1.00
0
20
40
60
80
100
120
Time, msec

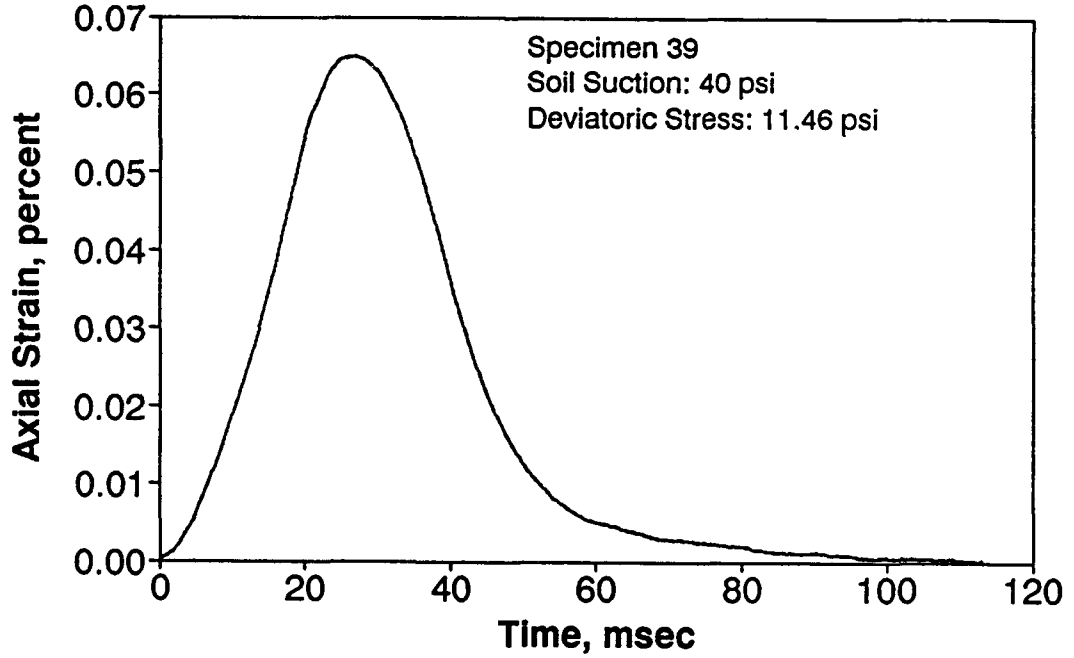
Specimen 39
Soil Suction: 40 psi
Deviatoric Stress: 11.46 psi
Axial Strain, percent
0.07
0.06
0.05
0.04
0.03
0.02
0.01
0.00
0
20
40
60
80
100
120
Time, msec

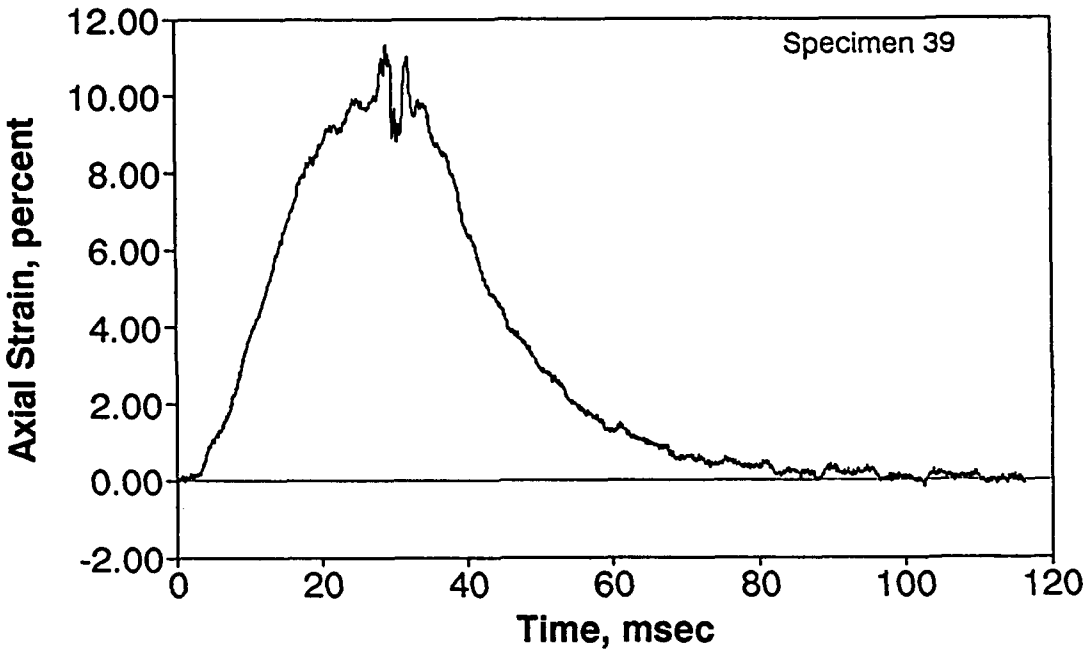
Specimen 39
12.00
10.00
8.00
6.00
4.00
2.00
0.00
-2.00
Axial Strain, percent
0
20
40
60
80
100
120
Time, msec

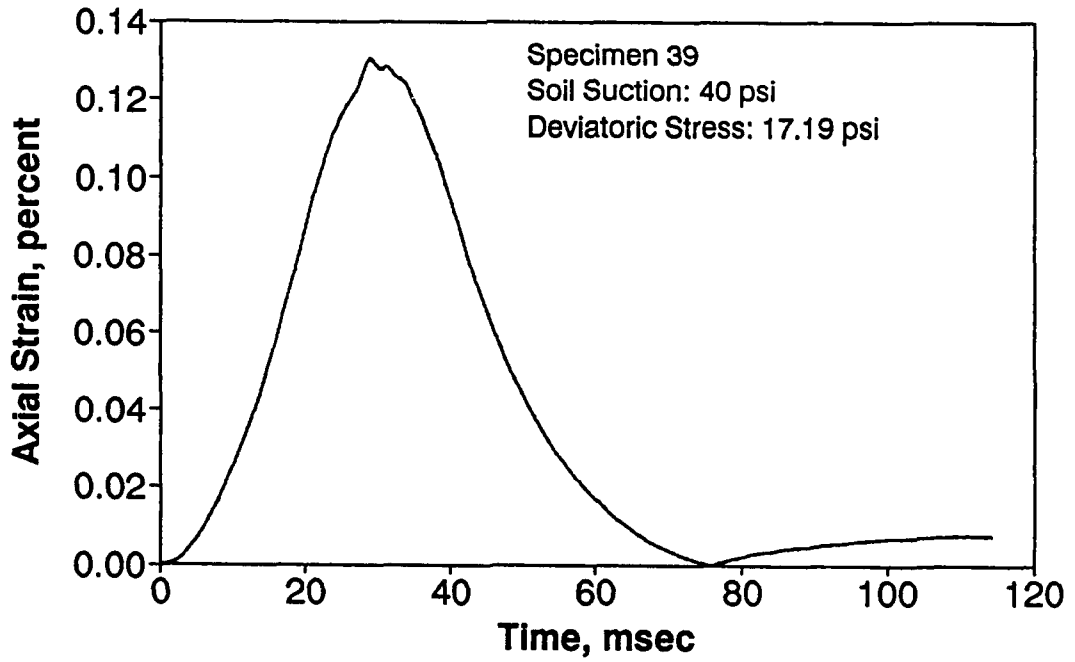
Specimen 39
Soil Suction: 40 psi
Deviatoric Stress: 17.19 psi
0.14
0.12
0.10
0.08
0.06
0.04
0.02
0.00
Axial Strain, percent
0
20
40
60
80
100
120
Time, msec

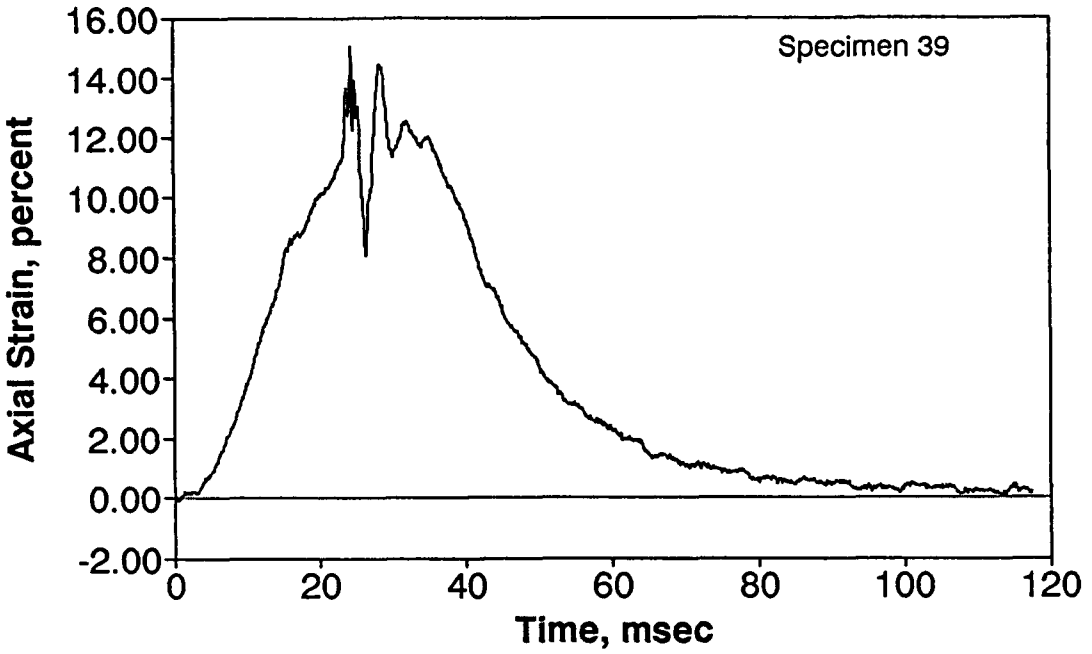
Specimen 39
Axial Strain, percent
16.00
14.00
12.00
10.00
8.00
6.00
4.00
2.00
0.00
-2.00
0
20
40
60
80
100
120
Time, msec

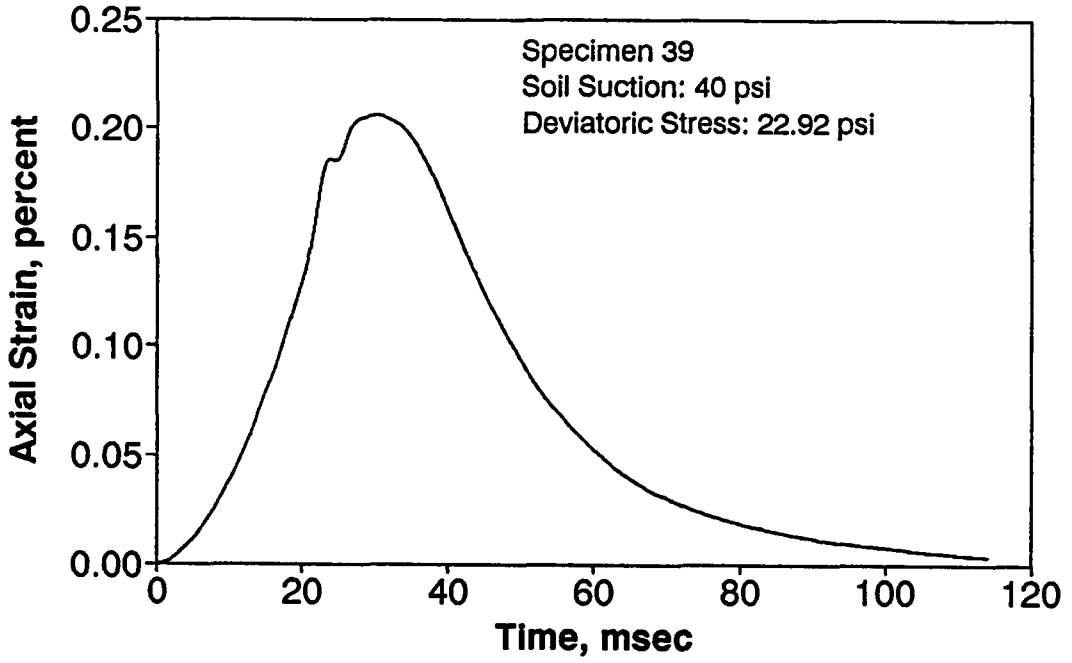
Specimen 39
Soil Suction: 40 psi
Deviatoric Stress: 22.92 psi
Axial Strain, percent
0.25
0.20
0.15
0.10
0.05
0.00
0
20
40
60
80
100
120
Time, msec

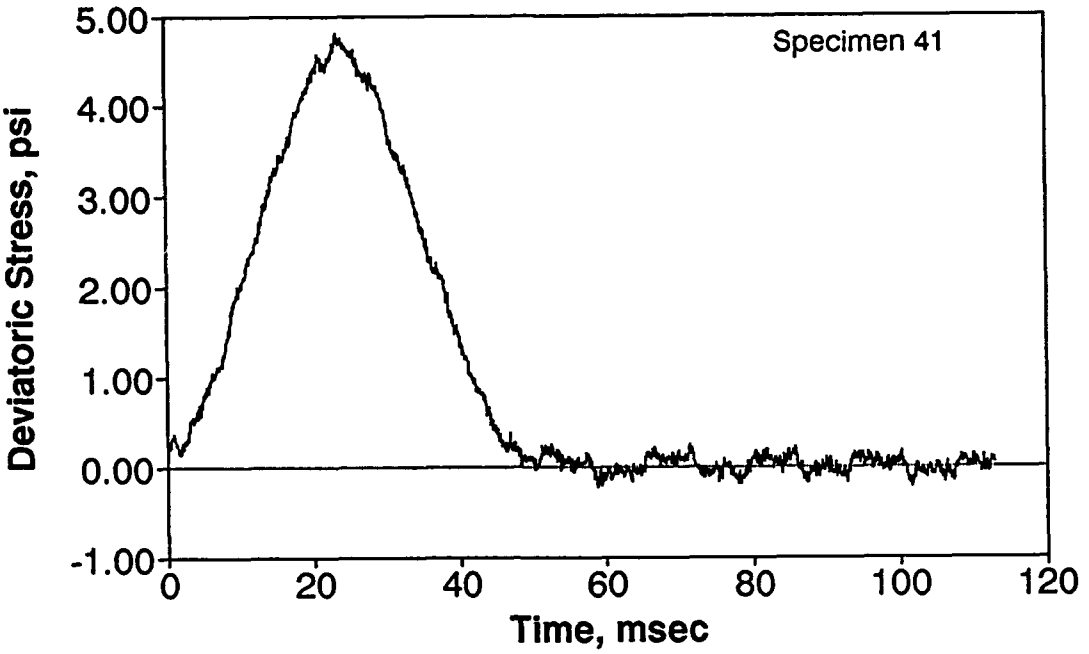
Specimen 41
Deviatoric Stress, psi
5.00
4.00
3.00
2.00
1.00
0.00
-1.00
0
20
40
60
80
100
120
Time, msec

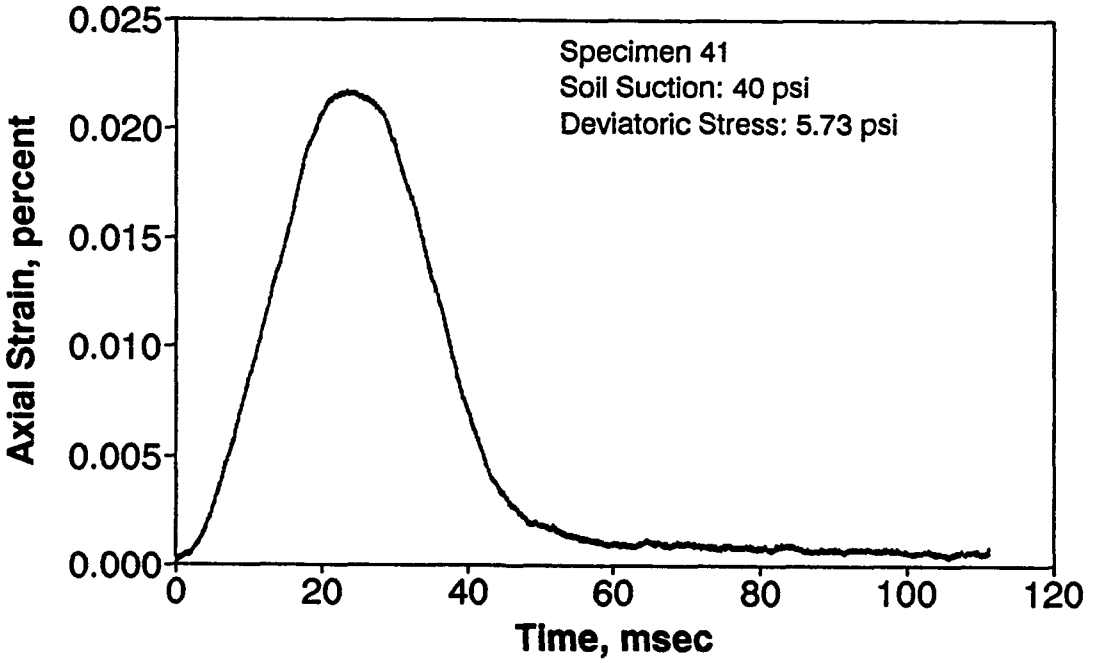
Specimen 41
Soil Suction: 40 psi
Deviatoric Stress: 5.73 psi
Axial Strain, percent
0.025
0.020
0.015
0.010
0.005
0.000
0
20
40
60
80
100
120
Time, msec

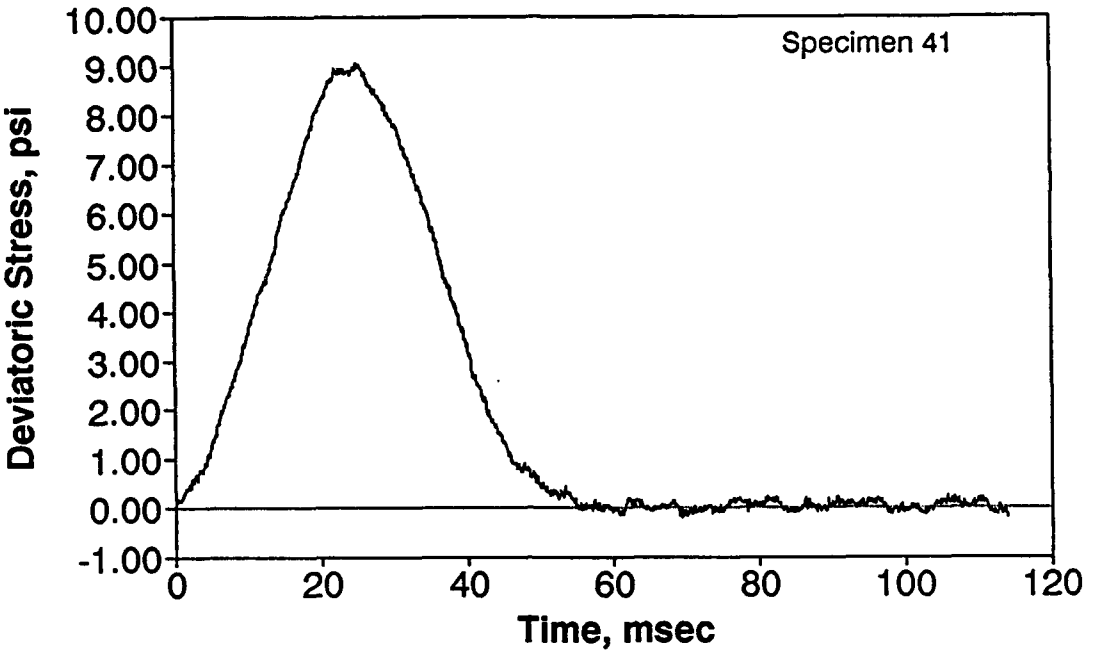
Specimen 41
Deviatoric Stress, psi
10.00
9.00
8.00
7.00
6.00
5.00
4.00
3.00
2.00
1.00
0.00
-1.00
0
20
40
60
80
100
120
Time, msec

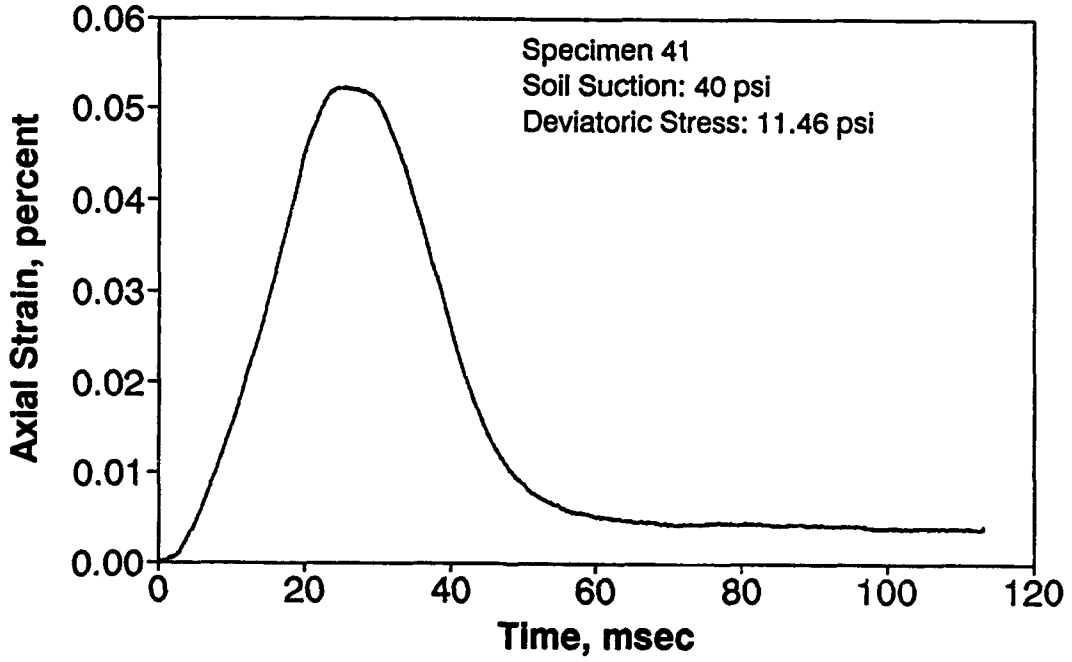
Specimen 41
Soil Suction: 40 psi
Deviatoric Stress: 11.46 psi
Axial Strain, percent
0.06
0.05
0.04
0.03
0.02
0.01
0.00
0
20
40
60
80
100
120
Time, msec

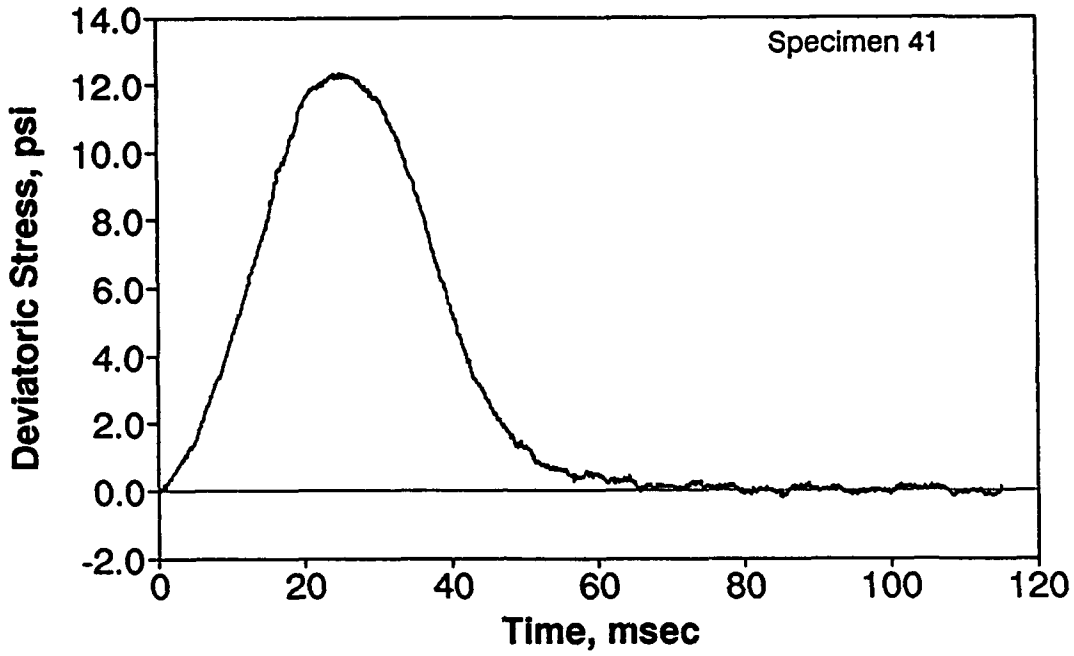
Specimen 41
Deviatoric Stress, psi
14.0
12.0
10.0
8.0
6.0
4.0
2.0
0.0
-2.0
0
20
40
60
80
100
120
Time, msec

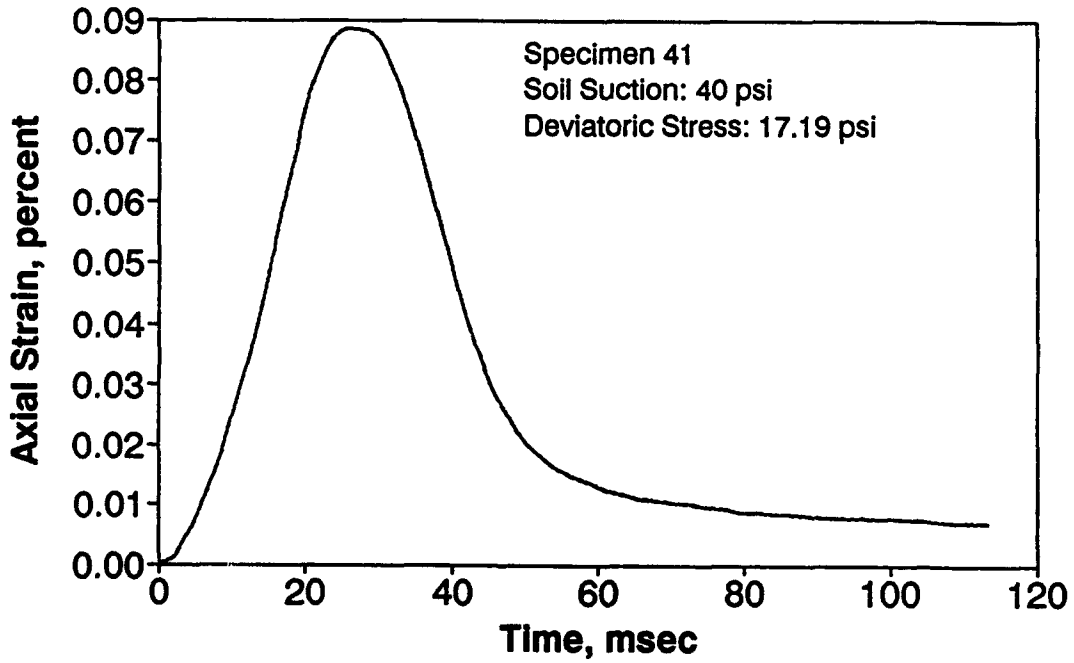
Specimen 41
Soil Suction: 40 psi
Deviatoric Stress: 17.19 psi
Axial Strain, percent
0.09
0.08
0.07
0.06
0.05
0.04
0.03
0.02
0.01
0.00
0
20
40
60
80
100
120
Time, msec

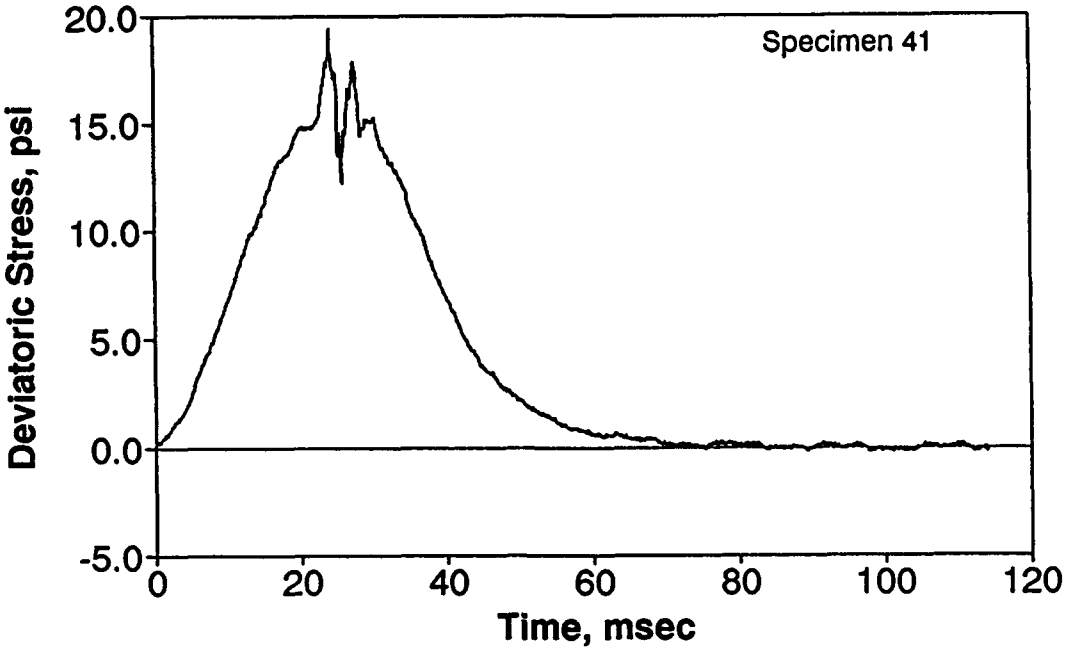
Specimen 41
Deviatoric Stress, psi
20.0
15.0
10.0
5.0
0.0
-5.0
0
20
40
60
80
100
120
Time, msec

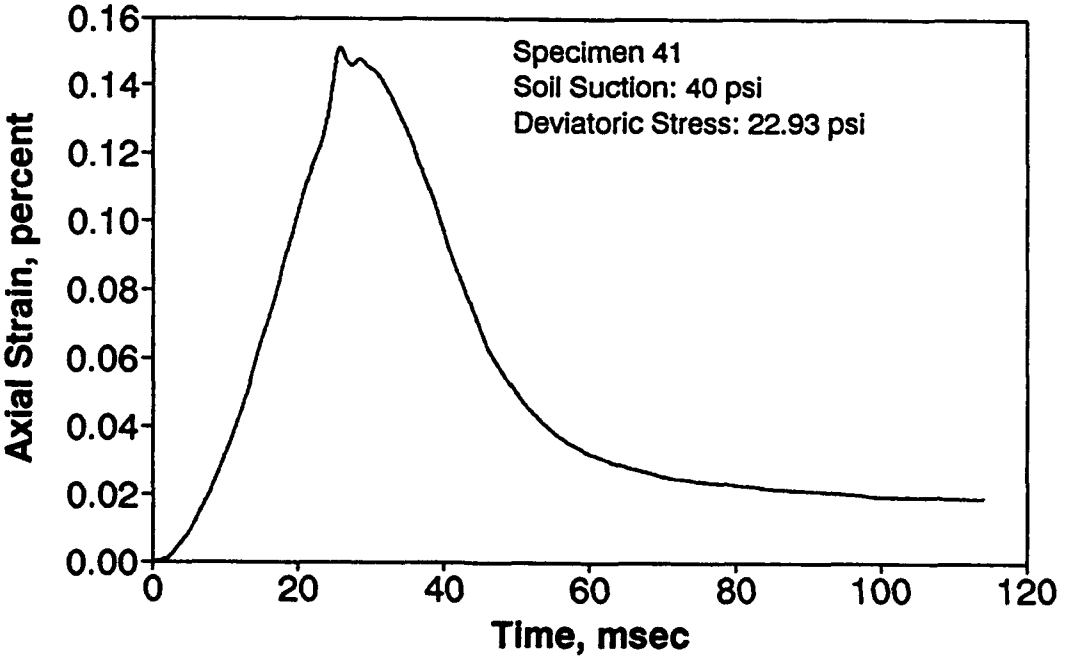
Specimen 41
Soil Suction: 40 psi
Deviatoric Stress: 22.93 psi
Axial Strain, percent
0.16
0.14
0.12
0.10
0.08
0.06
0.04
0.02
0.00
0
20
40
60
80
100
120
Time, msec

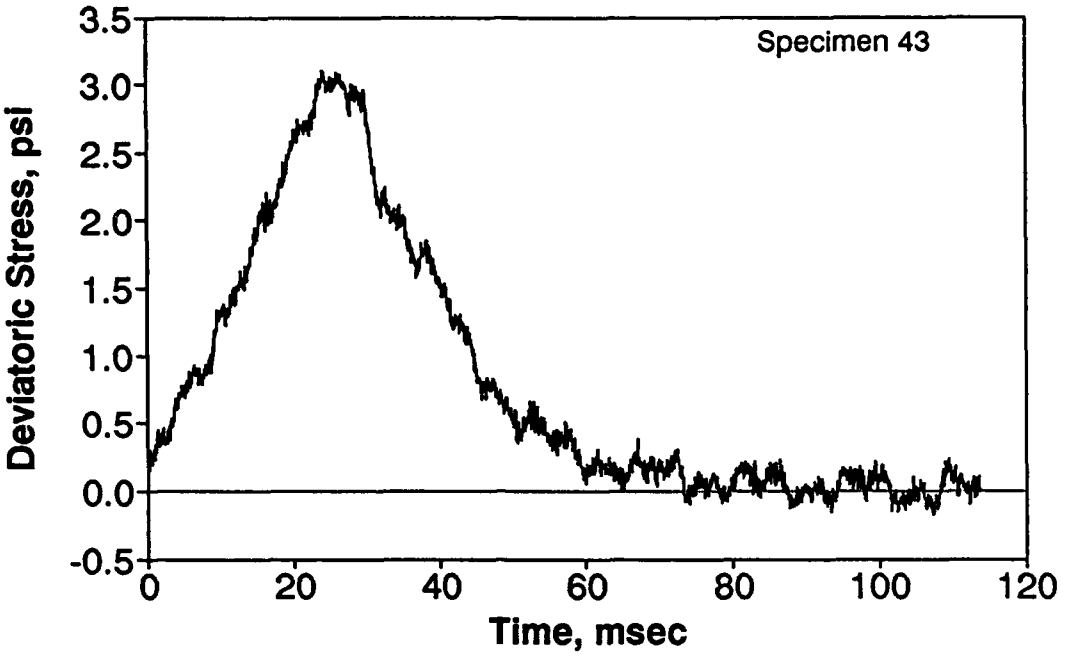
Specimen 43
Deviatoric Stress, psi
3.5
3.0
2.5
2.0
1.5
1.0
0.5
0.0
-0.5
0
20
40
60
80
100
120
Time, msec

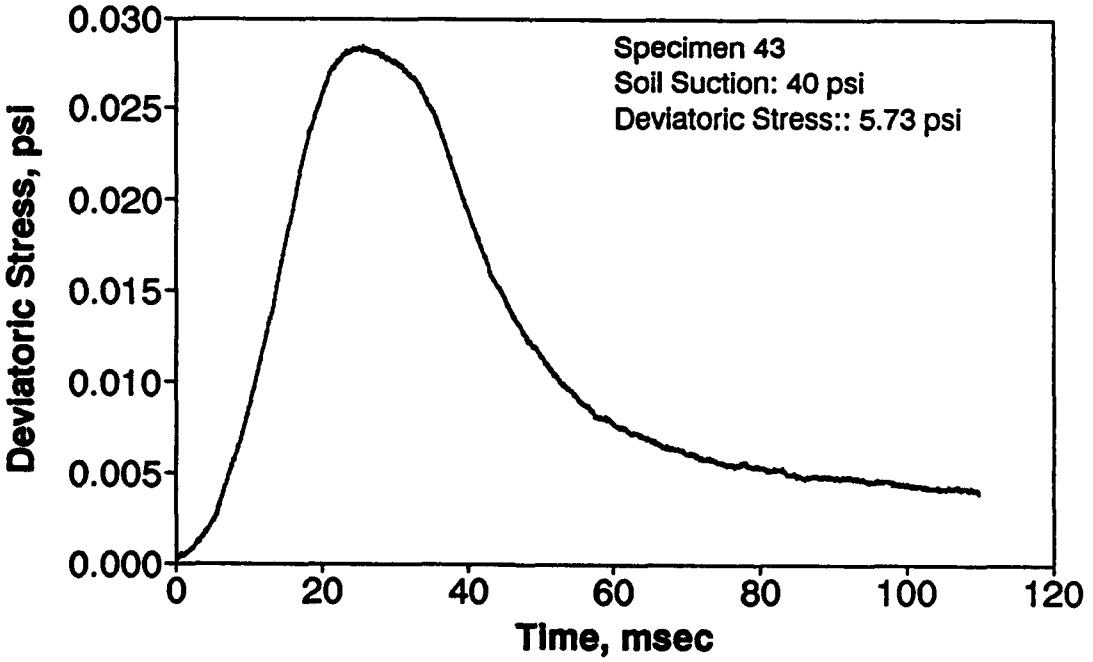
Specimen 43
Soil Suction: 40 psi
Deviatoric Stress:: 5.73 psi
Deviatoric Stress, psi
0.030
0.025
0.020
0.015
0.010
0.005
0.000
0
20
40
60
80
100
120
Time, msec

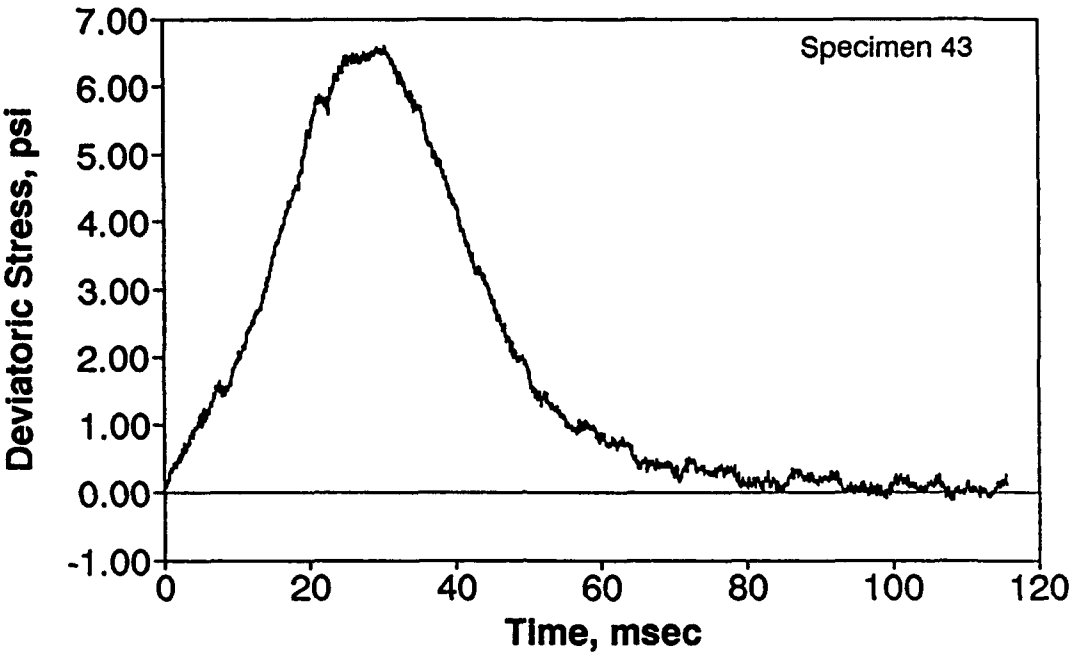
Specimen 43
Deviatoric Stress, psi
7.00
6.00
5.00
4.00
3.00
2.00
1.00
0.00
-1.00
0
20
40
60
80
100
120
Time, msec

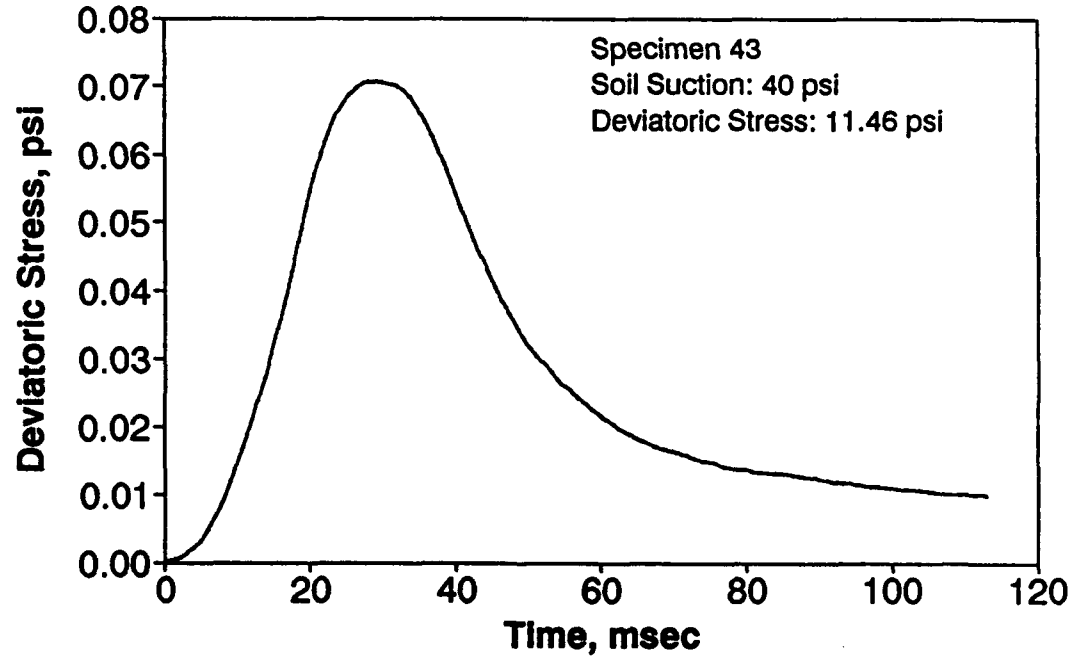
Specimen 43
Soil Suction: 40 psi
Deviatoric Stress: 11.46 psi
Deviatoric Stress, psi
0.08
0.07
0.06
0.05
0.04
0.03
0.02
0.01
0.00
0
20
40
60
80
100
120
Time, msec

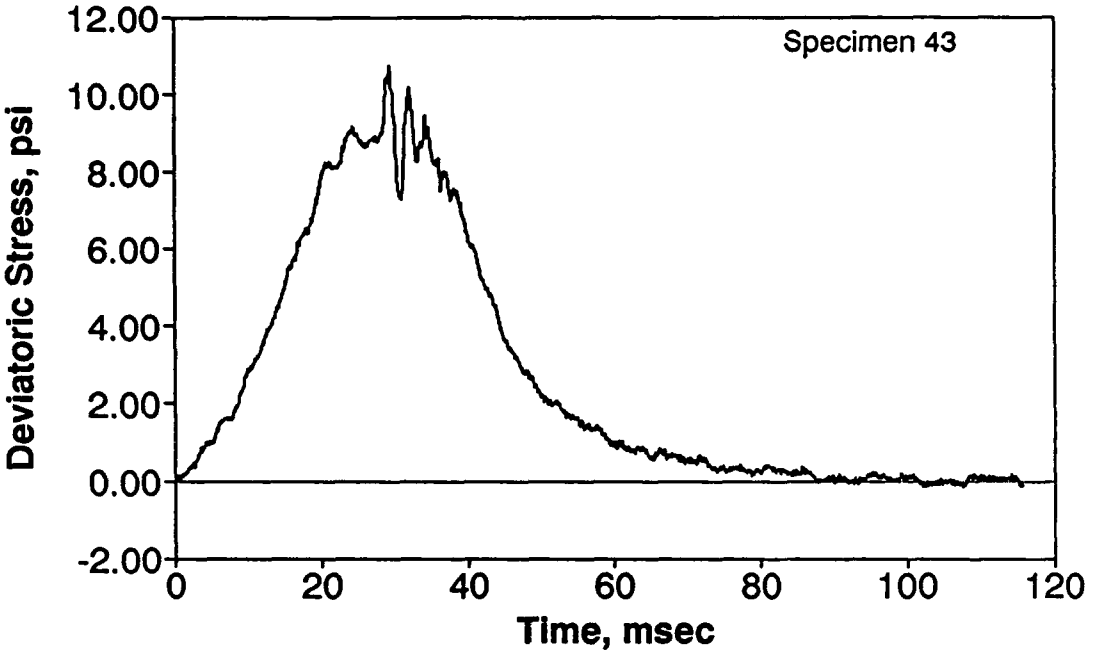
Specimen 43
Deviatoric Stress, psi
12.00
10.00
8.00
6.00
4.00
2.00
0.00
-2.00
0
20
40
60
80
100
120
Time, msec

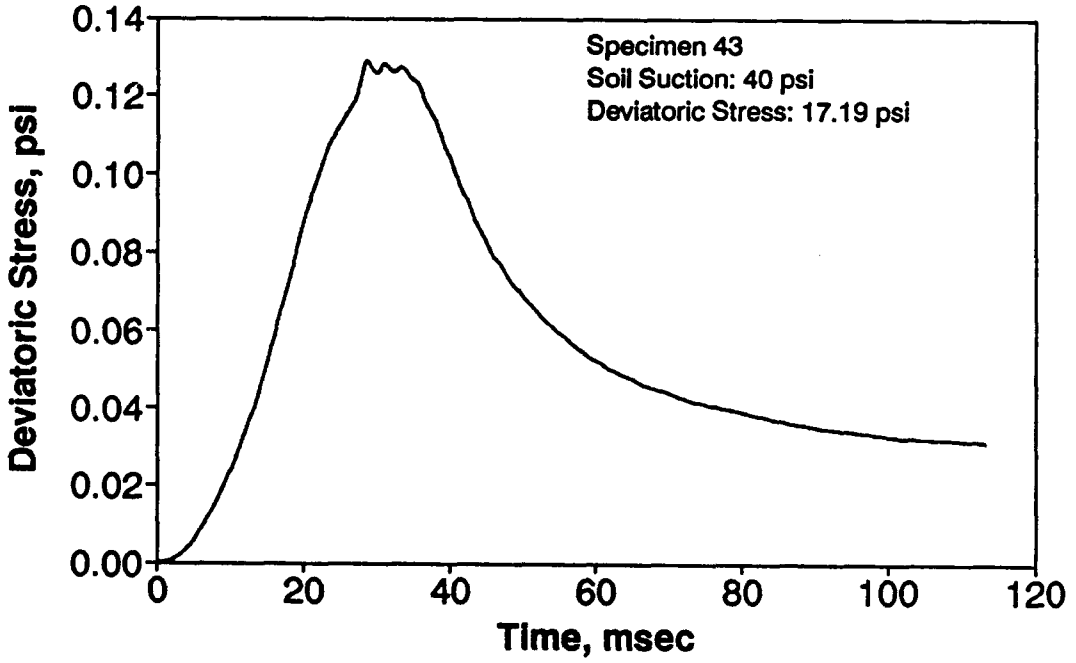
Specimen 43
Soil Suction: 40 psi
Deviatoric Stress: 17.19 psi
Deviatoric Stress, psi
0.14
0.12
0.10
0.08
0.06
0.04
0.02
0.00
0
20
40
60
80
100
120
Time, msec

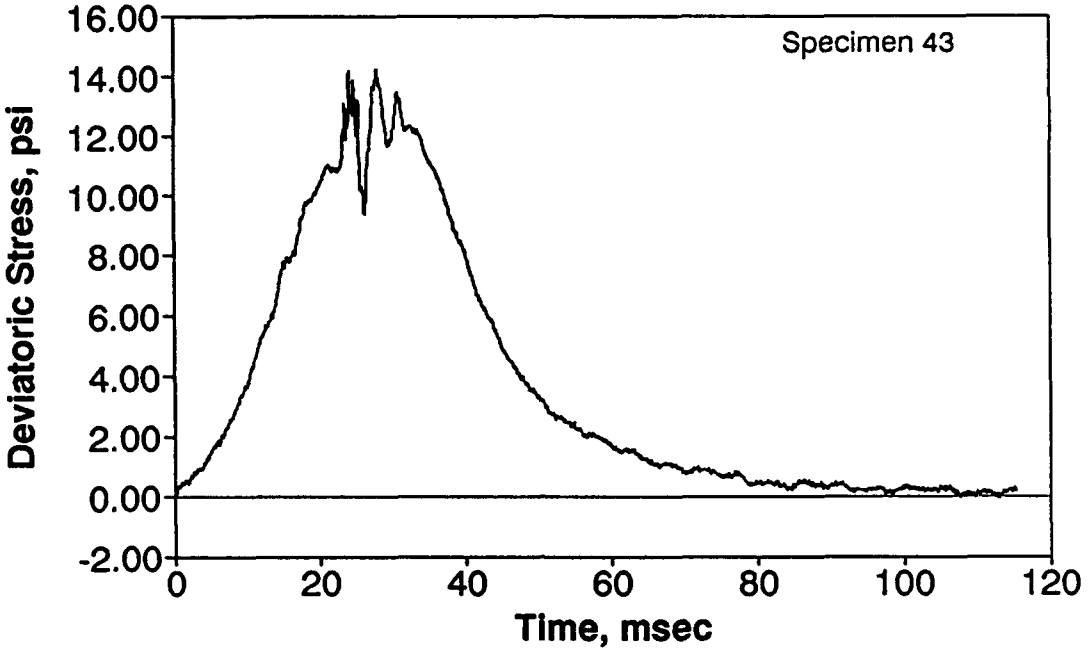
Specimen 43
Deviatoric Stress, psi
16.00
14.00
12.00
10.00
8.00
6.00
4.00
2.00
0.00
-2.00
0
20
40
60
80
100
120
Time, msec

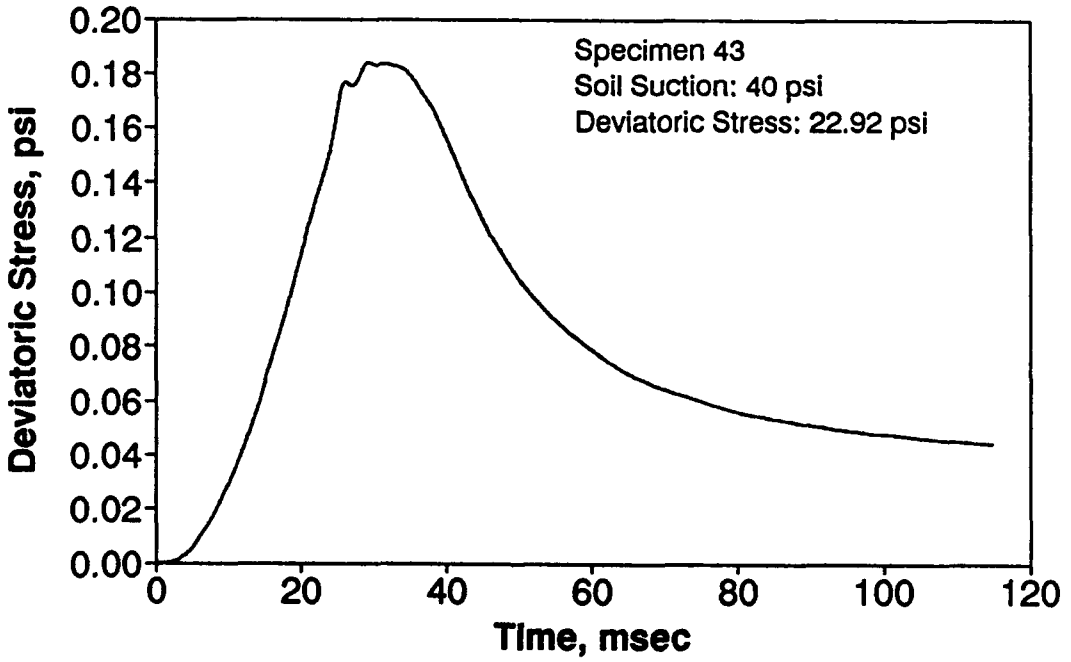
Specimen 43
Soil Suction: 40 psi
Deviatoric Stress: 22.92 psi
Deviatoric Stress, psi
0.20
0.18
0.16
0.14
0.12
0.10
0.08
0.06
0.04
0.02
0.00
0
20
40
60
80
100
120
Time, msec

APPENDIX M

SELECTED RESULTS OF DYNAMIC TESTS

ON

SPECIMENS AT 70 PSI SOIL SUCTION

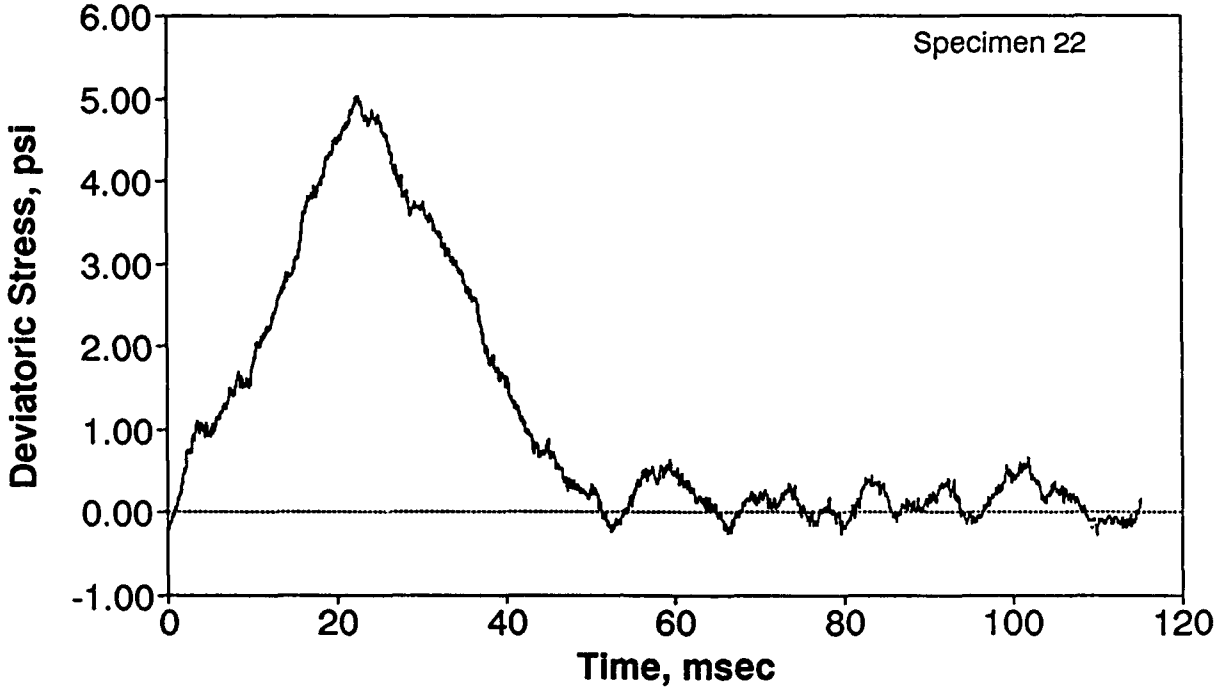
Specimen 22
Deviatoric Stress, psi
6.00
5.00
4.00
3.00
2.00
1.00
0.00
-1.00
0
20
40
60
80
100
120
Time, msec

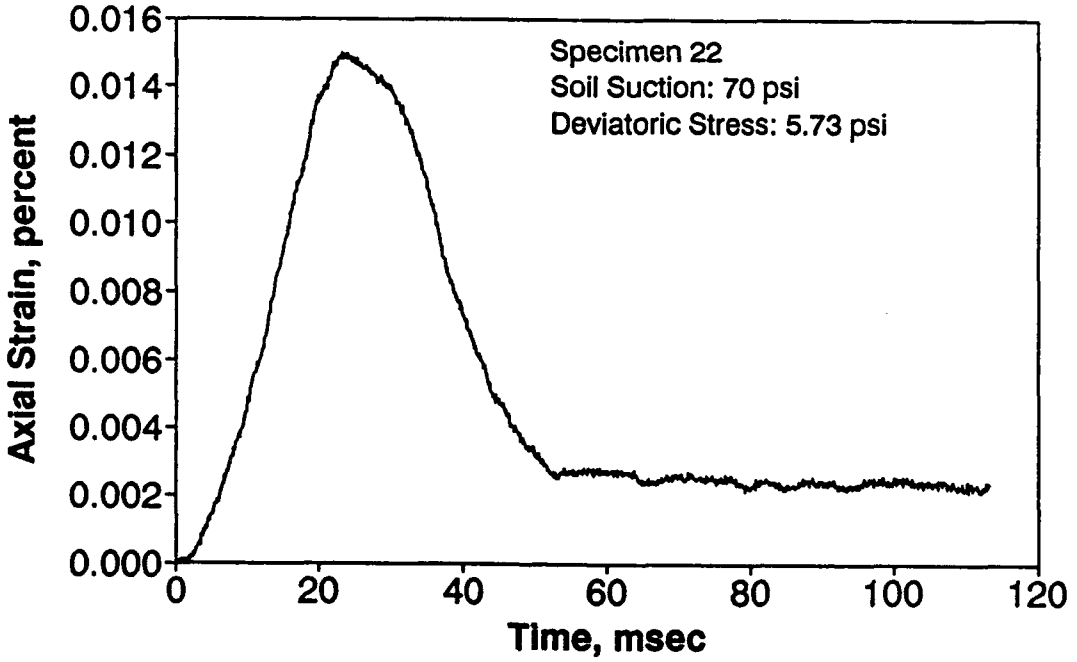
Specimen 22
Soil Suction: 70 psi
Deviatoric Stress: 5.73 psi
Axial Strain, percent
0.016
0.014
0.012
0.010
0.008
0.006
0.004
0.002
0.000
0
20
40
60
80
100
120
Time, msec

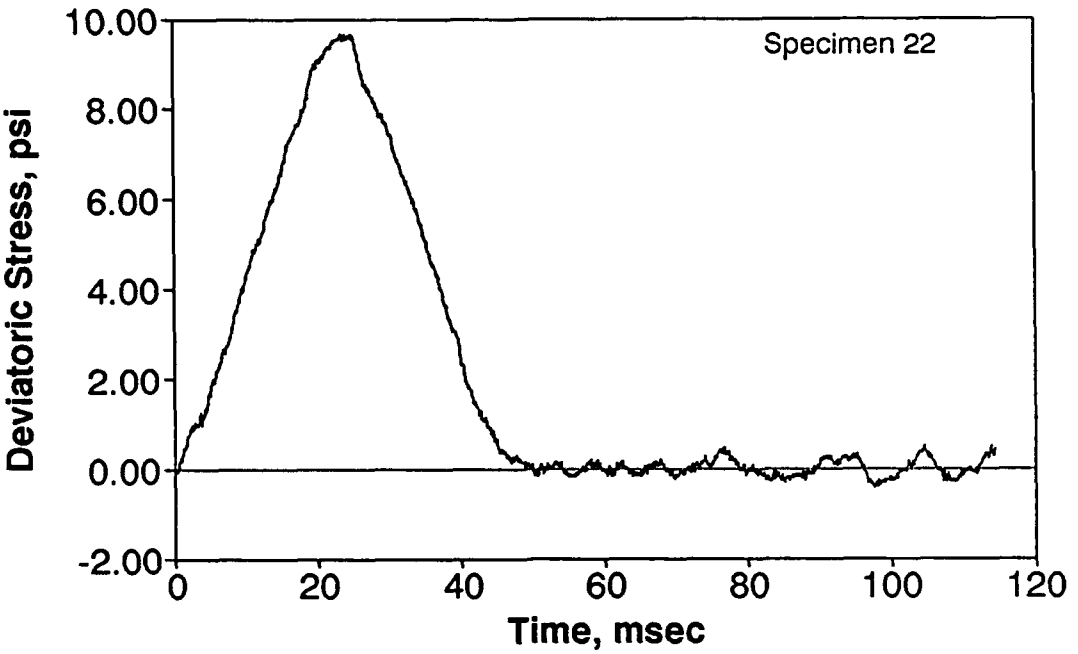
Specimen 22
Deviatoric Stress, psi
10.00
8.00
6.00
4.00
2.00
0.00
-2.00
0
20
40
60
80
100
120
Time, msec

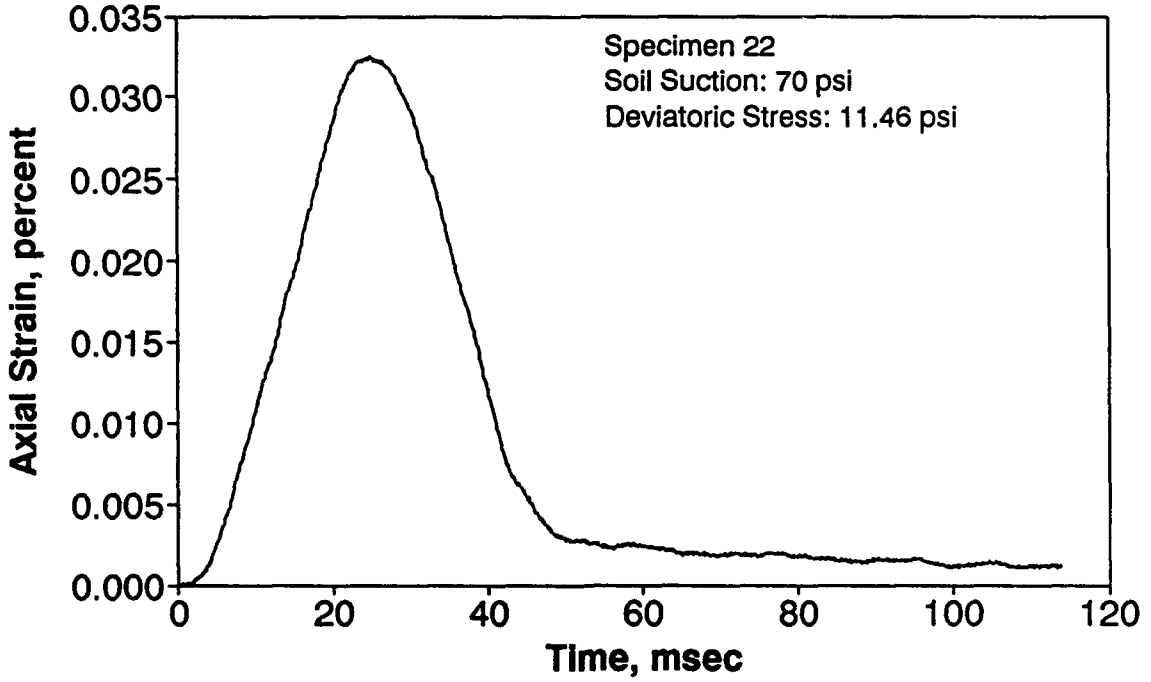
Specimen 22
Soil Suction: 70 psi
Deviatoric Stress: 11.46 psi
Axial Strain, percent
0.035
0.030
0.025
0.020
0.015
0.010
0.005
0.000
0
20
40
60
80
100
120
Time, msec

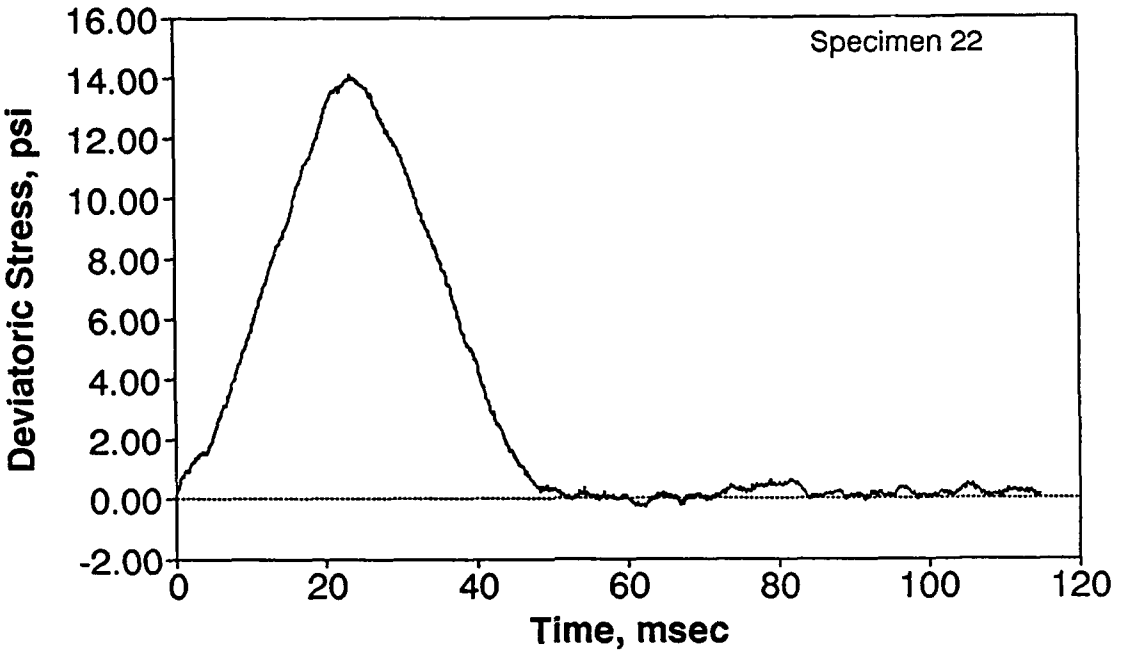
Specimen 22
Deviatoric Stress, psi
16.00
14.00
12.00
10.00
8.00
6.00
4.00
2.00
0.00
-2.00
0
20
40
60
80
100
120
Time, msec

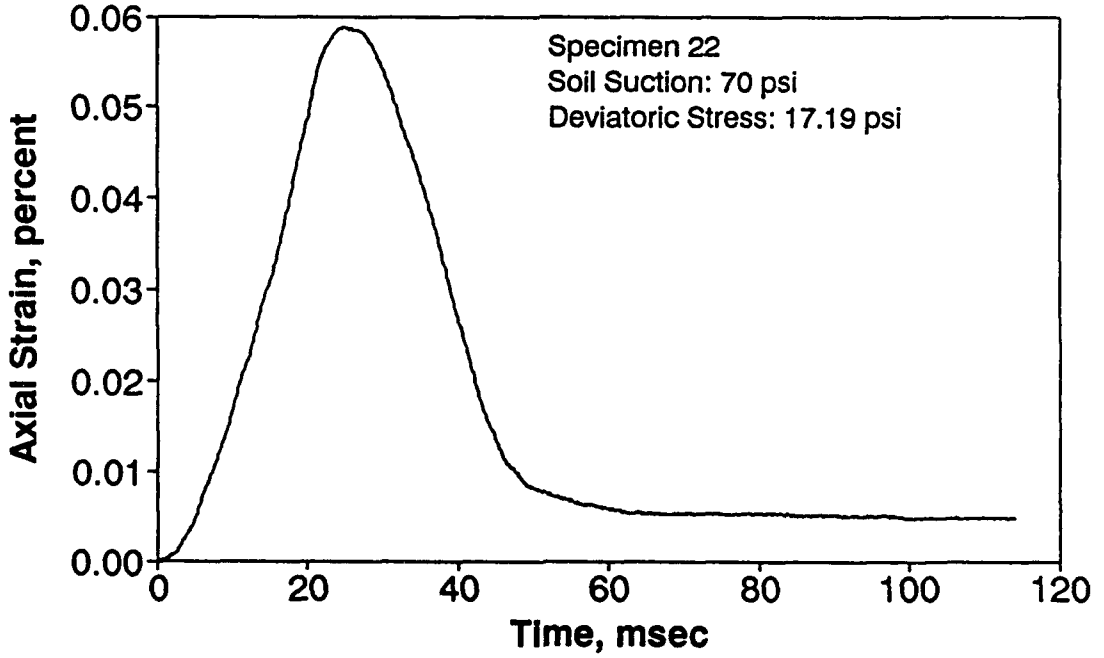
Specimen 22
Soil Suction: 70 psi
Deviatoric Stress: 17.19 psi
Axial Strain, percent
0.06
0.05
0.04
0.03
0.02
0.01
0.00
0
20
40
60
80
100
120
Time, msec

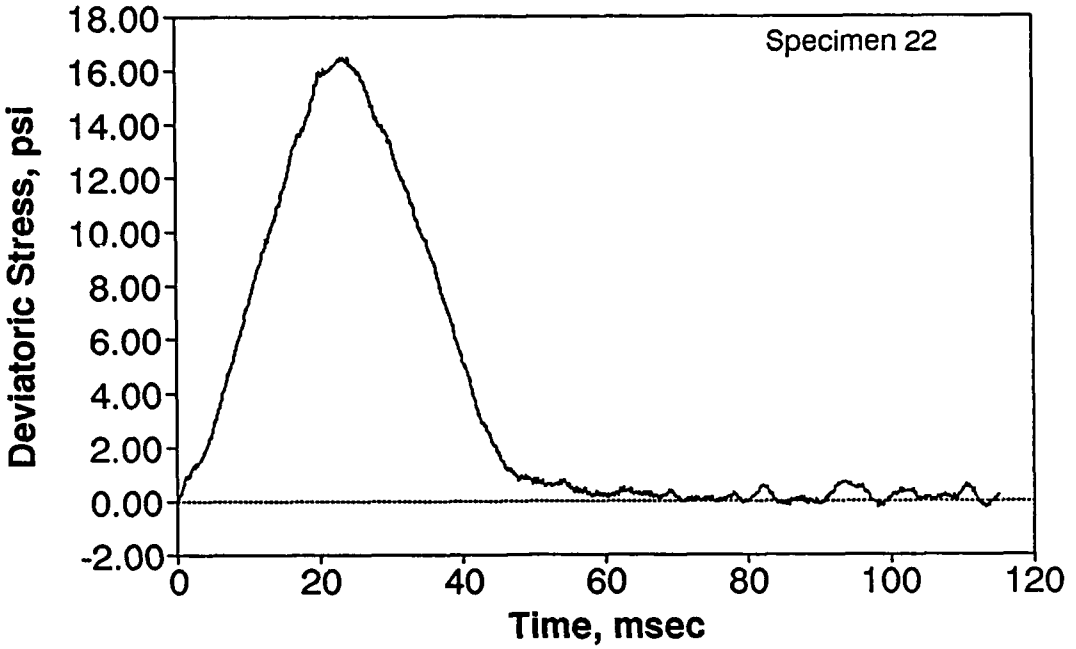
Specimen 22
Deviatoric Stress, psi
18.00
16.00
14.00
12.00
10.00
8.00
6.00
4.00
2.00
0.00
-2.00
0
20
40
60
80
100
120
Time, msec

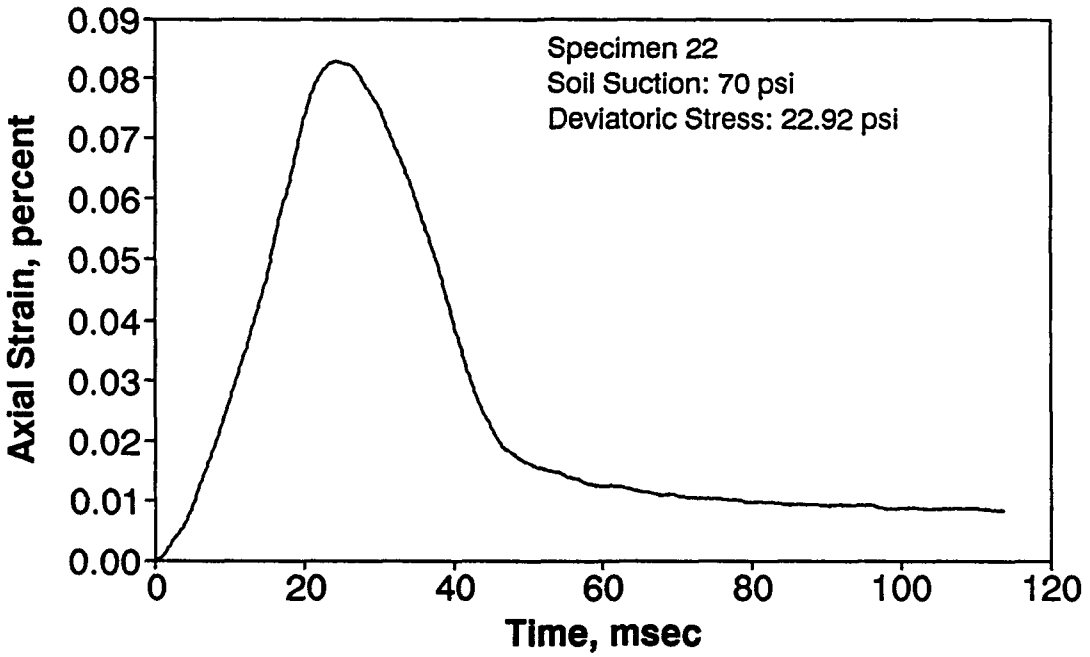
Specimen 22
Soil Suction: 70 psi
Deviatoric Stress: 22.92 psi
Axial Strain, percent
0.09
0.08
0.07
0.06
0.05
0.04
0.03
0.02
0.01
0.00
0
20
40
60
80
100
120
Time, msec

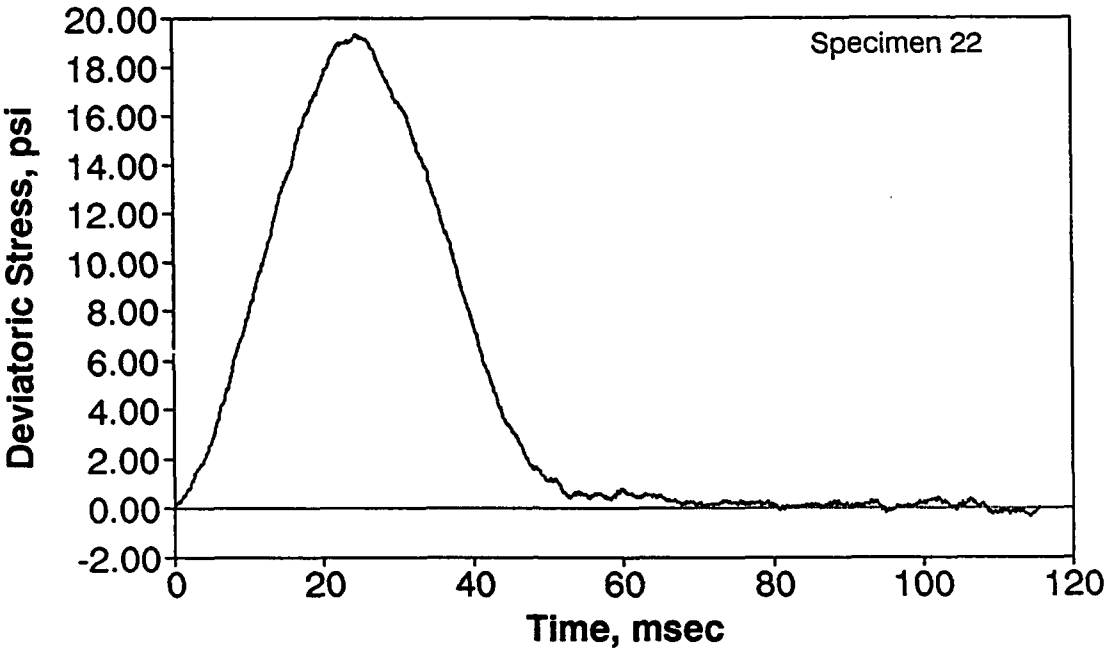
Specimen 22
Deviatoric Stress, psi
20.00
18.00
16.00
14.00
12.00
10.00
8.00
6.00
4.00
2.00
0.00
-2.00
0
20
40
60
80
100
120
Time, msec

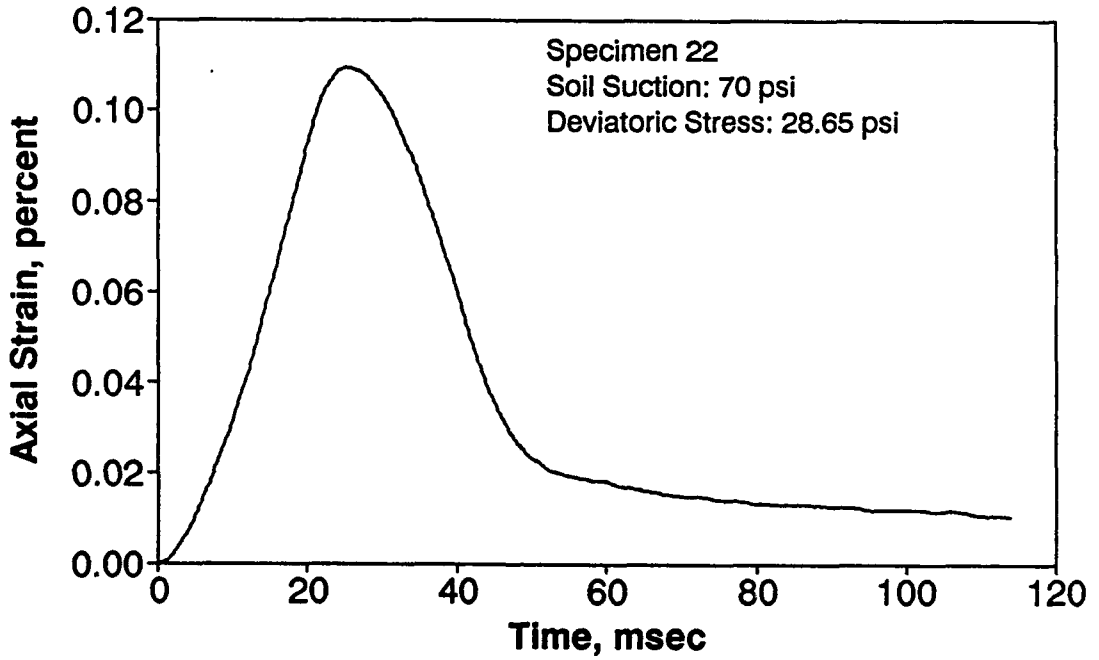
Specimen 22
Soil Suction: 70 psi
Deviatoric Stress: 28.65 psi
Axial Strain, percent
0.12
0.10
0.08
0.06
0.04
0.02
0.00
0
20
40
60
80
100
120
Time, msec

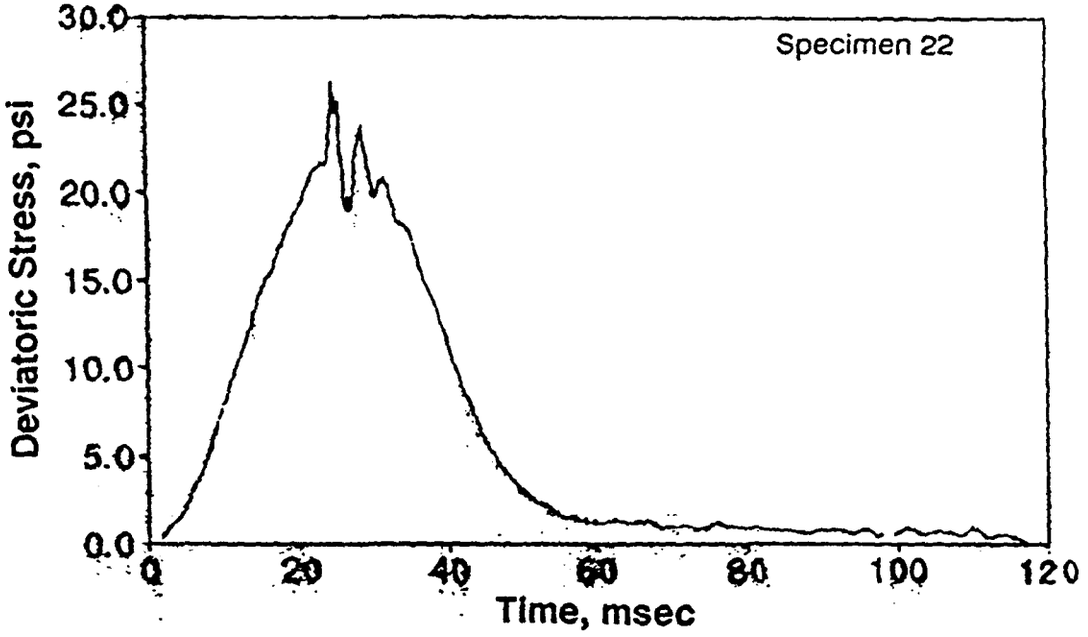
Specimen 22
Deviatoric Stress, psi
30.0
25.0
20.0
15.0
10.0
5.0
0.0
0
20
40
60
80
100
120
Time, msec

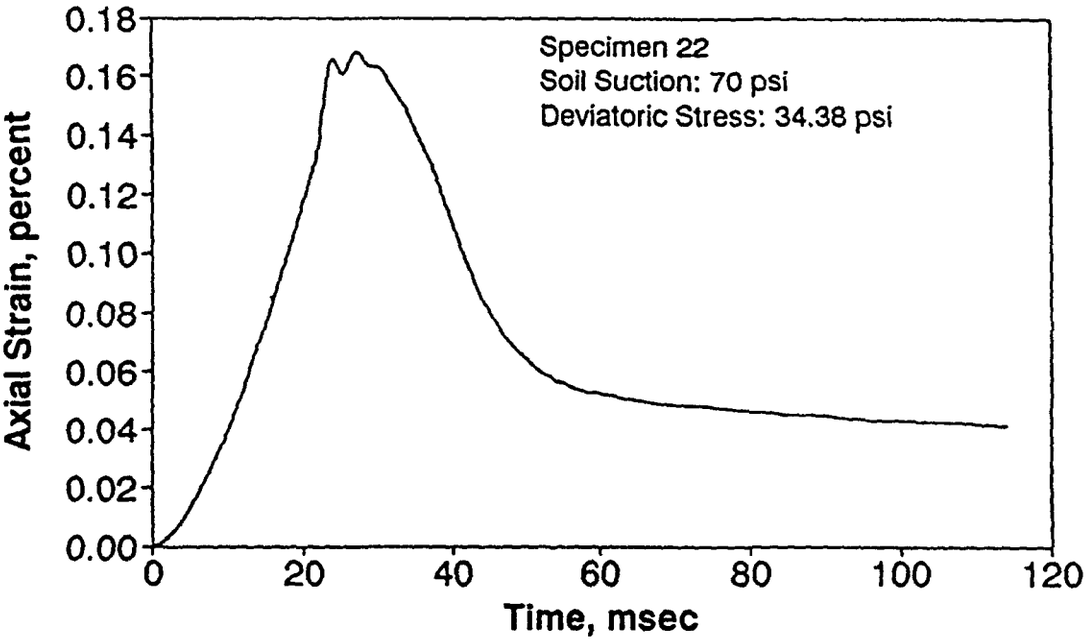
Specimen 22
Soil Suction: 70 psi
Deviatoric Stress: 34.38 psi
Axial Strain, percent
0.18
0.16
0.14
0.12
0.10
0.08
0.06
0.04
0.02
0.00
0
20
40
60
80
100
120
Time, msec

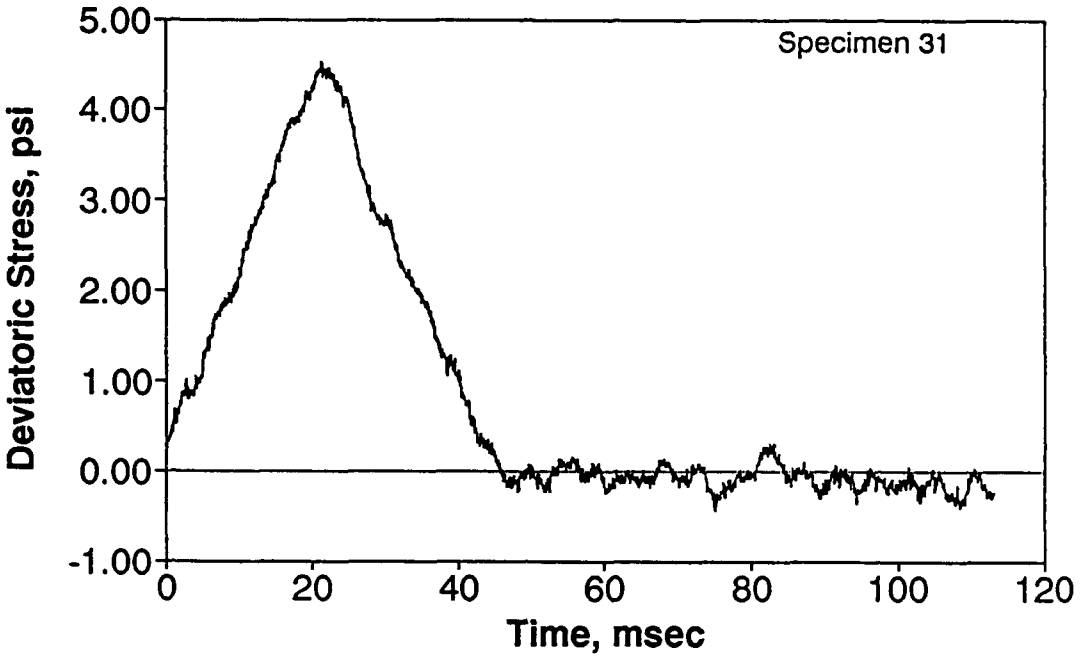
Specimen 31
Deviatoric Stress, psi
5.00
4.00
3.00
2.00
1.00
0.00
-1.00
0
20
40
60
80
100
120
Time, msec

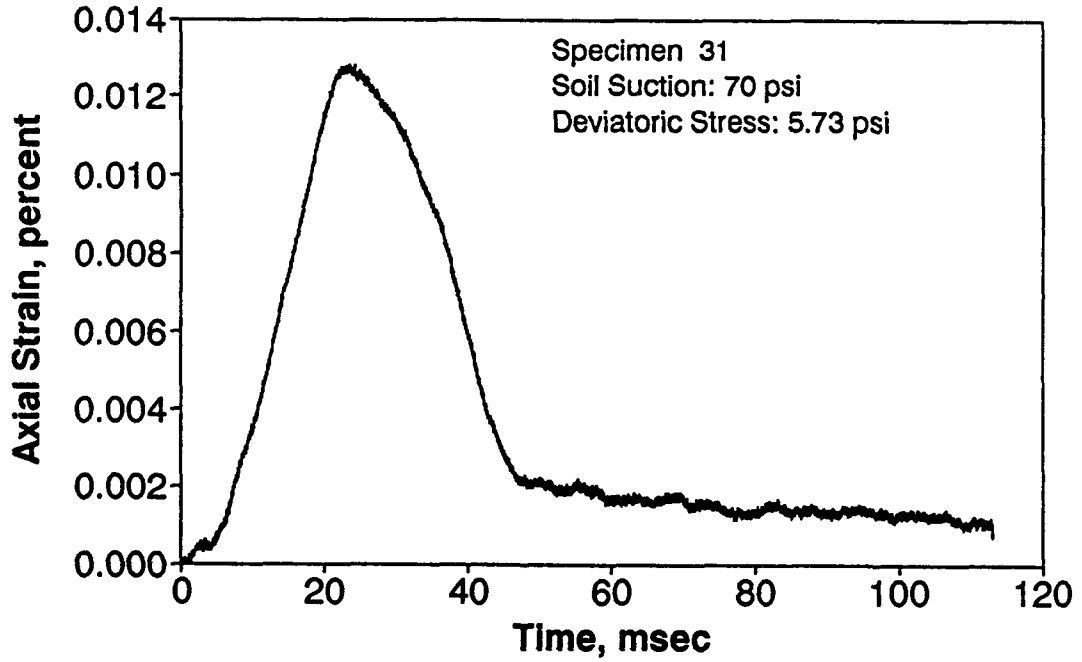
Specimen 31
Soil Suction: 70 psi
Deviatoric Stress: 5.73 psi
Axial Strain, percent
0.014
0.012
0.010
0.008
0.006
0.004
0.002
0.000
0
20
40
60
80
100
120
Time, msec

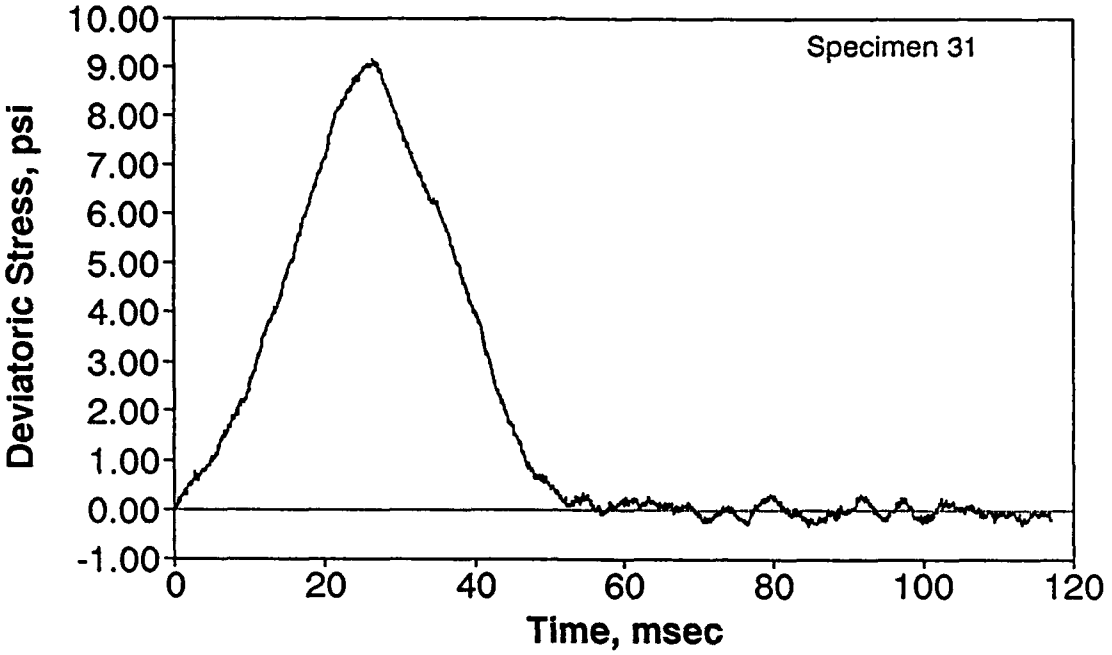
Specimen 31
Deviatoric Stress, psi
10.00
9.00
8.00
7.00
6.00
5.00
4.00
3.00
2.00
1.00
0.00
-1.00
0
20
40
60
80
100
120
Time, msec

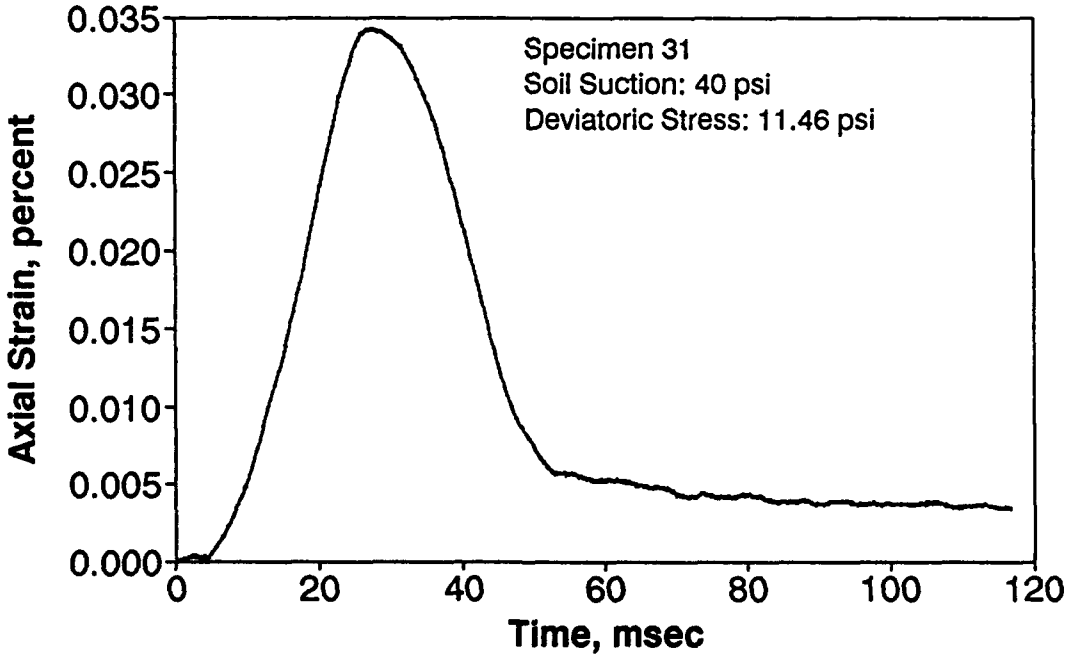
Specimen 31
Soil Suction: 40 psi
Deviatoric Stress: 11.46 psi
Axial Strain, percent
0.035
0.030
0.025
0.020
0.015
0.010
0.005
0.000
0
20
40
60
80
100
120
Time, msec

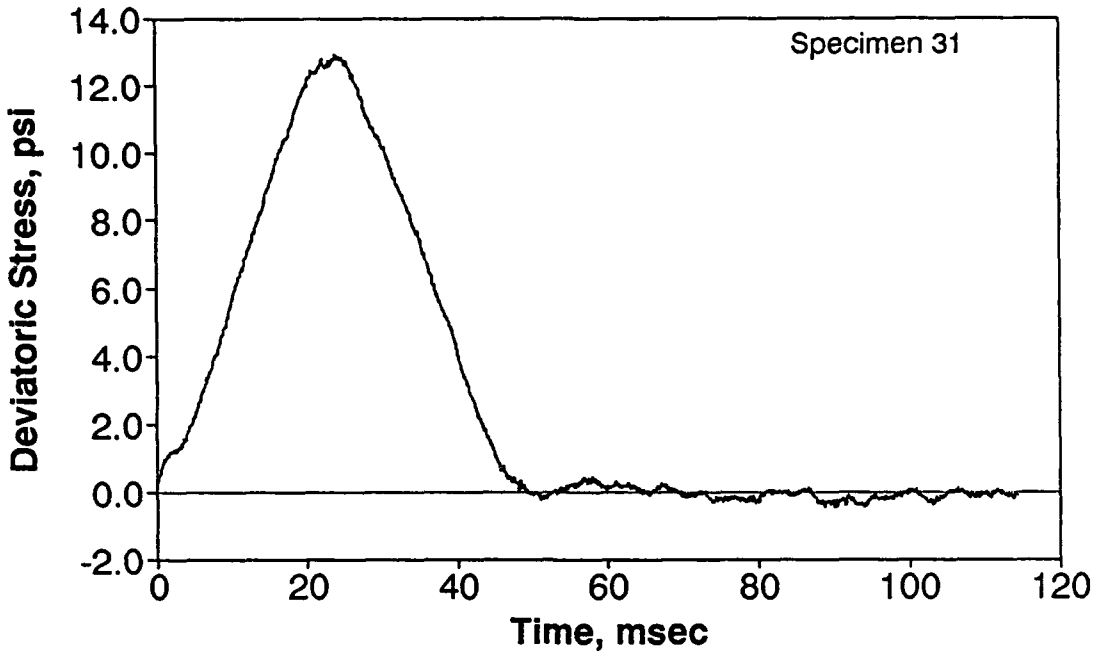
Specimen 31
Deviatoric Stress, psi
14.0
12.0
10.0
8.0
6.0
4.0
2.0
0.0
-2.0
0
20
40
60
80
100
120
Time, msec

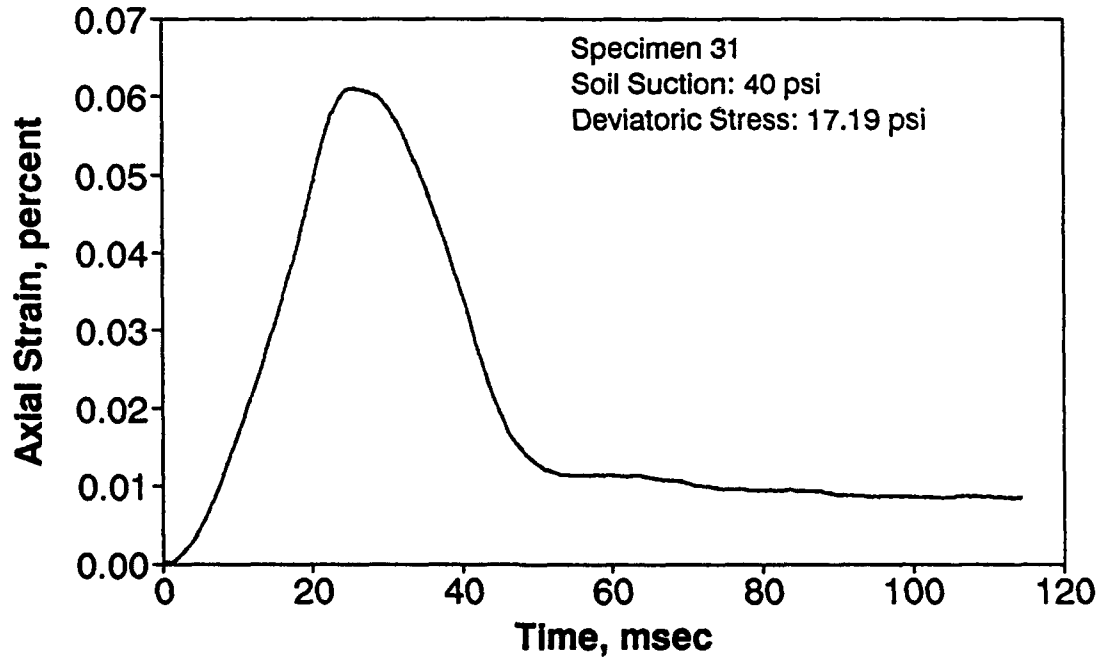
Specimen 31
Soil Suction: 40 psi
Deviatoric Stress: 17.19 psi
Axial Strain, percent
0.07
0.06
0.05
0.04
0.03
0.02
0.01
0.00
0
20
40
60
80
100
120
Time, msec

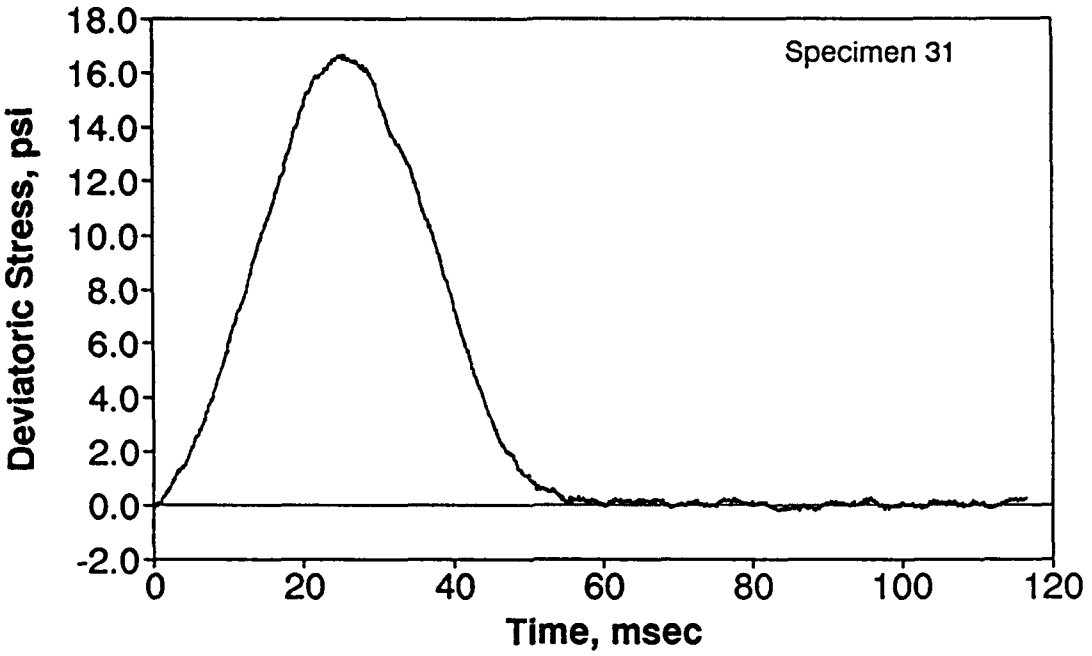
Specimen 31
Deviatoric Stress, psi
18.0
16.0
14.0
12.0
10.0
8.0
6.0
4.0
2.0
0.0
-2.0
0
20
40
60
80
100
120
Time, msec

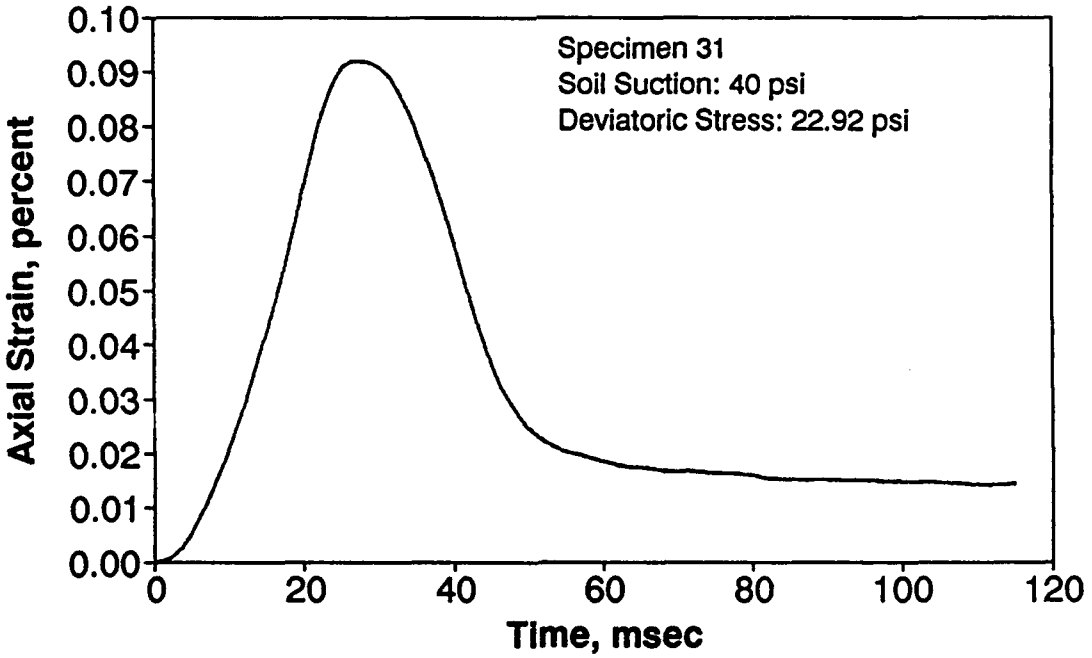
Specimen 31
Soil Suction: 40 psi
Deviatoric Stress: 22.92 psi
Axial Strain, percent
0.10
0.09
0.08
0.07
0.06
0.05
0.04
0.03
0.02
0.01
0.00
0
20
40
60
80
100
120
Time, msec

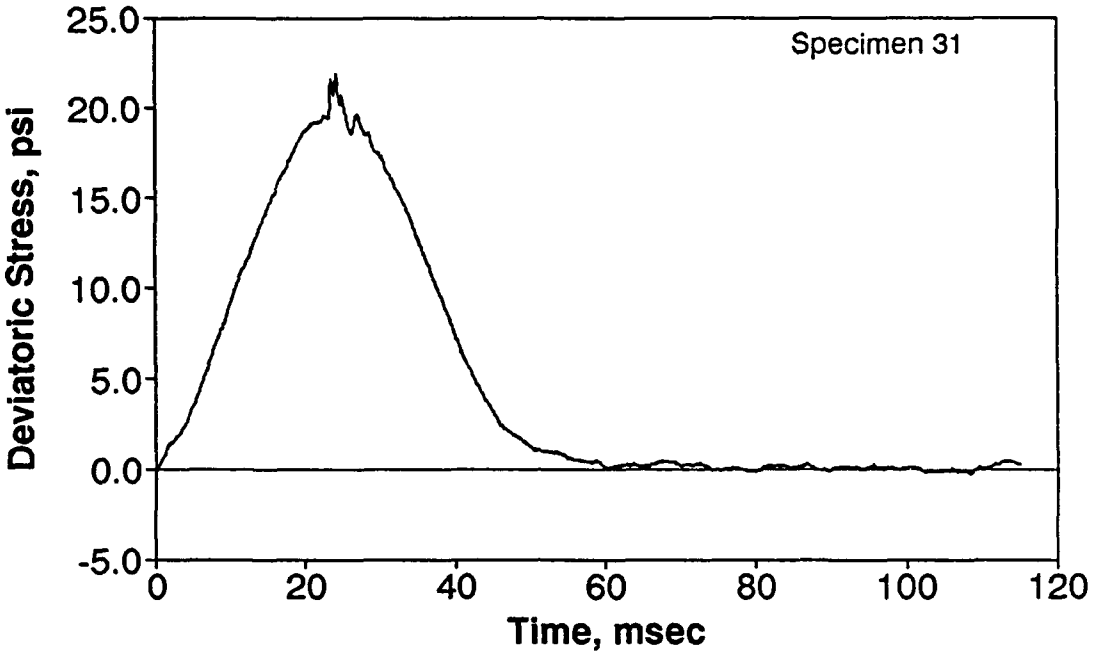
Specimen 31
Deviatoric Stress, psi
25.0
20.0
15.0
10.0
5.0
0.0
-5.0
0
20
40
60
80
100
120
Time, msec

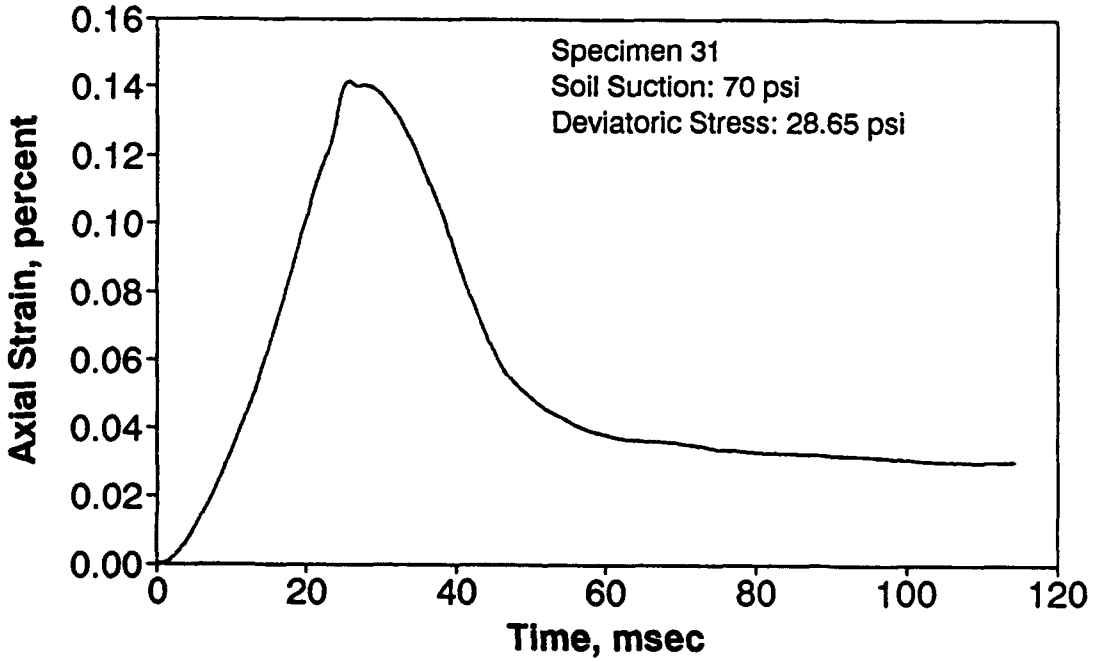
Specimen 31
Soil Suction: 70 psi
Deviatoric Stress: 28.65 psi
Axial Strain, percent
0.16
0.14
0.12
0.10
0.08
0.06
0.04
0.02
0.00
0
20
40
60
80
100
120
Time, msec